FORMATION AND METAMORPHISM OF ALUMINOUS UPPER MANTLE AND LOWER CRUSTAL ROCKS: A CASE STUDY ON WEBSTERITE AND GRANULITE XENOLITHS FROM BASANITES OF THE CHYULU HILLS VOLCANIC FIELD, KENYA

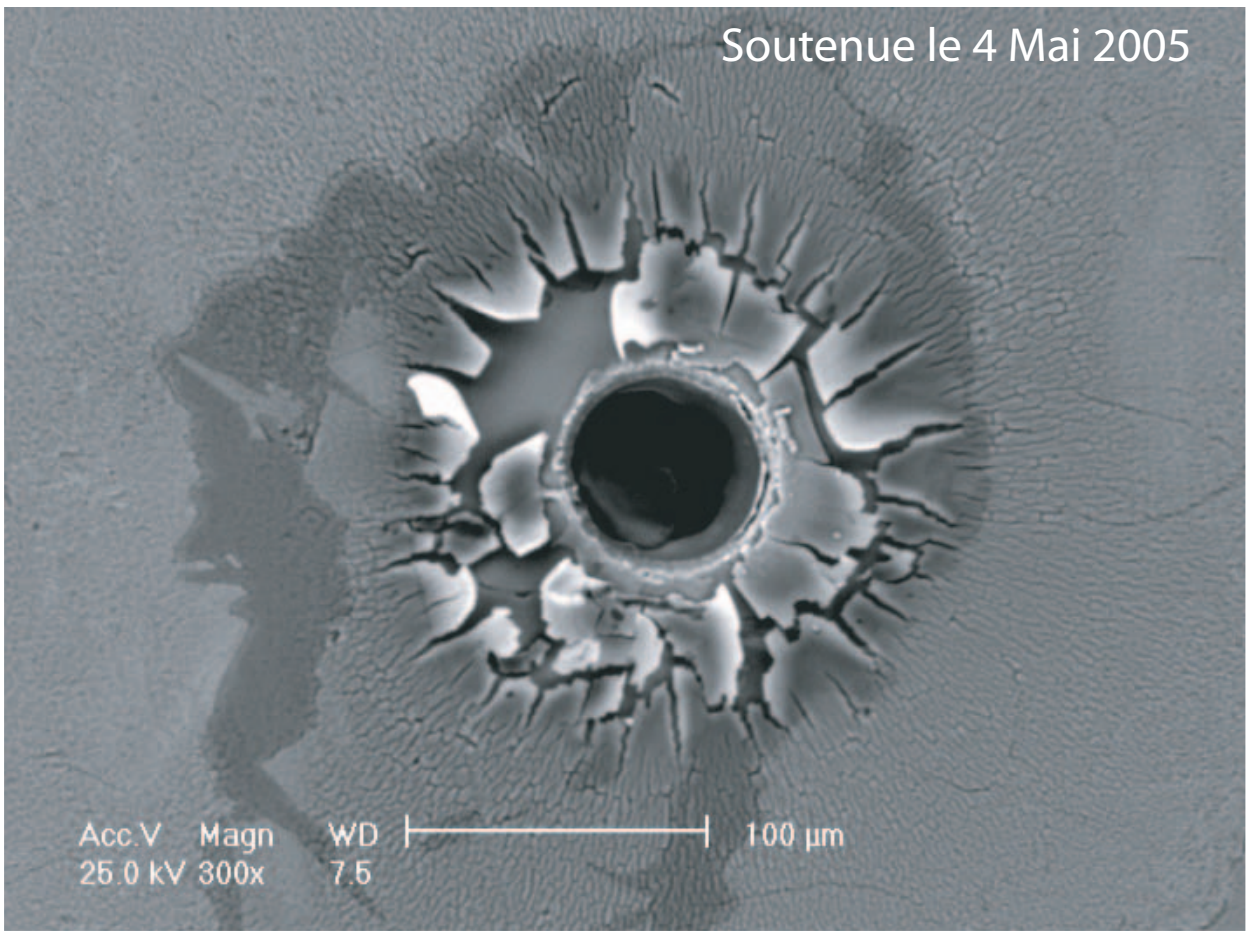
Thèse présentée à la Faculté des Sciences
Institut de Géologie
Université de Neuchâtel

Pour l'obtention du grade de doctor ès sciences
Par

ALEXEY ULIANOV

Acceptée sur proposition du jury:
Prof. Angelika Kalt (Neuchâtel; Supervisor)
Prof. Rainer Altherr (Heidelberg)
Prof. Hilary Downes (London)
Prof. Othmar Müntener (Bern)
Prof. Martin Burkhard (Neuchâtel)

Soutenue le 4 Mai 2005



Université de Neuchâtel
- 2005 -

Abstract

Mots clés: manteau supérior, croûte inférieure, xénolithes, série magmatique, métamorphisme, troctolite, websterite, granulite, sapphirine, hibonite, Mozambique orogène, Les Chyulu Hills, Kenya

Keywords: upper mantle, lower crust, xenoliths, magmatic series, metamorphism, troctolite, websterite, granulite, sapphirine, hibonite, Mozambique mobile belt, Chyulu Hills, Kenya

The Chyulu Hills volcanic field is located on the eastern flank of the Kenya rift some 150 km to the east of the Kenya Rift Valley. It lies on the Pan-African crystalline basement of the Mozambique mobile belt. Quaternary basanites of the Chyulu Hills contain peridotite, pyroxenite and granulite xenoliths entrained from the underlying upper mantle and lower crust. This study focuses on a suite of garnet-spinel olivine websterite, Mg-Al sapphirine-bearing and Ca-Al hibonite-bearing granulite xenoliths from several volcanic cones of the Chyulu Hills. In terms of protoliths, they form an igneous suite linked by fractionation. High bulk rock Mg#'s and very low concentrations of most incompatible elements indicate that the rocks represent a sequence of cumulates rather than crystallized melts. The websterites are the most magnesian part of this sequence, while the granulites are less magnesian and more rich in aluminum, calcium and alkalis. Along with constraints from postmagmatic *P-T* evolution, low HSFE abundances, LILE enrichment and fractionation of LREE over HREE in whole rock samples suggest that the protoliths of the xenoliths may represent arc cumulates, which implies that they should be of Pan-African age.

The normative compositions of the granulites are dominated by plagioclase and olivine. This, as well as the elevated abundances of Ni, low concentrations of Cr and HFSE and positive Eu anomalies in REE patterns suggests that the protoliths of the granulites were troctolitic cumulates. The original mineral assemblages were almost completely transformed by subsolidus processes. Mg-Al granulites contain the minerals spinel, sapphirine, sillimanite, plagioclase, corundum, clinopyroxene, orthopyroxene and garnet, while Ca-Al granulites are characterized by hibonite, spinel, sapphirine, mullite, sillimanite, plagioclase, quartz, clinopyroxene, corundum, and garnet. In the Mg-Al granulites, the first generation of orthopyroxene and some spinel may be of igneous origin. In the Ca-Al granulites, hibonite (and eventually some spinel) are the earliest mineral in the crystallization sequence and may represent igneous relicts. Most pyroxene and spinel as well as corundum in both Mg-Al and Ca-Al granulites have formed by subsolidus reactions. The qualitative *P-T* path derived from metamorphic reactions corresponds to subsolidus cooling accompanied or followed by compression. Final equilibration was achieved at $T \approx 600\text{-}740$ °C and $P < 8$ kbar, the pressure range being constrained by the stability of sillimanite. The early coexistence of corundum and pyroxenes (± spinel) as well as the association of sillimanite and sapphirine with clinopyroxene and the occurrence of hibonite makes both types of the studied granulite lithologies rare. The Ca-Al hibonite-bearing granulites are unique. Both types enlarge the spectrum of known Ca-Al-Mg-rich granulites worldwide.

Hibonite found in two xenoliths of the Ca-Al granulites occurs as small grains in the inner parts of complex corona textures where it forms intergrowths with spinel and sapphirine and shows reaction relationships with later mullite and sillimanite. Chemically, the analyzed hibonite is close to the idealized formula $Ca(Al,Cr,Ti,Si,Mg,Fe^{2+})_{12}O_{19}$ and does not contain other major components. It is similar to terrestrial hibonite in its (Fe+Mg) contents but shows the elevated Al and Ca abundances as well as the relative depletion in Ti and REE typical of meteoritic hibonite. Silica contents are high and exceed those in any other terrestrial and meteoritic hibonite. In order to evaluate the possibility of magmatic crystallization of hibonite in the igneous protoliths of the studied rocks, we compare some of the measured element abundances with those expected from element partitioning data for hibonite and Ca,Al-rich silicate melt. Based on this comparison, formation of low-Ti hibonite that is relatively rich in LREE appears consistent with magmatic crystallization, whereas hibonite with elevated Ti contents, low in LREE, is obviously the result of diffusion re-equilibration in the course of subsolidus cooling.

For the websterite xenoliths, there is an apparent contradiction between the textural-mineralogical data and results of *P-T* calculations that appear to suggest high-P igneous crystallization of pyroxenes under upper mantle conditions on the one hand and the positive Eu anomaly that suggests shallow-level plagioclase accumulation on the other hand. This contradiction can in part be reconciled by a model of compression of a plagioclase-bearing (gabbroic) protolith at near-igneous temperatures to mantle depth where it obtained its ultramafic phase assemblage. This would require foundering of dense lower crustal material into the mantle towards the end of Pan-African subduction and accretion, a process that is possible in areas with high geothermal gradients such as arcs.

The subsequent *P-T* evolution of the websterites as well as of most other types of upper mantle xenoliths from the Chyulu Hills is defined by a long period of cooling that may in some specimens be followed by (a) recent heating event(s). The chemical zoning patterns of orthopyroxene are either flat (suggesting complete subsolidus diffusion reequilibration) or show a core-to-rim decrease of Al and Ca indicating cooling. In both cases, Al and Ca may show a rimwards increase in the outermost zones of the orthopyroxene grains that is consistent with heating. Results from diffusion modeling for pyroxenes, albeit highly approximate, suggest that the rimwards increase in Al and Ca associated with heating is temporally related to the young volcanic activity of the Chyulu Hills, whereas the duration of cooling is much longer and may correspond to the age of the Pan-African orogeny (ca. 600 Ma).

Pressure-temperature data on equilibrated xenoliths suggest a geotherm beneath the Chyulu Hills similar to a $\sim$60–70 mW m^{-2} steady-state model geotherm. The lithospheric thickness is constrained to ca. 115 km. The late heating affected xenoliths derived from depths of ca. 80-40 km. It represents a local feature most probably related to small magma intrusions in the lithospheric mantle.

Preface

This thesis is part of a research project that aims to build a better understanding of the origin and evolution of the upper mantle and lower crust in the area of the East African Rift System via the study of deep-seated xenoliths from alkali volcanic rocks. This project was initiated by Prof. Angelika Kalt some four years ago and represents part of a long-standing research on xenoliths and alkali volcanics from the East African Rift that is rooted in her doctoral thesis and has never been forgotten ever since. It is currently being supported by the Swiss National Science Foundation grant 200021-100647/1 and housed at the Institute of Geology of the University of Neuchâtel.

During my bachelor and master theses at the University of St. Petersburg I have been specialized in diamond geology and xenolith petrology and doing anything else appeared unthinkable. This study is on the divide between the rather specific field of xenolith research and conventional magmatic and metamorphic petrology. Although first lessons of swimming in the pool were not always to my liking, now I appreciate this and believe that otherwise I would have deprived myself from many delights petrology can offer.

I also appreciate the opportunity to learn different cultures and languages that has always been open during the course of this study. This turned to be a painful experience at the beginning but becomes a source of enjoyment now. Although I may have been a rather negligent scholar, I tried to go this way as far as I could. All errors and failures I made *en route* are certainly mine, whereas the successes should be sheared with many other people.

I would sincerely like to thank:

Angelika Kalt for offering me the opportunity to do research at the University of Neuchâtel and thus making my further progress possible, which may have not been the case if I would not have left from St Petersburg for abroad. I thank her for offering specimens for this study, providing toward circumstances during its course and managing this research in cases I was less capable of doing that. Our professional relationships eventually turned to be productive, and this is to a significant extent her merit.

Rainer Altherr for offering specimens used in this study and microprobe facilities at Heidelberg to analyze them, discussing the results and valuable comments on earlier versions of the manuscripts included in the thesis. His continuous interest in my research and help on countless occasions resulted in improving the quality of the whole work and in speeding it up. I am particularly indebted to him for his help at the beginning of the thesis when many questions have remained open.

Othmar Müntener for those significant adjustments I have been making to my style of work under his influence during the course of the Ph.D. project, and for valuable comments on one of the manu-

scripts this thesis is made of. On a more personal basis, I would also like to thank him for helping me with learning German.

Valery Ivanikov for introducing me to alkaline and mantle petrology during my study at St. Petersburg.

Edwin Gnos, Thomas Burry and Philipp Hunziker for fixing malfunctions on the electron microprobe at Bern.

Hans-Peter Meyer for fixing malfunctions on the electron microprobe at Heidelberg.

Massoud Dadras for excellence in maintaining the scanning electron microscope at Neuchâtel.

Thomas Pettke and *Vincent Serneels* for help with LA-ICPMS and XRF measurements, respectively, and *André Villard* for preparing high-quality thin sections.

On a personal basis, I would also like to thank:

Flurin Vils, my roommate at the Institute of Geology, for creating a friendly environment and maintaining good partnership during the last stage of my Ph.D. project, and for providing his computer when mine has failed at the very end of work on the thesis. Without his help, the latter would have unlikely been printed out!

Benjamin Kaeser, my fellow doctoral student, for his professional friendship and also for helping me with learning German.

Other Staff, doctoral, graduate and undergraduate students at the Institute of Geology of the University of Neuchâtel: Thierry Adatte, Martin Burkhard, Erwan Bourdon, Christophe Dupraz, Giafranca Cerrito, Roberto Costa, Sabine Erb, Raymond Flinn, Karl Föllmi, Elisabeth Kuster, Virginie Matera, Jean-Paul Schaer, Pierre-André Schnegg, Manuel Da Silva, Philipp Steinmann, Christian Sue, Pierre Tissot, Eric Verrecchia, Francois Zwalen, Alexis, Baba, Barbara, Bastien, Bernd, Cécile, Charles, Claire, Cyril, Ellen, Federica, Guillaume, Kaspar, Laure, Mahmoud, Mary-Alix, Nicolas, Pascal, Rachel, Ronny, Stéphane, Cédric, Géraldine, Laureline, Marina, Michael, Michèle, Naomi, Tomaso.

My parents.

TABLE OF CONTENTS

CHAPTER I: Introduction

Background and aim of this study	I- 1
Geological overview	I- 4
Organization of the thesis	I- 7
Relative contribution of workers	I- 8
References	I- 8

CHAPTER II: Aluminous websterite and granulite xenoliths from the Chyulu Hills volcanic field, Kenya: Metamorphosed gabbroic cumulates from a Pan-African arc environment

Paper submitted to Contributions to Mineralogy and Petrology

Abstract	II- 1
Introduction	II- 1
Geological setting	II- 2
Analytical techniques	II- 3
Petrography, major element composition of minerals and P-T evolution	II- 4
Trace elements in minerals	II- 12
Whole-rock major and trace element composition	II- 16
Discussion	II- 18
Conclusions	II- 25
Acknowledgements	II- 25
References	II- 26

CHAPTER III: Mg-Al sapphirine and Ca-Al hibonite-bearing granulite xenoliths from the Chyulu Hills volcanic field, Kenya

Paper submitted to Journal of Petrology

Abstract	III- 1
Introduction	III- 1
Geological setting	III- 2
Analytical techniques	III- 4
General chemical and petrographic features	III- 5
Textures and mineral compositions	III- 7
Pre-metamorphic vs. metamorphic mineral assemblages	III- 20
Thermobarometric constraints	III- 21
Metamorphic reactions in the Mg-Al sapphirine-bearing granulites	III- 23
Metamorphic reactions in the Ca-Al hibonite-bearing granulites	III- 26
Mineral zoning as indicator of the metamorphic evolution	III- 28
Discussion	III- 29
Summary and conclusions	III- 31
Acknowledgements	III- 32
References	III- 32

CHAPTER IV: Hibonite, $Ca(Al,Cr,Ti,Si,Mg,Fe^{2+})_{12}O_{19}$, in granulite xenoliths from the Chyulu Hills volcanic field, Kenya

Paper published in European Journal of Mineralogy (2005). V. 17(1-2), 357-366

Abstract IV- 357
Introduction IV- 357
Analytical techniques IV- 358
Chemical composition of whole-rock samples IV- 359
Petrography IV- 359
Textural relations of hibonite IV- 359
Chemical composition of hibonite IV- 359
Mode of formation of hibonite IV- 362
Concluding remark IV- 365
Acknowledgements IV- 365
References IV- 365

CHAPTER V: Composition and thermal evolution of the lithospheric mantle beneath the Chyulu Hills (Southern Kenya, East African Rift) as deduced from xenoliths

Paper submitted to Journal of Petrology

Abstract V- 1
Introduction V- 1
Geological setting V- 3
Analytical techniques V- 5
Xenolith types and mineral composition V- 5
Metamorphic evolution and geothermobarometry V- 30
Discussion V- 39
Conclusions V- 43
Acknowledgements V- 44
References V -44

CHAPTER VI: General conclusions VI- 1

APPENDIX

Photomicrographs of the studied specimens i-viii

Electron microprobe analyses of minerals from the studied specimens

Ca-Al granulites: 1904-1 1
1904-9 19
1906-2 37

Mg-Al granulites: 1904-3 51
1904-7 73

Websterites: 1910-11 107
1910-1 133
1535-3 159
1906-4 169

CHAPTER I

Introduction

CHAPTER I

Introduction

Background and aim of this study

Alkali volcanic rocks often contain fragments of the Earth's upper mantle and lower crust entrained from the walls of the magma conduit during fast ascent of the magma to the surface. Such fragments, so-called xenoliths, typically bear no genetic relationship to the transporting magma. They are used to directly access the composition, properties, and evolution of the lithosphere beneath volcanic edifices. The xenoliths represent chaotic 'snapshots' of the lithosphere sampled by the host magma and are not necessarily genetically related. They may correspond to protoliths of different age, origin and metamorphic history, which hampers using them for deciphering petrogenetic processes in the lithosphere.

Sometimes, however, genetic relationships between xenoliths can be recognized. The geochemical study of such xenoliths leads to a better understanding of petrogenetic processes in the lithosphere, while the study of their metamorphic history helps to better understand the subsequent evolution of the lithosphere.

Meta-igneous comagmatic suites of mafic and ultramafic rocks linked by fractionation represent an important petrologic association in the lower crust and underlying upper mantle that may account for significant volumes of rocks and define the very nature of the crust-mantle boundary. Such mafic-ultramafic associations overprinted by the events of subsolidus thermal relaxation and metamorphism and consisting mainly of pyroxenite and granulite occur in some xenolith suites related to intraplate alkaline volcanism (e.g. Grégoire *et al.*, 1998; Upton *et al.*, 2001). This study focuses on a comagmatic suite of aluminous meta-igneous cumulates found as xenoliths in basanites of the Chyulu Hills volcanic field formed in Quaternary times on the eastern flank of the Kenya Rift and located within the Pan-African Mozambique mobile belt.

The studied rock suite includes garnet-spinel olivine websterites, Mg-Al two-pyroxene sapphirine-bearing granulites and Ca-Al clinopyroxene hibonite-bearing granulites. Mineralogical and geochemical characteristics of these rocks indicate that they cannot be considered as cumulates of alkaline magmatism related to the development of the Kenya Rift. The major and trace element data on minerals and whole rock samples as well as the subsolidus (metamorphic) history of the rocks appear most consistent with their origin as cumulates of Pan-African arc-type magmatism.

The geochemical and mineralogical characteristics of the websterite xenoliths suggest that their protoliths may have formed at a relatively shallow (lover crustal) depth and originally represented plagioclase-bearing mafic cumulates, with subsequent foundering of this dense material into the mantle after the cessation of Pan-African subduction. The Pan-African arc lithosphere may, therefore, have been thinned by some foundering process such as described for the southern Sierra Nevada today (Ducea, 2001; Zandt *et al.*, 2004). There, xenolith evidence suggests that the eastern Sierra Nevada has lost about half of its original 'petrologic' crust due to the convective removal of dense pyroxene- and garnet-dominated rocks localized at the base of the crust (e.g., Ducea & Saleeby, 1996; Zandt *et al.*, 2004), while seismic

tomography reveals a dense keel descending into the upper mantle, imaging the process of foundering in action (Boyd *et al.*, 2004). Foundering dense lower crustal lithologies into the mantle is also in line with the reaction sequences inferred from metamorphic textures in the granulite xenoliths, which indicate postmagmatic cooling followed by compression towards the end of the reaction path.

The study of the granulites is complementary to that of the websterites. Granulites are traditionally considered as the key to the understanding of the nature of high-temperature to ultrahigh-temperature metamorphism in the Earth's crust, as reaction textures and the *P-T* evolution of granulites can be used to unravel metamorphic processes and their causes (e.g. Bohlen, 1987, 1991; Harley, 1989). Granulites are also a major tool for investigating the chemical composition of the Earth's lower crust (e.g. Jan & Howie, 1981; Downes, 1993; Kempton *et al.*, 2001).

Historically, studying granulites from outcropping metamorphic complexes was never the same as studying granulite xenoliths in volcanic rocks. The study of outcropping granulites often benefits from the incorporation of the both approaches, 'metamorphic' and 'geochemical' (e.g. Osanai *et al.*, 1998; Möller *et al.*, 1998; Bhattacharya & Kar, 2002). Granulite xenoliths from volcanic rocks are traditionally considered in the context of their chemical composition (e.g. Rudnick *et al.*, 1986; Rudnick, 1992; Downes, 1993; Huang *et al.*, 1995; Kempton *et al.*, 2001), with far less attention being paid to their metamorphic evolution (Christy, 1989; Dawson *et al.*, 1997). The overwhelming dominance of the geochemical approach to granulitic xenoliths is partly justified, as a given section of the Earth's middle to lower crust, sampled by an ascending magma, may include rocks of different provenance, age and metamorphic evolution, juxtaposed by various tectonic processes (e.g. Downes *et al.*, 1990; Kempton *et al.*, 1990). This, however, is not the case if comagmatic meta-igneous xenolith suites are concerned. Blending the both stereotypes, which does not seem to encounter insurmountable difficulties *a priori*, is the thinking that defines the organization and outcome of this work.

In terms of chemical and mineralogical composition of the protoliths, the studied granulites belong to the same sequence of magmatic fractionation as the websterites. The websterites are the most mafic and magnesian members of this sequence, while the Mg-Al sapphirine-bearing granulites are more Si- and Al-rich and less magnesian. They consist of ortho- and clinopyroxene, corundum, spinel, sapphirine, sillimanite, plagioclase and garnet. The Ca-Al hibonite-bearing granulites are most enriched in Si and Al. They are dominated by clinopyroxene and plagioclase and may contain hibonite closely associated with spinel, mullite, sapphirine and sillimanite. Hibonite [$CaAl_{12}O_{19}$], which is very rare in terrestrial rocks, is the earliest mineral in the crystallization sequence. All rocks are poor in REE, HFSE and Cr and enriched in LILE and Ni. The C.I.P.W. normative compositions of the granulites are dominated by olivine and plagioclase that, together with the trace element data, suggests troctolitic cumulates as their protoliths. The igneous mineral association has to a large degree been replaced by metamorphic assemblages. The only relicts survived metamorphism appear to be some orthopyroxene grains in the Mg-Al sapphirine-bearing and hibonite in the Ca-Al hibonite-bearing granulites.

In terms of the metamorphic evolution, the studied granulites display a wealth of early, prograde reaction textures, whereas convincing indications of the post-peak evolution and retrogression are lacking. The reaction path of the granulites is defined by cooling and compression, with no clear evidence for subsequent decompression. It distinguishes them from granulites in outcropping metamorphic complexes (most of which show at least some retrogression) and allows one to better understand the early metamorphic evolution in the course of granulite facies metamorphism.

Hibonite occurring in the Ca-Al granulites is an oxide mineral of the magnetoplumbite group. The latter includes about ten end-member minerals with the general formula $AB_{12}O_{19}$, many of which are very rare. Given considerable variations in the chemical composition of hibonite, its generalized chemical formula can be represented as follows: $(Ca,REE,Th,U)(Al,Cr,Ti,Si,Fe^{2+},Fe^{3+},Mg,Zn)_{12}O_{19}$ (e.g. Burns & Burns, 1984). In the terrestrial environment, hibonite is known only from four localities: Tranomaro, Madagascar (Curien *et al*., 1956; Rakotondrazafy *et al*., 1996), Gornaya Shoriya, Siberia (Yakovlevskaya, 1961), Furua Complex, Tanzania (Maaskant *et al*., 1980), and Punalur, South India (Santosh *et al*., 1991). All these localities are represented by strongly Si-undersaturated amphibolite (Gornaya Shoriya) and granulite (all other occurrences) facies metamorphic rocks, most of them showing evidence for metasomatism (Letuvninkas, 1971; Maaskant *et al*., 1980; Rakotondrazafy *et al*., 1996). In all cases, hibonite is interpreted as metamorphic (possibly metasomatic) mineral. Apart from its terrestrial occurrences, hibonite is known and relatively common in interplanetary dust and Ca-,Al-rich inclusions and microspherules from chondrite meteorites. Hibonite in these objects, accompanied by other refractory phases such as fassaite, melilite and spinel, represents either a relict of an early condensate that survived melting event(s) or product of liquidus crystallization on cooling (for overview, see Keil & Fuchs, 1971; Bischoff *et al*., 1985; Fahey *et al*., 1987; Kimura *et al*., 1993; Rietmeijer, 1998; Russel *et al*., 1998).

Although hibonite from the studied granulite xenoliths is similar to hibonite from other terrestrial occurrences in its (Fe+Mg) contents, it shows the relative enrichment in Al and Ca as well as complementary impoverishment in Ti, Th, Y and REE typical of meteoritic hibonite. High silica contents in the studied hibonite exceed those in any other terrestrial and meteoritic hibonite and are best comparable with the abundances of silica in synthetic hibonite produced by liquidus crystallization from Ca-,Al-rich silicate melts (e.g. Beckett & Stolper, 1994). Thus, the geochemical characteristics of hibonite from the Ca-Al granulite xenoliths from the Chyulu Hills better compare with those of meteoritic and synthetic 'igneous' hibonite. This, as well as the textural setting of hibonite, seems most consistent with magmatic crystallization of this mineral in the terrestrial environment.

Whilst the textural characteristics and reaction paths demonstrated by the granulites are defined by ancient metamorphism, the websterites (as well as other ultramafic xenoliths from Chyulu) often show evidence for young chemical reequilibration recorded in mineral zoning patterns. Petrographically similar rocks equilibrated in the same *P-T* range may show opposite styles of zoning, indicating local thermal heterogeneity of the mantle. The

Al content in pyroxenes either decreases rimwards, suggesting cooling to the ambient mantle temperatures, or increases towards the rim that indicates heating. In the case of heating, diffusion modeling reveals young ages of diffusion that mostly do not exceed few million years. It strongly suggests that young alkaline magmatism and not older Pan-African or platformal processes are the cause of these local heating phenomena in the uppermost mantle beneath Chyulu. Against the background outlined above, this study seeks to build a better understanding of the formation and subsolidus history of comagmatic meta-igneous gabbro-troctolitic and troctolitic cumulates in the lover crust via the investigation of deep-seated xenoliths found in alkali volcanic rocks of Chyulu. Important aspects of the study include:

(I) the ancient evolution of the most basic and dense part of the cumulate sequence represented by the websterite xenoliths;

(II) the ancient evolution of the granulitic part of the sequence represented by the Mg-Al sapphirine-bearing and Ca-Al hibonite-bearing granulite xenoliths;

(III) the formation of hibonite;

(IV) the role of deep processes related to the young volcanism of Chyulu, in the evolution of the studied websterite xenoliths and the upper mantle beneath the Chyulu Hills as a whole.

Geological overview

The Chyulu Hills volcanic field

The Chyulu Hills volcanic field is located on the eastern flank of the Kenya rift. It lies some 150-200 km east of the rift axis and 50 km northeast of

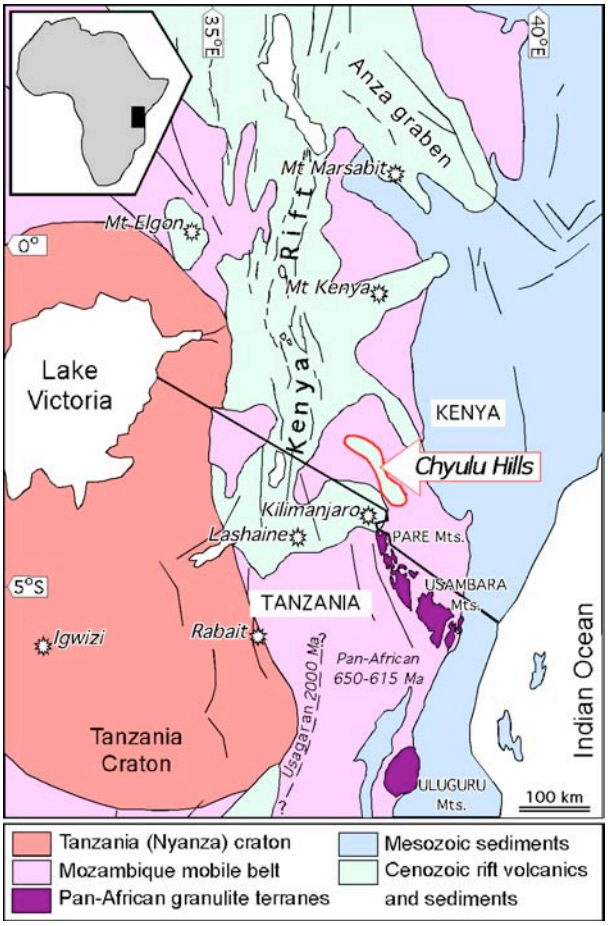


Fig. 1. Geological map of Kenya and northern Tanzania. Shown are principal tectonic units and volcanic areas as well as the location of the Chyulu Hills. The outcropping granulite complexes of NW Tanzania are after Möller *et al.* (2000), the distribution of Cenozoic volcanic and sedimentary rocks in the region is shown according to Williams (1970) and Baker *et al.* (1971).

Mt. Kilimanjaro, close to the border with Tanzania (Fig. 1). The Chyulu Hills include several hundred volcanic cones predominantly aligned in a NW-SE direction and forming a chain approximately 100 km long. This volcanic chain has no direct connection to the major rift structures of Kenya or Tanzania. For the last decade, the Chyulus have been the target of many petrological (xenoliths and alkaline volcanics), structural and geophysical studies (e.g. Henjes-Kunst & Altherr, 1992; Haug & Strecker 1995; Ritter & Kaspar 1997; Novak *et al.*, 1997a, b; Späth *et al.*, 2001).

The general structure of the lithosphere beneath the Chyulu Hills was investigated by a wide-angle reflection and refraction experiment and by seismic tomography. The Moho has been detected at a depth of 40 km and 44 km beneath the northwestern and the southeastern Chyulu Hills, respectively. The thickness of the lower crust amounts to ca. 20 km for (Ritter & Kaspar, 1997; Novak *et al*., 1997b). The seismic lithosphere-asthenosphere boundary is not detected. High-pressure porphyroclastic garnet lherzolite xenoliths from the Chyulu basanites yield geobarometric estimates in the range of 33-36 kbar, which may suggest a lithospheric thickness of 107-120 km (Henjes-Kunst & Altherr, 1992).

In the northwest of the Chyulu Hills, no velocity perturbation in the lithosphere is found (Pn velocity = 8.1 km/s). At the same time, the lithosphere beneath the central and southeastern Chyulu Hills is characterised by a prominent low-velocity zone that extends from c. 23 km depth in the lower crust to 70 km depth in the mantle (Pn velocity ≈ 7.9 km/s). The origin of this zone is assigned to elevated temperature or even the presence partial melt (Novak *et al*., 1997; Kaspar & Ritter, 1997).

Volcanism of the Chyulu Hills is of Quaternary age. Main types of volcanic rocks include foidites, less silica undersaturated basanites, and fractionated alkali basalts (Haug & Srecker, 1995; Späth *et al*., 2001). Foidites are the oldest (1.4 Ma) rocks, localized in the northwestern part of the field. Basanites are younger, they partly intrude and overlap basanites and partly form a volcanic cluster adjoining to basanites from the SE. Holocene alkali basalts occur in the southeastern part of the Chyulus; some of them were erupted in Historical time (Haug & Strecker, 1995). Most upper mantle and lower crustal xenoliths are hosted in basanites. This study is based on xenoliths collected from the Oldoinyo Lengai and Kwa Nthuku volcanic cones situated in the northwestern part of the Chyulu Hills. Except for the Quaternary alkali volcanics, no manifestations of magmatism younger than the Pan-African have yet been found within or in the vicinity of the Chyulu Hills. Karoo rocks are absent.

The crystalline basement of the Chyulu Hills

The Chyulu Hills lie on the crystalline basement of the Pan-African Mozambique mobile belt. (Holmes, 1951) which extends from the Arabian-Nubian Shield in the north via Ethiopia, Uganda, Kenya and Tanzania to Mozambique, Malawi and Madagascar in the south. The belt is now shown to include several metamorphic domains with different ages and *P-T* histories (e.g. Shackleton, 1973; Key *et al*. 1989; Stern & Dawoud 1991; Pinna *et al.,* 1993; Appel *et al*., 1998; Möller *et al*., 1998 and references therein). It results from a complex series of subduction, collision and accretion events between approximately 750 and 615 Ma (e.g. Coolen *et al*., 1982; Kröner et al., 1987; Stern & Dawoud 1991; Muhongo & Lenoir, 1994; Möller *et al*., 1998, 2000, Muhongo *et al*., 2001; Kröner *et al*., 2003; Meert, 2003), related to the closure of the Mozambique Ocean. The younger events within this time span are commonly termed 'Pan-African' (e.g. Möller *et al*., 2000) while the older ones are often related related to an 'East African orogen' (e.g. Stern, 1994; Meert, 2003). The older history of the Mozambique
belt seems to vary with geographic position. Magmatic and metamorphic events took place at 800-

800-820 Ma (e.g. Key *et al.* 1989; Kebede *et al.* 2001), at approximately 1000-1250 Ma (e.g. Pinna *et al.* 1993; Kröner *et al.*, 1997; Evans *et al.*, 1999), at around 2000 Ma (e.g. Möller *et al.*, 1995; Möller *et al.*, 1998) and in the Archean (Bell & Dodson, 1981; Cahen *et al.*, 1984; Muhongo *et al.*, 2001).

Lithologically, the Mozambique belt is dominated by amphibolite-facies and low grade metamorphic rocks and granitoids, but it also contains numerous granulite complexes. Together with the igneous complexes, the latter were the focus of most of the geochronological studies cited above and the subject of extensive petrological and geochemical investigations (e.g. Maaskant *et al.*, 1980; Sandiford *et al.*, 1987; Gichile, 1992; Pinna *et al.*, 1993; Möller *et al.*, 1995, 2000; Appel *et al.*, 1998). Therefore, the outcropping granulites play a major role in reconstructing Proterozoic metamorphic and geodynamic processes in the Mozambique belt. In contrast, few data are available on granulite xenoliths in volcanic edifices situated within the Mozambique belt of East Africa. They were described from Neogene volcanics of the Lashaine volcano in Tanzania (Dawson, 1977; Jones *et al.*, 1983). As is the case with the granulite xenoliths from this study, those of Lashaine represent relics of an igneous suite metamorphosed into granulite (Jones *et al.*, 1983), but with a different chemical and mineralogical composition.

The local basement consists of hornblende and hornblende-biotite gneisses, migmatized and granitoid gneisses and subordinate garnet amphibolites and marbles (Saggerson, 1963; Omenge & Okelo, 1992). Granulites are rare. They form thin bands in gneisses, few of which are traceable for great distances (Saggerson, 1963). The granulites are calc-silicate in composition and are made of andesine plagioclase, pyroxene (especially clinopyroxene), scapolite, garnet, epidote and in some cases quartz. They are lithologically different from the granulite xenoliths sampled by the young basanitic magmas. Due to the lack of thermobarometric, isotopic and age data, both the outcropping basement granulites and the granulite xenoliths of the Chyulu Hills volcanic field cannot be *a priori* assigned to any of the above-described granulite occurrences in East Africa.

Outcropping granulites
of the Mozambique mobile belt

On the basis of petrological and geochronological studies of granulites in Tanzania, Möller *et al.* (2000) proposed to divide the Mozambique belt into a western part where the main metamorphic event occurred at about 2000 Ga (Usagaran belt; see above) and an eastern (Pan-African) part with the major metamorphic events related to the formation of Gondwana at 650-550 Ma. For metapelitic granulites of the Usagaran belt, Möller *et al.* (1995) deduced a clockwise P-T path with near isothermal decompression from peak conditions of about 750°C and 1.8 GPa. Similar results were obtained by Muhongo *et al.* (2002) on mafic granulites of the Usagaran belt. For metasedimentary and meta-igneous granulites of the Pan-African belt (Pare, Usambara and Uluguru; Fig. 1), Appel *et al.* (1998) propose an anticlockwise *P-T* path that includes early compression to the peak conditions of approximately 810°C and 1 GPa.

Appel *et al.* (1998) suggested that Pan-African and Paleoprotoerozoic granulites in Tanzania could be distinguished on the basis of the different

P-T paths. This hypothesis is supported by the fact that granulites of the Pan-African Furua complex (Maaskant *et al*., 1980) in southern Tanzania and - presumably - Pan-African meta-igneous and metasedimentary granulites of the Sagan and Konso localities in southern Ethiopia (Gichile, 1992) are characterised by the anticlockwise *P-T* paths dominated by cooling from high temperatures. However, petrologic study on the Archean meta-igneous granulites from Labwor Hills in Uganda also revealed (near isobaric) cooling from very high temperatures (Sandiford *et al*., 1987). Only very brief descriptions of meta-igneous and metasedimentary granulites of Proterozoic ages are available for occurrences in Mozambique (Pinna *et al*. 1993) and Kenya (Key *et al*. 1989).

The reaction sequences and *P-T* estimates for the studied granulites do not allow us to clearly distinguish whether their *P-T* trends under post-peak conditions are clock- or anticlockwise. In contrast to exposed granulites where the both types of *P-T* evolution are often characterized by pronounced decompression in the course of tectonic exhumation, almost no indications of retrogression are found in our samples. Nevertheless, the inferred reaction sequence appears more consistent with an anticlockwise *P-T* evolution. This accords with the detailed results of Appel *et al*. (1998) and Möller *et al*. (1998) on the Pan-African granulite terranes of E-NE Tanzania (Pare, Usambara and Uluguru mountains) located S-SW of the Chyulu Hills (Fig. 1). For metasedimentary and meta-igneous granulites from these localities, Appel *et al*. (1998) propose an anticlockwise *P-T* path with the peak conditions of approximately 810°C and 9.5-11 kbar. As the cause of the granulite metamorphism, these authors and Möller *et al*. (2000) put forward a model of magmatic underplating in the environment of arc terranes forming the Mozambique belt in Pan-African times.

Organization of the thesis

The thesis includes an introduction, four petrology / geochemistry chapters, a general conclusion, and an appendix. The four petrology / geochemistry chapters represent manuscripts, which have been submitted to international journals during the course of the thesis. Three out of four manuscripts focus on the studied suite of comagmatic websterite and granulite xenoliths from the Chyulu Hills, their magmatic / geochemical (Chapter I) and metamorphic (Chapter II) history, as well as on the detailed petrography and geochemistry of hibonite in the Ca-Al hibonite-bearing granulite xenoliths. These manuscripts were written by the author of the thesis in close collaboration with his scientific supervisor, Prof. Dr. Angelika Kalt (Chapters I-III), and with the participation of Dr. Thomas Pettke who provided excellent LA-ICPMS facilities (Chapters I and III). These manuscripts are based on original observations obtained on (sometimes unique) specimens that were never studied before. The last manuscript (Chapter IV) is concerned with the *P-T* evolution of the lithospheric upper mantle beneath the Chyulu Hills. This manuscript focuses on the petrography and *P-T* evolution of a representative set of mantle xenoliths from beneath Chyulu and does not consider granulites. Basically, it was written by Prof. Dr. Rainer Altherr. Aluminous garnet-spinel olivine websterite xenoliths investigated in detail in the framework of this thesis represent four out of 59 xenoliths used by Rainer. Another four ultramafic xenoliths investigated by the author and bearing no relevance to the studied comagmatic websterite-

granulite suite are also included in this manuscript. Incorporating the latter in the thesis is justified by the petrographic complexity of the websterite xenoliths that does not allow to interpret the observed mineralogies and mineral zoning patterns on the basis of a few xenoliths only and requires data on a more representative set of xenoliths.

The relative contribution of all parties involved in this study could be summarized as follows:

	Chapter II	Chapter III	Chapter IV	Chapter V
Petrography, including optical microscopy and modal analyses	Ulianov: 90% Kalt: 10%	Ulianov: 90% Kalt: 10%	Ulianov: 90% Kalt: 10%	Ulianov: 15%
SEM documentation	Ulianov: 100%	Ulianov: 100%	Ulianov: 100%	Ulianov: 100%
EMP analyses	Ulianov: 100%	Ulianov: 100%	Ulianov: 100%	Ulianov: 15%
LA ICPMS analyses	Ulianov: 40% Pettke: 60%	Ulianov: 40% Pettke: 60%	Ulianov: 40% Pettke: 60%	No LA ICPMS data
Data processing (EMP and LA ICPMS)	Ulianov: 100%	Ulianov: 100%	Ulianov: 100%	Ulianov: 15%
Thermobarometric calculations	Ulianov: 100%	Ulianov: 100%	No calculations	Ulianov: 15%
Interpretation of data	Ulianov: 50% Kalt: 50%	Ulianov: 60% Kalt: 40%	Ulianov: 60% Kalt: 40%	Ulianov: 15%
Writing manuscript text	Ulianov: 40% Kalt: 60%	Ulianov: 70% Kalt: 30%	Ulianov: 70% Kalt: 30%	Ulianov: 15%
Making manuscript tables and figures	Ulianov: 90% Kalt: 10%	Ulianov: 90% Kalt: 10%	Ulianov: 90% Kalt: 10%	Ulianov: 15%

References

Appel, P., Möller, A. & Schenk, V. (1998). High-pressure granulite facies metamorphism in the Pan-African belt of eastern Tanzania: *P-T*-t evidence against granulite formation by continent collision. *Journal of Metamorphic Geology* **16**, 491-509.

Baker, B. H., Williams, L. A. J., Miller, J. A. & Fitch, F. J. (1971). Sequence and geochronology of the Kenya rift volcanics. *Tectonophysics* **11**, 191-215.

Bell, K. & Dodson, M. H. (1981). The geochronology of the Tanzanian Shield. *Journal of Geology* **89**, 109-128.

Bhattacharya, S. & Kar, R. (2002). High-temperature dehydration melting and decompressive *P-T* path in a granulite complex from the Eastern Ghats, India. *Contributions to Mineralogy and Petrology* **143**, 175-191.

Beckett, J. R. & Stolper, E. (1994). The stability of hibonite, melilite and other aluminous phases in silicate melts: implications for the origin of hibonite-bearing inclusions from carbonaceous chondrites. *Meteoritics*, **29**, 41-65.

Bischoff, A., Keil, K. & Stöffler, D. (1985). Perovskite-hibonite-spinel-bearing inclusions and aluminum-rich chondrules and

fragments in enstatite chondrites. *Chemie der. Erde*, **44**, 97-106.

Bohlen, S. R. (1987). Pressure-temperature-time path and a tectonic model for the evolution of granulites. *Journal of Geology* **95**, 617-632.

Bohlen, S. R. (1991). On the formation of granulites. *Journal of Metamorphic Geology* **9**, 223-229.

Boyd, O. S., Craig, H. J. & Sheehan, A. F. (2004). Foundring lithosphere imaged beneath the southern Sierra Nevada. *Science* **305**, 660-662.

Burns, R. G. & Burns, V. M. (1984). Crystal chemistry of meteorite hibonites. Proceeding of the 15th Planetary Science Conference. *Journal of Geophysical Research*, *Supplement Issue* **89**, C313-321.

Cahen, L., Snelling, N. J., Delhal, J. & Vail, J. R. (1984*). The geochronology and evolution of Africa*. Oxford: Clarendon Press, 512 pp.

Christy, A. G. (1989). The stability of sapphirine+clinopyroxene: implications for phase relations in the CaO-MgO-Al_2O_3-SiO_2 system under deep-crustal and upper mantle conditions. *Contributions to Mineralogy and Petrology* **102**, 422-428.

Coolen, J. J. M. M. M., Priem, H. N. A., Verdurmen, E. A. T. & Verschure, R. H. (1982). Possible zircon U-Pb evidence for Pan-African granulite-phacies metamorphism in the Mozambique Belt of southern Tanzania. *Precambrian Research* **17**, 31-40.

Curien, H., Guillemin, C., Orcel, J. & Steinberg, M. (1956). La hibonite, nouvelle espèce minérale. *Comptes Rendus de l'Académie des Sciences (Paris)*, **242**, 2845-2847.

Downes, H. (1993). The nature of the lower continental crust of Europe: petrological and geochemical evidence from xenoliths. *Physics of the Earth and Planetary Interiors* **79**, 195-218.

Downes, H., Dupuy, C. & Leyreloup, A. F. (1990) Crustal evolution of the Hercynian belt of western Europe: evidence from lower-crustal granulitic xenoliths (French Massif Central). *Chemical Geology* **83**, 209-231.

Ducea, M.N. & Saleeby, J.B. (1996). Buoyancy sources for a large unrooted mountain range, the Sierra Nevada, California: Evidence from xenolith thermobarometry. Journal of Geophysical Research **101**, 8229-8244.

Dawson, J. B. (1977). Sub-cratonic crust and upper mantle models based on xenolith suites in kimberlite and nephelinitic diatremes. *Journal of the Geological Society, London* **134**, 173-184.

Dawson, J. B., Harley S. L., Rudnick R. L. & Ireland T. R. (1997). Equilibration and reaction in Archean quartz-sapphirine granulite xenoliths from the Lace kimberlite pipe, South Africa. *Precambrian Research* **104**, 123-146.

Ducea, M.N. (2001). The California arc: thick granitic batholiths, eclogitic residues, lithospheric-scale thrusting, and magmatic flare-ups. *GSA Today* **11**, 4-10.

Evans, R. J., Ashwal, L. D. & Hamilton, M. A. (1999). Mafic, ultramafic, and anorthositic rocks of the Tete Complex, Mozambique:

petrology, age, and significance. South African Journal of Geology **102**, 153-166.

Fahey, A. J., Goswani, J. N., McKeegan, K. D. & Zinner, E. (1987). ^{26}Al, ^{244}Pu, ^{50}Ti, REE and trace element abundances in hibonite grains from CM and CV meteorites. *Geochimica et Cosmochimica Acta* **51**, 329-350.

Gichile, S. (1992). Granulites in the Precambrian basement of southern Ethiopia: geochemistry, *P-T* conditions of metamorphism and tectonic setting. *Journal of African Earth Sciences* **15**, 251-263.

Grégoire, M., Cottin, J. Y., Giret, A., Mattielli, N. & Weis, D. (1998). The meta-igneous granulite xenoliths from Kerguelen Archipelago: evidence of a continent nucleation in an oceanic setting. *Contributions to Mineralogy and Petrology* **133**, 259-283.

Harley, S. L. (1989). The origin of granulites: a metamorphic perspective. *Geological Magazine* **126(3)**, 215-247.

Haug, G. H., Strecker, M. R. (1995). Volcanotectonic evolution of the Chyulu Hills and implication for the regional stress field in Kenya. *Geology* **23**, 165-168.

Henjes-Kunst, F. & Altherr, R. (1992). Metamorphic petrology of xenoliths from Kenya and Northern Tanzania and implications for geotherms and lithospheric structure. *Journal of Petrology* **33**, 1125-1156.

Hermann, J., Müntener, O. & Günter, D. (2001). Differentiation of mafic magma in a continental crust-to-mantle transition zone. *Journal of Petrology* **42**, 189-206.

Holmes, A. (1951). The sequence of Precambrian orogenic belts in south and central Africa. *Proceedings of the 18th International Geological Congress, Vol. 14*. London: Assoc. Seros. Geol. Afr., pp. 254-269.

Huang, Y.-M., Van Calsteren, P. & Hawkesworth, C. J. (1995). The evolution of the lithosphere in southern Africa: a perspective on the basic granulite xenoliths from kimberlites in South Africa. *Geochimica et Cosmochimica Acta* **59**, 4905-4920.

Jan, M. Q. & Howie, R. A. (1981). The mineralogy and geochemistry of the metamorphosed basic and ultrabasic rocks of the Jijal complex, Kohistan, NW Pakistan. *Journal of Petrology* **22(1)**, 85-126.

Jones, A. P., Smith, J. V., Hansen, E. C. & Dawson, J. B. (1983). Metamorphism, partial melting and K-metasomatism of garnet-scapolite-kyanite granulite xenoliths from Lashaine, Tanzania. *Journal of Geology* 91, 143-165.

Keil, K. & Fuchs, L. H. (1971). Hibonite ($Ca_2(Al,Ti)_{24}O_{38}$) from the Leoville and Allende chondritic meteorites. *Earth and Planet*ary *Sci*ence *Lett*ers, **12**, 184-190.

Kempton, P. D., Downes H., Neymark L. A., Wartho J. A., Zartman, R. E. & Sharkov E. V. (2001). Garnet granulite xenoliths from the Northern Baltic Shield—the underplated lower crust of a palaeoproterozoic large igneous province? *Journal of Petrology* **42**, 731-763.

Kempton, P. D., Harmon, R. S., Hawkesworth C. J. & Moorbath S. (1990). Petrology and geochemistry of lower crustal granulites from the Geronimo Volcanic Field, southern Arizona. *Geochimica et Cosmochimica Acta* **54**, 3401-3426.

Kebede, T., Kloetzli U. S. & Koeberl, C. (2001). U/Pb and Pb/Pb zircon ages from granitoid rocks of Wallagga area: constraints on magmatic and tectonic evolution of Precambrian rocks of western Ethiopia. *Mineralogy and Petrology* **71**, 251-271.

Keil, K. & Fuchs, L. H. (1971). Hibonite ($Ca_2(Al,Ti)_{24}O_{38}$) from the Leoville and Allende chondritic meteorites. *Earth and Planetary Science Letters*, **12**, 184-190.

Kempton, P. D., Downes, H., Neymark, L. A., Wartho, J. A., Zartman, R. E. & Sharkov, E. V. (2001). Garnet granulite xenoliths from the Northern Baltic Shield - the underplated lower crust of a palaeoproterozoic large igneous province. *Journal of Petrology* **42**, 731-763.

Key, R. M., Charsley, T. J., Hackman, B. D., Wilkinson, A. F. & Rundle, C. C. (1989). Superimposed Upper Proterozoic collision-controlled orogenies in the Mozambique Orogenic Belt of Kenya. Precambrian Research **44**, 197-225.

Kimura, M., El Goresy, A., Palme, H. & Zinner, E. (1993). Ca-Al-rich inclusions in the unique chondrite ALH 85085 – Petrology, chemistry, and isotopic composition. *Geochimica et Cosmochimica Acta*, **57**, 2329-2359.

Kröner, A., Greiling, R., Reischmann, T., Hussein, I.M., Stern, R. J., Dürr, S., Krüger J. & Zimmer, M. (1987). Pan-African crustal evolution in the Nubian segment of northeast Africa. In: Kröner, A. (ed.) *Proterozoic Lithospheric Evolution*. American Geophysical Union, Washington, DC, Geodynamic Series **17**, 235-257.

Kröner, A., Muhongo, S., Hegner, E. & Wingate, M. T. D. (2003). Single zircon geochronology and Nd isotopic systematics of Proterozoic high-grade rocks from the Mozambique belt of southern Tanzania (Masasi area): implications for Gondwana assembly. *Journal of the Geological Society, London* **160**, 745-758.

Letuvninkas, A. I. (1971). Metasomatism in Proterozoic carbonate rocks from Gornaya Shoriya. *Geologiya i Geofizika*, **1**, 58-64. In Russian.

Maaskant, P., Coolen, J. J. M. & Burke, E. A. J. (1980). Hibonite and coexisting zoisite and clinozoisite in a calc-Silicate granulite from southern Tanzania. *Mineralogical Magazine* **43**, 995-1003.

McGuire, A. V. & Stern, R. J. (1993). Granulite xenoliths from western Saudi Arabia: the lower crust of the late Precambrian Arabian-Nubian Shield. *Contributions to Mineralogy and Petrology* **114**, 395-408.

Meert, J. G. (2003). A synopsis of events related to the assembly of eastern Gondwana. *Tectonophysics*, **362**, 1-40.

Möller, A., Appel, P., Mezger, K. & Schenk, V. (1995). Evidence for a 2 Ga subduction zoned: eclogites in the Usaragan Belt of Tanzania. *Geology* **23**, 1067-1070.

Möller, A., Mezger, K. & Schenk, V. (1998). Crustal age domains and the evolution of the continental crust in the Mozambique Belt of Tanzania: Combined Sm-Nd, Rb-Sr and Pb-Pb isotopic evidence. *Journal of Petrology* **39**, 749-783

Möller, A., Mezger, K. & Schenk, V. (2000). U-Pb dating of metamorphic minerals: Pan-

African metamorphism and prolonged slow cooling of high pressure granulites in Tanzania, East Africa. *Precambrian Research* 104: 123-146.

Muhongo, S. M., Kröner, A. & Nemchin, A. A. (2001). Zircon ages from granulite facies rocks in the Mozambique belt of Tanzania and implications for Gondwana assembly. *Journal of Geology* **109**, 171-189.

Muhongo, S. M. & Lenoir, J.-L. (1994). Pan-African granulite-facies metamorphism in the Mozambique belt of Tanzania: U-Pb zircon geochronology. *Journal of the Geological Society, London* **151**, 343-347.

Muhongo, S., Tuisku, P., Mnali, S., Temu, E., Appel, P. & Stendal, H. (2002). High-pressure granulite-facies metagabbros in the Ubendian Belt of SW Tanzania: preliminary petrography and P,T estimates. *Journal of African Earth Sciences* **34**, 279-285.

Novak, O., Prodehl, C., Jacob, A. W. B. & Okoth, W. (1997a). Crustal structure of the southern flank of the Kenya rift deduced from wide-angle P-wawe data. *Tectonophysics* **278**, 171-186.

Novak, O., Ritter, J. R. R., Altherr, R., Garasic, V., Volker, F., Kluge, C., Kaspar, T., Byrne, G. F., Sobolev, S. V. & Fuchs, K. (1997b). An integrated model for the deep structure of the Chyulu Hills volcanic field, Kenya. *Tectonophysics* **278**, 187-209.

Omenge, J. M. & Okelo, R. E. (1992). Geology of the Chyulu-Oloitokitok area. Kenya Mines and Geology Department, Nairobi, Report 112, 51 pp.

Osanai Y., Hammamoto, T., Maishima, O. & Kagami, H. (1998). Sapphirine-bearing granulites and related high-temperature metamorphic rocks from the Higo metamorphic terrane, west central Kyushu, Japan. *Journal of Metamorphic Geology* **16**, 53-66.

Pinna, P., Jourde, G., Calvez, J. Y. & Mroz, J. P. (1993). The Mozambique Belt in northern Mozambique: Neoproterozoic (1100-850 Ma) crustal growth and tectogenesis, and superimposed Pan-African (800-550 Ma) tectonism. *Precambrian Research* **62**, 1-59.

Rakotondrazafy, M. A. F., Moine, B. & Cuney, M. (1996). Mode of formation of hibonite ($CaAl_{12}O_{19}$) within the U-Th skarns from the granulites of S-E Madagascar. *Contributions to Mineralogy and Petrology* **123**, 190-201.

Rietmeijer, F. G. M. (1998). Interplanetary dust particles. In: Papike J.J. (ed.) *Planetary Materials*. Reviews in Mineralogy, Mineralogical Society of America, Washington DC, **36**, (2-)1-95.

Ritter, J. R. R. & Kaspar, T. (1997). A tomography study of the Chyulu Hills, Kenya. *Tectonophysics* **278**, 149-169.

Rudnick, R. L. (1992). Xenoliths – samples of the lower continental crust. In: Fountain D.M., Arculus R. & Kay R.W. (eds.) *Continental Lower Crust*. New York: Elsevier, pp. 269-316.

Rudnick R. L., McDonough W. F., McCulloch M. T. & Taylor S. R. (1986). Lower crustal xenoliths from Queensland, Australia: evidence for deep crustal assimilation and fractionation of continental basalts. *Geochimica et Cosmochimica Acta* **50**, 1099-1155.

Russel, S. S., Huss, G. R., Fahey, A. J., Greenwood, R. C., Hutchison, R. & Wasserburg, G. J. (1998). An isotopic and petro-

logic study of calcium-aluminum-rich inclusions from CO3 meteorites. *Geochimica et Cosmochimica Acta*, **62**, 689-714.

Saggerson, E. P. (1963). Geology of the Simba-Kibwezi area. *Geological survey of Keny*a **58**, 70 pp.

Sandiford, M., Neall, F. B. & Powell R. (1987). Metamorphic evolution of aluminous granulites from Labwor Hills, Uganda. *Contributions to Mineralogy and Petrology* **95**, 217-225.

Santosh, M., Sandiford, M. & Reed, S. J. B. (1991). Zoned hibonite from Punalur, South India. *Mineral Magazine* **55**, 159-162.

Shackleton, R. M. (1973). Correlation of structures across Precambrian orogenic belts in Africa. In: Tarling, D.H. & Runcorn, S.K. (eds.) *Implications of Continental Drift to the Earth Sciences*. London: Academic Press, pp. 1091-1095.

Späth, A., Le Roex, A. P. & Opiyo-Akech, N. (2001). Plume-lithosphere interaction and the origin of continental rift-related alkaline volcanism – the Chyulu Hills Volcanic field, Southern Kenya. *Journal of Petrology* **42**, 765-787.

Stern, R. J. & Dawoud, A. S. (1991). Late Precambrian (740 Ma) charnockite, enderbite, **431**, 41-46.

and granite from Jebel Moya, Sudan: a link between the Mozambique Belt and the Arabian-Nubian Schield? *Journal of Geology* **99**, 648-659.

Stern, R. J. (1994). Arc assembly and continental collision in the Neoproterozoic East African orogen: implications for the conditions of Gondwanaland. *Annual Review of Earth and Planetary Sciences* **22**, 319-351.

Upton, B. G. J., Aspen, P. & Hinton, R.W. (2001). Pyroxenite and granulite xenoliths from beneath the Scottish Northern Highlands Terrane: evidence for lower-crust/upper mantle relationships. Contributions to Mineralogy and Petrology **142**, 178-197.

Williams, L.A.J. (1970). The volcanics of the Gregory Rift Valley, East Africa. *Bulletin Volcanologique* **34**, 439-465.

Yakovlevskaya, T. A. (1961). Hibonite from Gornaya Shoriya. *Zapiski Vsesoyuznogo Mineralogicheskogo Obshchestva* **90**, 458-461. In Russian.

Zandt, G., Gilbert, H., Owens T. J., Ducea, M., Saleeby, J. & Jones, C. H. (2004). Active foundering of a continental arc root beneath the southern Sierra Nevada in California. *Nature*

CHAPTER II

Aluminous websterite and granulite xenoliths from the Chyulu Hills volcanic field, Kenya: Metamorphosed gabbroic cumulates from a Pan-African arc environment

A. Ulianov[1,*], A. Kalt[1], T. Pettke[2]

[1]University of Neuchâtel, Institute of Geology, Rue Emile-Argand 11, CH-2007 Neuchâtel, Switzerland

[2]Institut für Isotopengeologie und Mineralische Rohstoffe, ETH Zentrum, Sonneggstrasse 5, CH-8092 Zürich, Switzerland

*Corresponding author:
alexey.ulyanov@unine.ch

submitted to **Contributions to Mineralogy and Petrology**

CHAPTER II

Abstract

Major and trace element abundances analysed on whole rock glass pellets and minerals from aluminous garnet-spinel websterite, sapphirine-bearing Mg-Al granulite and hibonite-bearing Ca-Al granulite xenoliths of the Chyulu Hills volcanic field, Kenya, show that the investigated websterites and granulites represent a meta-igneous suite linked by fractionation. High bulk rock Mg# and very low concentrations of most incompatible elements indicate that they are cumulates rather than crystallized melts. Along with constraints from postmagmatic *P-T* evolution, low HSFE abundances, LILE enrichment and fractionation of LREE over HREE in whole rock samples suggest that the protoliths of the xenoliths may represent arc cumulates, which implies that they should be of Pan-African age. The textures and metamorphic reaction paths recorded in the granulites are in line with igneous emplacement in the crust and cooling from igneous to ambient crustal temperatures accompanied or followed by compression. For the websterite xenoliths, there is an apparent contradiction between the textural-mineralogical data and results of P-T calculations that appear to suggest high-P igneous cristallisation of pyroxenes on the one hand and the positive Eu anomaly that suggests shallow-level plagioclase accumulation on the other hand. This contradiction can in part be reconciled by a model of compression of a plagioclase-bearing protolith at near-igneous temperatures to mantle depth where it obtained its ultramafic phase assemblage. Such a P-T path would also be in line with textures and compositions of the granulite xenoliths. It would require foundering of dense lower crustal material into the mantle towards the end of Pan-African subduction and accretion, a process that is possible in areas with high geothermal gradients such as mature arcs.

Introduction

Mafic-ultramafic rock associations make up important volumes of island and continental arc lithosphere. They represent crystallised melts / cumulates formed at deep or shellow levels and give important geochemical-petrological insights into the formation of the Earth's crust and the evolution of the continental crust and uppermost mantle (e.g. Conrad and Kay 1984; DeBari et al. 1987; Ducea and Saleeby 1996; Weber et al. 2002; Spandler et al. 2003; Claeson and Meurer 2004; Topuz et al. 2004). Metamorphosed mafic-ultramafic complexes consisting mainly of pyroxenite and granulite are common in the exhumed cores of orogenic belts. There, they may represent either fossil continental crust-to-mantle transitions (e.g. Hermann et al. 2001) or continental arc crust (e.g. Cesare et al. 2002), but often they are indicative of subducted and subsequently exhumed oceanic sequences (e.g. Girardeau and Ibarguchi 1991; Takazawa et al. 1999; Morishita et al. 2003). Pyroxenites and granulites also occur in xenolith suites related to continental intraplate volcanism (e.g. Kempton et al. 2001; Embey-Isztin et al. 2003; Dessai et al. 2004; Sutherland et al. 2004). Some of such pyroxenite-granulite associations have been interpreted as comagmatic crystal fractionation sequences of basaltic liquids, often overprinted by subsolidus thermal relaxation and metamorphism (e.g. Upton et al. 2001; Dessai et al. 2004).

This study focuses on a suite of comagmatic aluminous meta-igneous cumulates from the Chyulu Hills volcanic field (eastern flank of the Kenya Rift), located on the Pan-African Mozambique Belt. Comagmatic aluminous pyroxenite-granulite xenolith suites are rare but known from several localities in the East African Rift / Arabian Plate where Tertiary to Recent volcanism samples the lithosphere of the Mozambique Belt. These suites are considered to be of Pan-African age and calc-alkaline affinity (McGuire and Stern 1993; Nasir 1995; Al-Mishwat and Nasir 2004).

The rock series investigated here includes garnet-spinel websterite, two-pyroxene sapphirine-bearing granulite and clinopyroxene hibonite-bearing granulite. Mineralogy and geochemical characteristics of these rocks indicate that they cannot represent cumulates of Tertiary to Recent alkaline magmatism related to the Kenya Rift. The major and trace element data on whole rock samples and minerals presented in this paper appear consistent with their interpretation as cumulates of Pan-African arc-type magmatism. The geochemical and textural features of the websterite xenoliths, along with the complex subsolidus reaction textures of the granulite xenoliths (Ulianov et al. 2005; Ulianov & Kalt 2005) further suggest that the Pan-African arc lithosphere may have been thinned by some foundering process such as that described for the southern Sierra Nevada today (Ducea 2001; Zandt et al. 2004). There, xenolith evidence suggests that the eastern Sierra Nevada has lost about half of its original crust due to convective removal of dense garnet-bearing lowermost crustal rocks (e.g. Ducea & Saleeby 1996), while seismic tomography reveals a descending keel of ultramafic-mafic crust and mantle lithosphere beneath the southern Sierra Nevada (Boyd et al. 2004) and thus images this process in action.

Geological setting

The Chyulu Hills volcanic field is located on the eastern flank of the Kenya rift. It lies some 150-200 km east of the rift axis and 50 km northeast of Mt. Kilimanjaro, close to the border with Tanzania (Fig. 1). The Chyulu Hills include several hundred volcanic cones predominantly aligned in a NW-SE direction, forming a ca. 100 km long chain that has no direct connection to the major rift structures of Kenya or Tanzania. The Chyulu Hills have been the target of petrological studies on mantle xenoliths (Henjes-Kunst and Altherr 1992; Altherr et al. 2005) and on alkaline volcanics (Haug and Strecker 1995; Späth et al. 2001) as well as of structural and geophysical studies (Haug and Strecker 1995; Ritter and Kaspar 1997; Novak et al. 1997a, b).

The general structure of the lithosphere beneath the Chyulu Hills was investigated by a wide-angle reflection and refraction experiment and by seismic tomography. The Moho was detected at a depth of ~44 km, with a thickness of ca. 20 km assigned to the lower crust (Ritter and Kaspar 1997; Novak et al. 1997b). The lithosphere-asthenosphere boundary was not detected seismically. However, porphyroclastic garnet lherzolite and depleted garnet-spinel harzburgite xenoliths from the northwestern Chyulu Hills yield geothermobarometric estimates of 1300-1350°C and 3.3-3.6 GPa, which suggests a lithospheric thickness of approximately 115 km (Henjes-Kunst and Altherr, 1992; Altherr et al. 2005).

Volcanism of the Chyulu Hills is of Quaternary age. Main types of volcanic rocks include foi-

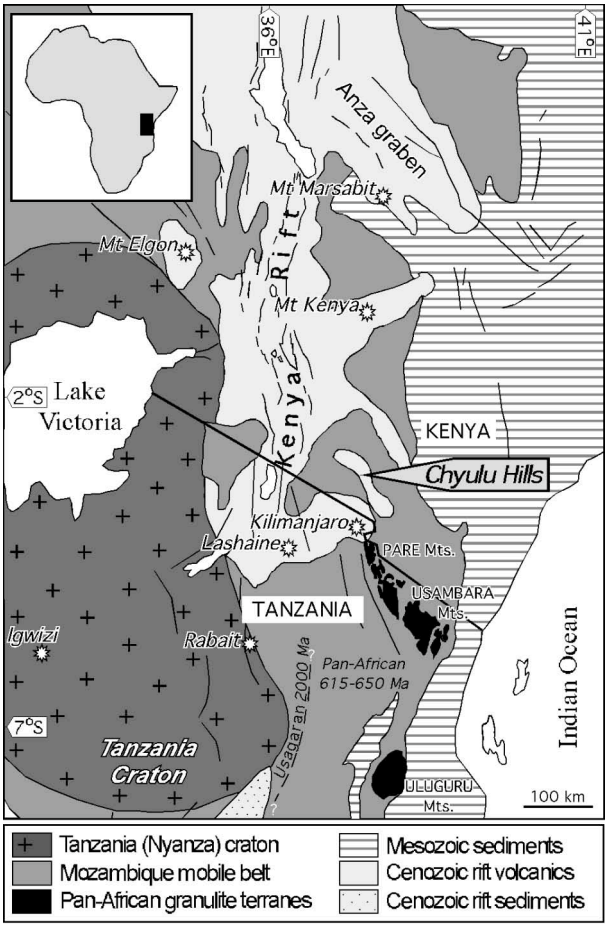


Fig. 1 Simplified geological map of Kenya and northern Tanzania. Shown are principal tectonic units and volcanic areas as well as the location of the Chyulu Hills. The outcropped granulite complexes of NW Tanzania are after Möller et al. (2000), the distribution of Cenozoic volcanic and sedimentary rocks in the region is after Williams (1970) and Baker et al. (1971).

dite, less silica-undersaturated basanite, and fractionated alkali basalt (Haug and Strecker 1995; Späth et al. 2001). The oldest (1.4 Ma) rocks are foiditic and found in the northwestern part of the volcanic field. Basanitic rocks are younger; they partly intrude and overlie basanites and also form a volcanic cluster adjoining to basanite edifices from the SE. Holocene alkali basalt occurs in the southeastern part of the Chyulu Hills, with some eruptions in Historical time (Haug and Strecker 1995). Most upper mantle and lower crustal xenoliths are hosted in basanite. This study is based on xenoliths collected from basanite of several volcanic edifices in the northwestern part of the Chyulu Hills. Apart from the Quaternary alkali volcanics, no manifestations of magmatism younger than the Pan-African have yet been found within or in the vicinity of the Chyulu Hills.

The Chyulu Hills lie on the crystalline basement of the Mozambique belt. Main local basement lithologies include amphibolite-facies gneiss, amphibolite and migmatite (Saggerson 1963; Omenge and Okelo 1992). Pyroxenites were not reported and granulites are rare. They are calc-silicate, dominated by andesitic plagioclase, pyroxenes, scapolite, garnet and epidote (Saggerson 1963). Corundum, sapphirine or other Al-rich phases are not mentioned (Saggerson 1963). In local outcrops, no granulites comparable to the specimens used in this study have ever been described.

Analytical techniques

Major elements in minerals were analyzed using a CAMECA SX50 electron microprobe equipped with four wavelength-dispersive spectrometers (Mineralogisch-Petrographisches Institut, University of Bern), and a CAMECA SX51 electron microprobe with five wavelength-dispersive spectrometers (Mineralogisches Institut, University of Heidelberg). Results from these two laboratories are consistent. Operating conditions for routine analyses included a 15 kV accelerating voltage and a 20 nA beam current on both instruments. The analyzed area was ~2 μm in diameter for mafic phases, and 5-10 μm for plagioclase. Counting times for most elements were 20 s. Raw spectrometer data were reduced with the PAP program.

To reintegrate the major element compositions of strongly exsolved early generation pyroxenes in the studied websterite xenoliths, modal proportions of the exsolved garnet were estimated using back-scattered electron images, while the 'bulk' chemical compositions of finely exsolved orthopyroxenes in the granulite xenoliths were obtained by electron microprobe operated with a defocused beam.

Trace element abundances in minerals were determined on a LA-ICPMS instrument equipped with a 193 nm ArF excimer laser (Lambda Physik, Germany) coupled to an ELAN 6100 quadrupole ICP-MS (Perkin Elmer, USA) at the Institut für Isotopengeologie und Mineralische Rohstoffe, ETH Zürich (for capabilities of the instrument and analytical technique, see Günther et al. 1997; Heinrich et al. 2003). The spot size ranged from 14 to 110 μm, depending on grain size and on whether core areas or rims of mineral grains were analysed. For core areas, except for plagioclase with abundant inclusions, a 110 μm spot size was used, resulting in improved precision. Raw data were reduced off-line using the LAMTRACE program.

Two sets of analyses of major element concentrations were performed on bulk rock samples. The first set was obtained on an XRF spectrometer Philips PW2400 at the Institut de Minéralogie et de Pétrographie, University of Fribourg. The second set was made on glass pills (see Ulianov et al. 2005) using a CAMECA SX50 electron microprobe at the Mineralogisch-Petrographisches Institut, University of Bern. The beam was rastered over an area of ca. 15×20 μm, operating conditions were the same as for minerals. The two sets of measurements are in good agreement with each other. In the discussion, we will use the microprobe data because of their somewhat better totals. Whole-rock trace element abundances were measured on glass pills using the same LA-ICPMS technique as for minerals. A spot size of 110 μm was used. Cr, Ni, Co, Sr and Ba were also determined by XRF at the University of Fribourg, together with major elements.

Petrography, major element composition of minerals and P-T evolution

Each of the studied rock groups, garnet-spinel websterite, Mg-Al sapphirine-bearing granulite and Ca-Al hibonite-bearing granulite, consists of petrographically similar rocks. No lithologies intermediate between these groups were found. Textures and P-T calculations are given in detail in Altherr et al. (2005) for the websterite xenoliths and in Ulianov & Kalt (2005) for the granulite xenoliths. Mineral compositions are given in Tables 1-3.

All studied xenoliths show pronounced subsolidus re-equilibration. Their igneous mineral assemblages are either completely replaced or obliterated. The studied xenoliths are also modified by late-stage heating and decompression in the host basanites. Garnet is usually replaced by kelyphite, only rare relicts are preserved. Clinopyroxene suffered incongruent melting and is often decomposed into micro-aggregates of secondary diopside, plagioclase and quenched melt. Numerous microprobe profiles performed for all minerals in all samples enable us, however, to distinguish these effects from primary major element variations (Altherr et al. 2005; Ulianov & Kalt 2005). Henceforth, we will refer to non-modified compositions only (see Tables 1-3).

Table 1 Representative major element compositions of minerals from garnet-spinel websterite xenoliths

	1910-11											1910-1								
	SPL	SPL	OL		OPX I gar lam.	OPX II		CPX I gar lam.	CPX II		GRT incl. in	OL	OL	OPX I cpx lam.	OPX II		CPX I gar lam.	CPX II		GRT incl. in
	core	core	core	core	integr.	core	rim	integr.	core	rim	OPX I	core	core	integr.	core	rim	integr.	core	rim	OPX I
SiO_2	0.05	0.05	39.95	39.94	51.71	55.52	55.34	49.66	53.69	53.08	41.86	39.53	39.37	54.56	56.10	55.27	50.36	53.21	53.58	42.25
TiO_2	0.03	0.05	n.d.	0.01	0.03	0.02	0.01	0.07	0.07	0.04	0.04	0.01	n.d.	0.05	0.06	0.04	0.08	0.11	0.08	0.02
V_2O_3	0.02	n.d.																		
Al_2O_3	61.93	62.02	0.01	0.03	8.27	2.19	3.27	10.13	4.29	4.76	23.43	0.02	0.01	3.37	1.92	2.99	9.35	5.15	5.41	22.98
Cr_2O_3	0.63	0.34	n.d.	n.d.	0.00	n.d.	n.d.	0.01	0.01	0.01	0.03	0.02	0.02	0.05	0.02	n.d.	0.04	0.05	0.08	0.07
FeO_t	16.42	17.36	14.71	14.30	10.09	9.60	9.52	6.91	4.21	4.56	11.78	16.10	15.80	9.96	9.66	10.19	6.65	5.28	5.09	11.96
MnO	0.04	0.05	0.05	0.07	0.08	0.06	0.04	0.10	0.10	0.09	0.19	0.07	0.08	0.09	0.12	0.06	0.08	0.09	0.04	0.21
NiO	1.57	1.36	0.86	1.04	0.16	0.22	0.23	0.09	0.09	0.12	0.02	0.62	0.59	0.14	0.16	0.13	0.05	0.10	0.07	0.02
ZnO	0.32	0.38																		
MgO	18.93	18.74	45.13	45.10	28.21	31.88	31.61	16.37	15.44	15.22	18.57	44.44	44.37	30.63	31.74	31.27	15.58	14.80	14.62	18.24
CaO	n.d.	n.d.	0.05	0.06	1.62	0.64	0.63	15.88	20.14	20.53	4.67	0.02	0.04	1.36	0.62	0.62	16.27	19.70	19.46	4.56
Na_2O	0.01	n.d.	n.d.	n.d.	0.05	0.08	0.05	0.92	1.64	1.62	0.02	n.d.	0.01	0.18	0.07	0.10	1.44	1.94	2.00	0.01
K_2O	n.d.	0.01	n.d.	n.d.	0.01	n.d.	n.d.	n.d.	n.d.	n.d.	0.02	0.02	n.d.	n.d.	n.d.	n.d.	0.01	n.d.	n.d.	n.d.
Total	99.95	100.36	100.76	100.54	100.23	100.20	100.70	100.14	99.67	100.02	100.61	100.85	100.27	100.39	100.48	100.68	99.91	100.41	100.42	100.32
Si	0.001	0.001	0.997	0.998	1.819	1.943	1.925	1.799	1.953	1.931	2.990	0.992	0.992	1.914	1.956	1.929	1.830	1.931	1.938	3.026
Ti	0.001	0.001	0.000	0.000	0.001	0.001	0.000	0.002	0.002	0.001	0.002	0.000	0.000	0.001	0.002	0.001	0.002	0.003	0.002	0.001
V	0.000	0.000																		
Al	1.870	1.869	0.000	0.001	0.343	0.090	0.134	0.433	0.184	0.204	1.973	0.001	0.000	0.139	0.079	0.123	0.400	0.220	0.231	1.940
Cr	0.013	0.007	0.000	0.000	0.000	0.000	0.000	0.000	0.000	0.000	0.002	0.000	0.000	0.001	0.001	0.000	0.001	0.002	0.002	0.004
Fe^{3+}	0.113	0.120																		
Fe^{2+}	0.238	0.251	0.307	0.299	0.297	0.281	0.277	0.209	0.128	0.139	0.704	0.338	0.333	0.292	0.282	0.297	0.202	0.160	0.154	0.716
Mn	0.001	0.001	0.001	0.002	0.002	0.002	0.001	0.003	0.003	0.003	0.012	0.002	0.002	0.003	0.004	0.002	0.002	0.003	0.001	0.013
Ni	0.032	0.028	0.017	0.021	0.005	0.006	0.006	0.003	0.003	0.004	0.001	0.013	0.012	0.004	0.004	0.004	0.001	0.003	0.002	0.001
Zn	0.006	0.007																		
Mg	0.723	0.714	1.679	1.680	1.479	1.663	1.639	0.884	0.837	0.826	1.978	1.662	1.667	1.602	1.650	1.627	0.844	0.800	0.788	1.948
Ca	0.000	0.000	0.001	0.002	0.061	0.024	0.023	0.616	0.785	0.800	0.357	0.001	0.001	0.051	0.023	0.023	0.633	0.766	0.754	0.350
Na	0.000	0.000	0.000	0.000	0.003	0.005	0.003	0.065	0.116	0.114	0.002	0.000	0.000	0.012	0.005	0.007	0.101	0.136	0.140	0.001
K	0.000	0.000	0.000	0.000	0.000	0.000	0.000	0.000	0.000	0.000	0.001	0.001	0.000	0.000	0.000	0.000	0.000	0.000	0.000	0.000
Sum	3.000	3.000	3.003	3.001	4.011	4.014	4.010	4.015	4.011	4.022	8.022	3.008	3.008	4.020	4.005	4.012	4.018	4.024	4.013	8.001
Mg#	75.2	74.0	84.5	84.9	83.3	85.60	85.50	80.9	86.7	85.6	73.8	83.1	83.4	84.9	85.4	84.5	80.7	83.3	83.7	73.1
Al^{IV}					0.171	0.042	0.066	0.186	0.036	0.046				0.065	0.040	0.059	0.152	0.046	0.049	
Al^{VI}					0.172	0.048	0.069	0.247	0.148	0.158				0.074	0.040	0.064	0.248	0.174	0.183	

Table 1 (Contd.)

	1535-3									1906-4											
	SPL	OL	OPX I cpx lam.	OPX II		CPX I gar lam.	CPX II		GRT incl. in	SPL	SPL	OL	OPX I gar lam.	OPX II		CPX I gar lam.	CPX II		GRT	CRN	KFS
	core	core	integr.	core	rim	integr.	core	rim	CPX II	core	core	core	integr.	core	rim	integr.	core	rim	relic	core	core
SiO_2	0.03	40.05	55.19	55.60	56.04	51.35	53.30	54.05	41.99	0.01	0.01	40.33	52.49	55.21	55.80	50.34	52.52	53.17	41.45	n.d.	62.88
TiO_2	0.04	n.d.	0.03	0.02	0.06	0.14	0.13	0.16	0.05	0.04	0.02	0.01	0.03	0.06	0.04	0.09	0.12	0.09	0.05	0.01	
V_2O_3																					
Al_2O_3	64.32	0.04	3.14	2.77	2.54	9.46	6.44	5.34	23.70	59.85	64.98	0.01	6.96	2.54	2.15	8.10	4.66	3.29	22.72	99.11	20.05
Cr_2O_3	0.50	n.d.	n.d.	0.01	0.03	0.05	0.03	0.05	0.05	0.27	0.13	0.07	0.01	n.d.	n.d.	0.01	n.d.	0.02	0.01	0.06	
FeO_t	14.87	14.51	9.26	9.04	8.88	5.79	4.16	4.11	11.60	19.35	14.06	13.93	10.39	9.19	9.17	6.51	4.34	4.11	13.78	0.00	0.08
MnO	0.01	0.07	0.10	0.04	0.05	0.11	0.06	0.11	0.11	0.11	0.07	0.06	0.11	0.09	0.04	0.09	n.d.	0.06	0.21	0.51	
NiO	1.34	0.93	0.30	0.31	0.26	0.09	0.12	0.12	n.d.	1.10	0.69	0.55	0.16	0.08	0.03	0.05	0.10	0.07	n.d.	0.04	
ZnO	0.32									0.42	0.29										
MgO	19.31	44.98	31.31	31.58	32.02	15.71	13.99	14.88	18.61	17.99	19.47	46.16	29.34	32.25	32.67	16.27	14.88	15.80	17.38	0.03	
CaO	n.d.	0.06	1.07	0.78	0.51	16.30	19.04	19.70	4.52	n.d.	n.d.	0.02	1.40	0.25	0.25	17.84	21.77	22.34	5.10	n.d.	0.52
SrO																					1.99
BaO																					0.81
Na_2O	n.d.	n.d.	0.15	0.15	0.07	1.75	2.51	2.26	0.00			0.02	0.02	0.02	0.01	0.83	1.44	1.16	0.02	n.d.	1.75
K_2O	n.d.	n.d.	n.d.	0.01	0.01	n.d.	n.d.	n.d.	n.d.			n.d.	n.d.	n.d.	0.01	0.01	0.02	0.01	n.d.	n.d.	12.84
Total	100.74	100.65	100.54	100.00	100.45	100.75	99.77	100.78	100.64	99.14	99.70	101.19	100.92	99.68	100.17	100.14	99.86	100.12	100.73	99.76	100.92
Si	0.001	1.000	1.925	1.939	1.947	1.842	1.932	1.943	2.992	0.000	0.000	0.997	1.836	1.935	1.945	1.832	1.920	1.940	2.992	0.000	2.904
Ti	0.001	0.000	0.001	0.001	0.001	0.004	0.004	0.004	0.003	0.001	0.000	0.000	0.001	0.001	0.001	0.002	0.003	0.002	0.003	0.000	
V																					
Al	1.914	0.001	0.129	0.114	0.104	0.400	0.275	0.226	1.991	1.839	1.942	0.000	0.287	0.105	0.088	0.347	0.201	0.141	1.933	1.991	1.092
Cr	0.010	0.000	0.000	0.000	0.001	0.001	0.001	0.001	0.003	0.006	0.003	0.002	0.000	0.000	0.000	0.000	0.000	0.001	0.001	0.001	
Fe^{3+}	0.073									0.154	0.055									0.007	0.003
Fe^{2+}	0.241	0.303	0.270	0.264	0.258	0.174	0.126	0.124	0.691	0.268	0.244	0.288	0.304	0.269	0.267	0.198	0.133	0.125	0.832	0.000	0.000
Mn	0.000	0.001	0.003	0.001	0.001	0.003	0.002	0.003	0.007	0.002	0.001	0.001	0.003	0.003	0.001	0.003	0.000	0.002	0.013	0.001	
Ni	0.027	0.019	0.008	0.009	0.007	0.003	0.003	0.003	0.000	0.023	0.014	0.011	0.004	0.002	0.001	0.001	0.003	0.002	0.000	0.000	
Zn	0.006									0.008	0.005										
Mg	0.727	1.674	1.628	1.642	1.659	0.840	0.756	0.797	1.976	0.699	0.736	1.701	1.530	1.685	1.697	0.883	0.811	0.859	1.870	0.001	
Ca	0.000	0.001	0.040	0.029	0.019	0.626	0.739	0.759	0.345	0.000	0.000	0.001	0.052	0.010	0.009	0.696	0.853	0.873	0.394	0.000	0.026
Sr																					0.053
Ba																					0.015
Na	0.000	0.000	0.010	0.010	0.005	0.122	0.176	0.157	0.000			0.001	0.001	0.001	0.000	0.059	0.102	0.082	0.003	0.000	0.156
K	0.000	0.000	0.000	0.000	0.000	0.000	0	0	0.000			0.000	0.000	0.000	0.001	0.000	0.001	0.000	0.000	0.000	0.756
Sum	3.000	3.000	4.015	4.009	4.002	4.015	4.015	4.018	8.008	3.000	3.000	3.002	4.020	4.012	4.011	4.021	4.027	4.028	8.040	2.000	5.005
Mg#	75.1	84.7	85.8	86.1	86.5	82.8	85.7	86.5	74.1	72.3	75.1	85.5	83.4	86.2	86.4	81.7	85.9	87.3	69.2		
Al^{IV}			0.061	0.053	0.051	0.144	0.054	0.039					0.144	0.053	0.045	0.146	0.052	0.032			
Al^{VI}			0.069	0.061	0.053	0.257	0.221	0.187					0.143	0.052	0.044	0.201	0.149	0.109			

Mg# = Mg/[Mg+Fe^{2+}]. For spinel, corundum, and potassium feldspar, Fe^{3+} and Fe^{2+} were calculated from stoichiometry. For other minerals, all Fe was taken as FeO. Al^{IV} in pyroxenes = (Al+Cr+2Ti-Na-K)/2; Al^{VI} = Al^{total}-Al^{IV}. integr. = integrated composition (see section 'analytical techniques').

Table 2 Representative major element compositions of minerals from Mg-Al sapphirine-bearing granulites

	1910-11									1910-1								
	OPX I cpx lam. integr.	OPX II		CPX II		SPL	SPR	PL	GRT	OPX I cpx lam. integr.	OPX II		CPX II		SPL	SPR	PL	GRT
		core	rim	core	rim	core		core	relic		core	rim	core	rim	core		core	relic
SiO_2	54.15	56.47	56.48	52.87	54.09	0.01	12.29	59.20	41.74	55.58	55.68	55.84	53.57	53.86	0.01	11.25	62.74	41.11
TiO_2	0.01	0.01	n.d.	0.05	0.03	n.d.	n.d.		n.d.	n.d.	0.01	0.04	n.d.	n.d.	n.d.	0.04		n.d.
V_2O_3															0.03			
Al_2O_3	3.08	1.15	1.66	6.82	8.98	65.86	65.74	26.04	23.25	2.54	1.97	2.08	8.12	11.49	66.92	66.30	23.71	23.19
Cr_2O_3	0.03	0.01	n.d.	0.08	0.01	0.67	0.12		0.05	0.01	n.d.	0.03	0.00	0.06	0.14	0.07		0.07
FeO_t	9.37	9.77	9.37	3.26	2.32	12.25	3.32	n.d.	13.63	9.92	10.25	9.94	3.28	2.61	12.80	4.07	0.07	14.89
MnO	0.06	n.d.	0.04	0.05	0.06	0.02	0.07		0.18	0.03	0.08	0.04	0.05	0.03	0.04	0.01		0.26
NiO	0.16	0.24	0.13	0.01	n.d.	1.20	0.26		0.01	0.21	0.25	0.28	0.03	0.11	1.62	0.53		n.d.
ZnO						0.37									0.67			
MgO	30.7	32.87	32.81	14.35	12.59	19.76	18.32		17.90	30.55	31.85	31.92	12.70	10.76	18.49	17.30		16.11
CaO	1.43	0.27	0.20	21.4	18.61	n.d.	n.d.	7.49	4.18	1.16	0.16	0.47	19.59	17.14	n.d.	0.03	4.38	4.97
SrO								0.15									0.29	
BaO								0.05									0.07	
Na_2O	0.43	0.05	0.11	1.71	3.68	n.d.	0.01	7.20	n.d.	0.41	0.11	0.09	3.20	4.82	n.d.	0.00	8.56	0.23
K_2O	n.d.	n.d.	n.d.	n.d.	0.02	n.d.	n.d.	0.40	0.02	n.d.	n.d.	n.d.	n.d.	n.d.	n.d.	0.02	0.99	0.01
Total	99.42	100.86	100.79	100.60	100.39	100.14	100.16	100.53	100.97	100.40	100.36	100.71	100.54	100.89	100.74	99.62	100.81	100.86
Si	1.917	1.962	1.958	1.903	1.927	0.000	1.435	2.634	2.993	1.946	1.949	1.946	1.921	1.907	0.000	1.327	2.768	2.980
Ti	0.000	0.000	0.000	0.001	0.001	0.000	0.000		0.000	0.000	0.000	0.001	0.000	0.000	0.000	0.003		0.000
V															0.001			
Al	0.128	0.047	0.068	0.289	0.377	1.955	9.046	1.366	1.965	0.105	0.081	0.085	0.343	0.480	1.986	9.219	1.233	1.981
Cr	0.001	0.000	0.000	0.002	0.000	0.013	0.011		0.003	0.000	0.000	0.001	0.000	0.002	0.003	0.006		0.004
Fe^{3+}						0.031		0.000							0.010		0.003	
Fe^{2+}	0.277	0.284	0.272	0.098	0.069	0.227	0.324	0.000	0.817	0.291	0.300	0.290	0.098	0.077	0.260	0.401		0.903
Mn	0.002	0.000	0.001	0.002	0.002	0.000	0.007		0.011	0.001	0.002	0.001	0.001	0.001	0.001	0.001		0.016
Ni	0.005	0.007	0.004	0.000	0.000	0.024	0.024		0.001	0.006	0.007	0.008	0.001	0.003	0.033	0.051		0.000
Zn						0.007									0.013			
Mg	1.620	1.702	1.695	0.770	0.669	0.742	3.189		1.913	1.595	1.661	1.658	0.679	0.568	0.694	3.043		1.741
Ca	0.054	0.010	0.007	0.825	0.710	0.000	0.000	0.357	0.321	0.044	0.006	0.018	0.752	0.650	0.000	0.004	0.207	0.386
Sr								0.004									0.007	
Ba								0.001									0.001	
Na	0.029	0.003	0.007	0.120	0.254	0.000	0.002	0.621	0.000	0.028	0.008	0.006	0.222	0.330	0.000	0.000	0.733	0.033
K	0.000	0.000	0.000	0.000	0.001	0.000	0.000	0.022	0.002	0.000	0.000	0.000	0.000	0.000	0.000	0.002	0.056	0.001
Sum	4.033	4.016	4.012	4.010	4.011	3.000	14.038	5.005	8.025	4.015	4.014	4.013	4.019	4.018	3.000	14.058	5.008	8.045
Mg#	85.4	85.7	86.2	88.7	90.7	76.6			70.1	84.6	84.7	85.1	87.4	88.1	72.7			65.8
Al^{IV}	0.050	0.022	0.031	0.087	0.062					0.039	0.037	0.041	0.061	0.076				
Al^{VI}	0.078	0.025	0.038	0.203	0.315					0.067	0.045	0.044	0.283	0.404				

Mg# = Mg/[Mg+Fe^{2+}]. For spinel and plagioclase, Fe^{3+} and Fe^{2+} were calculated from stoichiometry. For other minerals, all Fe was taken as FeO.
Al^{IV} in pyroxenes = (Al+Cr+2Ti-Na-K)/2; Al^{VI} = Al^{total}-Al^{IV}. integr. = integrated composition (see section 'analytical techniques').

Table 3 Representative major element compositions of minerals from Ca-Al hibonite-bearing granulite xenoliths

	1906-2						1904-1								1904-9						
	CPX I	CPX II		SPL	PL	GRT	CPX I	CPX II		SPL	SPR	HIB	PL	GRT	CPX I	CPX II		SPL	HIB	PL	GRT
	core	core	rim	core	core	relic	core	core	rim	core		core	core	relic	core	core	rim	core	core	core	relic
SiO_2	54.65	53.31	51.76	n.d.	60.88	40.73	54.31	53.27	52.23	0.02	10.40	3.04	59.46	40.34	52.82	53.51	51.94	0.02	2.99	60.20	40.18
TiO_2	n.d.	0.05	0.03	0.03		0.03	0.02	0.10	0.14	0.01	0.01	0.37		0.00	n.d.	0.02	n.d.	0.03	0.06		0.02
V_2O_3				0.02														n.d.			
Al_2O_3	4.81	8.24	9.56	62.83	25.14	23.07	5.28	7.47	10.5	64.20	67.85	83.81	26.12	22.50	4.67	8.02	10.77	65.00	84.05	25.63	22.58
Cr_2O_3	0.06	0.08	0.34	3.38		0.06	n.d.	0.00	0.01	1.73	1.08	0.23		0.00	0.00	0.01	n.d.	0.49	0.18		n.d.
FeO_t	3.56	3.83	3.35	14.03	0.03	14.6	2.78	3.91	2.23	14.59	3.90	2.02	0.02	13.66	3.12	3.59	2.65	14.54	2.27	0.01	14.23
MnO	0.04	0.04	0.01	n.d.		0.26	n.d.	0.03	n.d.	0.03	0.02	n.d.		0.14	0.02	0.04	n.d.	0.10	0.01		0.16
NiO	0.16	0.13	0.14	2.19		n.d.	0.16	0.12	0.11	1.61	0.39			0.05	0.20	0.15	0.14	2.02			0.01
ZnO				1.86						1.51		0.22						1.69	0.21		
MgO	13.95	11.89	11.46	16.37		14.2	14.18	12.69	12.1	16.82		1.67		11.73	14.63	11.99	10.83	16.52	1.48		11.90
CaO	20.2	18.54	19.49	n.d.	6.37	8.00	20.37	20.74	20.71	n.d.	16.75	8.57	7.68	11.06	23.38	19.39	19.94	n.d.	8.50	6.89	10.82
SrO					0.11						0.03		0.03							0.04	
BaO					n.d.								0.01							n.d.	
Na_2O	2.55	3.62	3.40	0.04	8.11	0.01	2.40	2.45	2.62	n.d.	n.d.	0.02	7.16	0.01	0.97	3.13	3.17	0.04	n.d.	7.55	0.01
K_2O	n.d.	n.d.	0.01	0.02	0.29	0.01	n.d	n.d.	0.02	n.d.	n.d.	0.01	0.43	0.00	n.d.	n.d.	n.d.	n.d.	n.d.	0.39	n.d.
Total	99.97	99.72	99.53	100.77	100.92	100.97	99.50	100.77	100.67	100.53	100.42	99.96	100.91	99.49	99.80	99.84	99.43	100.45	99.75	100.72	99.91
Si	1.976	1.93	1.882	0.000	2.688	2.971	1.966	1.916	1.866	0.000	1.219	0.343	2.634	2.999	1.927	1.933	1.879	0.001	0.338	2.665	2.982
Ti	0.000	0.001	0.001	0.001		0.001	0.001	0.003	0.004	0.000	0.000	0.031		0.000	0.000	0.001	0.000	0.001	0.005		0.001
V				0.000														0.000			
Al	0.205	0.351	0.409	1.913	1.308	1.983	0.225	0.317	0.442	1.944	9.373	11.130	1.364	1.972	0.201	0.341	0.459	1.967	11.187	1.337	1.975
Cr	0.002	0.002	0.010	0.069		0.003	0.000	0.000	0.000	0.035	0.100	0.021		0.000	0.000	0.000	0.000	0.010	0.016		0.000
Fe^{3+}				0.020	0.001					0.020			0.001					0.023		0.000	
Fe^{2+}	0.108	0.116	0.102	0.284	0.000	0.891	0.084	0.118	0.067	0.294	0.382	0.190	0.000	0.849	0.095	0.108	0.080	0.289	0.214	0.000	0.883
Mn	0.001	0.001	0.000	0.000		0.016	0.000	0.001	0.003	0.001	0.001	0.000		0.009	0.001	0.001	0.000	0.002	0.001		0.010
Ni	0.005	0.004	0.004	0.045		0.000	0.005	0.003	0.000	0.033	0.037			0.003	0.006	0.004	0.004	0.042			0.001
Zn				0.035						0.029		0.018						0.032	0.018		
Mg	0.752	0.641	0.621	0.630		1.544	0.765	0.680	0.644	0.644	2.926	0.280		1.300	0.795	0.646	0.584	0.632	0.249		1.317
Ca	0.783	0.719	0.759	0.000	0.301	0.625	0.790	0.799	0.793	0.000	0.004	1.034	0.364	0.881	0.914	0.751	0.773	0.000	1.028	0.327	0.86
Sr					0.003								0.001							0.001	
Ba					0.000								0.000							0.000	
Na	0.179	0.254	0.240	0.002	0.694	0.001	0.168	0.171	0.181	0.000	0.000	0.005	0.615	0.002	0.068	0.219	0.222	0.002	0.000	0.648	0.001
K	0.000	0.000	0.000	0.001	0.016	0.001	0.000	0.000	0.001	0.000	0.000	0.002	0.025	0.000	0.000	0.000	0.000	0.000	0.000	0.022	0.000
Sum	4.010	4.019	4.028	3.000	5.012	8.036	4.005	4.008	4.001	3.000	14.044	13.054	5.003	8.015	4.007	4.005	4.002	3.000	13.056	5.001	8.030
Mg#	87.4	84.7	85.9	68.9		63.4	90.1	85.2	90.6	68.7				60.5	89.3	85.7	88.0	68.6			59.9
Al^{IV}	0.014	0.051	0.091				0.030	0.076	0.134						0.067	0.062	0.119				
Al^{VI}	0.191	0.301	0.319				0.196	0.241	0.308						0.135	0.279	0.341				

Mg# = Mg/[Mg+Fe^{2+}]. For spinel and plagioclase, Fe^{3+} and Fe^{2+} were calculated from stoichiometry. For other minerals, all Fe was taken as FeO. Al^{IV} in pyroxenes = (Al+Cr+2Ti-Na-K)/2; $Al^{VI} = Al^{total}-Al^{IV}$.

Garnet-spinel websterite xenoliths

The minerals found in these xenoliths are ortho- and clinopyroxene, garnet, as well as subordinate olivine and spinel and accessory pyrrhotite (Fig. 2a-c). One xenolith (1906-4) consists of two websteritic parts separated by a thin vein of potassium feldspar with frequent needle-like inclusions of corundum.

The earliest mineral assemblage consists of large clinopyroxene (cpx Ia) and orthopyroxene (opx Ia) grains including some garnet (grt Ia, Fig. 2a), and large individual grains and aggregates of spinel (Fig. 2b). Spinel is relatively rich in Ni and poor in Cr and Ti (Table 1). Pyroxenes Ia usually bear exsolution lamellae of garnet (grt Ib) in their cores. Re-integrated core compositions of opx Ia are rich in Al and Ca as compared to rims and to a younger generation of smaller opx grains (opx Ib, Table 1). Re-integrated core compositions of cpx Ia are rich in Al and low in Ca contents and X_{Mg} as compared to rims and to a slightly younger generation of smaller cpx grains (cpx Ib, Table 1). Textures and zoning patterns are interpreted to reflect cooling from very high, possibly igneous temperatures with pyroxenes continuously crystallising and adjusting their compositions. Estimates that may approximate peak or early cooling temperatures, based on re-intergated opx Ia core compositions and the presence of garnet, are around 1230°C / 2.0 GPa. Partial re-equilibration after cooling is calculated to have taken place at 930-1010°C / 1.8-2.2 GPa, using px Ia rim and px Ib compositions for three samples (1535-3, 1910-1, 1910-11) and at conditions of approximately 740-840°C / 1.4-1.8 GPa for sample 1906-4 (Altherr et al. 2005). In two of the websterite xenoliths (1910-1 and 1910-11), the outermost pyroxene rims record a very young heating event related to rift magmatism (Altherr et al. 2005).

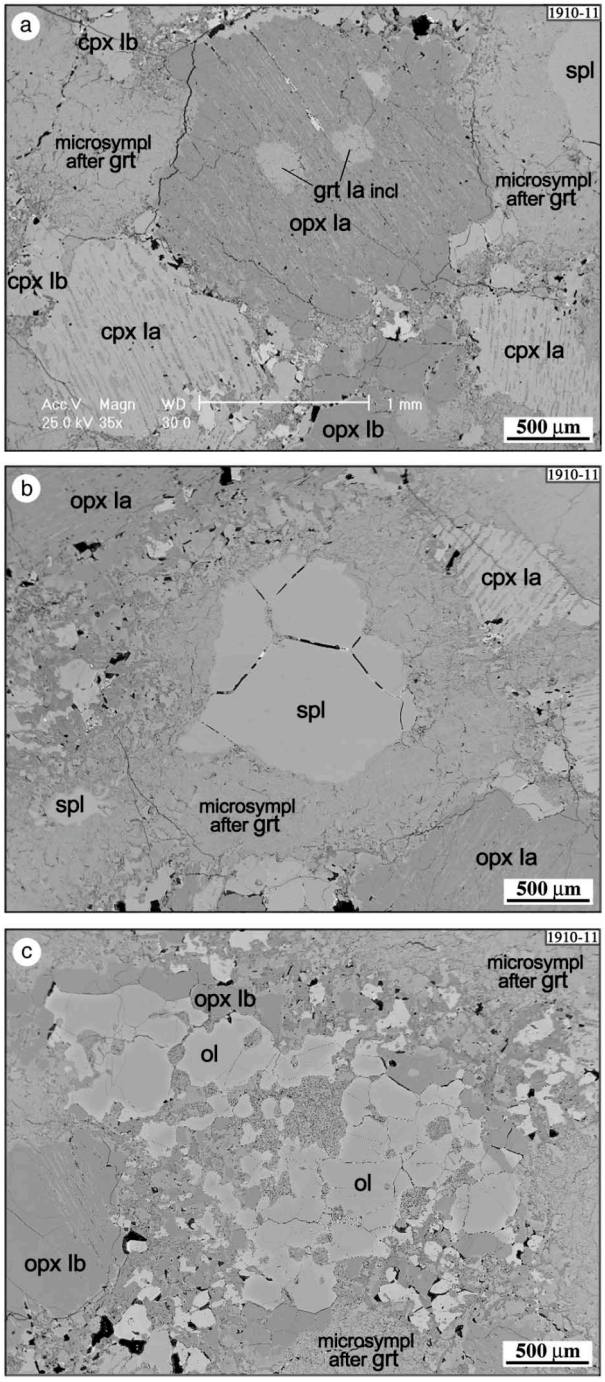


Fig. 2 Back-scattered electron images showing textures and different generations of the major mineral phases in garnet spinel websterite xenoliths. (a) General texture defined by two generations of pyroxene (Ia and Ib). (b) Tightly packed ¨glomeroporphyritic¨ aggregate of spinel I partially replaced by garnet. (c) Olivine and its relationships with garnet and orthopyroxene. Mineral abbreviations after Kretz (1983).

Olivine occurs either as distinct grains or as angular aggregates (Fig 2c). It is characterized by moderate Mg# (83.1-85.5) and very high NiO contents (Table 1). Garnet (grt Ib) forms a more or less continuous network around pyroxene grains. Both, olivine and network garnet are interpreted to have formed in the course of cooling by partial or complete replacement of spinel and pyroxenes.

Mg-Al sapphirine-bearing granulite xenoliths

Xenoliths of this type (1904-3 and 1904-7) consist of ortho- and clinopyroxene, corundum, spinel, sapphirine, sillimanite, garnet and plagioclase (Fig. 3a-c).

Large orthopyroxene grains with abundant exsolution lamellae of clinopyroxene (opx I, see Fig. 3a) represent early relicts. Plagioclase (1904-3: An_{21-16}; 1904-7: An_{40-30}) occurs as large grains and polycrystalline aggregates and contains abundant inclusions of sillimanite. Smaller grains of opx II and cpx II without exsolution texture often form coarse-grained intergrowths with spinel (Fig. 3b) that are interpreted to result from the reaction olivine + plagioclase = clinopyroxene + orthopyroxene + spinel (Ulianov and Kalt 2005). Opx I analyzed with a defocused beam shows a pronounced rimward decrease in Ca and Al. Opx II is less calcic and more homogeneous (Table 2). Cpx II shows an Al plateau in the core and a rimward increase in Al content and Mg#'s (Table 2). Spinel forms individual grains and core parts of complex corona structures that include sapphirine, sillimanite and garnet (Fig. 3c). Garnet forms a more or less continuous network around corona structures and individual grains of pyroxenes, spinel, corundum and plagioclase (Fig. 3a-c).

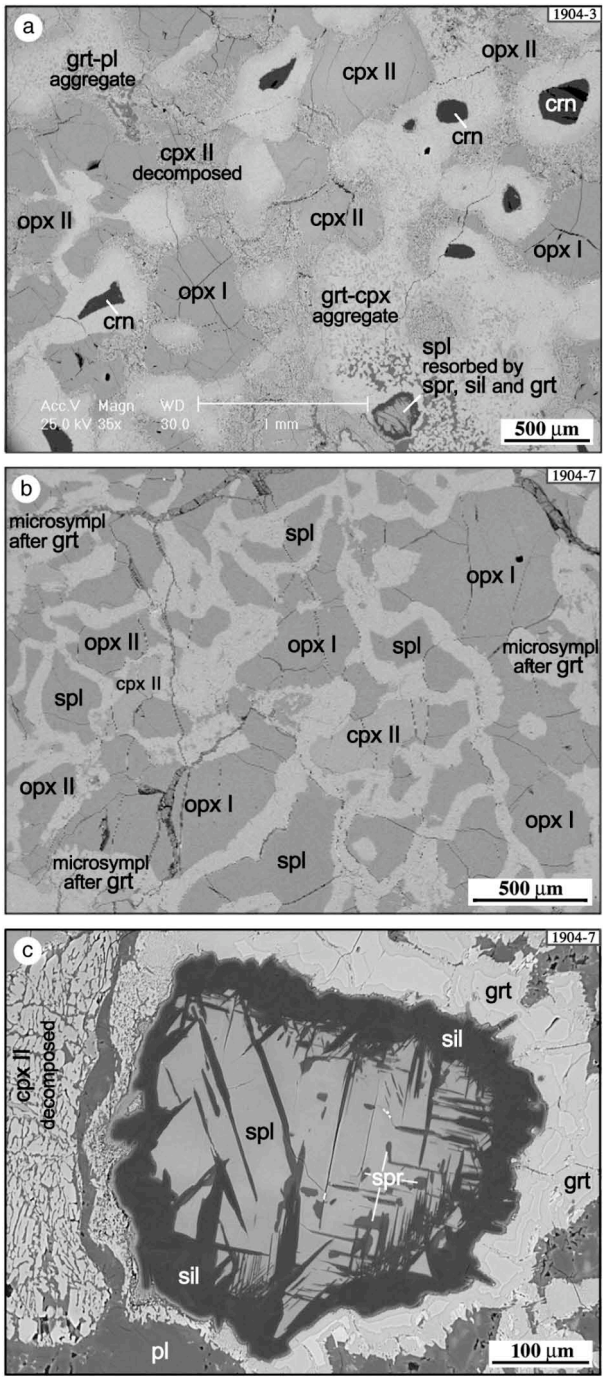


Fig. 3 Back-scattered electron images illustrating textures and different generations of the major mineral phases in Mg-Al sapphirine-bearing granulites. (a) General texture dominated by pyroxene, corundum and garnet. (b) Coarse-grained symplectite aggregates of orthopyroxene, clinopyroxene and spinel. (c) Sapphirine, sillimanite and garnet replacing spinel. Mineral abbreviations after Kretz (1983).

Metamorphic reaction textures in the Mg-Al granulites point to cooling accompanied or fol-

lowed by compression (Ulianov and Kalt 2005). Pressure calculations are hampered by the lack of quartz which would allow us to use the qtz-pl-cpx-grt equilibrium. For the exsolved cores of opx I analyzed with a defocused beam, we obtained estimates of 1090 and 1135 ºC (Ulianov and Kalt 2005) that may approximate early cooling. For the last stage of equilibration, the estimates range widely from 514 to 784 ºC depending on the geothermometer used (Ulianov and Kalt 2005).

Ca-Al hibonite-bearing granulite xenoliths

Xenoliths of this type (1904-1, 1904-9 and 1906-2) consist of abundant clinopyroxene and plagioclase (Fig. 4a), less abundant garnet and corundum (Fig. 4a, b), of minor spinel, quartz and sillimanite, and of accessory mullite and hibonite (Fig. 4c). Hibonite major and trace element composition is reported in Ulianov et al. (2005).

The earliest mineral seems to be hibonite accompanied by spinel, mullite, sapphirine, and sillimanite, forming complex corona structures (Fig. 4c, Ulianov et al. 2005), and clinopyroxene (cpx I) intergrown with quartz in the cores of large complex clinopyroxene grains (Fig. 4b). The cpx-qtz cores are mantled by an outer zone of clinopyroxene that lacks quartz and is similar in composition to isolated smaller grains devoid of quartz (cpx II). Cpx I is less aluminous, more magnesian and calcic than Cpx II (Table 3). Cpx II is zoned with a core plateau in Al and a rimward increase in Al content and Mg# (Table 3). Plagioclase (1904-1: An_{39-34}; 1904-9: An_{35-32}; 1906-2: An_{31-26}) forms large grains and polycrystalline aggregates. Corundum grains are closely associated with cpx II (Fig. 4a). Garnet forms networks at the expense of

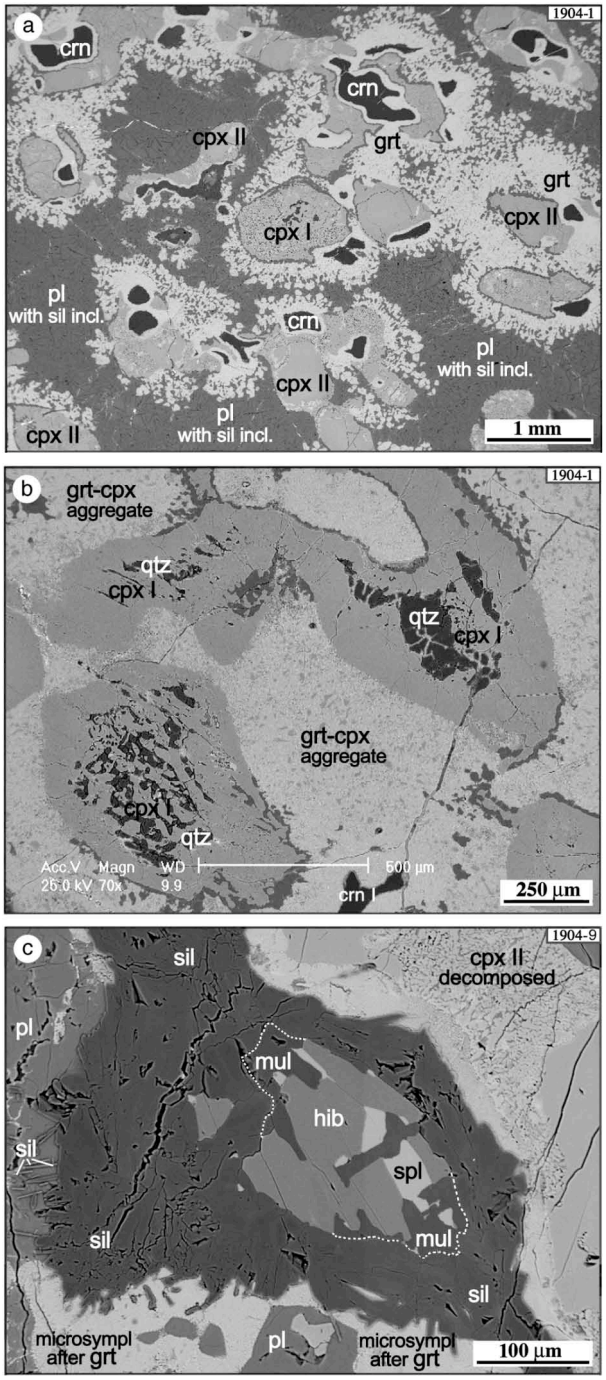


Fig. 4 Back-scattered electron images illustrating textures and different generations of the major mineral phases in Ca-Al hibonite-bearing granulites. (a) General texture dominated by clinopyroxene and plagioclase. (b) Large complex grains of clinopyroxene with quartz in the inner parts. (c) Aggregate of hibonite, spinel, mullite and sillimanite partially resorbed by garnet. Mineral abbreviations after Kretz (1983).

all other minerals except for hibonite and does not form independent grains. It has fairly high Ca contents (Table 3).

Metamorphic reaction textures in the Ca-Al granulites are interpreted to reflect cooling accompanied or followed by compression (Ulianov and Kalt 2005). Quartz never shows direct contact with garnet and plagioclase, thus excluding calculations using the qtz-pl-cpx-grt equilibrium. Temperatures obtained with the Fe-Mg garnet-clinopyroxene geothermometers are 635-639 ºC for specimen 1904-1 and 725-741 ºC for specimens 1904-9 and 1906-2 (Ulianov and Kalt 2005). Given the presence of sillimanite in both xenoliths, we fixed a maximum pressure for all temperature calculations at 0.8 GPa.

Trace elements in minerals

The results of trace-element analyses by LA ICP-MS are given in Table 4. In full agreement with the microprobe measurements (see Tables 1-3), all silicate minerals in both websteritic and granulitic lithologies show extremely low abundances of Ti and Cr and elevated contents of Ni. Spinel is also strongly depleted in Ti and, in most cases, has low Cr contents. It may contain some Pb and Nb. Spinel and olivine are important hosts of Ni, Co and Zn but play no significant role for the LILE, HFSE and REE budget.

In silicates, strong fractionation of LILE over HFSE and REE is observed, with Sr and Ba being particularly enriched (Table 4). Sr is hosted preferentially by plagioclase (and clinopyroxene). Clinopyroxene from xenoliths depleted in plagioclase (granulite 1904-3) or devoid of plagioclase (websterite samples 1910-11 and 1535-3) is very rich in Sr (up to 250 μg/g), whereas clinopyroxene from plagioclase-rich granulite xenoliths shows only moderate enrichment in Sr (<90 μg/g) that accumulates in plagioclase (up to 3000 μg/g). Plagioclase is also the major carrier of K and Ba (K_2O <1.5 wt%, Ba <480 μg/g).

HFSE abundances are generally very low. Their major host mineral is clinopyroxene (Zr <8.3 μg/g and <1 μg/g, Nb <0.8 μg/g and < 0.04 μg/g in websteritic and granulitic clinopyroxene, respectively).

REE abundances are also rather low with clinopyroxene being their major host (Table 4). Websteritic clinopyroxene shows a considerable fractionation of LREE over HREE (Fig. 5a). In granulitic clinopyroxene, the REE patterns are less fractionated (Fig. 5b) or nearly flat (sp. 1904-9, Fig. 5c). Positive Eu anomalies are weakly pronounced in websteritic clinopyroxene and accentuated in granulitic clinopyroxene, the latter due to the presence of abundant plagioclase. In the granulite xenoliths, plagioclase also accounts for a considerable fraction of the bulk rock REE content as well as for the fractionation of LREE over HREE (Table 4).

Websteritic clinopyroxene shows elevated abundances of most incompatible elements compared to clinopyroxene from granulites (Fig. 6a-c). Both websterite- and granulite-hosted clinopyroxene show negative anomalies of Nb, Zr and Hf and enrichment in Sr and Eu. No significant difference in trace element abundances is found neither between different generations of clinopyroxene nor between core and rim zones of clinopyroxene grains with clear major element zonation (see Table 4, Fig. 5 and 6). For websteritic pyroxenes I with abundant exsolution lamellae of garnet (kelyphitized), reintegrated compositions were obtained by averaging data from several shots per grain (maximum spot size of 110 μm). The obtained patterns are generally similar to those of

Table 4 Trace-element analyses (in μg/g) of minerals from the studied websterite and granulite xenoliths

websterite 1910-11

	SPL I	OL	OPX I		OPX II		CPX I		CPX II	GRT	kelyphites	
	core	core	core, reint.	rim	core	rim	core, reint.	rim	small grain	relic		
Li	1.4	1.9	1.1	0.30	0.87	0.42	0.40	0.52	1.1	<1.16	1.0	0.47
B	3.6	2.0	2.2	1.7	0.74	1.4	1.8	1.7	0.92	<12.60	2.4	3.9
K	<1.5	<0.70	97	<0.53	<0.40	0.68	60	2.3	4.3	<14.9	7.4	232
Ti	162	7.5	141	121	122	125	333	408	390	139	153	633
Cr	1851	5.0	68	48	46	49	119	119	91	184	205	115
Ni	11814	7164	1322	1735	1440	1526	585	762	755	110	90	232
Co	598	340	123	134	120	122	58	49	48	122	96	90
Zn	3137	161	93	112	92	98	23	25	27	38	28	37
V	107	0.81	18	19	16	18	50	63	57	15	15	24
Sc	0.18	0.53	3.3	0.75	0.75	0.75	4.7	2.1	2.8	13	11	7.1
Rb	<0.023	<0.013	0.13	<0.010	<0.011	<0.018	0.077	<0.025	<0.014	<0.40	<0.051	0.29
Sr	0.034	<0.010	4.2	0.21	1.3	0.23	114	145	138	<0.25	0.24	35
Y	<0.018	<0.008	0.30	<0.013	0.005	<0.011	0.42	0.065	0.064	1.1	1.2	0.86
Zr	0.063	<0.030	1.1	0.081	0.063	0.070	2.0	1.8	1.9	1.5	1.5	4.8
Nb	0.045	<0.013	0.18	0.017	0.018	<0.015	0.25	0.23	0.18	0.19	0.048	0.54
Cs	<0.014	<0.007	0.005	<0.008	<0.006	<0.008	0.004	<0.014	<0.007	<0.27	<0.011	<0.004
Ba	<0.059	<0.053	217	0.315	0.048	0.872	203	0.28	29	<1.11	0.28	127
La	<0.013	<0.007	0.18	<0.007	0.014	0.011	1.24	1.6	1.6	<0.22	0.018	0.62
Ce	<0.017	<0.005	0.139	0.014	0.025	0.016	2.36	3.0	2.9	<0.16	0.083	1.0
Pr	<0.006	<0.007	0.018	<0.005	<0.002	<0.005	0.25	0.26	0.32	<0.12	0.020	0.12
Nd	<0.037	<0.044	0.11	<0.029	<0.010	<0.018	0.93	1.4	1.3	0.78	0.14	0.53
Sm	<0.060	<0.027	0.040	<0.019	<0.011	<0.029	0.15	0.13	0.17	<0.46	0.18	0.14
Eu	0.020	<0.012	0.048	0.007	<0.005	<0.012	0.14	0.19	0.16	0.31	0.14	0.15
Gd	<0.085	<0.034	0.036	<0.020	<0.012	<0.021	0.061	0.14	0.043	<0.93	0.22	0.13
Tb	<0.013	<0.005	0.006	<0.004	<0.003	<0.005	0.011	<0.008	0.009	<0.13	0.014	0.029
Dy	<0.037	<0.021	0.042	<0.012	0.011	<0.018	0.070	<0.022	<0.025	<0.56	0.18	0.14
Ho	<0.012	<0.006	0.012	<0.003	<0.002	<0.008	0.020	<0.008	<0.005	0.12	0.070	0.033
Er	<0.019	<0.023	0.034	<0.015	<0.007	<0.022	0.033	<0.045	<0.008	<0.21	0.14	0.14
Tm	<0.006	<0.005	0.005	<0.004	<0.003	<0.003	0.008	<0.008	<0.003	<0.069	<0.019	0.009
Yb	<0.043	<0.038	0.038	<0.028	<0.020	<0.021	0.088	<0.051	<0.032	<0.47	<0.13	0.073
Lu	<0.018	<0.004	<0.003	<0.003	<0.002	<0.005	0.009	<0.011	<0.005	<0.10	0.039	0.016
Hf	<0.065	0.019	0.019	0.015	0.014	<0.013	0.085	0.059	0.085	<0.70	0.054	0.061
Ta	<0.008	<0.006	0.005	<0.007	<0.002	<0.004	0.014	0.013	<0.009	<0.18	<0.022	0.029
Pb	0.078	0.080	0.078	0.050	0.041	0.046	0.12	0.072	0.12	<0.56	<0.072	0.12
Th	<0.007	<0.003	0.045	0.004	0.023	<0.005	0.18	0.21	0.20	<0.11	<0.015	0.059
U	<0.007	<0.007	0.029	0.009	0.005	<0.003	0.049	0.059	0.047	<0.10	<0.023	0.023

websterite 1535-3

	SPL I	OL	OPX I		OPX II		CPX I	CPX II		CPX II	GRT	kelyphite
	core	core	core, reint.	rim	core	rim	core, reint.	core	rim	small grain	relic	
Li	1.9	3.9	2.0	0.9	2.0	1.3	1.0	1.6	2.1	3.0	<0.23	0.16
B	5.8	1.5	2.1	1.9	1.5	1.9	3.7	2.0	2.8	1.6	2.7	2.2
K	<1.4	<1.3	<0.36	<0.52	<0.28	2.1	89	5.4	10.6	9.7	<2.0	<0.62
Ti	194	5.3	158	129	126	128	475	809	836	514	165	151
Cr	3832	<3.1	124	83	74	79	199	223	253	249	200	199
Ni	12397	7634	2054	1523	1669	1518	778	783	871	759	96	92
Co	575	333	127	96	107	98	40	38	42	41	108	98
Zn	3478	158	88	67	79	71	17	19	21	20	23	21
V	127	0.92	24	19	20	19	67	64	94	88	21	19
Sc	<0.172	0.358	0.770	0.525	0.658	0.559	2.886	2.883	3.233	2.658	14.101	14.162
Rb	<0.044	0.020	<0.006	<0.017	<0.005	0.010	0.40	<0.007	<0.020	<0.009	<0.036	<0.023
Sr	<0.034	0.10	0.26	0.16	0.20	0.22	184	218	229	241	0.16	0.16
Y	<0.030	<0.009	0.008	<0.007	0.006	<0.008	0.35	0.16	0.16	0.12	1.3	1.2
Zr	<0.039	0.051	0.18	0.11	0.13	0.16	4.2	6.1	8.3	3.5	1.1	1.4
Nb	<0.028	<0.012	0.017	0.014	<0.006	<0.012	0.55	0.80	0.65	0.76	0.073	0.070
Cs	<0.014	<0.014	<0.005	<0.006	<0.002	<0.005	0.004	<0.004	<0.012	0.003	<0.015	<0.007
Ba	<0.17	<0.051	<0.017	<0.024	<0.014	0.047	1.3	0.029	<0.11	0.094	<0.093	<0.030
La	0.019	0.020	0.006	<0.006	<0.004	<0.006	3.3	4.7	4.7	4.7	0.028	0.009
Ce	<0.026	0.012	0.024	0.007	0.015	0.028	10.4	13.6	13.8	13.4	0.14	0.21
Pr	<0.014	<0.008	0.004	0.007	0.003	0.006	1.4	1.8	1.7	1.7	0.057	0.086
Nd	<0.10	<0.032	0.019	0.030	0.029	0.020	6.4	7.3	7.4	7.2	0.78	0.75
Sm	<0.049	<0.051	<0.020	<0.029	0.014	<0.025	0.82	0.83	0.90	0.87	0.29	0.31
Eu	0.049	<0.011	<0.005	<0.005	<0.003	<0.004	0.37	0.35	0.38	0.36	0.24	0.38
Gd	0.055	<0.073	<0.017	<0.017	<0.014	<0.015	0.25	0.34	0.22	0.24	0.34	0.35
Tb	<0.011	<0.008	<0.003	<0.003	<0.002	<0.003	0.026	0.024	0.025	0.016	0.060	0.05
Dy	<0.044	<0.032	<0.011	<0.011	<0.009	<0.016	0.11	0.083	0.052	0.078	0.25	0.26
Ho	<0.008	<0.008	<0.002	<0.003	<0.002	<0.002	0.017	0.009	0.011	0.004	0.045	0.062
Er	<0.032	<0.028	<0.005	<0.011	<0.006	<0.010	0.022	0.007	<0.017	<0.011	0.17	0.15
Tm	<0.013	<0.005	<0.002	<0.004	<0.002	0.003	0.003	<0.002	<0.006	<0.003	0.021	0.022
Yb	<0.087	<0.037	<0.012	<0.017	<0.010	<0.021	0.015	<0.014	<0.056	<0.027	<0.147	0.17
Lu	<0.014	<0.006	<0.004	<0.004	<0.002	<0.002	<0.004	<0.003	<0.012	<0.003	0.050	0.043
Hf	0.034	<0.033	<0.011	<0.011	<0.006	<0.013	0.13	0.075	0.23	0.076	<0.072	0.025
Ta	<0.010	<0.007	<0.002	<0.008	<0.004	<0.004	0.067	0.13	0.081	0.095	<0.018	<0.004
Pb	0.10	<0.039	0.034	0.042	0.028	<0.016	0.15	0.16	0.19	0.22	<0.076	0.047
Th	<0.014	<0.009	0.006	<0.003	0.007	<0.006	0.10	0.22	0.21	0.17	<0.011	<0.006
U	<0.017	<0.014	<0.002	<0.005	<0.003	<0.003	0.034	0.077	0.063	0.062	<0.010	0.019

Table 4 (Contd.)

	Mg-Al two-pyroxene granulite1904-7							Mg-Al two-pyroxene granulite1904-3						
	OPX I	CPX II		SPL	GRT	kely-	PL	OPX I	CPX II		SPL	GRT	kely-	PL
	core	core	rim	core	relic	phite	core	core	core	rim	core	relic	phite	
Li	0.28	0.18	0.22	1.7	<1.5	<3.3	<1.6	2.4	1.7	3.3	6.0	<1.1	0.77	<0.67
B	1.7	1.1	2.6	9.6	<12	<4.5	<19	1.3	1.9	3.0	4.3	<7.5	3.7	<8.8
K	0.47	6.6	8.5	<2.1	<15	17	3209	<0.40	6.9	7.3	<3.1	24.9	33.6	12094
Ti	43	242	222	<2.1	<19	4.3	<19	6.4	48	52	3.8	12	15	<10
Cr	102	231	176	4020	<43	39	<46	46	42	42	1085	210	175	<24
Ni	1040	360	454	10943	70	92	<14	1917	723	810	16272	69	107	<9.4
Co	107	32	33	835	124	113	<0.96	154	42	41	991	187	169	<0.35
Zn	27.9	7.0	6.8	2676	14	21	<2.8	174	23	24	8125	48	44	<1.6
V	7.8	20	16	4.3	<2.1	<0.49	<2.2	2.2	6.0	7.5	3.9	1.2	1.6	<0.96
Sc	0.67	14	12	<0.18	<1.6	0.55	<1.69	0.71	4.9	4.5	<0.29	3.8	3.3	1.4
Rb	<0.011	<0.011	<0.040	<0.047	<0.25	<0.075	<0.31	<0.010	0.010	<0.047	<0.053	<0.20	<0.078	0.22
Sr	2.0	27	61	0.032	<0.16	2.9	1418	9.5	98	116	<0.058	0.24	10	3073
Y	<0.008	0.080	0.045	0.020	0.15	<0.092	0.24	0.004	0.055	<0.027	<0.035	<0.16	<0.037	<0.12
Zr	<0.013	<0.008	<0.033	<0.061	<0.26	<0.095	<0.44	0.013	0.049	<0.043	<0.11	<0.26	<0.10	<0.22
Nb	<0.004	<0.015	<0.026	0.025	<0.15	<0.093	<0.40	<0.005	0.005	<0.018	<0.077	<0.11	<0.058	<0.17
Cs	<0.003	<0.003	<0.016	0.019	<0.15	<0.047	<0.20	<0.004	<0.005	<0.015	<0.035	<0.085	<0.029	<0.044
Ba	0.066	0.21	0.11	<0.078	<0.64	<0.29	184	<0.017	<0.021	<0.17	<0.24	<0.74	0.28	479
La	0.013	0.33	0.36	0.026	<0.21	0.026	0.54	0.035	0.31	0.25	<0.046	<0.051	<0.038	0.33
Ce	0.022	0.54	0.45	<0.011	<0.156	0.040	0.36	0.026	0.48	0.45	<0.028	<0.084	<0.042	0.17
Pr	<0.002	0.075	0.058	<0.018	<0.159	<0.025	<0.142	<0.002	0.042	0.033	<0.015	<0.069	<0.015	<0.078
Nd	<0.010	0.38	0.32	<0.12	<0.40	<0.10	<0.84	<0.017	0.12	0.16	<0.17	<0.29	<0.090	<0.40
Sm	<0.017	0.038	<0.034	0.062	<0.64	<0.12	<0.56	<0.020	<0.024	<0.076	<0.20	<0.63	<0.20	<0.54
Eu	<0.008	0.25	0.18	<0.040	<0.33	0.20	<0.17	0.010	0.26	0.17	<0.041	0.26	0.11	<0.16
Gd	<0.024	0.046	<0.090	<0.11	<0.46	<0.12	<0.58	<0.017	<0.024	<0.055	<0.10	<0.68	<0.15	<0.39
Tb	<0.002	0.005	<0.005	<0.015	<0.12	<0.033	<0.089	<0.003	0.004	<0.012	<0.031	<0.053	<0.016	<0.043
Dy	<0.008	<0.012	0.031	<0.049	<0.40	<0.076	<0.50	<0.007	<0.007	<0.058	<0.12	<0.21	<0.091	<0.24
Ho	0.003	<0.006	<0.010	<0.013	<0.074	<0.028	<0.13	<0.002	0.003	<0.012	<0.038	<0.067	<0.017	<0.044
Er	<0.006	<0.011	<0.022	<0.043	<0.21	<0.055	<0.26	<0.005	<0.014	<0.042	<0.064	<0.11	0.053	<0.12
Tm	<0.003	0.002	<0.007	<0.008	<0.12	<0.018	<0.085	<0.002	0.004	<0.008	<0.015	<0.036	<0.022	<0.091
Yb	<0.024	0.034	<0.068	<0.078	<0.65	<0.21	<0.80	<0.017	<0.019	0.076	<0.20	<0.34	<0.18	<0.27
Lu	<0.003	0.005	<0.005	<0.015	<0.074	<0.033	<0.13	<0.003	<0.004	0.015	<0.022	<0.039	0.029	<0.044
Hf	<0.017	<0.012	<0.022	<0.049	<0.29	<0.19	<0.70	<0.015	<0.007	<0.035	<0.063	<0.15	<0.066	<0.17
Ta	<0.002	<0.004	<0.007	<0.018	<0.15	<0.023	<0.11	<0.002	<0.004	<0.011	<0.033	<0.13	0.023	<0.092
Pb	0.063	0.092	0.084	0.13	<0.57	<0.14	1.1	0.038	0.11	0.066	<0.11	<0.29	<0.13	1.6
Th	<0.002	<0.002	<0.006	<0.013	<0.076	<0.028	<0.094	0.011	<0.003	<0.009	<0.023	<0.068	0.019	<0.064
U	0.009	<0.002	<0.008	<0.017	<0.072	<0.019	<0.15	<0.005	<0.002	<0.008	<0.016	<0.053	<0.016	<0.043

	Ca-Al two-pyroxene granulite1904-1							Ca-Al two-pyroxene granulite1904-9						
	CPX I	CPX II		SPL	HIB	PL		CPX I	CPX II		SPL	kely-	PL	
		core	rim	core	core	core	rim		core	rim	core	phite	core	rim
Li	4.2	6.6	8.9	15	n.a.	3.0	<3.0	3.4	3.4	3.7	21	0.49	21	<0.90
B	<10	3.9	2.0	13	n.a.	<18	<31	3.4	3.2	2.7	<5.8	6.9	2.5	<15
K	9.4	6.9	5.9	<7.1	n.a.	4117	4782	19	4.8	4.3	<4.5	124	1531	4598
Ti	54	458	321	36	1265	11	<26	4.9	56	44	8.7	9.8	0.83	<8.3
Cr	277	252	214	10788	n.a.	<46	<73	35	82	89	4265	93	<1.4	<30
Ni	923	770	824	16469	n.a.	<22	<54	1381	1038	1150	19915	71	<1.0	21
Co	51	47	46	1248	n.a.	<0.75	<1.3	70	58	59	1288	108	0.031	0.38
Zn	49	45	42	18108	n.a.	<5.1	<7.8	67	54	56	19801	52	0.48	<3.4
V	60	68	63	100	184	<1.7	<3.8	5.7	10	11	11	2.0	<0.078	<1.4
Sc	1.7	16	14	<0.70	n.a.	<1.9	<3.5	0.47	2.7	2.3	<0.54	1.5	0.37	<1.5
Rb	<0.21	0.009	<0.043	<0.13	n.a.	<0.37	<0.59	0.11	<0.009	<0.029	<0.089	0.61	<0.022	<0.30
Sr	37	18	26	<0.14	80	747	689	40	33	31	0.26	36	630	789
Y	<0.090	1.4	0.84	<0.11	0.22	<0.11	<0.46	<0.026	0.028	0.016	<0.049	0.025	<0.011	0.14
Zr	<0.28	0.25	0.20	<0.21	n.a.	<0.50	<1.04	<0.041	0.27	0.13	<0.18	0.14	<0.031	<0.41
Nb	<0.14	0.010	<0.031	0.088	n.a.	<0.28	<0.42	<0.046	<0.009	<0.019	<0.088	<0.006	<0.009	<0.18
Cs	<0.12	<0.004	0.37	<0.067	n.a.	<0.12	<0.30	<0.017	<0.004	<0.006	0.18	0.016	<0.006	<0.13
Ba	<0.69	0.096	<0.23	<0.69	8.9	209	184	1.8	0.020	<0.069	0.44	36	120	203
La	0.34	0.32	0.25	<0.079	2.9	0.46	0.62	0.060	0.086	0.10	<0.047	0.019	0.23	<0.16
Ce	0.56	0.77	0.59	0.090	4.9	0.30	<0.37	0.14	0.16	0.16	<0.039	0.016	0.13	0.14
Pr	<0.052	0.14	0.072	<0.028	0.46	<0.067	<0.35	0.017	0.024	0.024	<0.033	0.006	0.013	<0.070
Nd	<0.31	0.66	0.20	<0.23	2.0	<0.67	<1.1	<0.13	0.070	<0.089	<0.14	<0.030	<0.031	<0.42
Sm	<0.50	0.25	<0.096	<0.27	0.26	<0.78	1.6	<0.13	<0.018	<0.060	<0.12	<0.035	<0.029	<0.34
Eu	0.13	0.39	0.28	<0.12	0.72	<0.26	<0.28	0.12	0.18	0.19	<0.094	0.46	0.079	<0.10
Gd	<0.44	0.23	<0.097	<0.33	0.26	<0.65	<0.96	<0.11	<0.026	0.072	<0.20	<0.029	<0.021	<0.35
Tb	<0.040	0.038	<0.015	<0.043	<0.053	<0.12	<0.36	<0.017	<0.004	<0.014	0.038	0.004	<0.009	<0.055
Dy	<0.16	0.32	0.16	<0.12	0.18	<0.49	<1.16	<0.079	<0.014	<0.022	<0.10	<0.013	<0.022	<0.21
Ho	<0.041	0.075	0.027	<0.031	<0.037	<0.073	<0.22	<0.017	<0.004	<0.010	<0.026	<0.003	<0.005	<0.096
Er	<0.12	0.12	0.11	<0.088	<0.28	<0.21	<0.85	<0.067	<0.008	<0.035	<0.053	<0.009	<0.010	<0.27
Tm	<0.038	0.017	0.010	<0.029	<0.027	<0.15	<0.14	<0.016	<0.002	<0.013	0.083	<0.003	<0.003	<0.10
Yb	<0.26	0.092	<0.057	<0.19	<0.30	0.62	<1.3	<0.15	<0.013	<0.036	<0.12	<0.021	<0.021	<0.35
Lu	<0.041	0.023	0.028	<0.031	<0.021	<0.074	<0.15	<0.012	<0.003	<0.006	0.034	<0.006	<0.006	<0.056
Hf	<0.28	0.020	<0.036	<0.12	n.a.	<0.50	<0.85	<0.12	<0.008	<0.032	<0.105	<0.026	0.023	<0.31
Ta	<0.049	0.011	<0.015	<0.037	n.a.	<0.12	<0.26	<0.028	0.003	<0.011	<0.061	<0.007	<0.006	<0.093
Pb	<0.32	0.17	0.11	<0.23	1.5	0.81	<1.0	<0.11	0.074	<0.058	<0.17	0.067	0.31	0.89
Th	<0.060	0.004	<0.013	<0.055	n.a.	<0.076	<0.16	<0.012	<0.003	<0.006	<0.028	<0.006	<0.005	<0.082
U	<0.056	0.003	<0.009	<0.042	<0.034	<0.071	<0.15	<0.020	<0.003	<0.010	<0.019	<0.006	<0.005	<0.14

< values represent analyses below the limit of detection.

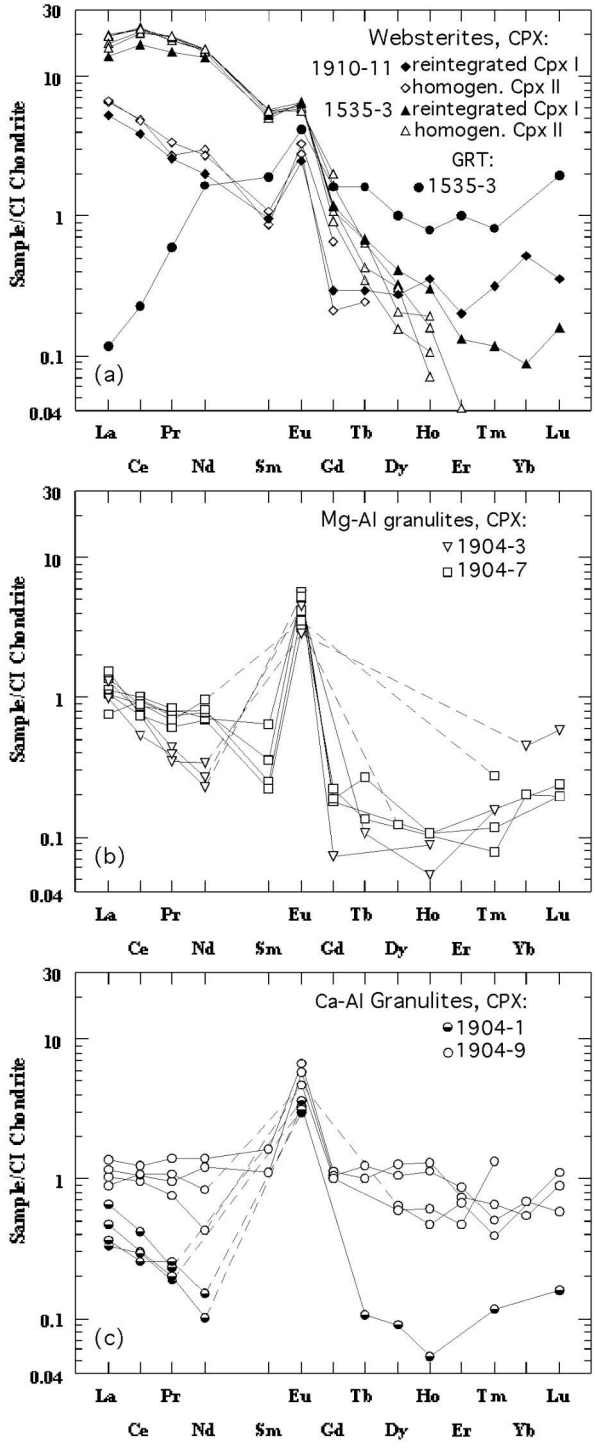


Fig. 5 Chondrite-normalized rare earth element patterns in clinopyroxene and garnet from the studied xenoliths. Normalization values are from Sun and McDonough (1989).

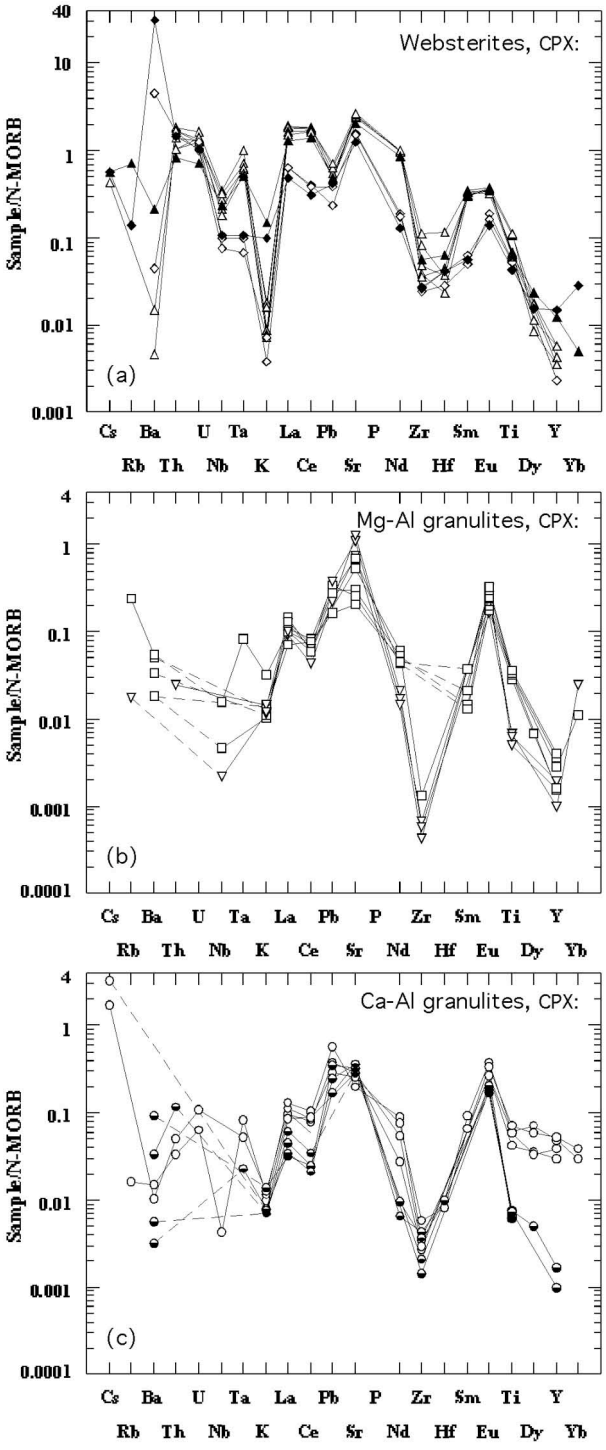


Fig. 6 MORB-normalized multi-element patterns of clinopyroxene from the studied xenoliths. Normalization values are from Sun and McDonough (1989). Symbols as in Fig. 5.

homogeneous clinopyroxene II (Fig. 5a and 6a). Exceptions are HREE, Ba and K (higher than in cpx II).

Only one relict of unaltered interstitial garnet (from websterite 1535-3) turned out to be large enough to be analysed by LA-ICPMS. Its REE

pattern (Fig. 5a) is characterised by only moderate fractionation of HREE over LREE and by a positive Eu anomaly. Kelyphite was also analysed for trace elements. Although major element concentrations hardly differ between garnet and adjacent kelyphite, trace elements in kelyphite show a considerable scatter. Some kelyphite areas have trace element abundances which are similar to those observed in garnet relicts, whereas others are strongly enriched in incompatible elements (cf. garnet and two kelyphites in websterite 1910-11, Table 3).

Whole-rock major and trace element composition

The major and trace element compositions of the studied xenoliths are given in Table 5. The rocks are basic, with SiO_2 ranging from 44.9 to 50.2 wt% and MgO ranging from 21.3 to 6.1 wt%. Their Mg# calculated on the basis of divalent iron are high (69.4-80.6). They are relatively rich in calcium and very rich in aluminum (15.5-24.6 wt% Al_2O_3). Alkalies are Na-dominated. Ni and Co contents are remarkably high and vary between 209-1061 and 113-238 μg/g, respectively. The Sr content reaches 872 μg/g and is often accompanied by high concentrations of Ba (up to 1155 μg/g). The contents of Ti and Nb are low (<360 μg/g and <4.1 μg/g, respectively). All studied xenoliths have very low abundances of REE, including the LREE.

Strong correlations are observed between MgO and all major and some trace elements (Fig. 7). At the same time, other trace elements, especially Cr, V, Nb, Zr and REE, are not correlated. The chondrite-normalized REE patterns (Fig. 8a) show fractionation of the LREE over the HREE

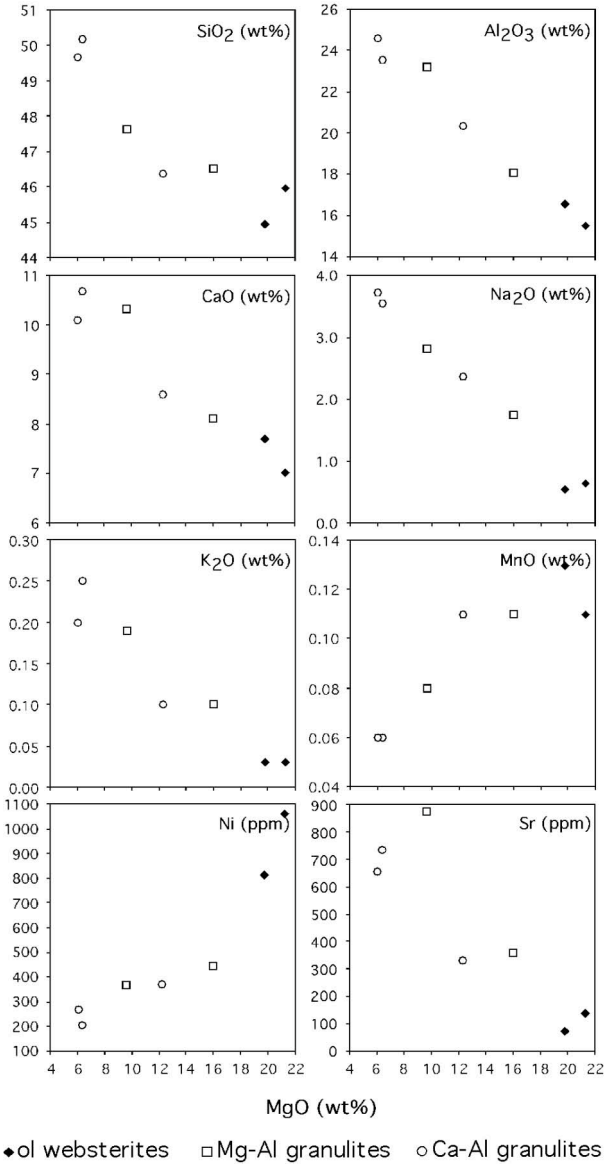


Fig. 7 Variation diagrams for major and selected trace elements in the studied xenoliths.

$[(La/Yb)_{CIn}$ 3-33] and are characterized by positive Eu anomalies, accentuated in granulites and much less pronounced in websterites. The abundances of the REE elements in granulites are generally lower than in websterites, with some granulite xenoliths being inferior to CI chondrite with respect to La and Ce contents.

The multi-element distribution patterns of all studied xenoliths are similar in their configuration and demonstrate a fractionation of LILE over HFSE and REE and pronounced positive anomalies of Ba,

Table 5 Major-element (in wt% oxides) and trace-element (in μg/g) composition of websterite and granulite whole rock samples

	1535-3	1910-11	1904-3	1904-7	1906-2	1904-9	1904-1
SiO_2	45.98	44.94	46.51	47.65	46.39	50.18	49.66
TiO_2	0.04	0.06	0.01	0.01	0.01	0.05	0.01
Al_2O_3	15.51	16.55	18.09	23.20	20.34	23.58	24.59
FeO_t	9.09	9.88	9.27	5.39	9.39	4.57	4.76
MnO	0.11	0.13	0.11	0.08	0.11	0.06	0.06
MgO	21.25	19.76	16.01	9.61	12.25	6.34	6.06
CaO	7.01	7.69	8.12	10.32	8.59	10.68	10.11
Na_2O	0.65	0.55	1.74	2.82	2.37	3.55	3.72
K_2O	0.03	0.03	0.10	0.19	0.10	0.25	0.20
P_2O_5	0.03	0.02	0.02	0.06	0.01	0.05	0.03
L.O.I.	0.16	0.37	0.11	0.41	0.12	0.43	0.28
Total	99.86	99.98	100.09	99.74	99.68	99.74	99.48
Mg#	80.64	78.09	75.48	76.06	69.93	71.2	69.41
XRF:							
Cr	331	156	87	65	919	238	102
Ni	1061	812	445	367	374	209	271
Cu	28	10	<2	<2	<2	<2	<2
Sr	138	73	357	872	332	733	657
Ba	82	138	102	627	60	1155	955
LA-ICP-MS (averages from 4-5 shots):							
TiO_2	0.041 (0.001)	0.060 (0.001)	0.005 (0.001)	0.019 (0.001)	0.013 (0.001)	0.048 (0.002)	0.004 (0.001)
MnO	0.119 (0.003)	0.131 (0.002)	0.115 (0.006)	0.072 (0.002)	0.102 (0.002)	0.063 (0.002)	0.053 (0.002)
K_2O	0.036 (0.003)	0.037 (0.001)	0.098 (0.004)	0.25 (0.02)	0.117 (0.004)	0.30 (0.01)	0.227 (0.009)
P_2O_5	0.021 (0.004)	0.013 (0.001)	0.010 (0.001)	0.039 (0.003)	0.010 (0.001)	0.033 (0.003)	0.020 (0.002)
Li	1.21 (0.07)	1.4 (0.2)	1.5 (0.2)	1.0 (0.1)	2.6 (0.2)	4.1 (0.3)	1.7 (0.2)
B	2.0 (0.3)	2.0 (0.2)	1.4 (0.2)	1.7 (0.4)	1.2 (0.3)	1.11 (0.03)	1.6 (0.1)
Cr	334 (9)	167 (1)	84 (5)	62 (6)	948 (67)	261 (14)	108 (12)
Co	188 (19)	238 (9)	225 (9)	155 (3)	222 (6)	113 (5)	222 (7)
Zn	55 (27)	68 (13)	57 (7)	35 (11)	58 (9)	22 (2)	28 (13)
Sc	8.6 (0.9)	6.6 (0.3)	2.5 (0.1)	1.8 (0.1)	4.3 (0.1)	6.0 (0.3)	1.4 (1.0)
V	44 (0.8)	31 (1)	4.4 (0.1)	7.1 (0.4)	77 (2)	37 (1)	5.8 (0.8)
Rb	0.9 (0.1)	0.38 (0.01)	0.69 (0.03)	4.4 (0.4)	3.8 (0.1)	2.8 (0.1)	1.02 (0.05)
Sr	146 (5)	74 (1)	344 (7)	855 (32)	313 (14)	718 (12)	651 (8)
Y	0.9 (0.1)	1.1 (0.1)	0.04 (0.01)	0.44 (0.02)	0.06 (0.01)	0.72 (0.02)	0.13 (0.03)
Zr	12.8 (0.6)	3.8 (0.2)	0.1 (0.1)	3.7 (0.1)	0.7 (0.2)	3.56 (0.08)	1.1 (0.9)
Nb	4.1 (0.1)	1.51 (0.04)	0.49 (0.02)	1.8 (0.1)	0.48 (0.03)	0.91 (0.08)	0.8 (0.1)
Cs	0.007 (0.003)	0.02 (0.01)	0.02 (0.01)	0.023 (0.005)	0.193 (0.019)	0.020 (0.005)	0.030 (0.006)
Ba	63 (7)	149 (3)	143 (6)	613 (30)	57 (1)	1049 (24)	939 (16)
La	2.0 (0.4)	2.0 (0.2)	0.34 (0.01)	1.53 (0.06)	0.07 (0.02)	1.23 (0.04)	0.42 (0.04)
Ce	4.0 (0.2)	2.4 (0.2)	0.31 (0.02)	2.0 (0.1)	0.11 (0.02)	2.01 (0.09)	0.21 (0.05)
Pr	0.6 (0.1)	0.32 (0.03)	0.025 (0.003)	0.25 (0.02)	0.012 (0.002)	0.23 (0.02)	0.03 (0.01)
Nd	2.5 (0.4)	1.17 (0.04)	0.07 (0.02)	0.91 (0.07)	0.06 (0.02)	1.05 (0.04)	0.14 (0.02)
Sm	0.6 (0.2)	0.21 (0.02)	<0.03	0.15 (0.03)	<0.05	0.19 (0.05)	<0.05
Eu	0.24 (0.03)	0.21 (0.01)	0.16 (0.01)	0.22 (0.02)	0.05 (0.01)	0.46 (0.02)	0.40 (0.02)
Gd	0.5 (0.3)	0.23 (0.06)	<0.03	0.10 (0.03)	<0.04	0.21 (0.02)	0.06 (0.01)
Tb	0.04 (0.02)	0.03 (0.01)	<0.005	0.016 (0.003)	0.004 (0.000)	0.024 (0.005)	0.004 (0.001)
Dy	0.18 (0.02)	0.18 (0.03)	0.015 (0.007)	0.07 (0.01)	0.017 (0.001)	0.16 (0.02)	0.023 (0.004)
Ho	0.037 (0.007)	0.040 (0.005)	<0.005	0.015 (0.003)	<0.005	0.029 (0.002)	0.005 (0.001)
Er	0.09 (0.02)	0.11 (0.02)	<0.02	0.04 (0.01)	<0.03	0.09 (0.02)	<0.03
Tm	0.015 (0.002)	0.014 (0.001)	<0.004	<0.005	<0.007	0.010 (0.001)	<0.004
Yb	0.085 (0.015)	0.104 (0.004)	0.013 (0.004)	0.033 (0.004)	0.015 (0.005)	0.061 (0.003)	0.018 (0.001)
Lu	<0.024	0.016 (0.006)	<0.004	<0.006	<0.006	0.008 (0.001)	<0.005
Hf	0.22 (0.02)	0.09 (0.02)	<0.016	0.04 (0.01)	0.037 (0.002)	0.07 (0.01)	0.03 (0.02)
Pb	0.090 (0.008)	0.11 (0.02)	0.27 (0.07)	0.40 (0.07)	0.33 (0.02)	0.28 (0.08)	0.3 (0.1)
Th	0.2 (0.2)	0.17 (0.02)	0.005 (0.001)	0.12 (0.01)	0.006 (0.001)	0.083 (0.005)	0.006 (0.005)
U	0.038 (0.003)	0.041 (0.003)	0.007 (0.003)	0.14 (0.01)	0.009 (0.001)	0.046 (0.009)	0.030 (0.009)

< values represent analyses below the limit of detection.

Sr and Eu (Fig. 8b). In the granulites, less pronounced positive anomalies of K are also observed (Fig. 8b). Different specimens of the same petrographic group may significantly differ from each other in trace element contents.

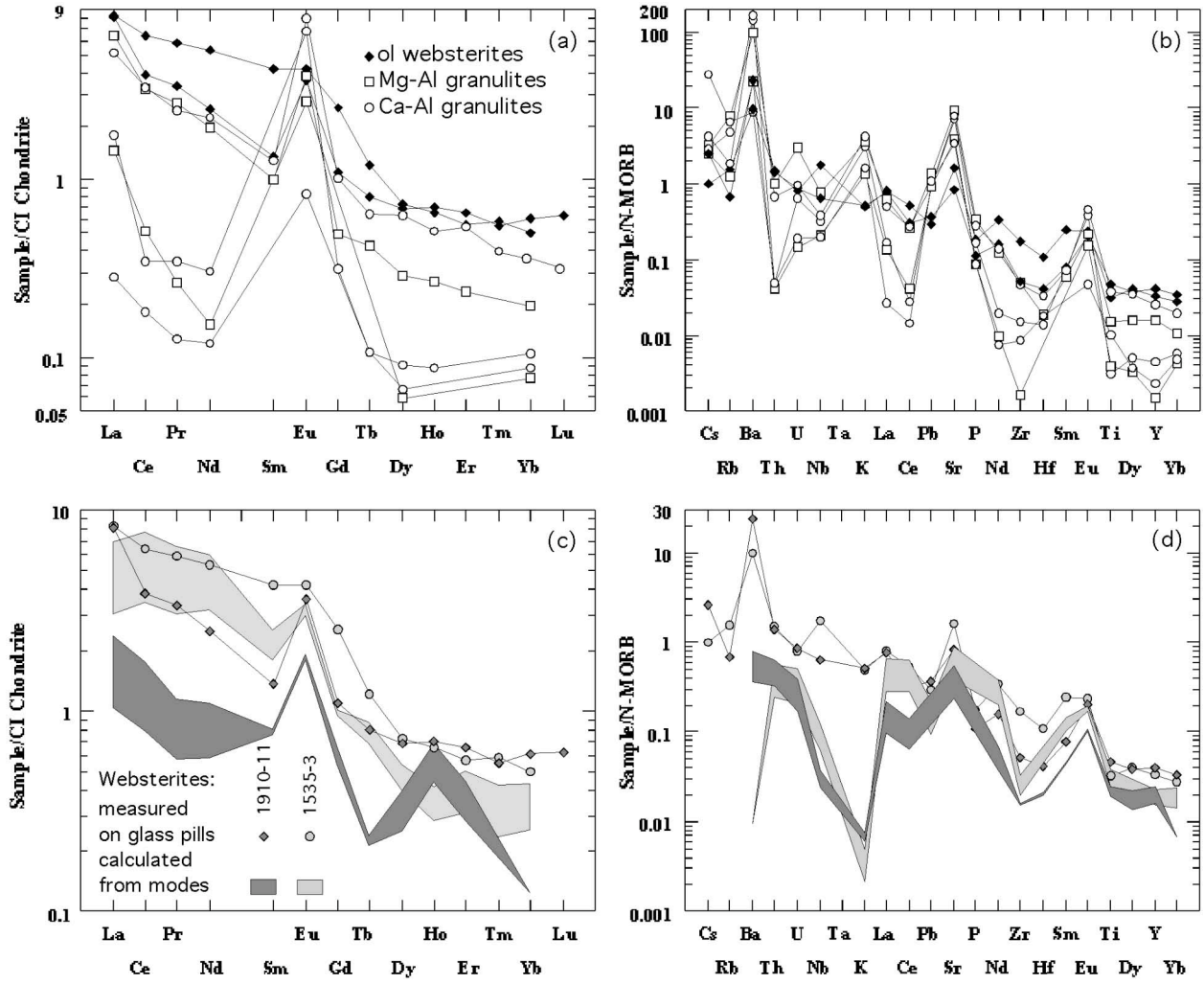


Fig. 8 Normalized bulk rock REE patterns (a) and multi-element patterns (b) of the studied xenoliths. Comparative plots showing REE (c) and multi-element patterns (d) of websterite xenoliths obtained by LA-ICPMS on glass pills (filled diamonds and circles) and calculated from modal abundances and trace element compositions of garnet and clinopyroxene (error ±10%). Granulites are not plotted, since many elements in their minerals are below the detection limits. Normalization values are from Sun and McDonough (1989).

Discussion

Significance of the trace element patterns: late-stage metasomatic effects vs. primary geochemical signature

Mineral and whole-rock trace element data reveal an apparent mismatch between the abundances of LILE, HFSE and LREE in the xenoliths and their minerals. For instance, websterite 1910-11 contains 1.5 μg/g of Nb. At the same time, the Nb content in its minerals does not exceed 0.25 μg/g. Granulite 1904-9 contains 3.6 μg/g of Zr, 0.91 μg/g of Nb, and 1.2 μg/g of La, whereas the maximum contents of these elements in the minerals are <0.32, <0.04, and <0.24 μg/g, respectively (cf. Tables 4 and 5). Among the rock-forming minerals of the xenoliths, only garnet, clinopyroxene and plagioclase may account for significant amounts of incompatible elements (see Table 4). Based on their modes and trace element compositions, we have calculated the expected bulk rock abundances for a selected set of incompatible ele-

ments, of which the concentrations are mostly above the detection limits (see Table 6). A comparison of the normalized REE and multi-element patterns of websterite xenoliths 1910-11 and 1535-3, obtained by LA-ICPMS on glass pills and calculated from modes, is given in Fig. 8c and d.

The results of these calculations confirm that although the concentrations of incompatible elements (particularly HFSE and REE) measured on glass pills are fairly low, the abundances expected from modes and mineral compositions are even lower. For example, xenoliths 1910-11, 1904-7 and 1904-1 are up to ten times richer in Zr, Nb, La and Ce than expected from their modal compositions and trace element abundances in garnet, clinopyroxene and plagioclase (cf. Tables 5 and 6). The presence of accessory phases such as rutile, titanite, zircon or REE-epidote appears unlikely due to both careful documentation of all specimens on the SEM and because of very low bulk rock abundances of the elements in question. We assign the observed mismatch to the presence the infiltration of fluids / melts shortly prior to or during the transport of the xenoliths to the Earth's surface.

In the studied xenoliths, there is no evidence of modal metasomatism related to host magmatism. However, there is evidence of late-stage heating and reaction with fluids / melts in some websterite xenoliths, such as zoning patterns of outermost pyroxene rims (Altherr et al. 2005), decomposition of early clinopyroxene and replacement of garnet by kelyphite (see above). LA-ICPMS analyses of kelyphite clearly show that its composition varies but that it may be enriched in HFSE, LREE and LILE (see Table 4). The basanites of the Chyulu Hills generally show very high abundances of these elements (Späth et al. 2001).

Table 6 Selected whole rock trace element abundances in the studied xenoliths obtained by calculations based on mineral modes and mineral compositions

	1535-3 25% cpx 40% grt	1910-11 25% cpx 45% grt	1904-3 7% pl 30% cpx 20% grt	1904-7 25% pl 20% cpx 20% grt	1904-9 45% pl 30% cpx 10% grt	1904-1 50% pl 25% cpx 10% grt
K_2O (wt%)	0.0003	0.0005	0.103	0.097	0.102	0.248
TiO_2	0.041	0.028	0.003	0.008	0.003	0.017
Sr (ppm)	57	36	247	363	356	379
Zr	2.0	1.2	<0.082	<0.16	0.060	<0.31
Nb	0.21	0.073	<0.035	<0.13	<0.008	<0.14
Ba	0.061	3.7	34	46	66	105
La	1.2	0.40	0.11	0.20	0.15	0.30
Ce	3.5	0.79	0.15	0.19	0.12	0.32
Pr	0.46	0.082	<0.030	<0.08	0.014	<0.059
Eu	0.19	0.11	<0.13	0.15	0.098	<0.21
Pb	0.047	<0.057	0.14	0.30	0.19	0.44

Orthopyroxene, spinel, corundum, sillmanite and other minerals with low concentrations of incompatible elements are not included because of textural complexity of the studied rocks that hampers the calculation of mineral modes.

Late addition of these elements by metasomatism related to host magmatism could also account for the observed lack of correlation between MgO and Nb, Zr, and LREE. We believe, therefore, that for most specimens the abundances of the LREE and HFSE elements, remarkably low in general and therefore especially sensitive to late-stage alteration, may have been significantly modified via the interaction with the host basanitic magma.

On the other hand, the behavior of the LILE is better accounted for by the involvement of (a) LILE-rich phase(s). In websterite xenoliths, a dramatic difference between the contents of K and Ba measured on glass pills and calculated from the modes and trace element composition of garnet and clinopyroxene is observed (cf. Tables 5 and 6), with the mineral-based values being much lower. Sr demonstrates a similar although less pronounced tendency. In specimen 1535-3, despite the measured and calculated abundances of La and Ce are well matched (rather an exception than a rule), the K and Ba contents obtained by direct

measurements (Table 5) are three orders of magnitude higher than those based on the compositions of garnet and clinopyroxene (Table 6). In granulites, in spite of plagioclase accounting for a significant general enrichment in the LILE, the mineral-based abundances of Ba and Sr are also substantially lower. At the same time, K and Sr are well correlated with MgO over the entire set of the studied xenoliths (Fig. 7). Ba, except for one specimen, also shows a good correlation with MgO (not plotted). Ba-Sr-rich potassium feldspar (Table 1) occurs as layer in websteritic xenolith 1906-4. An inclusion of potassium feldspar armored in clinopyroxene was also found in websterite 1535-3. In granulite 1904-7, submicroscopic inclusions of celsian in plagioclase were observed. In both cases, no qualitative analyses were made due to small size of the inclusions. Accessory inclusions of K-feldspar in early pyroxene and in garnet are also reported from other websterite xenoliths of the Chyulu Hills (Altherr et al. 2005). Therefore, the LILE contents, which are two to three orders of magnitude higher than REE and HFSE, may have undergone minor changes during late-stage metasomatism related to host magmatism, but seem to be largely controlled by the presence of minor amounts of (a) early K-Ba-Sr-rich phase(s), most likely potassium feldspar.

Major and trace element constraints on the protoliths

The good correlation between MgO and other oxides (Fig. 7) leads to the conclusion that the suite of investigated xenoliths is meta-igneous and can be considered as a sequence of magmatic fractionation. The overall high bulk rock Mg#'s (80.6-69.4) suggest that not only websteritic but also granulitic xenoliths represent cumulates rather than crystallized melts. Several lines of evidence exclude that the xenoliths are cumulates of rift-related alkaline magmatism and suggest that they are related to subduction zone / arc magmatism (see below).

Contrary to arc settings, cumulates related to alkaline rift magmatism are generally rich in clinopyroxene (e.g. Dawson et al. 1995) and devoid of orthopyroxene because the latter requires elevated SiO_2 or H_2O contents in the magmas (e.g. Grove et al. 2003). Rare cognate cumulates in basanites from the Chyulu Hills are clinopyroxene-dominated and non-metamorphic whereas the studied xenoliths are rich in orthopyroxene (except Ca-Al granulites) and metamorphosed. In classification diagrams for basalts, the compositions of the analysed xenoliths mainly plot in the field of subalkalic (TAS) or high-alumina / calc-alkaline (Alkali index versus Al_2O_3) rocks. In the AFM diagram and in Fe_{tot}/Mg versus SiO_2 plots, they are intermediate between the calc-alkaline and the tholeiitic trends. Clinopyroxene from alkaline igneous rock generally shows fairly high TiO_2/Al^{IV} ratios (LeBas 1962) whereas clinopyroxene related to arc magmatism is characterised by low TiO_2/Al^{IV} ratios (e.g. Jan and Howie 1981; Conrad and Kay 1984; DeBari et al. 1987; DeBari and Coleman 1989; Mukhopadhay and Manton 1994, Himmelberg and Loney 1995). Al^{IV} and TiO_2 contents of cpx I from websterite xenoliths of the Chyulu Hills, interpreted to have formed at igneous or near-igneous temperatures, clearly follow the trend defined by arc cumulates (Loucks 1990, Fig. 9) but not the alkaline trend (LeBas 1962, Fig. 9). The same holds true for cpx I and II of granulite xenoliths, but their compositions are probably

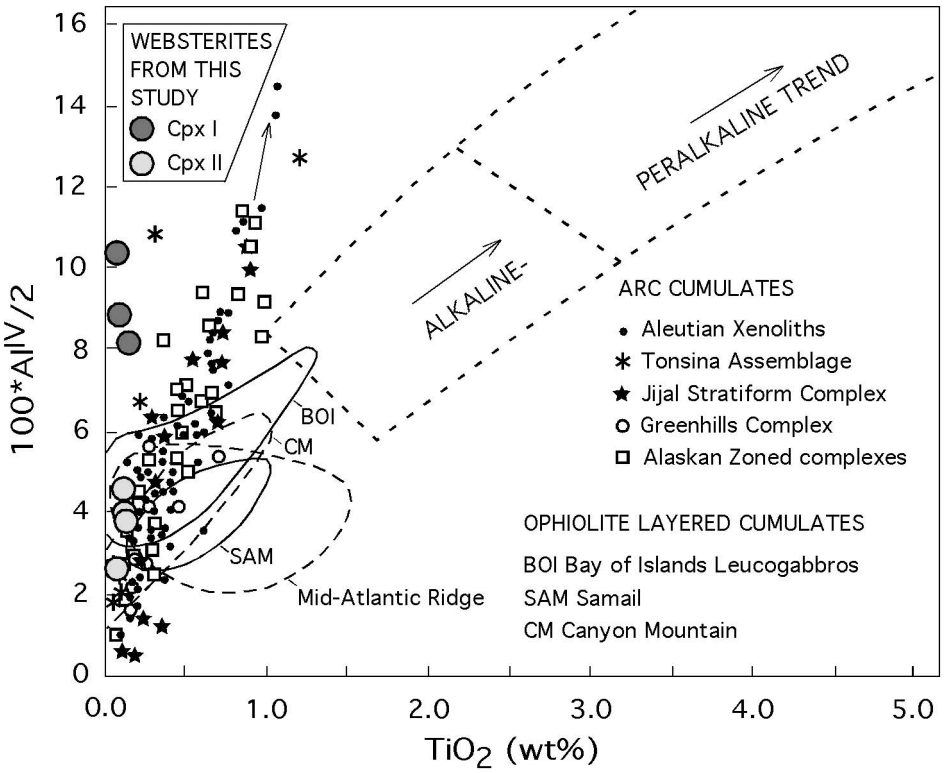


Fig. 9 Tetrahedral Al (in %) versus TiO_2 contents in clinopyroxene of the websterite xenoliths from the Chyulu Hills (diagram modified after Loucks 1990). Fields for alkaline and peralkaline trends are taken from LeBas (1962). Fields for cumulates from ophiolites as compiled by Loucks (1990). Also shown are data from arc cumulates: Aleutian xenoliths (DeLong et al. 1975; Conrad and Kay 1984; DeBari et al. 1987), Tonsina (DeBari and Coleman 1989), Jijal (Jan and Howie 1982), Greenhills Complex (Spandler et al. 2003), Alaskan zoned complexes (Ruckmick and Noble 1959; Findlay 1969; Irvine 1974; Himmelberg and Loney 1995).

entirely metamorphic. Rift-related alkaline magmas, and in particular those erupted in Quaternary times in the Chyulu Hills, are strongly enriched in HFSE and LREE (Späth et al. 2001). TiO_2 contents may be up to 8 wt% (Altherr, unpublished data). The studied xenoliths are characterised by extremely low abundances of these elements.

Subduction- or arc-related magmas usually show enrichment of LILE and fractionation of LREE over HREE (e.g. Tatsumi and Eggins 1995). The whole rock REE and multi-element patterns of the analysed xenoliths also reveal these features, but some of the LILE and LREE fractionation is interpreted to represent metasomatic additions (see previous section). Out of the seven analysed specimens only one can be considered virtually free of the late-stage overprints (Ca-Al granulite 1906-2). It is characterized by extremely low abundances of REE and a low degree of their fractionation (Fig. 8a, lowermost pattern). Detailed investigation of metamorphic phase relations in the Ca-Al granulite xenoliths (Ulianov and Kalt 2005) led to the conclusion that plagioclase and olivine were the solidus phase assemblage. The (La/Yb)n ratio of specimen 1906-2 is 3.4. Assuming that plagioclase carries the major part of the REE, and applying published partition coefficients for plagioclase (e.g., Dunn and Sen 1994) to the whole-rock composition of this specimen raises the $(La/Yb)_{CIn}$ ratio to ~20-60, the values of ca. 20-

40 being more consistent with most of the available partition coefficients (see Dunn and Sen 1994; Bindeman et al. 1998 and references therein). These values constrain the upper limit of the possible range of fractionation of LREE over HREE in the parental magma. In conclusion, moderately elevated contents of LREE and (possibly) a fractionation of LILE over HFSE are expected in the parental magma(s) of the studied rock suite.

Positive Eu anomalies are consistent with a cumulate nature of the rocks. The Eu anomalies in whole rock samples generally match those observed in minerals (Fig. 5). Accentuated positive Eu (and Sr) anomalies in granulites suggest massive fractional crystallization of plagioclase (see Bindeman et al. 1998). Extreme fractionation of Eu in granulitic clinopyroxene (Fig. 5b and c) points to subsolidus crystallization via metamorphic reactions involving plagioclase, well in accordance with petrographic data (Ulianov and Kalt 2005). In websterites, Eu anomalies are less well expressed. They are nevertheless confirmed by the elevated abundances of Eu in garnet and clinopyroxene (Fig. 5a). This suggests the involvement of at least some plagioclase during fractional crystallization of the protolith, with subsequent replacement by mafic phases at subsolidus conditions. Moreover, very high abundances of Ni and remarkably low Cr and Ti contents in bulk rock and minerals of all samples suggest that also olivine was important during the course of igneous crystallization, i.e. the original protoliths were close to gabbro-troctolites (websterites) or troctolites (granulites). In the granulites, the troctolitic assemblage (plagioclase + olivine) accounts for >89.6 % of the normative C.I.P.W. composition.

Major and trace element composition of mafic and ultramafic cumulates in arc settings are variable in terms of concentration levels and fractionation patterns. Nevertheless, most arc cumulates are characterised by fairly low chondrite-normalised REE, by a low to moderate fractionation of LREE over HREE, by low HFSE (Ti) and by positive Pb, Sr, (Ba and Eu) anomalies (e.g. Himmelburg and Loney 1995; Cesare et al. 2002; Spandler et al. 2003; Claeson and Meurer 2004). Most of these features are also displayed by the websterite and granulite xenoliths of the Chyulu Hills when 'substracting' metasomatic effects, although the concentration levels in the granulites are extremely low. MORB or MORB-type cumulates may have similar features such as low concentration levels and positive Ba, Sr and Eu anomalies, but are often characterised by flat REE patterns or depletion of LREE and lack positive Pb and negative Ti anomalies (e.g. Kornprobst et al. 1990; Benoit et al. 1996; Morishita et al. 2003).

Nature and evolution of the igneous protoliths

In the Mg-Al sapphirine-bearing granulites, plagioclase and some spinel grains may mineralogically represent igneous relicts (Ulianov & Kalt 2005), although the actual composition of these phases is controlled by metamorphism. The former presence of olivine is clearly indicated by coarse-grained symplectite aggregates of opx, cpx and spl which formed by the subsolidus reaction ol + pl = opx + cpx + spl (Fig. 3b). The 'primary' assemblage deduced for the Mg-Al sapphirine-bearing granulites from their textures is thus in line with the bulk rock major and trace element data that suggest a troctolitic protolith. In the Ca-Al hibon-

ite-bearing granulites, only hibonite may chemically and mineralogically represent an igneous relict. The actual chemical composition of plagioclase, which apparently belongs to the solidus assemblage, is defined by metamorphism. In general, textures and bulk rock major and trace element characteristics of these rocks also suggest a plagioclase-rich troctolitic protolith.

The P-T path deduced for the granulite xenoliths is characterised by cooling and some compression (Ulianov & Kalt 2005). It involves crystallisation of pyroxene and lateron of garnet. The highest temperature obtained on early opx I in Mg-Al sapphirine-bearing granulites is 1090 and 1135 ºC; for the last stage of equilibration, the estimates are between 510 and 780 ºC. Some textures related to the formation of garnet at the expense of corundum can be best interpreted as reflecting compression (Ulianov & Kalt 2005). However, as there is no evidence for early kyanite in the samples, the entire P-T evolution of the granulites seems to be limited to the sillimanite stability field.

The geological setting as well as major and trace element compositions of the analysed bulk rocks and minerals suggest that the igneous protoliths of granulite and websterite xenoliths may represent arc cumulates. The Mozambique Belt, which represents the lithosphere beneath the Chyulu Hills, was the site of multiple subduction and accretion in Pan-African times, e.g. between 750 and 615 Ma (e.g., Coolen et al. 1982; Kröner et al. 1987; Stern and Dawoud 1991; Muhongo and Lenoir 1994; Möller et al. 1998, 2000, Muhongo et al. 2001; Kröner et al. 2003), finally consuming the Mozambique Ocean by the collision of East and West Gondwana (e.g., Meert 2003). Between the Pan-African events and Tertiary to Recent rift formation, the Mozambique lithosphere was not subject to major overprints. Therefore, the igneous protoliths of the granulite and websterite xenoliths from the Chyulu Hills most likely cristallised in the context of Pan-African arc magmatism. The P-T paths, textures and mineral zoning patterns of the granulites are in line with igneous emplacement in the crust and slow cooling from igneous temperatures in Pan-African times to ambient crustal temperatures. Provided that cooling was constrained to the sillimanite stability field, perhaps accompanied or followed by some compression, and given the slope and position of the sillimanite-kyanite phase boundary, the protoliths of the granulite xenoliths must have intruded at rather shallow depths close to the Al_2SiO_5 triple point (approximately 0.6 GPa). The actual thickness of the crust is approximately 44 km, and there is no evidence for major crustal thinning since Pan-African times as observed in northern Kenya (Henjes-Kunst and Altherr 1992). Thus, if the granulite protoliths were compressed, this is limited to 44 km or approximately 1.2 GPa.

For the websterite xenoliths, there is an apparent contradiction between the textural-mineralogical data and results of P-T calculations on the one hand and some trace element data on the other hand. Large grain size, exsolution lamellae of garnet, high Al contents in cores of opx I and cpx I and pyroxene zoning patterns indicate cooling from near-igneous temperatures at 1.9 - 2.0 GPa (Altherr et al. 2005) and suggest that the investigated websterites are high-pressure cumulates that directly cristallised pyroxene. This is in line with the bulk rock major element compositions that imply a considerable fraction of mafic

minerals and do not suggest much plagioclase accumulation. Igneous crystallisation at deep levels is also in line with the Al_2O_3 contents versus X_{Mg} of clinopyroxene that clearly follows the trend defined by high-P igneous rocks (Fig. 10; e.g. Jan and Howie 1981; DeBari and Coleman 1989; Müntener et al. 2001) as opposed to low-P igneous rocks (e.g. Beard and Day 1988; Topuz et al. 2004). On the other hand, the positive Eu anomalies in bulk rock, clinopyroxene and garnet argue for plagioclase-bearing protoliths, whereas high Ni contents may point to early olivine. The stability of plagioclase and olivine in mafic arc magmas as a function of pressure, H_2O and oxygen fugacity has been explored in a number of experimental studies (e.g. Holloway and Burnham, 1972; Johnston 1986; Bartels et al. 1991; Draper and Johnston 1992; Sisson and Grove, 1993; Panjasawatwong et al., 1995; Müntener et al., 2001; Grove et al., 2003). In anhydrous systems, plagioclase (and olivine) stability as liquidus phase is usually limited to pressures below 1.0 - 1.2 GPa. Only in some dry high-alumina basaltic systems plagioclase was found as a liquidus phase up to 1.7 GPa (Johnston 1986). The effect of H_2O is to suppress plagioclase crystallisation and to expand the olivine stability field at low and medium pressures. It is very unlikely that the positive Eu anomalies observed in the websterites is due to early plagioclase (and olivine) cristallisation at pressures of approximately 2.0 GPa.

As the granulite and websterite xenoliths seem to be related to an arc setting and as the P-T paths of the granulites allow for some compression, subduction could in principle be a viable process for transporting the websterite protoliths (crustal plagioclase-bearing cumulates) to asthenospheric mantle depth where they transformed to pyroxenites. This process is invoked for pyroxenites of orogenic mafic-ultramafic complexes from several localities (e.g., Beni Bousera: Kornprobst 1990; Ronda: Morishita et al. 2003; Horoman: Morishita et al. 2004). All these rocks are tholeiitic and represent former oceanic crust metamorphosed during subduction. In our case, however, the 'classical' subduction setting with high P/T gradients for the rocks carried to depth

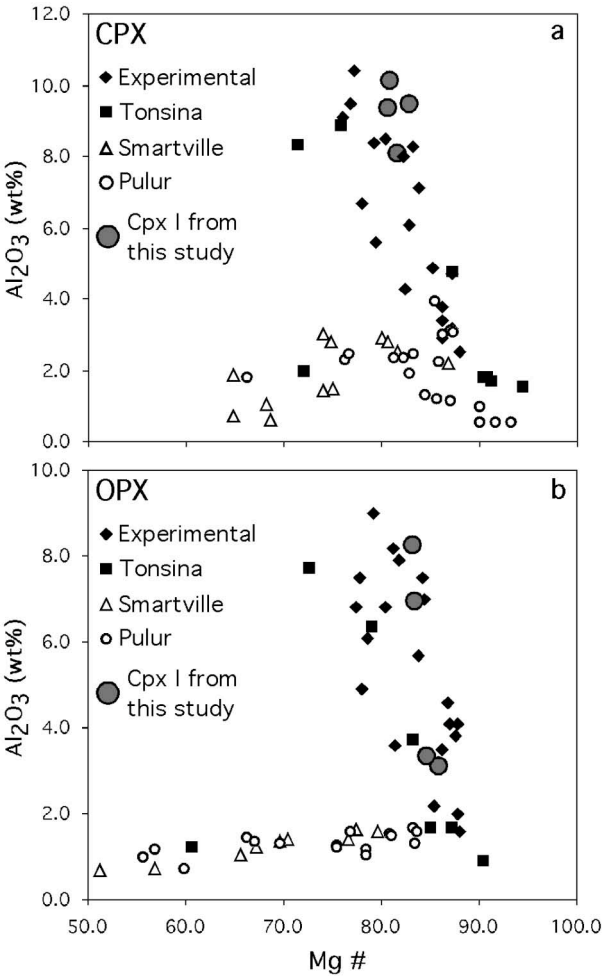


Fig. 10 (a) Al_2O_3 contents versus X_{Mg} in clinopyroxene of the websterite xenoliths from the Chyulu Hills. (b) Al_2O_3 contents versus X_{Mg} in orthopyroxene of the websterite xenoliths from the Chyulu Hills. Also shown are data from experimental igneous pyroxenites at 1.2 GPa (Müntener et al. 2001) and from arc cumulates: Tonsina (DeBari and Coleman 1989), Smartville (Beard and Day 1988), and Pulur (Topuz et al. 2004).

seems unlikely. Firstly, the chemical characteristics of websterite and granulite xenoliths are more in line with arc cumulates. Secondly, textures and mineral compositions / zoning patterns suggest that at least the websterites were hot at depth, whereas there is no evidence that they have undergone earlier cooling. Thirdly, almost no eclogite xenoliths are found as xenoliths in the Chyulu Hills, which would be expected in a classical subduction scenario.

We believe that the most viable model to account for the observed textures, mineral compositions and bulk rock chemistry is a model where granulites and websterites represent crustal plagioclase-bearing mafic cumulates that were carried to depth (granulites to a lesser degree) while cooling from igneous temperatures. Convective instability of dense hot ultramafic-mafic lower crust is in principle possible in regions of elevated heatflow such as arcs (Jull and Kelemen 2001). Such a process is currently being observed beneath the Sierra Nevada. There, evidence from volcanic rocks indicates that mantle sources have changed from eclogite-facies garnet pyroxenite to spinel peridotite (e.g. Farmer et al. 2002; Zandt 2003). Xenolith (e.g. Ducea & Saleeby 1996) and seismic evidence (Boyd et al. 2004, Zandt et al. 2004) suggest that mafic lower crust is dragged into the mantle down to at least 70 km in the central / southern Sierra Nevada, while in adjacent areas (eastern Sierra Nevada) the crust is only about 35 km thick and hot peridotite is found at shallow levels. In these areas, the Sierra Nevada has lost about half of its original crust due to convective removal of dense garnet-bearing lowermost crustal rocks (e.g. Ducea & Saleeby 1996, Lee et al. 2001).

Conclusions

Major and trace element data on aluminous websterite and granulite xenoliths from the Chyulu Hills volcanic field, Kenya, suggest that these rocks were formed in a Pan-African arc environment. Textures, metamorphic reactions and P-T estimates for the granulite xenoliths are in line with subsolidus cooling accompanied or followed by compression. In order to reconcile apparently contradictory features of the websterite xenoliths, e.g. high P-T near-igneous major element composition of pyroxenes versus positive bulk rock and mineral Eu anomalies suggesting shallow-level plagioclase accumulation, it is necessary to invoke a model that accounts for down-dragging of hot crustal material into the mantle. The protoliths of the websterite and granulite xenoliths from the Chyulu Hills could thus have been part of a dense Pan-African lithospheric arc root that started to founder into the mantle when subduction ceased after closure of the Mozambique ocean.

Acknowledgements

We would like to thank Rainer Altherr and Othmar Müntener for fruitful discussions and for help in improving the first version of this manuscript (RA). Thanks also go to Hans-Peter Meyer and Edwin Gnos for assistance with electron microprobe analysis, to Vincent Serneels for providing XRF analyses and to Hans-Michael Seitz for preparing the glass pills. Permission and help for field sampling provided by the Office of the President, Kenya Wildlife Service, and the Kenya Agricultural Research Institute in Kiboko are gratefully acknowledged. This research was supported by the Swiss National Science Foundation grant 200021-100647/1.

References

Al-Mishwat AT, Nasir SJ (2004) Composition of the lower crust of the Arabian plate: a xenolith perspective. Lithos 72:45-72

Altherr R, Garasic V, Ulianov A, Kalt A (2005) Composition and thermal evolution of the lithospheric mantle beneath the Chyulu Hills (southern Kenya) as deduced from xenoliths. J Petrol, *to be submitted*

Baker BH, Williams LAJ, Miller JA, Fitch FJ (1971) Sequence and geochronology of the Kenya rift volcanics. Tectonophysics 11:191-215

Bartels KS, Kinzler RJ, Grove TL (1991) High pressure phase relations of primitive high-alumina basalts from Medicine Lake volcano, northern California. Contrib Mineral Petrol 108:253-270

Beard JS, Day HW (1988) Petrology and emplacement of reversely zoned gabbro-diorite plutons in the Smartville complex, Northern California. J Petrol 29:965-995

Bindeman IL, Davis AM, Drake MJ (1998) Ion microprobe study of plagioclase-basalt partition experiments at natural concentration levels of trace elements. Geochim Cosmochim Acta 62:1175-1193

Boyd OS, Craig HJ, Sheehan AF (2004) Foundring lithosphere imaged beneath the southern Sierra Nevada. Science 305:660-662

Burg JP, Bodinier JL, Chaudhry S, Hussain S, Dawood, H (1998) Infra-arc mantle-crust transition and intra-arc mantle diapirs in the Kohistan Complex (Pakistani Himalaya): petro-structural evidence. Terra Nova 10:74-80

Burns LE (1985) The Border Ranges ultramafic and mafic complex, south-central Alaska: cumulate fractionates of island-arc volcanics. Can J Earth Sci 22:1020-1038

Cesare B, Rubatto D, Hermann J, Barzi L (2002) Evidence for Late Carboniferous subduction-type magmatism in mafic-ultramafic cumulates of the SW Tauern window (Eastern Alps). Contrib Mineral Petrol 142:449-464

Claeson DT, Meurer WP (2004) Fractional crystallization of hydrous basaltic "arc-type" magmas and the formation of amphibole-bearing gabbroic cumulates. Contrib Mineral Petrol 147:288-304

Conrad WK, Kay RW (1984) Ultramafic and mafic inclusions from Adak island: crystallization history, and implications for the nature of primary magmas and crustal evolution in the Aleutian arc. J Petrol 25:88-125

Coolen JJMMM, Priem HNA, Verdurmen EAT, Verschure RH (1982) Possible zircon U-Pb evidence for Pan-African granulite-phacies metamorphism in the Mozambique Belt of southern Tanzania. Precambrian Res 17:31-40

Dawson JB, Smith JV, Steele IM (1995) Petrology and mineral chamistry of the plutonic igneous xenoliths from the carbonatite volcano Oldoinyo lengai, Tanzania. J Petrol 36:797-826

DeBari SM, Mahlburg Kay S, Kay RW (1987) Ultramafic xenoliths from Adagdak volcano, Adak, Aleutian Islands, Alaska: deformed igneous cumulates from the MOHO of an island arc. J Geol 95:329-341

DeBari SM, Coleman RG (1989) Examination of the deep levels of an island arc: evidence from the Tonsina ultramafic-mafic assem-

blage, Tonsina, Alaska. J Geophys Res 94:4373-4391

DeLong SE, Hodges FN, Arculus RJ (1975) Ultramafic and mafic inclusions, Kanaga Island, Alaska, and the occurrence of alkaline rocks in island arcs. J Geol 83:721-736

Dessai AG, Markwick A, Vaselli O, Downes H (2004) granulite and pyroxenite xenoliths from the Deccan Trap: insight into the nature and composition of the lower lithosphere beneath cratonic India. Lithos 78:263-290

Draper DS, Johnston AD (1992) Anhydrous PT phase relations of Aleutian high MgO-basalt: an investigation of the role of olivine-liquid reaction in the generation of arc high-alumina basalts. Contrib Mineral Petrol 112:501-519

Ducea MN (2001) The California arc: thick granitic batholiths, eclogitic residues, lithospheric-scale thrusting, and magmatic flare-ups. GSA Today 11:4-10

Ducea MN (2002) Constraints on the bulk composition and root foundering rates of continental arcs: a California perspective. J Geophys Res 107: B11, 2304, doi: 10.1029/2001JB000643

Ducea MN, Saleeby JB (1996) Buoyancy sources for a large unrooted mountain range, the Sierra Nevada, California: Evidence from xenolith thermobarometry. J Geophys Res 101:8229-8244

Dunn T, Senn C (1994) Mineral / matrix partition coefficients for orthipyroxene, plagioclase and olivine in basaltic to andesitic systems: a combined analytical and experimental study. Geochim Cosmochim Acta 58:717-733

Elthon D, Scarfe CM (1984) High-pressure phase equilibria of a high-magnesia basalt and the genesis of primary oceanic basalts. Am Mineral 69:1-15

Embey-Isztin A, Downes H, Kempton PD (2003) Lower cerustal granulite xenoliths from the Pannonian Basin, Hungary. Part I: mineral chemistry, thermobarometry and petrology. Contrib Mineral Petrol 144: 652-670

Findlay DC (1969) Origin of the Tulameen ultramafic-gabbro complex, southern British Columbia. Can J Earth Sci 6:219-232

Gaetani GA, Grove TL (1998) The influence of water on melting mantle peridotite. Contrib Mineral Petrol 131:323-346

Gaetani GA, Grove TL, Bryan WB (1993) The influence of water on the petrogenesis of subduction-related igneous rocks. Nature 365:332-334

Girardeau J, Ibarguchi JIL (1991) Pyroxenite-rich paridotites of the Cabo Ortegal Complex (northwestern Spain): Evidence for large-scale upper mantle heterogeneiity. J Petrol Special Lherzolite Issue: 135-154

Grove TL, Elkins-Tanton LT, Parman SW, Chatterjee N, Müntener O, Gaetani GA (2003) Fractional crystallization and mantle-melting controls on calc-alkaline differentiation trends. Contrib Mineral Petrol 145:515-533

Günther D, Frischknecht R, Heinrich CA (1997) Capabilities of a 193 nm ArF excimer laser for LA-ICPMS micro analysis of geological materials. J Anal At Spectrom 12:939-944

Haug GH, Strecker MR (1995) Volcano-tectonic evolution of the Chyulu Hills and implication for the regional stress field in Kenya. Geology 23:165-168

Heinrich CA, Pettke T, Halter WE, Aigner-Torres M, Audétat A, Günther D, Hattendorf B,

Bleiner D, Guillong M, Horn I (2003) Quantitative multi-element analysis of minerals, fluid and melt inclusions by laser-ablation inductively-coupled-plasma mass-spectrometry, Geochim Cosmochim Acta 67:3473-3496

Henjes-Kunst F, Altherr R (1992) Metamorphic petrology of xenoliths from Kenya and Northern Tanzania and implications for geotherms and lithospheric structure. J Petrol 33:1125-1156

Hermann J, Müntener O, Günter D (2001) Differentiation of mafic magma in a continental crust-to-mantle transition zone. J Petrol 42:189-206

Himmelberg GR, Loney RA (1995) Characteristics and petrogenesis of Alaskan-type ultramafic-mafic intrusions, southeastern Alaska. US Geol Surv Prof Pap 1564: 47 p

Holloway JR, Burnham CW (1972) Melting relations of basalt with equilibrium water pressure less than total pressure. J Petrol 13: 1-29

Holmes A (1951) The sequence of Pre-Cambrian orogenic belts in south and central Africa. In: Sandford KS, Blondel F (Eds), 18th International Geological Congress. Association of African Geological Surveys, London, pp 254-269

Irvine TN (1974) Petrology of the Dyke Island ultramafic complex, southeastern Alaska. Geol Soc Am Memoir 138: 240 p

Jan MQ, Howie RA (1981) The mineralogy and geochemistry of the metamorphosed basic and ultrabasic rocks of the Jijal Complex, Kohistan, NW Pakistan: J Petrol 22:85-126

Jan MQ, Windley BF (1990) Chromian spinel-silicate chemistry in ultramafic rocks of the Jijal Complex, Northwest Pakistan. J Petrol 31:667-715

Johnston AD (1986) Anhydrous P-T relations of near-primary high-alumina basalt from the South Sandwich Islands. Contrib Mineral Petrol 92:368-382

Jull M, Kelemen PB (2001) On the conditions of lower crustal convective instability. J Geophys Res 106:6423-6446

Kempton PD, Downes H, Neymark LA, Wartho JA, Zartman RE, Sharkov EV (2001) Garnet granulite xenoliths from the Northern Baltic Shield - the underplated lower crust of a palaeoproterozoic large igneous province. J Petrol 42:731-763

Khan MA, Jan MQ, Weaver BL (1993) Evolution of the lower arc crust in Kohistan, N. Pakistan: temporal arc magmatism through early, mature and intra-arc rift stages. In: Treloar PJ, Searle MP (Eds), Himalayan Tectonics. Geol Soc Lond Spec Publ 74:123-138

Kornprobst J, Piboule M, Roden M, Tabit A (1990) Corundum-bearing garnet clinopyroxenites at Beni Bousera (Morocco): Original plagioclase-rich gabbros recrystallized at depth within the mantle? J Petrol 31:717-745

Kretz R (1983) Symbols for rock-forming minerals. Am Mineral 68:277-279

Kröner A, Greiling R, Reischmann T, Hussein IM, Stern RJ, Dürr S, Krüger J, Zimmer M (1987). Pan-African crustal evolution in the Nubian segment of northeast Africa. In: Kröner A (Ed) Proterozoic Lithospheric Evolution. American Geophysical Union, Washington, DC, Geodynamic Series 17:235-257

Kröner A, Muhongo S, Hegner E, Wingate MTD (2003) Single zircon geochronology and Nd

isotopic systematics of Proterozoic high-grade rocks from the Mozambique belt of southern Tanzania (Masasi area): implications for Gondwana assembly. J Geol Soc, London 160:745-758

LeBas MJ (1962) The role of aluminium in igneaous clinopyroxenes with relation to their parentage. Amer J Sci 260:267-288

Lee CT, Rudnick RL, Brimhall GH (2001) Deep lithospheric dynamics beneath the Sierra Nevada during the Mesozoic and Cenozoic as inferred from xenolith petrology. Geochem Geophys Geosys 2: 2001GC000152

Leyreloup A, Bodiner JL, Dupuy C, Dostal J (1982) Petrology and geochemistry of granulite xenoliths from Central Hoggar (Algeria) – implications for the lower crust. Contrib Mineral Petrol 79:68-75

Liu IC, Presnall DC (1990) Liquidus phase relations in the join anorthite-forsterite-quartz at 20 kbar with applications to basalt petrogenesis and igneous sapphirine. Contrib Mineral Petrol 104:735-742

Liu IC, Presnall DC (2000) Liquidus phase relations in the system CaO-MgO-Al_2O_3-SiO_2 at 2.0 GPa: applications to basalt fractionation, eclogites and igneous sapphirine. J Petrol 41:3-20

Loucks RR (1990) Discrimination of ophiolitic from nonophiolitic ultramafic-mafic allochthons in orogenic belts by the Al/Ti ratio in clinopyroxene. Geology 18:346-349

McGuire AV, Stern RJ (1993) Granulite xenoliths from western Saudi Arabia: the lower crust of the late Precambrian Arabian-Nubian Shield. Contrib Mineral Petrol 114:395-408

Meert JG (2003) A synopsis of events related to the assembly of eastern Gondwana. Tectonophysics 362:1-40

Möller A, Mezger K, Schenk V (1998) Crustal age domains and the evolution of the continental crust in the Mozambique Belt of Tanzania: Combined Sm-Nd, Rb-Sr and Pb-Pb isotopic evidence. J Petrol 39:749-783

Möller A, Mezger K, Schenk V (2000) U-Pb dating of metamorphic minerals: Pan-African metamorphism and prolonged slow cooling of high pressure granulites in Tanzania, East Africa. Precambrian Res 104:123-146

Montanini A, Tribuzio R (1996) Gabbro-derived granulites from the northern Appenines (Italy): evidence for lower-crustal emplacement of tholeiitic liquids in Post-Variscan Times. J Petrol 42:2259-2277

Moore G, Carmichael ISE (1998) The hydrous phase equilibria (to 3 kbar) of an andesite and basaltic andesite from western Mexico: constraints on water content and conditions of phenocryst growth. Contrib Mineral Petrol 130:304-319

Morishita T, Arai S, Gervilla F, Green D (2003) Closed-system geochemical recycling of crustal materials in alpine-type peridotite. Geochim Cosmochim Acta 67:303-310

Morishita T, Arai S, Green D (2004) Possible non-melted remnants of subducted lithosphere: experimental and geochemical evidence from corundum-bearing mafic rocks in the Horoman Peridotite Complex, Japan. J Petrol 45:235-252

Müntener O, Kelemen PB, Grove TL (2001) The role of H_2O during crystallization of primitive arc magmas under uppermost mantle condi-

tions and genesis of igneous pyroxenites: an experimental study. Contrib Mineral Petrol 141:643-658

Mukhopadhyay B, Manton WI (1994) Upper-mantle fragments from beneath the Sierra Nevada Batholith: partiel fusion, fractional crystallization, and metasomatism in a subduction-related ancient lithosphere. J Petrol 35:1417-1450

Muhongo SM, Kröner A, Nemchin AA (2001) Zircon ages from granulite facies rocks in the Mozambique belt of Tanzania and implications for Gondwana assembly. J Geol 109:171-189

Muhongo SM, Lenoir J-L (1994) Pan-African granulite facies metamorphism in the Mozambique belt of Tanzania: U-Pb zircon geochronology. J Geol Soc London 151:343-347

Nasir S (1995) Mafic lower crustal xenoliths from the northwestern part of the Arabian Plate. Eur J Mineral 7:217-230

Novak O, Prodehl C, Jacob AWB, Okoth W (1997a) Crustal structure of the southern flank of the Kenya rift deduced from wide-angle P-wawe data. Tectonophysics 278:171-186

Novak O, Ritter JRR, Altherr R, Garasic V, Volker F, Kluge C, Kaspar T, Byrne GF, Sobolev SV, Fuchs K (1997b) An integrated model for the deep structure of the Chyulu Hills volcanic field, Kenya. Tectonophysics 278:187-209

Omenge JM, Okelo RE (1992) Geology of the Chyulu-Oloitokitok area. Kenya Mines and Geology Department, Nairobi, Rep 112, 51 pp

Panjasawatwong Y, Danyushevsky LV, Crawford AJ, Harris KL (1995) An experimental study of the effects on melt composition on plagioclase-melt equilibria at 5 and 10 kilobar: implications for the origin of magmatic high-An plagioclase. Contrib Mineral Petrol 118:420-432

Ritter JRR, Kaspar T (1997) A tomography study of the Chyulu Hills, Kenya. Tectonophysics 278:149-169

Ruckmick JC, Noble JA (1959) Origin of the ultramafic complex at Union Bay, southeastern Alaska. Geol Soc Am Bull 70:981-1018

Saggerson EP (1963) Geology of the Simba-Kibwezi area. Geological survey of Kenya, Rep 58, 70 pp

Sisson TW, Grove TL (1993) Experimental investigations of the role of H_2O in calc-alkaline differentiation and subduction zone magmatism. Contrib Mineral Petrol 113:143-166

Spandler CJ, Arculus RJ, Eggins SM, Mavrogenes J, Price RC, Reay AJ (2003) Petrogenesis of the Greenhills Complex, Southland, New Zealand: magmatic differentiation and cumulate formation at the roots of a Permian island-arc volcano. Contrib Mineral Petrol 144:703-721

Späth A, Le Roex AP, Opiyo-Akech N (2001) Plume-lithosphere interaction and the origin of continental rift-related alkaline volcanism – the Chyulu Hills Volcanic field, Southern Kenya. J Petrol 42:765-787

Stern RJ, Dawoud AS (1991) Late Precambrian (740 Ma) charnockite, enderbite, and granite from Jebel Moya, Sudan: a link between the Mozambique Belt and the Arabian-Nubian Schield? J Geol 99:648-659

Sun SS, McDonough WF (1989) Chemical and isotopic systematics of oceanic basalts: implications for mantle composition and processes. In: Saunders AD, Norry MJ (Eds) Magmatism in ocean basins. Geol Soc Spec Publ 42:313-345

Sutherland FL, Hollis JD, Birch WD, Pogson RE, Raynor LR (2004) Cumulate-rich xenolith suite in Late Cenozoic basaltic eruptives, Hepburn Lagoon, newlyn, in relation to western Victorian lithosphere. Austral J Earth Sci 51:319-337

Takazawa E, Frey EA, Shimizu N, Saal A, Obata M (1999) Polybaric petrogenesis of mafic layers in the Horoman peridotite complex, Japan. J Petrol 40:1827-1851

Tatsumi Y, Eggins SM (1995) Subduction zone magmatism. Blackwell, Oxford: 211 p

Tenthorey EA, Ryan JC, Snow EA (1996) Petrogenesis of sapphirine-bearing metatroctolites from the Buck Creek ultramafic body, southern Appalachian. J Metamorph Geol 14:103-114

Topuz G, Altherr R, Schwarz WH, Meyer HP, Eyüboglu Y, Sen C (2004) Ultramafic-mafic intrusions of the Pulur region (NE Turkey): products of shallow-level differentiation and cumulate formation beneath a late Liassic continental arc. Lithos, *submitted*

Ulianov A, Kalt A (2005) Metamorphism of Mg-Al sapphirine- and Ca-Al hibonite-bearing granulite xenoliths from the Chyulu Hills volcanic field, Kenya. J Petrol, *submitted*

Ulianov A, Kalt A, Pettke T (2005) Hibonite, $Ca(Al,Cr,Ti,Si,Mg,Fe^{2+})_{12}O_{19}$, and its mineral assemblage in Ca-Al meta-igneous granulite xenoliths from the Chyulu Hills volcanic field, Kenya. Eur J Mineral 17: 357-366

Upton BGJ, Aspen P, Hinton RW (2001) Pyroxenite and granulite xenoliths from beneath the Scottish Northern Highlands Terrane: evidence for lower-crust/upper mantle relationships. Contrib Mineral Petrol 142:178-197

Weber MBI, Tarney J, Kempton PD, Kent RW (2002) Crustal make-up of the northern Andes: evidence based on deep crustal xenolith suites, Mercaderes, SW Colombia. Tectonophys 345:49-82

Williams LAJ (1970) The volcanics of the Gregory Rift Valley, East Africa. Bull Vol 34:439-465

Zandt G, Gilbert H, Owens TJ, Ducea M, Saleeby J, Jones CH (2004) Active foundering of a continental arc root beneath the southern Sierra Nevada in California. Nature 431:41-46

CHAPTER III

Mg-Al sapphirine- and Ca-Al hibonite-bearing granulite xenoliths from the Chyulu Hills volcanic field, Kenya

A. Ulianov*, A. Kalt

University of Neuchâtel, Institute of Geology, Rue Emile-Argand 11, CH-2007 Neuchâtel, Switzerland

*Corresponding author:
alexey.ulyanov@unine.ch

submitted to **Journal of Petrology**

returned to **Journal of Petrology**
after a moderate revision

CHAPTER III

ABSTRACT

Basanites of the Chyulu Hills (Kenya Rift) bear mafic Mg-Al and Ca-Al granulite xenoliths. A recent geochemical study showed that together with garnet-spinel websterites, those xenoliths most likely represent cumulates from magmas formed in a subduction-related tectonic setting. The granulite protoliths were plagioclase-dominated troctolitic cumulates, but the original mineral assemblages were almost completely transformed by subsolidus reactions. Mg-Al granulites contain the minerals spinel, sapphirine, sillimanite, plagioclase, corundum, clinopyroxene, orthopyroxene and garnet, while Ca-Al granulites are characterized by hibonite, spinel, sapphirine, mullite, sillimanite, plagioclase, quartz, clinopyroxene, corundum, and garnet. In the Mg-Al granulites, the first generation of orthopyroxene and some spinel may be of igneous origin. In the Ca-Al granulites, hibonite (and eventually some spinel) are the earliest mineral in the crystallization sequence and may represent igneous relicts. Most pyroxene and spinel as well as corundum in both Mg-Al and Ca-Al granulites formed by subsolidus reactions. The qualitative *P-T* path derived from metamorphic reactions corresponds to subsolidus cooling accompanied or followed by compression. Final equilibration was achieved at $T \approx$ 600-740 °C and $P <$ 8 kbar, the pressure range being constrained by the stability of sillimanite. The early coexistence of corundum and pyroxenes (± spinel) as well as the association of sillimanite and sapphirine with clinopyroxene and the occurrence of hibonite makes both types of the studied granulite lithologies rare. The Ca-Al hibonite-bearing granulites are unique. Both types enlarge the spectrum of known Ca-Al-Mg-rich granulites worldwide.

INTRODUCTION

The study of granulites provides important constraints on the nature of high-temperature to ultra-high-temperature metamorphism in the Earth's crust. On the one hand, the chemical and isotopic compositions of granulites are useful tools for deciphering their origin and geodynamic setting (e.g. Jan & Howie, 1981; Downes, 1993; Kempton *et al*., 2001). On the other hand, reaction textures and the *P-T* paths of granulites serve to unravel metamorphic processes and their causes (e.g. Bohlen, 1987, 1991; Harley, 1989; Kriegsman & Schumacher, 1999; Rickers *et al*., 2001). The study of granulites from metamorphic terranes often benefits from the incorporation of both approaches (e.g. Osanai *et al*., 1998; Möller *et al*., 1998; Bhattacharya & Kar, 2002). Granulites are also a major tool for investigating the composition of the Earth's lower crust. Granulite xenoliths from volcanic rocks are traditionally considered in this context (e.g. Rudnick *et al*., 1986; Rudnick, 1992; Downes, 1993; Huang *et al*., 1995; Kempton *et al*., 2001), with far less attention being paid to their metamorphic reaction paths (Christy, 1989; Dawson *et al*., 1997). The overwhelming dominance of the geochemical approach to the study of granulitic xenoliths is partly justified, as a given section of the Earth's middle to lower crust, sampled by an ascending magma, may include rocks of different provenance, age and metamorphic evolution, juxtaposed by various tectonic processes (e.g. Downes *et al*., 1990; Kempton *et al*., 1990).

The studied granulite xenoliths from the Chyulu Hills, East African Rift, can yield informa-

tion on both issues, the chemical composition of the Earth's lower crust, in this case beneath the East African Rift, and the nature and conditions of metamorphic processes that affected it. Recent major and trace element studies on minerals and whole rock samples have shown that Mg-Al granulite, Ca-Al granulite and garnet-spinel websterite xenoliths of the Chyulu Hills represent a series of gabbroic to troctolitic cumulates related to arc magmatism (Ulianov *et al.*, submitted; see 'General chemical and petrographic features'). Combined with similarities to certain granulite terranes in Tanzania (see discussion) this geochemical signature suggests the xenoliths and hence the crust and upper mantle beneath the Chyulu Hills to be of Pan-African age.

The igneous minerals in the Mg-Al and Ca-Al granulite xenoliths have to a large degree been replaced by subsolidus assemblages that provide important information on the *P-T* path and on phase relations in mafic Ca-Mg-Al rich bulk compositions. Meta-igneous granulitic rocks rich in Mg, Al and Ca are rare. They tend to crystallize sapphirine and clinopyroxene and apparently represent a special paragenetic family of granulites that was recognized by Christy (1989). It includes xenoliths from Stockdale (Meyer & Brookins, 1976), Delegate (Griffin & O'Reilly, 1986) and the Kerguelen Archipelago (Grégoire *et al.*, 1998) and granulites from the metamorphic terranes of Finero (Lensch, 1971; Sills *et al.*, 1983), Roan (Johansson & Möller, 1986), Dunkelsteinerwald (Carswell *et al.*, 1989), Central Gneiss Belt of Grenville (Grant, 1989), Ullared-Gällared (Möller, 1999) and several other, less well-characterized terranes.

The purpose of this paper is (1) to contribute to the general understanding of mineral assemblages and reactions in Ca-Mg-Al-rich mafic igneous protoliths under granulite-facies conditions and (2) to decipher the reaction paths of the studied granulites and discuss their possible geologic significance. For this purpose, mineral assemblages, mineral compositions and reaction sequences are carefully described, *P-T* conditions are quantified when possible, and a qualitative *P-T* path is inferred.

GEOLOGICAL SETTING

The Chyulu Hills volcanic field is situated on the eastern flank of the Kenya rift some 150-200 km east of the rift axis, about 50 km northeast of Mt. Kilimanjaro (Fig. 1). It consists of several hundred volcanic cones and lava flows forming a NW-SE aligned chain ~100 km long. For the last decade, the Chyulus have been subject to a number of detailed petrological (focused on xenoliths and alkaline volcanics) and geophysical (gravity and seismological) studies (e.g. Henjes-Kunst & Altherr, 1992; Ritter & Kaspar, 1997; Novak *et al.*, 1997; Späth *et al.*, 2001). The seismic Moho has been detected at a depth of 44 km (the divide is not sharp) with a thickness of 20 km for the lower crust (Ritter & Kaspar, 1997). The lithosphere-asthenosphere boundary lies at ~107-120 km depth as suggested by the geobarometric estimates for high-P porphyroclastic garnet lherzolite xenoliths from the Chyulu volcanics (Henjes-Kunst & Altherr, 1992; Altherr *et al.*, submitted).

Volcanic activity within the Chyulu Hills is very young. The compositional spectrum of rocks ranges from foidites through less silica-undersaturated basanites to fractionated alkali ba-

salts (Haug & Strecker, 1995; Späth *et al*., 2001). Foidites are the oldest (1.4 Ma), whereas some of the alkali basalts were erupted in Historical times (Haug & Strecker, 1995). The xenoliths used for this study were sampled from basanites of the Kwa Nthuku volcano in the northwestern part of the Chyulu Hills. Despite its young volcanicity, there are no indications for a recent asthenospheric upwelling or upwarping of the MOHO beneath the Chyulu Hills volcanic field (Ritter & Kaspar, 1997; Novak *et al*., 1997).

The Chyulu Hills are located within the Pan-African Mozambique mobile belt. (Holmes, 1951) which extends from the Arabian-Nubian Shield in the north via Ethiopia, Uganda, Kenya and Tanzania to Mozambique, Malawi and Madagascar in the south. The belt is now shown to include several metamorphic domains with different ages and *P-T* histories (e.g. Shackleton, 1973; Key *et al*. 1989; Stern & Dawoud 1991; Pinna *et al*., 1993; Appel *et al*., 1998; Möller *et al*., 1998 and references therein). It results from a complex series of subduction, collision and accretion events between approximately 750 and 615 Ma (e.g. Coolen *et al*., 1982; Kröner et al., 1987; Stern & Dawoud 1991; Muhongo & Lenoir, 1994; Möller *et al*., 1998, 2000, Muhongo *et al*., 2001; Kröner *et al*., 2003; Meert, 2003), related to the closure of the Mozambique ocean. The younger events within this time span are commonly termed 'Pan-African' (e.g. Möller *et al*., 2000) while the older ones are often related to an 'East African orogen' (e.g. Stern, 1994; Meert, 2003). The older history of the Mozambique belt seems to vary with geographic position. Magmatic and metamorphic events have been dated at at 800-820 Ma (e.g. Key *et al*. 1989; Kebede *et al*. 2001), at approximately 1000-1250 Ma

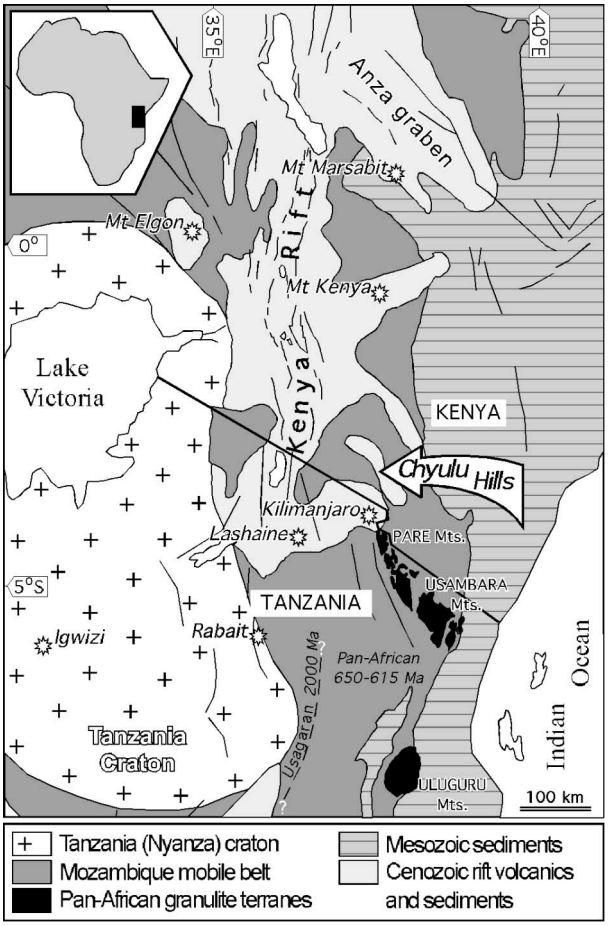


Fig. 1. Generalized geological map of Kenya, northern Tanzania, and parts of Uganda and Ethiopia showing the principal tectonic units and the location of the Chyulu Hills volcanic field. The outcropping granulite terranes of NW Tanzania are after Möller et al. (2000) and the distribution of Cenozoic volcanic and sedimentary rocks in the region is after Williams (1970) and Baker *et al*. (1971).

(e.g. Pinna *et al*. 1993; Kröner *et al*., 1997; Evans *et al*., 1999), at around 2000 Ma (e.g. Möller *et al*., 1995; Möller *et al*., 1998) and in the Archean (Bell & Dodson, 1981; Cahen *et al*., 1984; Muhongo *et al*., 2001).

Lithologically, the Mozambique belt is dominated by amphibolite-facies and lower grade metamorphic rocks and granitoids, but it also contains numerous granulite complexes. Together with the igneous complexes, the latter were the focus of most of the geochronological studies cited above and the subject of extensive petrological and

geochemical investigations (e.g. Maaskant *et al.*, 1980; Sandiford *et al.*, 1987; Gichile, 1992; Pinna *et al.* 1993; Möller *et al.*, 1995, 2000; Appel *et al.*, 1998). Therefore, the outcropping granulites play a major role in reconstructing Proterozoic metamorphic and geodynamic processes in the Mozambique belt. In contrast, few data are available on granulite xenoliths in volcanic edifices situated within the Mozambique belt of East Africa. They were described from Neogene volcanics of the Lashaine volcano in northern Tanzania (Dawson, 1977; Jones *et al.*, 1983). As is the case with the granulite xenoliths of this study, those of Lashaine represent relics of an igneous suite metamorphosed into granulite (Jones *et al.*, 1983), but with a different chemical and mineralogical composition compared to the Chyulu xenoliths.

The local basement consists of hornblende and hornblende-biotite gneisses, migmatized and granitoid gneisses and subordinate garnet amphibolites and marbles (Saggerson, 1963; Omenge & Okelo, 1992). Granulites are rare. They form thin bands in gneisses, few of which are traceable for great distances (Saggerson, 1963). The granulites are calc-silicate in composition and contain andesine plagioclase, pyroxene (especially clinopyroxene), scapolite, garnet, epidote and in some cases quartz. They are lithologically different from the granulite xenoliths sampled by the young basanitic magmas. Due to the lack of thermobarometric, isotopic and age data, both the outcropping basement granulites and the granulite xenoliths of the Chyulu Hills volcanic field cannot be *a priori* assigned to any of the above described granulite occurrences in East Africa.

ANALYTICAL TECHNIQUES

Mineral analyses were made on a CAMECA SX50 microprobe equipped with four wavelength-dispersive spectrometers at the Mineralogisch-Petrographisches Institut, University of Bern, and a CAMECA SX51 microprobe with five wavelength-dispersive spectrometers at the Mineralogisches Institut, University of Heidelberg. No systematic deviations were found in the control analyses performed on both machines. The microprobes were operated at a 15 kV accelerating voltage and a 20 nA beam current. The beam was focused to 1.5-2 μm for mafic phases, and to 5 or 10 μm – for plagioclase. PAP correction was applied to the raw data. Natural and synthetic oxide and silicate standards were used for calibration. For spinel, corundum, sillimanite and plagioclase, Fe^{3+} and Fe^{2+} were calculated from stoichiometry. For other minerals, all Fe was taken as FeO.

Whole rock major element abundances were determined on glass pills (for preparation technique, see Ulianov *et al.*, 2005) using a CAMECA SX50 microprobe at the Mineralogisch-Petrographisches Institut, University of Bern. The beam was rastered over an area of ~15×20 μm, operating conditions were the same as for minerals. Another set of analyses was obtained on fused discs using an XRF spectrometer Philips PW2400 at the Institut de Minéralogie et de Pétrographie, University of Fribourg. The results from both techniques appear consistent. In the following, we will use the microprobe measurements because of their slightly better totals. Cr, Ni, Sr and Ba were also determined by XRF at the University of Fribourg.

GENERAL CHEMICAL AND PETROGRAPHIC FEATURES

The major element compositions and C.I.P.W. norms of the studied granulite xenoliths are presented in Table 1. The rocks are slightly silica-undersaturated, rich in Al and relatively enriched in Ca. The overall high Mg# and very low abundances of HFSE and LREE (Ulianov *et al.*, submitted) suggest that the rocks represent a sequence of cumulates rather than crystallized melts. The C.I.P.W. normative compositions are dominated by plagioclase and olivine, with the normative 'troctolitic' component (*plagioclase* + *olivine*) ranging from 89.6 to 98.7 %. The high Ni and very low Ti abundances in the rocks accord well with a troctolitic mineralogy of the protoliths.

The cumulate sequence also includes websteritic lithologies finally equilibrated under mantle pressures and temperatures. They belong to the same major and trace element fractionation trend as the granulites, but are more magnesian and depleted in Si, Al, Ca and alkalies (Ulianov *et al.*, submitted). Low HSFE abundances, LILE enrichment and fractionation of LREE over HREE in websteritic and granulitic whole rock samples suggest that the protoliths may represent arc cumulates (Ulianov *et al.*, submitted). For the websterite xenoliths, there is an apparent contradiction between their ultramafic mineralogies and high pressures of final equilibration (14-23 kbar), on the one hand, and the positive Eu anomaly that suggests shallow-level plagioclase accumulation, on the other. This contradiction can be reconciled by a model of compression of a plagioclase-bearing protolith at near-igneous temperatures to mantle depth where plagioclase has reacted out (Ulianov *et al.,* submitted). This requires foundering of dense lower crustal material into the mantle, a process that is possible in areas with high geothermal gradients such as arcs (Jull and Kelemen 2001) and which is observed today in the southern Sierra Nevada (Ducea, 2001; Boyd *et al.*, 2004; Zandt *et al.*, 2004).

Table 1: Major element analyses (in wt%) of the studied xenoliths and their C.I.P.W. normative compositions

	1904-3	1904-7	1906-2	1904-9	1904-1
SiO_2	46.51	47.65	46.39	50.18	49.66
TiO_2	0.01	0.01	0.01	0.05	0.01
Al_2O_3	18.09	23.20	20.34	23.58	24.59
FeO_t	9.27	5.39	9.39	4.57	4.76
MnO	0.11	0.08	0.11	0.06	0.06
MgO	16.01	9.61	12.25	6.34	6.06
CaO	8.12	10.32	8.59	10.68	10.11
Na_2O	1.74	2.82	2.37	3.55	3.72
K_2O	0.10	0.19	0.10	0.25	0.20
P_2O_5	0.02	0.06	0.01	0.05	0.03
L.O.I.	0.11	0.41	0.12	0.43	0.28
Total	100.09	99.74	99.68	99.74	99.48
Mg#	75.5	76.1	69.9	71.2	69.4
Cr	87	65	919	238	102
Ni	445	367	374	209	271
Sr	357	872	332	733	657
Ba	102	627	60	1155	955
Quartz	no	no	no	no	no
Orthose	0.59	1.13	0.59	1.49	1.19
Albite	14.71	22.22	20.12	29.63	29.90
Anorthite	40.20	50.36	42.77	47.94	50.15
Corundum	0.37	no	0.71	no	no
Nepheline	no	0.96	no	0.31	0.97
Diopside (Wo)	no	0.36	no	2.15	0.11
Diopside (En)	no	0.24	no	1.32	0.07
Diopside (Fs)	no	0.10	no	0.70	0.04
Hypersthene (En)	6.95	no	1.69	no	no
Hypersthene (Fs)	2.98	no	0.96	no	no
Olivine (Fo)	23.16	16.77	20.35	10.25	10.64
Olivine (Fa)	10.98	7.71	12.77	6.00	6.84
Ilmenite	0.02	0.02	0.02	0.10	0.02
Apatite	0.04	0.13	0.02	0.11	0.07

Mg# = 100 × Mg/(Mg+Fe), all Fe as Fe^{2+}.

The mineral assemblage of the two studied Mg-Al sapphirine-bearing granulites (1904-3 and 1904-7) is spinel, sapphirine, sillimanite, plagioclase, ortho- and clinopyroxene, corundum, and garnet (Fig. 2a, b). The three studied Ca-Al hibonite-bearing granulites (1904-1, 1904-9, 1906-2) always show the assemblage spinel, sillimanite,

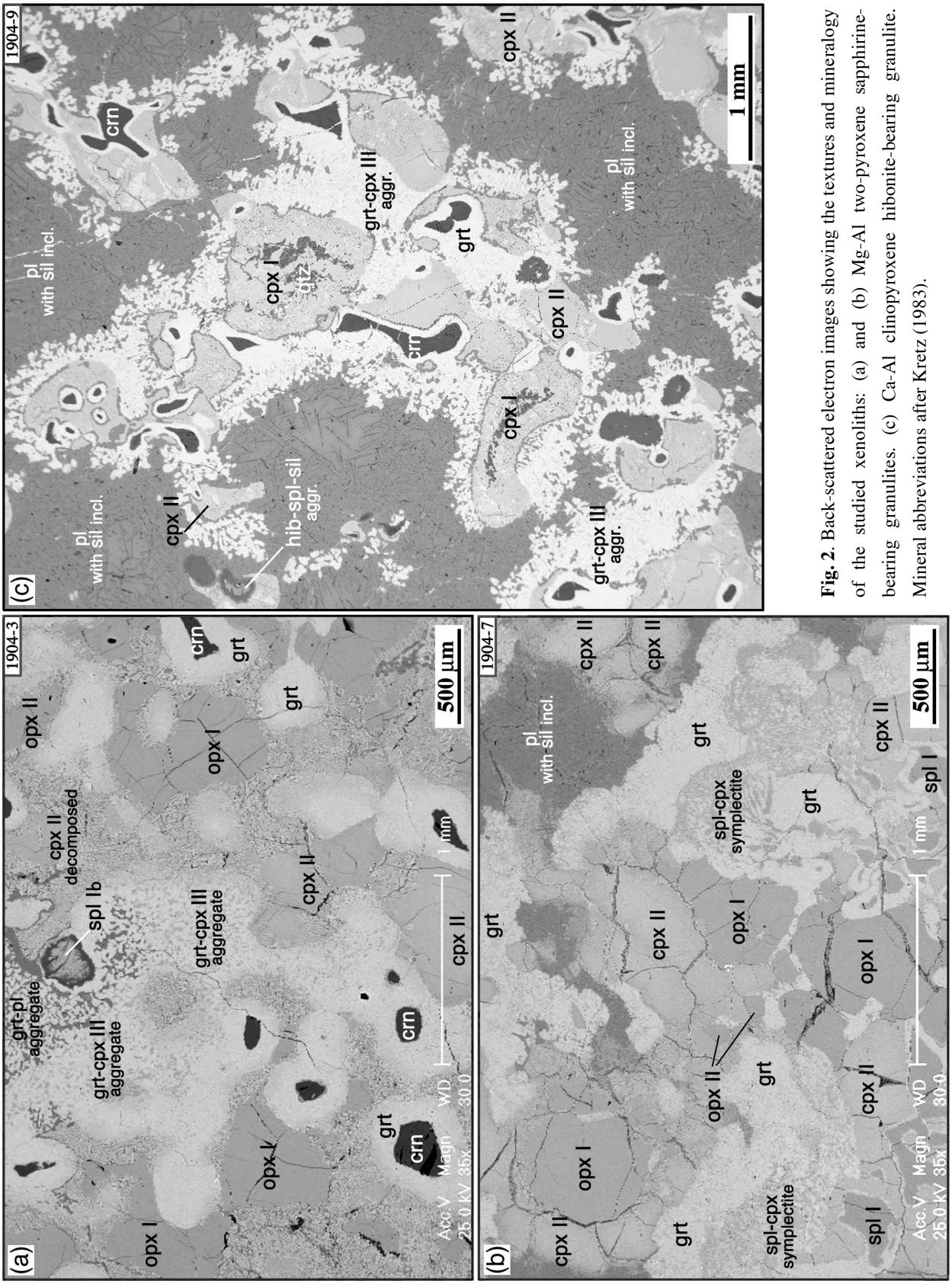


Fig. 2. Back-scattered electron images showing the textures and mineralogy of the studied xenoliths: (a) and (b) Mg-Al two-pyroxene sapphirine-bearing granulites. (c) Ca-Al clinopyroxene hibonite-bearing granulite. Mineral abbreviations after Kretz (1983).

clinopyroxene, quartz, plagioclase, corundum and garnet (Fig. 2c) but may additionally bear hibonite ($(Ca(Al,Cr,Ti,Si,Mg,Fe^{2+})_{12}O_{19}$, 1904-1, 1904-9), mullite (1904-9) and sapphirine (1904-1). Both rock types display a wealth of reaction textures.

Two out of five granulite xenoliths used in this study are banded, composed of layers of more mafic and more felsic granulite. Mafic and felsic layers bear the same minerals but their modes differ. We interpret this banding to be of magmatic origin as there are no indications of metamorphic differentiation processes or deformation (e.g. foliation) that could in principle also produce banding. Fabrics within the layers are isotropic and all of the reaction textures described in the section on textures and mineral compositions have developed in the absence of anisotropic stress.

The studied xenoliths are greatly affected by late-stage alteration. As a rule, garnet is replaced by kelyphite. The kelyphite is always extremely fine-grained. It consists of very Al-rich orthopyroxene, plagioclase and spinel. Clinopyroxene suffered incongruent melting and is often decomposed into a mixture of secondary diopside, plagioclase and quenched melt. Similar phenomena were described, e.g., in some lherzolite xenoliths from Hawaii (White, 1966), in garnet lherzolites from South African kimberlites (Carswell, 1975) and in a sapphirine-bearing granulite xenolith from the Delegate pipe in New South Wales, Australia (Griffin & O'Reilly, 1986). Most likely, these overprints are caused by fast heating and decompression in the host basanitic magma. Henceforth, we refer to the primary mineral compositions only (see Table 2 and 3).

TEXTURES AND MINERAL COMPOSITIONS

Mg-Al sapphirine-bearing granulites

The two studied Mg-Al sapphirine-bearing granulites (specimens 1904-3 and 1904-7) are petrographically similar to each other, although with distinctions. Xenolith 1904-3 is rather fine-grained, more mafic and appears mineralogically homogeneous. Xenolith 1904-7 is clearly banded, with more mafic (pyroxene-dominated) and more felsic (plagioclase-dominated) layers. Pyroxenes, plagioclase and garnet dominate, corundum and spinel are essential (5-15 vol.%), sapphirine is relatively rare. The rocks are characterized by various types of reaction domains:

(A) Worm-like clusters of clinopyroxene and corundum rimming and often completely replacing spinel (A1, Fig. 3a) and coarse-grained to worm-like aggregates of orthopyroxene, clinopyroxene and spinel often accompanied by corundum (A2, Fig. 3b and c);

(B) Sapphirine-sillimanite-garnet coronas on spinel (Fig. 3d and e);

(C) Garnet developed at the expense of all mafic phases and forming 'flaky' garnet-plagioclase and massive garnet-clinopyroxene aggregates after plagioclase (Fig. 2a and b and 3a-e);

(D) Clusters of Tschermak-rich clinopyroxene intergrown with sillimanite and embedded in plagioclase (Fig. 3f).

Orthopyroxene occurs in two generations. Opx I forms large, often elongated xenomorphic grains (Fig. 2a and b). It is exsolved and contains abundant microlamellae of clinopyroxene visible in high-magnification backscattered electron images only. In specimen 1904-7, Opx I is often deformed.

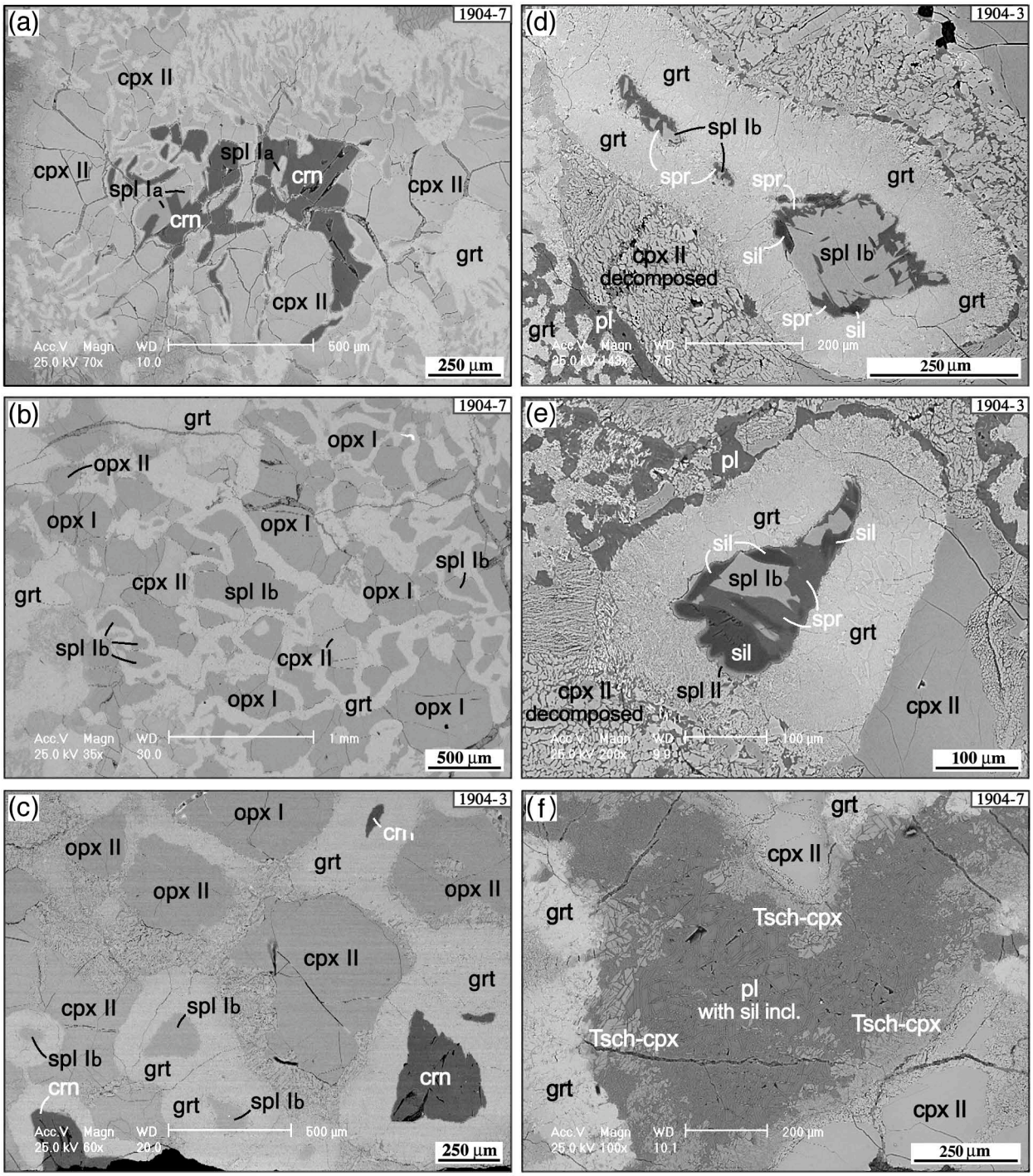


Fig. 3. Back-scattered electron images illustrating different generations of the major mineral phases and important reaction domains in Mg-Al granulites. (a) Spinel Ia partially replaced by corundum and clinopyroxene and resorbed by garnet (domain A1). (b) Coarse-grained symplectites of orthopyroxene, clinopyroxene and spinel resorbed by garnet (domain A2). (c) Coarse-grained aggregate of orthopyroxene, clinopyroxene, spinel and corundum resorbed by garnet (domain A2). (d and e) Sapphirine-sillimanite-garnet coronas around spinel I (domain B). (f) Clusters of Tschermak-rich clinopyroxene (domain D). [For further details, see text.]

It may show undulose extinction and sometimes initial recrystallization. Analyzed with a defocused beam, Opx I shows a pronounced decrease in Ca coupled with a moderate decrease in Al towards the rim (Fig 4a). The Mg# [= $Mg/(Mg+Fe_{tot})$] remains unchanged. Opx II occurs in two subtypes.

The first subtype is common in both specimens (Fig. 2a and b). It occurs as rather small, more or less isometric grains with no deformation, recrystallization or exsolution. The second one is found in specimen 1904-7 only. It forms aggregates of small strain-free grains apparently produced by recrystallization of Opx I. These aggregates may be rather large and are always corroded by thin rims of clinopyroxene. All transitions in the degree of exsolution from large exsolved grains of Opx I to relatively small exsolution-free grains of Opx II may be found. Opx II in specimen 1904-3 is nearly homogeneous in all elements (Fig. 4b). In specimen 1904-7, the Al content in Opx II either steadily increases from the core rimwards (Fig. 4c) or increases and then again decreases within the rim (Fig. 4e). The Ca content may slightly decrease rimwards (Fig. 4c). The Mg#'s of orthopyroxene range from 84.0 to 86.0. CaO in Opx I analyzed with a defocused beam reaches 1.2-1.5 wt%, whereas the CaO content in Opx II is much lower (0.16-0.24 wt%; Table 2).

Clinopyroxene forms two (1904-3) or three (1904-7) generations. The first generation is in equilibrium with Opx II and will therefore be further referred to as Cpx II (Fig. 2a and b). Cpx II grains occur as part of reaction domains A (Fig. 3a-c). They do not show any exsolution effects, with the larger grains showing chemically homogeneous cores. Towards the rim, an increase in Al and Na as well as Mg# and a decrease in Ca are observed (Fig. 4e and f). The zonation is systematic and regular in specimen 1904-3, where all grains of Cpx II display very similar profiles (Fig. 4e). In specimen 1904-7, however, the zonation is irregular (Fig. 4f). The rim contents of Al vary in a wide range from profile to profile. Cpx III occurs in reaction domains C (Fig. 2a) or as mantles on Opx II and is compositionally similar to the rims or intermediate zones of Cpx II grains (Table 2). Cpx IV is unusual. Found in specimen 1904-7 only, it forms part of reaction domains D (Fig. 3f). It is extremely rich in Tschermak components and has 18-23 wt% Al_2O_3 (Table 2). The Mg#'s of clinopyroxene range from 85.9 to 92.2. CaO ranges from 17.0 to 21.6 wt% (Table 2).

Spinel forms two textural generations. Spl I is common and occurs as large, more or less isometric grains in reaction domains A and B (Fig. 3a-c). Two subtypes of Spl I can be distinguished. Spl Ia is present in specimen 1904-7 only, where it forms individual grains enclosed in plagioclase and partially or completely replaced by clinopyroxene and corundum (reaction domain A1, Fig. 3a). It does not show any evidence for earlier coexistence with ortho- and clinopyroxene. Spl Ib is ubiquitous and occurs as part of reaction domains A2 (Spl + Opx + Cpx ± Crn, Fig. 3b and c) and B (Spl + Spr + Sil + Grt, Fig. 3d and e) in both specimens. Chemically, the two subtypes of spinel are not well distinguishable. Cr tends to concentrate in Spl Ia (0.30-0.77 wt% Cr_2O_3 at 0.90-1.30 wt% NiO), while Ni preferably concentrates in Spl Ib (up to 1.74 wt% NiO, but at 0.10-0.35 wt% Cr_2O_3). The Mg# ranges from 71.8 to 76.6 (Table 1). Spl I is not zoned but some grains may show a decrease in the Mg# restricted to the outermost 10-20 μm. Spl II forms very thin rims on sillimanite in some of reaction domains B (Fig. 3d and e). It cannot be analyzed due to small size.

Corundum forms worm-like intergrowths with clinopyroxene and platy aggregates with spinel in

Table 2: Representative microprobe analyses of minerals from the Mg-Al sapphirine-bearing granulites

	1904-3																				
	OPX I	OPX II		CPX II			CPX III	SPL Ib associated with:				CRN I		SPR	SIL	PL				GRT	
	cpx lam.				10 μm		aggr/	pyroxene		spr and sil				mantle	mantle		grt-pl	enve-	enve-	aggr/	relict
	integr.	core	rim	core	from rim	rim	grt	core	rim	core	rim	core	rim	on SPL	on SPL	core	aggr.	lope	lope	cpx	
SiO_2	55.27	56.21	55.92	53.85	53.68	53.39	54.99	0.02	0.05	0.02	0.02	0.02	0.02	11.17	36.82	62.74	63.14	63.91	63.64	41.20	40.99
TiO_2	-	-	0.01	0.04	0.02	-	-	0.01	0.01	0.01	-	-	0.02	0.02	-					0.01	-
V_2O_3										-	-										
Al_2O_3	2.69	2.03	2.17	8.02	11.56	11.25	8.83	65.95	65.85	66.92	67.42	99.37	100.06	66.19	62.39	23.71	23.33	22.93	23.13	23.14	22.67
Cr_2O_3	0.02	0.01	0.01	-	0.05	-	0.08	0.15	0.25	0.13	0.15	0.03	0.11	0.14	0.01					0.02	0.04
FeO_t	9.87	10.08	9.90	3.11	2.60	2.75	3.10	13.02	13.20	12.72	12.37	0.23	0.37	4.29	0.55	0.07	0.40	0.18	0.13	14.45	14.91
MnO	0.07	0.02	0.10	0.02	0.04	-	0.10	0.08	0.07	0.03	0.01	-	0.04	-	-					0.29	0.27
NiO	0.25	0.27	0.23	0.13	0.08	0.03	0.12	1.40	1.42	1.66	1.63			0.53	0.02					0.05	0.01
ZnO								0.85	0.60	0.69	0.68										
MgO	30.21	32.04	32.01	12.70	10.85	10.97	12.22	18.85	19.15	18.50	18.08	0.01	-	17.05	-					17.80	17.25
CaO	1.29	0.21	0.23	19.38	17.45	17.47	16.66	-	-	-	-	-	0.01	-	0.01	4.38	4.11	3.64	3.89	3.86	4.19
SrO																0.29	0.26	0.16	0.32		
BaO																0.07	0.05	-	-		
Na_2O	0.45	0.07	0.11	3.23	4.58	4.56	4.57			0.01	0.01	0.02	0.01	0.02	0.01	8.56	8.62	9.01	8.91	-	-
K_2O	0.02	-	-	0.01	0.00	-	-			-	-	-	-	-	-	0.99	1.09	1.02	0.96	-	-
Total	100.13	100.95	100.70	100.49	100.91	100.42	100.66	100.33	100.61	100.69	100.37	99.69	100.64	99.41	99.81	100.81	101.00	100.85	100.97	100.81	100.33
Si	1.943	1.952	1.947	1.929	1.900	1.901	1.953	0.001	0.001	0.000	0.001	0.000	0.000	1.322	0.997	2.768	2.781	2.810	2.799	2.972	2.981
Ti	0.000	0.000	0.000	0.001	0.001	0.000	0.000	0.000	0.000	0.000	0.000	0.000	0.000	0.002	0.000					0.000	0.000
Al	0.111	0.083	0.089	0.339	0.482	0.472	0.369	1.965	1.955	1.986	2.005	1.995	1.992	9.232	1.991	1.233	1.211	1.188	1.198	1.967	1.943
Cr	0.001	0.000	0.000	0.000	0.002	0.000	0.002	0.003	0.005	0.003	0.003	0.000	0.001	0.013	0.000					0.001	0.002
Fe^{3+}								0.031	0.037	0.010	0.000	0.003	0.005		0.012	0.003	0.015	0.006	0.005	0.000	
Fe^{2+}	0.290	0.293	0.288	0.093	0.077	0.082	0.092	0.244	0.241	0.257	0.261	0.000	0.000	0.425	0.000	0.000	0.000	0.000	0.000	0.872	0.907
Mn	0.002	0.001	0.003	0.001	0.001	0.000	0.003	0.002	0.001	0.001	0.000	0.000	0.001	0.000	0.000					0.017	0.017
Ni	0.007	0.007	0.006	0.004	0.002	0.001	0.003	0.028	0.029	0.034	0.033			0.051	0.000					0.003	0.001
Zn								0.016	0.011	0.013	0.013				0.000						
Mg	1.583	1.659	1.661	0.678	0.573	0.582	0.647	0.710	0.719	0.695	0.680	0.000	0.000	3.009	0.000					1.914	1.870
Ca	0.049	0.008	0.009	0.744	0.662	0.666	0.634	0.000	0.000	0.000	0.000	0.000	0.000	0.000	0.000	0.207	0.194	0.172	0.183	0.298	0.326
Sr																0.007	0.007	0.004	0.008		
Ba																0.001	0.001	0.000	0.000		
Na	0.031	0.005	0.007	0.225	0.314	0.315	0.315	0.000	0.000	0.001	0.001	0.001	0.000	0.004	0.001	0.733	0.736	0.768	0.760	0.000	0.000
K	0.001	0.000	0.000	0.000	0.000	0.000	0.000	0.000	0.000	0.000	0.000	0.000	0.000	0.000	0.000	0.056	0.061	0.057	0.054	0.000	0.000
Sum	4.017	4.008	4.012	4.013	4.014	4.019	4.018	3.000	3.000	3.000	2.997	2.000	1.999	14.058	3.002	5.008	5.006	5.005	5.007	8.044	8.047
Mg#	84.5	84.99	85.22	87.9	88.2	87.7	87.6	74.4	74.9	73.0	72.3									68.7	67.3
Al^{IV}	0.040	0.039	0.041	0.058	0.086	0.079	0.028														
Al^{VI}	0.071	0.044	0.048	0.281	0.396	0.394	0.341														

Table 2: Cntd.

	1904-7																					
	OPX I	OPX II		OPX II		CPX II			CPX III	Tsch-CPX		SPL Ia		SPL Ib		CRN I		SPR	SIL	PL		GRT
	cpx lam. integr.	core	rim	recrystallized core	rim	core	rim	rim	OPX II	core	rim	core	core	core	core	core	rim	mantle on SPL	mantle on SPL	core	rim	relict
SiO_2	54.12	56.59	56.47	56.55	56.36	53.09	54.52	50.84	55.68	46.03	49.08	-	-	0.02	-	-	0.04	12.28	36.96	59.20	59.7	41.54
TiO_2	-	-	0.01	-	0.02	0.05	0.04	0.03	0.03	0.01	-	0.01	-	0.02	0.01	-	0.02	-	0.01			-
V_2O_3																						
Al_2O_3	3.04	1.17	1.63	1.27	1.97	6.81	9.39	14.49	8.53	22.78	19.55	66.05	66.82	66.58	66.25	99.41	98.84	65.32	61.67	26.04	25.79	23.16
Cr_2O_3	-	0.03	0.02	-	-	0.03	-	0.01	-	-	0.03	0.63	0.33	0.28	0.30	0.11	0.10	0.06	0.02			-
FeO_t	9.19	9.84	9.78	9.58	9.81	3.15	2.10	1.80	2.53			12.37	12.68	12.21	13.06	0.10	0.30	3.31	0.29	-	0.01	13.70
MnO	0.10	0.04	0.02	0.08	0.06	0.10	0.05	0.00	0.02	1.64	1.40	0.06	0.02	0.01	0.04	0.05	-	-	-			0.27
NiO	0.21	0.21	0.17	0.13	0.15	0.04	0.07	0.14	0.05	-	0.03	1.23	0.90	1.32	1.50			-	-			0.05
ZnO										0.03	0.05	0.36	0.23	0.30	0.37			0.39	0.03			
MgO	30.53	32.73	32.6	32.6	32.89	14.37	12.36	9.96	12.56	6.95	7.91	19.42	19.78	19.26	19.25	-	0.01	18.16	0.14			17.83
CaO	1.49	0.26	0.22	0.30	0.20	21.27	18.21	18.81	16.41	18.83	17.87	-	-	0.01	-	0.01	0.01	-	0.06	7.49	7.34	4.32
SrO																				0.15	0.13	
BaO																				0.05	0.08	
Na_2O	0.48	0.03	0.04	0.05	0.04	1.73	3.94	3.89	4.73	3.75	4.42							0.03	0.02	7.20	7.33	-
K_2O	-	-	-		0.01	0.01	-	0.02	-	0.01	0.02							-	0.01	0.40	0.39	-
Total	99.17	100.91	100.96	100.57	100.93	100.66	100.69	100.00	100.53	100.03	100.36	100.14	100.77	100.00	100.79	99.68	99.32	99.55	99.20	100.53	100.77	100.89
Si	1.920	1.965	1.958	1.967	1.946	1.908	1.932	1.818	1.97	1.645	1.740	0.000	0.000	0.000	0.000	0.000	0.001	1.443	1.006	2.634	2.648	2.986
Ti	0.000	0.000	0.000	0.000	0.000	0.001	0.001	0.001	0.001	0.000	0.000	0.000	0.000	0.000	0.000	0.000	0.000	0.000	0.000			0.000
Al	0.127	0.048	0.067	0.052	0.080	0.288	0.392	0.611	0.356	0.959	0.817	1.963	1.969	1.979	1.961	1.996	1.993	9.041	1.979	1.366	1.348	1.962
Cr	0.000	0.001	0.000	0.000	0.000	0.001	0.000	0.000	0.000	0.000	0.001	0.013	0.007	0.006	0.006	0.001	0.001	0.006	0.000			0.000
Fe^{3+}										0.000	0.000	0.024	0.025	0.014	0.033	0.001	0.004	0.000	0.007			0.000
Fe^{2+}	0.273	0.286	0.283	0.279	0.283	0.095	0.062	0.054	0.075	0.049	0.042	0.237	0.240	0.244	0.241	0.000	0.001	0.325	0.000	0.000	0.000	0.824
Mn	0.003	0.001	0.000	0.002	0.002	0.003	0.001	0.000	0.001	0.000	0.001	0.001	0.000	0.000	0.001	0.001	0.000	0.000	0.000			0.017
Ni	0.006	0.006	0.005	0.004	0.000	0.001	0.002	0.004	0.001	0.001	0.001	0.025	0.018	0.027	0.030			0.037	0.001			0.003
Zn												0.007	0.004	0.006	0.007							
Mg	1.615	1.694	1.685	1.690	1.693	0.770	0.653	0.531	0.663	0.370	0.418	0.730	0.737	0.724	0.721	0.000	0.000	3.179	0.006			1.910
Ca	0.057	0.010	0.008	0.011	0.007	0.819	0.691	0.721	0.622	0.721	0.679	0.000	0.000	0.000	0.000	0.000	0.000	0.000	0.002	0.357	0.349	0.333
Sr																				0.004	0.003	
Ba																				0.001	0.001	
Na	0.033	0.002	0.003	0.004	0.003	0.121	0.270	0.270	0.325	0.260	0.304					0.000	0.000	0.006	0.001	0.621	0.630	0.000
K	0.000	0.000	0.000	0.000	0.000	0.000	0.000	0.001	0.000	0.000	0.001					0.000	0.000	0.000	0.000	0.022	0.022	0.000
Sum	4.033	4.012	4.010	4.009	4.015	4.007	4.006	4.011	4.013	4.005	4.003	3.000	3.000	3.000	3.000	2.000	2.000	14.037	3.001	5.005	5.001	8.034
Mg#	85.5	85.6	85.6	85.8	85.7	89.0	91.3	90.8	89.8	88.3	90.9	75.5	75.4	74.8	74.9							69.9
Al^{IV}	0.047	0.024	0.032	0.024	0.039	0.085	0.062	0.171	0.017	0.350	0.256											
Al^{VI}	0.080	0.025	0.035	0.028	0.042	0.203	0.330	0.440	0.340	0.610	0.561											

Mg# = 100 × Mg/(Mg+Fe^{2+}). ¨ - ¨ not detected.

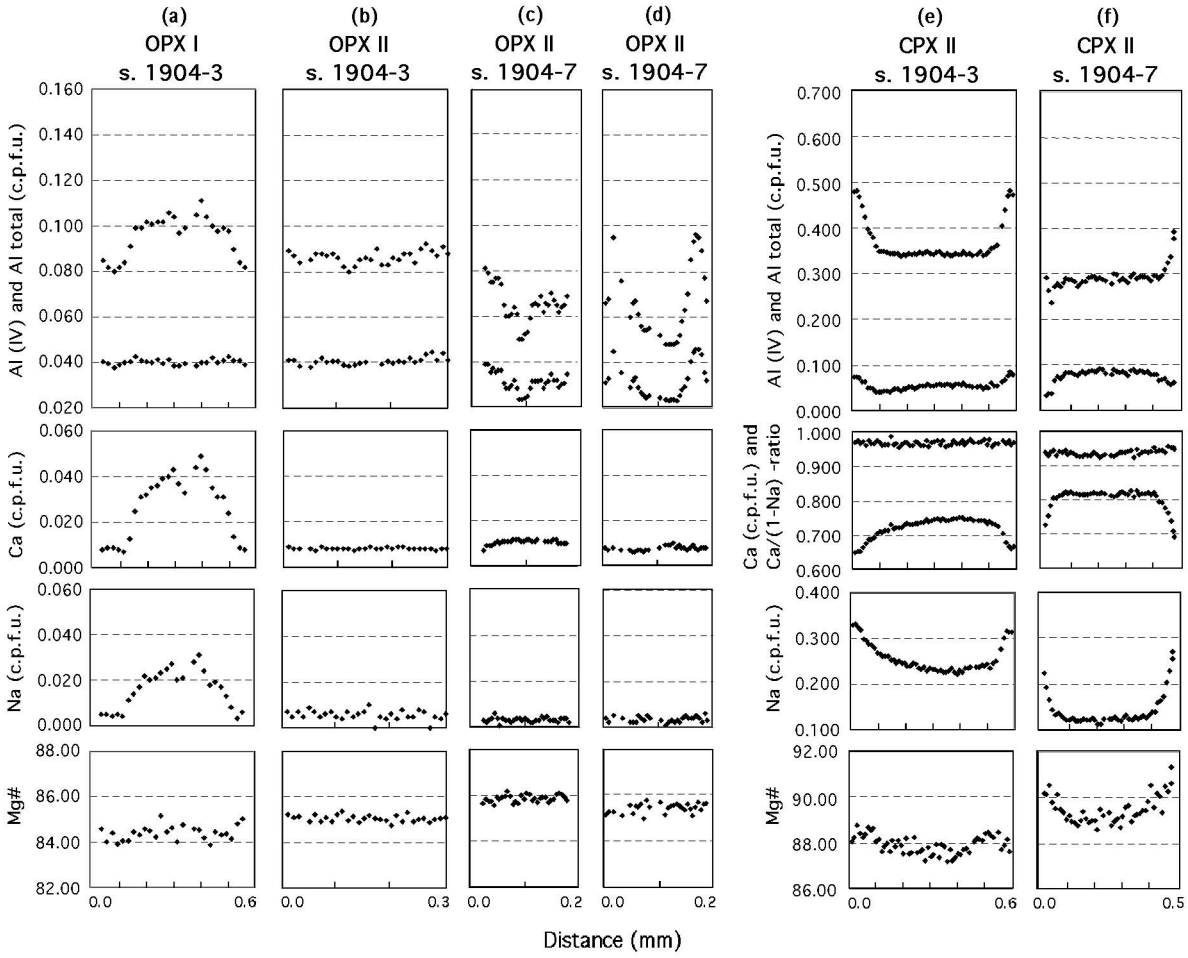


Fig. 4. Zoning patterns in pyroxenes in Mg-Al granulites. [For further explanation, see text.]

reaction domains A1 (Fig. 3a) as well as large individual grains in reaction domains A2 (Fig. 2a and 3c). Corundum contains up to 0.50 wt% Fe_2O_3 and 0.16 wt% Cr_2O_3 (Table 2). Some grains are slightly zoned whereby Cr and Fe increase and Al decreases rimwards.

Plagioclase forms large grains and granular aggregates with frequent sillimanite inclusions. In the rim parts of such aggregates, it is often intimately intergrown with garnet forming 'flaky' Grt-Pl aggregates. Plagioclase also occurs as thin envelopes mimicking the borders of some Cpx II grains. Plagioclase is relatively Na-rich (1904-3: An_{21-16}; 1904-7: An_{40-30}; Table 2). It may show some enrichment in Na in the envelopes around clinopyroxene II (Table 2).

Garnet replaces almost all other minerals, forming a network-like structure around pyroxene, spinel and corundum grains, 'flaky' aggregates with plagioclase and massive aggregates with Cpx III (Fig. 2a and b and 3a-e). As garnet itself is normally replaced by kelyphite, only its rare relicts are available for analysis. The Mg# ranges from 62.6 to 70.1 and CaO from 4.2 to 6.0 wt% (Table 2).

Sapphirine forms small platy inclusions in the outermost zones of spinel I grains or rims spinel I in reaction domains B (Fig. 3d and e). In the latter case, sapphirine apparently resorbs spinel and, in turn, is being replaced by sillimanite or directly by garnet. Sapphirine compositions are close to the ideal composition $7(Fe,Mg)O \times 9(Fe,Al,Cr)_2O_3 \times$

$3SiO_2$ (Table 2). NiO reaches 0.50 wt % and is the only minor component.

Sillimanite rims sapphirine and spinel in reaction domains B (Fig. 3d and e) and forms frequent needle-like inclusions in plagioclase (Fig. 2b and 3f). If associated with spinel and sapphirine, sillimanite tends to replace spinel, always replaces sapphirine and, in turn, is being resorbed by garnet. Sillimanite hosted in plagioclase seems equilibrated with the latter. Fe_2O_3 contents are < 0.65 wt% (Table 2).

Ca-Al hibonite-bearing granulites

The three studied samples (1904-1, 1904-9, 1906-2) are very similar to each other. Xenolith 1904-1 is relatively coarse-grained (plagioclase grains reach 3-4 mm, mafic minerals are smaller in size) and banded. Xenoliths 1904-9 and 1906-2 are more fine-grained and homogenous. Specimen 1906-2 is more mafic compared to the others. Major minerals in all samples are clinopyroxene and plagioclase, while corundum and garnet are essential (~10-15 vol.% each) and quartz, spinel and sillimanite subordinate (5-7 vol.%). In addition, sapphirine in sample 1904-1 and hibonite in samples 1904-1 and 1904-9 occur as rare accessories. Mullite is very rare. It is encountered in one specimen (1904-9), and only in three grains.

Textures are characterized by felsic and mafic domains. The felsic domains consist of plagioclase and the mafic domains are dominated by clinopyroxene, corundum, garnet, spinel, sillimanite and quartz (Fig. 2c). Both domains are normally separated by a fine-grained corona that consists of garnet and recrystallized plagioclase, grading locally, as in the Mg-Al granulites, into a massive zone of intimately intergrown micrograins of garnet and clinopyroxene (Fig. 2c and 5a-b).

Clinopyroxene can be divided into three generations. Cpx I occurs in close association with quartz. Together, they form granular cores of large complex clinopyroxene grains (Fig. 5a and b). Typically, such cores contain either one to several large (0.2-0.3 mm) or 10-20 small (<0.1 mm) drop-like inclusions of quartz with different optical orientations. Worm-like intergrowth of quartz and Cpx I may occur as well. Apart from this texture, the rocks are devoid of quartz. The core is always mantled by an outer zone of clinopyroxene that lacks quartz. Normally, the whole grain is embedded in plagioclase. Cpx II forms smaller grains that do not have quartz. Cpx III forms very small (<10 μm) grains intergrown and texturally equilibrated with garnet in the massive fine grained Grt-Cpx zones developed after plagioclase (Fig. 2c).

In general, clinopyroxene is characterized by moderate to high Mg# (86.3-91.2 in Cpx I, 83.6-90.7 in Cpx II and III). CaO ranges from 18.05 to 21.68 wt% (Table 3). Chemically, Cpx I is easily distinguishable from Cpx II and III. It is more magnesian than Cpx II, more Ca-rich, less aluminous and much less tschermakitic than Cpx II and III (Table 3). Cpx II is zoned (Fig. 6). If no inclusions are present, the core parts of the largest grains display plateaus in Al (Fig. 6a and b). Closer to the rims, the Al content increases and then always slightly decreases again within the outermost 10 μm. The Na zonation mimics that of Al but is less extreme; Ca shows the inverse pattern to Na (Fig. 6). The Mg# increases rimwards, sometimes with a slight tendency to decrease again within the outermost rim (Fig. 6). In smaller grains,

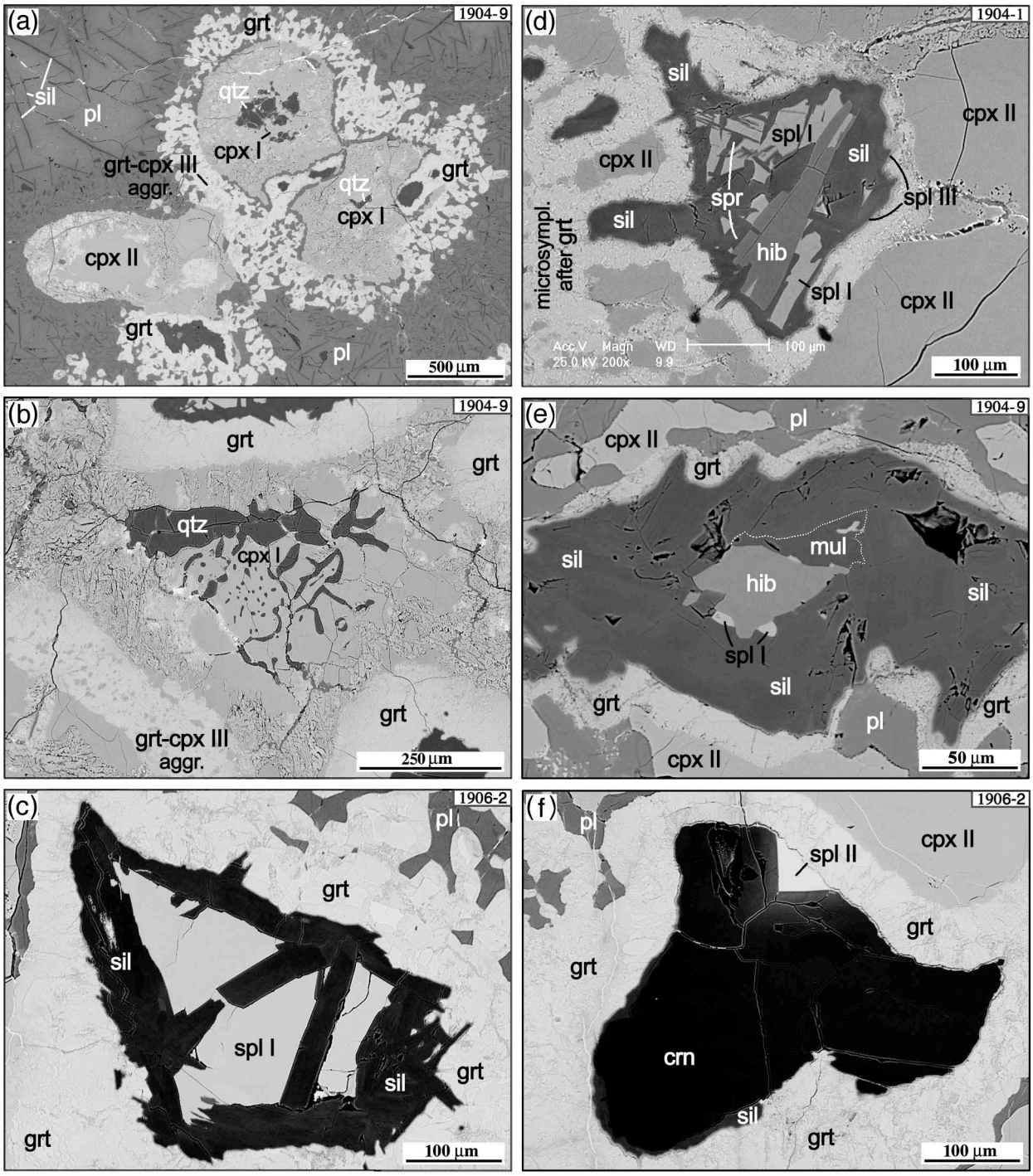


Fig. 5. Back-scattered electron images demonstrating the different mineral generations and important reaction domains in Ca-Al granulites. (a, b) Large complex grains of clinopyroxene I with quartz in the cores. (c) Spinel I aggregated with and rimmed by sillimanite. (d) Aggregate of hibonite, spinel, sapphirine and sillimanite partially resorbed by garnet. (e) Aggregate of hibonite, spinel, mullite and sillimanite partially resorbed by garnet. (f) Corundum aggregated with spinel II, partially rimmed by sillimanite and strongly resorbed by garnet. [For further explanation, see section on textures and mineral compositions and section on metamorphic reactions.]

Cpx II shows the same style of zonation, but with no plateau (Fig. 6c-e). Cpx III has a composition intermediate between the core and the rim zones of Cpx II (Table 3).

Plagioclase forms large isometric or elongated grains with abundant needle-like inclusions of sillimanite and late inclusion-free envelope-like zones mimicking the borders of clinopyroxene II in contact with the 'flaky' Grt-Pl or massive Grt-Cpx aggregates (Fig. 2c and 5a). As an exception, plagioclase occurs as ameboidal inclusions in clinopyroxene. Plagioclase is Na-rich (1904-1: An_{39-34}; 1904-9: An_{35-32}; 1906-2: An_{31-26}). It is slightly inhomogeneous and shows a tendency towards higher Ab in the envelopes (Table 3).

Corundum forms grains of variable shape. It is always closely associated with clinopyroxene and often occurs as inclusions in the latter (Fig. 2c). Isolated grains of corundum are Cr-poor and almost unzoned. Rare corundum grains intergrown with Spl II demonstrate strong chemical zonation towards Spl II: the content of Cr_2O_3 reaches ~7.0 wt%, while the Al content decreases (Table 3).

Garnet resorbs almost all other minerals and does not form independent grains. Most garnet is developed at the expense of corundum and plagioclase. As a rule, garnet is altered into kelyphite, only rare relics are preserved. The Mg# ranges from 58.6 to 65.5, CaO – from 7.90 to 11.45 wt% (Table 3).

Spinel can be subdivided into three generations. Spl I is common. It forms relatively large grains always associated with sillimanite, sometimes also with sapphirine, hibonite, mullite. The textural relationships between Spl I, Sil and other minerals are not easily discernible. Almost all grains of Spl I are completely mantled by platy crystals of sillimanite (Fig. 5c and d). Besides that, sillimanite tends to separate spinel into individual blocks, and all transitional forms from single grains of Spl I with a Sil mantle to well developed mosaic intergrowths of Spl I and Sil are observed (e.g. Fig. 5c). Some of these aggregates show clear textural indications of sillimanite replacing spinel. In others, these minerals seem to be in textural equilibrium. Sapphirine, mullite and / or hibonite, if present, occur in the core areas of the Spl-Sil aggregates (Fig. 5d and e). Of these minerals, only mullite apparently resorbs spinel (Fig. 5e). Hibonite shows linear contacts with spinel with no clear indications of resorbtion, although spinel often rims hibonite and not *vice versa*. The aggregates are always corroded by garnet (Fig. 5c-e). Except for one case of direct contact with spinel, garnet resorbs only the outer sillimanite mantle, but not the inner mineral assemblage (Fig. 5c-e). In thin section, the described aggregates are always closely associated with Cpx I and II (Fig. 2c, Fig. 5d and e).

Spinel II is rare. It forms small grains localized directly at the rims of the larger corundum grains, or penetrating corundum from the rim inwards (Fig. 5f). Late spinel III occurs as very thin mantles picking out borders of corundum and sillimanite in the various aggregates (e.g. Fig. 5d).

Individual Spl I grains are nearly homogeneous but they show considerable inter-grain variations in Cr_2O_3 contents and Mg#, depending on their textural position (Table 3). Cr_2O_3 typically ranges from 0.3 to 6.0 wt%, but is lower (0.3-2.7 wt%) in Spl I associated with hibonite and much higher (up to 22 wt%) in some of the Spl I-Sil ag-

Table 3: Representative microprobe analyses of minerals from the Ca-Al hibonite-bearing granulites

	1906-2																					
	CPX I		CPX II			CPX III	SPL I				SPL II		CRN				SIL		PL		GRT	
				20 μm		aggr/	grain 1		grain 2				individual		with spl II		rim/	rim/		enve-	aggr/	relict
	core	core	core	from rim	rim	grt	core	rim	core	rim	core	rim	core	rim	core	rim	Cr-spl I	spl I	core	lope	cpx	near spl
SiO_2	54.74	54.76	53.19	52.67	52.58	52.71	-	0.02	0.01	0.01	0.06	0.06	-	0.04	0.03	-	37.05	37.12	60.88	61.52	40.83	40.67
TiO_2	-	0.01	0.06	0.04	0.03	0.05	0.01	-	-	-	0.02	0.02	-	-	-	-	-	0.01			0.03	0.02
V_2O_3							0.04	-	0.04	-	0.09	0.10					-					
Al_2O_3	4.80	5.30	8.17	10.11	9.18	9.4	63.08	63.19	55.40	55.27	25.08	24.32	98.91	99.36	92.28	98.68	60.75	62.96	25.14	24.21	22.97	22.95
Cr_2O_3	0.05	-	0.10	0.28	0.45	-	3.27	3.13	11.18	10.82	39.69	39.44	0.23	0.71	6.95	0.28	1.96	0.06			-	0.05
FeO_t	3.57	3.60	3.90	3.25	3.29	3.42	13.94	14.10	15.38	15.18	24.71	25.14	0.35	0.55	0.90	0.53	0.64	0.37	0.03	0.29	14.29	14.65
MnO	0.03	-	0.02	-	0.06	0.04	0.04	-	-	-	0.15	0.01	-	-	-	-	-	0.02			0.26	0.15
NiO	0.16	0.13	0.12	0.13	0.17	0.18	2.13	2.08	1.63	1.59	0.39	0.47	0.01	-	0.02	0.03	-	0.03			0.02	-
ZnO							1.84	1.79	2.76	2.64	1.63	1.66					-				-	
MgO	13.92	13.65	11.74	11.29	11.72	11.98	16.41	16.44	14.14	14.20	8.54	8.37	0.02	-	0.02	0.01	0.01	0.01			14.95	14.35
CaO	20.50	20.13	18.65	19.24	19.55	19.37	0.01	-	-	-	0.01	-	-	0.02	-	-	-	0.03	6.37	5.59	7.64	7.94
SrO																			0.11	0.15		
BaO																			-	0.02		
Na_2O	2.42	2.71	3.64	3.5	3.27	3.4	0.06	0.05	0.09	0.08	0.04	0.05	-	-	0.02	-	-	-	8.11	8.30	0.03	0.01
K_2O	-	-	0.01	0.01	0.01	0.01	-	0.01	-	-	-	-	0.02	0.01	-	0.01	-	-	0.29	0.36		-
Total	100.19	100.29	99.59	100.51	100.31	100.56	100.83	100.82	100.62	99.78	100.40	99.65	99.54	100.69	100.21	99.54	100.82	100.60	100.92	100.44	101.03	100.79
Si	1.976	1.973	1.929	1.890	1.895	1.893	0.000	0.001	0.000	0.000	0.002	0.002	0.000	0.001	0.000	0.000	1.004	0.997	2.688	2.726	2.969	2.971
Ti	0.000	0.000	0.002	0.001	0.001	0.001	0.000	0.000	0.000	0.000	0.000	0.001	0.000	0.000	0.000	0.000	0.000	0.000			0.002	0.001
V							0.001	0.000	0.001	0.000	0.002	0.003										
Al	0.204	0.225	0.349	0.427	0.390	0.398	1.917	1.920	1.755	1.761	0.922	0.903	1.991	1.981	1.890	1.988	1.939	1.993	1.308	1.264	1.969	1.976
Cr	0.001	0.000	0.003	0.008	0.013	0.000	0.067	0.064	0.238	0.231	0.979	0.982	0.003	0.010	0.095	0.004	0.042	0.001			0.000	0.003
Fe^{3+}							0.018	0.018	0.011	0.011	0.096	0.110	0.005	0.008	0.013	0.008	0.012	0.008	0.001	0.011		
Fe^{2+}	0.108	0.108	0.118	0.098	0.099	0.103	0.283	0.286	0.334	0.332	0.549	0.552	0.000	0.000	0.000	0.000	0.003	0.000	0.000	0.000	0.869	0.895
Mn	0.001	0.000	0.001	0.000	0.002	0.001	0.001	0.000	0.000	0.000	0.004	0.000	0.000	0.000	0.000	0.000	0.000	0.000			0.016	0.009
Ni	0.005	0.004	0.003	0.004	0.005	0.005	0.044	0.043	0.035	0.035	0.010	0.012	0.000	0.000	0.000	0.000		0.001			0.001	0.000
Zn							0.035	0.034	0.055	0.053	0.038	0.039										
Mg	0.749	0.733	0.635	0.604	0.630	0.641	0.631	0.632	0.566	0.572	0.397	0.393	0.000	0.000	0.000	0.000	0.000	0.000			1.621	1.562
Ca	0.793	0.777	0.725	0.739	0.755	0.745	0.000	0.000	0.000	0.000	0.000	0.000	0.000	0.000	0.000	0.000	0.000	0.001	0.301	0.265	0.595	0.621
Sr																			0.003	0.004		
Ba																			0.000	0.000		
Na	0.170	0.189	0.256	0.243	0.229	0.237	0.003	0.002	0.005	0.004	0.002	0.003	0.000	0.000	0.001	0.000	0.000	0.000	0.694	0.713	0.004	0.001
K	0.000	0.000	0.001	0.001	0.000	0.000	0.000	0.000	0.000	0.000	0.000	0.000	0.000	0.000	0.000	0.000	0.000	0.000	0.016	0.020	0.000	0.000
Sum	4.007	4.009	4.021	4.014	4.019	4.025	3.000	3.000	3.000	3.000	3.000	3.000	2.000	2.000	2.000	2.000	3.000	3.002	5.012	5.004	8.046	8.039
Mg#	87.4	87.2	84.3	86.0	86.4	86.2	69.0	68.8	62.9	63.3	42.0	41.6									63.6	63.6
Al^{IV}	0.018	0.018	0.050	0.097	0.088	0.082																
Al^{VI}	0.187	0.207	0.300	0.331	0.302	0.317																

Table 3: Cntd.

	1904-1																					
	CPX I		CPX II 10 μm		CPX III aggr/	SPL I grain 1		SPL I grain 2		SPL II		CRN individual		with Spl II		SIL mantle	SPR	HIBONITE		PL		GRT incl.
	core	core	from rim	rim	grt	core	rim	core	rim	core	rim	core	rim	core	rim	on spl I		core	rim	core	envelope	in cpx
SiO_2	54.26	53.32	52.03	52.23	51.46	0.05	0.01	0.01	0.03	0.04	0.01	-	0.04	0.04	0.10	36.92	10.97	2.33	2.28	59.46	59.71	40.34
TiO_2	0.01	0.08	0.14	0.14	0.06	0.01	-	-	0.02	0.05	-	0.01	0.02	0.02	0.01	-	-	2.14	2.46			0.00
V_2O_3																						
Al_2O_3	5.10	7.52	11.33	10.50	9.93	64.89	65.21	63.15	63.01	28.00	27.99	99.43	98.95	99.31	92.64	62.59	66.53	82.27	81.97	26.12	26.11	22.50
Cr_2O_3	0.08	-	0.02	0.01	0.00	1.72	1.86	3.02	2.94	39.31	39.07	0.16	0.14	0.45	7.70	0.32	0.81	0.38	0.40			0.00
FeO_t	2.87	3.87	2.19	2.23	2.87	13.22	13.28	14.41	14.46	21.75	22.33	0.20	0.27	0.26	0.43	0.25	4.06	2.12	2.17	0.02	0.06	13.66
MnO	0.01	0.03	0.03	-	0.04	0.03	0.07	0.04	0.01	0.09	0.08	-	0.03	-	-	0.01	0.03	0.01	0.02			0.14
NiO	0.14	0.12	0.15	0.11	0.09	1.51	1.51	1.44	1.51	0.31	0.34						0.40					0.05
ZnO						1.40	1.25	1.68	1.73	1.35	1.29							0.16	0.26			
MgO	14.30	12.64	11.61	12.10	12.15	17.46	17.32	16.75	16.94	9.56	9.57	0.01	-	-	0.01	0.03	17.14	2.00	2.04			11.73
CaO	20.43	20.79	20.47	20.71	20.11	-	-	0.01	0.01	0.04	0.10	-	0.02	0.01	0.04	0.04	0.02	8.45	8.40	7.68	7.27	11.06
SrO																				0.03	0.15	
BaO																				0.01	0.06	
Na_2O	2.45	2.48	2.83	2.62	2.63							-	-	0.01	0.01	-	0.02	0.04	0.01	7.16	7.28	0.01
K_2O	0.01	0.01	-	0.02	0.01							0.01	-	-	-	-	-	-	-	0.43	0.46	0.00
Total	99.66	100.85	100.79	100.67	99.35	100.30	100.54	100.50	100.67	100.50	100.79	99.82	99.47	100.10	100.93	100.16	99.98	99.91	100.00	100.91	101.09	99.49
Si	1.964	1.916	1.855	1.866	1.868	0.001	0.000	0.000	0.001	0.001	0.000	0.000	0.001	0.001	0.002	0.996	1.292	0.264	0.258	2.634	2.641	2.999
Ti	0.000	0.002	0.004	0.004	0.002	0.000	0.000	0.000	0.000	0.001	0.000	0.000	0.000	0.000	0.000	0.000	0.000	0.183	0.209			0.000
V																						
Al	0.218	0.319	0.476	0.442	0.425	1.957	1.962	1.920	1.913	1.011	1.007	1.995	1.993	1.989	1.886	1.991	9.233	10.982	10.945	1.364	1.361	1.972
Cr	0.002	0.000	0.001	0.000	0.000	0.035	0.038	0.062	0.060	0.952	0.944	0.002	0.002	0.006	0.105	0.007	0.075	0.034	0.036			0.000
Fe^{3+}						0.006	0.000	0.018	0.025	0.033	0.049	0.003	0.004	0.003	0.006	0.006		0.000	0.000	0.001	0.002	
Fe^{2+}	0.087	0.116	0.065	0.067	0.087	0.277	0.284	0.293	0.286	0.524	0.522	0.000	0.000	0.000	0.000	0.000	0.399	0.201	0.206	0.000	0.000	0.849
Mn	0.000	0.001	0.001	0.003	0.001	0.001	0.002	0.001	0.000	0.002	0.002	0.000	0.000	0.000	0.000	0.000	0.002	0.001	0.001			0.009
Ni	0.004	0.003	0.004	0.000	0.003	0.031	0.031	0.030	0.031	0.008	0.008	0.000					0.038					0.003
Zn						0.026	0.024	0.032	0.033	0.031	0.029							0.013	0.022			
Mg	0.771	0.677	0.617	0.644	0.657	0.666	0.659	0.644	0.650	0.437	0.436	0.000	0.000	0.000	0.000	0.001	3.009	0.338	0.345			1.300
Ca	0.793	0.801	0.782	0.793	0.782	0.000	0.000	0.000	0.000	0.001	0.003	0.000	0.000	0.000	0.001	0.001	0.003	1.025	1.019	0.364	0.344	0.881
Sr																				0.001	0.004	
Ba																				0.000	0.001	
Na	0.172	0.173	0.195	0.181	0.185							0.000	0.000	0.000	0.000	0.000	0.004	0.009	0.002	0.615	0.624	0.002
K	0.001	0.000	0.000	0.001	0.000							0.000	0.000	0.000	0.000	0.000	0.000	0.000	0.000	0.025	0.026	0.000
Sum	4.012	4.008	4.000	4.001	4.011	3.000	3.000	3.000	3.000	3.000	3.000	2.000	2.000	2.000	2.000	3.002	14.056	13.050	13.044	5.003	5.003	8.015
Mg#	89.9	85.4	90.5	90.6	88.3	70.6	69.9	68.7	69.4	45.5	45.5											60.5
Al^{IV}	0.024	0.075	0.145	0.134	0.122																	
Al^{VI}	0.195	0.244	0.331	0.308	0.303																	

Table 3: Cntd.

	1904-9																					
	CPX I		CPX II		CPX III	SPL I		SPL I		CRN		SIL	MULLITE		HIBONITE				PL		GRT	
					aggr/	grain 1		grain 2				mantle			grain 1		grain 2			enve-	aggr/	relict
	core	core	core	rim	grt	core	rim	core	rim	core	rim	on SPL	core	rim	core	rim	core	rim	core	lope	cpx	near spl
SiO_2	54.91	54.76	53.45	52.82	52.13	0.04	0.06	0.04	0.02	0.02	-	37.03	22.54	22.83	3.02	2.99	2.81	2.84	60.20	60.86	40.74	40.08
TiO_2	-	-	0.04	0.03	0.03	-	-	0.02	-	0.02	0.01	-	-	-	0.06	0.09	0.64	0.88			0.02	0.03
V_2O_3						0.03	0.02	0.01	-													
Al_2O_3	4.19	4.01	7.88	10.23	9.68	65.49	65.54	65.88	66.13	99.21	99.05	62.59	76.88	76.94	83.83	83.88	83.37	83.54	25.63	24.80	22.44	22.81
Cr_2O_3	0.05	-	-	0.03	0.02	0.62	0.63	0.98	1.06	0.03	0.08	0.21	0.26	0.37	0.10	0.24	0.13	0.11			0.00	0.03
FeO_t	3.31	3.11	3.54	2.86	3.12	14.59	14.67	13.66	13.41	0.29	0.43	0.28	0.38	0.42	2.38	2.31	2.47	2.28	0.01	0.04	14.36	14.41
MnO	-	-	-	0.01	0.05	0.03	0.01	0.02	0.05	-	0.02	-	0.02	0.02	0.00	0.03	0.00	0.00			0.20	0.20
NiO	0.20	0.22	0.12	0.12	0.15	2.15	2.21	1.96	1.98	0.02	0.01	-	-	0.05							0.00	0.07
ZnO						1.69	1.68	2.07	2.11						0.25	0.22	0.19	0.25				
MgO	14.31	14.24	11.95	11.24	12.03	16.17	16.09	16.18	16.19	-	-	-	0.05	0.01	1.51	1.51	1.59	1.68			11.98	11.45
CaO	21.57	21.68	19.48	19.30	19.69	-	-	0.02	-	0.01	0.02	0.03	0.01	0.05	8.43	8.45	8.38	8.43	6.89	6.23	10.38	11.45
SrO																			0.04	0.03		
BaO																			-	0.02		
Na_2O	2.01	2.00	3.07	3.38	3.04	0.05	0.06	0.05	0.07	0.01	-	-	-	-	-	-	0.02	0.02	7.55	7.99	0.03	0.01
K_2O	-	-	-	0.02	0.00	-	0.02	-	0.01	0.01	-	0.01	0.02	0.01	-	-	0.01	0.01	0.39	0.42	0.01	0.01
Total	100.54	100.02	99.51	100.04	99.94	100.86	100.98	100.87	101.02	99.61	99.62	100.14	100.16	100.70	99.60	99.73	99.61	100.05	100.72	100.38	100.14	100.52
Si	1.977	1.982	1.937	1.897	1.882	0.001	0.002	0.001	0.000	0.000	0.000	0.999	1.188	1.198	0.342	0.338	0.318	0.320	2.665	2.700	3.011	2.965
Ti	0.000	0.000	0.001	0.001	0.001	0.000	0.000	0.000	0.000	0.000	0.000	0.000	0.000	0.000	0.005	0.008	0.055	0.075			0.001	0.002
V						0.001	0.000	0.000	0.000													
Al	0.178	0.171	0.336	0.433	0.412	1.977	1.977	1.985	1.988	1.994	1.992	1.990	4.777	4.761	11.180	11.173	11.132	11.104	1.337	1.297	1.955	1.989
Cr	0.001	0.000	0.000	0.001	0.001	0.012	0.013	0.020	0.021	0.000	0.001	0.004	0.011	0.016	0.009	0.021	0.012	0.010			0.000	0.002
Fe^{3+}					0.000	0.011	0.011	0.000	0.000	0.004	0.006	0.006	0.017	0.018					0.000	0.001		
Fe^{2+}	0.100	0.094	0.107	0.086	0.094	0.302	0.303	0.292	0.286	0.000	0.000	0.000	0.000	0.000	0.225	0.218	0.234	0.215	0.000	0.000	0.887	0.891
Mn	0.000	0.000	0.000	0.000	0.001	0.001	0.000	0.000	0.001		0.000	0.000	0.001	0.001	0.000	0.003	0.000	0.000			0.012	0.012
Ni	0.006	0.006	0.003	0.003	0.004	0.044	0.045	0.040	0.041	0.000	0.000	0.000	0.000	0.002							0.000	0.004
Zn						0.032	0.032	0.039	0.040						0.021	0.018	0.016	0.021				
Mg	0.768	0.769	0.645	0.602	0.648	0.618	0.614	0.617	0.616	0.000	0.000	0.000	0.004	0.001	0.255	0.254	0.269	0.282			1.320	1.263
Ca	0.832	0.841	0.756	0.743	0.762	0.000	0.000	0.000	0.000	0.000	0.000	0.001	0.000	0.002	1.022	1.023	1.017	1.019	0.327	0.296	0.822	0.908
Sr																			0.001	0.001		
Ba																			0.000	0.000		
Na	0.140	0.140	0.216	0.235	0.213	0.002	0.003	0.002	0.004	0.000	0.000	0.000	0.000	0.000	0.000	0.000	0.004	0.004	0.648	0.688	0.004	0.001
K	0.000	0.000	0.000	0.001	0.000	0.000	0.001	0.000	0.000	0.000	0.000	0.000	0.001	0.001	0.000	0.000	0.001	0.001	0.022	0.024	0.001	0.000
Sum	4.003	4.003	4.002	4.002	4.017	3.000	3.000	2.998	2.997	2.000	2.000	3.001	6.000	6.000	13.059	13.057	13.058	13.051	5.001	5.007	8.013	8.037
Mg#	88.5	89.1	85.8	87.5	87.3	67.2	67.0	67.9	68.3												59.8	58.6
Al^{IV}	0.020	0.016	0.061	0.100	0.101																	
Al^{VI}	0.159	0.156	0.275	0.333	0.311																	

$Mg\# = 100 \times Mg/(Mg+Fe^{2+})$. ¨ - ¨ not detected.

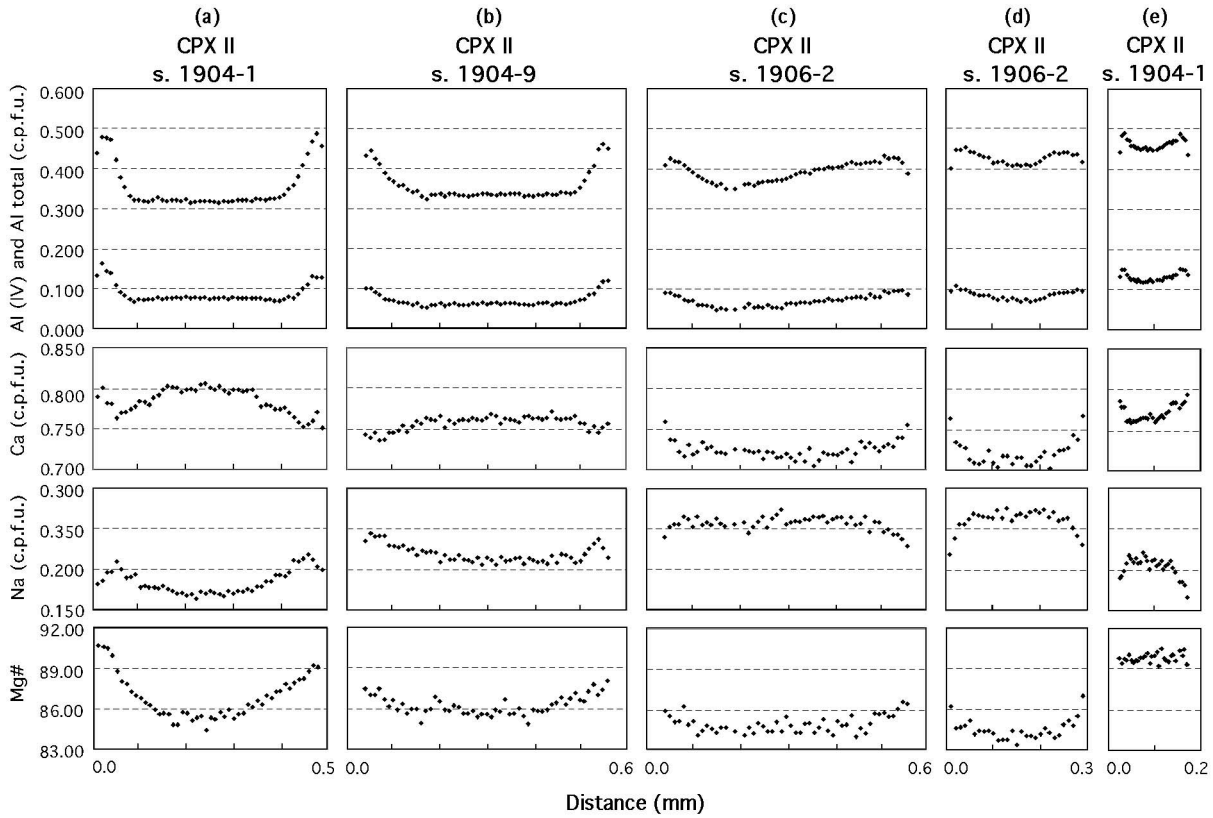


Fig. 6. Zoning patterns of clinopyroxenes of Ca-Al granulites. [For further explanation, see text.]

gregates. Mg# ranges from 66.5 to 70.9 (Table 3). NiO and ZnO are generally high (1.1-2.3 and 1.0-2.6 wt%, respectively). Spinel II is also nearly homogeneous in individual grains. It is extremely rich in Cr (33-40 wt% Cr_2O_3) and has lower NiO contents and Mg# than Spl I (Fig. 7; Table 3). The composition of spinel III is not easily measurable due to small grain size.

Sillimanite forms platy aggregates with spinel I (Fig. 5c), outer zones on spinel I and its aggregates with hibonite, mullite, sapphirine (Fig. 5d and e), as well as frequent needle-like inclusions in plagioclase (e.g. Fig. 5a). In the aggregates, sillimanite apparently resorbs hibonite, may resorb spinel I, sapphirine and mullite (Fig. 5d and e) and, in turn, is resorbed by garnet. Sillimanite shows a spectrum of compositions from nearly ideal in most cases to Cr-rich (up to ~2.0 wt% Cr_2O_3) in contact with Cr-rich Spl I. Fe_2O_3 may amount to 0.65 wt% (Table 3).

Sapphirine occurs as a rare accessory phase and is identified with confidence in specimen 1904-1 only. In specimen 1906-2, it may be present as micro-relicts enclosed in sillimanite in the outer parts of Spl-Sil aggregates, but the grains are too small to be analyzed by microprobe. Sapphirine in specimen 1904-1 is closely associated with spinel, hibonite and sillimanite (e.g. Fig. 5d). It may show straight borders with Spl I with no indications of resorbtion, but more often it resorbs Spl I. In turn, it is always resorbed by sillimanite, and in cases directly by garnet. The analyzed sapphirine is close to the ideal composition $7(Fe,Mg)O \times 9(Fe,Al, Cr)_2O_3 \times 3SiO_2$. Cr_2O_3 may reach 1.12 wt%, NiO - 0.47 wt% (Table 3).

Mullite occurs in specimen 1904-9 only. It is found in the cores of three spinel-hibonite-sillimanite aggregates, one of which is shown in Fig. 5e. Mullite apparently resorbs hibonite and spinel I and, in turn, is replaced by sillimanite. Chemically, it belongs to the 2:1 type ($2Al_2O_3$:$1SiO_2$). In the mullite solid solution series $Al_{4+2x}Si_{2-2x}O_{10-x}$ (Cameron, 1977), it is characterized by $x \approx 0.40$ (Table 3). The mullite is nearly homogeneous. It may contain limited amounts of Cr_2O_3 and FeO_t (<0.50 wt% each, see Table 3).

Hibonite occurs as accessory phase in xenoliths 1904-1 and 1904-9. Its absence in xenolith 1906-2 may be due to the relative depletion of its bulk chemical composition in Al and Ca compared to xenoliths 1904-1 and 1904-9 (see Table 1). Hibonite forms small isometric or elongated, often complexly indented grains intergrown with spinel I in the cores of complex corona textures made of hibonite, spinel, mullite, sapphirine and sillimanite (Fig. 5d and e). Neither hibonite nor spinel and sapphirine resorb each other. At the same time, the petrographic relationships of hibonite with spinel and sapphirine point to early crystallization of hibonite, since both spinel and sapphirine tend to localize on the border of hibonite grains, whereas hibonite never rims neither spinel nor sapphirine (Fig. 5d and e). Mullite, when present, apparently resorbs hibonite, as well as sillimanite does (Fig. 5e).

Chemically, the studied hibonite is close to the ideal formula $Ca(Al,Ti,Si,Mg,Fe^{2+})_{12}O_{19}$. Ca, Al, Si, Mg and Fe contents vary in a narrow range. SiO_2 ranges from 2.32 to 3.10 wt%. Some TiO_2 is always present (0.05-0.74 wt% in specimen 1904-1, 0.26-2.29 wt% in specimen 1904-9). Significant intergrain variations and a systematic rimwards increase in Ti are also common. Cr_2O_3 ranges from 0.03 to 0.52 wt%, ZnO does not exceed 0.25 wt% (Table 3). Ca contents vary from 1.016 to 1.048 c.p.f.u. and are somewhat excessive compared to the ideal stoichiometry of hibonite. An excess of Ca has been found in both terrestrial (e.g. Maaskant *et al.*, 1980) and meteoritic (e.g. Keil and Fuchs, 1971; MacDougall, 1979) hibonite and is common for this mineral. It additionally corroborates that an exchange of (Mg,Fe^{2+}) and Ca in site A of the hibonite structure is unlikely. At the same time, the classical substitution $(Ti,Si)+(Mg,Fe^{2+})\leftrightarrow 2(Al,Cr)$ in site B (e.g. Burns & Burns, 1984) and the common exchange $Ti\leftrightarrow 2(Mg, Fe^{2+})$ were operative (Ulianov *et al.*, 2005). The studied hibonite is very poor in REE ($\sum$REE from 1.5 to ~30 μg/g) with positive Eu anomalies and variable enrichment in LREE and very low abundances (<1-2 μg/g) of Nb, Ta, Zr, Hf and Th (Ulianov *et al.*, 2005).

PRE-METAMORPHIC VS. METAMORPHIC MINERAL ASSEMBLAGES

The studied xenoliths appear to have undergone nearly complete subsolidus recrystallization. Although their C.I.P.W. normative compositions are troctolitic, modal olivine is absent. It seems to have completely reacted out during subsolidus cooling, as discussed below. The plagioclase grains actually present show indications of metamorphic reequilibration and thus do not represent igneous relicts, neither texturally nor compositionally.

In the Mg-Al sapphirine-bearing granulites, the only potential igneous relicts are the largest grains of orthopyroxene (Opx I), of which the reintegrated composition is very rich in calcium and

aluminum (Table 2), and possibly a minor part of spinel texturally independent of pyroxenes (Spl 1a). Spinel 1a compositions, however, re-equilibrated under subsolidus conditions and are almost indistinguishable from those of metamorphic spinel Ib (see section 'Textures and mineral compositions'). Sapphirine never forms individual grains and is only found as a constituent of the complex corona textures developed around the grains of Spl I, most of which being metamorphic in origin (see section on Metamorphic reactions). Therefore, we do not interpret sapphirine as magmatic, although it may be a liquidus phase in basic Al-rich bulk compositions (Liu & Presnall, 1990; Liu & Presnall, 2000). Corundum appears texturally equilibrated with metamorphic spinel and pyroxenes (Fig. 3c; see section 'Metamorphic reactions') and is hence not considered to be igneous even though it may also be a liquidus phase in basic Al-rich bulk compositions (Liu & Presnall, 1990; Liu & Presnall, 2000). Sillimanite and garnet form only reaction rims and are clearly of metamorphic origin.

In the Ca-Al hibonite-bearing granulites, hibonite and some spinel are the only phases that could be igneous relicts, hibonite in terms of composition and textures, spinel only texturally. The metamorphic transformation of the initial troctolitic assemblage *olivine* + *plagioclase* on cooling must have formed pyroxenes and spinel, as in the Mg-Al granulites (see section 'Metamorphic reactions'). Spinel grains intergrown with / rimmed by sillimanite are common in the studied specimens, although some of them may texturally represent relicts of the igneous stage. When hibonite is present together with spinel in such aggregates, spinel grains tend to localize on the border of hibonite grains and sometimes rim hibonite, whereas hibonite never rims spinel (see Fig. 5d and e and section 'Textures and mineral compositions'). Therefore, hibonite can be considered as the earliest mineral of the reaction sequence most likely to represent an igneous relict. The latter hypothesis is confirmed by experiments that show hibonite to be a liquidus phase in experimental systems relevant to Ca,Al-rich inclusions in chondrite meteorites (Drake & Boynton, 1988; Kennedy *et al*., 1994; Beckett & Stolper, 1994). Some hibonites from the liquidus experiments are markedly enriched in silica (up to 1.7 wt%) in spite of the strong silica undersaturation of the coexisting melt (Beckett & Stolper, 1994). This suggests that high silica contents (as in the studied hibonites, see Table 2) may be characteristic of igneous hibonite.

Hibonite in the studied xenoliths is characterized by significant chemical variations, particularly in Ti and REE. Hibonites with very low Ti contents may retain their pristine (igneous) chemical composition, whereas high-Ti hibonites were apparently reequilibrated during metamorphism (Ulianov *et al*., 2005).

THERMOBAROMETRIC CONSTRAINTS

In the Mg-Al sapphirine-bearing granulites, quartz is completely absent and thus no geobarometers based on Px-Pl-Grt-Qtz assemblages can be used. In the Ca-Al hibonite-bearing granulites, quartz is not equilibrated with garnet and plagioclase, thus excluding the application of Grt-An-Cpx-Qtz or Grt-An-Sil-Qtz geobarometers. Barometry based on the reaction Spl + Qtz = Grt + Sil (Bohlen *et al*., 1986; Nichols *et al*., 1992) is hampered by the lack of data on the equilibrium composition of garnet in the course of early metamorphism, to which

Table 4: P-T estimates for studied granulites

	Mg-Al sapphirine granulites		Ca-Al hibonite granulites		
	1904-7	1904-3	1904-1	1904-9	1906-2
Reintegrated core compositions of opx I in two-px granulites **P is fixed at 8 kbar**					
T Ca-in-opx (Brey & Köhler, 1990)	1135	1090			
Rim compositions of px II; px III **P is fixed at 8 kbar**					
T two-px solvus (Brey & Köhler, 1990)	730 (26)	585 (24)			
T two-px solvus (Wells, 1977)	753 (27)	688 (22)			
T Ca-in-opx (Brey & Köhler, 1990)	714 (28)	737 (29)			
T opx-grt (Harley, 1984)	784 (37)	740 (27)			
T grt-cpx (Krogh Ravna, 2000)	559 (42)	642 (27)	639[a]	725 (30)	741 (29)
T grt-cpx (Ai, 1994)	514 (41)	616 (30)	635[a]	731 (33)	730 (31)

Values in parentheses are uncertainties.
[a] garnet is completely altered to kelyphite, only one small inclusion in the outer mantle of a Cpx I grain survived.

which this reaction is relevant. Given the presence of sillimanite and the absence of kyanite or textures indicating growth of sillimanite at the expense of kyanite in the studied xenoliths, the *P-T* evolution of the granulites seems limited to the sillimanite stability field. We thus fixed a maximum pressure of 8 kbar for all temperature calculations.

For the Mg-Al granulite xenoliths, we calculated temperatures using the cores of Opx I with the exsolved lamellae of Cpx. We obtained estimates of 1090 and 1135 ºC with the Ca-in-Opx thermometer of Brey & Köhler (1990; Table 4). These temperatures probably correspond to an early stage of subsolidus cooling rather than to the magmatic crystallization of the protolith because the original composition of Opx I was modified by diffusion owing to mineral reequilibration on cooling. For the latest stage of equilibration recorded in the pyroxene rims and in the aggregates of Cpx III and Grt, the temperature estimates range widely from 514 to 784 ºC, depending on the geothermometer used (Table 4). Discrepancies between the estimates based on the two-pyroxene solvus and on the Fe-Mg exchange between Grt and Cpx may indicate either unreliability of solvus geothermometry in this range of temperatures, or differences in the diffusivities of Ca, Fe and Mg. In specimen 1904-7, where phases are poorly equilibrated in general, the discrepancies are especially pronounced.

For the Ca-Al granulite xenoliths, temperatures may be evaluated with confidence only for the latest stage of equilibration recorded in the pyroxene rims and in the aggregates of Cpx III and Grt. The estimates from two conventional Fe-Mg Cpx-Grt geothermometers (Ai, 1994; Krogh Ravna, 2000) are shown in Table 4. Almost no

discrepancies between these two geothermometers are observed. Specimens 1904-9 and 1906-2 are 'hotter' (725-741 °C) than specimen 1904-1 (635-639 °C).

METAMORPHIC REACTIONS IN THE Mg-Al SAPPHIRINE-BEARING GRANULITES

The major metamorphic features of these rocks that have to be explained are reaction domains A and B as well as the ubiquitous formation of garnet (see section 'Textures and mineral compositions').

Reaction domain A1: formation of worm-like clusters of Cpx + Crn rimming and often completely replacing Spl (Fig. 3a): Spinel Ia in the cores of the clusters is early and has reacted with enclosing plagioclase. Obviously, the sapphirine- and sillimanite-forming reactions of domain B (described below) could not initiate due to the absence of adjacent pyroxenes. Instead, the reaction Spl + Pl = Cpx + Crn took place (see Fig. 7). The lack of pyroxenes around Spl Ia grains may also suggests that these grains were not produced by the reaction Ol + Pl = Opx + Cpx + Spl but that they represent earlier, perhaps igneous relicts (see section 'Pre-metamorphic vs. metamorphic mineral assemblages'). Metamorphic Cpx-Crn aggregates formed by the reaction Spl + Pl = Cpx + Crn have to our knowledge not yet been described from localities elsewhere. Assemblages of Spl and Pl formed at the expense of Cpx and Crn are known from mafic rocks within the Horoman Peridotite complex (Morishita & Arai, 2001). The reaction Spl + Pl = Cpx + Crn in the CMAS system has been calculated by these authors at approximately 800°C at the pressures relevant here (8 kbar). In the Mg-Al granulites, it was crossed towards the low-temperature side (Cpx + Crn) upon cooling.

Reaction domain A2: Formation of pyroxenes and spinel (± corundum): There is little doubt that the coarse-grained, worm-like or symplectitic aggregates of Opx II, Cpx II and Spl Ib (Fig. 2a and 3b) were formed at the expense of the primary igneous assemblage *olivine + plagioclase*. Such Opx-Cpx-Spl textures are well documented from several localities (e.g. Tenthorey *et al.*, 1996; Müntener *et al.*, 2000; Montanini & Tribuzio, 2001). The reaction Ol + Pl = Opx + Cpx + Spl in the CMAS system is univariant and has been determined experimentally by many workers (Kushiro & Yoder, 1966; Herzberg, 1978; Gasparik, 1984a). The high-temperature assemblage Ol + Pl is stable at 1250-1300 ºC at relatively low pressures (ca. 8 kbar; Kushiro & Yoder, 1966). In the Mg-Al granulites, it was replaced by Opx + Cpx + Spl most likely during cooling after igneous crystallization. In Fig. 7, this reaction is shown schematically, because iron in natural systems, preferably accommodated by spinel, displaces the reaction to lower pressures, whereas sodium in plagioclase causes the opposite effect, with the additional chemical components making the reaction at least divariant.

The Opx-Cpx-Spl aggregates may contain corundum forming individual grains (Fig. 2a and 3c) and, less frequently, intergrowths with Spl I. Since no indications for the growth of corundum at the expense of pyroxenes or spinel (and *vice versa*) in these domains are observed, corundum seems to have formed in equilibrium with pyroxenes and spinel. This points to the reaction Ol + Pl = Cpx + Opx + Spl + Crn that replaces Ol + Pl = Cpx + Opx + Spl upon cooling provided the pressure is

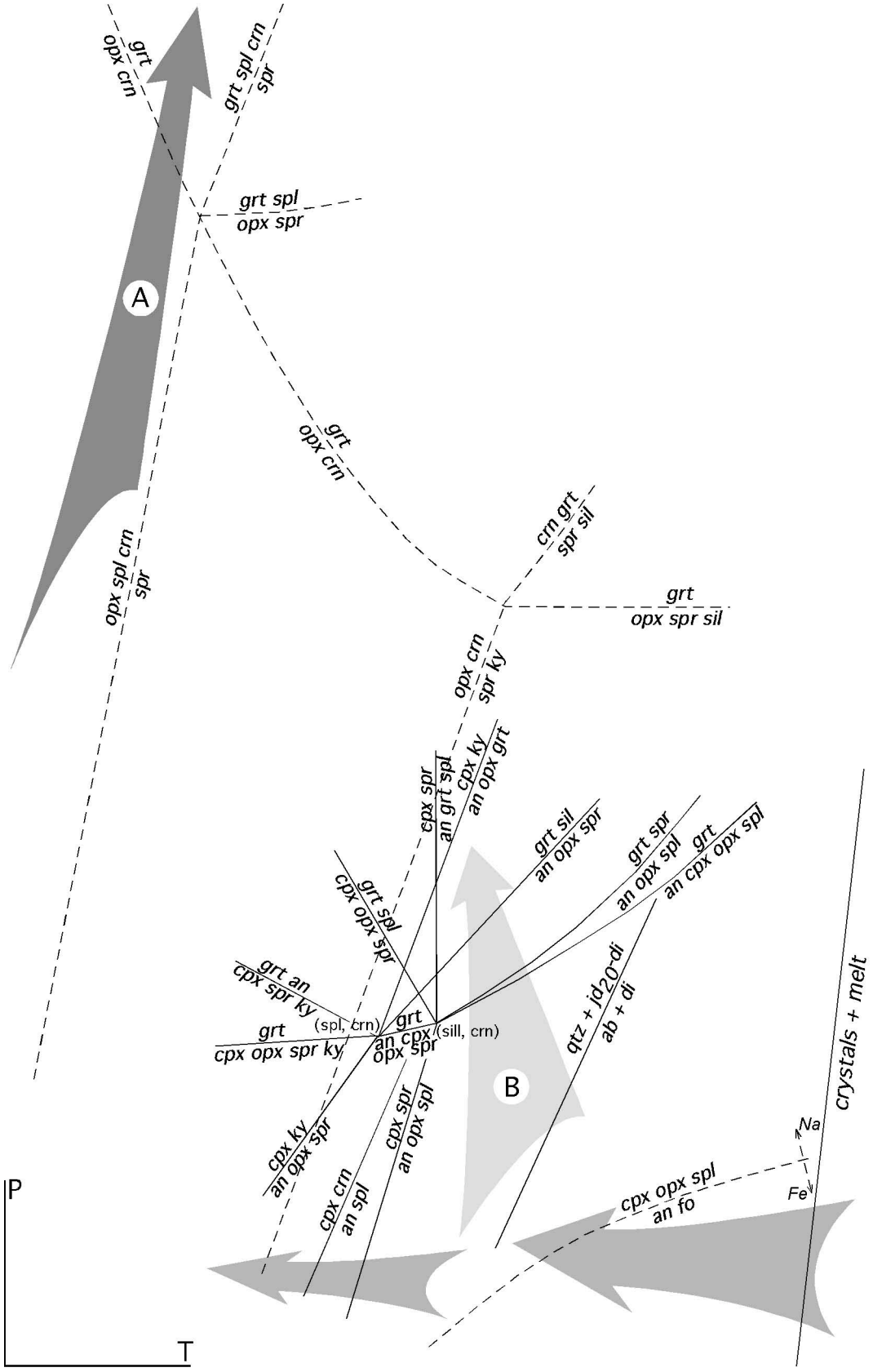


Fig. 7. Qualitative pressure-temperature diagram showing the inferred *P-T* path of the studied granulite xenoliths [Schreinemakers analysis for the CMAS and MAS systems after Christy (1989) and Ouzegane *et al*. (2003), respectively. Also shown are reactions: Spl + An = Crn + Di from Morishita & Arai (2001) and Ab + Cpx = Qtz + Jd_{20}-Cpx from Kushiro (1969)].

relatively low. To our knowledge, this reaction has been described neither from experiments nor from nature nor has it been calculated in any grid. It must, however, take place within the stability field of Opx + Crn that is limited to temperatures below approximately 850°C at the pressures of interest (ca. 8 kbar) in MAS grids (Gasparik, 2003; Ouzegane *et al*., 2003; Kelly & Harley 2004). The feasibility of this reaction for natural systems depends on the bulk chemical composition (e.g. Na and Fe contents) and its variations in local domains of the studied rocks that affects the stability of the assemblage Cpx + Opx + Spl + Crn in *P-T* space.

Reaction domain B. *Formation of sapphirine and sillimanite:* The sapphirine-sillimanite coronas on spinel I (Fig. 3d and e) occur only in cases where the initial spinel is situated near to both plagioclase and pyroxene. The key to the understanding of this texture is given by Fig. 3d and e. Although spinel I appears strongly resorbed by garnet, both sapphirine and sillimanite are present even on the smallest relicts of Spl I (Fig. 3d). This texture points to the co-crystallization of the assemblages Grt + Spr and Grt + Sil after spinel I, plagioclase and pyroxene. It argues against the formation of only sapphirine and sillimanite after spinel, with subsequent resorbtion of the resulting Spl-Spr-Sil coronas by garnet. A possible sequence of reactions during cooling, leading to the Spr-Sil-Grt corona textures after spinel, can be inferred from a Schreinemakers analysis in the CMAS system (Christy 1989; Fig. 7) as follows:

(1) An + Cpx + Opx + Spl = Grt and An + Opx + Spl = Grt + Spr,

(2) An + Opx + Spr = Grt + Sil.

Reactions (1), nearly degenerate, probably acted simultaneously and are responsible for sapphirine and garnet, whereas reaction (2) produced sillimanite and garnet once spinel was mantled by sapphirine and garnet. Reaction coronas similar to the ones described here are known in their fully developed forms only from Stockdale (Meyer & Brookins, 1976).

Reaction domain C. *Formation of garnet:* The occurrence of garnet in the corona textures with spinel, sillimanite and sapphirine (Fig. 3d and e) can be satisfactorily explained by the Schreinemakers diagram (Fig. 7), as discussed above. Garnet developed at the expense of corundum (Fig. 2a), can be attributed to the reaction Crn + Opx ± Cpx = Grt. The resorbtion of pyroxene grains located close to corundum by garnet can also be explained by this reaction. Garnet resorbing pyroxenes and spinel in reaction domains A (Fig. 3b) cannot have formed by the reaction Opx + Cpx + Spl = Grt as the latter requires additional silica in order to consume spinel. We speculate therefore that plagioclase participated in the reaction: Opx + Cpx + Spl + Pl = Grt (Gasparik, 1984a). The 'flaky' and massive zones of garnet or garnet and clinopyroxene propagating into and resorbing plagioclase (Fig. 2a) may also be explained by this reaction or by Opx + Spl + Pl = Grt + Cpx (Green & Ringwood, 1967) taking place simultaneously to the development of garnet in reaction domains A and B. Similar reaction zones of garnet after spinel, pyroxenes and plagioclase in metamorphosed metabasites have been described from many occurrences of mafic granulites throughout the world (e.g. Griffin, 1971; Irving, 1974; Indares & Rivers, 1995; Attoh, 1998; Indares, 2003), including meta-anorthosites and related rocks of E-NE Tanzania (Appel, 1996; Appel *et al*., 1998). Most of the above reactions can easily take place

during cooling, either isobaric or concomitant to / followed by compression, though only garnet-forming reaction Crn + Opx ± Cpx = Grt clearly necessitates compression (Fig. 7).

Although garnet seems generally stable and no textural evidence for its breakdown has been found, in specimen 1904-7 it may have started to decompose to the very end of the reaction path. A possible reaction (Pl + Grt = Cpx + Sil) involves also plagioclase and accounts for the formation of Cpx IV with its exceptional concentrations of Al (reaction domain D). Similar mineral relations are observed in sapphirine-bearing granulites from Stockdale (Meyer & Brookins, 1976).

It is worth stressing the importance of local chemical heterogeneities and additional chemical components in the studied rocks, which define the real dependence of the described mineral assemblages upon pressure and temperature. The key triggering the formation of spinel-sillimanite-sapphirine-garnet corona textures in reaction domains B instead of clinopyroxene-corundum aggregates A1 or pyroxene-spinel-garnet aggregates A2 is the availability of pyroxenes and plagioclase, respectively. Also, in the CMAS system, the well documented in the studied granulites reaction Pl + Ol = Cpx + Opx + Spl takes place at a maximum pressure of ca. 8 kbar at near-solidus temperature (Kushiro & Yoder, 1966; Gasparik, 1984a), but is displaced to lower pressures in Fe-rich compositions. Since the granulites are somewhat heterogeneous, the reaction does not take place in all reacting domains simultaneously and, on isobaric cooling, may proceed before the assemblage Crn + Opx + Cpx becomes stable. This appears to define the appearance of corundum in domains A2 (see above).

The MAS reaction Opx + Crn = Grt accounting for the formation of most garnet in the studied specimens lies at high pressures (>15 kbar in Fig. 7). However, the preferential enrichment of garnet in Fe displaces the reaction to lower pressures. Similarly, the reaction Opx + Spl + Crn = Spr limiting the stability field of the assemblage pyroxene-spinel-corundum from reaction domains A2 should be displaced to higher temperatures with increasing Fe content in spinel.

Obviously, the *P-T* evolution of reaction domains A (Px-Spl-Crn-Crt) is identical to that of domains B (Spl-Spr-Sil-Grt), and the metamorphic assemblages from both domains correspond to the same *P-T* path. The large mismatch in relative pressures and temperatures characterizing the metamorphic evolution of both domains in the MAS and CMAS petrogenetic grids shown in Fig. 7 is therefore not realistic and should disappear under the influence of additional chemical components (cf. Fig. 9 and 12 from Kelly & Harley, 2004, also illustrating the sensitivity of the simplified MAS and CMAS reactions to additional components). The overall *P-T* path of the Mg-Al granulites cannot be quantified but should be characterized by cooling, accompanied or followed by some compression.

METAMORPHIC REACTIONS IN THE Ca-Al HIBONITE-BEARING GRANULITES

The Ca-Al granulites correspond to troctolitic protoliths, with the normative abundances of olivine and plagioclase ranging from 95.3 to 98.7 %. Compared to the Mg-Al sapphirine-bearing granulites, they are less magnesian and more rich in Ca, Al and alkalies. They contain quartz, are relatively rich in clinopyroxene, whereas orthopyroxene is

absent. Xenoliths 1904-1 and 1904-9 bear hibonite that is probably a magmatic relict (see section 'Pre-metamorphic vs. metamorphic mineral assemblages'), whereas all other minerals, possibly with the exception of some spinel, were formed by subsolidus reactions. The major metamorphic features to be explained include:

(a) the mineral assemblage formed at the onset of metamorphism;

(b) the assemblage Qtz + Cpx I;

(c) the spinel I-sillimanite-garnet corona textures;

(d) the close association of corundum and Cpx II;

(e) the development of garnet at the expense of plagioclase and corundum;

(f) the association Spl II + Crn II enriched in Cr.

(a) Similarly to the Mg-Al granulites, the initial metamorphic mineral assemblage of the Ca-Al granulites may have been represented by pyroxenes, spinel and plagioclase formed at the expense of the igneous troctolitic assemblage *olivine + plagioclase*.

(b) The assemblage Qtz + Cpx I does not include any additional minerals. As plagioclase seems to have been stable throughout the entire evolution, a plausible explanation for this assemblage invokes the reaction Ab + Cpx = Qtz + Jd-Cpx. This continuous reaction first studied by Kushiro (1969) and subsequently considered by a number of researchers (see Anovitz, 1991 and references therein), has a positive *P-T* slope. Its isopleth for 20% of jadeite in clinopyroxene is shown in Fig. 7 relative to the CMAS simplified petrogenetic grid. Clinopyroxene I accommodates 14-19% jadeite and could thus have formed from plagioclase and a less Na-rich clinopyroxene by cooling and / or compression. At this stage, spinel from the initial metamorphic mineral assemblage (*a*) may have still been stable. Hibonite, of which the equilibrium assemblage with quartz is unknown in nature, may have been partially replaced by mullite and sillimanite.

(c) As temperature decreases and / or pressure increases, clinopyroxene I tends to accommodate more jadeite, until the competitive reaction Spl + Qtz = Sil + Grt is realized. The combined reaction Spl + Pl + Cpx I = Sil + Grt + Cpx II replaces Ab + Cpx = Qtz + Jd-Cpx. It is inferred to be responsible for both the sillimanite-garnet coronas after spinel I (Fig. 5c) and clinopyroxene II forming independent grains and mantling the Cpx I-Qtz cores (Fig. 2c and 5a). Similar mineral relations, although rather unusual for granulites in general, are known from granulite-facies rocks of the Parautochtonous Belt, Grenville (Indares & Rivers, 1995).

(d) The assemblage Crn + Cpx II (Fig. 2c) is consistent with the reaction Spl + Pl = Crn + Cpx, as observed in the Mg-Al granulite xenoliths (see previous section and Fig. 7). Since corundum is unstable with quartz under a vast range of metamorphic conditions (e.g. Shulters & Bohlen, 1989), this assemblage must be considered to have formed late with respect to quartz, when the latter had already been isolated in the core parts of the complexly formed grains of clinopyroxene I-II. The lack of orthopyroxene in this assemblage is probably due to temperatures too high to stabilize the assemblages Opx + Crn and Opx + Crn + Spl (see Fig. 7).

(e) The 'flaky' and massive zones of garnet or garnet and clinopyroxene propagating and resorbing plagioclase (Fig. 2c and 5a) are inferred to have formed from the reactions Di-Cpx + Spl + Pl = Grt and Di-Cpx + Spl + Pl = Grt + Tsch-rich

Cpx analogous to the reactions Cpx + Opx + Spl + Pl = Grt and Opx + Spl + Pl = Grt + Cpx in the Mg-Al granulites. Petrographically, garnet developed at the expense of corundum (Fig. 2c and 5f) can definitely be attributed to the reactions Cpx + Crn = Grt, as well as the resorbtion by garnet of those pyroxene grains that are located close to corundum. Similarly to the reaction Opx + Crn = Grt, this garnet-forming reaction is characterized by a negative *dP/dT* slope (Gasparik, 1984b) and may become operative during the course of metamorphic compression.

(f) The association Spl II + Crn II can be explained by the reaction Crn + Grt = Spl + Sil, again in good agreement with the petrography (Fig. 5f). Unusually high Cr contents in spinel II seem to stabilize the assemblage Spl + Sil at relatively high pressures and low temperatures that are inconsistent with its stability field in Cr-free system (e.g. Shulters & Bohlen, 1989).

In summary, the reaction textures observed in the Ca-Al granulites are consistent with cooling accompanied or followed by compression during the formation of garnet at the expense of corundum and clinopyroxene.

MINERAL ZONING AS INDICATOR OF THE METAMORPHIC EVOLUTION

In the Mg-Al sapphirine-bearing granulites, considerable chemical zonation is found in pyroxenes only (Fig. 4a-f). Opx I shows a rimwards decrease in Al, Ca and Na (Fig. 4a). Since the reaction Ol + Pl = Opx + Cpx + Spl ± Crn takes place at relatively high temperature, Opx I should equilibrate with clinopyroxene, spinel, and plagioclase. The Al content in Opx equilibrated with Spl and Pl is controlled by both pressure and temperature (Gasparik, 1984a; Berchova, 1996), whereas the Ca and Na contents in the case of equilibration with clinopyroxene are controlled chiefly by temperature (Brey & Köhler, 1990; Berchova, 1996). The concentrations of these elements decrease with the decrease of temperature. Thus, we suggest that cooling is mainly responsible for the observed chemical zonation in Opx I. Opx II is either nearly homogeneous (sp. 1904-3; Fig. 4b) or shows different patterns in the same textural context, indicating poor equilibration (sp. 1904-7; Fig. 4c and d).

Cpx II in the Mg-Al sapphirine-bearing granulites shows either a rimwards increase in the Al content (sp. 1904-3; Fig. 4e) or varying zoning patterns indicative of poor equilibration (sp. 1904-7; Fig. 4f). The largest grains of Cpx II are always characterized by plateaus in the core. It is therefore inferred that these grains record early metamorphic stabilization possibly corresponding to the reaction Ol + Pl = Cpx + Opx + Spl ± Crn during post-magmatic cooling / compression. Their further history involves the diopside and enstatite-consuming reactions Pl + Cpx + Opx + Spl = Grt and Cpx + Opx + Crn = Grt that cause the observed enrichment in Al and Na (Figs. 4e and f).

In the Ca-Al hibonite-bearing granulites, only Cpx II and Crn associated with Spl II show considerable zoning. In Cpx II, all available profiles are characterized by a rimwards increase in Al content that, however, tends to decrease again within the 20 μm outermost rim (Fig. 6a-e). Normally, the largest Cpx II grains have an Al plateau in the core (Fig. 6a and b). They are interpreted to record the reaction Spl + Ab + Cpx I = Sil + Grt + Cpx II in the course of early cooling and/or compression. Their subsequent history, similarly to

clinopyroxene from the Mg-Al granulites, involves the reactions Pl + Cpx + Spl = Grt and Cpx + Crn = Grt that consume the diopside component in clinopyroxene and cause its enrichment in the Tschermak and jadeite components (Fig. 6a-e).

In both Mg-Al and Ca-Al granulites, the Mg# in clinopyroxene increases rimwards. This is consistent with cooling in the presence of garnet, when clinopyroxene preferentially accommodates Mg, while garnet – Fe^{2+} (e.g. Ai, 1994; Krogh Ravna, 2000). In both rock types, the reaction Di + Ab + Spl = Sil + Grt + Jd-Di appears to have progressed in the reversed direction at the very end of the reaction path. More diopside-rich clinopyroxene (Al and Na decrease at the outermost rims of Cpx II in Fig. 6a-e), Na-rich plagioclase (thin Pl mantles around clinopyroxene) and 'secondary' spinel (thin rims of Spl II mantling sillimanite in the Spl-Sil-Grt corona textures) were formed. These indications of late retrogression are minor.

DISCUSSION

P-T path of the granulites and its geodynamic significance

The geothermometric estimates for the Mg-Al sapphirine-bearing granulites suggests cooling from near-solidus temperatures of at least 1090-1135 ºC to 514-784 ºC. The metamorphic reaction path is consistent with cooling associated with or followed by compression, the latter resulting in the development of garnet at the expense of mafic minerals, plagioclase and corundum. The sequence of reactions observed in the Ca-Al hibonite-bearing granulites is also consistent with subsolidus cooling down to approximately 640-740 °C and compression.

The observed reaction sequence and available *P-T* estimates do not allow us to evaluate the *P-T* trend of the studied granulites at the end of their *P-T* path, since no convincing petrographic evidence on their retrograde evolution exists. In contrast to exposed granulites where both clockwise and anticlockwise anticlockwise *P-T* paths are often characterized by pronounced decompression in the course of tectonic exhumation, no indications of this stage are found in our samples. The lack of hydrous minerals also argues against considerable retrogression.

Nevertheless, the inferred reaction sequence leading to the formation of sapphirine-sillimanite-garnet coronas on spinel (reaction domain B) and aggregates of Tschermak-rich clinopyroxene and sillimanite (reaction domain D) in the Mg-Al granulites may hint towards an anticlockwise *P-T* evolution (see section 'Metamorphic reactions' and Fig. 7). This mode of evolution accords with the detailed results of Appel *et al.* (1998) and Möller *et al.* (1998) on the Pan-African granulite terranes of E-NE Tanzania (Pare, Usambara and Uluguru mountains) situated S-SW of the Chyulu Hills (Fig. 1). For metasedimentary and meta-igneous granulites from these localities, Appel *et al.* (1998) propose an anticlockwise *P-T* path with the peak conditions of approximately 810°C and 9.5-11 kbar. As the cause of the granulite metamorphism, these authors and Möller *et al.* (2000) put forward a model of magmatic underplating in the environment of juvenile arc terranes forming the Mozambique belt in Pan-African times.

This model is in good agreement with the fact that the studied samples represent a former igneous suite. The inferred metamorphic reaction path associated with compression also accords with the

geochemical and petrographic characteristics of websterite xenoliths from the studied cumulate sequence. The geochemical features of the websterites, such as positive Eu anomalies and elevated Ni abundances, suggest plagioclase- and olivine-rich gabbroic protoliths and thus shallow-level plagioclase accumulation. At the same time, their actual mineral assemblages (pyroxenes, spinel, garnet and olivine) correspond to upper mantle pressures and temperatures (18-22 kbar / 927-1007 ºC for most specimens, see Ulianov *et al*., submitted). For reconciling this apparent contradiction, Ulianov *et al*. (submitted) favored a model of compression by foundering of dense lower crustal material into the mantle, probably towards the end of Pan-African subduction and accretion (Ulianov *et al*., submitted). Such a process is possible in areas with high geothermal gradients such as arcs (Jull and Kelemen 2001) and is observed today in the southern Sierra Nevada (Ducea 2001; Boyd et al. 2004; Zandt et al. 2004).

Mineral assemblages and their petrogenetic significance

Meta-igneous granulites rich in Mg, Al and Ca, such as the xenoliths from this study, are rare. Of all the xenolith localities studied, the *P-T* path responsible for the observed mineralogy has been specified only for Kerguelen (Grégoire *et al*., 1998). For the Stockdale and Delegate granulites, the reaction sequences and possible *P-T* paths were reviewed by Christy (1989) on the basis of a CMAS petrogenetic grid developed for the assemblage Cpx + Opx + Pl + Spr + Sil + Grt. All these paths are largely defined by cooling. In contrast, the mafic sapphirine-bearing granulites from metamorphic terranes, with the exception of Fiordero (Christy, 1989), demonstrate decompression-dominated reaction sequences and *P-T* paths, in which sapphirine occurs in symplectitic intergrowths with plagioclase found after kyanite (Johansson & Möller, 1986; Carswell *et al*., 1989; Christy, 1989; Grant, 1989; Möller, 1999).

The Mg-Al sapphirine-bearing granulite xenoliths have similarities with granulite xenoliths from the Stockdale kimberlite in Kansas (Meyer & Brookins, 1976). Except for the lack of corundum, their phase assemblage is the same and there are clear similarities in mineral chemistry. The Spl-Spr-Sil-Grt corona textures described from Stockdale are similar to ours and were interpreted as indicating a cooling-dominated metamorphic path (Christy, 1989).

The Ca-Al hibonite-bearing granulites are unique, both due to the geochemical pattern and mode of formation of hibonite unusual for its terrestrial occurrences and to the uncommon metamorphic reaction sequence observed in the host rocks. The studied hibonite is very poor in La, Ce, Th and Y. These low abundances are rather uncommon for terrestrial hibonites, since the latter, except for one locality (Punalur, India), are enriched in LREE and Th (Maaskant *et al*., 1980; Santosh *et al*., 1991; Rakotondrazafy *et al*., 1996). Low concentrations of La, Ce, Th and Y are typical, however, for hibonite from meteorites (e.g. Fahey *et al*., 1987). Si is higher than in any other terrestrial hibonite. All known terrestrial (Yakovlevskaya, 1961, Maaskant *et al*., 1980, Sandiford & Santosh, 1991, Rakotondrazafy *et al*., 1996) and extraterrestrial occurrences (e.g. Fahey *et al*., 1987) represent strongly silica-undersaturated lithologies. In the studied case, however, the rocks are not highly depleted in silica, resulting in modal

quartz formed in the course of metamorphism. Thus, strong Si-undersaturation is not universal for hibonite-bearing rocks. In all known terrestrial occurrences, hibonite is considered as metamorphic (possibly metasomatic) mineral. In the studied case, it seems to represent magmatic relict (see section 'Pre-metamorphic vs. metamorphic mineral assemblages'). The studied mullite represent the first finding of 2:1 mullite in nature. Synthetic mullite of such composition is common (e.g. Angel & Prewitt, 1986; Angel *et al*., 1991). Mullite from natural localities, however, is always more Si-rich, i.e. intermediate between the 3:2 and 2:1 types (Deer *et al*., 1982; Preston *et al*., 1999).

The early reaction sequence inferred from these granulites is rather uncommon. It is essentially based on the equilibria Ab + Cpx = Qtz + Jd-Cpx and Spl I + Qtz = Sil + Grt. Quartz seems arrested in the cores of clinopyroxene I and is not equilibrated with garnet. Corundum forms instead. Thus, despite being formally 'orthopyroxene-free garnet+clinopyroxene+quartz metabasites' these rocks deviate from the paragenetic definition and reaction model (based on the prograde equilibria Opx + Pl = Grt + Cpx + Qtz) for common representatives of this rock family (see O'Brien & Rötzler, 2003; Pattison, 2003).

In a more general sense, it is worth emphasizing that the studied granulites preserve high-temperature textures (especially the Spl-Cpx-Opx symplectitic intergrowth in the Mg-Al sapphirine-bearing and Qtz-Cpx I intergrowth in the Ca-Al hibonite-bearing granulites). At the same time, they show (almost) no petrographic evidence of retrograde evolution.

SUMMARY AND CONCLUSIONS

Together with spinel-garnet websterites entrained from the lithospheric mantle, the Mg-Al sapphirine-bearing and Ca-Al hibonite-bearing granulites from the Chyulu Hills volcanic field, Kenya represent a former igneous suite of gabbroic to troctolitic cumulates (Ulianov *et al*., submitted). All olivine has been removed by subsolidus reactions and plagioclase was texturally and compositionally modified in the course of metamorphism. Relicts of the igneous stage in the Mg-Al granulites may include calcium-rich orthopyroxene and some spinel. Geothermometric calculations based on the Ca contents in early orthopyroxene give a minimum estimate of 1090-1135 °C. In the Ca-Al granulites, hibonite and possibly some spinel are texturally the oldest minerals in the crystallization sequence, possibly igneous relicts.

The igneous minerals have, to a large degree, been replaced by metamorphic assemblages. Geothermobarometric estimates for metamorphic parageneses indicate cooling from (near) igneous temperatures down to conditions of ca. 600-740 °C. The observed reaction sequence is consistent with cooling accompanied or followed by compression. The distinctive reaction textures include Cpx-Opx-Spl(±Crn) intergrowths replacing igneous olivine and plagioclase and Crn-Cpx symplectites after spinel and plagioclase in the Mg-Al granulites, quartz-diopside intergrowths formed at the expense of early plagioclase and clinopyroxene in the Ca-Al granulites as well as the prominent corona textures observed in both rock types. All of these textures seem to have been acquired at granulite-facies conditions.

In a more general context, the studied granulite xenoliths have few direct analogues in both

xenolith suites and granulite terranes. The Mg-Al granulites are most comparable with granulite xenoliths from the Stockdale kimberlite in Kansas (Meyer & Brookins, 1976). The Ca-Al hibonite-bearing granulites are unique with respect to textures, whole rock composition and compositions of hibonite and mullite. Both rock types enlarge the spectrum of known Ca-Al-Mg rich granulites and contribute to the general understanding of reaction sequences in the CMAS system at granulite-facies conditions.

ACKNOWLEDGEMENTS

Hans-Peter Meyer and Edwin Gnos are thanked for assistance with electron microprobe analysis. Rainer Altherr is thanked for discussion and critical comments on the manuscript. We are grateful to Simon Harley and Tomoaki Morishita for their detailed and constructive reviews that helped us to significantly improve the earlier version of this paper, and Marjorie Wilson for her valuable comments and editorial handling of the manuscript. Permission and help for field sampling provided by the Office of the President, Kenya Wildlife Service, and the Kenya Agricultural Research Institute in Kiboko are gratefully acknowledged. Field work was financially supported by the Deutsche Forschungsgemeinschaft within the frame of the Collaborative Research Center 108 (SFB 108) at the University of Karlsruhe. The research was supported by the Swiss National Science Foundation grant 200021-100647/1.

REFERENCES

Altherr, R., Garasic, V., Ulianov, A. & Kalt, A. Composition and thermal evolution of the lithospheric mantle beneath the Chyulu Hills (Southern Kenya, East African Rift) as deduced from xenoliths. Submitted to *Journal of Petrology*.

Ai, Y. (1994). A revision of the garnet-clinopyroxene Fe^{2+}-Mg exchange geothermometer. *Contributions to Mineralogy and Petrology* **115**, 467-473.

Angel, R. J. & Prewitt, C. T. (1986). Crystal structure of mullite: a reexamination of the average structure. *American Mineralogist* **71**, 1472-1482.

Angel, R. J., McMullan, R. K. & Prewitt, C. T. (1991). Substructure and superstructure of mullite by neutron diffraction. *American Mineralogist* **76**, 332-342.

Anovitz, L. M. (1991). Al zoning in pyroxene and plagioclase: window on late prograde to early retrograde *P-T* path in granulite terranes. *American Mineralogist* **76**: 1328-1343.

Appel, P. (1996). Hochdruckgranulite und Eklogite im Mozambique Belt von Tanzania: eine petrologische und geochemische Studie. Dissertation, Christian-Albrechts-Universität Kiel, Germany.

Appel, P., Möller, A. & Schenk, V. (1998). High-pressure granulite facies metamorphism in the Pan-African belt of eastern Tanzania: *P-T*-t evidence against granulite formation by continent collision. *Journal of Metamorphic Geology* **16**, 491-509.

Attoh, K. (1998). Models for orthopyroxene-Plagioclase and other corona reactions in metanorites, Dahomeyide orogen, West Africa. *Journal of Metamorphic Geology* **16**, 345-362.

Beckett, J. R. & Stolper, E. (1994). The stability of hibonite, melilite and other aluminous phases in

silicate melts: implications for the origin of hibonite-bearing inclusions from carbonaceous chondrites. *Meteoritics*, **29**, 41-65.

Bell, K. & Dodson, M. H. (1981). The geochronology of the Tanzanian Shield. *Journal of Geology* **89**, 109-128.

Bhattacharya, S. & Kar, R. (2002). High-temperature dehydration melting and decompressive *P-T* path in a granulite complex from the Eastern Ghats, India. *Contributions to Mineralogy and Petrology* **143**, 175-191.

Bohlen, S. R. (1987). Pressure-temperature-time path and a tectonic model for the evolution of granulites. *Journal of Geology* **95**, 617-632.

Bohlen, S. R. (1991). On the formation of granulites. *Journal of Metamorphic Geology* **9**, 223-229.

Bohlen, S. R., Dollase, W. A. & Wall, V. J. (1986). Calibration and applications of spinel equilibria in the system FeO-Al_2O_3-SiO_2. *Journal of Petrology* **27**, 1143-1156.

Boyd, O. S., Craig, H. J. & Sheehan, A. F. (2004). Foundring lithosphere imaged beneath the southern Sierra Nevada. *Science* **305**, 660-662.

Brey, G. P. & Köhler, T. (1990). Geothermobarometry in four-phase lherzolites II. New thermobarometers, and practical assessment of existing thermobarometers. *Journal of Petrology* **31**, 1353-1378.

Cahen, L., Snelling, N. J., Delhal, J. & Vail, J. R. (1984*). The geochronology and evolution of Africa*. Oxford: Clarendon Press, 512 pp.

Cameron, W. E. (1977). Mullite: a substituted alumina. *American Mineralogist* **62**, 747-755.

Carswell, D. A. (1975). Primary and secondary phlogopites in garnet lherzolite xenoliths. *Physics and Chemistry of the Earth* **9**,417-430.

Carswell, D. A., Möller, C. & O'Brien, P. J. (1989). Origin of sapphirine-plagioclase symplectites in metabasites from Mitterbachgraben, Dunkelsteinerwald granulite complex, Lower Austria. *European Journal of Mineralogy* **1**, 455-466.

Christy, A. G. (1989). The stability of sapphirine+clinopyroxene: implications for phase relations in the CaO-MgO-Al_2O_3-SiO_2 system under deep-crustal and upper mantle conditions. *Contributions to Mineralogy and Petrology* **102**, 422-428.

Coolen, J. J. M. M. M., Priem, H. N. A., Verdurmen, E. A. T. & Verschure, R. H. (1982). Possible zircon U-Pb evidence for Pan-African granulite-facies metamorphism in the Mozambique Belt of southern Tanzania. *Precambrian Research* **17**, 31-40.

Dawson, J. B. (1977). Sub-cratonic crust and upper mantle models based on xenolith suites in kimberlite and nephelinitic diatremes. *Journal of the Geological Society, London* **134**, 173-184.

Dawson, J. B., Harley S. L., Rudnick R. L. & Ireland T. R. (1997). Equilibration and reaction in Archean quartz-sapphirine granulite xenoliths from the Lace kimberlite pipe, South Africa. *Precambrian Research* **104**, 123-146.

Deer, W. A., Howie, R. A. & Zussman, J. (1982). Rock-forming minerals. Volume 1A: orthosilicates, pp. 742-758. Longman Group Ltd, London – New York.

Downes, H. (1993). The nature of the lower continental crust of Europe: petrological and geo-

chemical evidence from xenoliths. *Physics of the Earth and Planetary Interiors* **79**, 195-218.

Downes, H., Dupuy, C. & Leyreloup, A. F. (1990) Crustal evolution of the Hercynian belt of western Europe: evidence from lower-crustal granulitic xenoliths (French Massif Central). *Chemical Geology* **83**, 209-231.

Drake, M. J. & Boynton, W. L. (1988). Partitioning of rare earth elements between hibonite and melt and implications for nebular condensation of the rare earth elements. *Meteoritics* **23**, 75-80.

Ducea, M. N. (2001). The California arc: thick granitic batholiths, eclogitic residues, lithospheric-scale thrusting, and magmatic flare-ups. *GSA Today* **11**, 4-10.

Evans, R. J., Ashwal, L. D. & Hamilton, M. A. (1999). Mafic, ultramafic, and anorthositic rocks of the Tete Complex, Mozambique: petrology, age, and significance. *South African Journal of Geology* **102**, 153-166.

Fahey, A. J., Goswani, J. N., McKeegan, K. D. & Zinner, E. (1987). ^{26}Al, ^{244}Pu, ^{50}Ti, REE and trace element abundances in hibonite grains from CM and CV meteorites. *Geochimica et Cosmochimica Acta* **51**, 329-350.

Gasparik, T. (2003). Phase diagrams for geoscientists: An atlas of the Earth's interior. Springer-Verlag, 462 pp.

Gasparik, T. (1984a). Two-pyroxene thermobarometry with new experimental data in the system CaO-MgO-Al_2O_3-SiO_2. *Contributions to Mineralogy and Petrology* **87**, 87-97.

Gasparik, T. (1984b). Experimental determined stability of clinopyroxene + garnet + corundum in the system CaO-MgO-Al_2O_3-SiO_2. American Mineralogist **69**, 1025-1035.

Gichile, S. (1992). Granulites in the Precambrian basement of southern Ethiopia: geochemistry, *P-T* conditions of metamorphism and tectonic setting. *Journal of African Earth Sciences* **15**, 251-263.

Grant, S. M. (1989). Tectonic implications from sapphirine-bearing lithologies, south-west Grenville Province, Canada. *Journal of Metamorphic Geology* **7**, 583-598.

Grégoire, M., Cottin, J. Y., Giret, A., Mattielli, N. & Weis, D. (1998). The meta-igneous granulite xenoliths from Kerguelen Archipelago: evidence of a continent nucleation in an oceanic setting. *Contributions to Mineralogy and Petrology* **133**, 259-283.

Green, D. H. & Ringwood, A. E. (1967). An experimental investigation of the gabbro to eclogite transformation and its petrologic application. *Geochimica et Cosmochimica Acta* **3**, 767-834.

Griffin, W. L. (1971). Genesis of coronas in anorthosites of the Upper Jotun Nappe, Indre Song, Norway. *Journal of Petrology* **12**, 219-243.

Griffin, W. L. & O'Reilly, S. Y. (1986). Mantle-derived sapphirine. *Mineralogical Magazine* **50**, 635-640.

Harley, S. L. (1984). An experimental study of the partitioning of Fe and Mg between garnet and orthopyroxene. *Contributions to Mineralogy and Petrology* **86**, 359-73.

Harley, S. L. (1989). The origin of granulites: a metamorphic perspective. *Geological Magazine* **126(3)**, 215-247.

Haug, G. H., Strecker, M. R. (1995). Volcano-tectonic evolution of the Chyulu Hills and implication for the regional stress field in Kenya. *Geology* **23**, 165-168.

Henjes-Kunst, F. & Altherr, R. (1992). Metamorphic petrology of xenoliths from Kenya and Northern Tanzania and implications for geotherms and lithospheric structure. *Journal of Petrology* **33**, 1125-1156.

Herzberg, C. T. (1978). Pyroxene geothermometry and geobarometry: experimental and thermodynamic evaluation of some subsolidus phase relations involving pyroxenes in the system CaO-MgO-Al_2O_3-SiO_2. *Geochimica et Cosmochimica Acta* **42**, 945-957.

Holmes, A. (1951). The sequence of Precambrian orogenic belts in south and central Africa. *Proceedings of the 18th International Geological Congress, Vol. 14*. London: Assoc. Seros. Geol. Afr., pp. 254-269.

Huang, Y.-M., Van Calsteren, P. & Hawkesworth, C. J. (1995). The evolution of the lithosphere in southern Africa: a perspective on the basic granulite xenoliths from kimberlites in South Africa. *Geochimica et Cosmochimica Acta* **59**, 4905-4920.

Indares, A. D. (2003). Metamorphic textures and *P-T* evolution of high-P granulites from the Lelukuau terrane, NE Grenville Province. *Journal of Metamorphic Geology* **21**, 35-48.

Indares, A. D. & Rivers, T. (1995). Textures, metamorphic reactions and thermobarometry of eclogitized metagabbros: a Proterozoic example. *European Journal of Mineralogy* **7**: 43-56.

Irving, A. J. (1974). Geochemical and high pressure experimental studies of garnet pyroxenite and pyroxene granulite xenoliths from the Delegate basaltic pipes, Australia. *Journal of Petrology* **15**, 1-40.

Jan, M. Q. & Howie, R. A. (1981). The mineralogy and geochemistry of the metamorphosed basic and ultrabasic rocks of the Jijal complex, Kohistan, NW Pakistan. *Journal of Petrology* **22(1)**, 85-126.

Johansson, L. & Möller C. (1986). Formation of sapphirine during retrogression of a basic high-pressure granulite, Roan, Western Gneiss Region, Norway. *Contributions to Mineralogy and Petrology* **94**, 29-41.

Jones, A. P., Smith, J. V., Hansen, E. C. & Dawson, J. B. (1983). Metamorphism, partial melting and K-metasomatism of garnet-scapolite-kyanite granulite xenoliths from Lashaine, Tanzania. *Journal of Geology* **91**, 143-165.

Jull, M. & Kelemen, P. B. (2001) On the conditions of lower crustal convective instability. *Journal of Geophysical Research* **106**, 6423-6446.

Kelly, N. M. & Harley, S. L. (2004) Orthopyroxene-corundum in Mg-Al-rich granulites from the Oygarden Islands, East Antarctica. *Journal of Petrology* **45**, 1481-1512.

Kempton, P. D., Downes H., Neymark L. A., Wartho J. A., Zartman, R. E. & Sharkov E. V. (2001). Garnet granulite xenoliths from the Northern Baltic Shield—the underplated lower crust of a palaeoproterozoic large igneous province? *Journal of Petrology* **42**, 731-763.

Kempton, P. D., Harmon, R. S., Hawkesworth C. J. & Moorbath S. (1990). Petrology and geochemistry of lower crustal granulites from the Geronimo Volcanic Field, southern Arizona. *Geochimica et Cosmochimica Acta* **54**, 3401-3426.

Kennedy, A. K., Lofgren, G. E. & Wasserburg, G. J. (1994). Trace-element partition coefficients

for perovskite and hibonite in meteorite compositions. *Chemical Geol*ogy **117**, 379-390.

Kebede, T., Kloetzli U. S. & Koeberl, C. (2001). U/Pb and Pb/Pb zircon ages from granitoid rocks of Wallagga area: constraints on magmatic and tectonic evolution of Precambrian rocks of western Ethiopia. *Mineralogy and Petrology* **71**, 251-271.

Key, R. M., Charsley, T. J., Hackman, B. D., Wilkinson, A. F. & Rundle, C. C. (1989). Superimposed Upper Proterozoic collision-controlled orogenies in the Mozambique Orogenic Belt of Kenya. *Precambrian Research* **44**, 197-225.

Kretz, R. (1983). Symbols for rock-forming minerals. *American Mineralogist* **68**, 277-279.

Kriegsman, L. M. & Schumacher, J. C. (1999). Petrology of sapphirine-bearing and associated granulites from central Sri Lanka. *Journal of Petrology* **40**, 1211-1239.

Krogh Ravna, E. (2000). The garnet-clinopyroxene Fe-Mg geothermometer: an updated calibration. *Journal of Metamorphic Geology* **18**, 211-219.

Kröner, A., Greiling, R., Reischmann, T., Hussein, I.M., Stern, R. J., Dürr, S., Krüger J. & Zimmer, M. (1987). Pan-African crustal evolution in the Nubian segment of northeast Africa. In: Kröner, A. (ed.) *Proterozoic Lithospheric Evolution*. American Geophysical Union, Washington, DC, Geodynamic Series **17**, 235-257.

Kröner, A., Muhongo, S., Hegner, E. & Wingate, M. T. D. (2003). Single zircon geochronology and Nd isotopic systematics of Proterozoic high-grade rocks from the Mozambique belt of southern Tanzania (Masasi area): implications for Gondwana assembly. *Journal of the Geological Society, London* **160**, 745-758.

Kushiro, I. (1969). Clinopyroxene solid solutions formed by reaction between diopside and plagioclase at high pressures. *Mineralogical Society of America, Special Paper* **2**, 179-191.

Kushiro, I. & Yoder, H. S. (1966). Anorthite-forsterite and anorthite-enstatite reactions, and their bearing on the basalt-eclogite transformation. *Journal of Petrology* **7**, 337-362.

Lensch, G. (1971). Das Vorkommen von Sapphirin im Peridotitkörper von Finero (Zone von Ivrea, Italienische Westalpen). *Contributions to Mineralogy and Petrology* **31**, 145-153.

Lui, I. C. & Presnall, D. C. (1990). Liquidus phase relations in the join anorthite-forsterite-quartz at 20 kbar with applications to basalt petrogenesis and igneous sapphirine. *Contributions to Mineralogy and Petrology* **104**, 735-742.

Liu, I. C. & Presnall, D. C. (2000). Liquidus phase relations in the system CaO-MgO-Al_2O_3-SiO_2 at 2.0 GPa: applications to basalt fractionation, eclogites and igneous sapphirine. *Journal of Petrology* **41**, 3-20.

Maaskant, P., Coolen, J. J. M. & Burke, E. A. J. (1980). Hibonite and coexisting zoisite and clinozoisite in a calc-Silicate granulite from southern Tanzania. *Mineralogical Magazine* **43**, 995-1003.

Meert, J. G. (2003). A synopsis of events related to the assembly of eastern Gondwana. *Tectonophysics*, **362**, 1-40.

Meyer, H. O. A. & Brookins, D. G. (1976). Sapphirine, sillimanite and garnet in granulite xenoliths from Stockdale kimberlite, Kansas. *American Mineralogist* **61**, 1194-1202.

Möller, A., Appel, P., Mezger, K. & Schenk, V. (1995). Evidence for a 2 Ga subduction zoned: eclogites in the Usaragan Belt of Tanzania. *Geology* **23**, 1067-1070.

Möller, A., Mezger, K. & Schenk, V. (1998). Crustal age domains and the evolution of the continental crust in the Mozambique Belt of Tanzania: Combined Sm-Nd, Rb-Sr and Pb-Pb isotopic evidence. *Journal of Petrology* **39**, 749-783

Möller, A., Mezger, K. & Schenk, V. (2000). U-Pb dating of metamorphic minerals: Pan-African metamorphism and prolonged slow cooling of high pressure granulites in Tanzania, East Africa. *Precambrian Research* 104: 123-146.

Möller, C. (1999). Sapphirine in SW Sweden: a record of Sveconorwegian (-Grenvillian) late-orogenic tectonic exhumation. *Journal of Metamorphic Geology* **17**, 121-141.

Montanini, A. & Tribuzio, R. (1996). Gabbro-derived granulites from the northern Apennines (Italy): evidence for lower-crustal emplacement of tholeiitic liquids in Post-Variscan Times. *Journal of Petrology* **42**, 2259-2277.

Morishita, T. & Arai, S. (2001). Petrogenesis of corundum-bearing mafic rocks in the Horoman Peridotite complex, Japan. *Journal of Petrology* 42, 1279-1299.

Muhongo, S. M., Kröner, A. & Nemchin, A. A. (2001). Zircon ages from granulite facies rocks in the Mozambique belt of Tanzania and implications for Gondwana assembly. *Journal of Geology* **109**, 171-189.

Muhongo, S. M. & Lenoir, J.-L. (1994). Pan-African granulite-facies metamorphism in the Mozambique belt of Tanzania: U-Pb zircon geochronology. *Journal of the Geological Society, London* **151**, 343-347.

Müntener, O., Hermann, J. & Trommsdorff, V. (2000). Cooling history and exhumation of lower crustal granulites and upper mantle (Malenco, Eastern Central Alps). *Journal of Petrology* **41**, 175-200.

Nichols, G. T., Berry, R. F. & Green, D. H. (1992). Internally consistent gahnitic spinel-cordierite-garnet equilibria in the FMASHZn system: geothermobarometry and applications. *Contributions to Mineralogy and Petrology* **111**, 362-377.

Novak, O., Ritter, J. R. R., Altherr, R., Garasic, V., Volker, F., Kluge, C., Kaspar, T., Byrne, G. F., Sobolev, S. V. & Fuchs, K. (1997). An integrated model for the deep structure of the Chyulu Hills volcanic field, Kenya. *Tectonophysics* **278**, 187-209.

O'Brien, P. J. & Rötzler J. (2003). High-pressure granulites: formation, recovery of peak conditions and implications for tectonics. *Journal of Metamorphic Geology* **21**, 3-20.

Ouzegane, K., Guiraud, M. & Kienast, J. R. (2003). Prograde and retrograde evolution in high-temperature corundum granulites (FMAS and KFMASH systems) from In Ouzzal Terrane (NW Hoggar, Algeria). *Journal of Petrology* **44**, 517-545.

Omenge, J. M. & Okelo, R. E. (1992). Geology of the Chyulu-Oloitokitok area. Kenya Mines and Geology Department, Nairobi, Report 112, 51 pp.

Osanai Y., Hammamoto, T., Maishima, O. & Kagami, H. (1998). Sapphirine-bearing granulites and related high-temperature metamorphic rocks from the Higo metamorphic terrane,

west central Kyushu, Japan. *Journal of Metamorphic Geology* **16**, 53-66.

Pattison, D. R. M. (2003). Petrogenetic significance of orthopyroxene-free garnet + clinopyroxene + plagioclase ± quartz-bearing metabasites with respect to the amphibolite and granulite facies. *Journal of Metamorphic Geology* **21**, 21-34.

Pinna, P., Jourde, G., Calvez, J. Y. & Mroz, J. P. (1993). The Mozambique Belt in northern Mozambique: Neoproterozoic (1100-850 Ma) crustal growth and tectogenesis, and superimposed Pan-African (800-550 Ma) tectonism. *Precambrian Research* **62**, 1-59.

Preston, J. P., Dempster, T. J., Bell, B. R. & Rogers, G. (1999). The petrology of mullite-bearing peraluminous xenoliths: implications for contamination processes in basaltic magmas. *Journal of Petrology* **40**, 549-573.

Rakotondrazafy, M. A. F., Moine, B. & Cuney, M. (1996). Mode of formation of hibonite ($CaAl_{12}O_{19}$) within the U-Th skarns from the granulites of S-E Madagascar. *Contributions to Mineralogy and Petrology* **123**, 190-201.

Rickers, K, Raith, M. & Dasgupta, S. (2001). Multistage reaction textures in xenolithic high Mg-Al granulites at Anakapalle, eastern Ghats Belt, India: examples of contact polymetamorphism and infiltration-driven metasomatism. *Journal of Metamorphic Geology* **19**, 563-582.

Ritter, J. R. R. & Kaspar, T. (1997). A tomography study of the Chyulu Hills, Kenya. *Tectonophysics* **278**, 149-169.

Rudnick, R. L. (1992). Xenoliths – samples of the lower continental crust. In: Fountain D. M., Arculus R. & Kay R. W. (eds.) *Continental Lower Crust*. New York: Elsevier, pp. 269-316.

Rudnick R. L., McDonough W. F., McCulloch M. T. & Taylor S. R. (1986). Lower crustal xenoliths from Queensland, Australia: evidence for deep crustal assimilation and fractionation of continental basalts. *Geochimica et Cosmochimica Acta* **50**, 1099-1155.

Saggerson, E. P. (1963). Geology of the Simba-Kibwezi area. *Geological Survey of Keny*a **58**, 70 pp.

Sandiford, M., Neall, F. B. & Powell R. (1987). Metamorphic evolution of aluminous granulites from Labwor Hills, Uganda. *Contributions to Mineralogy and Petrology* **95**, 217-225.

Sandiford, M. & Santosh, M. (1991). A granulite-facies kalsilite-leucite-hibonite association from Punalur, South India. *Mineralogy and Petrology* **43**, 225-236.

Santosh, M., Sandiford, M. & Reed, S. J. B. (1991). Zoned hibonite from Punalur, South India. *Mineral Magazine* **55**, 159-162.

Shackleton, R. M. (1973). Correlation of structures across Precambrian orogenic belts in Africa. In: Tarling, D. H. & Runcorn, S. K. (eds.) *Implications of Continental Drift to the Earth Sciences*. London: Academic Press, pp. 1091-1095.

Shulters, J. C. & Bohlen, S. R. (1989). The stability of hercynite and hercynite-gahnite spinels in corundum- or quartz-bearing assemblages. *Journal of Petrology* **30**, 1017-1031.

Sills, J. D., Ackermand, D., Herd, R. K. & Windley, B. F. (1983). Bulk composition and mineral parageneses of sapphirine-bearing rocks along a gabbro-lherzolite contact at Fin-

ero, Ivrea Zone, Northern Italy. *Journal of Metamorphic Geology* **1**, 337-351.

Späth, A., Le Roex, A. P. & Opiyo-Akech, N. (2001). Plume-lithosphere interaction and the origin of continental rift-related alkaline volcanism – the Chyulu Hills Volcanic field, Southern Kenya. *Journal of Petrology* **42**, 765-787.

Stern, R. J. & Dawoud, A. S. (1991). Late Precambrian (740 Ma) charnockite, enderbite, and granite from Jebel Moya, Sudan: a link between the Mozambique Belt and the Arabian-Nubian Shield? *Journal of Geology* **99**, 648-659.

Stern, R. J. (1994). Arc assembly and continental collision in the Neoproterozoic East African orogen: implications for the conditions of Gondwanaland. *Annual Review of Earth and Planetary Sciences* **22**, 319-351.

Tenthorey, E. A., Ryan, J. C. & Snow, E. A. (1996). Petrogenesis of sapphirine-bearing metatroctolites from the Buck Creek ultramafic body, southern Appalachian. *Journal of Metamorphic Geology* **14**, 103-114.

Ulianov, A. G., Kalt, A. & Pettke, T. (2005). Hibonite, $Ca(Al,Cr,Ti,Si,Mg,Fe^{2+})_{12}O_{19}$, in granulite xenoliths from the Chyulu Hills volcanic field, Kenya. *European Journal of Mineralogy* **17/2**, 355-364.

Ulianov, A. G., Kalt, A. & Pettke, T. Aluminous websterite and granulite xenoliths from the Chyulu Hills volcanic field, Kenya: Metamorphosed gabbroic cumulates from a Pan-African arc environment. Submitted to *Contributions to Mineralogy and Petrology*.

Wells, P. R. A. (1977). Pyroxene thermometry in simple and complex systems. *Contributions to Mineralogy and Petrology* **62**, 129-139.

White, R. W. (1966). Ultramafic inclusions in basaltic rocks from Hawaii. *Contributions to Mineralogy and Petrology* **12**, 245-314.

Yakovlevskaya, T. A. (1961). Hibonite from Gornaya Shoriya. *Zapiski Vsesoyuznogo Mineralogicheskogo Obshchestva* **90**, 458-461. In Russian.

Zandt, G., Gilbert, H., Owens, T. J., Ducea, M. & Saleeby, J., Jones, C. H. (2004). Active foundering of a continental arc root beneath the southern Sierra Nevada in California. *Nature* **431**, 41-46.

CHAPTER IV

Hibonite, $Ca(Al,Cr,Ti,Si,Mg,Fe^{2+})_{12}O_{19}$, in granulite xenoliths from the Chyulu Hills volcanic field, Kenya

A. Ulianov[1,*], A. Kalt[1], T. Pettke[2]

[1]University of Neuchâtel, Institute of Geology, Rue Emile-Argand 11, CH-2007 Neuchâtel, Switzerland

[2]Institut für Isotopengeologie und Mineralische Rohstoffe, ETH Zentrum, Sonneggstrasse 5, CH-8092 Zürich, Switzerland

*Corresponding author:
alexey.ulyanov@unine.ch

published in **European Journal of Mineralogy,** 2005. V. 17(1-2), 357-366.

Eur. J. Mineral.
2005, **17**, 357-366

Hibonite, $Ca(Al,Cr,Ti,Si,Mg,Fe^{2+})_{12}O_{19}$, in granulite xenoliths from the Chyulu Hills volcanic field, Kenya

ALEXEY ULIANOV[1,*], ANGELIKA KALT[1] and THOMAS PETTKE[2]

[1]Institut de Géologie, Université de Neuchâtel, Rue Emile-Argand 11, CH-2007 Neuchâtel, Switzerland
[2]Institut für Isotopengeologie und Mineralische Rohstoffe, ETH Zentrum,
Sonneggstrasse 5, CH-8092 Zürich, Switzerland

Abstract: In basanites of the Chyulu Hills volcanic field, Kenya, hibonite is found in two xenoliths of mafic meta-igneous granulites dominated by clinopyroxene and plagioclase. It occurs as small grains in the inner parts of complex corona textures where it forms intergrowths with spinel and sapphirine and shows reaction relationships with later mullite and sillimanite. Hibonite and whole-rock samples were analyzed for major and trace elements by electron microprobe, XRF and LA-ICPMS. Chemically, the analyzed hibonite grains are close to the idealized formula $Ca(Al,Cr,Ti,Si,Mg,Fe^{2+})_{12}O_{19}$ and do not contain other major components. They are similar to terrestrial hibonite in their (Fe+Mg) contents but show the elevated Al and Ca abundances as well as the relative depletion in Ti and REE typical of meteoritic hibonite. Silica contents are high and exceed those in any other terrestrial and meteoritic hibonite. In order to evaluate the possibility of magmatic crystallization of hibonite in the igneous protoliths of the studied rocks, we compare some of the measured element abundances with those expected from element partitioning data for hibonite and Ca,Al-rich silicate melt. Based on this comparison, formation of low-Ti hibonite that is relatively rich in LREE appears consistent with magmatic crystallization, whereas hibonite with elevated Ti contents, low in LREE, is obviously the result of diffusion re-equilibration in the course of subsolidus cooling.

Key-words: hibonite, mafic granulite, trace elements, East African Rift, LA-ICPMS.

Introduction

Hibonite is an oxide mineral of the magnetoplumbite group. The latter includes about ten end-member minerals with the general formula $AB_{12}O_{19}$, many of which are very rare. In the crystalline structure of the magnetoplumbite group minerals, larger cations reside in site A, whereas smaller ones occupy site B. Given considerable variations in the chemical composition of hibonite, its generalized crystal chemical formula can be written as $(Ca,REE,Th,U)(Al,Cr,Ti,Si,Fe^{2+},Fe^{3+},Mg,Zn)_{12}O_{19}$ (*e.g.*, Burns & Burns, 1984; Maaskant *et al*., 1980; Rakotondrazafy *et al*., 1996).

In the terrestrial environment, hibonite is rare and found only at four localities. In Madagascar, in the area of Tranomaro from where it was first described by Curien *et al*. (1956), it commonly occurs in thorianite-bearing skarns with scapolite, spinel, corundum, diopside, anorthite and calcite (Rakotondrazafy *et al*., 1996). In Gornaya Shoriya, Siberia, it is found in calcite-dominated calc-silicate rocks containing nests of idocrase, diopside, titanite, hercynite, rutile, corundum, sillimanite and magnetite and regionally associated with migmatized amphibolites and garnet-biotite gneisses (Kuzmin, 1960; Yakovlevskaya, 1961). In Tanzania, it is described from a calc-silicate grossular-anorthite rock bearing titanite, (clino-)zoisite, hercynite, apatite, ilmenite and corundum, associated with biotite-garnet gneisses, granulites and quartzites of the Furua Complex (Maaskant *et al*., 1980). In South India, near Punalur, it was discovered in a highly aluminous gneiss consisting of kalsilite, leucite, spinel, corundum and perovskite forming part of a sequence of supracrustal gneisses interlayered with charnockites (Santosh *et al*., 1991; Sandiford & Santosh, 1991). All these occurrences are high-grade metamorphic rocks. The occurrence in Gornaya Shoriya corresponds to the upper amphibolite facies, the others are in the granulite facies. The calc-silicate rocks are interpreted to be of metasomatic origin (Letuvninkas, 1971; Maaskant *et al*., 1980; Rakotondrazafy *et al.*, 1996). As with the feldspathoid gneisses of Punalur, they represent extremely Si-undersaturated lithologies.

Apart from its rare findings in the terrestrial environment, hibonite is known in meteorites and interplanetary dust. It is rather common in Ca,Al-rich inclusions and microspherules in chondrites (*e.g.*, Keil & Fuchs, 1971; Bischoff *et al*., 1985; Fahey *et al*., 1987; Kimura *et al*., 1993; Russell *et al*., 1998). In these objects, hibonite is associated with primary refractory oxides and silicates

*E-mail: alexey.ulyanov@unine.ch

DOI: 10.1127/0935-1221/2005/0017-0357
0935-1221/05/0017-0357 $ 4.50
© 2005 E. Schweizerbart'sche Verlagsbuchhandlung. D-70176 Stuttgart

Table 1. Whole-rock major and trace element analyses of the studied xenoliths.

Specimen	1904-9	1904-1
SiO_2	50.18	49.66
TiO_2	0.05	0.01
Al_2O_3	23.58	24.59
FeO	4.57	4.76
MnO	0.06	0.06
MgO	6.34	6.06
CaO	10.68	10.11
Na_2O	3.55	3.72
K_2O	0.25	0.20
P_2O_5	0.05	0.03
L.O.I.	0.43	0.28
Total	99.74	99.48
Mg#	71.2	69.4
TiO_2	0.048 (.002)	0.004 (.000)
MnO	0.063 (.002)	0.053 (.002)
K_2O	0.303 (.014)	0.227 (.009)
P_2O_5	0.033 (.003)	0.020 (.002)
Li	4.10 (.30)	1.66 (.21)
B	1.11 (.03)	1.65 (.12)
Cr	261 (14)	108 (12)
Co	113 (5)	222 (7)
Zn	22 (2)	28 (13)
Sc	6.0 (.3)	1.4 (1)
V	37.3 (.9)	5.8 (.8)
Rb	2.76 (.13)	1.02 (.05)
Sr	718 (12)	651(8)
Y	0.72 (.02)	0.13 (.03)
Zr	3.56 (.08)	1.10 (.84)
Nb	0.91 (.08)	0.76 (.10)
Cs	0.020 (.005)	0.030 (.006)
Ba	1049 (24)	939 (16)
La	1.23 (.04)	0.42 (.04)
Ce	2.01 (.09)	0.21 (.05)
Pr	0.23 (.02)	0.03 (.01)
Nd	1.05 (.04)	0.14 (.02)
Sm	0.19 (.05)	<0.05
Eu	0.46 (.02)	0.40 (.02)
Gd	0.21 (.02)	0.06 (.01)
Tb	0.024 (.005)	0.004 (.001)
Dy	0.16 (.02)	0.023 (.004)
Ho	0.029 (.002)	0.005 (.001)
Er	0.090 (.016)	<0.030
Tm	0.010 (.001)	<0.004
Yb	0.061 (.003)	0.018 (.001)
Lu	0.008 (.001)	<0.005
Hf	0.067 (.010)	0.028 (.015)
Pb	0.28 (.08)	0.28 (.10)
Th	0.083 (.005)	0.006 (.005)
U	0.046 (.009)	0.030 (.009)

Major element oxides (wt%) by electron microprobe on glass pellets; additional values for TiO_2, MnO, K_2O and P_2O_5 (wt%) by LA-ICPMS; trace elements (ppmw) by LA-ICPMS. Averages from 4-5 laser ablation shots are shown; standard deviations (1σ) are given in parentheses. See text for details.
FeO corresponds to total Fe; Mg# = MgO/(MgO+FeO_{total}), on a molar basis.

such as spinel, perovskite, melilite and fassaite. Glass may also be present. Secondary minerals include grossular, feldspathoids, phyllosilicates, wollastonite and calcite. The Ca,Al-rich inclusions have been studied extensively for more than twenty years now, because they are considered to be the first and most primitive condensed material formed in the solar system. Hibonite from the Ca,Al-rich inclusions may have complex post-condensation history. The latter includes: (1) heating responsible for partial-to-nearly-complete melting of primary minerals and element fractionation during evaporation of the molten material (*e.g.*, Wark & Lowering, 1982; Richter *et al.*, 2002); (2) cooling and liquidus crystallization (*e.g.*, Kennedy *et al.*, 1997; Russell *et al.*, 1998; Richter *et al.*, 2002); (3) alteration (Nomura & Miyamoto, 1998 and references therein). Hibonite, as well as the other refractory minerals in the Ca, Al-rich inclusions, may represent either relicts of an early condensate which survived melting event(s) or products of liquidus crystallization on cooling. The experimentally derived liquidus temperatures are of the order of 1600-1200°C (Stolper, 1982). Hibonite in interplanetary dust forms aggregate particles with other refractory phases, mainly perovskite and melilite. These extremely small objects (< 15 μm, often much less) have much in common with refractory inclusions from chondrite meteorites and also preserve the accretion history of the solar nebula (for a review, see Rietmeijer, 1998).

Synthetic hibonite has been produced by liquidus crystallization from a Tschermak-rich composition along the Diopside-Ca-Tschermakite join (Drake & Boynton, 1988) as well as from silica-undersaturated Ca,Al-rich compositions of the CMASTi system similar to those of Ca,Al-rich inclusions and hibonite-bearing microspherules in chondrites (Kennedy *et al.*, 1994; Beckett & Stolper, 1994).

Hibonite considered in this study is found as rare small grains in xenoliths of basic meta-igneous granulites. Neither hibonite nor the whole mineral assemblage of these rocks show evidence for formation by metasomatism. The granulites are rich in Mg, Ca and Al and slightly silica-undersaturated (normative olivine < 10 %). This geochemical pattern is relatively uncommon for terrestrial granulites (see review by Christy, 1989). In its utmost form, it is more typical of Ca,Al-rich inclusions in chondrites.

Analytical techniques

Analysis of hibonite for major elements was carried out on a CAMECA SX50 microprobe equipped with four wavelength-dispersive spectrometers (Mineralogisch-Petrographisches Institut, University of Bern). Operating conditions were a 15 kV acceleration voltage, 20 nA beam current, and counting times of 20-40 s. The beam was focused to 1.5-2 μm. Data were reduced with the PAP correction routine.

Trace element abundances in hibonite were determined using a LA-ICPMS instrument equipped with an Excimer 193 nm ArF laser complex and an ELAN 6100 quadrupole ICP mass spectrometer at the Institut für Isotopengeologie und Mineralische Rohstoffe, ETH Zürich (for capabilities

of the instrument, see Heinrich *et al*., 2003). Operating conditions were similar to those described by Pettke *et al*. (2004). Two sets of major element whole-rock analyses of the studied xenoliths were made. The first set was obtained on an XRF spectrometer Philips PW2400 (Institut de Minéralogie et de Pétrographie, University of Fribourg) using lithium-borate fused disks. The second set was made on glass pellets prepared by fusion of rock powders (30 mg) without flux on an iridium strip heater (a thin strip of iridium metal connected to copper electrodes, heated by electric current *via* a potentiometer). The pellets were then analysed on a CAMECA SX50 microprobe (Mineralogisch-Petrographisches Institut, University of Bern). The beam was set at 20 μm, other operating conditions were the same as for minerals. The two sets of measurements are in good agreement with each other. In the following, the microprobe data are preferred because the lithium-borate fused disks for XRF analysis were somewhat inhomogeneous (corundum not completely dissolved). Whole-rock trace element abundances were determined by LA-ICPMS on the same glass pellets that were used for major element microprobe analysis. The analytical technique was the same as for hibonite.

Chemical composition of whole-rock samples

Major and trace element compositions of the studied granulite xenoliths are given in Table 1. They correspond to basic protoliths, with SiO_2 ranging from 46.4 to 50.2 wt% and MgO ranging from 12.3 to 6.1 wt%. The Mg#'s calculated on the basis of divalent iron are high (69.4-71.2). The rocks are relatively calcium-rich and display strong enrichment in Al_2O_3 (20.3-24.6 wt%). Alkalies are sodium-dominated. The Sr and Ba contents reach 733 ppmw and 1155 ppmw, respectively, whereas the abundances of TiO_2 (< 0.05 wt%) and Nb (< 0.91 ppmw) are low. The absolute concentrations of rare earth elements (REE) are very low. Significant fractionation of LREE over HREE [$(La/Yb)_{Cn}$ 14-17] and positive Eu anomalies are observed.

The studied rocks are meta-igneous. In terms of the chemical composition of protoliths, they belong to a crystal accumulation sequence that also includes olivine websterites and magnesian sapphirine-bearing orthopyroxene granulites. The granulites record cooling under granulite-facies conditions possibly accompanied by some compression (Ulianov & Kalt, submitted). Their P-T path is consistent with those of outcropping granulites of Pan-African age in Tanzania (Pare, Uluguru, Usambara complexes). Regional geodynamic reconstructions for these granulite complexes include magmatic underplating / magma loading in the environment of an active continental margin during the Pan-African (Appel *et al*., 1998; Möller *et al*., 1998, 2000).

Petrography

The studied xenoliths of hibonite-bearing granulites (specimens 1904-1 and 1904-9) are mineralogically and petrographically similar to each other. Xenolith 1904-1 is rather coarse-grained (plagioclase porphyroblasts reach 3-4 mm, mafic minerals are smaller in size) and banded. Xenolith 1904-9 is more fine-grained and texturally more homogeneous. Mineral assemblages are as follows (mineral abbreviations from Kretz, 1983):

1904-1: cpx, pl, grt, crn, spl, qtz, sil, spr, hibonite;

1904-9: cpx, pl, grt, crn, spl, qtz, sil, mullite, hibonite.

Plagioclase (30-35 %), clinopyroxene (25-30 %) and garnet (~ 15 %) dominate, corundum and spinel do not exceed 10 % each (Fig. 1). Several generations of clinopyroxene, corundum and spinel are observed. Quartz and sillimanite are subordinate (5-7 %). Sapphirine, mullite and hibonite are rare minerals of these rocks.

The xenoliths show late-stage alterations that include pervasive kelyphitization of garnet and incongruent melting of clinopyroxene. Most likely, these overprints are caused by fast heating and decompression in the host basanite.

Textural relations of hibonite

Hibonite forms small (< 80-100 μm) isometric or elongated, often complexly indented grains always associated with spinel and sometimes accompanied by sapphirine or mullite in the core parts of the corona aggregates shown in Fig. 1a-f. The relationships of hibonite and spinel in these aggregates are somewhat uncertain. Neither hibonite nor spinel apparently resorbs each other. On the other hand, spinel normally occurs on the borders of hibonite grains (Fig. 1b and c), sometimes rimming them almost completely (Fig. 1f). Growth relationships of hibonite with sapphirine are also uncertain (Fig. 1e and f). Mullite resorbs both hibonite and spinel. Sillimanite forms after mullite and seems to have grown at the expense of all other minerals of this assemblage. In turn, it is being replaced by garnet in the outermost parts of the corona aggregates. (Fig. 1a and c).

Chemical composition of hibonite

Major element composition and stoichiometry

The studied hibonites are close to the idealized formula $Ca(Al,Cr,Ti,Si,Mg,Fe^{2+})_{12}O_{19}$. Ca, Al, Si, Mg and Fe contents do not show significant variations. The abundances of SiO_2 vary in the range of 2.32-3.10 wt% (Table 2). The content of TiO_2 is low (0.05-0.74 wt% in specimen 1904-1, 0.26-2.29 wt% in specimen 1904-9). In both specimens, considerable intergrain variations and a rimward increase in Ti are observed (Table 2).

Ca abundances range from 1.016 to 1.048 c.p.f.u. (Table 2) and appear therefore somewhat excessive in spite of the thorough calibration of the microprobe. An excess of Ca has been reported for both meteoritic (*e.g*., Keil & Fuchs, 1971; MacDougall, 1979) and terrestrial (Yakovlevskaya, 1961; Maaskant *et al*., 1980) hibonite and seems common for this mineral. It additionally corrobo-

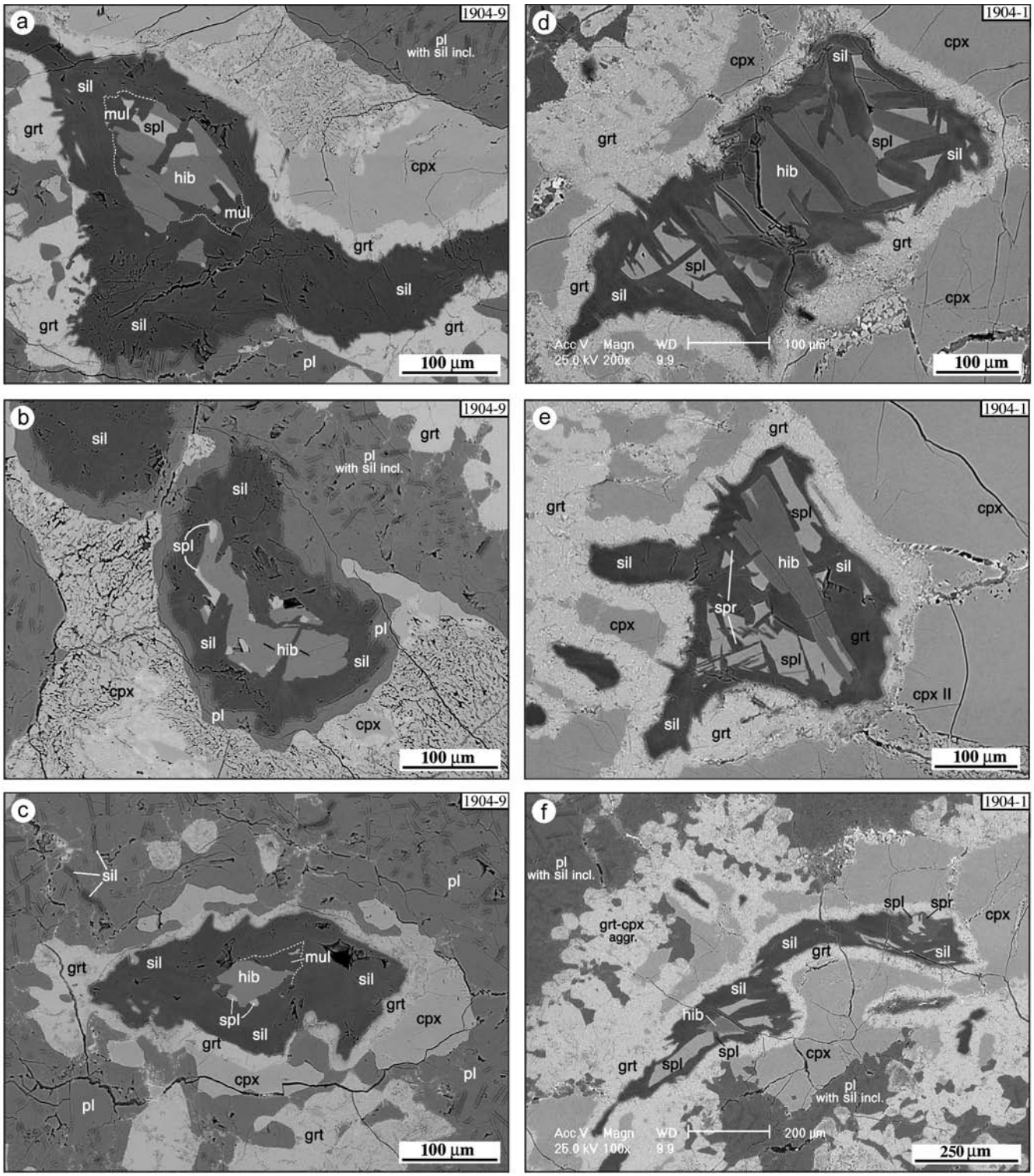


Fig. 1. Back-scattered electron images of granulite xenoliths from the Chyulu Hills volcanic field, southern Kenya, showing textural relationships of hibonite in corona aggregates. **a-f**: hibonite intergrown with spinel (± sapphirine) and rimmed by mullite (when present) and sillimanite. The relationships of hibonite with spinel and sapphirine are uncertain. Both spinel and sapphirine often appear to have formed later than hibonite, although no direct indications of resorbtion of hibonite by these minerals are observed. Mullite apparently replaces hibonite. Sillimanite also shows reaction relationships with hibonite as well as minerals associated with the latter. In the outermost parts of the corona aggregates, sillimanite is being replaced by garnet. Mineral abbreviations following Kretz (1983).

rates that an exchange between (Mg,Fe^{2+}) and Ca in site A of the hibonite structure is unlikely. On the other hand, the classical exchange $(Ti,Si) + (Mg,Fe^{2+}) \leftrightarrow 2(Al,Cr)$ in site B (*e.g.*, Burns & Burns, 1984; Santosh *et al.*, 1991) is well

Table 2. Chemical composition (wt%) and structural formulae of hibonite in specimens 1904-9 and 1904-1.

Aggregate	A					B			C			
	single grain					two grains separated by Sil			single grain		single grain	
	1	2	3	4	5	6	7	8	9	10	11	12
	core	core	rim	core	rim	core	intermed.	rim	core	rim	core	rim
SiO_2	2.98 (06)	2.95 (04)	2.98 (03)	2.99 (02)	2.97 (01)	2.98 (03)	2.92 (02)	2.97 (04)	3.00 (03)	3.02 (04)	2.92 (02)	2.90 (06)
TiO_2	0.07 (01)	0.05 (02)	0.09 (02)	0.14 (01)	0.19 (04)	0.15 (01)	0.32 (03)	0.41 (08)	0.19 (02)	0.24 (02)	0.48 (02)	0.74 (11)
Al_2O_3	83.78 (28)	83.73 (17)	83.79 (12)	83.74 (18)	83.76 (21)	83.79 (14)	83.62 (14)	83.57 (21)	83.74 (26)	83.77 (20)	83.35 (11)	83.42 (18)
Cr_2O_3	0.21 (04)	0.33 (04)	0.18 (04)	0.11 (03)	0.06 (02)	0.09 (02)	0.09 (03)	0.08 (02)	0.09 (02)	0.06 (04)	0.11 (02)	0.12 (02)
FeOt	2.22 (03)	2.30 (08)	2.17 (10)	2.29 (07)	2.24 (09)	2.33 (07)	2.19 (11)	2.27 (13)	2.29 (05)	2.17 (09)	2.33 (05)	2.30 (05)
ZnO	0.20 (05)	0.20 (10)	0.17 (03)	0.20 (06)	0.21 (07)	0.21 (07)	0.21 (03)	0.18 (06)	0.21 (03)	0.22 (09)	0.22 (08)	0.24 (01)
MgO	1.49 (02)	1.47 (01)	1.50 (03)	1.52 (01)	1.51 (03)	1.52 (01)	1.55 (03)	1.61 (05)	1.53 (02)	1.55 (04)	1.56 (03)	1.66 (03)
CaO	8.41 (04)	8.42 (01)	8.48 (06)	8.50 (07)	8.52 (06)	8.52 (04)	8.49 (09)	8.46 (02)	8.46 (06)	8.44 (07)	8.40 (06)	8.42 (03)
Total	99.36	99.45	99.36	99.49	99.46	99.59	99.39	99.55	99.51	99.47	99.37	99.80
Si	0.338	0.334	0.338	0.339	0.336	0.337	0.331	0.336	0.340	0.342	0.331	0.328
Ti	0.006	0.004	0.008	0.012	0.016	0.013	0.027	0.035	0.016	0.020	0.041	0.063
Al	11.190	11.182	11.188	11.175	11.179	11.174	11.169	11.147	11.172	11.173	11.144	11.111
Cr	0.019	0.030	0.016	0.010	0.005	0.008	0.008	0.007	0.008	0.005	0.010	0.011
Fe^{2+}	0.210	0.218	0.206	0.217	0.212	0.220	0.208	0.215	0.217	0.205	0.221	0.217
Zn	0.017	0.017	0.014	0.017	0.018	0.018	0.018	0.015	0.018	0.018	0.018	0.020
Mg	0.252	0.248	0.253	0.257	0.255	0.256	0.262	0.272	0.258	0.261	0.264	0.280
Ca	1.021	1.022	1.029	1.031	1.034	1.033	1.031	1.026	1.026	1.023	1.021	1.019
Sum	13.052	13.056	13.052	13.057	13.055	13.059	13.053	13.052	13.054	13.049	13.051	13.049

Aggregate	D						E		F			
	two grains separated by Sil						single elongated grain		single grain		single grain	
	13	14	15	16	17	18	19	20	21	22	23	24
	core	rim	core	rim	core	rim	intermed.	rim	core	rim	core	rim
SiO_2	3.13 (01)	2.98 (03)	3.10 (01)	2.98 (08)	2.93 (02)	2.62 (02)	2.72 (09)	2.81 (16)	2.54 (06)	2.32 (12)	2.64 (03)	2.35 (06)
TiO_2	0.26 (02)	0.34 (08)	0.33 (01)	0.39 (05)	1.17 (03)	1.47 (06)	1.20 (03)	1.32 (05)	1.86 (02)	2.29 (20)	1.40 (13)	2.21 (11)
Al_2O_3	83.27 (15)	83.79 (24)	83.47 (18)	83.58 (13)	82.47 (16)	82.40 (16)	82.36 (18)	82.48 (38)	82.10 (19)	82.08 (34)	82.66 (09)	81.82 (06)
Cr_2O_3	0.40 (02)	0.36 (07)	0.29 (03)	0.29 (04)	0.24 (04)	0.27 (03)	0.25 (04)	0.24 (04)	0.29 (03)	0.31 (02)	0.40 (10)	0.33 (00)
FeOt	2.03 (07)	1.96 (05)	1.96 (07)	1.94 (08)	2.09 (10)	2.14 (06)	2.22 (12)	2.14 (08)	2.09 (04)	2.06 (06)	2.08 (06)	2.13 (01)
ZnO	0.12 (05)	0.10 (07)	0.13 (06)	0.12 (03)	0.15 (09)	0.16 (02)	0.11 (03)	0.13 (05)	0.20 (05)	0.18 (05)	0.16 (02)	0.20 (07)
MgO	1.71 (02)	1.67 (03)	1.72 (01)	1.70 (02)	1.96 (03)	1.94 (04)	2.02 (18)	1.89 (06)	2.02 (04)	2.07 (06)	1.90 (05)	2.02 (04)
CaO	8.54 (03)	8.58 (06)	8.66 (10)	8.64 (04)	8.47 (05)	8.43 (09)	8.46 (17)	8.46 (05)	8.41 (04)	8.36 (04)	8.52 (05)	8.44 (03)
Total	99.47	99.80	99.69	99.68	99.51	99.45	99.37	99.51	99.58	99.72	99.78	99.52
Si	0.354	0.336	0.350	0.337	0.332	0.298	0.309	0.319	0.288	0.263	0.299	0.267
Ti	0.022	0.029	0.028	0.033	0.100	0.126	0.103	0.113	0.159	0.195	0.119	0.189
Al	11.111	11.140	11.114	11.130	11.022	11.031	11.033	11.029	10.990	10.976	11.030	10.968
Cr	0.036	0.032	0.026	0.026	0.022	0.024	0.022	0.022	0.026	0.028	0.036	0.030
Fe^{2+}	0.192	0.185	0.185	0.183	0.198	0.203	0.211	0.203	0.199	0.195	0.197	0.203
Zn	0.010	0.008	0.011	0.010	0.013	0.013	0.009	0.011	0.017	0.015	0.013	0.017
Mg	0.289	0.281	0.290	0.286	0.331	0.328	0.342	0.320	0.342	0.350	0.321	0.342
Ca	1.036	1.037	1.048	1.046	1.029	1.026	1.030	1.028	1.023	1.016	1.034	1.029
Sum	13.050	13.049	13.052	13.052	13.046	13.049	13.060	13.044	13.044	13.039	13.049	13.045

*denotation of aggregates as in Fig. 1.
Structural formulae were calculated on the basis of 19 O. MnO and K_2O contents are below detection limits for most analyses. Standard deviations (1σ) in parentheses.

expressed (Fig. 2a). The common substitution Ti ↔ 2(Mg, Fe^{2+}) seems operative as well (Fig. 2b).

Trace elements

The studied hibonite contains some amount of Zn, V, Sr and Ba (Tables 2 and 3). The ZnO content measured on the electron microprobe reaches *ca*. 0.2 wt% (Table 2). V abundances are between 42 and 192 ppmw. The abundances of Sr and Ba analyzed by LA-ICPMS show considerable scatter. Their highest values (*e.g.*, hibonite A from specimen 1904-9, Table 3) appear to reflect the contamination of hibonite through the interaction with late fluids in the outermost rims and inner cracks. Analyzing these areas

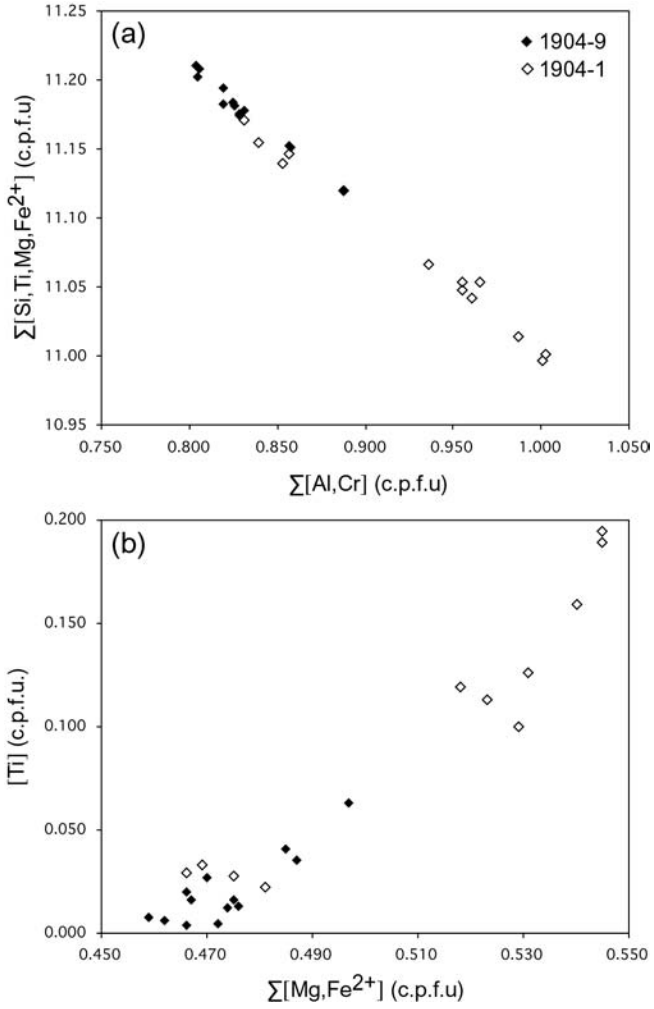


Fig. 2. Substitutions in hibonites. **a**: [Si+Ti+Mg+Fe^{2+}] for [Al+Cr]. **b**: Ti for [Mg+Fe^{2+}].

could not be completely avoided due to the small size of the hibonite grains. The abundances of Nb, Ta, Zr, Hf and Th measured in two hibonite grains are all extremely low, < 1-2 ppmw. The abundances of REE are low, with the values for HREE often being below detection limit (Table 3). The REE patterns of the hibonite grains show variable enrichment in LREE and positive Eu anomalies (Fig. 4).

Comparison with other terrestrial hibonite and hibonite from chondrite meteorites

Representative chemical compositions of hibonite from other terrestrial occurrences are given in Table 4, data on hibonite from chondrite meteorites are shown in Table 5. Compared to hibonite from terrestrial occurrences, hibonite from meteorites displays higher Al and Ca contents at lower abundances of Si, Ti, Fe, Mg, and REE. Hibonite from the Chyulu Hills is similar to other terrestrial hibonite in its (Fe+Mg) contents but show the high Al and Ca contents and relatively low Ti and REE abundances typical of meteoritic hibonite. Compared to both terrestrial and meteoritic hibonite, it is enriched in silica.

Mode of formation of hibonite

Subsolidus *vs.* igneous mineral assemblages in the studied granulite xenoliths

The igneous protoliths of the granulites were significantly modified by subsolidus mineral reactions. Minerals preceding subsolidus processes include some plagioclase and mafic silicates, of which the compositions are unknown, and those relicts, *i.e*. hibonite, spinel and sometimes sapphirine, that are preserved in the cores of the aggregates mantled by sillimanite and garnet (Fig. 1a-f). Experimental data on Ca,Al-rich silicate melts show that sapphirine and spinel represent liquidus phases close to the $CaAl_2Si_2O_8$-apex of the join Mg_2SiO_4-SiO_2-$CaAl_2Si_2O_8$ (Liu & Presnall, 1990, 2000), whereas hibonite appears as a liquidus phase in experimental systems relevant to Ca,Al-rich inclusions in chondrite meteorites (Drake & Boynton, 1988; Kennedy *et al*., 1994; Beckett & Stolper, 1994). Some hibonites from the liquidus experiments are markedly enriched in silica (up to 1.7 wt%) in spite of the strong silica undersaturation of the coexisting melt (Beckett & Stolper, 1994). This suggests that high silica contents (as in the studied hibonites, see Table 2) may be characteristic of igneous hibonite.

Crystallization and re-equilibration of hibonite

In order to further evaluate the possibility of magmatic crystallization of hibonite, we compare the measured trace element abundances of hibonite with those expected from the partition coefficients between hibonite and Ca,Al-rich silicate melt, using the whole rock trace element data. This approach is *a priori* controversial for several reasons. First, there is no proof that the protolith of the studied specimens represents the melt the hibonites were crystallized from. In the sequence of comagmatic meta-igneous xenoliths from the Chyulu Hills that includes the studied granulites, all other lithologies represent igneous cumulates modified by subsolidus processes. One xenolith petrographically similar to specimens from this study but lacking hibonite is also cumulate in origin, since it is very magnesian, relatively rich in Cr and characterized by very low LREE abundances. Strong positive Eu anomalies clearly indicate the accumulation of plagioclase. We have supposed therefore that the whole comagmatic sequence including xenoliths 1904-9 and 1904-1 from this study represents cumulates (Ulianov *et al.*, submitted).

Another source of controversy deals with the uncertainty of the partition coefficients for hibonite and their dependence on the composition of host melt, especially on the activity of Al (Russell *et al*., 1998). The partitioning of trace elements between hibonite and melt has been studied by several workers in both chondritic hibonite-glass microspherules from meteorites (Ireland *et al*., 1991; Russell *et al*., 1998) and simplified experimental chemical compositions (Drake & Boynton, 1988; Kennedy *et al*., 1994; Beckett & Stolper, 1994). Within the framework of this study, we applied partition coefficients from Ireland *et al*. (1991), Kennedy *et al*. (1994) and Russell *et al*. (1998). As

Table 3. Trace element composition of hibonite (ppmw, determined by LA-ICPMS).

Specimen					1904-9			1904-1
Aggregate*		A		B	C	D	E	F
	core	core	core	intermed.	core	core	core	core
	1	2	6	7	9	13	19	21
Na	104	111	104	126	89	67	89	156
V	43	51	52	44	42	184	192	129
Y	<0.15	<0.21	<0.27	0.30	<0.15	0.22	<0.30	<0.32
Ba	63.9	100.2	8.9	12.5	7.6	8.9	3.4	14.1
Sr	672	1343	43	55	34	80	50	184
La	10.4	12.1	2.7	1.6	0.23	2.9	1.0	0.16
Ce	8.8	11.0	2.1	1.6	0.6	4.9	2.5	0.2
Pr	0.47	0.43	0.16	<0.27	0.07	0.45	0.36	<0.08
Nd	0.84	<0.78	<0.88	1.25	<0.43	1.96	1.51	1.31
Sm	<0.51	<0.79	<0.46	<1.74	<0.58	0.26	<1.11	<0.68
Eu	3.26	3.25	0.42	0.41	0.58	0.72	1.00	2.04
Gd	<0.76	<1.00	<0.64	<1.30	<0.57	0.26	0.41	0.94
Tb	<0.09	<0.12	<0.16	<0.10	<0.11	<0.05	<0.18	<0.10
Dy	<0.26	<0.40	<0.64	<0.42	<0.26	0.18	<0.25	<0.54
Ho	<0.10	<0.13	<0.13	<0.15	<0.13	<0.04	<0.09	0.09
Er	<0.51	<0.60	<0.67	<1.28	<0.62	<0.28	<0.73	<0.95
Tm	<0.08	<0.10	<0.07	<0.17	<0.11	<0.03	<0.12	<0.13
Yb	<0.73	<0.92	<0.93	<0.95	<0.72	<0.29	0.62	<0.79
Lu	<0.05	<0.10	<0.21	<0.19	<0.05	<0.02	<0.07	<0.06
Pb	4.14	5.40	<1.04	<1.69	0.74	1.49	<1.10	2.52
U	<0.08	<0.12	<0.12	<0.38	<0.11	<0.03	<0.10	<0.14

*denotation of aggregates as in Fig. 1; analyses numbers correspond to that in Table 2. Elevated detection limits result from the small laser ablation pit sizes (20-30 μm) used due to the small size of the studied hibonite grains.

Table 4. Representative analyses (in wt%) of hibonite from terrestrial occurrences.

	Madagascar[1]		Siberia[2]		Tanzania[3]	India[4]
SiO_2	0.88	0.67	1.03	0.75	0.14	0.25
TiO_2	2.45	6.03	5.10	5.6	1.99	9.49
Al_2O_3	78.08	76.31	73.67	72.8	76.78	74.87
Cr_2O_3	n.a.	n.a.	n.a.	n.a.	n.a.	n.a.
Fe_2O_3	n.a.	n.a.	9.90	2.7	n.a.	n.a.
FeO	3.58	3.21	0.35	7.3	1.98	2.62
MnO	n.a.	n.a.	n.a.	n.a.	<0.03	0.03
ZnO	b.d.	b.d.	n.a.	n.a.	n.a.	n.a.
MgO	2.05	2.80	1.59	0.27	3.24	2.62
CaO	5.89	7.33	8.67	6.2	2.59	7.11
Na_2O	n.a.	n.a.	n.a.	n.a.	0.08	0.24
La_2O_3	1.68	0.38	n.a.	1.8	4.68	<0.01
Ce_2O_3	2.23	0.70	n.a.	2.1	7.44	<0.01
Nd_2O_3	0.48	0.12	n.a.	0.2	<0.06	<0.02
Sm_2O_3	0.04	0.08	n.a.	n.a.	0.13	<0.02
ThO_2	1.38	0.30	n.a.	b.d.	n.a.	n.a.
Total	98.74	97.93	100.31	99.72	99.05	97.23

n.a. not analysed; b.d. below detection limit.
[1]Rakotondrazafy *et al*. (1996); [2]Yakovlevskaya (1961); [3]Maaskant *et al*. (1980); [4]Santosh *et al*. (1991).

Table 5. Representative analyses (in wt% for oxides and in ppmw for trace elements) of hibonite from chondrites.

	Murchison[1]	Colony[2]	Murchison[3]	Allende[4]	Isna[5]	Lancé[6]
SiO_2	b.d.	0.13	b.d.	<0.01	b.d.	0.07
TiO_2	2.30	1.38	5.14	0.29	0.07	1.75
Al_2O_3	87.90	87.50	83.28	90.30	91.10	88.80
Cr_2O_3	n.a.	n.a.	n.a.	<0.01	n.a.	<0.02
FeO	n.a.	0.15	b.d.	0.61	0.39	0.18
ZnO	n.a.	n.a.	n.a.	n.a.	n.a.	<0.02
MgO	1.20	0.72	2.63	<0.04	0.04	0.99
CaO	8.60	8.88	8.46	8.34	8.80	8.40
Total	100.00	98.77	99.51	99.54	100.39	100.19
La	10.8	116.4	n.a.	14.0	98.6	3.8-6.5
Ce	25	115.9	n.a.	0.05	0.2	5.0-11.2
Nd	19	111.4	n.a.	15.86	68.5	6.9-10.6
Sm	5.3	102.6	n.a.	2.79	44.9	1.8-2.9
Eu	0.28	16.5	n.a.	0.88	27.3	0.5-1.4
Tb	1.3	127.5	n.a.	0.29	100.6	1.3-1.8
Yb	1.3	2.9	n.a.	0.16	189.8	0.3-2.1

n.a. not analysed; b.d. below detection limit.
[1,2]Microspherules: [1]Ireland *et al.* (1991); [2]Russell *et al.* (1998). [3-6]Ca,Al-rich inclusions: [3]Ireland (1988); [4]Fahey *et al.* (1987); [5]Russell *et al.* (1998); [6]Fahey *et al.* (1994).

the U, Th, Nb and Zr abundances of the studied hibonites are extremely low and because of the possible late-stage redistribution of Sr and Ba, only Ti and the REE (see Fig. 5) are used.

Since the partition coefficient for Ti between hibonite and silicate melt is close to unity (although it varies as a function of chemical composition of the melt, ranging from 0.8 to 2.1 in Ca,Al-rich melts, see Beckett & Stolper,

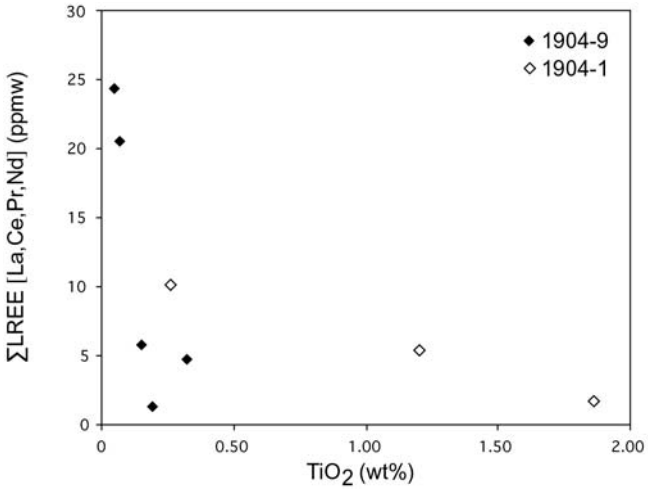


Fig. 3. Diagram TiO_2 *vs*. LREE for the studied hibonite.

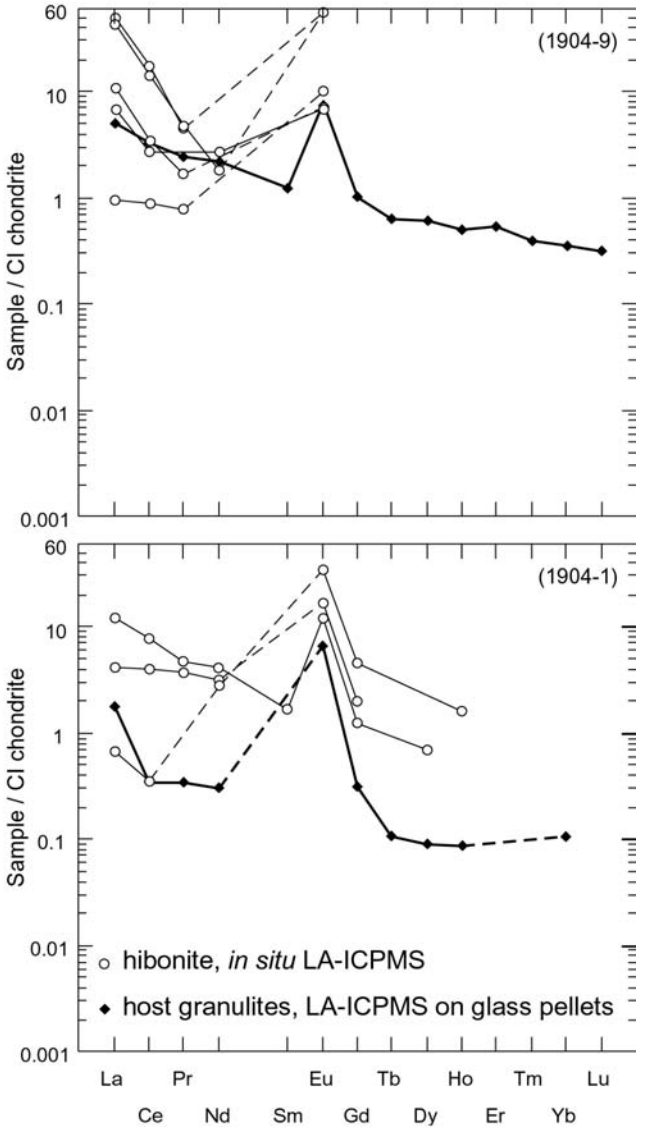


Fig. 4. Chondrite-normalized REE patterns of hibonite and the host granulite. Normalization values from Sun & McDonough (1989). Patterns are not complete because of REE abundances below detection limits (see Tables 1 and 3).

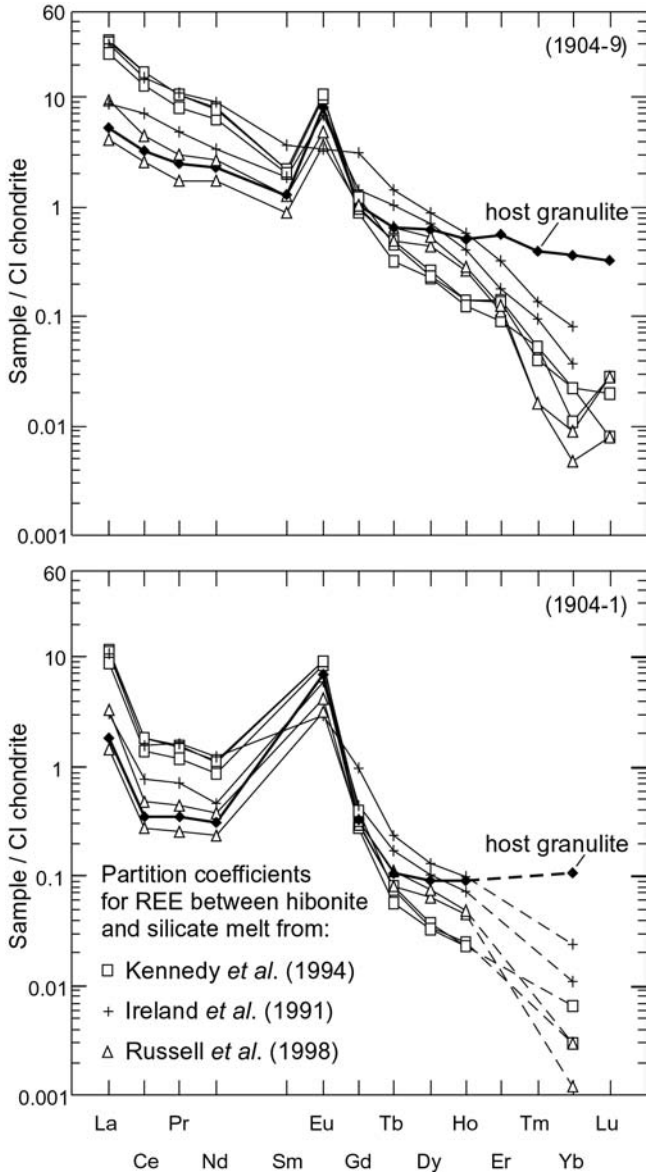


Fig. 5. Chondrite-normalized REE patterns calculated for hibonite from the bulk rock REE abundances and partition coefficients between hibonite and melt [Kennedy *et al*. (1994), experimental runs HB-6#1, 7#1 and 7#2; Ireland *et al.* (1991), hibonite-bearing microspherules in Lancé 3413-1/31 and Murchison 7-228; Russell *et al*. (1998), hibonite-bearing microspherules in Colony SP1 and ALH82101 SP15]. Whole-rock REE patterns of the host granulites are shown for comparison. Normalization values from Sun & McDonough (1989).

1994), hibonites that may have retained their magmatic trace element abundances are expected to be very poor in Ti, of which the abundances should be broadly similar to those in the parental magma (Table 1). Such hibonite is indeed present (see Table 3, hibonite A in 1904-9 and hibonite D and E in 1904-1).

Plotted against TiO_2, the analyzed hibonite shows a scatter in LREE contents (Fig. 3). Although all REE patterns of hibonite shown in Fig. 4 are in principle compatible with those calculated from the bulk rock REE

abundances of the host granulites and the partition coefficients used (see Fig. 5), higher partition coefficients (*e.g.*, Kennedy *et al*., 1994) and hence higher REE concentrations in hibonite should be more realistic estimates, given the cumulate nature of the studied protoliths. LREE abundances in the low-Ti hibonite are roughly compatible with these patterns. Hibonite with elevated Ti abundances appears re-equilibrated under subsolidus conditions (*e.g.*, hibonite F in 1904-1). In turn, this hibonite has very low LREE abundances that appear to be less compatible with magmatic crystallization.

We believe, therefore, that the low-Ti hibonite retained its pristine abundances of Ti and LREE defined by magmatic crystallization. In turn, the observed negative correlation between LREE and Ti and the rimwards increase in Ti (Tables 2 and 3, Fig. 3) appear to be due to diffusion re-equilibration of hibonite in the course of subsolidus processes. The latter almost completely define mineralogy and mineral relations in the studied granulitic xenoliths. The corresponding P-T path is essentially defined by cooling in the sillimanite stability field to ~ 725-730°C and ~ 630-640°C for specimens 1904-9 and 1904-1, respectively (see details in Ulianov & Kalt, submitted).

Concluding remark

The Chyulu Hills hibonite is significantly enriched in silica and, compared to other terrestrial occurrences of this mineral, exhibits relatively low Ti contents at very low REE abundances. Chemically, it better compares with hibonite from meteorites. Although meteoritic hibonite may form in several ways, in some meteorites it appears equilibrated with / crystallized from melt. In turn, our data seem most consistent with magmatic crystallization of hibonite in the terrestrial environment.

Acknowledgements: We thank Vincent Serneels for performing the XRF analyses. Thanks go to Thomas Armbruster for his help with recognizing hibonite. Michael Seitz is thanked for preparing the glass pellets. Constructive reviews by Rainer Altherr and Stephan Klemme significantly improved the quality of the manuscript. Permission and help for field sampling provided by the Office of the President, Kenya Wildlife Service, and the Kenya Agricultural Research Institute in Kiboko are gratefully acknowledged. This research was supported by the Swiss National Science Foundation grant 200021-100647/1.

References

Appel, P., Möller, A., Schenk, V. (1998): High-pressure granulite facies metamorphism in the Pan-African belt of eastern Tanzania: P-T-t evidence against granulite formation by continent collision. *J. metamorphic Geol.*, **16**, 491-509.

Beckett, J.R. & Stolper, E. (1994): The stability of hibonite, melilite and other aluminous phases in silicate melts: implications for the origin of hibonite-bearing inclusions from carbonaceous chondrites. *Meteoritics*, **29**, 41-65.

Bischoff, A., Keil, K., Stöffler, D. (1985). Perovskite-hibonite-spinel-bearing inclusions and aluminum-rich chondrules and fragments in enstatite chondrites. *Chem. Erde*, **44**, 97-106.

Burns, R.G. & Burns, V.M. (1984): Crystal chemistry of meteorite hibonites. Proceeding of the 15th Planetary Science Conference. *J. Geophys. Res., Suppl. Issue* **89**, C313-321.

Christy, A.G. (1989): The stability of sapphirine+clinopyroxene: implications for phase relations in the CaO-MgO-Al_2O_3-SiO_2 system under deep-crustal and upper mantle conditions. *Contrib. Mineral. Petrol.*, **102**, 422-428.

Curien, H., Guillemin, C., Orcel, J., Steinberg, M. (1956): La hibonite, nouvelle espèce minérale. *C. R. Acad. Sc. Paris*, **242**, 2845-2847.

Drake, M.J. & Boynton, W.L. (1988): Partitioning of rare earth elements between hibonite and melt and implications for nebular condensation of the rare earth elements. *Meteoritics*, **23**, 75-80.

Fahey, A.J., Goswani, J.N., McKeegan, K.D., Zinner, E. (1987): ^{26}Al, ^{244}Pu, ^{50}Ti, REE and trace element abundances in hibonite grains from CM and CV meteorites. *Geochim. Cosmochim. Acta*, **51**, 329-350.

Fahey, A.J., Zinner, E., Kurat, G., Kracher, A. (1994): Hibonite-hercynite inclusion HH-1 from the Lancé (CO3) meteorite: The history of an ultrarefractory CAI. *Geochim. Cosmochim. Acta*, **58**, 4779-4793.

Heinrich, C.A., Pettke, T., Halter, W.E., Aigner-Torres, M., Audétat, A., Günther, D., Hattendorf, B., Bleiner, D., Guillong, M., Horn, I. (2003): Quantitative multi-element analysis of minerals, fluid and melt inclusions by laser-ablation inductively-coupled-plasma mass-spectrometry. *Geochim. Cosmochim. Acta*, **67**, 3473-3496.

Ireland, T.R. (1988): Correlated morphological, chemical, and isotopic characteristics of hibonites from the Murchison carbonaceous chondrite. *Geochim. Cosmochim. Acta*, **52**, 2827-2839.

Ireland, T.R., Fahey, E.K., Zinner, E.K. (1991): Hibonite-bearing microspherules: A new type of refractory inclusions with large isotopic anomalies. *Geochim. Cosmochim. Acta*, **55**, 367-379.

Keil, K. & Fuchs, L.H. (1971): Hibonite ($Ca_2(Al,Ti)_{24}O_{38}$) from the Leoville and Allende chondritic meteorites. *Earth Planet. Sci. Lett.*, **12**, 184-190.

Kennedy, A.K., Lofgren, G.E., Wasserburg, G.J. (1994): Trace-element partition coefficients for perovskite and hibonite in meteorite compositions. *Chemical Geol.*, **117**, 379-390.

Kennedy, A.K., Beckett, J.R., Edwards, D.A., Hutcheon, I.D. (1997): Trace element disequilibria and magnesium isotope heterogeneity in 3655A: Evidence for a complex multistage evolution of a typical Allende Type B1 CAI. *Geochim. Cosmochim. Acta*, **61**, 1541-1561.

Kimura, M., El Goresy, A., Palme, H., Zinner, E. (1993): Ca-Al-rich inclusions in the unique chondrite ALH 85085 – Petrology, chemistry, and isotopic composition. *Geochim. Cosmochim. Acta*, **57**, 2329-2359.

Kretz, R. (1983): Symbols for rock-forming minerals. *Am. Mineral.*, **68**, 277-279.

Kuzmin, A.M. (1960): Högbomite from Gornaya Shoriya. *Geologiya i Geofizika*, **4**, 63-75. (Russian).

Letuvninkas, A.I. (1971): Metasomatism in Proterozoic carbonate rocks from Gornaya Shoriya. *Geologiya i Geofizika*, **1**, 58-64. (Russian).

Liu, I.C. & Presnall, D.C. (1990): Liquidus phase relations in the join anorthite-forsterite-quartz at 20 kbar with applications to basalt petrogenesis and igneous sapphirine. *Contrib. Mineral. Petrol.*, **104**, 735-742.

—, — (2000): Liquidus phase relations in the system CaO-MgO-Al_2O_3-SiO_2 at 2.0 GPa: applications to basalt fractionation, eclogites and igneous sapphirine. *J. Petrol*., **41**, 3-20.

Maaskant, P., Coolen, J.J.M., Burke, E.A.J. (1980): Hibonite and coexisting zoisite and clinozoisite in a calc-silicate granulite from southern Tanzania. *Mineral. Mag.*, **43**, 995-1003.

MacDougall, J.D. (1979): Refractory-element-rich inclusions in CM meteorites. *Earth Planet. Sci. Lett.*, **42**, 1-6.

Möller, A., Mezger, K., Schenk, V. (1998): Crustal age domains and the evolution of the continental crust in the Mozambique Belt of Tanzania: Combined Sm-Nd, Rb-Sr and Pb-Pb isotopic evidence. *J. Petrol.*, **39**, 749-783.

Möller, A., Mezger, K., Schenk, V. (2000): U-Pb dating of metamorphic minerals: Pan-African metamorphism and prolonged slow cooling of high pressure granulites in Tanzania, East Africa. *Precambrian Research*, **104**, 123-146.

Nomura, K. & Miyamoto, M. (1998): Hydrothermal experiments on alteration of Ca-Al-rich inclusions (CAIs) in carbonaceous chondrites: Implications for aqueous alteration in parent asteroids. *Geochim. Cosmochim. Acta*, **62**, 3575-3588.

Pettke, T., Halter, W.E., Webster, J.D., Aigner-Torres, M., Heinrich, C.A. (2004): Accurate quantification of melt inclusion chemistry by LA-ICPMS: A comparison with EMP and SIMS and advantages and possible limitations of these methods. *Lithos*, **78**, 333-361.

Rakotondrazafy, M.A.F., Moine, B., Cuney, M. (1996): Mode of formation of hibonite ($CaAl_{12}O_{19}$) within the U-Th skarns from the granulites of S-E Madagascar. *Contrib. Mineral. Petrol.*, **123**, 190-201.

Richter, F.M., Davis, A.M., Ebel, D.S., Hashimoto, A. (2002): Elemental and isotopic fractionation of Type B calcium-, aluminum-rich inclusions: Experiments, theoretical considerations, and constraints on their thermal evolution. *Geochim. Cosmochim. Acta*, **66**, 521-540.

Rietmeijer, F.G.M. (1998): Interplanetary dust particles. in ¨Planetary Materials¨, J.J. Papike, ed. *Rev. Min*., Min. Soc. Amer.,Washington DC, **36**, (2-)1-95.

Russell, S.S., Huss, G.R., Fahey, A.J., Greenwood, R.C., Hutchison, R., Wasserburg, G.J. (1998): An isotopic and petrologic study of calcium-aluminum-rich inclusions from CO3 meteorites. *Geochim. Cosmochim. Acta*, **62**, 689-714.

Sandiford, M. & Santosh, M. (1991): A granulite-facies kalsilite-leucite-hibonite association from Punalur, South India. *Mineral. Petrol.*, **43**, 225-236.

Santosh, M., Sandiford, M., Reed, S.J.B. (1991): Zoned hibonite from Punalur, South India. *Mineral. Mag*., **55**, 159-162.

Stolper, E. (1982): Crystallization sequences of calcium-aluminum-rich inclusions from Allende: An experimental study. *Geochim. Cosmochim. Acta*, **46**, 2159-2180.

Sun, S.S. & McDonough, W.F. (1989): Chemical and isotopic systematics of oceanic basalts: implications for mantle composition and processes. *In*: Saunders A.D., Norry M.J. (eds). «Magmatism in ocean basins». *Geol. Soc. Spec. Publ*., **42**, 313-345.

Wark, D.A. & Lowering, J.F. (1982): The nature and origin of type B1 and B2 Ca-Al-rich inclusions in the Allende meteorite. *Geochim. Cosmochim. Acta*, **46**, 2581-2594.

Yakovlevskaya, T.A. (1961): Hibonite from Gornaya Shoriya. *Zapiski Vsesoyuznogo Mineralogicheskogo Obshchestva*, **90**, 458-461. (Russian)

Received 2 March 2004
Modified version received 17 September 2004
Accepted 22 November 2004

CHAPTER V

Composition and thermal evolution of the lithospheric mantle beneath the Chyulu Hills (Southern Kenya, East African Rift) as deduced from xenoliths

R. Altherr[1,*], V. Garasic[1,2], A. Ulianov[3], A. Kalt[3]

[1]Institute of Mineralogy, University of Heidelberg, Im Neuenheimer Feld 236, D-69121 Heidelberg, Germany

[2]Institute of Mineralogy, Petrology and Mineral Deposits, RGN Faculty, University of Zagreb, Pierottijeva 6, HR-10000 Zagreb, Croatia

[3]Geological Institute, University of Neuchâtel, Rue Emile-Argand 11, CH-2007 Neuchâtel, Switzerland

*Corresponding author:
raltherr@min.uni-heidelberg.de

to be submitted to **Journal of Petrology**
on April 15th

CHAPTER V

ABSTRACT

The Chyulu Hills are a Quaternary volcanic field located approximately 150 km to the east of the Kenya Rift Valley close to the border of Tanzania, about 40 km north of Mt. Kilimanjaro. In the northwestern part of the volcanic field, several denuded cinder cones formed by eruption of basanitic magma contain abundant mantle and crustal xenoliths. Apart from meta-igneous granulite, various types of lherzolite, harzburgite, websterite and orthopyroxenite occur. We investigated 59 mantle-derived xenoliths for their textures and mineral compositions. The aim of our study was to constrain the thermal and metamorphic evolution of the xenoliths and their lithospheric source regions by applying geothermobarometric considerations and calculations as well as diffusion modelling. Xenoliths of garnet lherzolite and porphyroclastic harzburgite equilibrated in the lowermost lithosphere at ~ 3.5 GPa and 1350 °C. All other xenoliths (garnet- and/or spinel-bearing websterite and harzburgite, spinel lherzolite, orthopyroxenite) derive from depths of less than ~ 80 km and are characterized by textural and chemical disequilibrium. Coarse-grained harzburgite xenoliths contain fingerprint-like intergrowths of spinel and orthopyroxene (± clinopyroxene) formed by decompression-induced breakdown of low-Ca garnet + olivine. Relict garnet is present in some of these xenoliths. Exsolution of spinel (and clinopyroxene) from orthopyroxene suggests cooling during/after decompression. Chemical zoning patterns of orthopyroxene grains are either flat or show a core-to-rim decrease of Al and Ca; in both cases, Al and Ca may show a rimward increase in the outermost zones of the opx grains, indicating a relatively young heating event prior to entrainment into the transporting basanitic magmas. In websterite and orthopyroxenite xenoliths, pyroxene grains are characterized by exsolution of garnet, complementary pyroxene and spinel. Chemical zoning patterns of pyroxene grains are broadly similar to those of the coarse-grained harzburgite and suggest a similar metamorphic evolution (cooling, in part followed by heating). Cooling of the lithospheric mantle started during/after the formation of the Mozambique fold belt in the late Proterozoic. In a number of xenoliths, chemical equilibrium was attained during cooling. Pressure-temperature (*P-T*) data on these xenoliths suggest a geotherm similar to a ~ 60–70 mW m^{-2} steady-state model beneath the Chyulu Hills volcanic field. The lithospheric thickness is constrained to ~ 115 km. The late heating that affected the source regions of many xenoliths derived from depths of ~ 80-40 km is a local feature and was most probably related to small magma intrusions in the lithospheric mantle. The uppermost mantle (~ 40 – 60 km depth) comprises very depleted harzburgite together with websterite and orthopyroxenite. Due to considerable scatter of the geothermobarometric data obtained on low-temperature xenoliths, the temperature at the seismically defined Moho (at a depth of 40 km) cannot be well constrained (600 – 750 °C).

INTRODUCTION

Being one of the Earth's largest active continental rifts, the East African Rift System (EARS) has been the site of many studies intended to enhance our understanding of why and how continents rift apart. Any model to explain the origin of Cenozoic

rifting and volcanism in East Africa must account for several characteristic surface features, including the East African Plateau (EAP) with a mean elevation of about 1100 m, an only small amount of extension (≤ 15 km) across East Africa (Ebinger, 1989; Ebinger *et al*., 1999) and large volumes of volcanic rocks in the Eastern Rift (> 900,000 km^3; Morley, 1999) as opposed to small amounts in the Western Rift (Ebinger, 1989; Pasteels *et al*., 1989; Burke, 1996; Kampunzu *et al*., 1998). These features are not well consistent with a passive mode of rifting, entirely due to extensional stresses caused by plate-boundary forces. Consequently, the EARS has commonly been explained by active rifting in the context of one or more mantle plumes (e.g. Latin *et al*., 1993; Slack *et al*., 1994; Burke, 1996; Simiyu & Keller, 1997; Zeyen *et al*., 1997; Ebinger & Sleep, 1998; George *et al*., 1998; Nyblade *et al*., 2000; Rogers *et al*., 2000; Macdonald *et al*., 2001; Späth *et al*., 2001; Nyblade, 2002).

Global seismic tomography models consistently show a broad region of low seismic wave velocities that extends from the lowermost mantle beneath the southeastern Atlantic Ocean and southwestern Africa to the upper mantle under East Africa (e.g. Grand *et al*., 1997; Ritsema *et al*., 1999; Ritsema & van Heijst, 1999; Helmberger *et al*., 2000; Ni & Helmberger, 2003). This feature has been interpreted as a broad, NE-directed thermal upwelling and is often termed the 'African Superplume'. Recent surface wave tomography studies revealed extraordinarily low seismic velocities beneath the lithosphere of the Archean Tanzania craton (Ritsema & van Heijst, 1999; Weeraratne et al., 2003) and beneath NE Africa/Arabia (Debayle *et al*., 2001). Under the Kenya rift, imposed on a late Proterozoic orogenic belt, there is a broad (200 – 300 km) low-velocity anomaly that extends to depths greater than 400 km (Green *et al*., 1991; Achauer *et al*., 1994; Simiyu & Keller, 1997) The transition zone beneath this region is thinned by a downward deflection of the 410 km discontinuity, which points to anomalously high temperatures as the cause of low seismic velocities (Owens *et al*., 2000). In conjunction with the plateau uplift and the pattern of long-wavelength, low Bouguer gravity anomalies on the EAP, these findings are broadly in line with the hypotheses that a plume rises beneath the Tanzanian craton and spreads out beneath the adjacent western and eastern branches of the EARS (Weeraratne *et al*., 2003). Such a model can easily explain the plateau uplift and the pattern of long-wavelength, low Bouguer anomalies on the EAP (Ebinger et al., 1989; Simiyu & Keller, 1997; Lithgow-Bertelloni & Silver, 1998) as well as observed seismic anisotropy variations across the EAP and the whole African plate (Behn *et al*., 2004; Walker *et al*., 2004).

Investigations on mantle xenoliths are a powerful tool to refine the upper mantle model deduced from geophysical observations. In particular, they can significantly contribute to decipher the thermal and chemical evolution of the lithospheric mantle during rifting. As such xenoliths are transported to the surface within hours to days, they provide instantaneous snapshots of their lithospheric source regions. Since chemical diffusion is much slower than thermal diffusion, most xenoliths are in chemical disequilibrium, whereby chemical zoning patterns of their mineral grains reflect temporal variations in chemical potentials due to changes in pressure (*P*), temperature (*T*) and chemical composition. For example, xenoliths from the Quater-

nary Labait volcano located on the eastern edge of the Tanzanian craton at its intersection with the eastern branch of the EARS indicate that refractory mantle with Re depletion ages of ~ 2.8 Ga persists to 150 km depth. At depths ≥ 120 km, more fertile xenoliths with younger Re depletion ages occur, suggesting that the lower cratonic lithosphere is chemically and thermally interacting with asthenospheric melts (Lee & Rudnick, 1999; Chesley *et al*., 1999; Dawson, 1999).

In this paper, we present the results of a detailed study on 59 mantle xenoliths from the Quaternary Chyulu volcanic field located on the eastern rift flank in southern Kenya. We use textures, mineral compositions, geothermobarometry and diffusion modelling to constrain the thermal evolution and the compositional structure of the lithosphere beneath this part of the EARS. In particular, we try to find out if and to which extent Tertiary-Quaternary rifting and plume activity have modified the thermal and chemical structure of the lithosphere.

GEOLOGICAL SETTING

In the eastern branch of the EARS (Kenya Rift), volcanic and tectonic activitiy started in northern Kenya in the Late Oligocene (McDougall & Watkins, 1988) and propagated south- and eastward with time (Baker, 1987; Morley, 1999). Quaternary to Recent volcanic activity is restricted to the southern central graben and the eastern rift shoulder.

The Chyulu Hills volcanic field in southern Kenya is located about 150-200 km east of the rift axis (Fig. 1a). The volcanic rocks were classified on the basis of surface morphology, relative age and composition (Haug & Strecker, 1995; Novak *et al*., 1997; Späth *et al*., 2000, 2001; Fig. 1b). Volcanism started about 1.4 Ma ago in the northwestern Chyulu Hills near Emali (Haug & Strecker, 1995). There, numerous denuded cinder cones and lava flows range in composition from Ti-rich foidites (groups I and II of Haug & Strecker, 1995) to less silica-undersaturated basanites (groups III and IV of Haug & Strecker, 1995). The central and southeastern Chyulu Hills are dominated by a prominent ridge of several hundred Quaternary volcanic cones and lava flows forming a NW-SE aligned chain of approximately 100 km length. The volcanic rocks are of Upper Pleistocene to Recent age (Omenge & Okelo, 1992) and of alkali basaltic composition (group V of Haug & Strecker, 1995; Novak *et al*., 1997; Fig. 1b). Mantle and lower crustal xenoliths only occur with some cinder cones of the northwestern Chyulu Hills. The samples taken for this study come from group-III basanites (Fig. 1b).

The Chyulu Hills are located on the Pan-African Mozambique Belt (Saggerson, 1963; Shackleton, 1993). The Pan-African basement consists of gneisses, migmatites and granulites with subordinate eclogites, garnet amphibolites and marbles (Saggerson, 1963; Omenge & Okelo, 1992; Möller *et al*., 1998). Structural trends in the basement rocks are mainly N-S. The alignment of the volcanoes in the southeastern Chyulu Hills seems to be controlled by late-orogenic shear zones and their joints that divide the basement into small segments (Smith & Mosely, 1993; Haug & Strecker, 1995).

The structure of the lithosphere beneath the Chyulu Hills has been studied by wide-angle reflection and refraction experiments as well as by gravity measurements and seismic tomography (Novak *et al*., 1997; Kaspar & Ritter, 1997). The

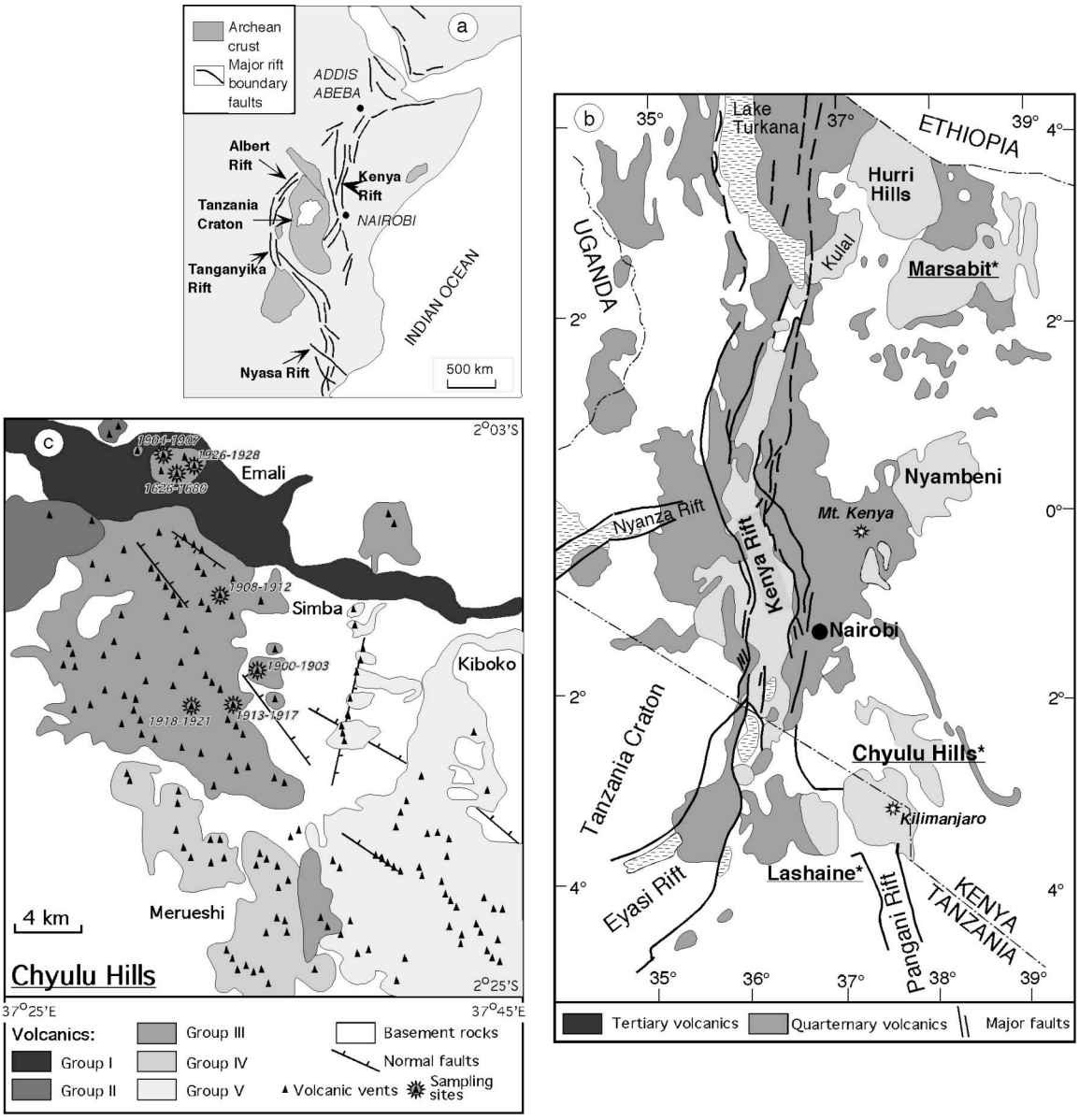


Fig. 1. Geological setting. (a) The Kenya Rift as part of the East African Rift System. (b) Distribution of Tertiary and Quaternary volcanic rocks in the Kenya Rift (modified after Baker (1987). Xenolith-bearing Quaternary volcanic fields are marked by asterisks. (c) Simplified geological map of the northwestern Chyulu Hills, with xenolith sample sites. Groups I-IV represent (from old to young) the sequence of Chyulu Hills volcanic edifices according to the classification by Haug & Strecker (1995). Group I and group II represent foiditic lavas with anomalously high Ti contents. Groups 3 and 4 are basanitic to alkali basaltic pyroclastic deposits that host most of the mantle xenoliths. Group 5 rocks are fractionated alkali basalts that contain abundant crustal-derived xenocrysts. For further explanation see 'Geological setting'.

Moho was detected at depths of 40 km and 44 km beneath the northwestern and the southeastern Chyulu Hills, respectively. While there is no velocity perturbation in the northwest (Pn velocity = 8.1 km/s), the lithosphere beneath the central and southeastern Chyulu Hills is characterised by a prominent low-velocity zone that extends from c. 23 km depth in the lower crust to 70 km depth in the mantle (Pn velocity ≈ 7.9 km/s). This zone is interpreted to be caused by elevated temperature or even partial melt (Novak *et al.*, 1997; Kaspar & Ritter, 1997).

Seismic anisotropy in the upper mantle beneath the Chyulu Hills as deduced from shear wave splitting is characterized by a consistent NNE-SSW orientation of the fast direction (Walker *et al*., 2004). This orientation is subparallel to the Pan-African N-S structural trends in the basement, but does not correspond to the ~ E-W orientation of olivine a axes that would result from extension-induced ductile stretching of the lithospheric mantle beneath southern Kenya (Walker *et al*., 2004, and references therein). This suggests that the lithospheric mantle beneath the Chyulu Hills was not significantly deformed during Cenozoic rifting and volcanism.

In a reconnaissance study on a restricted number of xenoliths from the northwestern Chyulu Hills, Henjes-Kunst & Altherr (1992) used the equilibration conditions deduced from major element mineral compositions to construct a geotherm for this part of the volcanic field. They found that *P-T* data obtained for (nearly) equilibrated garnet-bearing xenoliths plot along a 60 mW m^{-2} steady-state model geotherm (Pollack & Chapman, 1977) and estimated a lithospheric thickness of ~ 110 km.

ANALYTICAL TECHNIQUES

Minerals were analysed using a CAMECA SX50 microprobe equipped with four wavelength-dispersive spectrometers (Zentrum für Elektronenmikroskopie, University of Karlsruhe), and a CAMECA SX51 microprobe equipped with five wavelength-dispersive spectrometers (Mineralogisches Institut, University of Heidelberg). Operating conditions on both machines included a 15 kV accelerating voltage, a 20 nA beam current and a beam diameter of ~ 1 μm. Natural and synthetic silicate and oxide standards were used for calibration. Counting times were 10-30 s for silicates (30 s for Al, Ni, Ca; 20 s for Ti; 10 s for all other elements) and 10-100 s for spinels (100 s for Ti; 30 s for Ni, V, Zn; 10 s for all other elements). For checking the accuracy in silicates, particularly in olivine, some point analyses or profiles were run with enhanced counting times (60-100 s). The PAP routine (Pochou & Pichoir, 1984, 1985) was applied to the raw data.

XENOLITH TYPES AND MINERAL COMPOSITION

Overview and general remarks

The mantle xenoliths found are various types of lherzolite, harzburgite, websterite and orthopyroxenite. Most xenoliths are characterized by textural and chemical disequilibrium. Features such as porphyroclastic textures, kink bands in olivine, reaction coronas, intra- and intergrain exsolution and chemical zoning of mineral grains testify to variable metamorphic evolutions induced by deformation, changing *P–T* conditions and infiltration of melts and/or fluids. Primary garnet, for example, is in most cases replaced by symplectite and/or kelyphite, and only its relics are preserved. Furthermore, primary compositions of olivine, pyroxenes and spinel may be modified in contact with pseudomorphs after garnet or with intergranular glass.

In the petrographic descriptions given below, Roman numerals attributed to mineral names and abbreviations refer to different mineral generations recognized by textural evidence. A difference in Roman numerals does not necessarily imply a difference in chemical composition. The attribute “I” generally denotes ‘primary’ mineral grains; in case of porphyroclastic textures, “Ia” stands for porphyroclasts and “Ib” for neoblasts.

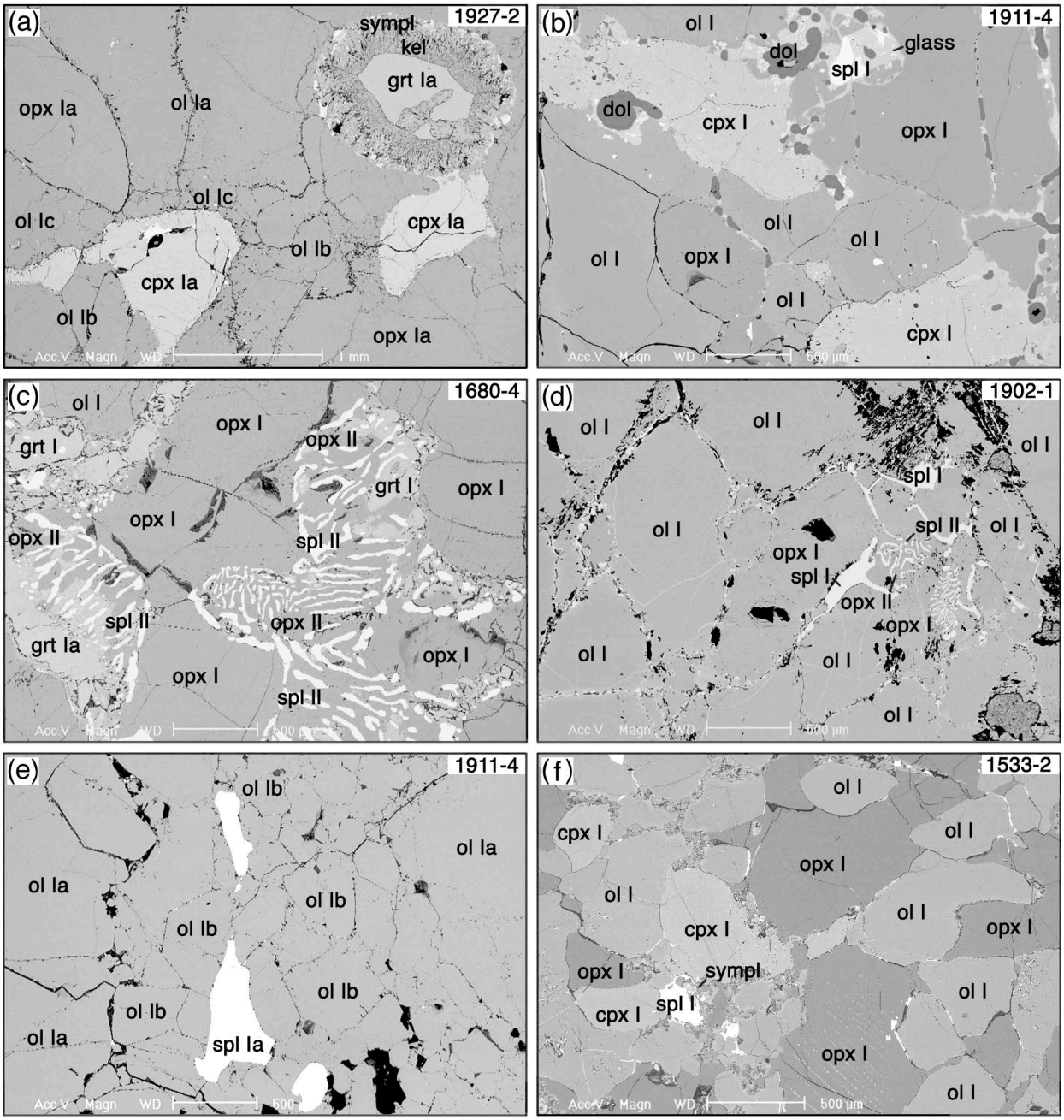


Fig. 2. BSE (back-scattered electron) images of peridotite and olivine websterite xenoliths from the Chyulu Hills, showing textural features and mineral generations. (a) Grt lherzolite. (b) Spl lherzolite. (c) Coarse-grained grt harzburgite. (d) Granular grt-spl harzburgite. (e) Porphyroclastic spl harzburgite. (f) Grt-spl olivine websterite. Mineral abbreviations after Kretz (1983); sympl: pyroxene-spinel (±plagioclase) symplectite after garnet; kel: fine-grained pyroxene-spinel-plagioclase kelyphite after garnet. For further explanation see 'Xenolith types and mineral composition'.

Minerals of reaction coronas (symplectites) and exsolved garnet or pyroxene (lamellar or intergranular) are always marked with "II". Finally, "III" is attributed to mineral domains that were modified by late-stage reaction with melt or fluid. In this paper, however, we will focus on the 'pre-metasomatic' evolution of the xenoliths. The various late-stage alterations related to the infiltration of melts and/or fluids into the rocks will be treated in a later contribution.

Garnet lherzolite

These rocks are characterised by porphyroclastic to heterogranular textures. Larger grains (porphyroclasts) of olivine (ol Ia), orthopyroxene (opx Ia) and clinopyroxene (cpx Ia) together with pseudomorphs after garnet (grt Ia) are embedded in a matrix of smaller neoblasts (ol Ib, opx Ib, cpx Ib; Fig. 2a). Pseudomorphs after grt Ia consist of kelyphite surrounded by a relatively thin symplectitic to granular zone that consists of orthopyroxene (opx II), clinopyroxene (cpx II), spinel (spl II) and minor plagioclase (pl II). Relics of grt I are only preserved in the center of some pseudomorphs (Fig. 2a). Olivine-Ia grains often show kink bands. Almost euhedral tabular grains of olivine Ic are mainly concentrated at the rims of ol Ia. At the contact to intergranular glass, cpx-Ia and Ib grains show sponge-like rims (cpx III), suggesting incongruent melting of clinopyroxene during the transport of the xenoliths in the host magma or a reaction with a late-stage fluid and/or melt. Orthopyroxene Ia, however, does not show any reaction with former melt.

At distances greater than ~ 300 μm from the pseudomorphs after garnet, pyroxene and olivine grains are chemically homogeneous, and there are no discernible differences in composition between porphyroclasts (Ia) and neoblasts (Ib, Ic). Relatively high contents of Ca and Na in opx Ia and Ib and low contents in cpx Ia and Ib (Table 1a) indicate high equilibration temperatures. Towards grt-Ia pseudomorphs, pyroxene-Ia/Ib grains may locally show increases in Al and Ti as well as decreases in Na, Mg and Si. In addition, opx-Ia/Ib grains may show an increase in Ca. Compared to cpx Ia and Ib, cpx-III domains are richer in Ca and Ti but poorer in Na and Al (Table 1a).

Olivine grains (Ia, Ib, Ic, II) are characterized by X_{Mg} values [= Mg/(Mg+Fe_{tot})] between 0.895 and 0.917, whereby the variation within individual samples is smaller. High contents of CaO (0.15-0.18 wt %; Table 1a) point to high equilibration temperatures (Köhler & Brey, 1990), while the elevated contents of Al_2O_3 (0.04-0.08 wt %) appear consistent with high-pressure equilibration in the presence of melt (Agee & Walker, 1990; Taura *et al*., 1998). Towards grt-Ia pseudomorphs, olivine grains often show increasing contents of Fe, Cr and decreasing contents of Mg.

Reliable analyses of the mineral grains replacing grt Ia were only possible in the coarser outer domains of the pseudomorphs. Pyroxene-II grains are highly aluminous and their X_{Mg} values are lower than those of pyroxenes Ia and Ib (Table 1a). Na and Ti contents of cpx II and opx II decrease systematically from the rim towards the interior of the pseudomorphs suggesting that these elements were metasomatically introduced during grt decomposition. X_{Cr} values [= Cr/(Cr+Al+Fe^{3+})] of spl II decrease from 0.295 in the outer parts of the pseudomorphs to 0.056 in the inner parts.

Spinel lherzolite

These rocks display coarse-grained heterogranular textures. Both pyroxenes contain exsolution lamellae of complementary pyroxene and spinel; clinopyroxene additionally has garnet lamellae. Olivine shows kink bands and contains inclusions of spinel that may themselves include tiny clinopyroxene grains. All minerals are relatively Mg-rich, similar to those of garnet lherzolite. A characteristic feature is interstitial glass that encloses euhedral microphenocrysts of olivine (ol III) and clinopyroxene (cpx III) as well as clusters of greenish spinel

Table 1a: Representative electron microprobe analyses of minerals from garnet lherzolite 1927-2

Mineral:	Opx Ia	Opx Ia	Opx Ia	Opx II	Cpx Ia	Cpx Ia	Cpx II	Ol Ia	Ol Ia	Ol Ib	Grt Ia	Grt Ib	Spl II	Pl II
Domain:	core	rim	c/kel	sym	core	rim	sym	core	rim	c/kel	core	rim	sym	sym
SiO_2	55.87	55.33	55.28	50.46	53.81	53.81	49.58	41.17	41.09	41.24	42.79	42.50	0.12	45.48
TiO_2	0.14	0.14	0.24	0.18	0.17	0.20	0.39	0.02	0.01	0.03	0.28	0.33	0.21	0.10
Al_2O_3	3.71	3.73	3.88	11.84	4.36	4.33	9.62	0.07	0.06	0.09	21.94	21.63	55.43	33.95
Cr_2O_3	0.75	0.80	0.76	1.18	1.17	1.28	1.40	0.06	0.06	0.09	2.58	2.78	11.44	0.08
Fe_2O_3	n.c.	n.c.	n.c.	n.c.	n.c.	n.c.	n.c.	n.c.	n.c.	n.c.	n.c.	n.c.	2.95	n.c.
FeO	5.13	5.42	5.48	5.97	3.69	3.74	3.59	8.14	8.37	8.48	5.53	5.83	7.40	0.59
MnO	0.12	0.08	0.13	0.26	0.18	0.13	0.19	0.13	0.09	0.13	0.23	0.21	0.18	0.00
NiO	n.a.	n.a.	n.a.	n.a.	n.a.	n.a.	n.a.	0.40	0.39	0.36	n.a.	n.a.	0.00	n.a.
MgO	33.19	32.99	32.64	29.24	20.11	20.33	16.66	50.55	50.60	50.36	21.95	21.88	21.79	0.64
CaO	1.85	1.90	2.01	1.85	15.89	15.60	17.15	0.15	0.18	0.18	5.25	5.39	0.01	19.00
Na_2O	0.23	0.22	0.17	0.01	1.15	1.16	0.97	0.01	0.00	0.01	0.02	0.04	0.00	0.08
K_2O	0.00	0.00	0.00	0.01	0.00	0.03	0.02	0.01	0.00	0.00	0.00	0.00	0.00	0.00
Total	100.97	100.61	100.59	100.99	100.52	100.60	99.57	100.70	100.86	100.96	100.56	100.58	99.51	99.93
Si	1.911	1.903	1.902	1.737	1.918	1.916	1.795	0.996	0.994	0.996	3.002	2.991	0.003	2.102
Ti	0.004	0.004	0.006	0.005	0.004	0.005	0.011	0.000	0.000	0.000	0.015	0.017	0.004	0.004
Al	0.149	0.151	0.157	0.480	0.183	0.182	0.410	0.002	0.002	0.002	1.814	1.794	1.694	1.849
Cr	0.020	0.022	0.021	0.032	0.033	0.036	0.040	0.001	0.001	0.002	0.143	0.155	0.235	0.003
Fe^{3+}	n.c.	n.c.	n.c.	n.c.	n.c.	n.c.	n.c.	n.c.	n.c.	n.c.	n.c.	n.c.	0.057	n.c.
Fe^{2+}	0.147	0.156	0.158	0.172	0.110	0.111	0.109	0.165	0.169	0.171	0.325	0.343	0.160	0.023
Mn	0.003	0.002	0.004	0.007	0.005	0.004	0.006	0.003	0.002	0.003	0.014	0.012	0.004	0.000
Ni	n.a.	n.a.	n.a.	n.a.	n.a.	n.a.	n.a.	0.008	0.008	0.007	n.a.	n.a.	0.000	n.a.
Mg	1.692	1.691	1.674	1.500	1.069	1.079	0.899	1.823	1.824	1.814	2.296	2.295	0.842	0.044
Ca	0.068	0.070	0.074	0.068	0.607	0.595	0.665	0.004	0.005	0.005	0.395	0.406	0.000	0.941
Na	0.015	0.015	0.012	0.001	0.079	0.080	0.068	0.001	0.000	0.001	0.003	0.005	0.000	0.008
K	0.000	0.000	0.000	0.001	0.000	0.001	0.001	0.000	0.000	0.000	0.000	0.000	0.000	0.000
Total	4.009	4.014	4.008	4.003	4.009	4.010	4.004	3.002	3.005	3.001	8.006	8.020	3.000	4.973
X_{Mg}	0.920	0.916	0.914	0.897	0.907	0.907	0.892	0.917	0.915	0.914	0.876	0.870	0.840	–
X_{Cr}	0.120	0.126	0.116	0.063	0.153	0.166	0.089	–	–	–	0.073	0.079	0.122	–

Formula calculations on the basis of 12 oxygens for grt, 6 oxygens for cpx and opx, 4 oxygens for olivine, 8 oxygens for plagioclase and 4 oxygens and 3 cations for spinel. X_{Mg} = Mg/(Mg+Fe^{2+}); X_{Cr} = Cr/(Cr+Al); c/kel = contact to kelyphite, sym = symplectite after garnet I (opx II + cpx II + spl II); n.a. = not analyzed, n.c. = not calculated.

Table 1b: Representative electron microprobe analyses of minerals from spinel lherzolite 1911–4

Mineral:	Opx I	Opx I	Opx III	Cpx I	Cpx I	Cpx III	Cpx III	Ol I	Ol I	Ol I	Ol III	Spl I	Spl I	Spl I	Spl III
Domain:	core	rim	in glass	core	rim	c/glass	in glass	core	rim	c/spl	in glass	core	rim	c/ol	in glass
SiO_2	55.54	55.31	52.28	52.39	52.59	51.32	50.65	40.92	40.78	40.35	39.72	0.00	0.00	0.09	0.00
TiO_2	0.00	0.06	0.10	0.13	0.15	0.33	0.77	0.00	0.05	0.04	0.03	0.31	0.33	0.31	0.13
Al_2O_3	2.53	2.78	8.02	3.84	3.65	4.84	4.91	0.02	0.03	0.02	0.07	33.21	33,50	32.00	57.99
Cr_2O_3	0.57	0.52	0.46	0.89	0.97	0.78	1.41	0.00	0.01	0.42	0.13	29.15	29.99	31.25	7.77
Fe_2O_3	n.c.	n.c.	n.c.	n.c.	n.c.	n.c.	n.c.	n.c.	n.c.	n.c.	n.c.	7.48	6.59	6.29	4.29
FeO	6.85	6.93	7.42	3.08	3.21	4.19	4.43	11.01	10.76	10.85	12.30	13.46	12.37	12.26	8.36
MnO	0.21	0.17	0.29	0.15	0.09	0.16	0.12	0.11	0.20	0.23	0.21	0.09	0.22	0.18	0.15
NiO	n.a.	n.a.	n.a.	n.a.	n.a.	n.a.	n.a.	0.40	0.35	0.26	0.20	0.00	0.00	0.00	0.00
MgO	32.74	32.71	29.11	16.17	16.15	17.82	16.87	48.45	48.13	48.66	46.48	15.46	16.11	15.94	21.40
CaO	0.68	0.64	1.80	21.35	21.33	19.06	19.41	0.04	0.18	0.21	0.28	0.00	0.01	0.03	0.02
Na_2O	0.06	0.06	0.13	1.22	1.13	0.69	0.42	0.00	0.01	0.02	0.00	n.a.	n.a.	n.a.	n.a.
K_2O	0.01	0.00	0.01	0.00	0.02	0.00	0.05	0.00	0.01	0.00	0.00	n.a.	n.a.	n.a.	n.a.
Total	99.19	99.18	99.62	99.22	99.30	99.18	99.04	100.94	100.52	101.08	99.41	99.16	99.11	98.35	100.12
Si	1.940	1.933	1.831	1.920	1.926	1.879	1.864	0.999	1.000	0.987	0.994	0.000	0.000	0.003	0.000
Ti	0.000	0.002	0.003	0.004	0.004	0.009	0.021	0.000	0.001	0.001	0.001	0.007	0.007	0.007	0.003
Al	0.104	0.115	0.331	0.166	0.158	0.209	0.213	0.000	0.001	0.001	0.002	1.146	1.150	1.113	1.754
Cr	0.016	0.014	0.013	0.026	0.028	0.023	0.041	0.000	0.000	0.008	0.003	0.675	0.691	0.729	0.158
Fe^{3+}	n.c.	n.c.	n.c.	n.c.	n.c.	n.c.	n.c.	n.c.	n.c.	n.c.	n.c.	0.165	0.144	0.140	0.083
Fe^{2+}	0.200	0.202	0.217	0.094	0.098	0.128	0.104	0.225	0.221	0.222	0.257	0.330	0.301	0.303	0.180
Mn	0.006	0.005	0.009	0.005	0.003	0.005	0.003	0.002	0.004	0.005	0.004	0.002	0.005	0.004	0.003
Ni	n.a.	n.a.	n.a.	n.a.	n.a.	n.a.	n.a.	0.008	0.007	0.005	0.004	0.000	0.000	0.000	0.000
Mg	1.705	1.704	1.520	0.884	0.882	0.973	0.926	1.764	1.759	1.774	1.734	0.675	0.700	0.701	0.819
Ca	0.025	0.024	0.067	0.838	0.837	0.747	0.765	0.001	0.005	0.005	0.008	0.000	0.000	0.001	0.001
Na	0.004	0.004	0.009	0.086	0.081	0.049	0.030	0.000	0.001	0.001	0.000	n.a.	n.a.	n.a.	n.a.
K	0.000	0.000	0.001	0.000	0.001	0.000	0.002	0.000	0.000	0.000	0.000	n.a.	n.a.	n.a.	n.a.
Total	4.002	4.003	3.999	4.023	4.018	4.021	4.003	3.000	2.999	3.009	3.007	3.000	3.000	3.000	3.000
X_{Mg}	0.895	0.894	0.875	0.904	0.900	0.884	0.871	0.887	0.889	0.889	0.871	0.672	0.699	0.699	0.820
X_{Cr}	0.131	0.111	0.037	0.135	0.151	0.098	0.162	–	–	–	–	0.371	0.375	0.396	0.082

Formula calculations on the basis of 6 oxygens for cpx and opx, 4 oxygens for olivine and 4 oxygens and 3 cations for spinel. X_{Mg} = Mg/(Mg+Fe^{2+}); X_{Cr} = Cr/(Cr+Al); c/glass = contact to glass, c/spl = contact to spinel, c/ol = contact to olivine; n.a. = not analyzed, n.c. = not calculated.

(spl III). In one sample, the glass also contains rounded aggregates of dolomite crystals (Fig. 2b). At the contacts with interstitial glass, clinopyroxene shows sponge-like rims (cpx III) similar to those described for garnet lherzolite.

Spinel-I grains are zoned with X_{Mg} increasing and X_{Cr} decreasing rimwards. Opx-I grains are characterized by a minor rimward increase in Al (from 0.10 to 0.13 cpfu) that may be followed by a slight decrease at the outermost rims (< 50 μm). Cpx I exhibits the complementary Al zoning pattern. In both pyroxenes, no significant zoning was found for Ca, Na, Mg and Fe. Cpx-III domains, however, have higher concentrations of Ti, Al, Fe and Mg and lower contents of Ca and Na than cpx I (Table 1b).

Coarse-grained garnet, garnet-spinel and spinel harzburgite

The xenoliths of this group display coarse-grained (up to 6 mm) heterogranular textures. Primary garnet (grt I) is largely replaced by coarse symplectitic aggregates of vermicular spinel (spl II) embedded in the marginal parts of larger orthopyroxene grains or, more seldom, in aggregates composed of orthopyroxene and minor clinopyroxene, rarely accompanied by relict olivine (Table 2). Frequently, these fingerprint-like intergrowths bulge towards neighbouring olivine, and vermicular spl II may be partially embedded in the outer zones of olivine grains (Fig. 2c). In three samples, these symplectites border on or contain relict garnet I, indicating the reaction grt I + ol I = spl II + opx II ± cpx II. In one of these samples (1920–23), garnet occurs in interstices between and as small isolated blebs within large orthopyroxene grains, suggesting an origin by exsolution from orthopyroxene. In the same sample, blebs and strips of garnet and olivine occur along contacts between coarse symplectitic spinel II and orthopyroxene II, suggesting the reaction spl + opx → grt + ol. No systematic compositional difference was found between these small garnet grains and relict grt-I grains. Within individual samples, X_{Mg} values of garnet are nearly constant but Ca and Cr may show minor variations (Table 3a). There are significant differences in garnet composition among the three samples. Garnet from sample 1917–4 that also contains cpx I, has high CaO contents of ~ 6.2 wt%, while garnets from samples that lack cpx I (1680–4 and 1920-23) are 'subcalcic' with CaO contents of ~ 4.3 and 2.7, respectively (Tables 3a and 3b). Garnet grains are generally rimmed by a thin (< 40 μm), late-stage kelyphitic corona composed of spl + opx ± cpx ± pl, irrespective of the type of neighbouring phase.

About half of the samples (e.g. 1917-4) contain minor primary spinel I (Table 2) that coexisted with garnet I. In xenoliths in which grt I is completely replaced by symplectite of spl II + opx II (± cpx II), spl-I and spl-II grains have similar compositions, but significant differences exist between different samples (Table 2). X_{Mg} and X_{Cr} values range from 0.64 to 0.83 and from 0.34 to 0.61, respectively, with both parameters showing a weak negative correlation. In samples with relict garnet, however, *s*pinel grains within individual samples show some compositional variation (Table 2).

Except for three samples, opx-I grains contain short (< 30 μm) and thin (< 6 μm) exsolution 'lamellae' of spinel that may be accompanied by cpx lamellae, the latter occurring only in 5 samples (Table 2). In all but 3 samples, opx-I

Table 2: Characteristics of harzburgite xenoliths from the Chyulu Hills

Rock type	Phases present				Exsolution		Mineral chemistry			Core-to-rim zoning of opx		Thermal evolution
Sample no.	Grt I	Spl I	Spl II	Cpx I	in opx		X_{Cr} (spl I/II)	X_{Cr} (grt I)	X_{Mg} (ol)	Al	Ca	
Coarse-grained spinel harzburgite												
1680–1	–	+	–	–	spl	0.34	–	0.923	flat, incr		flat, incr	cooling & equilibr, heating
1920–6	–	+	–	–	–	0.52	–	0.912	decr, incr		flat, incr	cooling, heating
1920–11	–	+	–	–	spl	0.40	–	0.922	flat, incr		flat, incr	cooling, equilibration, heating
Coarse-grained garnet-spinel harzburgite												
1680–2	(+)	+	+	–	spl	0.48	–	0.926	flat, incr		flat, incr	cooling, equilibration, heating
1911–6	(+)	+	+	–	–	0.49	–	0.925	flat		flat	equilibration
1917–4	+	+	+	+	spl, cpx	0.43–0.51		0.106	0.923		flat, decr	flat (decr) cooling
1920–17	(+)	+	+	–	spl, cpx	0.50	–	0.915	decr (flat)		flat	cooling, equilibration
1920–18	(+)	+	+	–	spl	0.42	–	0.926	decr (flat)		flat	cooling, equilibration
1920–23	+	+	+	–	spl	0.32–0.38		0.044	0.932		decr (flat), incr	flat cooling, heating
Coarse-grained garnet harzburgite												
1680–3	(+)	–	+	–	spl	0.48	–	0.922	flat, incr		flat, incr	cooling, equilibration, heating
1680–4	+	–	+	–	spl, cpx	0.37–0.46		0.058	0.931		flat, incr	flat cooling, equilibration, heating
1680–5	(+)	–	+	–	spl	0.37	–	0.930	flat, incr		flat, incr	cooling, equilibration, heating
1911–3	(+)	–	+	–	spl	0.45	–	0.905	flat, incr		flat, incr	cooling, equilibration, heating
1917–3	(+)	–	+	–	spl	0.44	–	0.925	flat, incr		flat	cooling, heating
1920–2	(+)	–	+	–	spl, cpx	0.51	–	0.922	flat, incr		flat, flat	cooling, equilibration, heating
1920–8	(+)	–	+	–	–	0.53	–	0.900	flat, incr		flat, incr	equilibration, heating
1920–10	(+)	–	+	–	spl, cpx	0.45	–	0.924	flat (decr), incr		flat (decr) incr	cooling, equilibration, heating
1920–22	(+)	–	+	–	spl	0.54	–	0.916	flat, incr		flat, incr	cooling, equilibration, heating
Granular garnet-spinel harzburgite												
1902–1	(+)	+	+	–	–	0.56	–	0.936	decr		flat	cooling
19026	(+)	+	+	–	–	0.53	–	0.938	decr, incr		flat, incr	cooling, heating
Porphyroclastic spinel harzburgite												
1927–5	–	+	–	+	–	0.57	–	0.915	flat		flat (incr)	equilibration (heating)
1927–15	–	+	–	+	–	0.61	–	0.911	flat		flat	equilibration

+ = present, (+) = garnet is completely transformed to fingerprint-like spl-opx(-cpx) intergrowths, – = absent. Exs lam opx = exsolution lamellae in opx; incr = increasing, decr = decreasing

Table 3a: Representative electron microprobe analyses of minerals from coarse-grained garnet-spinel harzburgite 1917–4

Mineral:	Opx I	Opx I	Opx IIa	Opx IIa	Opx IIb	Cpx IIa	Cpx IIa	Cpx IIb	Cpx III	Grt I	Grt I	Spl IIa	Spl IIa	Spl IIb	Ol I
Domain:	core	rim	core	c/spl	sym	core	c/spl	sym		core	rim	core	rim		
SiO_2	55.33	55.85	56.43	56.31	48.76	53.76	53.58	49.08	50.93	42.01	42.11	0.06	0.13	0.19	40.99
TiO_2	0.03	0.01	0.02	0.01	0.02	0.03	0.05	0.03	1.06	0.04	0.02	0.08	0.25	0.38	0.01
Al_2O_3	3.57	2.83	2.53	2.66	13.11	2.81	3.14	10.24	5.31	20.86	21.38	26.63	26.83	55.28	0.05
Cr_2O_3	1.16	0.94	0.54	1.09	1.92	1.23	1.52	2.22	1.36	3.48	3.25	41.24	40.58	10.92	0.02
Fe_2O_3	n.c.	n.c.	n.c	n.c.	n.c.	n.c.	n.c.	n.c.	n.c.	n.c.	n.c.	3.63	3.50	3.03	n.c.
FeO	4.90	4.85	4.96	5.16	6.40	2.41	2.46	4.59	3.49	6.18	6.39	11.99	12.12	7.32	7.65
MnO	0.11	0.08	0.13	0.13	0.36	0.04	0.06	0.39	0.11	0.30	0.34	0.12	0.01	0.08	0.14
NiO	n.a.	n.a.	n.a.	n.a.	n.a.	n.a.	n.a.	n.a.	n.a.	n.a.	n.a.	n.a.	n.a.	n.a.	0.37
MgO	34.05	34.19	34.68	34.17	28.02	17.30	17.38	18.73	18.07	20.46	20.62	15.70	15.78	21.96	51.08
CaO	0.81	0.73	0.74	0.77	1.18	21.14	20.67	15.51	18.46	6.35	6.11	0.01	0.08	0.00	0.05
Na_2O	0.07	0.05	0.05	0.07	0.00	0.92	0.93	0.09	0.85	0.00	0.00	0.01	0.00	0.00	0.01
K_2O	0.00	0.01	0.00	0.01	0.00	0.01	0.01	0.00	0.00	0.00	0.02	0.00	0.02	0.02	0.00
Total	100.03	99.54	100.09	100.38	99.78	99.65	99.79	100.88	99.63	99.69	100.24	99.45	99.30	99.16	100.36
Si	1.905	1.929	1.937	1.932	1.704	1.950	1.941	1.755	1.852	3.004	2.993	0.002	0.004	0.005	0.993
Ti	0.001	0.000	0.001	0.000	0.001	0.001	0.001	0.001	0.029	0.002	0.001	0.002	0.006	0.007	0.000
Al	0.145	0.115	0.103	0.108	0.540	0.120	0.134	0.432	0.228	1.758	1.791	0.938	0.944	1.693	0.002
Cr	0.032	0.026	0.015	0.030	0.053	0.035	0.043	0.063	0.039	0.197	0.183	0.974	0.958	0.224	0.000
Fe^{3+}	n.c.	n.c.	n.c.	n.c.	n.c.	n.c.	n.c.	n.c.	n.c.	n.c.	n.c.	0.082	0.079	0.059	n.c.
Fe^{2+}	0.141	0.140	0.142	0.148	0.187	0.073	0.074	0.137	0.106	0.370	0.380	0.300	0.303	0.159	0.155
Mn	0.003	0.002	0.004	0.004	0.011	0.001	0.002	0.012	0.004	0.018	0.020	0.003	0.000	0.002	0.003
Ni	n.a.	n.a.	n.a.	n.a.	n.a.	n.a.	n.a.	n.a.	n.a.	n.a.	n.a.	n.a.	n.a.	n.a.	0.007
Mg	1.748	1.760	1.775	1.748	1.460	0.936	0.938	0.999	0.979	2.181	2.185	0.699	0.703	0.851	1.845
Ca	0.030	0.027	0.027	0.028	0.044	0.822	0.802	0.595	0.719	0.487	0.465	0.000	0.002	0.000	0.001
Na	0.005	0.004	0.003	0.005	0.000	0.065	0.065	0.006	0.060	0.000	0.000	0.001	0.000	0.000	0.000
K	0.000	0.001	0.000	0.001	0.000	0.000	0.001	0.000	0.000	0.000	0.001	0.000	0.001	0.001	0.000
Total	4.009	4.003	4.006	4.002	3.999	4.004	4.002	3.999	4.016	8.017	8.020	3.000	3.000	3.000	3.006
X_{Mg}	0.925	0.926	0.926	0.922	0.886	0.928	0.927	0.879	0.902	0.855	0.852	0.700	0.699	0.843	0.923
X_{Cr}	0.179	0.182	0.126	0.216	0.089	0.226	0.245	0.127	0.146	0.101	0.093	0.509	0.504	0.117	–

Formula calculations on the basis of 12 oxygens for grt, 6 oxygens for cpx and opx, 4 oxygens for olivine and 4 oxygens and 3 cations for spinel. X_{Mg} = Mg/(Mg+Fe^{2+}); X_{Cr} = Cr/(Cr+Al); c/spl = contact to spinel IIa, sym = symplectite after garnet (opx IIb + cpx IIb + spl IIb); n.a. = not analyzed, n.c. = not calculated.

Table 3b: Representative electron microprobe analyses of minerals from coarse-grained harzburgite xenoliths 1920–23 and 1920–10

Sample no.	1920-23							1920–10						
Mineral:	Opx I	Opx I	Opx II	Grt I	Spl IIa	Spl IIb	Ol I	Opx I	Opx I	Opx II	Spl II	Spl II	Ol I	Ol I
Domain:	core	rim	core	core	core/rim		core/rim	core	rim	core	core	rim	core	rim
SiO_2	56.31	56.36	56.70	42.78	0.04	0.04	41.48	55.64	55.35	55.91	0.11	0.10	40.64	40.57
TiO_2	0.04	0.05	0.01	0.01	0.09	0.03	0.00	0.08	0.24	0.26	1.71	1.55	0.05	0.04
Al_2O_3	2.72	3.10	3.10	23.13	36.86	63.80	0.02	2.80	3.33	3.31	29.28	29.77	0.03	0.04
Cr_2O_3	0.64	0.54	0.68	1.38	31.21	4.23	0.05	0.88	0.67	0.89	36.21	35.05	0.03	0.10
Fe_2O_3	n.c.	n.c.	n.c.	n.c.	3.31	0.74	n.c.	n.c.	n.c.	n.c.	3.81	4.13	n.c.	n.c.
FeO	4.00	4.22	4.20	5.81	9.20	8.23	6.90	4.94	4.85	5.02	11.64	10.93	7.57	7.81
MnO	0.07	0.12	0.13	0.32	0.06	0.22	0.08	0.14	0.14	0.08	0.01	0.07	0.12	0.11
NiO	n.a.	n.a.	n.a.	n.a.	n.a.	n.a.	0.38	n.a.	n.a.	n.a.	n.a.	n.a.	0.44	0.37
MgO	35.13	34.95	35.36	23.77	18.54	21.84	51.90	34.27	33.97	33.95	17.41	17.61	51.40	50.78
CaO	0.35	0.38	0.35	2.71	0.00	0.00	0.07	0.90	1.08	1.01	0.02	0.02	0.09	0.17
Na_2O	0.07	0.07	0.10	0.00	0.02	0.01	0.01	0.12	0.17	0.13	0.00	0.00	0.00	0.03
K_2O	0.01	0.00	0.01	0.00	0.01	0.00	0.00	0.01	0.00	0.00	0.02	0.00	0.00	0.00
Total	99.33	99.78	100.64	99.89	99.34	99.14	100.88	99.78	99.80	100.57	100.23	99.24	100.37	100.02
Si	1.937	1.931	1.927	2.992	0.001	0.001	0.996	1.921	1.910	1.915	0.003	0.003	0.989	0.988
Ti	0.001	0.001	0.000	0.000	0.002	0.000	0.000	0.002	0.006	0.007	0.037	0.034	0.001	0.001
Al	0.110	0.125	0.124	1.907	1.228	1.899	0.000	0.114	0.135	0.134	1.004	1.025	0.001	0.001
Cr	0.017	0.015	0.018	0.076	0.697	0.084	0.001	0.024	0.018	0.024	0.833	0.810	0.000	0.002
Fe^{3+}	n.c.	n.c.	n.c.	n.c.	0.070	0.014	n.c.	n.c.	n.c.	n.c.	0.083	0.091	n.c.	n.c.
Fe^{2+}	0.115	0.121	0.119	0.340	0.217	0.174	0.138	0.143	0.140	0.144	0.283	0.267	0.154	0.159
Mn	0.002	0.003	0.004	0.019	0.002	0.005	0.002	0.004	0.004	0.002	0.000	0.002	0.002	0.002
Ni	n.a.	n.a.	n.a.	n.a.	n.a.	n.a.	0.007	n.a.	n.a.	n.a.	n.a.	n.a.	0.009	0.007
Mg	1.801	1.785	1.792	2.479	0.781	0.822	1.857	1.764	1.748	1.733	0.755	0.767	1.858	1.844
Ca	0.013	0.014	0.013	0.203	0.000	0.000	0.002	0.033	0.040	0.037	0.001	0.001	0.002	0.004
Na	0.004	0.004	0.007	0.000	0.001	0.000	0.000	0.008	0.011	0.009	0.000	0.000	0.000	0.001
K	0.001	0.000	0.001	0.000	0.000	0.000	0.000	0.000	0.000	0.000	0.001	0.000	0.000	0.000
Total	4.001	4.000	4.005	8.016	3.000	3.000	3.004	4.013	4.013	4.004	3.000	3.000	3.013	3.010
X_{Mg}	0.940	0.937	0.938	0.880	0.782	0.826	0.931	0.925	0.926	0.923	0.727	0.742	0.924	0.921
X_{Cr}	0.135	0.104	0.128	0.038	0.362	0.043	–	0.174	0.118	0.153	0.453	0.441	–	–

Formula calculations on the basis of 12 oxygens for grt, 6 oxygens for cpx and opx, 4 oxygens for olivine and 4 oxygens and 3 cations for spl. X_{Mg} = Mg/(Mg+Fe^{2+}); X_{Cr} = Cr/(Cr+Al). n.a. = not analyzed, n.c. = not calculated

Table 3c: Representative electron microprobe analyses of minerals from granular (1902–1) and porphyroclastic harzburgite (1927–15)

Sample no.:	Granular garnet-spinel harzburgite 1902–1								Porphyroclastic spinel harzburgite 1927–15						
Mineral:	Opx I	Opx I	Opx II	Ol I	Ol III	Spl I	Spl I	Cpx III	Opx I	Opx I	Cpx I	Cpx I	Cpx III	Ol I	Spl I
Domain:	core	rim	core	core	c/glass	core	rim		core	rim	core	rim		core/rim	core/rim
SiO_2	56.54	56.62	57.47	40.91	40.29	0.03	0.03	51.55	55.38	55.08	53.22	53.37	52.34	40.80	0.26
TiO_2	0.01	0.00	0.03	0.01	0.01	0.00	0.11	1.87	0.02	0.06	0.03	0.12	0.62	0.02	0.21
Al_2O_3	2.53	1.65	1.61	0.01	0.00	24.86	24.19	4.10	3.02	2.95	3.07	3.13	2.69	0.06	19.65
Cr_2O_3	0.74	0.41	0.71	0.03	0.04	46.60	45.08	1.26	1.24	1.21	1.43	1.55	2.36	0.10	44.99
Fe_2O_3	n.c.	n.c.	n.c.	n.c.	n.c.	1.15	3.10	n.c.	n.c.	n.c.	n.c.	n.c.	n.c.	n.c.	7.04
FeO	3.90	4.06	4.02	6.35	7.66	10.01	9.88	2.79	5.46	5.64	3.64	3.59	3.69	8.62	11.11
MnO	0.14	0.15	0.12	0.06	0.12	0.11	0.07	0.09	0.09	0.12	0.16	0.17	0.09	0.11	0.09
NiO	n.a.	n.a.	n.a.	0.39	0.34	n.a.	n.a.	n.a.	n.a.	n.a.	n.a.	n.a.	n.a.	0.33	n.a.
MgO	35.90	36.14	36.54	52.38	51.57	16.84	16.83	17.35	33.07	33.36	20.79	20.68	18.76	50.31	15.71
CaO	0.15	0.19	0.21	0.00	0.10	0.01	0.06	20.25	2.03	2.04	17.49	17.21	18.98	0.20	0.00
Na_2O	0.06	0.06	0.05	0.01	0.00	0.00	0.00	0.97	0.08	0.05	0.43	0.59	0.59	0.03	0.01
K_2O	0.00	0.01	0.00	0.01	0.01	0.00	0.00	0.00	0.00	0.01	0.02	0.03	0.00	0.02	0.00
Total	99.96	9.27	100.76	100.15	100.13	99.61	99.34	100.22	100.36	100.52	100.278	100.45	100.12	100.61	99.08
Si	1.932	1.949	1.949	0.988	0.980	0.001	0.001	1.868	1.912	1.903	1.913	1.914	1.901	0.991	0.008
Ti	0.000	0.000	0.001	0.000	0.000	0.000	0.002	0.051	0.000	0.002	0.001	0.003	0.017	0.000	0.005
Al	0.102	0.067	0.064	0.000	0.000	0.874	0.855	0.175	0.123	0.120	0.130	0.132	0.115	0.002	0.714
Cr	0.020	0.011	0.019	0.000	0.001	1.099	1.069	0.036	0.034	0.33	0.041	0.044	0.068	0.002	1.097
Fe^{3+}	n.c.	n.c.	n.c.	n.c.	n.c.	0.026	0.070	n.c.	n.c.	n.c.	n.c.	n.c.	n.c.	n.c.	0.163
Fe^{2+}	0.111	0.117	0.114	0.128	0.156	0.250	0.248	0.084	0.158	0.163	0.110	0.108	0.112	0.175	0.287
Mn	0.004	0.004	0.003	0.001	0.002	0.003	0.002	0.003	0.003	0.004	0.005	0.005	0.003	0.002	0.002
Ni	n.a.	n.a.	n.a.	0.008	0.007	n.a.	n.a.	n.a.	n.a.	n.a.	n.a.	n.a.	n.a.	0.006	n.a.
Mg	1.829	1.855	1.848	1.885	1.870	0.749	0.752	0.937	1.702	1.718	1.114	1.106	1.016	1.822	0.722
Ca	0.005	0.007	0.008	0.000	0.003	0.000	0.002	0.786	0.075	0.075	0.674	0.661	0.739	0.005	0.000
Na	0.004	0.004	0.003	0.000	0.000	0.000	0.000	0.068	0.005	0.003	0.030	0.041	0.042	0.001	0.001
K	0.000	0.000	0.000	0.000	0.000	0.000	0.000	0.000	0.000	0.001	0.001	0.001	0.000	0.001	0.000
Total	4.008	4.014	4.010	3.012	3.019	3.000	3.000	4.009	4.012	4.021	4.017	4.016	4.012	3.008	3.000
X_{Mg}	0.943	0.941	0.942	0.936	0.923	0.750	0.752	0.917	0.915	0.913	0.910	0.911	0.901	0.912	0.716
X_{Cr}	0.163	0.143	0.229	–	–	0.557	0.556	0.171	0.216	0.216	0.238	0.249	0.371	–	0.606

Formula calculations on the basis of 6 oxygens for cpx and opx, 4 oxygens for olivine and 4 oxygens and 3 cations for spl. X_{Mg} = Mg/(Mg+Fe^{2+}); X_{Cr} = Cr/(Cr+Al); c/glass = contact to glass; n.a. = not analyzed, n.c. = not calculated

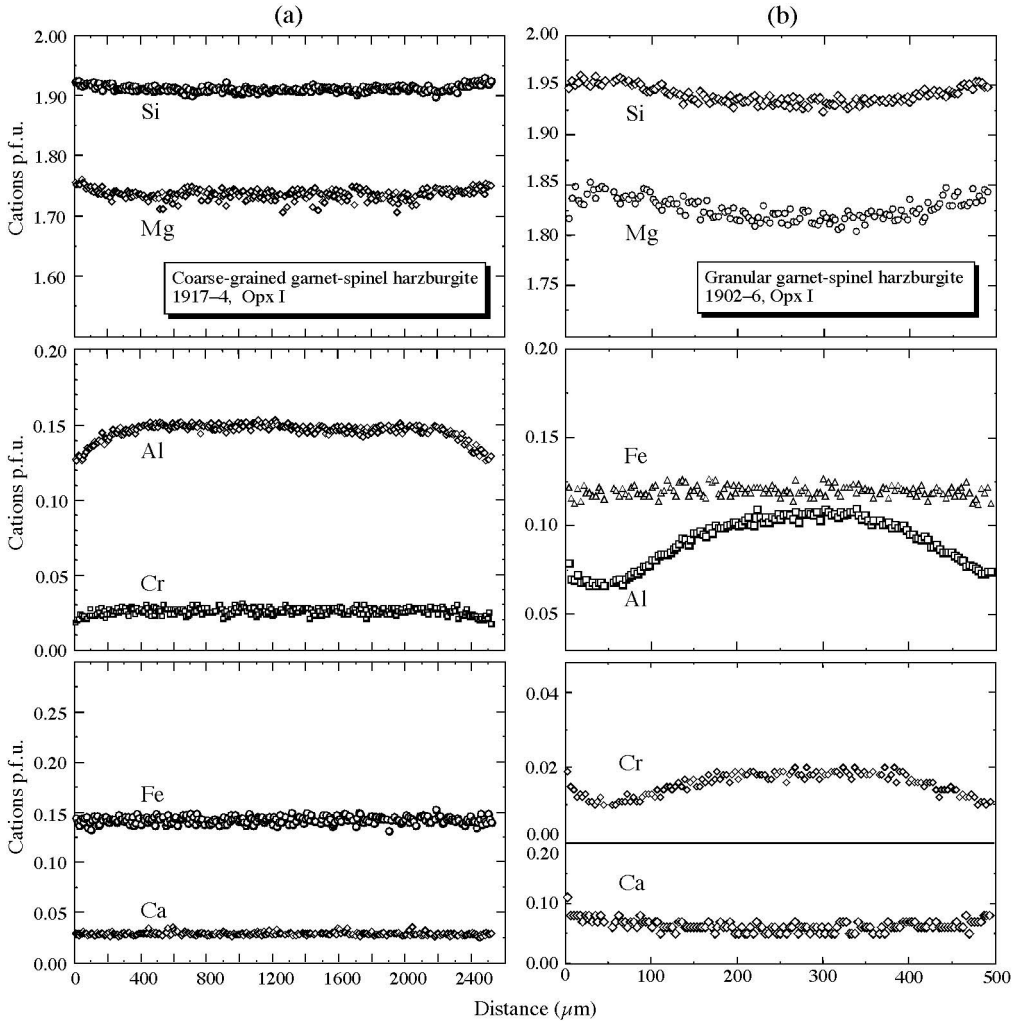


Fig. 3. Zoning patterns of opx I in coarse-grained grt-spl harzburgite 1917–4 (a) and in granular grt-spl harzburgite 1902–6 (b). For further explanation see 'Xenolith types and mineral composition'.

grains display minor chemical zoning. In most samples, the cores of opx-I grains are homogeneous and the outermost zones (< 300 μm) are characterized by increases in Al and Ca, suggesting a relatively short-lived heating event after a long period of cooling and attainment of chemical equilibrium. In one sample (1917-4), however, the outer zones (ca. 500 μm) of opx-I grains are characterized by a minor decrease in Al, suggesting simple cooling (Fig. 3a). Ca and Na, however, may be elevated in the outermost rims, due to interaction with an intergranular melt phase. In three samples (1917–3, 1920–6, 1920–23), opx-I grains are complexely zoned. From core to rim, Al first decreases slightly and then increases again at the outhermost rim (Fig. 4a). X_{Mg} and X_{Cr} values of opx-I grains are nearly constant within a sample, but vary among the samples (0.89–0.94 and 0.10–0.18, respectively; Table 2). The compositions of opx-II grains are similar to those of the outer zones of opx I grains. In most cases, Al increases slightly towards spl II (Tables 3a and 3b).

Olivine grains have kink bands. Within individual samples, olivine compositions are nearly constant, but there are compositional differences between different samples with X_{Mg} ranging

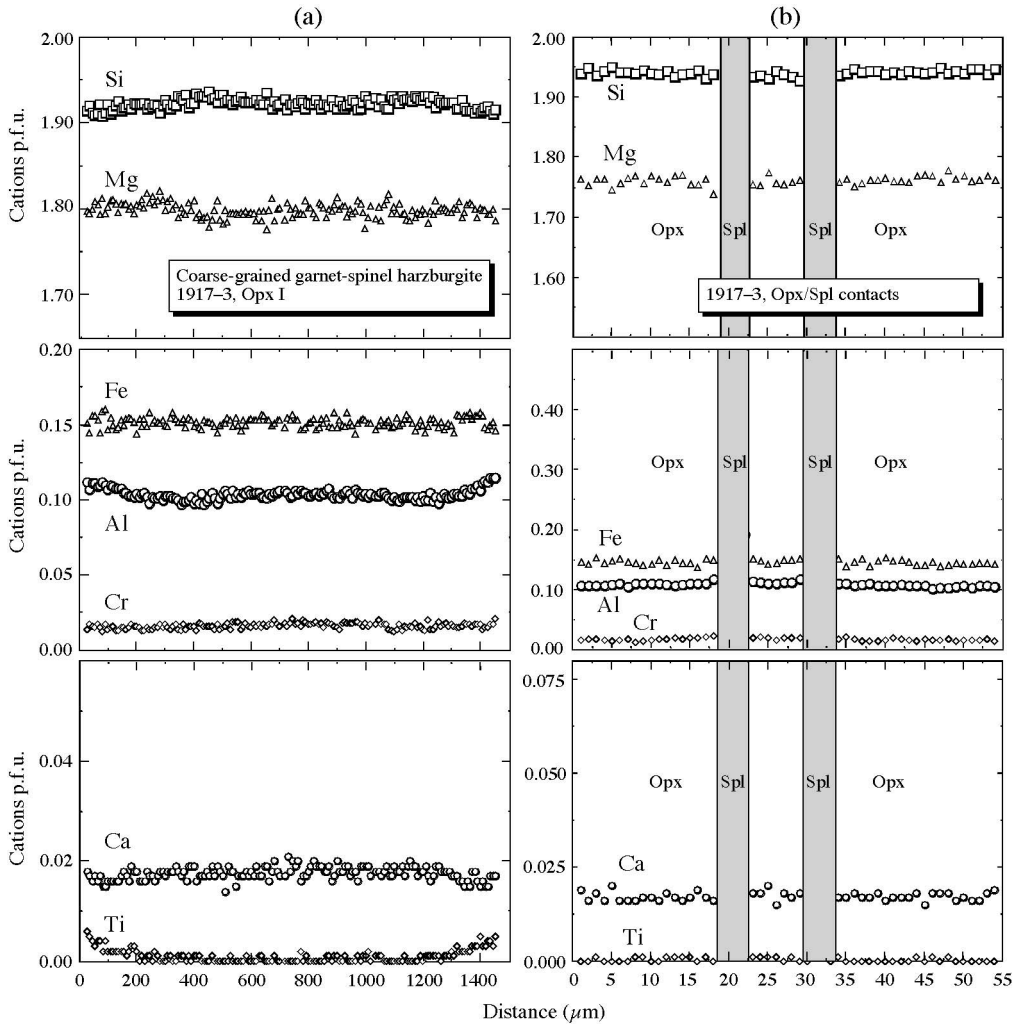


Fig. 4. Zoning patterns of opx I in harzburgite 1917–3. (a) Grain without spl exsolution lamellae. (b) Grain showing spl exsolution lamellae. For further explanation see 'Xenolith types and mineral composition'.

from 0.900 to 0.932 (Table 2). Among the samples, there is no correlation between X_{Mg} of olivine and X_{Cr} of spinel.

Only one coarse-grained harzburgite (1917-4) contains very minor primary clinopyroxene I. The small grains are characterized by low TiO_2 contents, while late-stage interstitial cpx–III grains have higher TiO_2 and Na_2O contents (Table 3a).

Granular garnet-spinel harzburgite

The two samples of granular garnet-spinel harzburgite (1902–1, 1902–6) are characterized by relatively fine-graind equigranular textures (Fig. 2d). Polygonal equidimensional shapes of most olivine and orthopyroxene grains (~ 120 ° triple points) indicate textural equilibrium. The rocks are devoid of primary clinopyroxene. Spinel occurs in two generations. Besides primary spinel (spl I) the rocks contain round, fingerprint-like intergrowths of vermicular spinel II and opx II, interpreted as former low-Ca garnet I. Locally, these intergrowths occur in contact with spl I, suggesting the former coexistence of garnet and spinel. Both spinel generations show similar compositions and are exceptionally rich in Cr (Tables 2 and 3c). Or-

thopyroxene-I grains do not contain exsolution lamellae and display a weak chemical zoning, whereby Al and Cr first decrease from core to rim and then increase again in the outermost zones of the grains (Fig. 3b; Table 3c). Orthopyroxene II has low contents of Al and relatively high abundances of Cr. Olivine-I grains are chemically homogeneous with X_{Mg} values of c. 0.937 that may decrease in the outermost zones to c. 0.923 (Table 3c).

Porphyroclastic spinel harzburgite

The two xenoliths of spinel harzburgite (1927-5, 1927-15) are characterized by porphyroclasts of olivine (ol Ia), orthopyroxene (opx Ia), spinel (spl Ia) and rare clinopyroxene (cpx Ia) embedded in a matrix of variably sized neoblasts of all four mineral phases (ol Ib, opx Ib, spl Ib, cpx Ib) (Fig. 2e). Fingerprint-like intergrowths of spl and opx are absent. Within each sample, mineral compositions are rather constant and no compositional difference between porphyroclasts and neoblasts was found. Orthopyroxene shows X_{Mg} values of ~ 0.92 and X_{Cr} values of ~ 0.21 (Table 2). Relatively high Ca contents (0.070–0.075 cpfu) in opx in conjunction with low Ca contents in cpx (0.671–0.674 cpfu) indicate high equilibration temperatures. Spinel displays high values of X_{Cr} (0.57–0.61) and X_{Mg} (~ 0.72), while olivine has normal X_{Mg} values of 0.911 and 0.915 (Tables 2 and 3c).

Garnet-spinel-olivine websterite

The two xenoliths of this type show granular textures (Fig. 2f). Their modes are dominated by olivine (ol I) and orthopyroxene (opx I); clinopyroxene (cpx I) amounts to 10–15 vol. %; spinel (spl I) is subordinate, and garnet (grt I) or pseudomorphs after garnet are subordinate to rare. X_{Mg} values of olivine, garnet and pyroxenes are considerably lower than those in the peridotites (Table 4).

Sample 1533–2 is fine-grained and heterogranular and contains relatively abundant spl I. Former grt-I grains are almost completely replaced by fine-grained symplectite/kelyphite consisting of spl II + opx II + cpx II. The cores of larger pyroxene-I grains contain exsolution lamellae of complementary pyroxene as well as of spinel and ilmenite. The outer parts of these large pyroxene grains and smaller px grains are free of exsolution lamellae. Both opx I and cpx I show considerable chemical zoning. In opx-I grains, Al and Ca first decrease and then increase again from core to rim (Fig. 5a, b). In cpx I, Al decreases but Ca increases slightly from core to rim (Fig. 5c).

Sample 1533–11 is more coarse-grained. Garnet I, often replaced by kelyphite, occurs in larger aggregates along grain boundaries or frames spinel-I grains. Near the boundary between spinel and garnet, tiny (< 50–60 μm) grains of orthopyroxene (opx II) may occur. These grains most probably represent 'left-overs' of the reaction spl I + opx I + cpx I = grt I + ol I. There are also isolated spl-I grains that are not in contact with garnet. Spinel-I grains are strongly zoned with a rimward increase in X_{Mg}, while X_{Cr} markedly decreases and the Ti content slightly decreases.

In their inner parts, opx-I grains contain very thin though frequent lamellae of clinopyroxene, and very often tiny intermittent lamellae of spinel or ilmenite. Cpx I may have coarser lamellae of garnet, and always contains tiny spinel and ilmenite lamellae. The outer zones of opx-I and cpx-I grains are free of exsolution phenomena.

Table 4: Characteristics of websterite xenoliths from the Chyulu Hills

Rock type (thermal evolution) Sample no.	Grt I	Spl I	Ol I	Grt II	Ol II	Inclusions in grt I	Inclusions in spl I	Exsolution lamellae in opx	Exsolution lamellae in cpx	Zoning of opx[a] Al	Zoning of opx[a] Ca*	Zoning of cpx[a] Al	Zoning of cpx[a] Ca*
Garnet-spinel-olivine websterite (cooling followed by heating)													
1533–2	+	+	+	–	–	–	grt, opx	spl, cpx, ilm	spl, opx, ilm	decr, incr	decr, incr	decr	incr
1533–11	+	+	+	–	–	–	grt, opx	spl, cpx, ilm	spl, opx, ilm	flat, incr	flat, incr	decr	flat
Coarse-grained websterite, group 1: (nearly) equilibrated after cooling													
1901–9	+	–	–	+	–	–	–	grt	grt	flat	flat	flat	flat
1906–1	+	+	–	+	–	kf, qtz, cpx	cor, rt (ilm)	grt, cpx	grt, rt (ilm)	flat	flat	flat	flat
1906–4	+	+	–	+	+	spl	–	grt, cpx	grt, opx, spl	flat (decr)	flat	flat (decr)	flat
1916–3	–	–	–	+	–	–	–	grt, cpx	grt, opx	decr	decr, (flat)	flat	flat
1916–20	–	–	–	–	–	–	_	grt, cpx	grt	decr, flat	flat	flat (decr)	flat
1921–4	+	–	–	+	+	–	–	grt	grt	flat	flat	flat	flat
1921–5	–	–	–	+	–	–	–	grt, spl	grt, spl	flat	flat	flat	flat
Coarse-grained websterite, group 2: cooling													
1533–6 (incr)	+	–	–	+	–	rt (ilm)	–	grt, cpx	grt, rt	decr, incr	flat	decr	flat
1533–12 (incr)	+	–	–	+	–	rt (ilm)	–	grt (very rare)	grt, rt	decr	flat	decr	flat
1535–2	+	–	–	+	–	–	–	grt	–	decr	decr	decr	flat
1535–3	+	+	+	+	+	–	–	grt, cpx	grt, opx	incr, decr	decr	decr	incr
1535–9	+	–	–	+	–	–	–	–	opx	decr	decr	flat	flat
1905–2 (incr)	+	–	–	+	–	kf, qtz	–	grt, cpx, rt	grt, opx, rt	flat	flat	decr	flat
Coarse-grained websterite, group 3: cooling followed by heating													
1910–1	+	–	+	+	+	–	–	grt	grt	decr, incr	flat	decr, incr	flat
1910–11	+	+	+	+	+	–	–	grt, cpx	grt	decr, incr	flat	decr, incr	flat
1916–13	+	+	+	+	+	spl, ol	–	grt, cpx	grt, opx	flat, incr	flat	decr, flat	incr

Table 5a: Representative electron microprobe analyses of minerals from (olivine) websterite xenoliths

Sample no.:	Garnet-spinel-olivine websterite 1533–11									Garnet websterite 1935–9				
Mineral:	Opx	Opx	Cpx	Cpx	Ol	Spl	Spl	Grt	Grt	Opx	Opx	Cpx	Cpx	Grt
Domain:	core	rim	core	rim	core/rim	core	rim	core	rim	core	rim	core	rim	core
SiO_2	55.41	55.04	51.90	52.63	39.34	0.03	0.05	40.53	40.70	54.54	55.31	52.98	53.42	40.85
TiO_2	0.18	0.21	0.77	0.54	0.01	1.79	1.49	0.15	0.05	0.12	0.13	0.36	0.41	0.11
V_2O_3	n.a.	n.a.	n.a.	n.a.	n.a.	0.23	0.23	n.a.	n.a.	n.a.	n.a.	n.a.	n.a.	n.a.
Al_2O_3	1.94	2.75	4.98	3.69	0.01	28.22	38.96	22.10	22.16	2.91	2.35	3.35	3.51	22.14
Cr_2O_3	0.32	0.37	0.50	0.74	0.03	30.14	21.76	1.35	1.17	0.36	0.31	0.63	0.61	1.08
Fe_2O_3	n.c.	n.c.	n.c.	n.c.	n.c.	7.36	4.73	n.c.	n.c.	n.c.	n.c.	n.c.	n.c.	n.c.
FeO	10.16	10.94	4.33	4.52	17.25	21.23	20.54	13.77	12.99	10.73	11.02	4.72	4.85	13.24
MnO	0.17	0.14	0.07	0.05	0.16	0.18	0.22	0.54	0.49	0.21	0.16	0.08	0.04	0.45
ZnO	n.a.	n.a.	n.a.	n.a.	n.a.	0.16	0.15	n.a.	n.a.	n.a.	n.a.	n.a.	n.a.	n.a.
NiO	n.a.	n.a.	n.a.	n.a	0.38	0.27	0.24	n.a.	n.a.	0.12	0.17	n.a.	n.a.	0.02
MgO	31.33	30.60	14.74	15.54	43.43	10.66	12.12	15.80	16.50	30.45	30.84	15.72	15.50	17.08
CaO	0.38	0.63	21.62	21.68	0.03	0.00	0.04	5.81	5.87	0.76	0.61	20.63	20.52	5.46
Na_2O	0.02	0.05	1.15	0.88	0.01	0.00	0.00	0.01	0.02	0.05	0.07	1.33	1.35	0.03
K_2O	0.00	0.00	0.00	0.00	0.00	0.00	0.00	0.02	0.00	0.01	0.02	0.00	0.00	0.00
Total	99.91	100.73	100.06	100.27	100.64	100.27	100.53	100.05	99.95	100.26	100.99	99.81	100.21	100.45
Si	1.948	1.928	1.896	1.919	0.993	0.001	0.001	2.971	2.974	1.921	1.935	1.938	1.944	2.969
Ti	0.005	0.006	0.021	0.015	0.000	0.041	0.032	0.008	0.003	0.003	0.003	0.010	0.011	0.006
V	n.a.	n.a.	n.a.	n.a.	n.a.	0.006	0.005	n.a.	n.a.	n.a.	n.a.	n.a.	n.a.	n.a.
Al	0.080	0.114	0.214	0.159	0.000	1.015	1.327	1.909	1.908	0.121	0.097	0.145	0.151	1.896
Cr	0.009	0.010	0.014	0.021	0.001	0.727	0.497	0.078	0.068	0.010	0.009	0.018	0.018	0.062
Fe^{3+}	n.c.	n.c.	n.c.	n.c.	n.c.	0.169	0.103	n.c.	n.c.	n.c.	n.c.	n.c.	n.c.	n.c.
Fe^{2+}	0.299	0.320	0.132	0.138	0.364	0.542	0.496	0.844	0.794	0.316	0.322	0.144	0.147	0.805
Mn	0.005	0.004	0.002	0.002	0.003	0.005	0.005	0.033	0.030	0.006	0.005	0.002	0.001	0.028
Zn	n.a.	n.a.	n.a.	n.a.	n.a.	0.004	0.003	n.a.	n.a.	n.a.	n.a.	n.a.	n.a.	n.a.
Ni	n.a.	n.a.	n.a.	n.a.	0.008	0.007	0.006	n.a.	n.a.	0.003	0.005	n.a.	n.a.	0.001
Mg	1.642	1.598	0.802	0.845	1.635	0.485	0.522	1.726	1.797	1.599	1.608	0.857	0.841	1.850
Ca	0.014	0.024	0.846	0.847	0.001	0.000	0.001	0.456	0.460	0.029	0.023	0.808	0.800	0.425
Na	0.001	0.003	0.081	0.062	0.000	0.000	0.000	0.001	0.003	0.003	0.004	0.095	0.095	0.004
K	0.000	0.000	0.001	0.000	0.000	0.000	0.000	0.002	0.000	0.000	0.001	0.000	0.000	0.000
Total	4.003	4.006	4.010	4.007	2.006	3.000	3.000	8.028	8.036	4-012	4.012	4.018	4.008	8.047
X_{Mg}	0.846	0.833	0.859	0.860	0.818	0.472	0.513	0.674	0.694	0.835	0.833	0.856	0.851	0.697
X_{Cr}	0.101	0.065	0.061	0.117	–	0.417	0.272	0.039	0.0344	0.076	0.085	0.110	0.107	0.032

Formula calculations on the basis of 12 oxygens for grt, 6 oxygens for cpx and opx, 4 oxygens for olivine and 4 oxygens and 3 cations for spl. $X_{Mg} = Mg/(Mg+Fe^{2+})$; $X_{Cr} = Cr/(Cr+Al)$; n.a. = not analyzed, n.c. = not calculated

Table 5b: Representative electron microprobe analyses of minerals from websterite

Sample no.:	Garnet websterite 1901–9						Garnet-spinel websterite 1906–1							
Mineral:	Opx	Opx	Cpx	Cpx	Grt	Grt	Opx	Opx	Cpx	Cpx	Cpx	Grt	Grt	Kfs
Domain:	core	rim	core	rim	l/opx	l/cpx	core	rim	core	rim	incl/grt	l/opx	l/cpx	incl/grt
SiO_2	54.35	54.40	52.55	52.37	41.31	40.68	54.96	54.64	54.33	53.86	54.27	40.06	39.47	64.89
TiO_2	0.14	0.16	0.60	0.55	0.16	0.22	0.03	0.05	0.16	0.19	0.17	0.04	0.00	0.00
Al_2O_3	3.43	3.50	5.07	5.09	22.69	22.63	1.13	1.20	3.66	3.76	3.36	22.14	22.48	18.56
Cr_2O_3	0.13	0.16	0.27	0.27	0.20	0.40	0.15	0.09	0.19	0.22	0.21	0.18	0.20	n.a.
Fe_2O_3	n.c.	n.c.	n.c.	n.c.	n.c.	n.c.	n.c.	n.c.	n.c.	n.c.	n.c.	n.c.	n.c.	n.c.
FeO	12.07	11.81	5.97	5.95	13.83	13.60	14.92	14.76	4.74	4.87	5.15	18.89	18.99	0.70
MnO	0.12	0.14	0.13	0.04	0.34	0.31	0.19	0.12	0.07	0.10	0.08	0.50	0.50	0.01
NiO	n.a.	n.a.	n.a.	n.a	n.a.	n.a.	n.a.	n.a.	n.a	n.a.	n.a.	n.a.	n.a.	n.a.
MgO	28.70	28.81	14.97	14.97	16.93	16.91	28.84	28.80	14.23	14.34	14.63	12.96	12.70	0.01
CaO	0.90	0.89	18.74	18.89	4.51	4.91	0.35	0.37	20.63	20.59	20.76	4.81	4.79	0.25
Na_2O	0.22	0.23	1.55	1.51	0.00	0.02	0.02	0.02	2.00	1.89	1.83	0.00	0.00	1.34
K_2O	0.00	0.03	0.02	0.00	0.04	0.01	0.00	0.01	0.01	0.02	0.00	0.01	0.01	14.30
Total	100.07	100.13	99.87	99.63	100.02	99.67	100.57	100.04	100.01	99.84	100.47	99.58	99.13	100.05
Si	1.926	1.925	1.919	1.917	3.001	2.972	1.961	1.959	1.977	1.966	1.971	3.000	2.973	2.985
Ti	0.004	0.004	0.017	0.015	0.009	0.012	0.001	0.001	0.004	0.005	0.005	0.002	0.000	0.000
Al	0.143	0.146	0.218	0.219	1.943	1.948	0.048	0.051	0.157	0.162	0.144	1.955	1.996	1.006
Cr	0.004	0.004	0.008	0.008	0.012	0.023	0.004	0.002	0.005	0.006	0.006	0.010	0.012	n.a.
Fe^{3+}	n.c.	n.c.	n.c.	n.c.	n.c.	n.c.	n.c.	n.c.	n.c.	n.c.	n.c.	n.c.	n.c.	n.c.
Fe^{2+}	0.358	0.349	0.182	0.182	0.840	0.831	0.445	0.442	0.144	0.149	0.156	1.183	1.196	0.027
Mn	0.004	0.004	0.004	0.001	0.021	0.019	0.006	0.003	0.002	0.003	0.003	0.032	0.032	0.000
Ni	n.a.	n.a.	n.a.	n.a.	n.a.	n.a.	n.a.	n.a.	n.a.	n.a.	n.a.	n.a.	n.a.	n.a.
Mg	1.516	1.520	0.815	0.817	1.834	1.841	1.534	1.539	0.772	0.780	0.792	1.446	1.426	0.001
Ca	0.034	0.034	0.733	0.741	0.351	0.384	0.013	0.014	0.804	0.805	0.808	0.386	0.386	0.012
Na	0.015	0.015	0.110	0.107	0.001	0.003	0.001	0.001	0.141	0.134	0.129	0.000	0.000	0.119
K	0.000	0.001	0.001	0.000	0.004	0.001	0.000	0.000	0.000	0.001	0.000	0.001	0.000	0.839
Total	4.004	4.004	4.007	4.008	8.015	8.033	4.013	4.014	4.008	4.012	4.014	8.015	8.023	4.991
X_{Mg}	0.809	0.813	0.817	0.818	0.686	0.689	0.775	0.777	0.842	0.840	0.835	0.550	0.544	–
X_{Cr}	0.024	0.030	0.035	0.034	0.006	0.012	0.079	0.046	0.033	0.038	0.040	0.005	0.006	–

Formula calculations on the basis of 12 oxygens for grt, 6 oxygens for cpx and opx and 8 oxygens for K-feldspar. X_{Mg} = Mg/(Mg+Fe^{2+}); X_{Cr} = Cr/(Cr+Al); l/opx = lamella in opx, l/cpx = lamella in cpx, incl/grt = inclusion in garnet; n.a. = not analyzed, n.c. = not calculated

Table 5c: Representative electron microprobe analyses of minerals from websterites

Sample no.:	Garnet-spinel websterite 1916-13													
Mineral:	Opx	Opx	Cpx	Cpx	Cpx*	Cpx*	Grt	Grt	Spl	Spl	Ol	Ol	Opx	Spl
Domain:	core	rim	core	rim	core	rim	l/opx	l/cpx	core	rim	core	rim	sym	sym
SiO_2	55.23	54.09	52.45	52.53	52.12	52.34	41.29	41.63	0.00	0.00	39.83	38.90	48.87	0.00
TiO_2	0.15	0.17	0.40	0.39	0.57	0.45	0.11	0.10	0.86	0.88	0.00	0.04	0.14	0.20
Al_2O_3	2.29	3.42	4.39	4.44	5.51	4.81	22.77	22.69	37.06	38.14	0.04	0.02	11.69	58.01
Cr_2O_3	0.09	0.29	0.47	0.53	0.46	0.55	0.68	0.82	19.09	18.86	0.00	0.03	0.54	3.76
Fe_2O_3	n.c.	n.c.	n.c.	n.c.	n.c.	n.c.	n.c.	n.c.	11.67	10.14	n.c.	n.c.	n.c.	6.33
FeO	9.84	10.35	5.06	4.72	5.06	4.75	11.80	12.08	17.60	18.96	15.86	18.94	12.74	14.72
MnO	0.15	0.13	0.12	0.14	0.06	0.01	0.36	0.33	0.08	0.18	0.11	0.36	0.35	0.30
NiO	n.a.	n.a.	n.a.	n.a.	n.a.	n.a.	n.a.	n.a.	n.a.	n.a.	0.51	0.40	n.a.	n.a.
MgO	31.83	31.08	15.53	15.42	15.12	15.34	17.53	17.52	13.61	12.77	44.81	42.55	25.05	17.26
CaO	0.76	0.69	20.72	20.67	20.44	20.71	5.40	5.53	0.00	0.03	0.05	0.10	1.37	0.05
Na_2O	0.06	0.04	1.05	1.15	1.25	1.26	0.01	0.01	0.00	0.00	0.00	0.03	0.03	0.00
K_2O	0.01	0.00	0.00	0.00	0.00	0.02	0.00	0.00	0.00	0.00	0.00	0.01	0.01	0.00
Total	100.40	100.25	100.19	99.98	100.59	100.23	99.95	100.71	99.98	99.95	101.21	101.36	100.79	100.62
Si	1.932	1.901	1.913	1.917	1.892	1.906	2.986	2.993	0.000	0.000	0.994	0.985	1.735	0.000
Ti	0.004	0.004	0.011	0.011	0.015	0.012	0.006	0.005	0.019	0.019	0.000	0.001	0.004	0.004
Al	0.094	0.142	0.189	0.191	0.236	0.207	1.941	1.922	1.269	1.307	0.001	0.001	0.489	1.790
Cr	0.002	0.008	0.014	0.015	0.013	0.016	0.039	0.047	0.438	0.433	0.000	0.001	0.015	0.078
Fe^{3+}	n.c.	n.c.	n.c.	n.c.	n.c.	n.c.	n.c.	n.c.	0.255	0.222	n.c	n.c.	n.c.	0.125
Fe^{2+}	0.288	0.304	0.154	0.144	0.153	0.145	0.713	0.726	0.428	0.461	0.331	0.401	0.378	0.322
Mn	0.004	0.004	0.004	0.004	0.002	0.000	0.022	0.020	0.002	0.004	0.002	0.008	0.011	0.007
Ni	n.a.	n.a.	n.a.	n.a.	n.a.	n.a.	n.a.	n.a.	n.a.	n.a.	0.010	0.008	n.a.	n.a.
Mg	1.660	1.629	0.844	0.839	0.818	0.833	1.890	1.877	0.589	0.553	1.666	1.606	1.325	0.674
Ca	0.029	0.026	0.810	0.808	0.795	0.808	0.419	0.426	0.000	0.001	0.001	0.003	0.052	0.001
Na	0.004	0.002	0.074	0.081	0.088	0.089	0.001	0.002	0.000	0.000	0.000	0.002	0.002	0.000
K	0.001	0.000	0.000	0.000	0.000	0.001	0.000	0.000	0.000	0.000	0.000	0.000	0.000	0.000
Total	4.018	4.021	4.012	4.010	4.012	4.016	8.018	8.018	3.000	3.000	3.006	3.015	4.011	3.000
X_{Mg}	0.852	0.843	0.846	0.853	0.842	0.852	0.726	0.721	0.579	0.546	0.834	0.800	0.778	0.676
X_{Cr}	0.025	0.054	0.067	0.074	0.053	0.071	0.020	0.024	0.257	0.249	–	–	0.030	0.042

Formula calculations on the basis of 12 oxygens for grt, 6 oxygens for cpx and opx, 4 oxygens for olivine and 4 oxygens and 3 cations for spinel.
X_{Mg} = Mg/(Mg+Fe^{2+}); X_{Cr} = Cr/(Cr+Al); sym = symplectite after garnet, l/opx = lamella in opx, l/cpx = lamella in cpx; Cpx* = Cpx without exsolution lamellae;
n.a. = not analyzed, n.c. = not calculated

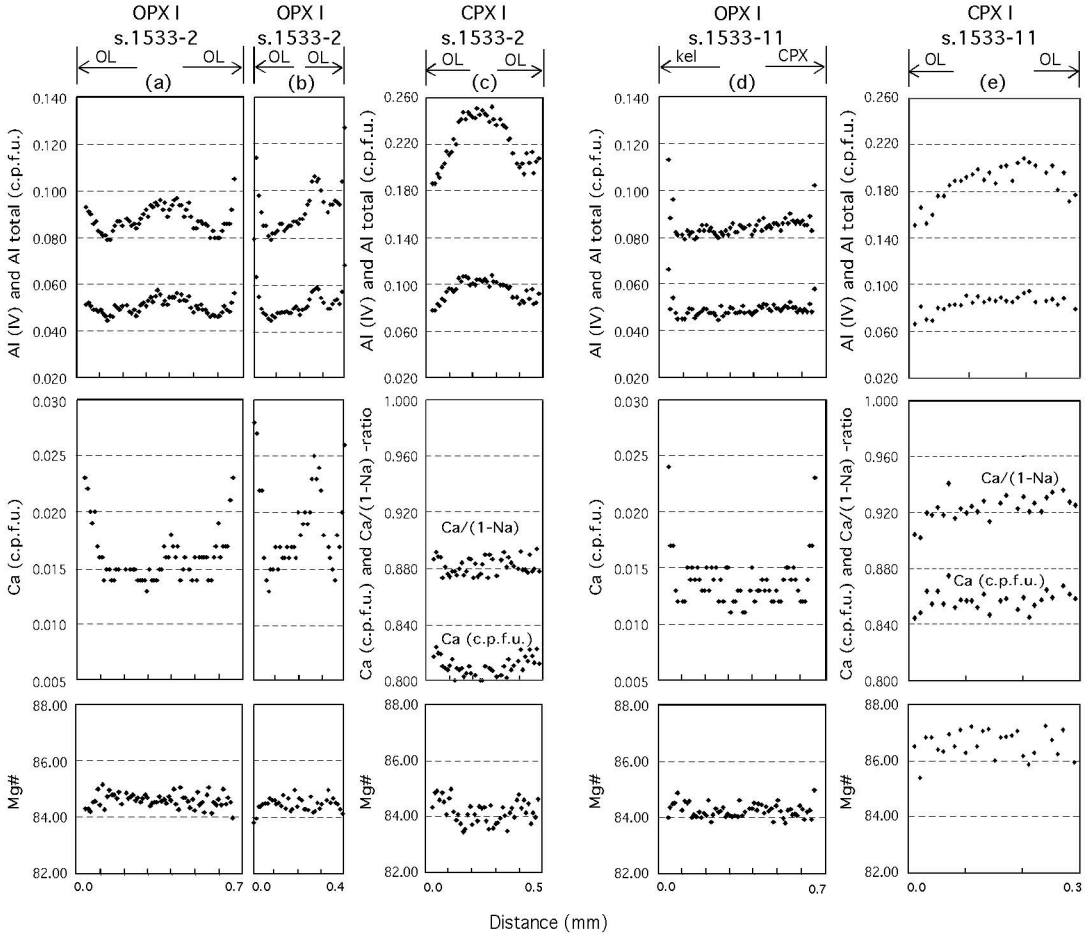


Fig. 5. Zoning patterns of opx (a-c) and cpx (d, e) in ol websterite xenoliths 1533-2 and 1533-11. For further explanation see 'Xenolith types and mineral composition'.

In opx I, Al and Ca decrease from the core through an intermediate zone, and then increase rimwards. In some grain sections, only the rimward increases in Al or Ca are evident (Fig. 5d), due to cross-section effects. X_{Mg} shows an indistinct tendency to decrease towards rims. In cpx I, the Al content decreases rimwards (Fig. 5e). Its behaviour at the rim is not clear: some profiles may suggest an increase in Al within the outermost zone, but the effect is weak. The zonation in Ca and X_{Mg} is also weak and somewhat inconsistent in different profiles (Fig. 5e). Compositions of smaller pyroxene grains are broadly similar to those of the rims of larger grains. Olivine forms large grains, sometimes with inclusions of spinel. Despite their size, these grains are fairly homogeneous. Some increase in Ca within the outermost rims may be observed, but its primary nature is questionable. Representative mineral analyses of sample 1533–11 are given in Table 5a.

Websterites

Most websterite xenoliths are coarse-grained (up to 5 mm). 'Primary' phases are orthopyroxene (opx I) and clinopyroxene (cpx I) that may be accompanied by variable amounts of garnet (grt I) and/or spinel (spl I). Grain boundaries of pyroxenes may vary from straight to curved or irregular, suggesting deformation-enhanced grain boundary migration. Pyroxene grains often show undulose

extinction and their exsolution lamellae may be bent. Garnet forms a more or less continuous, medium-grained network around pyroxene grains and also occurs within both pyroxenes. As a rule, garnet is replaced by kelyphite and/or symplectite (orthopyroxene, clinopyroxene, spinel, ± plagioclase) and only relics are preserved (Table 4; Fig. 6a).

Both pyroxenes appear in different phenotypes. Larger grains underwent extensive exsolution of second generation garnet (Fig. 6a) that can sometimes be accompanied by complementary pyroxene, rutile and spinel. In many cases, exsolution lamellae are confined to the cores of pyroxene grains, but in some samples garnet lamellae extend to the rims of host grains and merge into intergranular garnet aggregates (Fig. 6b). Smaller pyroxene grains mostly lack garnet lamellae (Fig. 6b), but tiny clinopyroxene lamellae may occur in opx. In addition, very small pyroxene grains may be developed at the outermost rims of larger pyroxene grains or along grain boundaries as a result of late recrystallization processes.

If present, primary garnet I grains occur as round inclusions in both pyroxenes (grt Ia) (Fig. 6a) and/or round interstitial aggregates (grt Ib). The latter may contain armoured relics of brown or green spinel. Since interstitial garnet Ib (or kelyphite) may also contain olivine, it was probably formed by the reaction spl I + opx I + cpx I = grt Ib + ol Ib.

Five websterite xenoliths are characterized by the occurrence of unusual inclusions in grt-Ia grains. In addition to spl I, we found inclusions of (i) K-feldspar accompanied by either quartz (sample 1905–2) or clinopyroxene (1906–1), (ii) rutile that is partially transformed to ilmenite (1906–1, 1535–6, 1535–12), and (iii) composite inclusions of rutile and corundum that are partly overgrown by brown spinel (1906–1, 1906–4). In some of these xenoliths, exsolved intergranular garnet II is accompanied by quartz.

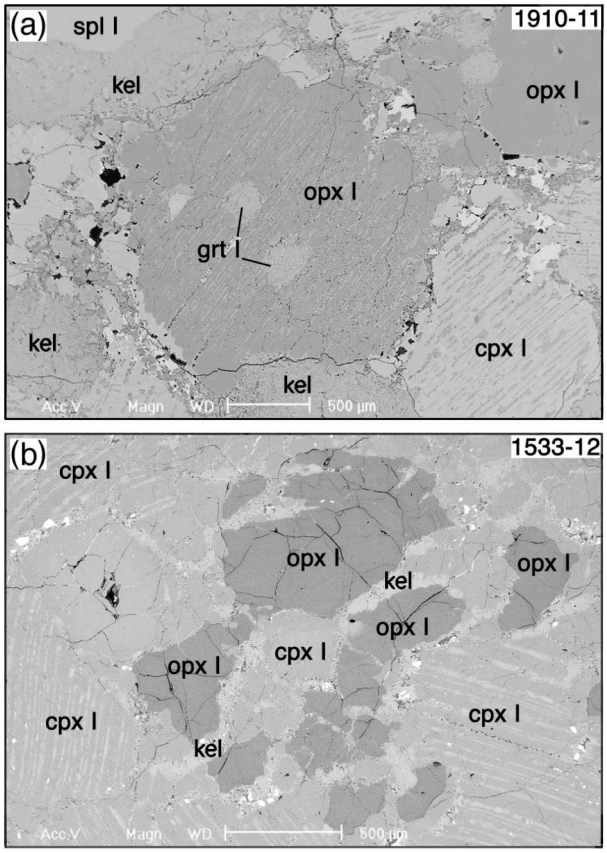


Fig. 6. BSE images of coarse-grained websterite dominated by pyroxene grains showing extensive exsolution of garnet (a) and of websterite containing both exsolved and homogeneous pyroxene (b). Mineral abbreviations after Kretz (1983); kel: fine-grained pyroxene-spinel-plagioclase kelyphite after garnet. For further explanation see 'Xenolith types and mineral composition'.

Pyroxene compositions are variable, depending on whole-rock composition, *P-T* evolution, grain size and distance from garnet. On the basis of chemical zoning patterns of pyroxene grains, the websterite xenoliths can be subdivided into three groups (Table 4). Xenoliths of the first group are characterized by (nearly) constant opx-I

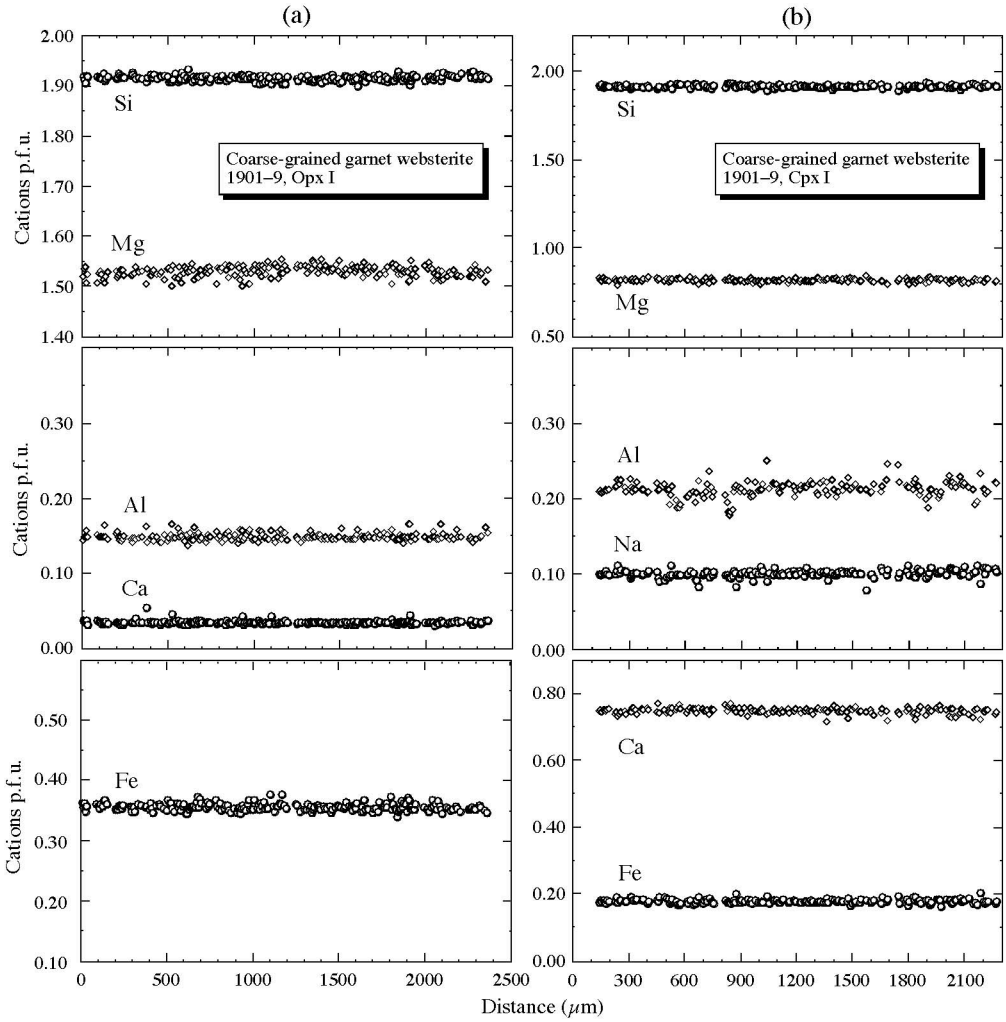


Fig. 7. Zoning patterns of opx and cpx in websterite (group 1). For further explanation see 'Xenolith types and mineral composition'.

and cpx-I compositions indicating chemical equilibration after garnet-Ib/II formation (Fig. 7; Table 5b). In websterites of the second group, larger pyroxene grains usually show core-to-rim decreases in Al (Figs. 8 and 9; Table 5a), and Al contents of smaller grains are similar to or slightly lower than those of the rims of larger pyroxene grains. Towards garnet-II lamellae in pyroxene cores, Al either decreases or is constant. These features suggest incomplete homogenization during/after cooling. In websterites of the third group, both pyroxenes may show an increase of Al towards grt I/II, whereby the compositions of opx-I and cpx-I domains in contact to grt are always constant within one sample, suggesting local equilibration between pyroxenes and garnet (Fig. 10; Table 5c). The spatial extent of equilibration is variable and tends to depend on the average distance to garnet reservoirs. In some samples, larger pyroxene grains with abundant closely spaced grt lamellae are homogeneous (i.e. totally equilibrated), while in the case of widely spaced lamellae, equilibrated high-Al zones of host pyroxenes may be relatively thin (Figs. 6a and10). Rarely, small opx grains may show a core-to-rim increase in Al, while neighbouring small cpx grains display

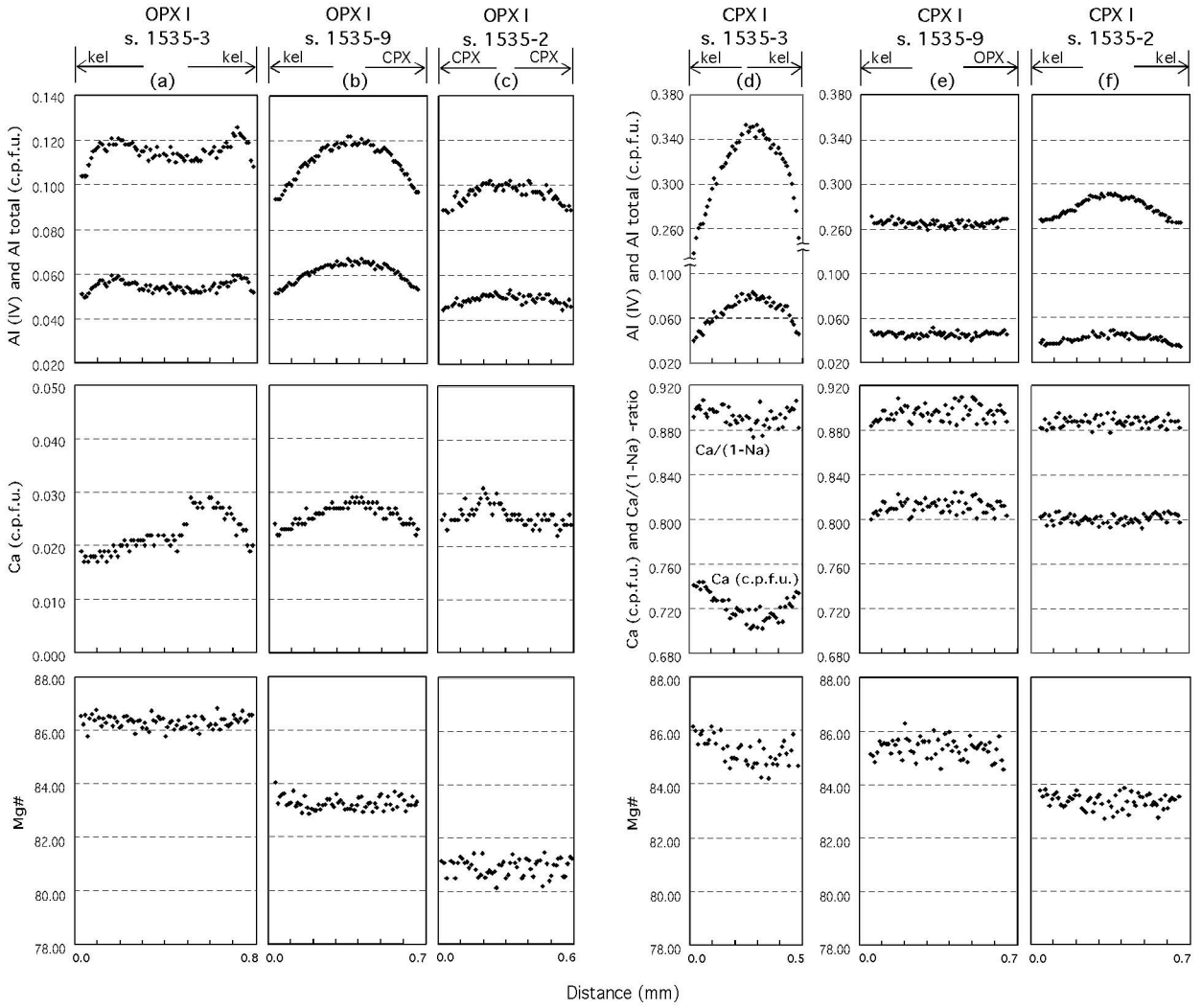


Fig. 8. Zoning patterns of opx (a-c) and cpx (d-f) in websterite (group 2). For further explanation see 'Xenolith types and mineral composition'.

a slight decrease in Al. Ca in opx grains generally tends to be more homogeneous than Al, but may also mimic Al zonation patterns (Fig. 10).

Within individual samples, compositions of garnet-I/II relics and of olivine II are constant. Towards kelyphite, however, X_{Mg} and the abundances of Ca in olivine may decrease and increase, respectively. Relict primary spinel is also homogeneous, except for a weak zonation with rimward decreases in Ni and Zn and an increase in Cr found in some samples. Sulfides are rare. Primary Ni-pyrrhotite may occur as globular inclusions in smaller opx grains of some samples.

Clinopyroxene-bearing orthopyroxenites

Xenoliths of this group (1680–7, 1901–1, 1901–8, 1907–1; Table 6; Fig. 11a) are coarse-grained and granular (up to 5 mm). Grain boundaries are relatively straight. Clinopyroxene (cpx I) and brown spinel (spl I, not in sample 1901–8) occur as rare interstitial grains between the large grains of orthopyroxene (opx I). Intergranular garnet (grt II) forms a thin network between the pyroxene grains and frames interstitial spinel, suggesting formation by exsolution from former pyroxenes. Garnet grains without armoured spinel that could be interpreted as primary garnet were only found in sam-

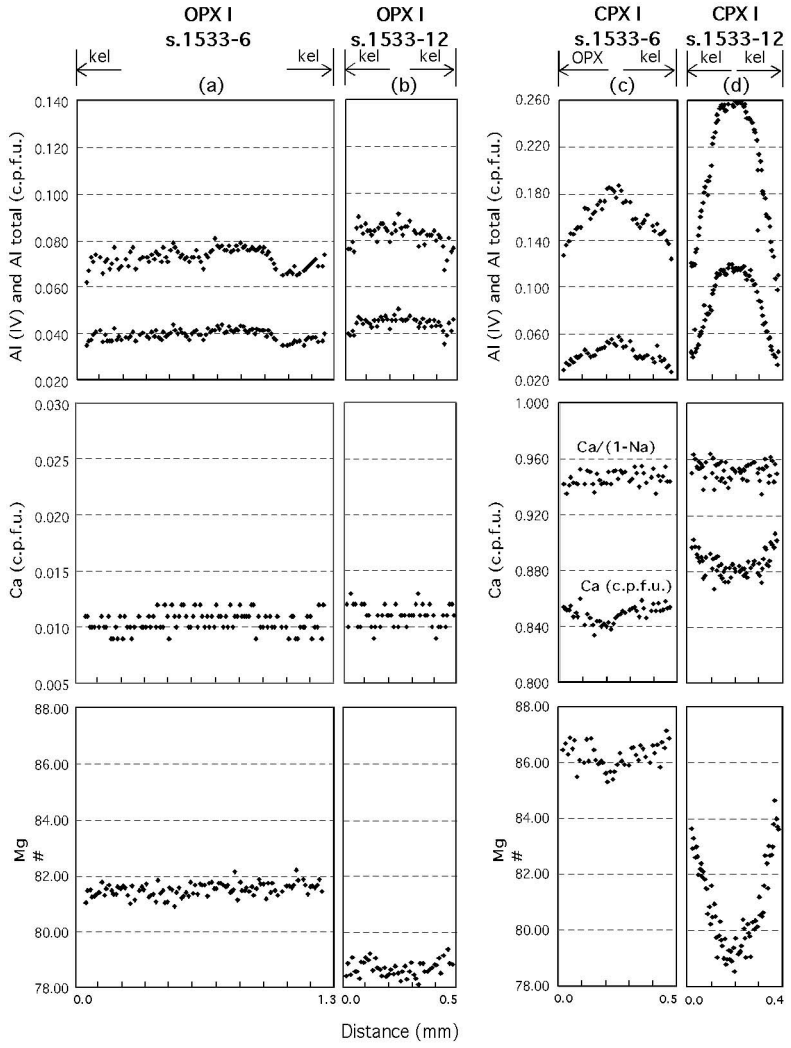


Fig. 9. Zoning patterns of opx (a, b) and cpx (c, d) in websterite (group 2). For further explanation see 'Xenolith types and mineral composition'.

ple 1680–7. Both pyroxenes underwent exsolution of garnet, complementary pyroxene, Mg-rich ilmenite and minor spinel. Garnet is often altered to extremely fine-grained kelyphite; at the contact to armoured spinel, it is transformed into a symplectite consisting of Al-rich opx II, Al-rich spl II, ± Al-rich cpx II and ± pl II.

In four samples, opx-I grains are chemically homogeneous. In particular, no chemical gradients were observed along profiles measured across opx/grt contacts (Table 7a). The relatively small cpx-I grains display a weak core-to-rim decrease in Al; a similar decrease may be observed towards exsolution lamellae of grt. Small variations in X_{Mg} of relict garnet domains within individual samples are due to the effects of late-stage kelyphitization.

Orthopyroxenites devoid of primary clinopyroxene

These xenoliths (1901-7, 1902-7, 1910–11a, 1911–15, Fig. 11b) are characterized by heterogranular textures and dynamically recrystallized grain boundaries. Some of these samples contain abundant primary garnet and intergranular grt II that are completely transformed into sym-

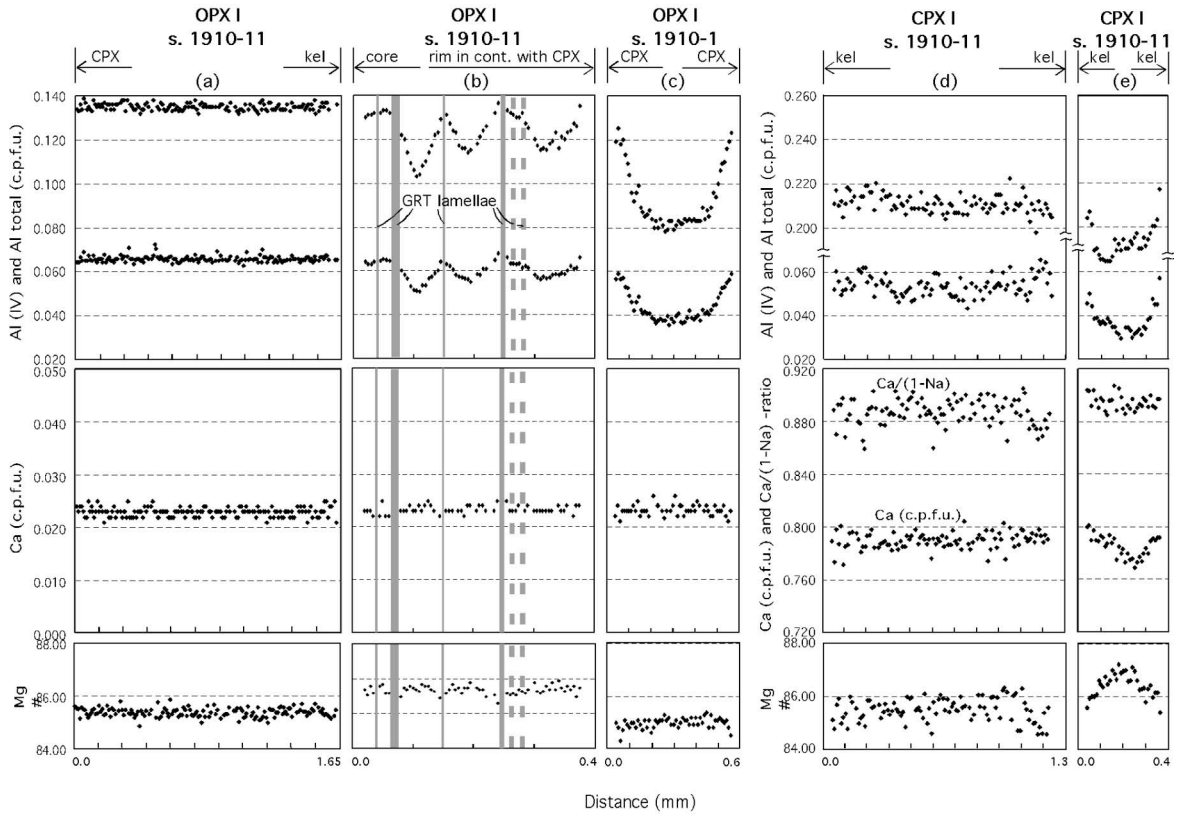


Fig. 10. Zoning patterns of opx in websterite (group 3). Mineral abbreviations after Kretz (1983); kel: fine-grained pyroxene-spinel-plagioclase kelyphite after garnet. For further explanation see 'Xenolith types and mineral composition'.

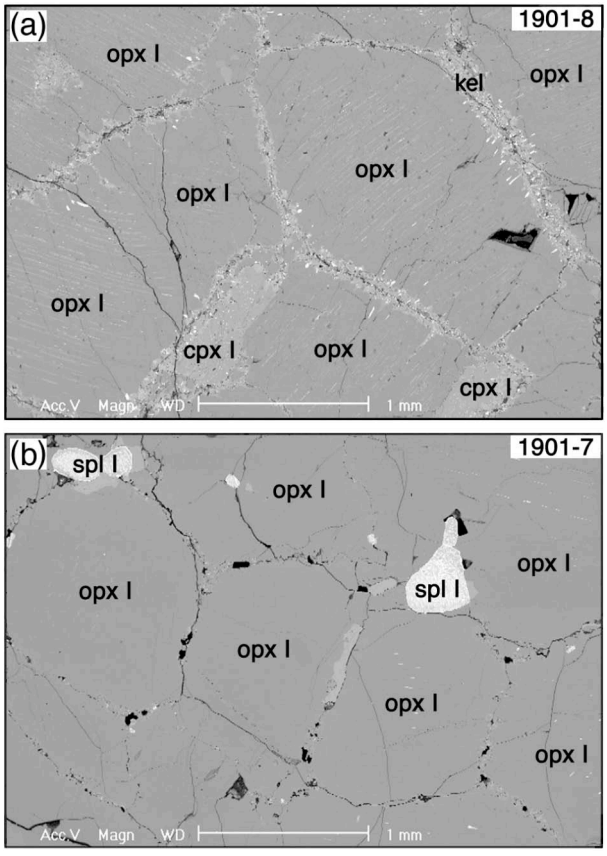


Fig. 11. BSE images of clinopyroxene-bearing orthopyroxenite (a) and of orthopyroxenite devoid of primary clinopyroxene (b). Mineral abbreviations after Kretz (1983); kel: fine-grained pyroxene-spinel-plagioclase kelyphite after garnet. For further explanation see 'Xenolith types and mineral composition'.

plectite (opx + spl ± pl). In only one of these samples, opx contains thin exsolution lamellae of grt (Table 6).

In all samples, large opx grains display complex chemical zoning. The cores may be (nearly) homogeneous with Al and Ca showing plateaus. Towards the rims, Al and Ca decrease continuously and then increase abruptly in the outermost zones. Small opx grains only show a rimward increase in Al and Ca (Fig. 12).

Table 6: Characteristics of orthopyroxenite xenoliths from the Chyulu Hills

Rock type / Sample no.	Phases present Grt I	Spl I	Cpx I	Grt II	Exsolution lamellae in opx	in cpx	Zoning of opx[a] Al & Ca*	Zoning of cpx[a] Al & Ca*	Thermal evolution
Clinopyroxene-bearing orthopyroxenite									
1680–7	+	+	+	+	grt, cpx, ilm, spl	grt, ilm, spl	– –	decr –	cooling, equilibration
1901–1	–	+	+	+	grt, cpx, ilm, spl	grt, ilm, spl	– –	decr –	cooling, equilibration
1901–8	–	–	+	+	grt, cpx, ilm, spl	grt, ilm, spl	– –	decr –	cooling, equilibration
1907–1	–	+	+	+	grt, cpx, ilm	grt, opx, ilm, spl	– –	decr –	cooling, equilibration
Orthopyroxenite devoid of primary clinopyroxene									
1901–7	+	+	–	+	cpx, spl	spl	decr, incr	– –	cooling, heating
1902–7	–	+	–	+	cpx, ilm, spl	–	decr, incr	– –	cooling, heating
1910–11a	+	–	–	+	grt	–	decr, incr	– –	cooling, heating
1911–15	+	–	–	+	–	–	decr, incr	– –	cooling, heating

+ = present, – = absent. [a] Zoning is from core to rim; incr = increasing, decr = decreasing. Ca* = Ca/(1-Na)

Table 7: Representative electron microprobe analyses of minerals from clinopyroxene-bearing orthopyroxenite

Sample no.:	Garnet-clinopyroxene orthopyroxenite 1907–1										Garnet-clinopyroxene orthopyroxenite 1901–8				
Mineral:	Opx I	Opx I	Opx II	Cpx I	Cpx I	Cpx II	Grt II	Grt II	Mg-Ilm	Spl	Opx I	Cpx I	Grt IIb	Grt IIb	Ilm
Domain:	core	rim	sym	core	rim	sym	l/opx	l/cpx	l/opx	sym	core/rim	core/rim	l/opx	incl/cpx	incl/cpx
SiO_2	55.0	54.63	48.54	52.43	52.86	49.68	40.47	40.45	0.08	0.08	54.87	52.71	40.42	40.71	0.18
TiO_2	0.06	0.08	0.91	0.50	0.33	1.64	0.04	0.08	51.41	0.75	0.08	0.36	0.05	0.06	40.37
Al_2O_3	1.95	1.94	9.09	4.42	3.45	9.07	21.86	21.73	0.40	56.37	2.06	3.68	21.71	21.69	0.22
Cr_2O_3	0.23	0.29	0.47	0.51	0.65	0.31	1.13	1.20	0.82	4.83	0.24	0.63	1.10	1.09	2.81
Fe_2O_3	n.c.	n.c.	n.c.	n.c.	n.c.	n.c.	n.c.	n.c.	5.28	2.94	n.c.	n.c.	n.c.	n.c.	23.06
FeO	12.00	12.37	15.86	5.77	5.57	11.10	15.60	16.31	32.48	20.09	12.22	5.93	15.35	15.91	24.98
MnO	0.19	0.18	0.57	0.03	0.02	0.55	0.48	0.50	0.31	0.32	0.17	0.08	0.51	0.56	0.19
NiO	n.a.	n.a.	n.a.	n.a.	n.a.	n.a.	n.a.	n.a.	n.a.	n.a.	n.a.	n.a.	n.a.	n.a.	n.a.
MgO	30.12	29.79	22.91	13.73	14.72	13.83	14.53	13.95	7.48	13.60	29.86	14.37	14.69	14.17	5.69
CaO	0.31	0.32	1.69	20.85	20.86	15.70	6.03	5.67	0.04	0.06	0.31	20.94	5.90	5.96	0.91
Na_2O	0.03	0.04	0.04	1.65	1.39	0.28	0.03	0.03	0.02	0.01	0.04	1.50	0.03	0.00	0.00
K_2O	0.00	0.00	0.00	0.01	0.01	0.01	0.00	0.01	0.02	0.02	0.01	0.02	0.02	0.00	0.01
Total	99.90	99.63	100.07	99.89	99.86	99.16	100.16	99.92	98.35	99.08	99.85	100.23	99.77	100.15	98.41
Si	1.949	1.946	1.767	1.926	1.941	1.754	2.987	3.000	0.002	0.002	1.948	1.934	2.992	3.007	0.004
Ti	0.002	0.002	0.025	0.014	0.009	0.046	0.002	0.004	0.937	0.015	0.002	0.010	0.003	0.004	0.751
Al	0.082	0.081	0.390	0.191	0.149	0.401	1.901	1.899	0.011	1.802	0.086	0.159	1.894	1.889	0.006
Cr	0.006	0.008	0.013	0.015	0.019	0.009	0.066	0.070	0.016	0.104	0.007	0.018	0.064	0.064	0.055
Fe^{3+}	n.c.	n.c.	n.c.	n.c.	n.c.	n.c.	n.c.	n.c.	0.096	0.060	n.c.	n.c.	n.c.	n.c.	0.429
Fe^{2+}	0.356	0.369	0.483	0.177	0.171	0.349	0.963	1.011	0.658	0.456	0.363	0.182	0.950	0.983	0.517
Mn	0.006	0.005	0.018	0.001	0.001	0.017	0.030	0.031	0.006	0.007	0.005	0.003	0.032	0.035	0.004
Ni	n.a.	n.a.	n.a.	n.a.	n.a.	n.a.	n.a.	n.a.	n.a.	n.a.	n.a.	n.a.	n.a.	n.a.	n.a.
Mg	1.592	1.582	1.243	0.752	0.806	0.775	1.599	1.542	0.270	0.550	1.580	0.786	1.621	1.560	0.210
Ca	0.012	0.012	0.066	0.821	0.821	0.632	0.476	0.450	0.001	0.002	0.012	0.823	0.468	0.472	0.024
Na	0.002	0.003	0.003	0.118	0.099	0.021	0.004	0.004	0.001	0.000	0.003	0.107	0.005	0.000	0.000
K	0.000	0.000	0.000	0.000	0.000	0.000	0.000	0.001	0.000	0.001	0.000	0.001	0.002	0.000	0.000
Total	4.006	4.009	4.007	4.016	4.016	4.005	8.029	8.014	2.000	3.000	4.005	4.022	8.030	8.013	2.000
X_{Mg}	0.817	0.811	0.720	0.809	0.825	0.690	0.624	0.604	0.291	0.547	0.813	0.812	0.630	0.613	0.289
X_{Cr}	0.074	0.090	0.033	0.072	0.112	0.022	0.034	0.036	–	0.054	0.073	0.103	0.033	0.033	–

Formula calculations on the basis of 12 oxygens for grt, 6 oxygens for cpx and opx and 4 oxygens and 3 cations for spl. X_{Mg} = Mg/(Mg+Fe^{2+}); X_{Cr} = Cr/(Cr+Al); sym = symplectite replacing grt II; incl/cpx = inclusions in cpx; l/opx = lamella in opx; n.a. = not analyzed, n.c. = not calculated

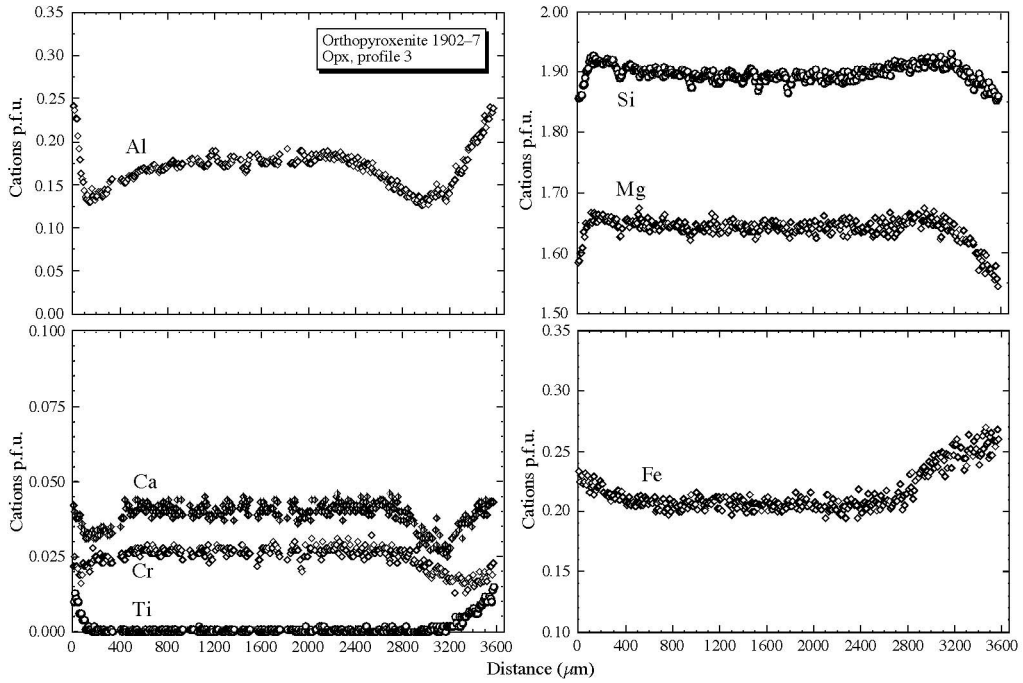


Fig. 12. Zoning pattern of opx in cpx-free orthopyroxenite 1902-7. For further explanation see 'Xenolith types and mineral composition'.

METAMORPHIC EVOLUTION AND GEOTHERMOBAROMETRY

General considerations

Continental rifting includes significant thermal modifications of the lithosphere. In principle, thinning of the lithosphere by mechanical extension and/or plume-induced thermal erosion will increase the geothermal gradient throughout the remaining lithosphere or, in other words, the lithosphere tends to approach the thickness that is in equilibrium with the heat flow from the underlying convective system. However, mantle convection is fast and thermal diffusion is slow, implying that the thermal structure of the lithosphere will hardly ever reach a steady state. Thus, significant conductive heating will most probably be confined to the lower levels of the lithosphere, while overlying levels may still undergo cooling after an earlier heating event. At all levels, the lithosphere may become locally heated by ephemeral melts. In general, an intruding magma can heat a lithospheric volume comparable to its own volume, and heat diffusion quickly resets these relatively small-sized volumes to ambient temperatures. Near the top of the rheological boundary layer in the lower lithosphere, however, large dike stockworks can build up (Parsons *et al.*, 1992; Sleep, 2003) resulting in a more regional-scale heating of this part of the lithosphere.

Models for the thermal structure and evolution of the lithospheric mantle depend on the reliability of geothermobarometry. For typical mantle rocks, such as peridotite and Mg-rich pyroxenite, a large number of potential thermometers and barometers are available and many of them have been extensively tested and evaluated (e.g. Carswell & Harley, 1990; Brey et al., 1990; Brey & Köhler, 1990; Werling & Altherr, 1997; Smith 1999; Krogh Ravna & Paquin, 2003). The most

widely used set of thermobarometers is that of Brey & Köhler (1990). This experimentally calibrated set has the great advantage of internal consistency. In this paper, we use the barometer based on the Al content in opx coexisting with grt ($P_{Al\text{-}opx}$) in combination with the thermometers based on the exchange of enstatite and diopside components between cpx and opx ($T_{2px\text{–}en\text{–}di}$), the partitioning of Na between cpx and opx ($T_{2px\text{–}Na}$), the Ca content in opx coexisting with cpx ($T_{Ca\text{-}opx}$) and the Fe^{2+}-Mg exchange between grt and opx ($T_{grt\text{-}opx}$). Additional information was obtained from the garnet-in barometer ($P_{grt\text{-}in}$; Webb & Wood, 1986), the thermometers based on the Fe^{2+}-Mg exchange between grt and cpx ($T_{grt\text{-}cpx}$; Krogh, 1988) and Cr-Al exchange between orthopyroxene and spinel ($T_{opx\text{-}spl}$; Sachtleben & Seck, 1981).

Fe^{2+}-Mg exchange thermometry is generally fraught with uncertainties in the $Fe^{3+}/\Box Fe$ ratios of the phases involved. However, it is now widely accepted that the experiments used to calibrate the Fe^{2+}-Mg exchange thermometers produced grt, opx and cpx with substantial amounts of Fe^{3+}, similar to those of natural samples (e.g. Brey & Köhler, 1990; Canil & O'Neill, 1996). Therefore, the application of these thermometers should yield meaningful temperature estimates, provided the mineral pairs were equilibrated with respect to Fe^{2+}-Mg and not subject to unusual oxygen fugacities.

Apart from the question of thermobarometer quality, it is important to be aware of the problems that can arise during evaluation of inter- and intraphase element partitioning. Chemical zoning patterns of mineral grains may be very complex, depending on both the *P–T–t* path of the host rock and different diffusivities of the elements involved (e.g. Paquin & Altherr, 2001a, b; Olker et al. 2003). Moreover, the different textural positions, sizes and shapes of mineral grains and the effects of grain section geometry have to be considered.

Garnet lherzolites

The ubiquitous breakdown of garnet I is tentatively attributed to decompression during transport in the host magmas. This hypothesis is corroborated by the observation that X_{Cr} of spl II decreases from the outer to the inner parts of the pseudomorphs after grt I. Such a variation suggests that grt I decomposition and spl II formation started at the rims of former garnet grains in contact with olivine, and continued inwards during progressive decompression. A further argument in favour of a relatively late decomposition of garnet follows from the fact that pyroxene-I grains and olivine-I grains still show chemical gradients within narrow zones towards the pseudomorphs. Apart from these local chemical heterogeneities of mineral grains, the garnet lherzolite xenoliths exhibit homogeneous mineral compositions, suggesting a former state of equilibration. This makes geothermobarometric calculations feasible.

For each garnet lherzolite xenolith, *P-T* conditions were estimated using all analyses of pyroxene-I grains and relict grt-I grains, except for those pyroxene domains located close to garnet pseudomorphs. We found a general consistency between *P-T* estimates based on the compositions of pyroxene cores and those based on pyroxene rims (Table 8). Furthermore, combinations of different pyroxene thermometers ($T_{2pxen\text{-}en\text{-}di}$, T_{2pxNa}, $T_{Ca\text{-}opx}$) with the barometer based on the aluminium content in opx coexisting with grt ($P_{Al\text{-}opx}$) yielded consistent results. However, *P-T* estimates obtained

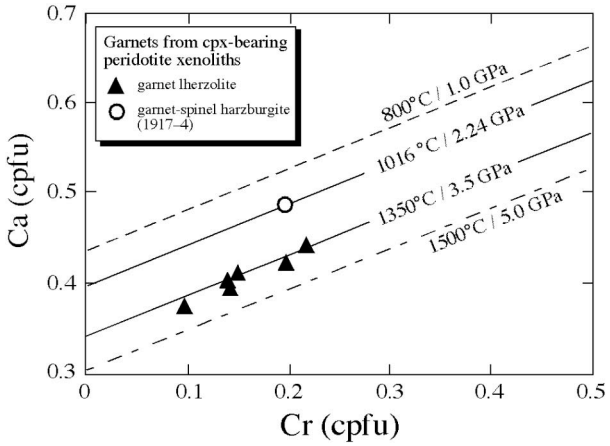


Fig. 13. Ca-Cr systematics of garnet in garnet lherzolite xenoliths. For further explanation see 'Xenolith types and mineral composition'.

by applying thermometers based on the Fe^{2+}-Mg exchange between grt and cpx ($T_{grt\text{-}cpx}$) and grt and opx ($T_{grt\text{-}opx}$) in combination with $P_{Al\text{-}opx}$ show a large scatter whereby temperatures are significantly higher than those derived from two-pyroxene thermometers. These discrepancies are likely due to the modification of primary Fe/Mg ratios of small garnet-I relics (< 200 μm) by the reaction ol + grt = opx + cpx + spl on the initial stage of garnet decomposition. We therefore assume that the *P-T* values derived from combinations of the various pyroxene thermometers with the Al-in-opx barometer are more reliable.

Another independent test for the consistency of estimated peak metamorphic conditions is provided by the Ca-Cr systematics of garnet. As shown by Brenker & Brey (1997), the Cr content in lherzolitic garnet is a function of the effective bulk composition only and does not depend on pressure and temperature. For constant Cr in grt, Ca in grt decreases with increasing *P* and *T*, and at constant *P* and *T*, Ca increases linearly with Cr. Figure 13 shows the Ca-Cr relationships of garnet-I relics from six garnet lherzolite xenoliths together with calculated isolines for various *P-T* conditions. It is evident that the data plot along the isoline for 1350 °C and 3.5 GPa representing the average *P-T* values that were derived for these rocks (Table 8). We therefore conclude that the garnet lherzolite xenoliths equilibrated at pressures between 3.3 and 3.6 GPa and temperatures between 1340 and 1370 °C.

Spinel lherzolites

Exsolution lamellae in pyroxenes indicate initial cooling at elevated pressures (exsolution of garnet and spinel in cpx). The weak, antithetic zoning patterns of Al in opx I and cpx I are difficult to interpret, but may, in part, be caused by the combined effects of exsolution and diffusion during and after cooling. Apart from the Al zoning patterns and the sponge-like rims of cpx I in contact with glass (cpx III), both pyroxenes are nearly homogeneous, suggesting that chemical equilibrium was almost reached after cooling.

Combinations of various pyroxene thermometers ($T_{2px\text{-}en\text{-}di}$, $T_{2px\text{-}Na}$, $T_{Ca\text{-}opx}$) with the $P_{grt\text{-}in}$ barometer yield similar temperature and pressure values of 928–990 °C and 2.11–2.25 GPa for core compositions (Table 9). Similar or slightly higher *P-T* estimates are obtained for rim compositions. These *P-T* estimates must be considered as maximum values, since no garnet is present in opx. However, since grt was exsolved from cpx, they probably approximate the *P-T* conditions reached after cooling. Slightly higher temperature values obtained with the $T_{opx\text{–}spl}$ thermometer (Table 9) can be explained by incomplete equilibration of Al and Cr between opx and spl during and after cooling. Both Cr and Al are characterized by relatively low diffusivities compared to Ca, Mg, Fe and Na.

Table 8: Temperature (°C) and pressure (GPa) estimates on garnet-bearing mantle xenoliths from the northwestern Chyulu Hills

Sample		$T_{2px\text{-}en\text{-}di}$ / $P_{Al\text{-}opx}$	$T_{2px\text{-}Na}$ / $P_{Al\text{-}opx}$	$T_{Ca\text{-}opx}$ / $P_{Al\text{-}opx}$	$T_{grt\text{-}cpx}$ / $P_{Al\text{-}opx}$	$T_{grt\text{-}opx}$ / $P_{Al\text{-}opx}$
Garnet lherzolite						
1911–2		1360 ± 10 / 3.60 ± 0.11	1341 ± 40 / 3.53 ± 0.24	1318 ± 28 / 3.43 ± 0.20	*1499 ± 17 / 4.21 ± 0.17*	*1602 ± 35 / 4.71 ± 0.35*
1911–5		1370 ± 05 / 3.54 ± 0.08	1382 ± 36 / 3.59 ± 0.20	1343 ± 12 / 3.41 ± 0.10	*1570 ± 24 / 4.46 ± 0.21*	*1830 ± 55 / 5.71 ± 0.60*
1911–11		1359 ± 08 / 3.52 ± 0.06	1342 ± 66 / 3.46 ± 0.31	1338 ± 10 / 3.44 ± 0.10	*1520 ± 30 / 4.25 ± 0.24*	*1650 ± 34 / 4.82 ± 0.33*
1911–17		1374 ± 19 / 3.65 ± 0.13	1392 ± 67 / 3.73 ± 0.35	1323 ± 12 / 3.41 ± 0.10	*1421 ± 41 / 3.88 ± 0.03*	*1642 ± 50 / 4.88 ± 0.05*
1927–1		1360 ± 06 / 3.41 ± 0.05	1352 ± 58 / 3.38 ± 0.28	1349 ± 16 / 3.35 ± 0.13	*1428 ± 29 / 3.71 ± 0.20*	*1432 ± 33 / 3.73 ± 0.28*
1927–2		1364 ± 07 / 3.43 ± 0.08	1365 ± 34 / 3.45 ± 0.19	1345 ± 22 / 3.38 ± 0.18	*1460 ± 44 / 3.88 ± 0.34*	*1529 ± 27 / 4.19 ± 0.30*
1927–3		1360 ± 04 / 3.47 ± 0.07	1367 ± 31 / 3.49 ± 0.17	1352 ± 21 / 3.41 ± 0.16	*1476 ± 24 / 3.96 ± 0.19*	*1502 ± 30 / 4.09 ± 0.28*
1927–8		1360 ± 20 / 3.37 ± 0.12	1379 ± 53 / 3.45 ± 0.27	1328 ± 18 / 3.22 ± 0.17	*1501 ± 38 / 4.00 ± 0.29*	*1564 ± 34 / 4.29 ± 0.34*
Websterite (group 1, equilibrated)						
1901–9*		1076 ± 17 / 2.29 ± 0.13	1128 ± 42 / 2.52 ± 0.22	1088 ± 14 / 2.34 ± 0.13	1125 ± 29 / 2.50 ± 0.23	*1188 ± 29 / 2.81 ± 0.29*
1906–1		776 ± 30 / 1.94 ± 0.33	676 ±104/ 1.36 ± 0.68	868 ± 17 / 2.49 ± 0.30	693 ± 11 / 1.45 ± 0.19	701 ± 14 / 1.50 ± 0.27
1906–4		633 ± 39 / 0.85 ± 0.24	652 ± 90 / 0.94 ± 0.48	762 ± 11 / 1.40 ± 0.12	868 ± 22 / 1.88 ± 0.20	723 ± 20 / 1.22 ± 0.18
1916–3		1014 ± 13 / 2.14 ± 0.13	1057 ± 95 / 2.39 ± 0.53	1064 ± 12 / 2.42 ± 0.14	1004 ± 17 / 2.10 ± 0.16	962 ± 20 / 1.86 ± 0.18
1916–20		954 ± 20 / 1.88 ± 0.18	1058 ± 98 / 2.39 ± 0.57	1030 ± 16 / 2.26 ± 0.17	1008 ± 15 / 2.13 ± 0.20	982 ± 29 / 2.00 ± 0.33
1921–4		1031 ± 22 / 2.24 ± 0.14	1036 ± 57 / 2.26 ± 0.29	995 ± 12 / 2.06 ± 0.12	1089 ± 18 / 2.48 ± 0.10	1052 ± 48 / 2.32 ± 0.23
1921–5		981 ± 14 / 1.81 ± 0.11	1076 ± 42 / 2.34 ± 0.31	1054 ± 10 / 2.19 ± 0.10	*1172 ± 42 / 2.81 ± 0.36*	1035 ± 19 / 2.09 ± 0.22
Websterite (group 2, cooling)						
1535–2	R	965 ± 19 / 2.11 ± 0.03		972 ± 28 / 2.14 ± 0.06	950 ± 21 / 2.03 ± 0.05	*1045 ± 17 / 2.56 ± 0.04*
1535–3	R	948 ± 18 / 2.16 ± 0.03		927 ± 22 / 2.07 ± 0.05	944 ± 22 / 2.14 ± 0.05	958 ± 25 / 2.20 ± 0.07
1535–9	R	960 ± 23 / 2.26 ± 0.04		1007 ± 31 / 2.52 ± 0.06	927 ± 26 / 2.11 ± 0.05	988 ± 32 / 2.42 ± 0.07
Websterite (group 3, late heating)						
1910–1	R	961 ± 36 / 1.99 ± 0.08		975 ± 32 / 2.04 ± 0.09	*1121 ± 46 / 2.67 ± 0.10*	*1054 ± 38 / 2.40 ± 0.09*
1910–11	R	947 ± 29 / 1.82 ± 0.05		959 ± 29 / 1.88 ± 0.05	962 ± 24 / 1.86 ± 0.06	990 ± 21 / 2.00 ± 0.05
1916–13	R	971 ± 32 / 1.88 ± 0.33	972 ± 78 / 1.88 ± 0.53	997 ± 12 / 1.92 ± 0.27	*1074 ± 19 / 2.35 ± 0.20*	989 ± 21 / 1.95 ± 0.38
Equilibrated clinopyroxene-bearing orthopyroxenite						
1901-1		919 ± 45 / 1.48 ± 0.42	935 ± 42 / 1.58 ± 0.33	998 ± 12 / 1.88 ± 0.32	*1118 ± 48 / 2.51 ± 0.39*	972 ± 24 / 1.75 ± 0.40
1901–8		812 ± 38 / 1.28 ± 0.36	843 ± 67 / 1.42 ± 0.47	837 ± 45 / 1.40 ± 0.45	*1011 ± 42 / 2.47 ± 0.37*	814 ± 20 / 1.23 ± 0.34
1907–1		802 ± 45 / 1.28 ± 0.38	769 ±120/ 1.03 ± 0.77	832 ± 48 / 1.40 ± 0.44	893 ± 34 / 1.79 ± 0.27	784 ± 35 / 1.11 ± 0.26
1680–7		725 ± 30 / 0.92 ± 0.30	742 ± 80 / 1.02 ± 0.54	773 ± 14 / 1.20 ± 0.18	892 ± 22 / 1.84 ± 0.21	661 ± 15 / 0.60 ± 0.24
Coarse-grained harzburgite with relict garnet				$T_{opx\text{-}spl}$ / $P_{Al\text{-}opx}$		
1680–4	C	no cpx I	no cpx I	931 ± 39 / 2.31 ± 0.15	866 ± 50 / 2.04 ± 0.20	*1094 ± 65 / 3.00 ± 0.26*
	R	no cpx I	no cpx I	875 ± 12 / 1.65 ± 0.20	930 ± 38 / 1.88 ± 0.28	*1059 ± 38 / 2.38 ± 0.40*
1917–4	C	1028 ± 20 / 2.30 ± 0.44	1031 ± 12 / 2.31 ± 0.15	1038 ± 36 / 2.35 ± 0.45	*1042 ± 35 / 2.36 ± 0.43*	1002 ± 70 / 2.18 ± 0.50
	R	*1161 ± 98 / 2.90 ± 0.72*	*1103 ± 86 / 2.65 ± 0.68*	1017 ± 26 / 2.25 ± 0.32	972 ± 37 / 2.05 ± 0.35	1025 ± 12 / 2.25 ± 0.14
1920–23	C	no cpx I	no cpx I	843 ± 18 / 1.78 ± 0.11	926 ± 36 / 2.09 ± 0.18	*1114 ± 50 / 2.81 ± 0.22*
	R	no cpx I	no cpx I	862 ± 11 / 1.82 ± 0.10	897 ± 38 / 1.95 ± 0.18	*1129 ± 50 / 2.86 ± 0.18*

Errors correspond to 1 σ. $T_{2px\text{-}en\text{-}di}$, $T_{2px\text{-}Na}$, $T_{Ca\text{-}opx}$, = two-pyroxene enstatite-diopside exchange, two-pyroxene Na exchange and Ca-in-opx thermometers, respectively, of Brey & Köhler (1990); $T_{grt\text{-}opx}$, = garnet-orthopyroxene Fe-Mg exchange thermometer of Brey & Köhler (1990); $T_{grt\text{-}cpx}$, = garnet-clinopyroxene Fe-Mg exchange thermometer of Krogh (1988); $P_{Al\text{-}opx}$ = Al-in-orthopyroxene barometer of Brey & Köhler (1990). * Only cpx domains free of plagioclase lamellae were used. C = pyroxene cores, R = pyroxene rims. *P-T* values in italics are thought to be not reliable due to high Na contents of pyroxenes and/or modification of Fe/Mg ratios in relict garnet during kelyphitization.

Table 9: Estimates of temperatures (°C) and maximum pressures (GPa) on garnet-free harzburgite xenoliths from the Chyulu Hills

Sample		$T_{opx\text{-}spl}$ / $P_{grt\text{-}in}$	$T_{Ca\text{-}opx}$ / $P_{grt\text{-}in}$	$T_{2px\text{-}en\text{-}di}$ / $P_{grt\text{-}in}$	$T_{2px\text{-}Na}$ / $P_{grt\text{-}in}$	$T_{ol\text{-}spl}$ / $P_{grt\text{-}in}$
Coarse-grained spinel harzburgite						
1680/1	C	884 ± 71 / 1.99 ± 0.07	910 ± 12 / 2.01 ± 0.03	no cpx	no cpx	1011 ± 10 / 2.11 ± 0.02
	R	1019 ± 37 / 2.09 ± 0.10	952 ± 14 / 2.02 ± 0.06	no cpx	no cpx	1007 ± 60 / 2.10 ± 0.12
1680/2	C	1011 ± 59 / 2.41 ± 0.13	979 ± 21 / 2.36 ± 0.06	no cpx		1026 ± 50 / 2.44 ± 0.13
	R	1028 ± 25 / 2.45 ± 0.07	1000 ± 12 / 2.40 ± 0.04	no cpx		1001 ± 50 / 2.40 ± 0.11
1680/3	C	899 ± 64 / 2.22 ± 0.08	1000 ± 17 / 2.38 ± 0.03	no cpx		1018 ± 63 / 2.41 ± 0.01
	R	920 ± 33 / 2.26 ± 0.05	995 ± 27 / 2.38 ± 0.04	no cpx		1005 ± 49 / 2.39 ± 0.09
1680/5	C	989 ± 15 / 2.19 ± 0.05	953 ± 19 / 2.15 ± 0.04	no cpx	no cpx	1005 ± 21 / 2.20 ± 0.05
	R	1049 ± 33 / 2.27 ± 0.07	953 ± 12 / 2.15 ± 0.03	no cpx		1006 ± 42 / 2.18 ± 0.09
1911/3	C	1021 ± 33 / 2.39 ± 0.10	1021 ± 20 / 2.40 ± 0.09	no cpx		986 ± 17 / 2.33 ± 0.07
	R	1068 ± 30 / 2.44 ± 0.12	*1179 ± 31 / 2.69 ± 0.12*	no cpx		1030 ± 14 / 2.39 ± 0.09
1911/6	C	926 ± 54 / 2.12 ± 0.10	985 ± 10 / 2.17 ± 0.08	no cpx	no cpx	966 ± 47 / 2.16 ± 0.14
	R	963 ± 65 / 2.15 ± 0.10	1010 ± 21 / 2.19 ± 0.04	no cpx	no cpx	997 ± 27 / 2.18 ± 0.05
1917/3	C	930 ± 29 / 2.18 ± 0.05	902 ± 10 / 2.13 ± 0.03	no cpx	no cpx	953 ± 11 / 2.20 ± 0.02
	R	978 ± 43 / 2.24 ± 0.05	888 ± 15 / 2.12 ± 0.02	no cpx	no cpx	924 ± 15 / 2.15 ± 0.03
1920/2	C	1062 ± 54 / 2.61 ± 0.13	1077 ± 41 / 2.63 ± 0.09			1067 ± 20 / 2.61 ± 0.04
	R	1073 ± 58 / 2.64 ± 0.14	*1160 ± 29 / 2.84 ± 0.04*			1062 ± 32 / 2.61 ± 0.07
1920/6	C	1093 ± 36 / 2.73 ± 0.08	1079 ± 23 / 2.71 ± 0.06			1047 ± 43 / 2.63 ± 0.09
	R	1028 ± 77 / 2.60 ± 0.16	*1187 ± 26 / 3.00 ± 0.11*			1020 ±113/ 2.59 ± 0.24
1920/8	C	1093 ± 31 / 2.71 ± 0.10	1065 ± 08 / 2.61 ± 0.05			1053 ± 23 / 2.61 ± 0.09
	R	1057 ± 55 / 2.65 ± 0.13	1074 ± 11 / 2.69 ± 0.05			1084 ± 25 / 2.70 ± 0.07
1920/10	C	1025 ± 19 / 2.36 ± 0.04	1052 ± 39 / 2.42 ± 0.09			968 ± 33 / 2.29 ± 0.05
	R	990 ± 38 / 2.30 ± 0.07	*1100 ± 13 / 2.50 ± 0.02*			983 ± 23 / 2.30 ± 0.03
1920/11	C	960 ± 82 / 2.20 ± 0.15	985 ± 06 / 2.22 ± 0.05			1006 ± 38 / 2.26 ± 0.08
	R	1006 ± 49 / 2.30 ± 0.13	1027 ± 33 / 2.33 ± 0.15			1017 ± 43 / 2.31 ± 0.15
1920/17	C	1040 ± 25 / 2.54 ± 0.10	1053 ± 33 / 2.56 ± 0.10			958 ± 25 / 2.39 ± 0.09
	R	1010 ± 28 / 2.48 ± 0.11	1092 ± 12 / 2.62 ± 0.15			926 ± 49 / 2.34 ± 0.15
1920/18	C	942 ± 26 / 2.20 ± 0.02	940 ± 19 / 2.20 ± 0.01			929 ± 17 / 2.19 ± 0.01
	R	914 ± 36 / 2.18 ± 0.04	946 ± 15 / 2.20 ± 0.01			960 ± 48 / 2.21 ± 0.06
1920/22	C	1043 ± 44 / 2.61 ± 0.12	1022 ± 29 / 2.59 ± 0.10			1014 ± 25 / 2.56 ± 0.07
	R	1081 ± 37 / 2.71 ± 0.12	1068 ± 10 / 2.70 ± 0.07			1052 ± 38 / 2.66 ± 0.10

Table 9: Continued

Sample		$T_{opx\text{-}spl}$ / $P_{grt\text{-}in}$	$T_{Ca\text{-}opx}$ / $P_{grt\text{-}in}$	$T_{2px\text{-}en\text{-}di}$ / $P_{grt\text{-}in}$	$T_{2px\text{-}Na}$ / $P_{grt\text{-}in}$	$T_{ol\text{-}spl}$ / $P_{grt\text{-}in}$
Granular spinel harzburgite						
1902/1	C	808 ± 54 / 2.25 ± 0.07	730 ± 27 / 2.19 ± 0.01	no cpx	no cpx	921 ± 67 / 2.42 ± 0.12
	R	640 ± 56 / 2.12 ± 0.04	778 ± 62 / 2.21 ± 0.03	no cpx	no cpx	923 ± 21 / 2.43 ± 0.12
1902/6	C	802 ± 37 / 2.20 ± 0.04	748 ± 24 / 2.16 ± 0.01	no cpx	no cpx	900 ± 29 / 2.34 ± 0.05
	R	692 ± 86 / 2.12 ± 0.04	809 ± 16 / 2.19 ± 0.01	no cpx	no cpx	955 ± 32 / 2.40 ± 0.05
Porphyroclastic spinel harzburgite						
1927/5	C	*1111 ± 59 / 2.90* ± 0.17	1371 ± 05 / 3.72 ± 0.01	1340 ± 35 / 3.61 ± 0.07		*1067 ± 14 / 2.79 ± 0.03*
	R	*1098 ± 42 / 2.85 ± 0.17*	1362 ± 11 / 3.68 ± 0.03	1307 ± 45 / 3.49 ± 0.09	1338 ± 94 / 3.60 ± 0.20	*1060 ± 21 / 2.76 ± 0.04*
1927/15	C	*1098 ± 48 / 3.03 ± 0.15*	1412 ± 10 / 4.06 ± 0.05	1340 ± 04 / 3.82 ± 0.05	1358 ± 54 / 3.88 ± 0.19	1102 ± 11 / 3.03 ± 0.05
	R	*1053 ± 80 / 2.85 ± 0.23*	1419 ± 08 / 4.06 ± 0.05	1331 ± 25 / 3.76 ± 0.05	1380 ± 98 / 3.91 ± 0.31	1046 ± 20 / 2.85 ± 0.05
Spinel lherzolite						
1911/4	C	1002 ± 36 / 2.25 ± 0.11	990 ± 10 / 2.22 ± 0.03	928 ± 24 / 2.15 ± 0.05	987 ± 37 / 2.22 ± 0.06	941 ± 50 / 2.19 ± 0.08
	R	963 ± 30 / 2.20 ± 0.02	967 ± 03 / 2.18 ± 0.02	975 ± 40 / 2.18 ± 0.04	940 ± 105 / 2.17 ± 0.12	1028 ± 40 / 2.27 ± 0.06
1911/7	C	1059 ± 95 / 2.29 ± 0.19	950 ± 21 / 2.18 ± 0.03	938 ± 26 / 2.12 ± 0.04	986 ± 85 / 2.18 ± 0.10	943 ± 25 / 2.11 ± 0.05
	R	1034 ± 62 / 2.33 ± 0.12	975 ± 13 / 2.21 ± 0.05	990 ± 53 / 2.25 ± 0.10	*1049 ± 99 / 2.35 ± 0.18*	1005 ± 65 / 2.29 ± 0.15

Errors correspond to 1 σ. $T_{opx\text{-}spl}$ = orthopyroxene-spinel Cr-Al exchange thermometer of Sachtleben and Seck (1981); $P_{grt\text{-}in}$ = maximum pressure of grt-free spl peridotite derived from spl composition according to Webb and Wood (1986); $T_{Ca\text{-}opx(BK90)}$, $T_{2px(BK90)}$, $T_{Na\text{-}px(BK90)}$, = Ca-in-orthopyroxene, two-pyroxene, Na exchange thermometers, respectively, of Brey and Köhler (1990); $T_{spl\text{-}ol(F79)}$ = Spl-ol Fe-Mg exchange thermometer of Fabriès et al. (1979). Temperature values refer to estimated maximum pressures after Webb and Wood (1986). C and R refer to P-T estimates derived from mineral core and rim compositions, respectively.

Fe-Mg zoning patterns of spinel grains, in particular of those that are in contact with olivine, indicate a significant but short-lived heating event that was most probably related to the infiltration of melts just before the xenoliths were sampled by ascending magmas. Average temperature values ($T_{ol\text{-}spl}$) obtained for spinel core compositions are similar to the values obtained by two-pyroxene thermometry but temperatures obtained from spinel rim compositions are approximately 60–80 °C higher (Table 9).

Coarse-grained garnet, garnet-spinel and spinel harzburgites

Apart from three samples (spinel harzburgites 1680–1, 1920-6, 1920-11), all xenoliths of this group are characterized by fingerprint-like spl-opx pseudomorphs after garnet I, and in three of these samples (1680–4, 1917–4, 1920–23) relict garnet has been preserved. Furthermore, the cores of large opx-I grains are either homogeneous or show a weak rimward decrease in Al (Table 3a), and in most samples opx I has exsolution lamellae of spl ± cpx. In combination, these features suggest that the rocks were first subject to decompression (grt I + ol I = spl II + opx II) followed by a relatively long period of cooling during which spl ± cpx were exsolved from opx I grains and the compositions of opx I and opx II grains became more homogeneous and (more) alike. Many samples experienced a short-lived heating event prior to sampling by the transporting magmas, as indicated by increases of Al (and partly also Ca) in the outermost zones of opx I/II grains. Still later, most harzburgites were infiltrated by melts that locally interacted with the mineral grains and, en route to the surface, started to crystallize cpx III.

Geothermobarometry on most of the xenoliths of this group is hindered by the lack of primary clinopyroxene and relict garnet I. Xenolith 1917–4, however, contains both primary cpx and relict grt. Application of pyroxene thermometers ($T_{2px\text{-}en\text{-}di}$, $T2px\text{-}Na$, $T_{Ca\text{-}opx}$) and of $T_{opx\text{-}grt}$ in combination with the Al-in-opx barometer ($P_{Al\text{-}opx}$) on core compositions of pyroxenes and relict garnet I yielded *P-T* estimates of 1002–1038 °C and 2.18–2.35 GPa, while the $T_{opx–spl}$ thermometer in combination with $P_{Al\text{-}opx}$ gave 1042 ± 35 °C / 2.36 ± 0.43 GPa. Similar or higher temperature values were obtained from rim compositions (Table 8). Ca-Cr systematics of garnet are in line with these estimates (Fig. 13).

The other two xenoliths with grt I relics (1680–4, 1920–23) are devoid of primary cpx. In sample 1680–4, however, cpx was exsolved from opx I, indicating saturation in diopside component (Table 8). We therefore applied combinations of the $T_{opx\text{-}spl}$ and $T_{Ca\text{-}opx}$ thermometers with the $P_{Al\text{-}opx}$ barometer. Both samples yield roughly similar *P-T* estimates of ~ 870 – 930 °C / 1.7 – 2.3 GPa (1680–4) and 840 – 930 °C / 1.8 – 2.1 GPa (1920–23) for opx I core and garnet I compositions (Table 8). Similar *P-T* conditions for these two xenoliths are also suggested by similar X_{Cr} values of garnet I and spinel I/II grains (Table 2). Both the relatively low X_{Cr} values of grt I (0.033–0.065) and spl I/II (0.326–0.463) and the *P-T* estimates of ~ 1100 °C and 2.9 GPa are roughly in line with experimental data (Brey *et al.*, 1999; Girnis & Brey, 1999; Girnis *et al.*, 2003; Klemme, 2004). Significantly higher *P-T* values were obtained with a combination of $T_{grt\text{-}opx}$ with $P_{Al\text{-}opx}$ (Table 8). Most probably, these values are caused by a secondary modification of Fe/Mg ratios in garnet, due to the

small size of garnet relics in these two samples, as compared to sample 1917–4.

For the other xenoliths of this group, that lack both relic garnet and primary cpx, only maximum *P-T* conditions can be given by using combinations of the $T_{opx\text{-}spl}$, $T_{Ca\text{-}opx}$, $T_{ol\text{-}spl}$ thermometers in combination with the $P_{grt\text{-}in}$ barometer (Table 9). For most of these xenoliths, P_{max}-T estimates for rim compositions are higher than those for core compositions reflecting the relatively late heating event deduced from the Al-Ca zoning patterns of opx grains. For three of the samples, however, there is no systematic difference between temperatures derived from core and rim compositions and the differences are in the order of the uncertainties resulting from both chemical heterogeneity of mineral grains and analytical precision (Table 9). P_{max}-T estimates for core compositions range from ~ 900 °C / 2.0 GPa to ~ 1080 °C / 2.7 GPa. Since garnet was present in these rocks and reacted with olivine to fingerprint-like intergrowths of spinel and opx, these *P-T* estimates may approximate actual *P-T* values reached during cooling.

Granular garnet-spinel harzburgites

The presence of spinel I and of fingerprint-like intergrowth of opx II and spl II suggest the former coexistence of low-Ca garnet and spinel. Most probably, the reaction grt I + ol I to opx II + spl II was caused by decompression. Subsequently, the rocks must have undergone a relatively long period of cooling and recrystallization as suggested by (i) Al zoning patterns of opx-I grains, (ii) granular rock textures (apart from fingerprint-like aggregates) and (iii) identical compositions of spl I and spl II.

Reliable temperature estimates for these xenoliths cannot be given. The lack of primary clinopyroxene and of cpx exsolution lamellae in opx excludes the application of two-pyroxene thermometers and qualifies temperature values derived from the Ca-in-opx thermometer (Brey & Köhler, 1990) as minimum temperatures. On the other hand, the absence of garnet only enables an estimate of maximum pressures with $P_{grt\text{-}in}$. Values obtained range from ~ 640 °C / 2.1 GPa to ~ 810 °C / 2.2 GPa derived from combinations of $T_{opx\text{-}spl}$ (Sachtleben & Seck, 1981) and $T_{Ca\text{-}opx}$ (Brey & Köhler, 1990) with the $P_{grt\text{-}in}$ barometer of Webb & Wood (1986) (Table 9).

Porphyroclastic spinel harzburgites

The homogeneity of all mineral phases in these two xenoliths suggests chemical equilibrium. We therefore applied the pyroxene thermometers of Brey & Köhler (1990) in combination with the $P_{grt\text{-}in}$ barometer of Webb & Wood (1986). Resulting *P-T* estimates range from 1338 °C / 3.40 GPa to 1371 °C / 3.72 GPa and from 1331 °C / 3.76 GPa to 1419 °C / 4.06 GPa for xenoliths 1927-5 and 1927-15, respectively (Table 9). These values represent maximum *P-T* conditions, since no garnet is present in the rocks. However, given the small pressure dependence of the $T_{2px\text{-}en\text{-}di}$ thermometer (~ 20 °C/GPa; Brey & Köhler, 1990), it can safely be assumed that these xenoliths are derived from the lowermost lithosphere.

Garnet-spinel-olivine websterites

Textures and mineral compositions indicate relatively complex but similar *P-T* evolutions of both samples. The original paragenesis was ol I + opx I + cpx I + spl I + grt I. Chemical zonation patterns

of and exsolution lamellae in pyroxene grains indicate a relatively long period of cooling followed by a relatively recent and short-lived heating event. During cooling, the equilibrium grt I + ol I = spl I + opx I + cpx I was shifted to the left, as suggested by rare opx grains between coexisting spl I and grt I grains. The small volume of exsolved phases in pyroxenes suggests limited cooling. A careful comparison of the Ca* [= Ca/(1-Na)] partitioning between the different cpx and opx domains (cores, intermediate low-Al zones, rims) with experimental data (Brey *et al.*, 1990) indicates that both pyroxenes were not in chemical equilibrium (with respect to Ca and Na) during cooling and after the short-lived heating event. Therefore, we only used the $T_{Ca\text{-}opx}$ and $T_{grt\text{-}opx}$ thermometers in combination with the $P_{Al\text{-}opx}$ barometer. Application of these thermobarometer combinations on the low-Al zones of pyroxene grains resulted in *P-T* values of ~ 850 °C / 1.75 GPa for both samples, while rim compositions yielded 970-1020 °C / 1.6-1.9 GPa (Table 8). These *P-T* estimates, however, should be used with caution.

Websterites

The websterites experienced a relatively long period of cooling indicated by exsolution of garnet ± complementary pyroxene ± rutile ± ilmenite from pyroxene-I grains in all samples and formation of garnet Ib by the reaction opx + cpx + spl = grt + ol in samples with primary spinel and olivine. Application of the $T_{2px\text{-}en\text{-}di}$ and $T_{Ca\text{-}opx}$ thermometers in combination with the $P_{Al\text{-}opx}$ barometer on re-integrated compositions of pyroxene-I cores of some samples yield original temperatures of ~ 1110–1270 °C and pressures of 1.3–2.3 GPa.

Websterite xenoliths of the first group that contain (nearly) homogeneous pyroxenes and were not subject to late-stage heating can be used to constrain the thermal state of the subcontinental lithosphere prior to Quaternary volcanism. We used various thermometers in combination with the $P_{Al\text{-}opx}$ barometer (Brey & Köhler, 1990) for *P-T* estimates (Table 8). Although Fe/Mg ratios of garnet relics might have been modified during late-stage kelyphitization, this procedure is justified because the $P_{Al\text{-}opx}$ barometer is not particularly sensitive to garnet composition. However, temperature estimates derived from the $T_{grt\text{-}opx}$ (Brey & Köhler, 1990) and $T_{grt\text{-}cpx}$ (Krogh, 1988) thermometers should be regarded with some caution.

For the two websterites 1906–1 and 1906–4 that both contain primary garnet and spinel, widely scattering but generally low *P-T* estimates between ~ 680 °C / 1.4 GPa and 870 °C / 1.9 GPa were obtained (Table 8). It is important to note that pyroxene "solvus" relationships at low temperatures (< 850 °C) are not well constrained due to the steepening of the solvus limbs at successively lower temperatures (Brey & Köhler, 1990). Moreover, as compared with clinopyroxenes produced in the experiments of Brey et al. (1990), cpx I grains of both samples are characterized by higher Na contents. Therefore, the relatively low temperature values obtained by the $T_{2p\text{-}en\text{-}di}$ and $T_{2px\text{-}Na}$ thermometers have to be treated with some caution. *P-T* estimates obtained on the other websterite xenoliths of the first group are significantly higher and more consistent (Table 8).

Websterite xenoliths of the second group were not equilibrated during/after cooling, as indicated by chemical zoning patterns of pyroxene

grains. Therefore, any *P-T* estimates derived from thermometers that are based on elements with relatively low diffusivities, such as Al, Cr and Ca, may be meaningless. *P-T* estimates obtained on pyroxene rim compositions of those xenoliths that have relatively flat pyroxene zoning patterns are given in Table 8 (samples 1535–2, –3, –9).

In websterites of the third group, a long period of cooling was followed by a relatively short-lived (recent) heating event leading to a significant increase in Al of pyroxene domains adjacent to grt I/II. As pyroxene compositions at the contact to garnet are constant within individual samples, we used these compositions for estimating pressures and temperatures that were reached during/after heating (Table 8). Intermediate zones of pyroxene grains that are characterized by minimum Al contents can be used to deduce upper limits for the temperatures reached after cooling but before heating. Using the pressure estimates obtained from pyroxene rims, temperature values of ~ 830-850 °C are obtained for all four samples.

Clinopyroxene-bearing orthopyroxenites

Exsolution textures and pyroxene compositions indicate that after a long period of cooling, chemical equilibrium was nearly reached in these rocks (except for Al in cpx that shows a decrease towards exsolved garnet). Since Fe/Mg ratios of garnet relics were most probably modified during kelyphitization, we applied the $T_{2pxen\text{-}di}$, T_{2pxNa} and $T_{Ca\text{-}opx}$ thermometers in combination with the $P_{Al\text{-}opx}$ barometer (Brey & Köhler, 1990) to average compositions of pyroxenes and garnet for each sample. This is justified, since the $P_{Al\text{-}opx}$ barometer is not particularly sensitive to Fe/Mg ratio of garnet. Three of the samples yielded relatively low values of ~ 800 °C / 1.2 GPa, while sample 1901–1 gave ~ 950 °C / 1.7 GPa (Table 8).

Orthopyroxenites devoid of primary clinopyroxene

Due to the lack of cpx and relict garnet in these xenoliths no geothermobarometric calculations could be performed. However, rock textures and chemical zoning patterns of opx grains suggest a relatively long period of cooling followed by a recent heating event.

DISCUSSION

Garnet lherzolites and porphyroclastic spinel harzburgites were chemically equilibrated at very high *P-T* conditions of ~ 3.5 GPa / 1350 C (Tables 8 and 9) that are typical for the lithosphere-asthenosphere transition. All the other xenoliths are characterized by textural and/or chemical disequilibrium documenting a *P-T* evolution. Fingerprint-like intergrowths of spl and opx, for example, testify to decompression, while exsolution phenomena and/or core-to-rim decreases of Al in pyroxene grains indicate cooling. Some xenoliths with exsolution textures show homogeneous mineral compositions, suggesting that a state of chemical equilibrium was reached during/after cooling. In many xenoliths, pyroxene grains show a rimward increase of Al in their outermost zones, pointing to a late, relatively short-lived heating event. In the following, we will try to put temporal constraints on both the late heating and the preceding cooling events and we will discuss the deduced *P-T* evolution of the xenoliths' source regions in the context of lithospheric processes.

Table 10: Calculated diffusion times for Al zoning patterns in orthopyroxene and clinopyroxene

Rock type Sample no	Mineral	$x_{1/2}$ (μm)	T_0 (°C)	D (T_0) $m^2\ s^{-1}$	t (T_0) (Ma)	T_e (°C)	D (T_e) $m^2 s^{-1}$	t (T_e) (ka)
Late heating event (rimward increase of Al in opx)								
Coarse-grained spinel harzburgite								
1680–1	Opx	48	884	xxxxxx	xx	1019	$4.84 * 10^{-22}$	150
1920–11	Opx	25	960	xxxxxx	xx	1010	$1.10 * 10^{-21}$	20
Coarse-grained garnet harzburgite								
1680–3	Opx	35	900	xxxxxx	xx	986	$5.92 * 10^{-23}$	670
1911–3	Opx	30	1020	xxxxxx	xx	1070	xxxxxxx	xx
1920–22	Opx	30	1040	xxxxxx	xx	1080	$1.83 * 10^{-21}$	16
Coarse-grained websterite (group 3)								
1910–1	Opx	26	834	$1.45 * 10^{-24}$	15	961	$1.27 * 10^{-22}$	170
1910–11	Cpx	11	843	$0.30 * 10^{-24}$	13	947	$9.56 * 10^{-24}$	400
Early cooling without equilibration and late heating (rimward decrease in Al in opx)								
Granular garnet-spinel harzburgite								(Ga)
1902–6	Opx	74	800	xxxxxx	xx	690	xxxxxx	0.50

D_{Al}(opx) = $6.27 * 10^{-25}$ $m^2\ s^{-1}$ at 812 °C and E_a = 400 kJ mol^{-1} (Smith & Barron, 1991); D_{Al}(cpx) = $3.7 * 10^{-21}$ $m^2\ s^{-1}$ at 1180 °C and E_a = 377 kJ mol^{-1} (Sautter *et al.*, 1988)

Late heating event

In many xenoliths, a late heating event is documented by rimward increases of Al and Ca in the outermost zones of orthopyroxene grains. In garnet-bearing websterites, relatively large domains of opx and cpx adjacent to (exsolved) garnet may show homogeneous compositions with elevated Al contents or Al may steadily increase towards garnet, suggesting a relatively young age and a rather short duration of the heating event. We estimated diffusion times for Al zoning patterns in pyroxene grains, based on a model for linear diffusion in a semi-infinite medium (Crank, 1975). Diffusion coefficients and activation energies were taken as follows: $D_{Al} = 6 \times 10^{-25}$ m^2 s^{-1} at 812 °C and E_a = 400 kJ mol^{-1} for opx (Smith & Barron, 1991), and $D_{Al} = 3.7 \times 10^{-21}$ m^2 s^{-1} at 1180 °C and E_a = 377 kJ mol^{-1} for cpx (Sautter *et al.*, 1988). Diffusion times were estimated according to the relationship $x_{1/2} = (Dt)^{0.5}$, with $x_{1/2}$ = width of diffusion profile corresponding to a half change in concentration, D = diffusion coefficient and t = duration of diffusion (Crank, 1975). As the diffusion coefficient is strongly dependent on temperature, all calculations were performed at the starting (T_0) and final (T_e) temperatures of the heating event. T_e was calculated by applying various thermometer and barometer combinations on pyroxene rim compositions, while T_0 was derived from compositions of pyroxene domains characterized by the lowest Al contents. In rocks that attained chemical equilibrium after cooling these low-Al domains correspond to the homogenous cores of pyroxene grains, while in rocks that did not reach chemical equilibrium, these low-Al domains correspond to the minimum of the Al zoning patterns. In the latter case, the calculated values of T_e are higher than the temperatures that were actually reached during cooling at the beginning of the heating event. For T_0, we found durations of ~ 17 – 10 Ma, while T_e values resulted in significantly shorter heating periods between ~ 1.4 ka and 0.50 Ma (Table 10). Although Al diffusivity in pyroxenes is not well constrained (e.g. Dimanov & Sautter, 2000, and references therein), these estimates strongly suggest that the rocks were heated before entrainment in the transporting magmas. Since $\Delta T = T_e - T_0$ does not correlate with T_0, heating was a local phenomenon and was most probably caused by relatively small volumes of intruding magma.

Decompression and cooling

Textures of coarse-grained and granular harzburgites indicate decompression accompanied and/or followed by cooling. Furthermore, exsolution phenomena and chemical zoning patterns of pyroxene grains from spinel lherzolites, (olivine) websterites and orthopyroxenites suggest that also these rocks were subject to a relatively long period of cooling, before most of them were heated. Zoning patterns that suggest simple cooling without subsequent heating were only observed in one coarse-grained harzburgite (and in the two granular spinel harzburgites. Whereas Al contents in the opx grains of these xenoliths decrease gradually from core to rim, Ca contents are in most cases constant, a feature that is most likely due to higher diffusivity of Ca as compared to that of Al (Sautter *et al.*, 1988; Witt-Eickschen & Seck, 1991; Dimanov & Sautter, 2000). For one of these samples (1902–6, granular harzburgite), we estimated the time needed to homogenize the observed Al zoning profile across opx. Our calculations resulted in a value of 0.5 Ga (Table 10), suggesting that cooling started

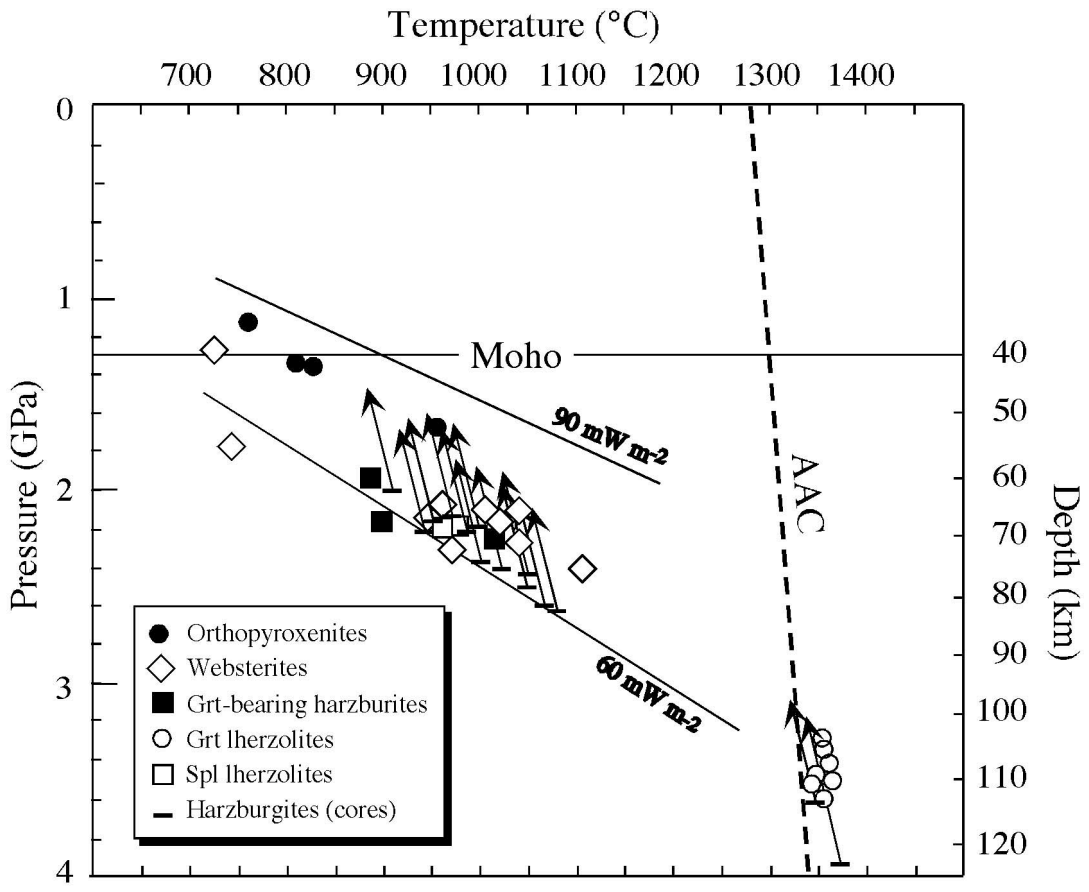


Fig. 14. Pressure-temperature diagram showing the results of thermobarometric calculations on xenoliths that are completely equilibrated or that attained homogeneous mineral compositions after an early cooling event (Tables 8 and 9). Also shown are the adiabatic upwelling curve for normal temperature asthenosphere (McKenzie & Bickle, 1989) as well as steady state model geotherms of Pollack & Chapman, 1977). For further explanation see 'Discussion'.

immediately after formation of the Mozambique collisional belt in the late Proterozoic. Such a long duration of cooling is compatible with our observation that chemical equilibrium was reached during cooling in a considerable number of xenoliths.

Geotherm

P-T estimates on mantle xenoliths can be used to constrain the geothermal gradient, if the rocks were equilibrated to the ambient *P-T* conditions of the respective upper-mantle portions before being sampled. We used those xenoliths that attained homogeneous mineral compositions during cooling for constructing a geotherm for the lithospheric mantle beneath the Chyulu Hills. A 'best estimate' for each xenolith was obtained by calculating the mean of the individual *P-T* values derived from the different geothermobarometer combinations (Tables 8 and 9), whereby values in italics were not considered. The data points for the garnet lherzolites scatter around 1360 °C / 3.5 GPa and plot slightly to the right of the adiabatic upwelling curve for normal temperature asthenosphere in the absence of significant amounts of melting with a potential surface temperature of 1280 °C (AAC; McKenzie & Bickle, 1989). Considering the pressure dependence of $T_{Ca\text{-}opx}$ ($dT/dP \approx 50$ °C/GPa; Brey & Köhler, 1990), *P-T* estimates on the two

porphyroclastic spinel harzburgites using a combination of $T_{Ca\text{-}opx}$ and $P_{grt\text{-}in}$ (= P_{max}) are in accordance with the *P-T* estimates on the garnet lherzolites (Fig. 14). All these values indicate an apparent lithospheric thickness of ~ 110 km, as was already suggested by Henjes-Kunst & Altherr (1992). Our *P-T* estimates for the other chemically equilibrated xenoliths scatter along a ~ 60-70 mW m^{-2} steady-state model geotherm as given by Pollack & Chapman (1977) (Fig. 14). At the low-temperature side of the 'geotherm' the scatter of the data points is larger. This may be due to incomplete chemical equilibration during cooling and or a higher uncertainty of thermometers that were experimentally calibrated at temperatures above 900 °C (see discussion in Krogh Ravna & Paquin, 2003).

Maximum *P-T* values on coarse-grained garnet-free spinel harzburgites estimated by combining $T_{Ca\text{-}opx}$ with $P_{grt\text{-}in}$ are in excellent agreement with the *P-T* data obtained for chemically equilibrated garnet-bearing xenoliths (Fig. 14). Fingerprint-like intergrowths of spinel and opx in these xenoliths testify to the former presence of garnet. Therefore maximum pressure estimates obtained by applying $P_{grt\text{-}in}$ should roughly correspond to ambient pressures as calculated by applying $P_{grt\text{-}in}$. As a whole, the *P-T* data array defines a lithospheric geotherm that is very similar to the one suggested by Henjes-Kunst & Altherr (1992).

Composition of the lithosphere beneath the Chyulu Hills

The xenolith population of the northwestern Chyulu Hills comprises a wide range of rock compositions such as fertile lherzolite, variably depleted harzburgite, olivine websterite, websterite and orthopyroxenite, testifying to a highly heterogeneous nature of the lithospheric mantle. The results of the geothermobarometric calculations allow for a correlation of xenolith types with depth. The lowermost lithosphere (~ 115 to 105 km depth) comprises fertile garnet lherzolites (8 xenoliths) and depleted porphyroclastic spinel harzburgites (2 xenoliths). Both xenolith types occur at the same cinder cone. There is no information on the depth range between ~ 105 and 80 km. Between ~ 80 and 60 km, depleted harzburgite and (olivine) websterite are the dominant rock types, accompanied by spinel lherzolite. The original relationship between websterites and peridotites is not known. The uppermost mantle (60–40 km depth) is dominated by orthopyroxenite, websterite and very depleted granular harzburgite. All rock types derived from the shallow lithospheric mantle (depth of 80 – 40 km) were subject to a long period of cooling that most probaby started during/after formation of the Pan-African Mozambique orogenic belt. Most likely, the websterites and orthopyroxenites, together with abundant mafic and Ca-Al-rich granulites, represent a former crystal accumulation sequence related to orogenic magmatic activity (Ulianov et al., 2005a, b).

CONCLUSIONS

The lithosphere beneath the Chyulu Hills volcanic field on the eastern flank of the Kenya Rift is appriximately 115 km thick. During Tertiary to Recent rifting processes, the lithospheric mantle did not experience a significant heat input, neither from the convecting mantle nor from a plume. The actual *P-T* gradient beneath Chyulu corresponds roughly to a 60-70 mW/m^2 steady-state model geotherm.

The absence of strongly foliated xenoliths at the base of the lithosphere suggests that the lithospheric mantle beneath Chyulu was not deformed during Tertiary to Recent rifting processes. This is in line with the results of a study on the seismic anisotropy of the mantle beneath Chyulu, showing that the fast axis of olivine is oriented subparallel to the major Pan-African structural trends (Walker *et al*., 2004).

The lithospheric mantle beneath the Chyulu Hills has a compositional structure with fertile garnet lherzolite and depleted porphyroclastic spinel harzburgite at the base, depleted harzburgite and (olivine) websterite accompanied by spinel lherzolite between ~ 80 and 60 km, followed by orthopyroxenite, websterite and very depleted granular harzburgite at the top (60–40 km depth). The lithosphere between 80 – 40 km depth most likely represents mantle rocks and magmatic intrusions of Pan-African age that may be related to orogenic processes (see also Ulianov et al., 2005a, b)

Heat input during Tertiary to recent rifting processes is a local phenomenon which seems to be confined to the shallow lithosphere. Heating was most probably caused by relatively small volumes of intruding magma. It remains yet open whether these melts come from the convecting mantle, from the lowermost lithosphere or from a plume.

ACKNOWLEDGEMENTS

This long-lasting study was funded by the Deutsche Forschungsgemeinschaft (DFG; German Research Foundation, grant to RA) and the Schweizerischer Nationalfond (SNF; Swiss National Science Foundation project 200021-100647, grant to AK). Hans-Peter Meyer provided superb microprobe facilities. Charly Wacker (†), Ilona Fin and Udo Geilenkirchen are thanked for preparing numerous high-quality polished thin sections. Additional technical support was given by Thomas Ludwig and Elke Weiher-Schröder. Discussions with Karl Fuchs, Tilo Kaspar, Stephan Klemme, Vladimir Majer, Olaf Novak, Claus Prodehl, Joachim R. R. Ritter, Alexander Rocholl, Hans-Michael Seitz, Stephan V. Sobolev, Frank Volker, Friederike Werling, Alan B. Woodland and Hermann Zeyen are gratefully acknowledged.

REFERENCES

Achauer, U., the KRISP Teleseismic Working Group (1994). New ideas on the Kenya Rift based on the inversion of the combined dataset of the 1985 and 1989/90 seismic tomography experiments. *Tectonophysics* **236**, 305-329.

Agee, C. B. & Walker, D. (1990). Aluminum partitioning between olivine and ultrabasic silicate liquid to 6 GPa. *Contributions to Mineralogy and Petrology* **105**, 243-254.

Baker, B. H. (1987). Outline of the petrology of the Kenya rift alkaline province. In: Fitton, J. G. & Upton, B. G. J. (eds) *Alkaline igneous rocks. Geological Society of London Special Publublications* 30, 293-311, Blackwell.

Behn, M. D., Conrad, C. P. & Silver, P. G. (2004). Detection of upper mantle flow associated with the African Superplume. *Earth and Planetary Science Letters* **224**, 259-274.

Brenker, F. E. & Brey, G. P. (1997). Reconstruction of the exhumation path of the Alpe Arami garnet peridotite body from depths exceeding 160 km. *Journal of Metamorphic Geology* **15**, 581-592.

Brey, G. P. & Köhler, T. (1990). Geothermobarometry in four-phase lherzolites II. New thermobarometers and practical assessment of existing thermobarometers. *Journal of Petrology* **31**, 1353-1378.

Brey, G. P., Köhler, T. & Nickel, K. G. (1990). Geothermobarometry in four-phase lherzolites I. Experimental results from 10 to 60 kb. *Journal of Petrology* **31**, 1313-1352.

Brey, G. P., Doroshev, A. M., Girnis, A. V. & Turkin, A. I. (1999). Garnet-spinel-olivine-orthopyroxene equilibria in the FeO-MgO-Al_2O_3-SiO_2-Cr_2O_3 system: I. Compositions and molar volumes of minerals. *European Journal of Mineralogy* **11**, 619-636.

Burke, K. (1996). The African Plate. *South African Journal of Geology* **99**, 341-409.

Canil, D. & O'Neill, H. St. C. (1996). Distribution of ferric iron in some upper-mantle assemblages. *Journal of Petrology* **37**, 609-365.

Carswell, D. A. & Harley, S. L. (1990). Mineral barometry and thermometry. In: Carswell, D. A. (Ed) *Eclogite Facies Rocks*, pp. 83-110, Blackie, Glasgow.

Chesley, J. T., Rudnick, R. L. & Lee, C. T. (1999). Re-Os systematics of mantle xenoliths from the east African rift: Age, structure and history of the Tanzanian Craton. *Geochimica Cosmochima Acta* **63**, 1203-1217.

Crank, J. (1975). The mathematics of diffusion. *Oxford University Press*, London.

Dawson, J. B. (1999). Metasomatism and Melting in Spinel Peridotite Xenoliths from Labait, Tanzania. In: Gurney et al. (eds.): *The Nixon volume, Proceedings of the 7th International Kimberlite Conference*, 164-173.

Debayle, E., Lévêque, J.-J. & Cara, M. (2001). Seismic evidence for a deeply rooted low-velocity anomaly in the upper mantle beneath the northeastern Afro/Arabian continent. *Earth and Planetary Science Letters* **193**, 423-436.

Dimanov, V. & Sautter, V. (2000). 'Average' interdiffusion of (Fe,Mn)-Mg in natural diopside. *European Journal of Mineralogy* **12**, 749-760.

Ebinger, C. J. (1989) Tectonic development of the western branch of the East African rift system. *Geological Society of America Bulletin* **101**, 885-903.

Ebinger, C. J. & Sleep, N. H. (1998). Cenozoic magmatism throughout East Africa resulting from impact of a single plume. *Nature* **395**, 788-791.

Ebinger, C. J., Bechel, T. D., Forsyth, D. W. & Bowin, C. O. (1989). Effective elastic thickness beneath the East African and Afar plateaus and dynamic compensation of uplift. *Journal of Geophysical Research* **94**, 2883-2901.

George, R. M. M., Rogers, N. W. & Kelley, S. (1998). Ealiest magmatism in Ethiopia: evidence for two mantle plumes in one flood basalt province. *Geology* **26**, 923-926.

Girnis, A. V. & Brey, G. P. (1999). Garnet-spinel-olivine-orthopyroxene equilibria in the FeO-MgO-Al_2O_3-SiO_2-Cr_2O_3 system: II. Thermodynamic analysis. *European Journal of Mineralogy* **11**, 619-636.

Girnis, A. V., Brey, G. P., Doroshev, A. M., Turkin, A. I. & Simon, N. (2003). The system MgO-Al_2O_3-SiO_2-Cr_2O_3 revisited: reanalysis of Doroshev et al.'s (1977) experiments and

new experiments. *European Journal of Mineralogy* **15**, 953-964.

Grand, S. P., van der Hilst, R. D. & Widiyantoro, S. (1997). Global seismic tomography: a snapshot of convection in the mantle. *GSA Today* **7**, 1-7.

Green, W. V., Achauer, U. & Meyer, R. P. (1991). A three-dimensional seismic image of the crust and upper mantle beneath the Kenya rift. *Nature* **354**, 199-203.

Harley, S. L. (1984). An experimental study of the partitioning of Fe and Mg between garnet and orthopyroxene. *Contributions to Mineralogy and Petrology* **86**, 359-373.

Haug, G. H. & Strecker, M. R. (1995). Volcanotectonic evolution of the Chyulu Hills and implications for the regional stress field in Kenya. *Geology* **23**, 165-168.

Helmberger, D., Ni, S., Wen, L. & Ritsema, J. (2000). Seismic evidence for ultralow-velocity zones beneath Africa and eastern Atlantic. *Journal of Geophysical Research* **105**, 23865-23878.

Henjes-Kunst, F. & Altherr, R. (1992). Metamorphic petrology of xenoliths from Kenya and northern Tanzania and implications for geotherms and lithospheric structures. *Journal of Petrology* **33**, 1125-1156.

Kampunzu, A. B., Bonhomme, M. G. & Kanika, M. (1998). Geochronology of volcanic rocks and evolution of the Cenozoic Western Branch of the East African Rift System. *Journal of African Earth Sciences* **26**, 441-446.

Kaspar, T. & Ritter, J. R. R. (1997). On the use of later teleseismic arrivals in ACH-tomography with an application in SE-Kenya. *Geophysical Research Letters* **24**, 1827-1830.

Klemme, S. (2004). The influence of Cr on the garnet–spinel transition in the Earth's mantle: experiments in the system MgO-Cr_2O_3-SiO_2 and thermodynamic modelling. *Lithos* **77**, 639-646.

Klemme, S. & O'Neill, H. St. C. (2000a). The effect of Cr on the solubility of Al in orthopyroxene: experiments and thermodynamic modelling. *Contributions to Mineralogy and Petrology* **140**, 84-98.

Klemme, S. & O'Neill, H. St. C. (2000b). The near-solidus transition from garnet lherzolite to spinel lherzolite. *Contributions to Mineralogy and Petrology* **138**, 237-248.

Köhler, T. P. & Brey, G. P. (1990). Calcium exchange between olivine and clinopyroxene calibrated as a geothermobarometer for natural peridotites from 2 to 60 kb with applications. *Geochimica et Cosmochimica Acta* **54**, 2375-2388.

Kretz, R. (1983). Symbols for rock-forming minerals. *American Mineralogist* **68**, 277-279.

Krogh, E. J. (1988). The garnet-clinopyroxene Fe-Mg geothermometer – a reinterpretation of existing experimental data. *Contributions to Mineralogy and Petrology* **99**, 44-48.

Krogh Ravna, E. J. & Paquin, J. (2003). Thermobarometric methodologies applicable to eclogites and garnet ultrabasites. In: Carswell, D. A., Compagnoni, R. (eds) *Ultra-high pressure metamorphism, EMU Notes in Mineralogy* **5**, 229-259, Eötvös University Press, Budapest.

Latin, D., Norry, M. J. & Tarzey, R. J. E. (1993). Magmatism in the Gregory Rift, East Africa: evidence for melt generation by a plume. *Journal of Petrology* **34**, 1007-1027.

Lee, C.-T. & Rudnick, R. L. (1999). Compositionally stratified cratonic lithosphere: petrology and geochemistry of peridotite xenoliths from the Labait tuff cone, Tanzania. In: Gurney et al. (eds.): *The Nixon volume, Proceedings of the 7th International Kimberlite Conference*, 503-521.

Lithgow-Bertelloni, C. & Silver, P. G. (1998). Dynamic topography, plate driving forces and the African superswell. *Nature* **395**, 269-272.

Macdonald, R., Rogers, N. W., Fitton, J. G., Black, S. & Smith, M. (2001). Plume-lithosphere interactions in the generation of the basalts of the Kenya rift, East Africa. *Journal of Petrology* **42**, 877-900.

McDougall, I. & Watkins, R. T. (1988). Potassium-argon ages of volcanic rocks from the northeast of Lake Turkana, northern Kenya. *Geological Magazine* **125**, 15-23.

McKenzie, D. & Bickle, M. J. (1988). The volume and composition of melt generated by extension of the lithosphere. *Journal of Petrology* **25**, 625-679.

Möller, A., Mezger, K. & Schenk, V. (1998). Crustal age domains and the evolution of the continental crust ion the Mozambique Belt of Tanzania: Combined Sm-Nd, Rb-Sr and Pb-Pb isotopic evidence. *Journal of Petrology* **39**, 749-783.

Morley, C.K. (1999). Tectonic evolution of the East African Rift system and the modifying influence of magmatism: a review. *Acta Vulcanologica* **11**, 1-19.

Ni, S., Helmberger, D. V. (2003). Seismological constraints on the South African superplume; could be the oldest distinct structure on Earth. *Earth and Planetary Science Letters* **206**, 119-131.

Novak, O., Ritter, J. R. R., Altherr, R., Garasic, V., Volker, F., Kluge, C., Kaspar, T., Byrne, G. F., Sobolev, S. V. & Fuchs, K. (1997). An integrated model for the deep structure of the Chyulu Hills volcanic field, Kenya. *Tectonophysics* **278**, 187-209.

Nyblade, A. A. (2002). Crust and upper mantle structure in East Africa: Implications for the origin of Cenozoic rifting and volcanism and the formation of magmatic rifted margins. In: Menzies, M. A., Klemperer, S. L., Ebinger, C. J., Baker, J. (eds) *Volcanic Rifted Margins*, *Geological Society of America Special Paper* 362. Boulder, Colorado, pp. 15-26.

Nyblade, A. A., Owens, T. J., Gurrola, H., Ritsema, J. & Langston, C. A. (2000). Seismic evidence for a deep upper mantle thermal anomaly beneath east Africa. *Geology* **28**, 599-602.

Olker, B., Altherr, R. & Paquin, J. (2003). Fast exhumation of the ultrahigh-pressure Alpe Arami garnet peridotite (Central Alps, Switzerland): constraints from geospeedometry and thermal modelling. *Journal of Metamorphic Geology* **21**, 395-402.

Omenge, J. M. & Okelo, R. E. (1992). Geology of the Chyulu-Oloitokitok area. *Kenya Mines and Geology Department, Nairobi, Report* **112**, 51 p.

Owens, T. J., Nyblade, A. A., Gurrola, H. & Langston, C. A. (2000). Mantle transition zone structure beneath Tanzania, East Africa. *Geophysical Research Letters* **27**, 827-830.

Paquin, J. & Altherr, R. (2001a). New constraints on the P-T evolution of the Alpe Arami garnet

peridotite body (Central Alps, Switzerland). *Journal of Petrology* **42**, 1119-1140.

Paquin, J. & Altherr, R. (2001b). 'New Constraints on the P-T Evolution of the Alpe Arami Garnet Peridotite Body (Central Alps, Switzerland)': Reply to Comment by Nimis & Trommsdorff (2001). *Journal of Petrology* **42**, 1781-1787.

Parsons, T., Sleep, N. H. & Thompson, G. T. (1992). Host rock rheology on the emplacement of tabular intrusions: Implications for underplating of extending crust. *Tectonics* **11**, 1348-1356.

Pasteels, P., Villeneuve, M., De Paepe. P. & Klerkx, J. (1989). Timing of the volcanism of the southern Kivu province: Implications for the evolution of the western branch of the East African rift system. *Earth and Planetary Science Letters* **94**, 353-363.

Pollack, H. N. & Chapman, D. S. (1977). On the regional variation of heat flow, geotherms and lithospheric thickness. *Tectonophysics* **38**, 279-296.

Pouchou, J. L. & Pichoir, F. (1984). A new model for quantitative analyses. I. Application to the analysis of homogeneous samples. *La Recherche Aérospatiale* **3**, 13-38.

Pouchou, J. L. & Pichoir, F. (1985). "PAP" □□□□□Z) correction procedure for improved quantitative microanalysis. In: Armstrong, J. T. (Ed) *Microbeam Analysis*, pp. 104-106.

Ritsema, J. & van Heijst, H. J. (1999). New seismic model of the upper mantle beneath Africa. *Geology* **28**: 63-66.

Ritsema, J., van Heijst, H. J. & Woodhouse, J. H. (1999). Complex shear wave velocity structure imaged beneath Africa and Iceland. *Science* **286**, 1925-1928.

Rogers, N., Macdonald, R., Fitton, J. G., George, R., Smith, M. & Barreiro, B. (2000). Two mantle plumes beneath the East African rift system: Sr, Nd and Pb isotope evidence from Kenya Rift basalts. *Earth and Planetary Science Letters* **176**, 387-400.

Sachtleben, T. & Seck, H. A. (1981). Chemical control of Al-solubility in orthopyroxene and its implications on pyroxene geothermometry. *Contributions to Mineralogy and Petrology* **78**, 157-165

Saggerson, E. P. (1963). Geology of the Simba-Kibwezi area. *Geological Survey of Kenya Report* **58**, 70 p.

Sautter, V., Jaoul, O. & Abel, F. (1988). Aluminium diffusion in diopside using the $^{27}Al(p,\square)^{28}Si$ nuclear reaction: preliminary results. *Earth and Planetary Science Letters* **89**, 109-114.

Shackleton, R. M. (1993). Tectonics of the Mozambique Belt in East Africa. In: Prichard, H. M., Alabaster, T., Harris, N. B. W., Neary, C. R. (eds.) *Magmatic Processes and Plate Tectonics, Geological Society of London Special Publications* 76, pp. 345-362.

Simiyu, S. M. & Keller, G. R. (1997). An integrated analysis of lithospheric structure across the east African plateau based on gravity anomalies and recent studies. *Tectonophysics* **278**, 291-313.

Slack, P. D. & Davis, P. M., the KRISP Teleseismic Working Group (1994). Attenuation and velocity of P-waves in the mantle beneath the East African Rift, Kenya. *Tectonophysics* **236**, 179-199.

Sleep, N. H. (2003). Geodynamic implications of xenolith geotherms. *Geochemistry Geophysics*

Geosystems **4**, 1079, doi: 10-1029/2003GC000511.

Smith, D. (1999). Temperatures and pressures of mineral equilibration in peridotite xenoliths: Review, discussion, and implications. In: Frei, Y., Bertka, C. M., Mysen, B. O. (eds.) *Mantle Petrology: Field Observations and High-Pressure Experimentation. A Tribute to Francis R. (Joe) Boyd. Geochemical Society Special Publications* **6**, 171-188.

Smith, D. & Barron, B. R. (1991). Pyroxene-garnet equilibration during cooling in the mantle. *American Mineralogist* **76**, 1950-1963.

Smith, M. & Mosley, P. (1993). Crustal heterogeneity and basement influence on the development of the Kenya Rift, East Africa. *Tectonics* **12**, 591-606.

Späth, A., Le Roex, A. P. & Opiyo-Akech, N. (2000). The petrology of the Chyulu Hills Volcanic Province, southern Kenya. *Journal of African Earth Sciences* **31**, 337-358.

Späth, A., Le Roex, A. P. & Opiyo-Akech, N. (2001). Plume-lithosphere interaction and the origin of continental rift-related alkaline volcanism – the Chyulu Hills volcanic province, southern Kenya. *Journal of Petrology* **42**, 765-787.

Taura, H., Yurimoto, H., Kurita, K. & Sueno, S (1998). Pressure dependence on partition coefficients for trace elements between olivine and the coexisting melts. *Physics and Chemistry of Minerals* **25**, 469-484.

Ulianov, A., Kalt, A. & Pettke, T. (2005). Aluminous websterite and granulite xenoliths from the Chyulu Hills volcanic field, Kenya: Metamorphosed gabbroic cumulates from a Pan-African arc environment. *Contributions to Mineralogy and Petrology*, submitted.

Walker, K. T., Nyblade, A. A., Klemperer, S. L., Bokelmann, G. H. R. & Owens, T. J. (2004). On the relationship between extension and anisotropy: Constraints from shear wave splitting across the East African Plateau. *Journal of Geophysical Research* **109**, B08302, doi: 10.1029/2003JB002866.

Webb, S. A. C. & Wood, B. J. (1986). Spinel-pyroxene-garnet relationships and their dependence on Cr/Al ratio. *Contributions to Mineralogy and Petrology* **92**, 471-480.

Weeraratne, D. S., Forsyth, D. W., Fischer, K. M. & Nyblade, A. A. (2003). Evidence for an upper mantle plume beneath the Tanzanian craton from Rayleigh wave tomography. *Journal of Geophysical Research* **108**, 2427, doi: 10.1029/2002JB002273.

Werling, F. & Altherr, R. (1997). Thermal evolution of the lithosphere beneath the French Massif Central as deduced from geothermobarometry on mantle xenoliths. *Tectonophysics* **275**, 119-142.

Zeyen, H., Volker, F., Wehrle, V., Fuchs, K., Sobolev, S. V. & Altherr, R. (1997). Styles of continental rifting: crust-mantle detachment and mantle plumes. *Tectonophysics* **278**, 329-352.

CHAPTER VI

General conclusions

CHAPTER VI

General conclusions

Petrographically, each granulite xenolith is unique, since the chemical composition and *P-T* path that define the observed mineralogies are rarely the same in specimens from different localities and may vary among xenoliths from one volcanic edifice. This does not mean, however, that common solutions do not exist. In terms of protolith, large volumes of geochemically and petrographically similar rocks can be emplaced in a similar environment. Gabbro-troctolitic and troctolitic cumulates in the lower crust are common in nature, as well as their subsolidus metamorphism on cooling. I hope that this study will help to better understand possible ways of postmagmatic evolution of such protoliths (Chapters II and III).

I believe that the geochemical study of comagmatic xenolith suites is truly complementary to the study of their postmagmatic evolution. The deeper the protolith is changed by subsolidus processes, the more valuable are constraints imposed by the geochemical data. This applies to the websterite xenoliths from this work, of which the geochemistry is the key to their origin (Chapter II). On the other hand, a wealth of reaction textures preserved in the granulites provides a better insight into their postmagmatic evolution than their geochemical characteristics do (Chapter III).

Although trying to compare a relatively limited dataset on one rock sequence investigated in this work, to the enormous amount of data on outcropping granulites might be a very large generalization, I would not say that undertaking a metamorphic study on granulite xenoliths yields a deficient version of what could be done on an outcropping granulite terrane. Outcropping granulites are often retrogressed due to the inevitable process of tectonic exhumation. The mechanism of exhumation of granulite xenoliths by ascending magmas is entirely different and acts much faster than tectonic processes. This allows one to expect a better preservation of early, prograde metamorphic reactions in granulite xenoliths and also reveals rocks (and phenomena) that cannot be easily 'brought to the surface' by tectonic processes, such as metagabbroic websterites, of which the formation is investigated in this study. I believe, therefore, that studying metamorphism in outcropping granulite terranes and on granulite and associated ultramafic xenoliths from volcanic rocks is also complementary (Chapter III).

The 'specific' question of the mineral association, chemical composition, and origin of hibonite associated with the Ca-Al granulites largely deals with the petrology of hibonite and stands somewhat apart from the main line of the whole study. I believe that its origin as an igneous relict, albeit uncommon for terrestrial hibonite, fits all petrographic and geochemical constraints best (Chapter IV).

However, although early igneous and prograde metamorphic processes define the petrography of the studied xenoliths, stating that they lack a late-stage evolution might not be true, particularly with respect to the pyroxenites. Tectonic exhumation in orogenic belts has the advantage to bring rocks out from the environment, where further mineralogical and geochemical modification is possible, in one orogenic cycle, whereas the time of residence of lower crustal and upper mantle rocks under elevated pressure and temperature before they are sampled owing to volcanism is unlimited. The

studied websterite xenoliths show indications of recent heating / cooling in mineral zoning patterns and possibly in the mineral modes. These processes are concerned with the young magmatic activity of the Chyulu Hills. Thus, the advantage of fast exhumation in the transporting magma is somewhat diminished by the reequilibration of the upper mantle (and possibly lower crustal) rocks by processes related to the volcanism (Chapter V), earlier postorogenic processes in the lithosphere as well as various overprints due to the interaction of xenoliths with the host magma set aside.

Against the background outlined above, the results of this study can be summarized as follows:

(1) The investigated comagmatic sequence of metaigneous cumulates from the Chyulu Hills consists of gabbro-troctolitic and troctolitic cumulates. The rocks are characterized by high contents of normative olivine and plagioclase, high Ni and low Ti abundances and positive Eu anomalies. All they belong to the same differentiation trend, of which the websterites are the most magnesian part, while granulites are represented by less magnesian and more Ca- and Al-rich compositions.

(2) Hibonite in the Ca-Al granulites seems to represent one of very few relict minerals indicative of the 'troctolitic' stage; its formation appears most consistent with igneous crystallization. The petrographic relationships of the hibonite with other minerals suggest that it represents the first mineral in the crystallization sequence. Compared to hibonite from terrestrial occurrences, it is strongly impoverished in Ti, Th and LREE and displays elevated contents of Al and Ca more typical of hibonite from chondrite meteorites where this mineral may represent a liquidus phase. The abundances of Si exceed those in any terrestrial and extraterrestrial hibonite and compare with those in synthetic hibonites crystallized from Ca-, Al-rich melts.

(3) The rocks have undergone metamorphism resulted in the formation of olivine garnet-spinel websterites, Mg-Al sapphirine-bearing and Ca-Al hibonite-bearing granulites at the expense of the gabbro-troctolitic and troctolitic cumulates. The websterites were finally equilibrated under upper mantle conditions (930-1010°C / 1.8-2.2 GPa), while geothermometric estimates for the granulites vary in the range of 720-780 °C, the pressure being defined by the sillimanite stability field (< 8 kbar).

(3.1) Formation of the websterites is most consistent with foundering dense mafic cumulates in the mantle at high temperatures and subsequent reequilibration to ambient temperatures of the mantle that had lasted until they were entrained and brought to the surface by the host basanite. The petrography of the websterites appears in contradiction with their geochemistry. On the one hand, these rocks are ultramafic and do not contain modal plagioclase. They were finally equilibrated under mantle conditions. On the other hand, they display positive Eu anomalies in whole rock samples, suggesting the accomulation of plagioclase. These characteristics can be explained by foundering dense mafic-ultramafic plagioclase-bearing cumulates formed at the base of the, into the mantle.

(3.2) Formation of the granulites is consistent with cooling and compression in the course of prograde metamorphism, while indications of metamorphic retrogression are nearly absent. The

petrography of the granulites is defined by the formation of pyroxenes, spinel and corundum after the initial troctolitic assemblage on cooling, and the subsequent development of garnet at the expense of corundum, pyroxenes and spinel towards the end of the reaction path, which is consistent with compression. In contrast to most granulites from outcropping metamorphic complexes, almost no petrographic evidence for subsequent retrogression is found.

(4) A Pan-African arc environment related to the formation of the Mozambique mobile belt of Kenya is the most probable tectonic setting for the studied rocks that largely defines their evolution.

The last conclusion addresses the tectonic environment, in which the investigated igneous sequence has formed. The studied rocks are cumulates, and their geochemical characteristics differ from those of crystallized melts. Thus, to decipher the tectonic environment of formation, their whole rock compositions are of a limited value. The availability of well-preserved igneous relicts devoid of subsolidus reequilibration is also limited, thus hampering geochemical reconstructions based on trace element partition coefficients. Nevertheless, geochemical data (Chapter II), metamorphic history (Chapter II and III), and the very geological setting of the Chyulu Hills seem to accord with a calc-alkaline source of the protoliths of the studied rocks and the environment of an arc terrane of the Mozambique belt in Pan-African times.

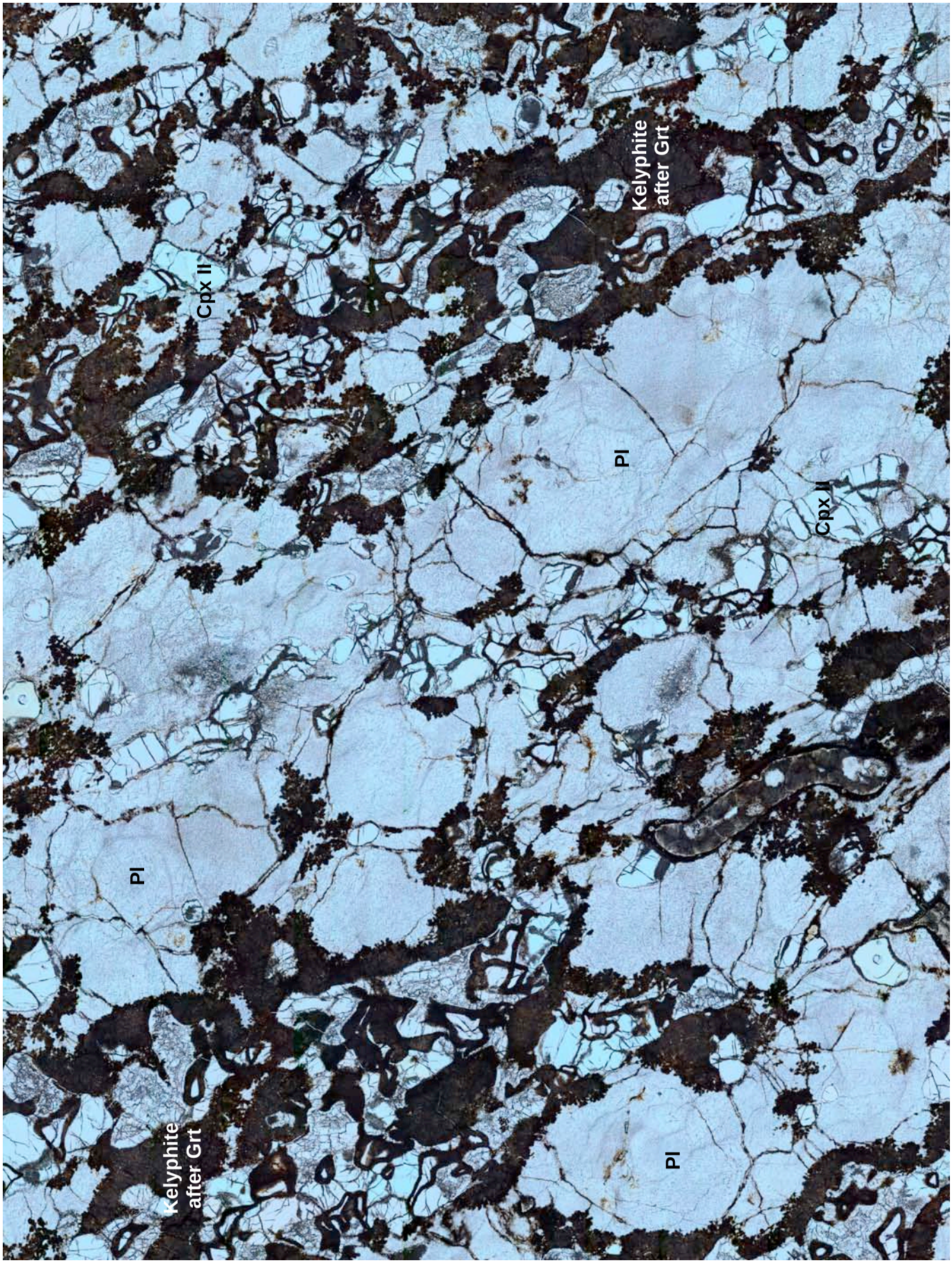
On the other hand, they virtually exclude the origin of the studied rocks as cumulates related to the young alkaline magmatism of the Chyulu Hills. Although a wealth of evidence, both geophysical (low-velocity perturbation in the uppermost mantle and lover crust) and petrographic (local heating / cooling), for the recent modification of the uppermost mantle and lover crust beneath the Chyulu Hills exists, rocks that would reflect geochemical consequences of these phenomena are lacking among xenolith used in this study. A more representative set of mantle xenoliths considered in Chapter V also does not give enough evidence for a large-scale chemical modification of the mantle underlying the Chyulu Hills. Thus, in spite of its intense recent volcanicity, the part of the East African Rift System in the area of the Chyulu Hills is (largely) characterized by old lithosphere, of which the origin and evolution appear to be concerned with the formation of the Pan-African orogenic belt.

APPENDIX

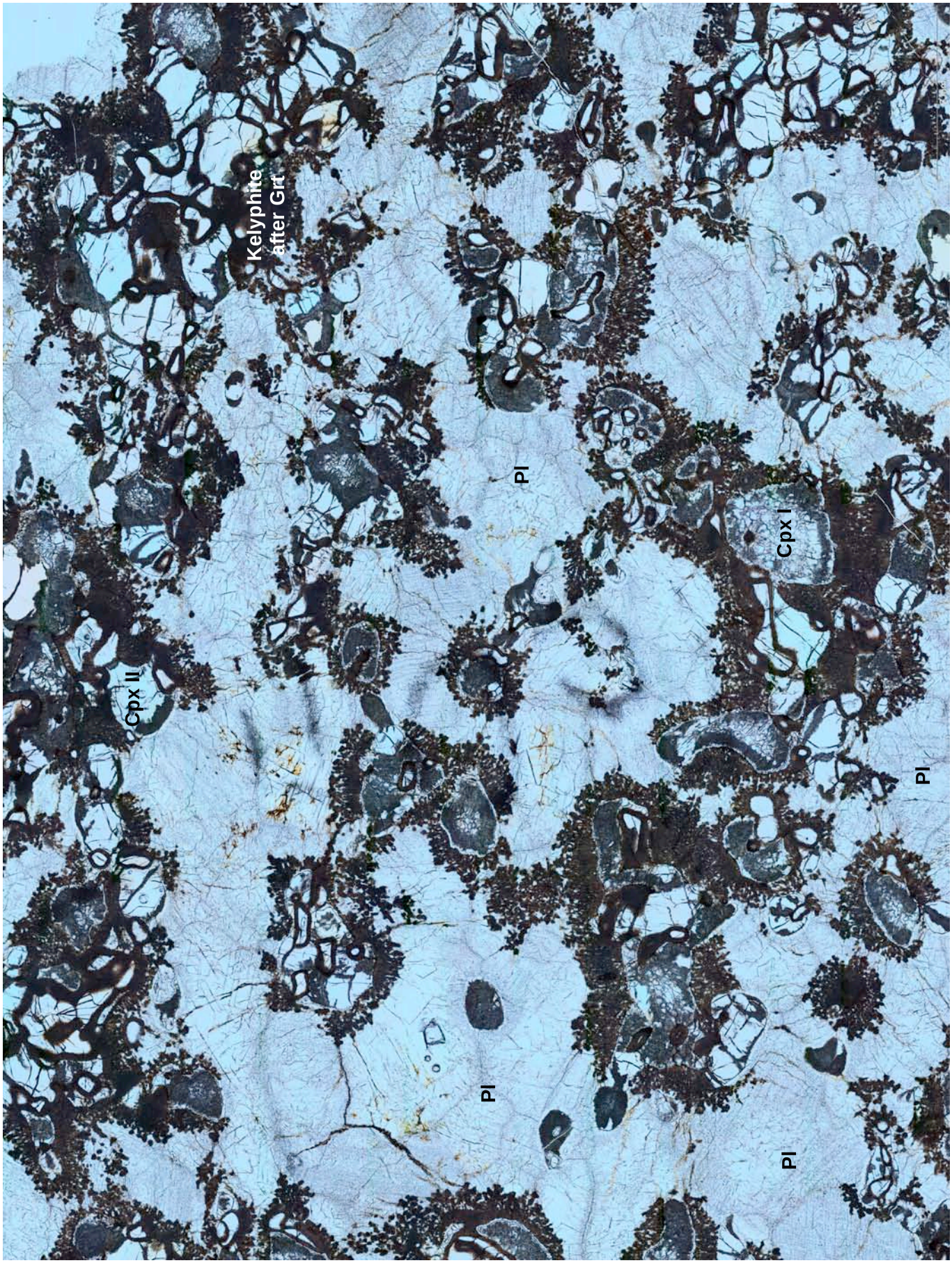
Photomicrographs of the studied specimens

*Field of view 8.5*14.5 mm, plane polarized light*

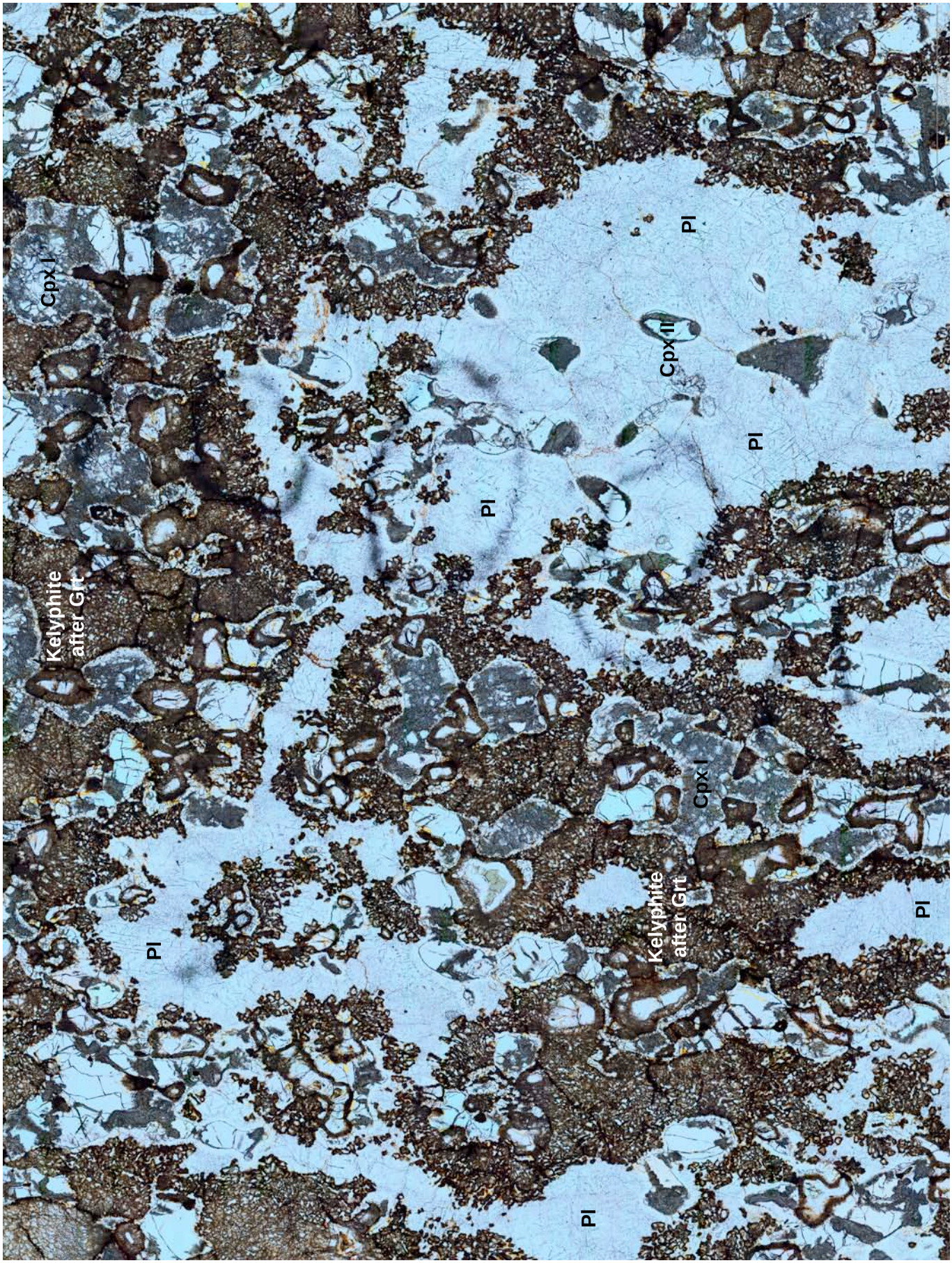
Ca-Al granulite **1904-1**



Ca-Al granulite **1904-9**



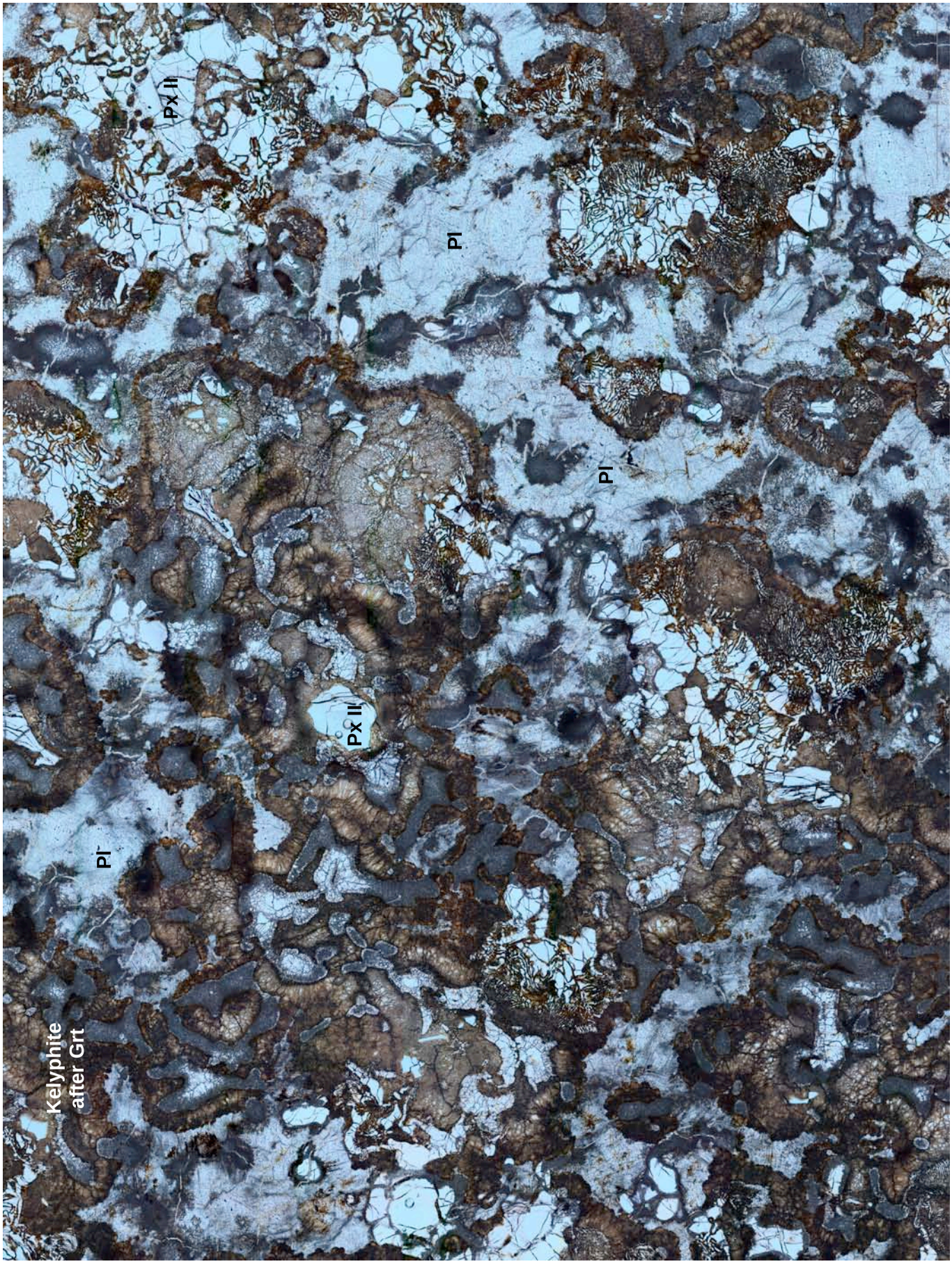
Ca-Al granulite **1906-2**



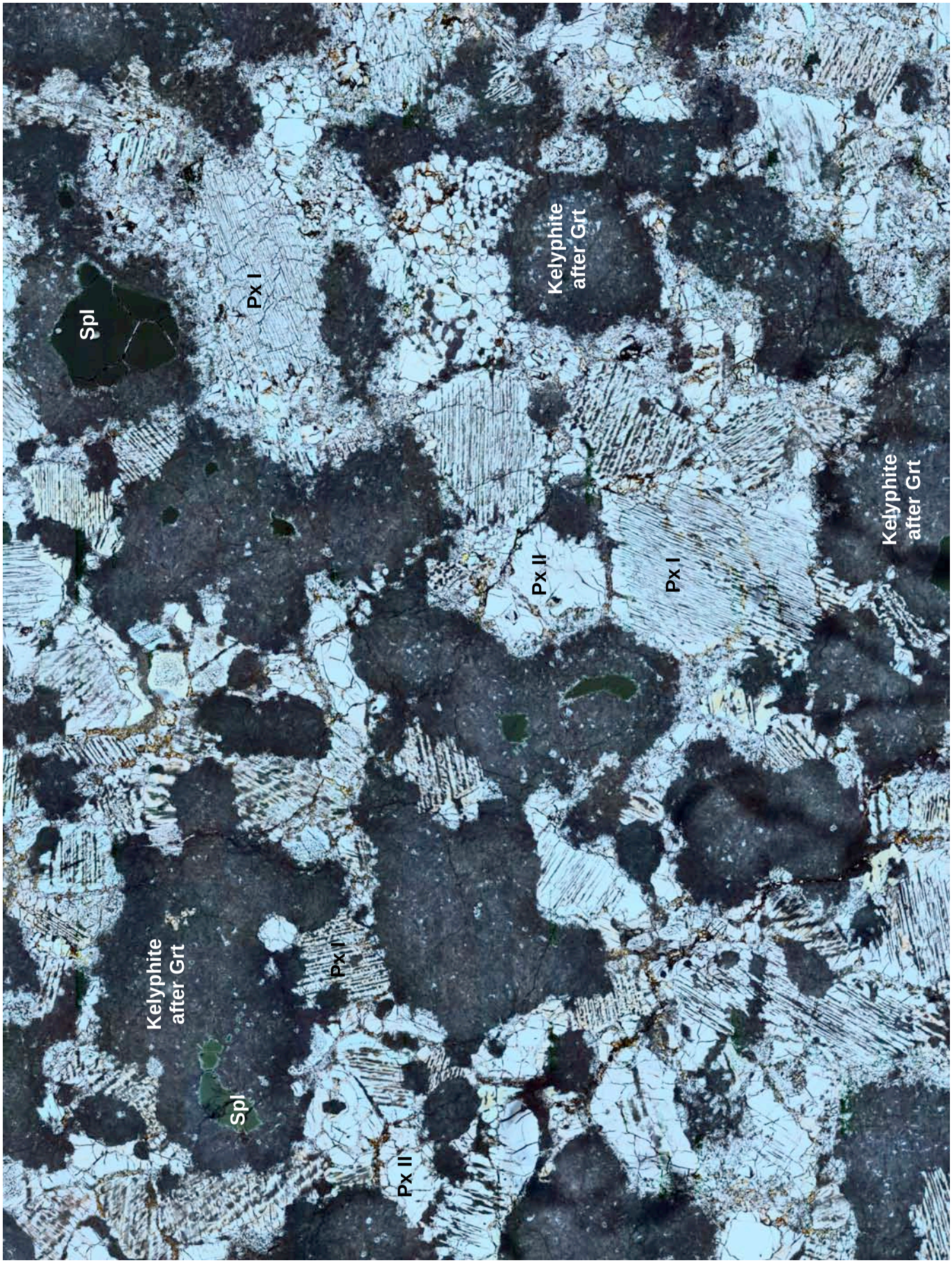
Mg-Al granulite **1904-3**



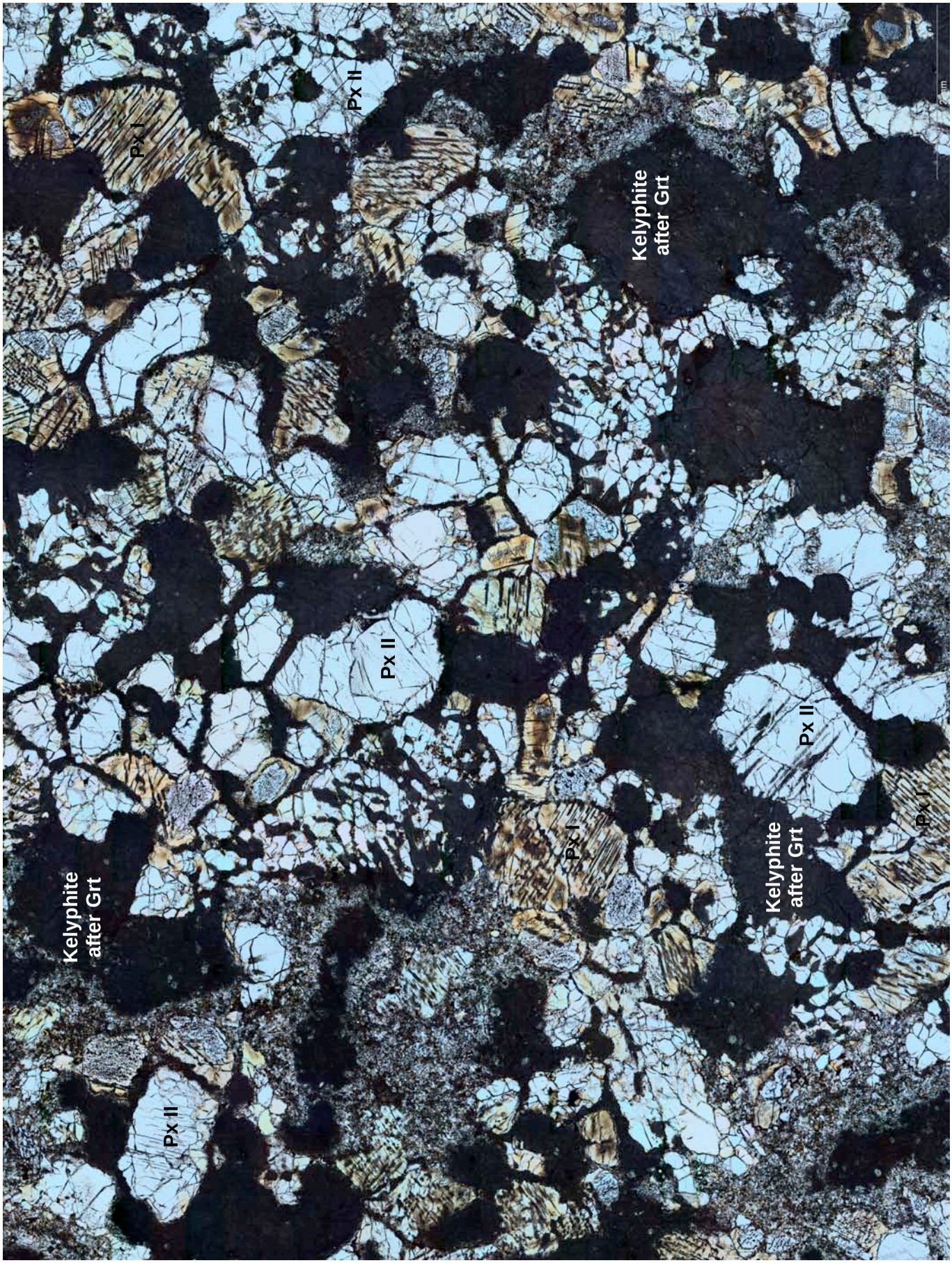
Mg-Al granulite **1904-7**



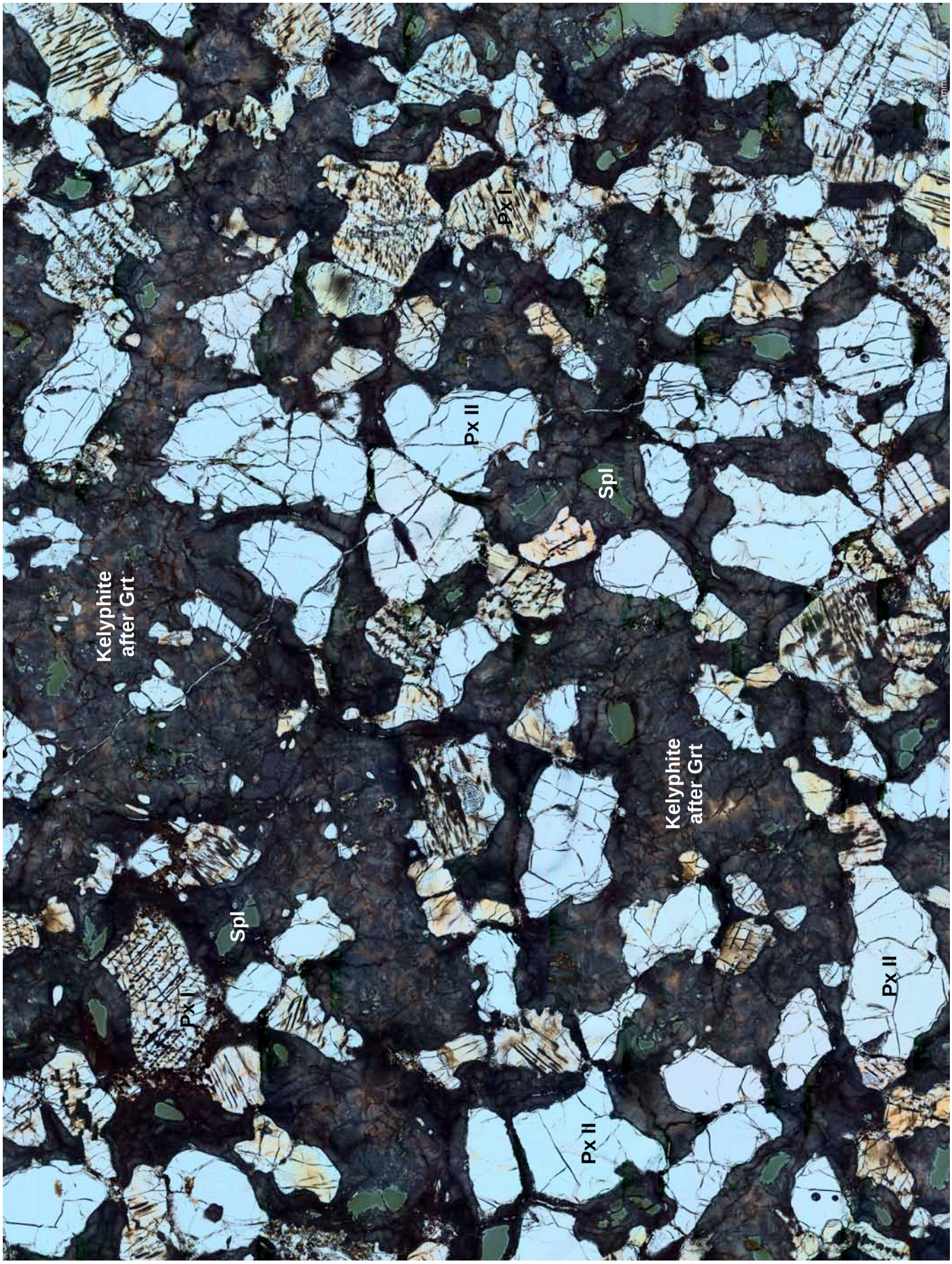
websterite **1910-11**



websterite **1910-1**

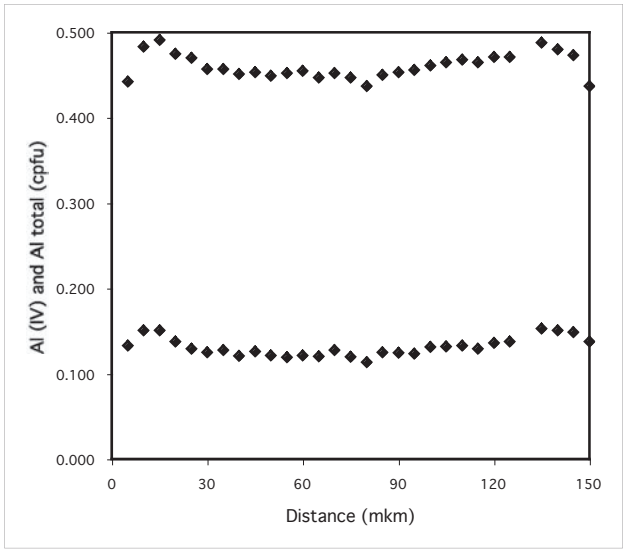


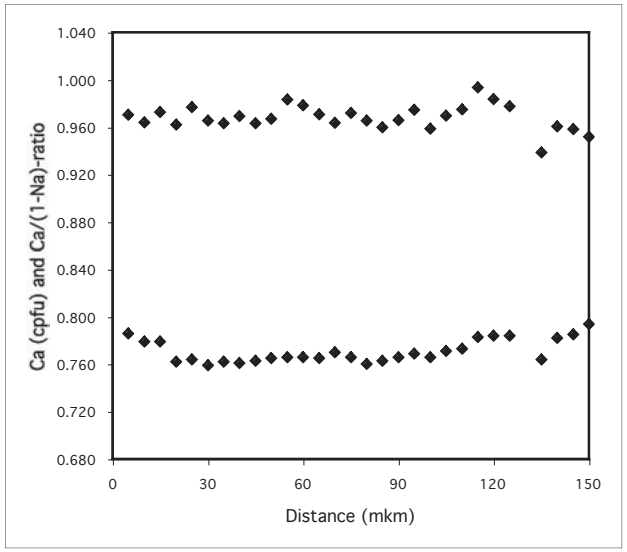
websterite **1535-3**

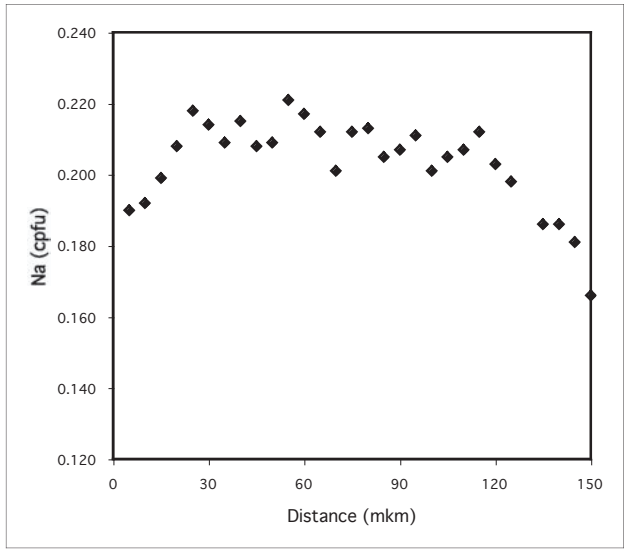


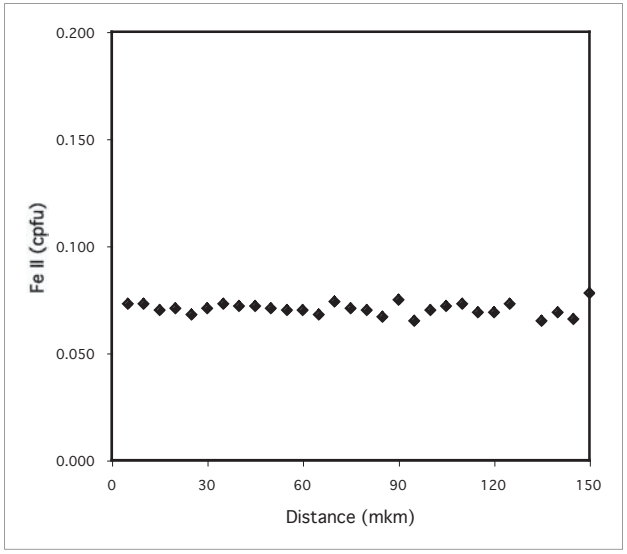
Electron microprobe analyses of minerals
from the studied specimens

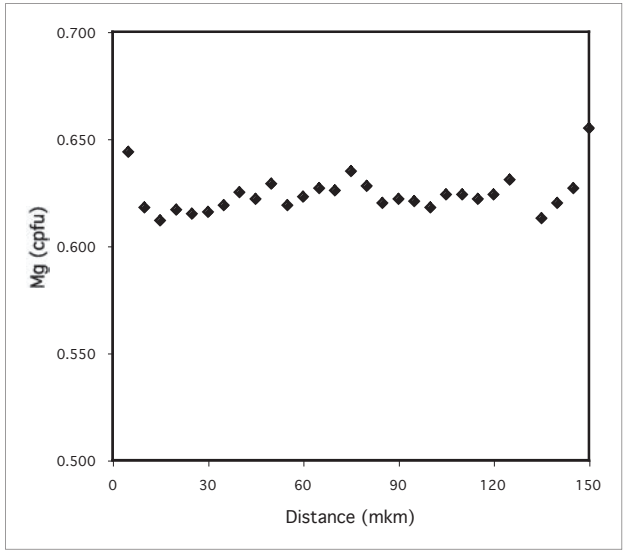
Ca-Al hibonite-bearing granulite 1904-1

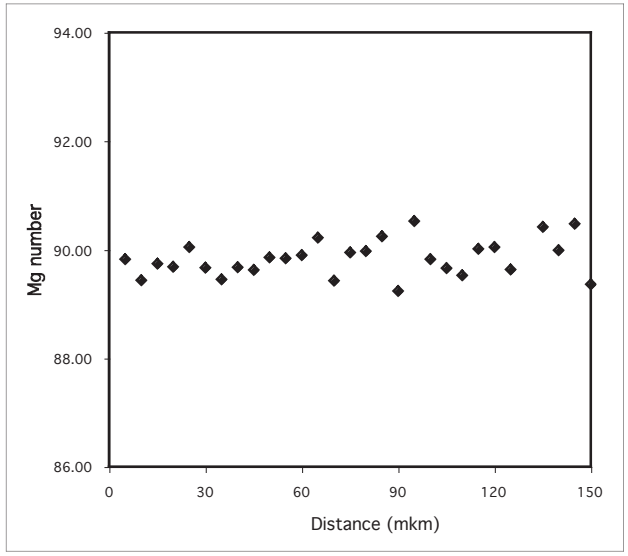












2

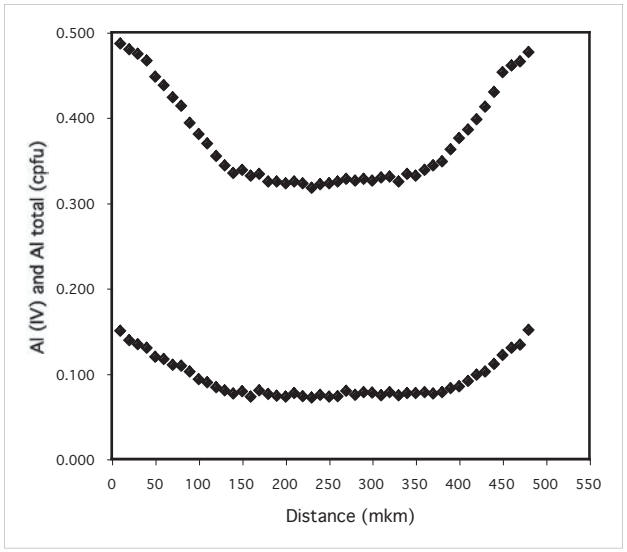
1904-1 Cpx II, profile 144

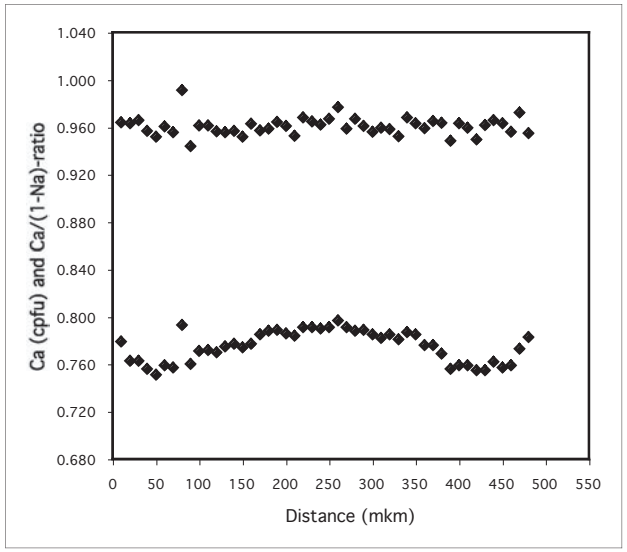
	5	10	15	20	25	30	35	40	45	50	55	60	65	70	75	80	85	90	95	100
SiO2	52.08	51.85	51.73	52.57	52.44	52.94	52.80	52.74	52.85	52.76	53.03	52.70	52.64	52.47	52.59	52.98	53.05	52.74	52.86	52.96
TiO2	0.10	0.07	0.07	0.08	0.05	0.05	0.07	0.06	0.08	0.04	0.07	0.08	0.06	0.05	0.06	0.04	0.07	0.06	0.05	0.04
Al2O3	10.50	11.51	11.70	11.39	11.23	10.96	10.93	10.77	10.85	10.73	10.88	10.88	10.65	10.76	10.66	10.42	10.77	10.82	10.90	11.05
Cr2O3	0.27	0.20	0.19	0.15	0.15	0.17	0.10	0.08	0.09	0.05	0.10	0.05	0.08	0.06	0.05	0.04	0.04	0.02	0.00	0.05
FeO	2.46	2.45	2.35	2.41	2.30	2.41	2.47	2.43	2.43	2.40	2.37	2.34	2.27	2.47	2.40	2.35	2.24	2.51	2.19	2.38
MnO	0.02	0.00	0.01	0.00	0.00	0.01	0.00	0.02	0.07	0.05	0.02	0.03	0.03	0.00	0.00	0.02	0.00	0.02	0.05	0.00
NiO	0.11	0.12	0.17	0.13	0.12	0.11	0.10	0.06	0.13	0.10	0.16	0.12	0.14	0.07	0.13	0.13	0.10	0.01	0.08	0.10
MgO	12.10	11.64	11.52	11.71	11.62	11.67	11.72	11.80	11.77	11.88	11.77	11.78	11.80	11.78	11.97	11.84	11.73	11.74	11.74	11.72
CaO	20.56	20.40	20.40	20.11	20.07	20.00	20.06	19.99	20.09	20.10	20.25	20.13	20.02	20.16	20.08	19.94	20.07	20.10	20.23	20.20
Na2O	2.75	2.78	2.88	3.04	3.16	3.11	3.04	3.12	3.03	3.04	3.23	3.15	3.07	2.91	3.07	3.09	2.97	3.00	3.07	2.94
K2O	0.00	0.01	0.01	0.00	0.00	0.00	0.00	0.00	0.01	0.00	0.01	0.01	0.00	0.00	0.00	0.00	0.01	0.00	0.00	0.00
Total	100.95	101.02	101.02	101.60	101.15	101.44	101.30	101.06	101.39	101.15	101.89	101.27	100.75	100.73	101.02	100.86	101.07	101.01	101.17	101.45
Si	1.859	1.847	1.843	1.859	1.863	1.874	1.872	1.875	1.873	1.874	1.871	1.870	1.876	1.872	1.871	1.886	1.882	1.875	1.875	1.873
Ti	0.003	0.002	0.002	0.002	0.001	0.001	0.002	0.002	0.002	0.001	0.002	0.002	0.002	0.001	0.002	0.001	0.002	0.001	0.001	0.001
Al	0.442	0.483	0.491	0.475	0.470	0.457	0.457	0.451	0.453	0.449	0.452	0.455	0.447	0.452	0.447	0.437	0.450	0.453	0.456	0.461
Cr	0.008	0.006	0.005	0.004	0.004	0.005	0.003	0.002	0.003	0.001	0.003	0.001	0.002	0.002	0.001	0.001	0.001	0.001	0.000	0.001
Fe2+	0.073	0.073	0.070	0.071	0.068	0.071	0.073	0.072	0.072	0.071	0.070	0.070	0.068	0.074	0.071	0.070	0.067	0.075	0.065	0.070
Mn	0.001	0.000	0.000	0.000	0.000	0.000	0.000	0.000	0.002	0.002	0.001	0.001	0.001	0.000	0.000	0.001	0.000	0.001	0.001	0.000
Ni	0.003	0.003	0.005	0.004	0.003	0.003	0.003	0.002	0.004	0.003	0.005	0.003	0.004	0.002	0.004	0.004	0.003	0.000	0.002	0.003
Mg	0.644	0.618	0.612	0.617	0.615	0.616	0.619	0.625	0.622	0.629	0.619	0.623	0.627	0.626	0.635	0.628	0.620	0.622	0.621	0.618
Ca	0.786	0.779	0.779	0.762	0.764	0.759	0.762	0.761	0.763	0.765	0.766	0.766	0.765	0.770	0.766	0.760	0.763	0.766	0.769	0.766
Na	0.190	0.192	0.199	0.208	0.218	0.214	0.209	0.215	0.208	0.209	0.221	0.217	0.212	0.201	0.212	0.213	0.205	0.207	0.211	0.201
K	0.000	0.000	0.000	0.000	0.000	0.000	0.000	0.000	0.000	0.000	0.000	0.000	0.000	0.000	0.000	0.000	0.000	0.000	0.000	0.000
Sum	4.009	4.003	4.006	4.003	4.007	4.000	4.001	4.005	4.001	4.004	4.010	4.008	4.003	4.000	4.009	4.001	3.993	4.000	4.001	3.995
Mg#	89.82	89.44	89.74	89.68	90.04	89.67	89.45	89.67	89.63	89.86	89.84	89.90	90.22	89.43	89.94	89.97	90.25	89.24	90.52	89.83
Al IV	0.133	0.151	0.151	0.138	0.129	0.125	0.128	0.121	0.126	0.122	0.119	0.122	0.121	0.128	0.120	0.114	0.125	0.125	0.124	0.132
Al VI	0.309	0.333	0.341	0.338	0.341	0.332	0.330	0.330	0.327	0.328	0.333	0.334	0.327	0.325	0.327	0.324	0.325	0.329	0.333	0.330

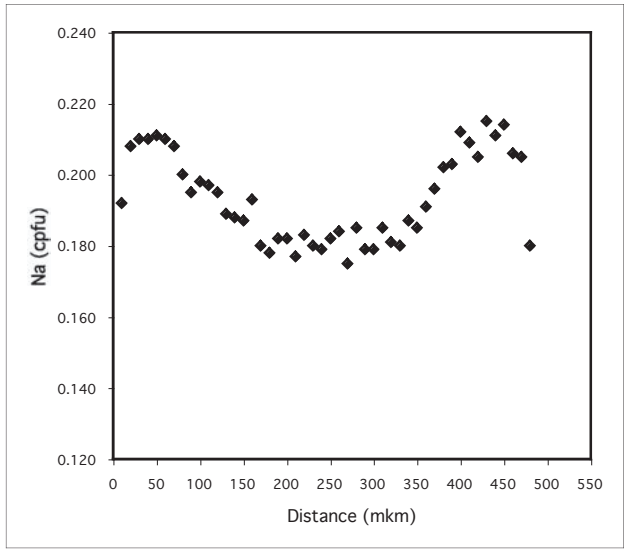
1904-1 Cpx II, profile 144

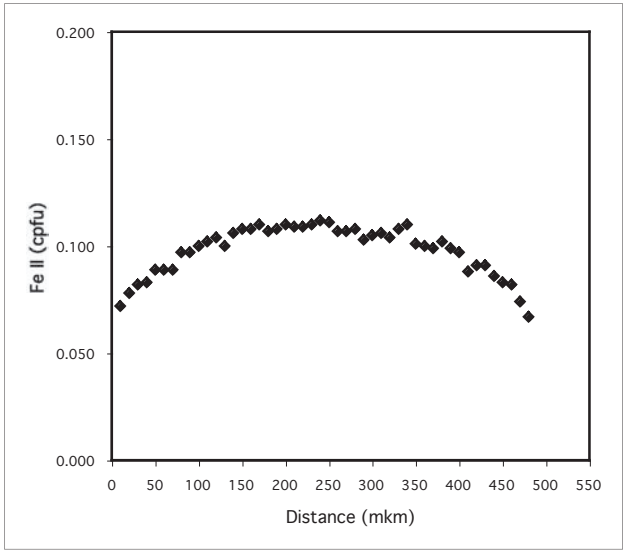
	105	110	115	120	125	130	135	140	145	150
SiO2	52.38	52.16	52.11	52.07	51.85	52.26	52.28	51.97	52.03	52.12
TiO2	0.07	0.07	0.07	0.07	0.03	0.09	0.06	0.12	0.07	0.09
Al2O3	11.12	11.15	11.06	11.24	11.19	10.38	11.61	11.42	11.26	10.38
Cr2O3	0.00	0.03	0.04	0.01	0.00	0.01	0.03	0.05	0.03	0.02
FeO	2.41	2.45	2.33	2.33	2.44	2.62	2.17	2.31	2.22	2.61
MnO	0.05	0.00	0.01	0.00	0.02	0.00	0.03	0.00	0.01	0.06
NiO	0.17	0.09	0.10	0.11	0.15	0.11	0.09	0.16	0.13	0.12
MgO	11.78	11.74	11.71	11.76	11.86	12.42	11.55	11.67	11.78	12.30
CaO	20.26	20.24	20.50	20.56	20.49	21.32	20.00	20.47	20.52	20.73
Na2O	2.97	2.99	3.06	2.94	2.86	2.10	2.70	2.70	2.62	2.40
K2O	0.01	0.01	0.00	0.01	0.00	0.00	0.03	0.00	0.00	0.01
Total	101.22	100.93	101.01	101.09	100.89	101.29	100.57	100.87	100.66	100.85
Si	1.861	1.859	1.857	1.853	1.850		1.863	1.852	1.857	1.862
Ti	0.002	0.002	0.002	0.002	0.001		0.002	0.003	0.002	0.002
Al	0.465	0.468	0.465	0.471	0.471		0.488	0.480	0.473	0.437
Cr	0.000	0.001	0.001	0.000	0.000		0.001	0.001	0.001	0.001
Fe2+	0.072	0.073	0.069	0.069	0.073		0.065	0.069	0.066	0.078
Mn	0.001	0.000	0.000	0.000	0.000		0.001	0.000	0.000	0.002
Ni	0.005	0.002	0.003	0.003	0.004		0.003	0.004	0.004	0.003
Mg	0.624	0.624	0.622	0.624	0.631		0.613	0.620	0.627	0.655
Ca	0.771	0.773	0.783	0.784	0.784		0.764	0.782	0.785	0.794
Na	0.205	0.207	0.212	0.203	0.198		0.186	0.186	0.181	0.166
K	0.000	0.000	0.000	0.000	0.000		0.001	0.000	0.000	0.001
Sum	4.007	4.008	4.014	4.010	4.012		3.986	3.998	3.995	4.000
Mg#	89.66	89.53	90.01	90.04	89.63		90.41	89.99	90.48	89.36
Al IV	0.132	0.133	0.129	0.136	0.138		0.153	0.151	0.149	0.138
Al VI	0.333	0.335	0.336	0.335	0.334		0.335	0.330	0.325	0.300

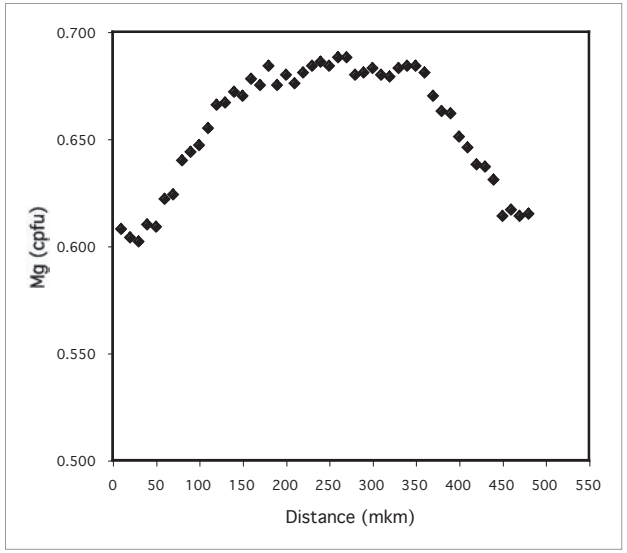
1904-1 Cpx II, profile 144

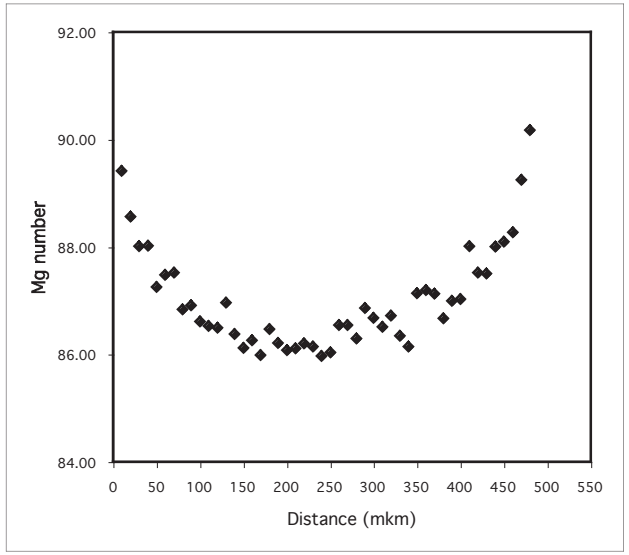












1904-1 Cpx II, profile 465

	10	20	30	40	50	60	70	80	90	100	110	120	130	140	150	160	170	180	190	200
SiO2	52.41	52.67	52.83	52.78	53.42	52.91	53.23	51.61	53.52	53.56	53.49	53.75	54.13	54.08	54.08	53.81	53.72	53.67	54.04	53.93
TiO2	0.09	0.09	0.05	0.06	0.05	0.10	0.08	0.08	0.10	0.09	0.10	0.10	0.10	0.08	0.11	0.10	0.11	0.09	0.11	0.08
Al2O3	11.70	11.54	11.42	11.18	10.79	10.47	10.14	9.70	9.41	9.10	8.84	8.47	8.25	8.01	8.11	7.91	7.95	7.71	7.76	7.70
Cr2O3	0.04	0.06	0.06	0.01	0.00	0.00	0.02	0.02	0.00	0.01	0.05	0.06	0.02	0.06	0.05	0.05	0.05	0.05	0.00	0.05
FeO	2.43	2.63	2.78	2.79	3.01	3.00	2.99	3.20	3.25	3.37	3.44	3.50	3.36	3.56	3.65	3.63	3.70	3.58	3.62	3.69
MnO	0.04	0.05	0.00	0.03	0.02	0.04	0.07	0.04	0.07	0.05	0.04	0.03	0.00	0.04	0.01	0.00	0.02	0.04	0.00	0.04
NiO	0.09	0.09	0.10	0.06	0.07	0.10	0.14	0.13	0.11	0.11	0.14	0.09	0.15	0.10	0.11	0.11	0.11	0.08	0.10	0.12
MgO	11.54	11.48	11.45	11.55	11.59	11.75	11.79	11.86	12.16	12.22	12.36	12.58	12.62	12.70	12.67	12.77	12.72	12.85	12.75	12.82
CaO	20.58	20.17	20.19	19.93	19.87	19.96	19.90	20.44	19.98	20.27	20.26	20.25	20.42	20.43	20.39	20.36	20.57	20.59	20.71	20.63
Na2O	2.81	3.03	3.07	3.05	3.08	3.06	3.02	2.85	2.84	2.88	2.86	2.84	2.75	2.74	2.72	2.80	2.61	2.58	2.64	2.64
K2O	0.00	0.01	0.00	0.01	0.00	0.01	0.01	0.02	0.00	0.00	0.01	0.01	0.01	0.01	0.00	0.00	0.00	0.01	0.02	0.01
Total	101.75	101.82	101.95	101.46	101.90	101.39	101.40	99.94	101.45	101.66	101.59	101.68	101.80	101.80	101.91	101.56	101.55	101.24	101.73	101.71
Si	1.852	1.860	1.864	1.870	1.884	1.879	1.889	1.869	1.900	1.901	1.902	1.909	1.918	1.919	1.917	1.916	1.914	1.917	1.921	1.919
Ti	0.002	0.002	0.001	0.002	0.001	0.003	0.002	0.002	0.003	0.002	0.003	0.003	0.003	0.002	0.003	0.003	0.003	0.002	0.003	0.002
Al	0.487	0.480	0.475	0.467	0.448	0.438	0.424	0.414	0.394	0.381	0.370	0.355	0.344	0.335	0.339	0.332	0.334	0.325	0.325	0.323
Cr	0.001	0.002	0.002	0.000	0.000	0.000	0.001	0.001	0.000	0.000	0.001	0.002	0.000	0.002	0.001	0.001	0.001	0.001	0.000	0.001
Fe2+	0.072	0.078	0.082	0.083	0.089	0.089	0.089	0.097	0.097	0.100	0.102	0.104	0.100	0.106	0.108	0.108	0.110	0.107	0.108	0.110
Mn	0.001	0.001	0.000	0.001	0.001	0.001	0.002	0.001	0.002	0.001	0.001	0.001	0.000	0.001	0.000	0.000	0.001	0.001	0.000	0.001
Ni	0.003	0.003	0.003	0.002	0.002	0.003	0.004	0.004	0.003	0.003	0.004	0.003	0.004	0.003	0.003	0.003	0.003	0.002	0.003	0.003
Mg	0.608	0.604	0.602	0.610	0.609	0.622	0.624	0.640	0.644	0.647	0.655	0.666	0.667	0.672	0.670	0.678	0.675	0.684	0.675	0.680
Ca	0.779	0.763	0.763	0.756	0.751	0.759	0.757	0.793	0.760	0.771	0.772	0.770	0.775	0.777	0.774	0.777	0.785	0.788	0.789	0.786
Na	0.192	0.208	0.210	0.210	0.211	0.210	0.208	0.200	0.195	0.198	0.197	0.195	0.189	0.188	0.187	0.193	0.180	0.178	0.182	0.182
K	0.000	0.000	0.000	0.001	0.000	0.000	0.000	0.001	0.000	0.000	0.000	0.000	0.000	0.000	0.000	0.000	0.000	0.000	0.001	0.000
Sum	3.998	4.001	4.001	4.000	3.996	4.005	4.000	4.022	3.998	4.005	4.009	4.008	4.001	4.005	4.003	4.011	4.006	4.007	4.005	4.008
Mg#	89.41	88.56	88.01	88.02	87.25	87.48	87.52	86.84	86.91	86.61	86.53	86.49	86.96	86.38	86.12	86.26	85.99	86.47	86.21	86.08
Al IV	0.150	0.139	0.135	0.130	0.120	0.117	0.111	0.109	0.103	0.094	0.090	0.084	0.081	0.077	0.080	0.073	0.081	0.076	0.074	0.073
Al VI	0.337	0.341	0.341	0.337	0.329	0.321	0.314	0.305	0.292	0.288	0.280	0.271	0.264	0.259	0.260	0.259	0.254	0.249	0.251	0.250

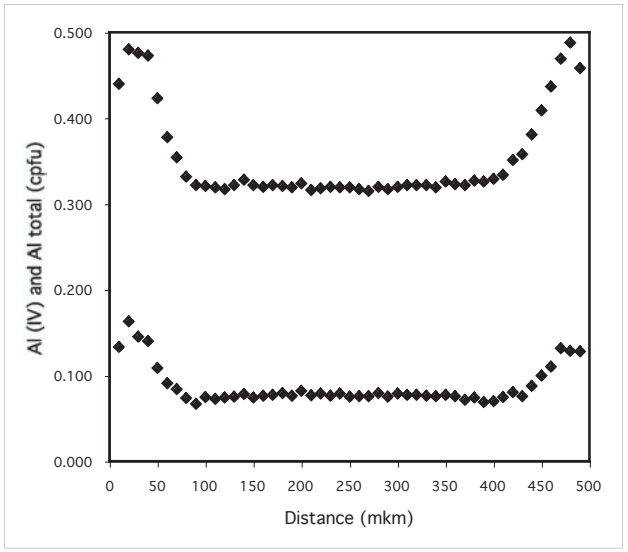
1904-1 Cpx II, profile 465

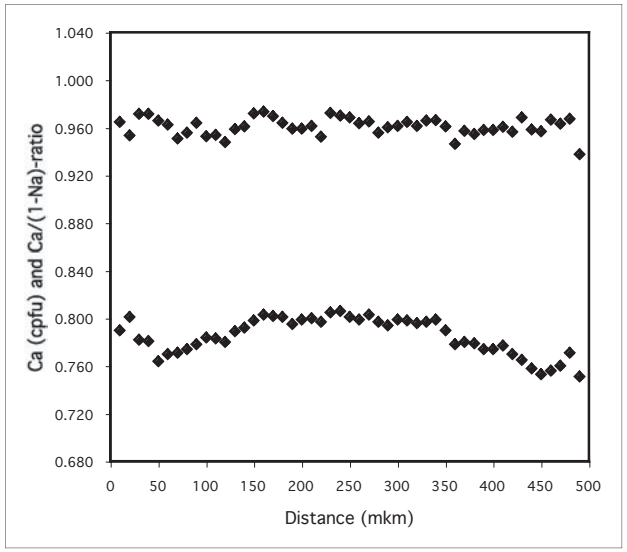
	210	220	230	240	250	260	270	280	290	300	310	320	330	340	350	360	370	380	390	400
SiO2	53.93	53.97	53.75	53.62	53.55	53.28	53.52	53.68	53.90	54.00	53.78	53.74	54.00	53.23	53.57	53.76	53.89	53.90	54.05	53.78
TiO2	0.10	0.13	0.11	0.12	0.09	0.13	0.11	0.10	0.10	0.12	0.09	0.11	0.09	0.11	0.10	0.11	0.09	0.10	0.12	0.13
Al2O3	7.73	7.71	7.56	7.67	7.68	7.71	7.79	7.76	7.83	7.79	7.84	7.86	7.75	7.93	7.88	8.08	8.20	8.34	8.70	8.99
Cr2O3	0.03	0.04	0.01	0.03	0.05	0.02	0.05	0.09	0.03	0.06	0.00	0.05	0.04	0.03	0.03	0.06	0.05	0.11	0.01	0.00
FeO	3.67	3.67	3.68	3.77	3.73	3.59	3.59	3.61	3.45	3.54	3.56	3.50	3.64	3.67	3.38	3.36	3.32	3.43	3.33	3.27
MnO	0.00	0.04	0.04	0.05	0.02	0.02	0.07	0.01	0.04	0.03	0.02	0.00	0.02	0.05	0.00	0.00	0.01	0.07	0.00	0.05
NiO	0.09	0.13	0.14	0.15	0.15	0.18	0.17	0.10	0.10	0.14	0.13	0.08	0.13	0.13	0.10	0.12	0.11	0.18	0.14	0.13
MgO	12.71	12.87	12.85	12.89	12.85	12.90	12.94	12.80	12.84	12.90	12.78	12.77	12.89	12.82	12.83	12.83	12.65	12.54	12.54	12.33
CaO	20.53	20.79	20.67	20.66	20.67	20.78	20.69	20.61	20.70	20.63	20.45	20.53	20.50	20.51	20.51	20.36	20.39	20.22	19.95	20.01
Na2O	2.56	2.66	2.60	2.59	2.62	2.66	2.53	2.67	2.60	2.60	2.68	2.62	2.61	2.69	2.67	2.77	2.84	2.93	2.96	3.09
K2O	0.03	0.00	0.00	0.00	0.00	0.01	0.01	0.00	0.00	0.00	0.01	0.00	0.01	0.00	0.01	0.00	0.00	0.01	0.01	0.00
Total	101.36	102.00	101.41	101.53	101.43	101.25	101.46	101.44	101.60	101.82	101.33	101.27	101.69	101.17	101.09	101.44	101.56	101.83	101.80	101.77
Si	1.923	1.916	1.919	1.913	1.913	1.907	1.910	1.915	1.917	1.917	1.918	1.917	1.920	1.906	1.915	1.914	1.915	1.912	1.913	1.905
Ti	0.003	0.003	0.003	0.003	0.002	0.003	0.003	0.003	0.003	0.003	0.002	0.003	0.002	0.003	0.003	0.003	0.002	0.003	0.003	0.003
Al	0.325	0.323	0.318	0.322	0.323	0.325	0.328	0.326	0.328	0.326	0.330	0.331	0.325	0.334	0.332	0.339	0.344	0.349	0.363	0.376
Cr	0.001	0.001	0.000	0.001	0.001	0.000	0.001	0.003	0.001	0.002	0.000	0.001	0.001	0.001	0.001	0.002	0.001	0.003	0.000	0.000
Fe2+	0.109	0.109	0.110	0.112	0.111	0.107	0.107	0.108	0.103	0.105	0.106	0.104	0.108	0.110	0.101	0.100	0.099	0.102	0.099	0.097
Mn	0.000	0.001	0.001	0.002	0.001	0.001	0.002	0.000	0.001	0.001	0.001	0.000	0.000	0.002	0.000	0.000	0.000	0.002	0.000	0.001
Ni	0.003	0.004	0.004	0.004	0.004	0.005	0.005	0.003	0.003	0.004	0.004	0.002	0.004	0.004	0.003	0.003	0.003	0.005	0.004	0.004
Mg	0.676	0.681	0.684	0.686	0.684	0.688	0.688	0.680	0.681	0.683	0.680	0.679	0.683	0.684	0.684	0.681	0.670	0.663	0.662	0.651
Ca	0.784	0.791	0.791	0.790	0.791	0.797	0.791	0.788	0.789	0.785	0.782	0.785	0.781	0.787	0.785	0.776	0.776	0.769	0.756	0.759
Na	0.177	0.183	0.180	0.179	0.182	0.184	0.175	0.185	0.179	0.179	0.185	0.181	0.180	0.187	0.185	0.191	0.196	0.202	0.203	0.212
K	0.001	0.000	0.000	0.000	0.000	0.000	0.000	0.000	0.000	0.000	0.000	0.000	0.001	0.000	0.000	0.000	0.000	0.000	0.000	0.000
Sum	4.001	4.011	4.009	4.012	4.013	4.019	4.010	4.010	4.005	4.005	4.007	4.004	4.005	4.017	4.009	4.009	4.007	4.010	4.004	4.010
Mg#	86.11	86.20	86.15	85.96	86.04	86.54	86.54	86.29	86.86	86.68	86.51	86.72	86.35	86.15	87.13	87.20	87.13	86.67	86.99	87.03
Al IV	0.077	0.074	0.072	0.075	0.073	0.074	0.080	0.075	0.078	0.078	0.075	0.079	0.075	0.077	0.077	0.078	0.077	0.078	0.083	0.085
Al VI	0.248	0.250	0.246	0.247	0.250	0.252	0.248	0.251	0.250	0.249	0.256	0.253	0.251	0.257	0.255	0.261	0.268	0.271	0.280	0.291

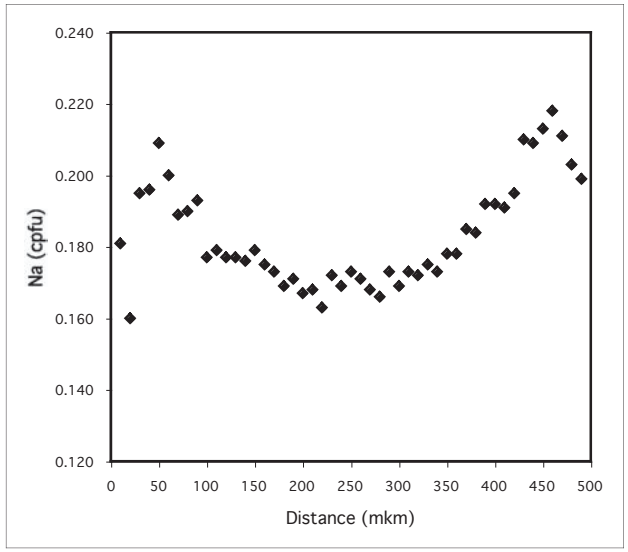
1904-1 Cpx II, profile 465

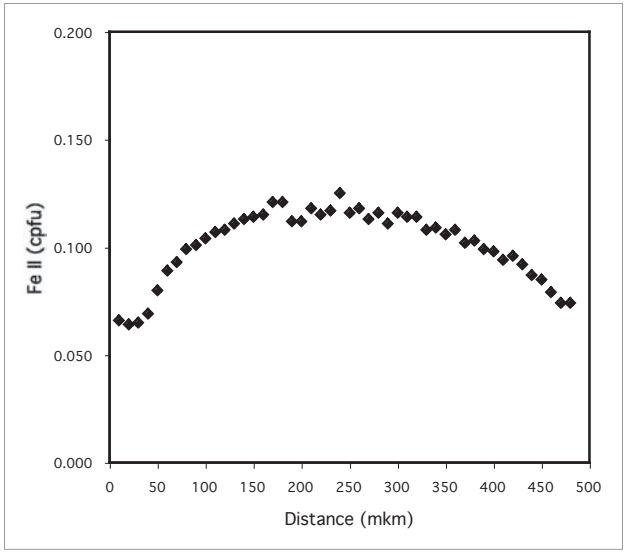
	410	420	430	440	450	460	470	480
SiO2	53.73	53.53	53.32	52.86	53.06	52.83	52.57	52.13
TiO2	0.10	0.06	0.10	0.06	0.09	0.08	0.10	0.12
Al2O3	9.23	9.49	9.90	10.24	10.88	11.06	11.17	11.37
Cr2O3	0.04	0.05	0.04	0.00	0.05	0.08	0.03	0.04
FeO	2.97	3.05	3.06	2.90	2.80	2.76	2.51	2.24
MnO	0.04	0.04	0.05	0.00	0.02	0.04	0.03	0.05
NiO	0.11	0.11	0.09	0.13	0.17	0.11	0.10	0.13
MgO	12.22	12.03	12.05	11.90	11.66	11.70	11.63	11.59
CaO	19.96	19.80	19.89	19.97	20.00	20.02	20.34	20.52
Na2O	3.03	2.98	3.13	3.05	3.13	3.00	2.98	2.61
K2O	0.02	0.00	0.01	0.00	0.01	0.01	0.00	0.01
Total	101.46	101.15	101.64	101.11	101.86	101.71	101.43	100.80
Si	1.906	1.904	1.889	1.882	1.874	1.868	1.863	1.857
Ti	0.003	0.002	0.003	0.002	0.002	0.002	0.003	0.003
Al	0.386	0.398	0.413	0.430	0.453	0.461	0.466	0.477
Cr	0.001	0.001	0.001	0.000	0.001	0.002	0.001	0.001
Fe2+	0.088	0.091	0.091	0.086	0.083	0.082	0.074	0.067
Mn	0.001	0.001	0.002	0.000	0.000	0.001	0.001	0.001
Ni	0.003	0.003	0.002	0.004	0.005	0.003	0.003	0.004
Mg	0.646	0.638	0.637	0.631	0.614	0.617	0.614	0.615
Ca	0.759	0.755	0.755	0.762	0.757	0.759	0.773	0.783
Na	0.209	0.205	0.215	0.211	0.214	0.206	0.205	0.180
K	0.001	0.000	0.000	0.000	0.000	0.001	0.000	0.001
Sum	4.003	3.998	4.008	4.007	4.004	4.001	4.003	3.991
Mg#	88.01	87.52	87.50	88.01	88.09	88.27	89.24	90.18
Al IV	0.092	0.099	0.103	0.112	0.122	0.130	0.134	0.152
Al VI	0.295	0.299	0.311	0.319	0.331	0.331	0.332	0.326

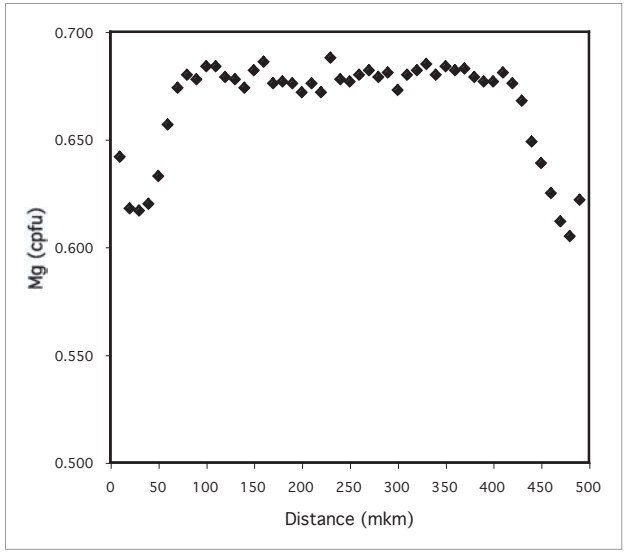
1904-1 Cpx II, profile 465

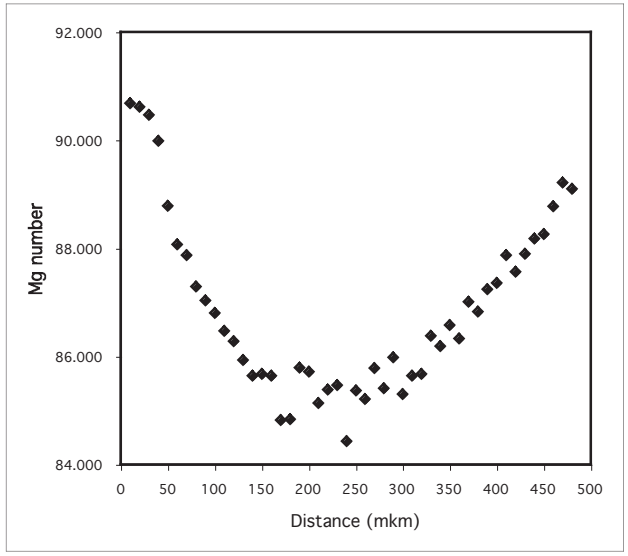












1904-1 Cpx II, profile 476

	10	20	30	40	50	60	70	80	90	100	110	120	130	140	150	160	170	180	190	200
SiO2	52.53	51.40	52.29	52.22	53.14	53.40	53.60	53.88	54.22	53.86	53.78	54.03	53.68	53.71	53.39	53.26	53.39	53.47	53.86	53.57
TiO2	0.14	0.09	0.14	0.06	0.05	0.07	0.06	0.07	0.08	0.11	0.09	0.10	0.08	0.08	0.09	0.10	0.09	0.10	0.09	0.11
Al2O3	10.50	11.30	11.39	11.29	10.09	9.00	8.39	7.91	7.69	7.64	7.58	7.53	7.65	7.82	7.65	7.57	7.63	7.62	7.58	7.69
Cr2O3	0.01	0.02	0.02	0.00	0.03	0.04	0.03	0.03	0.04	0.01	0.05	0.08	0.02	0.09	0.04	0.06	0.06	0.03	0.05	0.07
FeO	2.23	2.14	2.20	2.33	2.68	2.97	3.12	3.33	3.39	3.47	3.59	3.63	3.71	3.79	3.81	3.83	4.03	4.06	3.76	3.76
MnO	0.00	0.00	0.03	0.03	0.00	0.00	0.00	0.06	0.06	0.05	0.03	0.06	0.03	0.05	0.09	0.02	0.07	0.08	0.02	0.04
NiO	0.11	0.09	0.15	0.13	0.16	0.08	0.04	0.07	0.14	0.12	0.14	0.12	0.12	0.10	0.12	0.10	0.08	0.12	0.15	0.17
MgO	12.10	11.49	11.67	11.69	11.94	12.36	12.64	12.79	12.80	12.86	12.84	12.77	12.71	12.69	12.78	12.85	12.68	12.71	12.71	12.61
CaO	20.71	20.72	20.57	20.49	20.07	20.16	20.13	20.26	20.44	20.51	20.44	20.42	20.59	20.75	20.81	20.93	20.93	20.93	20.82	20.87
Na2O	2.62	2.28	2.84	2.85	3.03	2.90	2.73	2.74	2.80	2.55	2.58	2.57	2.55	2.55	2.58	2.52	2.49	2.43	2.47	2.41
K2O	0.02	0.02	0.00	0.02	0.00	0.01	0.00	0.00	0.00	0.01	0.01	0.00	0.00	0.02	0.01	0.00	0.00	0.00	0.00	0.01
Total	100.97	99.56	101.30	101.09	101.18	101.02	100.74	101.15	101.67	101.19	101.12	101.31	101.13	101.65	101.36	101.23	101.46	101.57	101.51	101.31
Si	1.870	1.854	1.855	1.857	1.889	1.904	1.916	1.922	1.926	1.923	1.923	1.927	1.920	1.914	1.910	1.909	1.910	1.911	1.921	1.916
Ti	0.004	0.003	0.004	0.002	0.001	0.002	0.001	0.002	0.002	0.003	0.002	0.003	0.002	0.002	0.002	0.003	0.002	0.003	0.002	0.003
Al	0.440	0.480	0.476	0.473	0.423	0.378	0.354	0.332	0.322	0.321	0.319	0.317	0.322	0.328	0.322	0.320	0.322	0.321	0.319	0.324
Cr	0.000	0.001	0.001	0.000	0.001	0.001	0.001	0.001	0.001	0.000	0.001	0.002	0.001	0.002	0.001	0.002	0.002	0.001	0.001	0.002
Fe2+	0.066	0.064	0.065	0.069	0.080	0.089	0.093	0.099	0.101	0.104	0.107	0.108	0.111	0.113	0.114	0.115	0.121	0.121	0.112	0.112
Mn	0.000	0.000	0.001	0.001	0.000	0.000	0.000	0.002	0.002	0.002	0.001	0.002	0.001	0.001	0.003	0.001	0.002	0.003	0.000	0.001
Ni	0.003	0.003	0.004	0.004	0.004	0.002	0.001	0.002	0.004	0.003	0.004	0.003	0.003	0.003	0.003	0.003	0.002	0.003	0.004	0.005
Mg	0.642	0.618	0.617	0.620	0.633	0.657	0.674	0.680	0.678	0.684	0.684	0.679	0.678	0.674	0.682	0.686	0.676	0.677	0.676	0.672
Ca	0.790	0.801	0.782	0.781	0.764	0.770	0.771	0.774	0.778	0.784	0.783	0.780	0.789	0.792	0.798	0.803	0.802	0.801	0.795	0.799
Na	0.181	0.160	0.195	0.196	0.209	0.200	0.189	0.190	0.193	0.177	0.179	0.177	0.177	0.176	0.179	0.175	0.173	0.169	0.171	0.167
K	0.001	0.001	0.000	0.001	0.000	0.001	0.000	0.000	0.000	0.001	0.000	0.000	0.000	0.001	0.000	0.000	0.000	0.000	0.000	0.001
Sum	3.997	3.983	4.000	4.003	4.003	4.005	4.000	4.004	4.007	4.002	4.004	3.999	4.005	4.007	4.015	4.015	4.012	4.010	4.002	4.002
Mg#	90.678	90.616	90.469	89.985	88.780	88.070	87.875	87.291	87.035	86.802	86.473	86.277	85.932	85.642	85.678	85.643	84.818	84.837	85.787	85.714
Al IV	0.133	0.163	0.145	0.140	0.109	0.091	0.084	0.074	0.067	0.075	0.073	0.074	0.075	0.079	0.074	0.077	0.078	0.080	0.077	0.082
Al VI	0.307	0.317	0.331	0.333	0.315	0.287	0.270	0.259	0.255	0.247	0.247	0.243	0.247	0.250	0.248	0.244	0.245	0.242	0.243	0.242

1904-1 Cpx II, profile 476

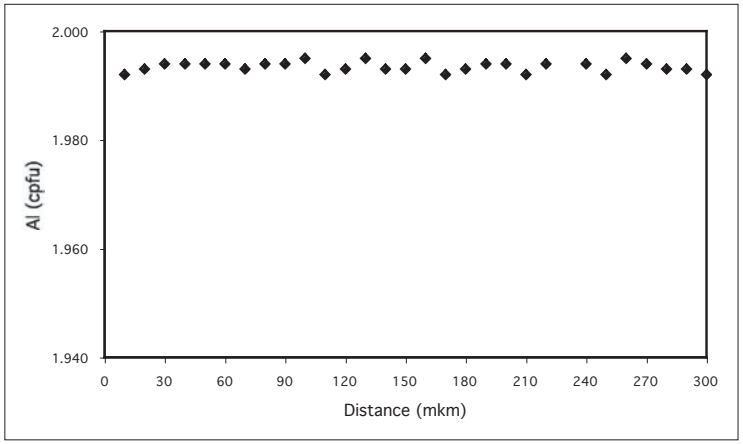
	210	220	230	240	250	260	270	280	290	300	310	320	330	340	350	360	370	380	390	400
SiO2	53.56	53.56	53.17	53.43	53.53	53.54	53.53	53.37	53.62	53.67	53.35	53.45	53.40	53.73	53.40	53.67	53.80	53.95	54.13	54.04
TiO2	0.08	0.06	0.09	0.11	0.08	0.10	0.08	0.06	0.06	0.11	0.12	0.06	0.08	0.08	0.12	0.09	0.08	0.08	0.07	0.05
Al2O3	7.49	7.50	7.58	7.59	7.55	7.51	7.47	7.57	7.50	7.61	7.61	7.64	7.63	7.60	7.70	7.65	7.65	7.79	7.75	7.82
Cr2O3	0.10	0.00	0.03	0.07	0.00	0.00	0.05	0.06	0.06	0.05	0.00	0.04	0.08	0.07	0.03	0.06	0.07	0.03	0.00	0.05
FeO	3.94	3.83	3.90	4.18	3.89	3.93	3.79	3.86	3.71	3.89	3.80	3.80	3.61	3.67	3.53	3.62	3.43	3.47	3.33	3.30
MnO	0.05	0.00	0.03	0.06	0.03	0.03	0.04	0.05	0.02	0.05	0.02	0.06	0.05	0.03	0.01	0.01	0.03	0.03	0.00	0.05
NiO	0.11	0.10	0.13	0.08	0.12	0.12	0.10	0.11	0.12	0.08	0.09	0.13	0.08	0.12	0.11	0.16	0.10	0.13	0.16	0.10
MgO	12.67	12.54	12.87	12.75	12.69	12.75	12.78	12.68	12.75	12.65	12.70	12.78	12.81	12.79	12.80	12.76	12.81	12.78	12.74	12.75
CaO	20.87	20.70	20.94	21.07	20.87	20.84	20.94	20.72	20.67	20.89	20.76	20.73	20.75	20.89	20.55	20.27	20.36	20.41	20.26	20.27
Na2O	2.42	2.35	2.47	2.45	2.49	2.46	2.43	2.38	2.50	2.44	2.48	2.48	2.51	2.50	2.55	2.57	2.67	2.66	2.77	2.77
K2O	0.01	0.01	0.00	0.00	0.01	0.00	0.00	0.02	0.01	0.01	0.00	0.00	0.00	0.01	0.00	0.00	0.00	0.00	0.01	0.00
Total	101.30	100.66	101.21	101.79	101.24	101.27	101.22	100.87	101.02	101.46	100.94	101.17	101.00	101.48	100.81	100.85	100.99	101.33	101.22	101.19
Si	1.917	1.925	1.907	1.907	1.916	1.916	1.917	1.917	1.921	1.917	1.915	1.914	1.914	1.917	1.916	1.923	1.924	1.923	1.929	1.926
Ti	0.002	0.002	0.002	0.003	0.002	0.003	0.002	0.002	0.002	0.003	0.003	0.002	0.002	0.002	0.003	0.002	0.002	0.002	0.002	0.001
Al	0.316	0.318	0.320	0.319	0.319	0.317	0.315	0.320	0.317	0.320	0.322	0.322	0.322	0.319	0.326	0.323	0.322	0.327	0.326	0.329
Cr	0.003	0.000	0.001	0.002	0.000	0.000	0.001	0.002	0.002	0.001	0.000	0.001	0.002	0.002	0.001	0.002	0.002	0.001	0.000	0.001
Fe2+	0.118	0.115	0.117	0.125	0.116	0.118	0.113	0.116	0.111	0.116	0.114	0.114	0.108	0.109	0.106	0.108	0.102	0.103	0.099	0.098
Mn	0.001	0.000	0.001	0.002	0.001	0.001	0.001	0.002	0.001	0.002	0.001	0.002	0.001	0.001	0.000	0.000	0.001	0.001	0.000	0.001
Ni	0.003	0.003	0.004	0.002	0.003	0.003	0.003	0.003	0.003	0.002	0.003	0.004	0.002	0.003	0.003	0.005	0.003	0.004	0.004	0.003
Mg	0.676	0.672	0.688	0.678	0.677	0.680	0.682	0.679	0.681	0.673	0.680	0.682	0.685	0.680	0.684	0.682	0.683	0.679	0.677	0.677
Ca	0.800	0.797	0.805	0.806	0.801	0.799	0.803	0.797	0.794	0.799	0.798	0.796	0.797	0.799	0.790	0.778	0.780	0.779	0.774	0.774
Na	0.168	0.163	0.172	0.169	0.173	0.171	0.168	0.166	0.173	0.169	0.173	0.172	0.175	0.173	0.178	0.178	0.185	0.184	0.192	0.192
K	0.001	0.001	0.000	0.000	0.000	0.000	0.000	0.001	0.000	0.000	0.000	0.000	0.000	0.001	0.000	0.000	0.000	0.000	0.000	0.000
Sum	4.006	3.996	4.016	4.014	4.009	4.008	4.007	4.004	4.005	4.004	4.008	4.008	4.009	4.007	4.007	4.001	4.004	4.003	4.003	4.003
Mg#	85.139	85.388	85.466	84.433	85.372	85.213	85.786	85.409	85.985	85.298	85.642	85.678	86.381	86.185	86.582	86.329	87.006	86.829	87.242	87.355
Al IV	0.077	0.079	0.077	0.079	0.075	0.076	0.076	0.080	0.075	0.079	0.078	0.078	0.077	0.076	0.078	0.076	0.072	0.074	0.069	0.070
Al VI	0.239	0.239	0.244	0.240	0.244	0.241	0.239	0.241	0.242	0.241	0.245	0.245	0.246	0.244	0.249	0.248	0.251	0.253	0.257	0.259

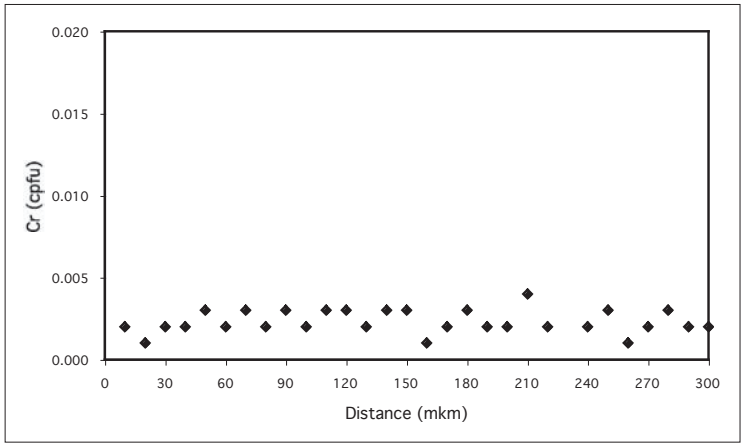
II

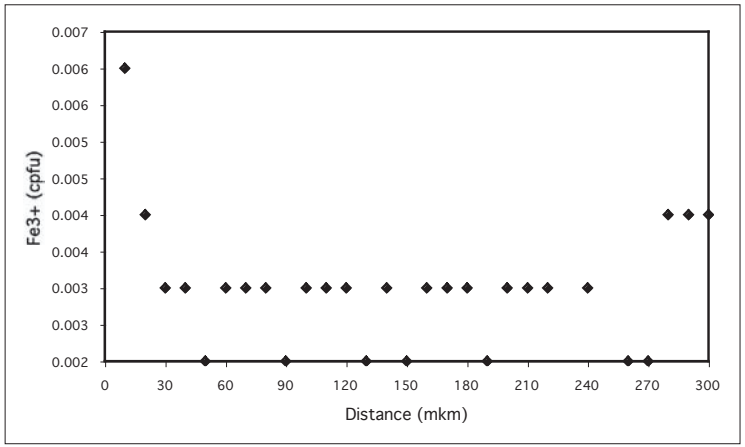
1904-1 Cpx II, profile 476

	410	420	430	440	450	460	470	480	490
SiO2	53.87	53.43	53.57	53.56	53.40	53.02	52.38	51.87	51.70
TiO2	0.07	0.08	0.08	0.05	0.07	0.05	0.07	0.08	0.09
Al2O3	7.95	8.32	8.52	9.06	9.75	10.45	11.17	11.64	10.87
Cr2O3	0.06	0.05	0.03	0.09	0.00	0.00	0.03	0.05	0.02
FeO	3.17	3.21	3.08	2.93	2.86	2.65	2.48	2.49	4.27
MnO	0.07	0.04	0.06	0.03	0.02	0.04	0.03	0.04	0.06
NiO	0.14	0.14	0.15	0.09	0.07	0.17	0.11	0.09	0.10
MgO	12.81	12.68	12.57	12.21	12.05	11.80	11.51	11.40	11.67
CaO	20.34	20.09	20.02	19.85	19.76	19.86	19.90	20.22	19.60
Na2O	2.76	2.82	3.03	3.03	3.09	3.17	3.05	2.94	2.86
K2O	0.00	0.00	0.02	0.01	0.01	0.00	0.00	0.72	0.20
Total	101.24	100.86	101.14	100.91	101.08	101.21	100.73	101.54	101.45
Si	1.920	1.911	1.910	1.910	1.899	1.883	1.868	1.845	
Ti	0.002	0.002	0.002	0.001	0.002	0.001	0.002	0.002	
Al	0.334	0.351	0.358	0.381	0.409	0.437	0.469	0.488	
Cr	0.002	0.001	0.001	0.002	0.000	0.000	0.001	0.001	
Fe2+	0.094	0.096	0.092	0.087	0.085	0.079	0.074	0.074	
Mn	0.002	0.001	0.002	0.001	0.001	0.001	0.001	0.001	
Ni	0.004	0.004	0.004	0.002	0.002	0.005	0.003	0.003	
Mg	0.681	0.676	0.668	0.649	0.639	0.625	0.612	0.605	
Ca	0.777	0.770	0.765	0.758	0.753	0.756	0.760	0.771	
Na	0.191	0.195	0.210	0.209	0.213	0.218	0.211	0.203	
K	0.000	0.000	0.001	0.000	0.000	0.000	0.000	0.033	
Sum	4.006	4.008	4.013	4.002	4.002	4.006	4.001	4.025	
Mg#	87.871	87.565	87.895	88.179	88.260	88.778	89.213	89.102	
Al IV	0.075	0.081	0.076	0.088	0.100	0.111	0.132	0.129	
Al VI	0.260	0.271	0.282	0.293	0.309	0.327	0.338	0.360	

1904-1 Cpx II, profile 476





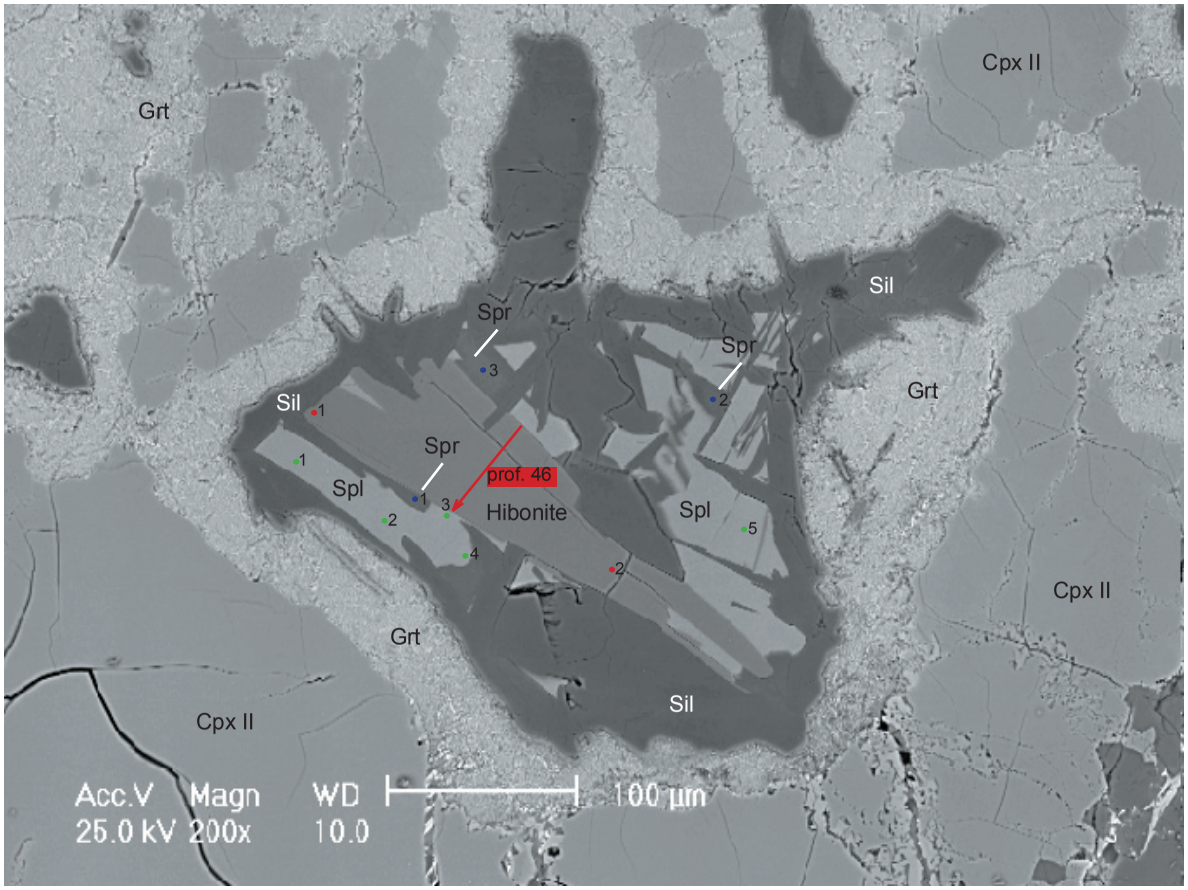


	10	20	30	40	50	60	70	80	90	100	110
SiO2	0.01	0.04	0.03	0.03	0.03	0.03	0.03	0.03	0.01	0.00	0.06
TiO2	0.00	0.00	0.00	0.01	0.02	0.01	0.02	0.01	0.00	0.01	0.00
Al2O3	100.95	100.48	100.28	100.10	100.04	99.89	99.40	99.39	99.38	99.43	99.25
Cr2O3	0.14	0.09	0.11	0.13	0.20	0.17	0.20	0.18	0.20	0.16	0.20
FeO	0.41	0.28	0.22	0.25	0.15	0.21	0.18	0.21	0.16	0.20	0.26
MnO	0.00	0.00	0.00	0.00	0.00	0.00	0.00	0.00	0.05	0.00	0.02
MgO	0.01	0.01	0.01	0.01	0.00	0.01	0.01	0.01	0.00	0.01	0.00
CaO	0.04	0.03	0.01	0.02	0.01	0.00	0.00	0.00	0.02	0.00	0.01
Na2O	0.00	0.00	0.01	0.00	0.00	0.00	0.02	0.00	0.00	0.00	0.00
K2O	0.01	0.00	0.01	0.00	0.01	0.00	0.00	0.01	0.00	0.01	0.00
Total	101.57	100.94	100.69	100.54	100.45	100.32	99.87	99.83	99.83	99.82	99.81
Si	0.000	0.001	0.001	0.001	0.001	0.000	0.000	0.001	0.000	0.000	0.001
Ti	0.000	0.000	0.000	0.000	0.000	0.000	0.000	0.000	0.000	0.000	0.000
Al	1.992	1.993	1.994	1.994	1.994	1.994	1.993	1.994	1.994	1.995	1.992
Cr	0.002	0.001	0.002	0.002	0.003	0.002	0.003	0.002	0.003	0.002	0.003
Fe3+	0.006	0.004	0.003	0.003	0.002	0.003	0.003	0.003	0.002	0.003	0.003
Fe2+	0.000	0.000	0.000	0.000	0.000	0.000	0.000	0.000	0.000	0.000	0.000
Mn	0.000	0.000	0.000	0.000	0.000	0.000	0.000	0.000	0.001	0.000	0.000
Mg	0.000	0.000	0.000	0.000	0.000	0.000	0.000	0.000	0.000	0.000	0.000
Ca	0.001	0.001	0.000	0.000	0.000	0.000	0.000	0.000	0.000	0.000	0.000
Na	0.000	0.000	0.000	0.000	0.000	0.000	0.001	0.000	0.000	0.000	0.000
K	0.000	0.000	0.000	0.000	0.000	0.000	0.000	0.000	0.000	0.000	0.000
Sum	2.000	2.000	2.000	2.000	2.000	2.000	2.000	2.000	2.000	2.000	2.000

1904-1 Corundum, profile 287

	120	130	140	150	160	170	180	190	200	210	220	230	240	250	260	270	280	290	300
SiO2	0.02	0.02	0.03	0.02	0.01	0.08	0.04	0.03	0.02	0.03	0.02	0.01	0.04	0.12	0.03	0.02	0.02	0.04	0.04
TiO2	0.02	0.01	0.00	0.01	0.00	0.02	0.00	0.01	0.02	0.00	0.00	0.00	0.01	0.04	0.00	0.03	0.01	0.02	0.03
Al2O3	99.50	99.57	99.55	99.41	99.59	99.10	99.13	99.27	98.89	98.54	99.04	98.46	99.15	98.82	99.31	99.18	99.25	98.95	98.53
Cr2O3	0.21	0.18	0.23	0.25	0.09	0.17	0.21	0.16	0.16	0.27	0.18	3.29	0.16	0.20	0.10	0.15	0.20	0.14	0.16
FeO	0.23	0.17	0.20	0.16	0.23	0.21	0.22	0.19	0.22	0.19	0.19	0.17	0.20	0.16	0.17	0.19	0.25	0.27	0.28
MnO	0.00	0.00	0.00	0.04	0.00	0.00	0.00	0.00	0.00	0.01	0.03	0.03	0.01	0.00	0.00	0.00	0.01	0.03	0.00
MgO	0.00	0.00	0.01	0.00	0.00	0.01	0.01	0.01	0.01	0.01	0.01	0.00	0.01	0.00	0.00	0.00	0.02	0.00	0.00
CaO	0.00	0.00	0.00	0.00	0.01	0.03	0.00	0.02	0.00	0.02	0.01	0.00	0.01	0.02	0.02	0.00	0.01	0.02	0.00
Na2O	0.00	0.01	0.00	0.00	0.00	0.01	0.00	0.00	0.00	0.00	0.01	0.00	0.00	0.00	0.01	0.01	0.00	0.00	0.00
K2O	0.00	0.00	0.00	0.01	0.00	0.00	0.00	0.00	0.00	0.01	0.00	0.00	0.00	0.00	0.00	0.00	0.01	0.00	0.02
Total	100.00	99.96	100.02	99.92	99.93	99.63	99.62	99.67	99.33	99.08	99.48	101.97	99.59	99.36	99.64	99.59	99.77	99.47	99.08
Si	0.000	0.000	0.000	0.000	0.000	0.001	0.001	0.001	0.000	0.000	0.000		0.001	0.002	0.000	0.000	0.000	0.001	0.001
Ti	0.000	0.000	0.000	0.000	0.000	0.000	0.000	0.000	0.000	0.000	0.000		0.000	0.000	0.000	0.000	0.000	0.000	0.000
Al	1.993	1.995	1.993	1.993	1.995	1.992	1.993	1.994	1.994	1.992	1.994		1.994	1.992	1.995	1.994	1.993	1.993	1.992
Cr	0.003	0.002	0.003	0.003	0.001	0.002	0.003	0.002	0.002	0.004	0.002		0.002	0.003	0.001	0.002	0.003	0.002	0.002
Fe3+	0.003	0.002	0.003	0.002	0.003	0.003	0.003	0.002	0.003	0.003	0.003		0.003	0.000	0.002	0.002	0.004	0.004	0.004
Fe2+	0.000	0.000	0.000	0.000	0.000	0.000	0.000	0.000	0.000	0.000	0.000		0.000	0.002	0.000	0.000	0.000	0.000	0.000
Mn	0.000	0.000	0.000	0.001	0.000	0.000	0.000	0.000	0.000	0.000	0.000		0.000	0.000	0.000	0.000	0.000	0.000	0.000
Mg	0.000	0.000	0.000	0.000	0.000	0.000	0.000	0.000	0.000	0.000	0.000		0.000	0.000	0.000	0.000	0.000	0.000	0.000
Ca	0.000	0.000	0.000	0.000	0.000	0.001	0.000	0.000	0.000	0.000	0.000		0.000	0.000	0.000	0.000	0.000	0.000	0.000
Na	0.000	0.000	0.000	0.000	0.000	0.000	0.000	0.000	0.000	0.000	0.000		0.000	0.000	0.000	0.000	0.000	0.000	0.000
K	0.000	0.000	0.000	0.000	0.000	0.000	0.000	0.000	0.000	0.000	0.000		0.000	0.000	0.000	0.000	0.000	0.000	0.000
Sum	2.000	2.000	2.000	2.000	2.000	2.000	2.000	2.000	2.000	2.000	2.000		2.000	2.000	2.000	2.000	2.000	2.000	2.000

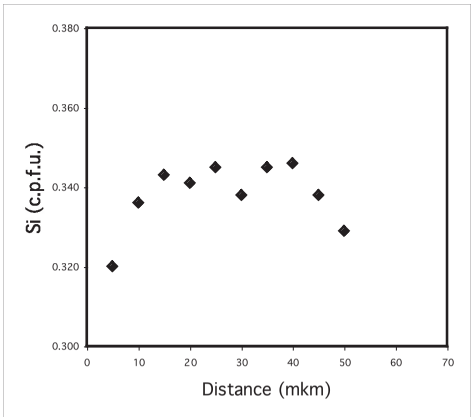
1904-1 Corundum, profile 287

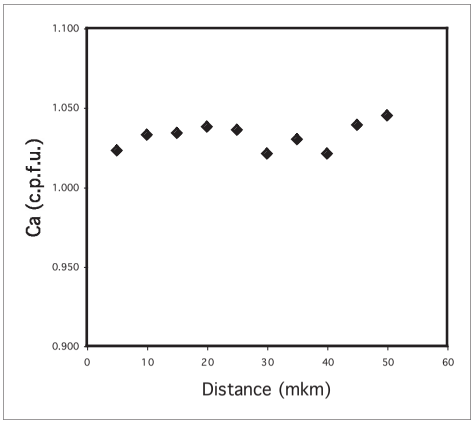


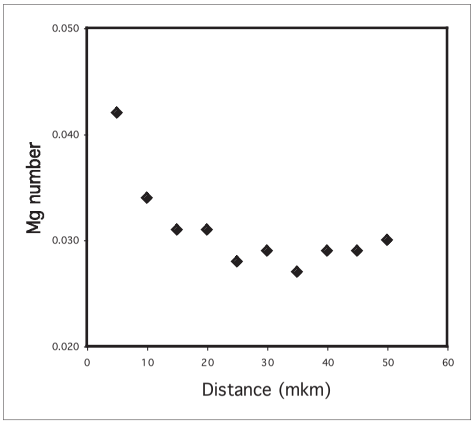
1904-1 Hibonite, profile 46

	5	10	15	20	25	30	35	40	45	50
SiO2	2.84	2.98	3.04	3.02	3.07	3.00	3.05	3.07	3.01	2.91
TiO2	0.49	0.40	0.37	0.37	0.33	0.34	0.32	0.34	0.35	0.35
Al2O3	83.87	83.90	83.81	83.74	84.03	83.84	83.67	83.93	84.00	83.58
Cr2O3	0.27	0.21	0.23	0.20	0.15	0.17	0.22	0.28	0.31	0.35
FeO	1.97	2.00	2.02	2.09	2.02	1.93	1.93	2.01	2.08	1.91
MnO	0.01	0.00	0.00	0.01	0.01	0.05	0.02	0.00	0.00	0.03
ZnO	0.17	0.13	0.22	0.07	0.07	0.10	0.00	0.17	0.13	0.10
MgO	1.65	1.75	1.67	1.72	1.74	1.72	1.68	1.71	1.71	1.55
CaO	8.46	8.56	8.57	8.59	8.60	8.44	8.50	8.47	8.63	8.61
Na2O	0.02	0.01	0.02	0.00	0.02	0.00	0.00	0.00	0.03	0.00
K2O	0.00	0.00	0.01	0.01	0.00	0.00	0.00	0.01	0.00	0.00
Total	99.76	99.94	99.97	99.81	100.03	99.59	99.40	100.00	100.26	99.41
Si	0.320	0.336	0.343	0.341	0.345	0.338	0.345	0.346	0.338	0.329
Ti	0.042	0.034	0.031	0.031	0.028	0.029	0.027	0.029	0.029	0.030
Al	11.157	11.138	11.130	11.133	11.139	11.158	11.152	11.134	11.125	11.157
Cr	0.024	0.019	0.021	0.018	0.013	0.015	0.020	0.025	0.028	0.031
Fe2+	0.186	0.188	0.190	0.197	0.190	0.183	0.183	0.189	0.195	0.181
Mn	0.001	0.000	0.000	0.001	0.001	0.005	0.001	0.000	0.000	0.003
Zn	0.014	0.011	0.018	0.005	0.006	0.008	0.000	0.014	0.011	0.009
Mg	0.278	0.294	0.280	0.289	0.291	0.289	0.284	0.287	0.286	0.262
Ca	1.023	1.033	1.034	1.038	1.036	1.021	1.030	1.021	1.039	1.045
Na	0.005	0.002	0.005	0.001	0.004	0.000	0.000	0.000	0.006	0.000
K	0.000	0.000	0.002	0.001	0.000	0.000	0.000	0.001	0.000	0.000
Sum	13.050	13.053	13.054	13.054	13.053	13.046	13.042	13.047	13.059	13.047

1904-1 Hibonite, profile 46







1904-1 Hibonite, an. 1 & 2

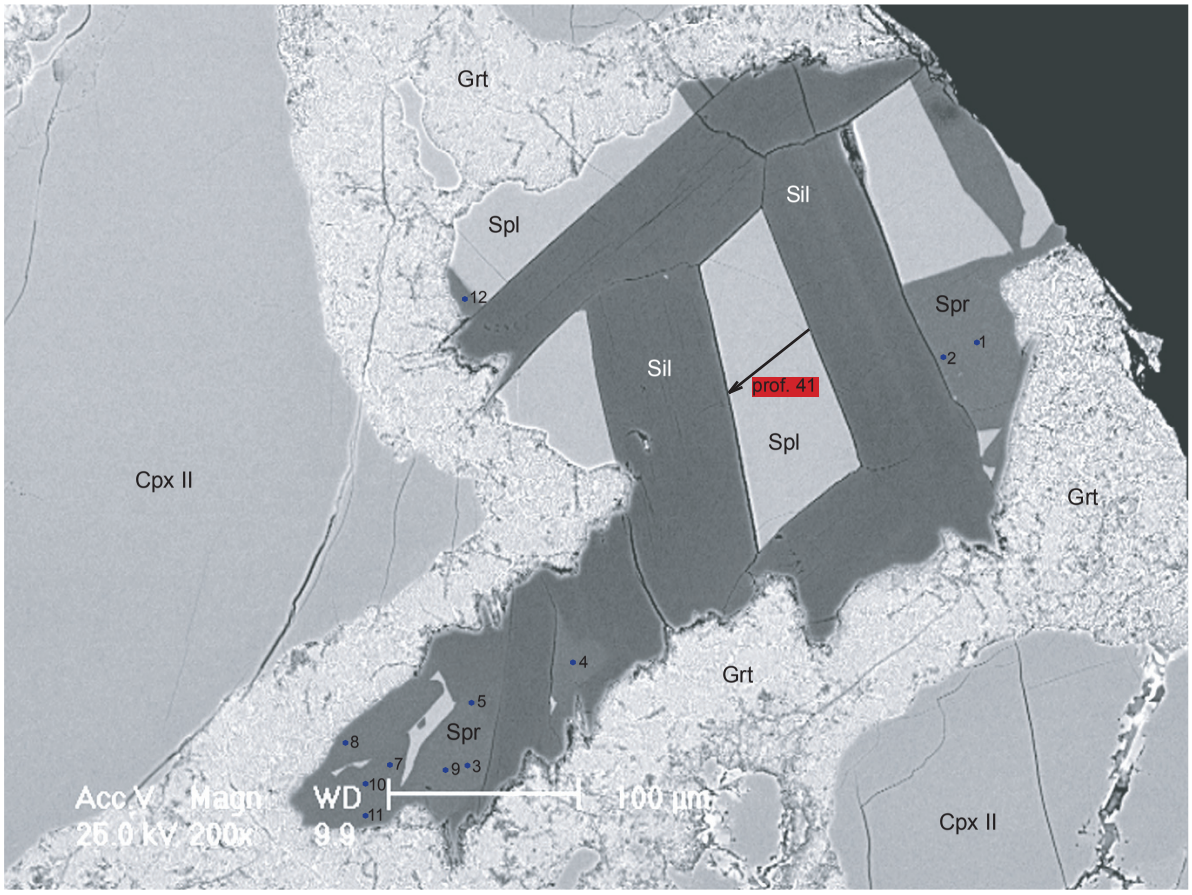
	1	2
SiO2	2.62	2.82
TiO2	1.33	1.30
Al2O3	83.48	82.58
Cr2O3	0.23	0.24
FeO	2.14	2.27
MnO	0.00	0.00
ZnO	0.13	0.17
MgO	1.84	2.00
CaO	8.36	8.43
Na2O	0.01	0.02
K2O	0.01	0.01
Total	100.14	99.84
Si	0.295	0.319
Ti	0.113	0.111
Al	11.081	11.012
Cr	0.020	0.021
Fe2+	0.202	0.215
Mn	0.000	0.000
Zn	0.011	0.014
Mg	0.309	0.337
Ca	1.009	1.022
Na	0.002	0.004
K	0.001	0.001
Sum	13.043	13.057

1904-1 Sapphirine, an. 1-3

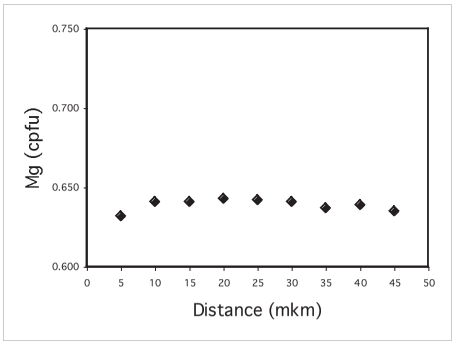
	1	2	3
SiO2	9.57	9.70	10.20
TiO2	0.01	0.00	0.00
Al2O3	69.44	69.85	68.88
Cr2O3	0.81	0.79	0.69
FeO	3.39	3.54	3.48
MnO	0.00	0.00	0.03
NiO	0.35	0.36	0.35
MgO	16.38	16.23	16.65
CaO	0.05	0.02	0.03
Na2O	0.00	0.00	0.01
K2O	0.00	0.01	0.00
Total	100.00	100.49	100.31
Si	1.123	1.132	1.192
Ti	0.001	0.000	0.000
Al	9.602	9.613	9.491
Cr	0.075	0.072	0.064
Fe2+	0.333	0.346	0.341
Mn	0.000	0.000	0.002
Ni	0.033	0.034	0.033
Mg	2.865	2.826	2.902
Ca	0.006	0.002	0.004
Na	0.000	0.000	0.002
K	0.000	0.002	0.000
Sum	14.038	14.026	14.031

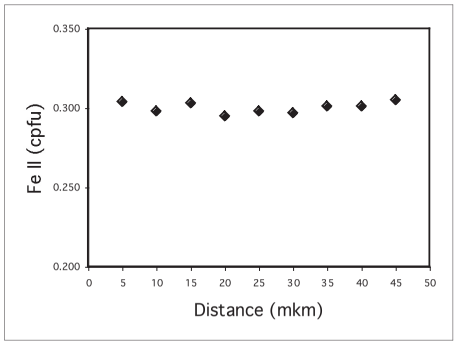
1904-1 Spinel, an. 1-5

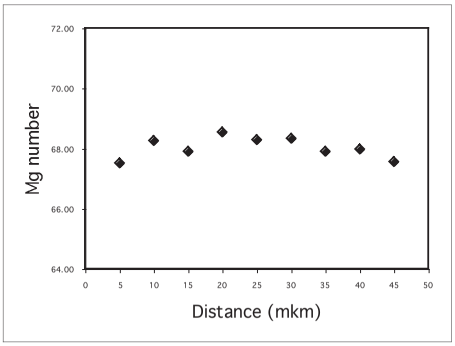
	1	2	3	4	5
SiO2	0.02	0.04	0.05	0.07	0.04
TiO2	0.00	0.01	0.04	0.00	0.02
Al2O3	65.29	65.15	64.88	65.05	65.60
Cr2O3	1.64	1.52	1.49	1.49	1.44
FeO	13.59	13.72	13.66	13.49	13.59
MnO	0.03	0.02	0.00	0.04	0.06
NiO	1.50	1.59	1.39	1.55	1.49
ZnO	1.01	1.10	1.26	1.06	1.13
MgO	17.37	17.44	17.36	17.40	17.36
CaO	0.02	0.01	0.04	0.02	0.00
Total	100.49	100.60	100.18	100.17	100.72
Si	0.001	0.001	0.001	0.002	0.001
Ti	0.000	0.000	0.001	0.000	0.000
Al	1.964	1.959	1.959	1.962	1.968
Cr	0.033	0.031	0.030	0.030	0.029
Fe3+	0.001	0.009	0.007	0.004	0.000
Fe2+	0.289	0.284	0.286	0.285	0.289
Mn	0.001	0.000	0.000	0.001	0.001
Ni	0.031	0.033	0.029	0.032	0.030
Zn	0.019	0.021	0.024	0.020	0.021
Mg	0.661	0.663	0.663	0.664	0.659
Ca	0.000	0.000	0.001	0.000	0.000
Sum	3.000	3.000	3.000	3.000	3.000
Mg/(Mg+Fe2+)	69.6	70.0	69.9	70.0	69.5

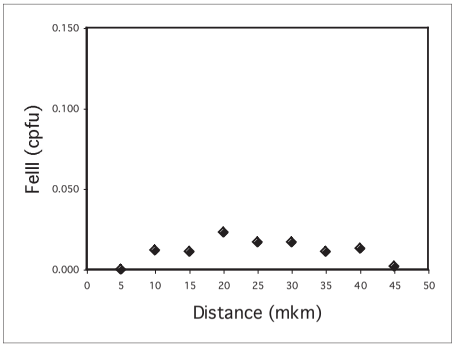


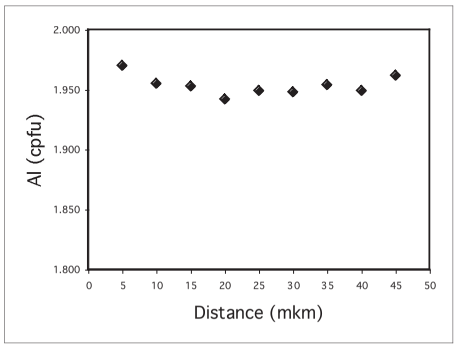
1904-1 Spinel, profile 41

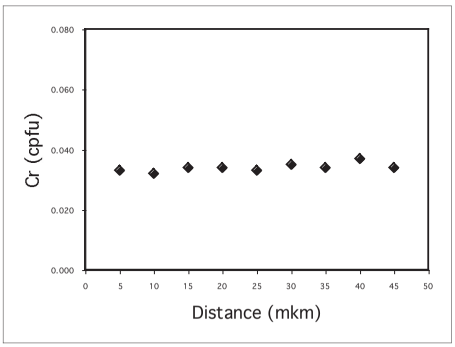


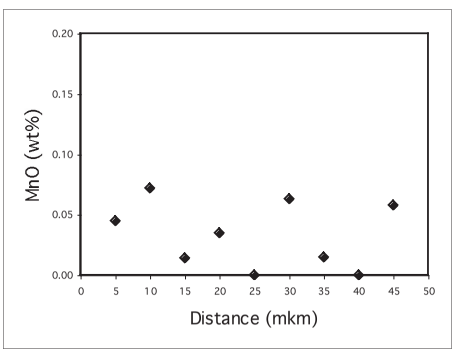


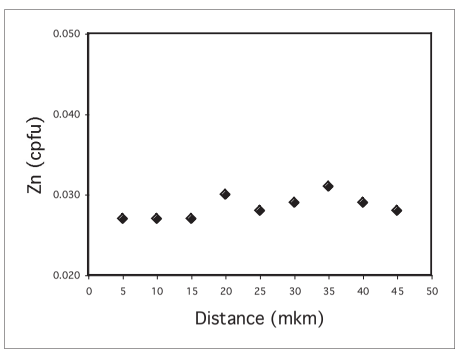


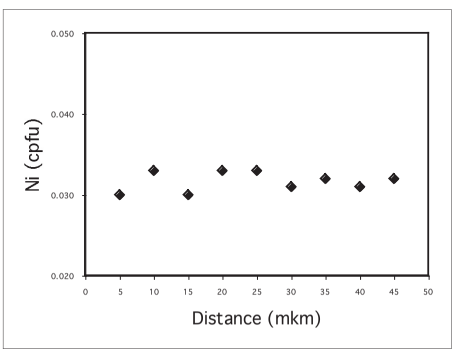












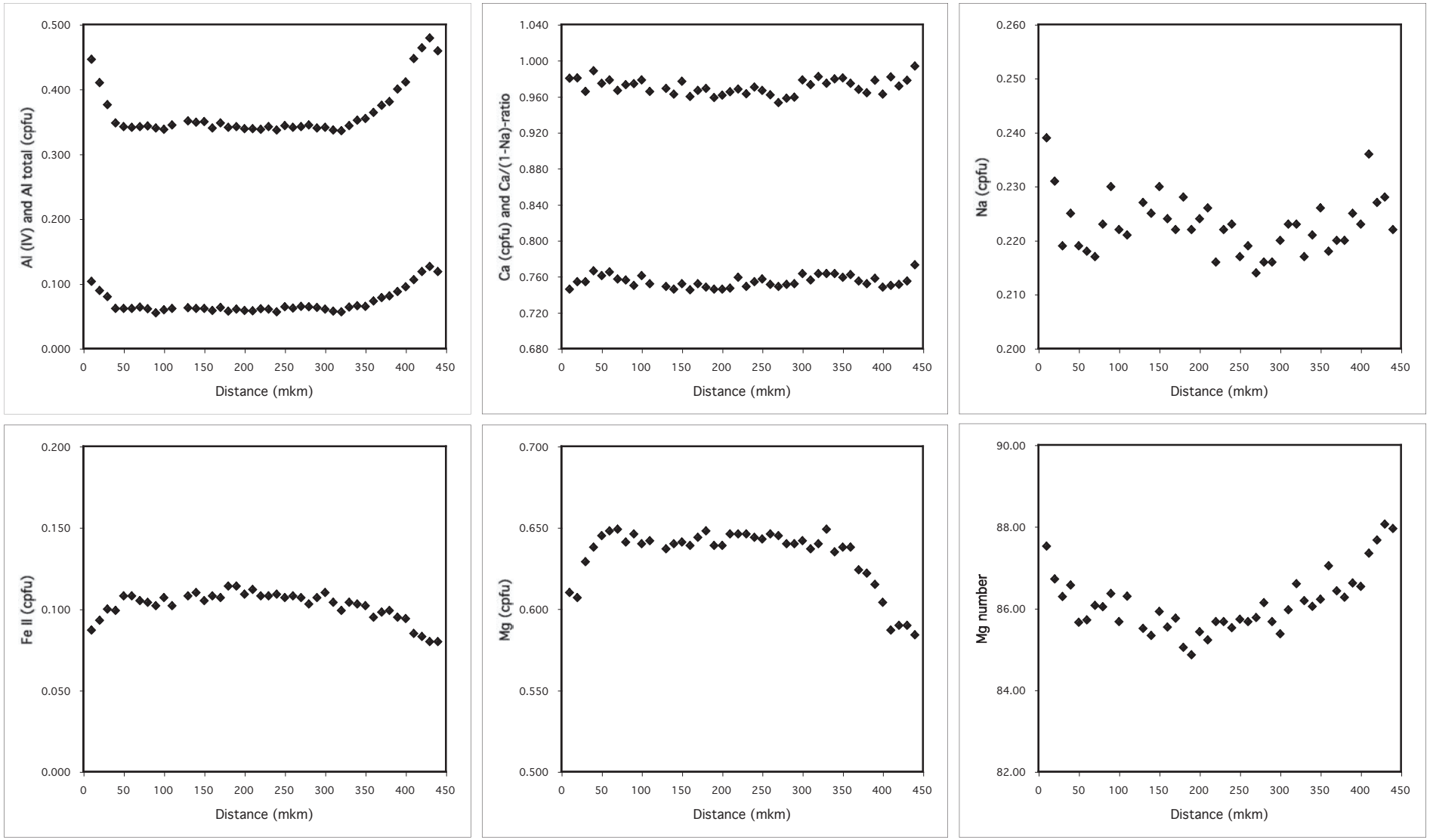
1904-1 Spinel, profile 41

	5	10	15	20	25	30	35	40	45
SiO2	0.04	0.03	0.04	0.03	0.02	0.02	0.01	0.02	0.03
TiO2	0.00	0.00	0.00	0.00	0.00	0.00	0.01	0.00	0.01
Al2O3	65.03	64.48	64.35	64.36	64.54	64.66	64.82	64.62	64.73
Cr2O3	1.63	1.55	1.67	1.68	1.61	1.73	1.68	1.81	1.68
FeO	14.14	14.43	14.55	14.84	14.71	14.68	14.59	14.71	14.28
MnO	0.05	0.07	0.01	0.04	0.00	0.06	0.02	0.00	0.06
NiO	1.45	1.60	1.44	1.59	1.59	1.52	1.55	1.49	1.53
ZnO	1.44	1.40	1.42	1.57	1.51	1.55	1.62	1.56	1.45
MgO	16.49	16.72	16.70	16.84	16.80	16.84	16.71	16.75	16.57
CaO	0.00	0.00	0.00	0.00	0.00	0.00	0.00	0.00	0.00
Total	100.27	100.29	100.19	100.96	100.78	101.07	101.01	100.96	100.34
Si	0.001	0.001	0.001	0.001	0.001	0.000	0.000	0.001	0.001
Ti	0.000	0.000	0.000	0.000	0.000	0.000	0.000	0.000	0.000
Al	1.970	1.955	1.953	1.942	1.949	1.948	1.954	1.949	1.962
Cr	0.033	0.032	0.034	0.034	0.033	0.035	0.034	0.037	0.034
Fe3+	0.000	0.012	0.011	0.023	0.017	0.017	0.011	0.013	0.002
Fe2+	0.304	0.298	0.303	0.295	0.298	0.297	0.301	0.301	0.305
Mn	0.001	0.002	0.000	0.001	0.000	0.001	0.000	0.000	0.001
Ni	0.030	0.033	0.030	0.033	0.033	0.031	0.032	0.031	0.032
Zn	0.027	0.027	0.027	0.030	0.028	0.029	0.031	0.029	0.028
Mg	0.632	0.641	0.641	0.643	0.642	0.641	0.637	0.639	0.635
Ca	0.000	0.000	0.000	0.000	0.000	0.000	0.000	0.000	0.000
Sum	2.998	3.000	3.000	3.000	3.000	3.000	3.000	3.000	3.000
100*Mg/(Mg+Fe2+)	67.52	68.26	67.90	68.55	68.30	68.34	67.91	67.98	67.55

1904-1 Sapphirine, an. 1-12

	1	2	3	4	7	8	9	10	11	12
SiO2	10.81	10.39	10.00	10.97	10.40	10.88	10.88	10.94	11.02	9.79
TiO2	0.00	0.00	0.03	0.00	0.01	0.00	0.00	0.03	0.00	0.02
Al2O3	64.07	67.85	68.61	66.53	67.85	67.35	67.11	66.59	66.34	68.36
Cr2O3	0.75	0.70	0.99	0.81	1.08	1.08	1.13	1.12	1.11	0.81
FeO	4.25	3.75	3.54	4.06	3.90	4.16	4.07	4.02	3.90	3.56
MnO	0.02	0.04	0.01	0.03	0.02	0.01	0.00	0.00	0.00	0.05
NiO	0.37	0.42	0.31	0.40	0.39	0.36	0.41	0.36	0.47	0.42
MgO	16.91	16.58	16.46	17.14	16.75	16.93	16.75	16.98	17.02	16.34
CaO	0.00	0.00	0.03	0.02	0.03	0.00	0.03	0.03	0.06	0.02
Na2O	0.01	0.00	0.00	0.02	0.00	0.00	0.00	0.01	0.02	0.00
K2O	0.00	0.00	0.01	0.00	0.00	0.01	0.02	0.01	0.01	0.00
Total	97.19	99.74	99.97	99.98	100.42	100.77	100.40	100.08	99.96	99.37
Si	1.311	1.224	1.174	1.292	1.219	1.271	1.277	1.287	1.299	1.157
Ti	0.000	0.000	0.002	0.000	0.000	0.000	0.000	0.002	0.000	0.001
Al	9.161	9.419	9.497	9.233	9.373	9.278	9.278	9.235	9.212	9.527
Cr	0.072	0.065	0.091	0.075	0.100	0.100	0.105	0.104	0.103	0.075
Fe2+	0.431	0.370	0.348	0.399	0.382	0.406	0.400	0.396	0.385	0.352
Mn	0.002	0.003	0.001	0.002	0.001	0.000	0.000	0.000	0.000	0.005
Ni	0.036	0.040	0.029	0.038	0.037	0.034	0.038	0.034	0.044	0.040
Mg	3.058	2.911	2.881	3.009	2.926	2.950	2.930	2.978	2.990	2.880
Ca	0.000	0.000	0.004	0.003	0.004	0.000	0.004	0.003	0.007	0.003
Na	0.002	0.001	0.000	0.004	0.000	0.001	0.000	0.002	0.004	0.000
K	0.000	0.000	0.001	0.000	0.000	0.001	0.003	0.002	0.002	0.000
Sum	14.073	14.034	14.029	14.056	14.044	14.041	14.033	14.043	14.046	14.040
O	20	20	20	20	20	20	20	20	20	20

Ca-Al hibonite-bearing granulite 1904-9



1904-9 Cpx II, profile 425

	10	20	30	40	50	60	70	80	90	100	110	120	130	140	150	160	170	180	190	200
SiO2	52.31	52.77	53.21	53.34	53.40	53.20	53.71	53.48	53.75	53.53	53.59	53.54	53.16	53.37	52.96	53.70	53.52	53.48	53.58	53.65
TiO2	0.01	0.00	0.02	0.00	0.00	0.02	0.03	0.02	0.00	0.03	0.01	0.00	0.05	0.01	0.03	0.02	0.01	0.03	0.01	0.02
Al2O3	10.51	9.63	8.85	8.17	8.04	7.99	8.08	8.06	8.01	7.95	8.11	10.39	8.20	8.19	8.16	7.99	8.19	8.03	8.04	7.95
Cr2O3	0.03	0.00	0.02	0.01	0.01	0.01	0.04	0.02	0.02	0.03	0.00	0.02	0.00	0.00	0.03	0.02	0.00	0.01	0.03	0.01
FeO	2.89	3.08	3.32	3.29	3.58	3.55	3.50	3.46	3.39	3.53	3.36	3.00	3.56	3.62	3.45	3.56	3.54	3.78	3.77	3.60
MnO	0.00	0.06	0.03	0.00	0.00	0.01	0.04	0.07	0.00	0.09	0.07	0.00	0.00	0.04	0.06	0.06	0.08	0.03	0.04	0.00
NiO	0.17	0.18	0.16	0.15	0.22	0.14	0.11	0.15	0.11	0.18	0.14	0.14	0.17	0.14	0.12	0.15	0.19	0.17	0.21	0.16
MgO	11.38	11.29	11.70	11.83	11.98	11.99	12.11	11.90	12.02	11.90	11.94	10.36	11.77	11.87	11.82	11.88	11.99	12.05	11.88	11.86
CaO	19.36	19.49	19.52	19.77	19.67	19.72	19.67	19.52	19.44	19.68	19.44	17.42	19.27	19.25	19.29	19.25	19.47	19.35	19.30	19.25
Na2O	3.42	3.30	3.13	3.21	3.14	3.10	3.11	3.18	3.29	3.17	3.15	2.86	3.23	3.22	3.26	3.20	3.18	3.26	3.17	3.20
K2O	0.02	0.00	0.00	0.00	0.01	0.00	0.00	0.00	0.00	0.00	0.01	0.06	0.02	0.02	0.00	0.01	0.00	0.00	0.00	0.01
Total	100.09	99.80	99.94	99.77	100.03	99.75	100.41	99.85	100.02	100.09	99.83	97.79	99.43	99.73	99.17	99.82	100.16	100.18	100.01	99.71
Si	1.881	1.905	1.918	1.929	1.928	1.927	1.930	1.932	1.936	1.932	1.935		1.929	1.931	1.927	1.939	1.928	1.928	1.934	1.940
Ti	0.000	0.000	0.001	0.000	0.000	0.000	0.001	0.001	0.000	0.001	0.000		0.001	0.000	0.001	0.000	0.000	0.001	0.000	0.001
Al	0.446	0.410	0.376	0.348	0.342	0.341	0.342	0.343	0.340	0.338	0.345		0.351	0.349	0.350	0.340	0.348	0.341	0.342	0.339
Cr	0.001	0.000	0.001	0.000	0.000	0.000	0.001	0.000	0.000	0.001	0.000		0.000	0.000	0.001	0.001	0.000	0.000	0.001	0.000
Fe2+	0.087	0.093	0.100	0.099	0.108	0.108	0.105	0.104	0.102	0.107	0.102		0.108	0.110	0.105	0.108	0.107	0.114	0.114	0.109
Mn	0.000	0.002	0.001	0.000	0.000	0.000	0.001	0.002	0.000	0.003	0.002		0.000	0.001	0.002	0.002	0.002	0.001	0.001	0.000
Ni	0.005	0.005	0.005	0.004	0.006	0.004	0.003	0.004	0.003	0.005	0.004		0.005	0.004	0.004	0.004	0.005	0.005	0.006	0.005
Mg	0.610	0.607	0.629	0.638	0.645	0.648	0.649	0.641	0.646	0.640	0.642		0.637	0.640	0.641	0.639	0.644	0.648	0.639	0.639
Ca	0.746	0.754	0.754	0.766	0.761	0.765	0.757	0.756	0.750	0.761	0.752		0.749	0.746	0.752	0.745	0.752	0.748	0.746	0.746
Na	0.239	0.231	0.219	0.225	0.219	0.218	0.217	0.223	0.230	0.222	0.221		0.227	0.225	0.230	0.224	0.222	0.228	0.222	0.224
K	0.001	0.000	0.000	0.000	0.000	0.000	0.000	0.000	0.000	0.000	0.001		0.001	0.001	0.000	0.000	0.000	0.000	0.000	0.000
Sum	4.015	4.006	4.002	4.010	4.010	4.011	4.006	4.007	4.008	4.009	4.003		4.008	4.008	4.012	4.002	4.009	4.014	4.005	4.002
Mg#	87.52	86.71	86.28	86.57	85.66	85.71	86.07	86.04	86.36	85.68	86.29		85.50	85.33	85.92	85.54	85.75	85.04	84.86	85.43
Al IV	0.104	0.090	0.080	0.062	0.062	0.062	0.064	0.061	0.055	0.060	0.062		0.063	0.062	0.062	0.059	0.063	0.058	0.061	0.059
Al VI	0.343	0.321	0.296	0.287	0.281	0.280	0.278	0.282	0.285	0.279	0.284		0.289	0.288	0.289	0.282	0.285	0.284	0.282	0.281

1904-9 Cpx II, profile 425

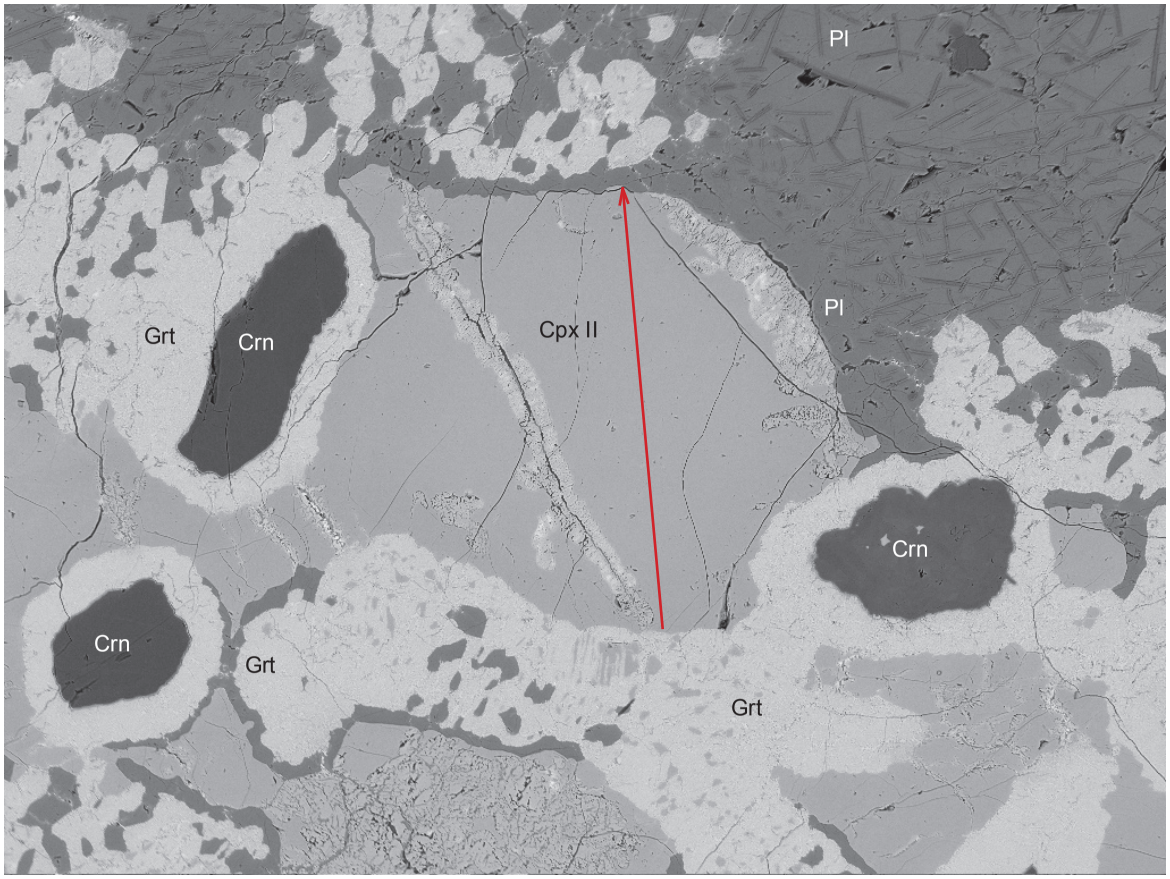
	210	220	230	240	250	260	270	280	290	300	310	320	330	340	350	360	370	380	390	400
SiO2	53.45	53.48	53.31	53.62	53.09	53.51	53.53	53.57	53.62	53.42	53.81	53.76	53.32	53.36	53.69	53.07	53.44	53.32	52.99	52.89
TiO2	0.02	0.00	0.00	0.00	0.03	0.02	0.03	0.00	0.01	0.00	0.01	0.00	0.00	0.05	0.00	0.00	0.03	0.00	0.01	0.04
Al2O3	7.95	7.94	8.02	7.92	8.04	8.02	8.03	8.10	8.00	8.01	7.92	7.89	8.08	8.28	8.40	8.51	8.85	8.98	9.43	9.66
Cr2O3	0.02	0.01	0.06	0.01	0.01	0.01	0.01	0.02	0.05	0.00	0.04	0.01	0.00	0.00	0.02	0.00	0.03	0.03	0.03	0.01
FeO	3.70	3.58	3.57	3.62	3.52	3.59	3.54	3.41	3.53	3.64	3.47	3.28	3.45	3.42	3.39	3.12	3.26	3.28	3.16	3.13
MnO	0.07	0.00	0.03	0.05	0.05	0.04	0.04	0.00	0.04	0.02	0.00	0.03	0.00	0.04	0.03	0.00	0.00	0.02	0.02	0.03
NiO	0.12	0.16	0.20	0.12	0.17	0.15	0.16	0.14	0.19	0.09	0.15	0.13	0.15	0.16	0.16	0.12	0.15	0.13	0.14	0.14
MgO	11.99	12.00	11.96	11.97	11.86	11.99	11.98	11.87	11.89	11.93	11.86	11.89	12.05	11.80	11.95	11.81	11.64	11.58	11.47	11.23
CaO	19.27	19.61	19.29	19.51	19.42	19.39	19.33	19.38	19.44	19.72	19.57	19.74	19.70	19.75	19.77	19.62	19.61	19.51	19.66	19.33
Na2O	3.23	3.09	3.16	3.19	3.08	3.13	3.06	3.09	3.08	3.14	3.19	3.19	3.10	3.17	3.25	3.10	3.16	3.15	3.23	3.19
K2O	0.00	0.00	0.01	0.02	0.00	0.00	0.00	0.01	0.01	0.00	0.00	0.00	0.00	0.03	0.01	0.00	0.01	0.00	0.00	0.00
Total	99.81	99.86	99.61	100.03	99.26	99.84	99.70	99.58	99.86	99.98	100.01	99.92	99.85	100.06	100.68	99.35	100.18	100.00	100.12	99.64
Si	1.933	1.933	1.932	1.935	1.930	1.933	1.935	1.937	1.936	1.930	1.940	1.939	1.927	1.925	1.924	1.924	1.921	1.920	1.907	1.909
Ti	0.001	0.000	0.000	0.000	0.001	0.001	0.001	0.000	0.000	0.000	0.000	0.000	0.000	0.001	0.000	0.000	0.001	0.000	0.000	0.001
Al	0.339	0.338	0.342	0.337	0.344	0.341	0.342	0.345	0.340	0.341	0.337	0.336	0.344	0.352	0.355	0.364	0.375	0.381	0.400	0.411
Cr	0.001	0.000	0.002	0.000	0.000	0.000	0.000	0.001	0.002	0.000	0.001	0.000	0.000	0.000	0.001	0.000	0.001	0.001	0.001	0.000
Fe2+	0.112	0.108	0.108	0.109	0.107	0.108	0.107	0.103	0.107	0.110	0.104	0.099	0.104	0.103	0.102	0.095	0.098	0.099	0.095	0.094
Mn	0.002	0.000	0.001	0.002	0.002	0.001	0.001	0.000	0.001	0.001	0.000	0.001	0.000	0.001	0.001	0.000	0.000	0.001	0.000	0.001
Ni	0.003	0.005	0.006	0.003	0.005	0.004	0.005	0.004	0.006	0.003	0.004	0.004	0.004	0.005	0.005	0.003	0.004	0.004	0.004	0.004
Mg	0.646	0.646	0.646	0.644	0.643	0.646	0.645	0.640	0.640	0.642	0.637	0.640	0.649	0.635	0.638	0.638	0.624	0.622	0.615	0.604
Ca	0.747	0.759	0.749	0.754	0.757	0.751	0.749	0.751	0.752	0.763	0.756	0.763	0.763	0.763	0.759	0.762	0.755	0.752	0.758	0.748
Na	0.226	0.216	0.222	0.223	0.217	0.219	0.214	0.216	0.216	0.220	0.223	0.223	0.217	0.221	0.226	0.218	0.220	0.220	0.225	0.223
K	0.000	0.000	0.001	0.001	0.000	0.000	0.000	0.001	0.000	0.000	0.000	0.000	0.000	0.001	0.000	0.000	0.001	0.000	0.000	0.000
Sum	4.010	4.006	4.008	4.009	4.005	4.005	4.000	3.998	4.000	4.010	4.003	4.004	4.009	4.009	4.011	4.004	4.000	3.999	4.005	3.996
Mg#	85.22	85.68	85.68	85.52	85.73	85.68	85.77	86.14	85.68	85.37	85.96	86.60	86.19	86.04	86.22	87.04	86.43	86.27	86.62	86.53
Al IV	0.058	0.061	0.061	0.057	0.065	0.062	0.065	0.065	0.063	0.061	0.058	0.057	0.064	0.066	0.065	0.073	0.079	0.081	0.088	0.095
Al VI	0.281	0.277	0.282	0.281	0.280	0.279	0.277	0.281	0.277	0.281	0.280	0.280	0.281	0.286	0.290	0.291	0.297	0.300	0.312	0.316

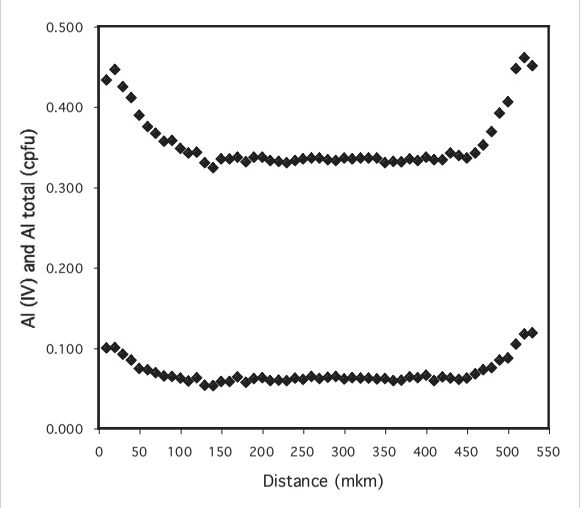
1904-9 Cpx II, profile 425

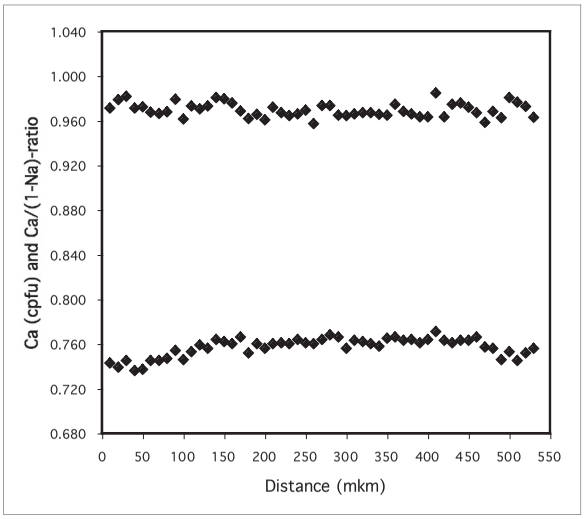
	410	420	430	440
SiO2	52.53	52.09	51.49	51.94
TiO2	0.00	0.01	0.03	0.00
Al2O3	10.55	10.91	11.20	10.77
Cr2O3	0.04	0.01	0.04	0.00
FeO	2.83	2.74	2.63	2.65
MnO	0.07	0.01	0.02	0.00
NiO	0.16	0.20	0.15	0.14
MgO	10.95	10.96	10.90	10.83
CaO	19.47	19.42	19.42	19.94
Na2O	3.39	3.24	3.24	3.17
K2O	0.00	0.00	0.02	0.00
Total	99.98	99.59	99.13	99.43
Si	1.890	1.880	1.868	1.879
Ti	0.000	0.000	0.001	0.000
Al	0.447	0.464	0.479	0.459
Cr	0.001	0.000	0.001	0.000
Fe3	0.000	0.000	0.000	0.000
Fe2	0.085	0.083	0.080	0.080
Mn	0.002	0.000	0.001	0.000
Ni	0.005	0.006	0.004	0.004
Mg	0.587	0.590	0.590	0.584
Ca	0.750	0.751	0.755	0.773
Na	0.236	0.227	0.228	0.222
K	0.000	0.000	0.001	0.000
Sum	4.004	4.001	4.006	4.002
Mg#	87.35	87.67	88.06	87.95
Al IV	0.106	0.119	0.127	0.119
Al VI	0.341	0.346	0.353	0.341

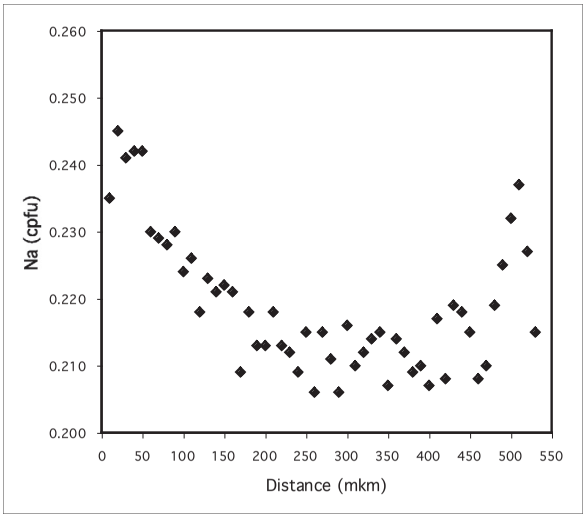
1904-9 Cpx II, profile 425

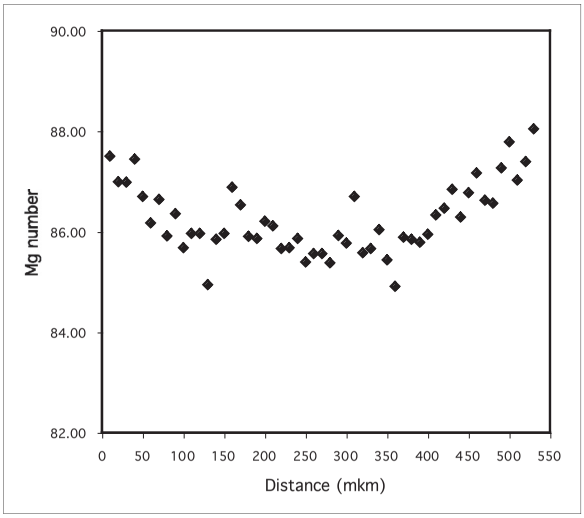
1904-9 Cpx II, profile 515











	10	20	30	40	50	60	70	80	90	100	110	120	130	140	150	160	170	180	190	200
SiO2	52.82	52.41	52.89	52.86	53.37	53.12	53.58	53.71	53.21	53.27	53.51	53.26	53.29	53.43	53.18	53.38	53.26	53.68	53.42	53.24
TiO2	0.03	0.00	0.02	0.02	0.00	0.00	0.02	0.01	0.02	0.01	0.00	0.00	0.01	0.03	0.02	0.03	0.00	0.02	0.00	0.01
Al2O3	10.23	10.44	10.01	9.64	9.14	8.78	8.60	8.41	8.37	8.13	8.04	8.00	7.71	7.55	7.83	7.82	7.89	7.80	7.91	7.86
Cr2O3	0.03	0.00	0.00	0.00	0.03	0.00	0.00	0.05	0.02	0.00	0.03	0.02	0.01	0.03	0.03	0.00	0.00	0.06	0.00	0.04
FeO	2.86	2.85	2.91	2.88	3.08	3.31	3.13	3.37	3.31	3.49	3.49	3.43	3.76	3.47	3.51	3.22	3.34	3.58	3.57	3.43
MnO	0.01	0.03	0.02	0.03	0.02	0.03	0.03	0.00	0.06	0.04	0.02	0.02	0.10	0.06	0.02	0.00	0.05	0.00	0.02	0.02
NiO	0.12	0.16	0.12	0.14	0.17	0.13	0.08	0.15	0.12	0.10	0.15	0.16	0.11	0.15	0.12	0.16	0.15	0.14	0.12	0.14
MgO	11.24	10.63	10.94	11.23	11.26	11.53	11.41	11.57	11.71	11.70	11.93	11.75	11.86	11.87	12.00	12.00	11.99	12.26	12.19	12.00
CaO	19.30	19.01	19.27	18.98	19.04	19.20	19.22	19.35	19.42	19.14	19.44	19.50	19.42	19.62	19.60	19.53	19.71	19.49	19.64	19.42
Na2O	3.38	3.48	3.44	3.45	3.46	3.27	3.26	3.26	3.27	3.18	3.22	3.09	3.17	3.13	3.15	3.13	2.97	3.12	3.04	3.02
K2O	0.02	0.00	0.00	0.00	0.01	0.00	0.00	0.01	0.00	0.00	0.00	0.00	0.00	0.00	0.00	0.00	0.00	0.01	0.01	0.01
Total	100.03	99.00	99.62	99.21	99.58	99.36	99.33	99.87	99.50	99.05	99.82	99.22	99.43	99.32	99.45	99.27	99.35	100.15	99.92	99.18
Si	1.897	1.901	1.908	1.914	1.927	1.925	1.938	1.936	1.928	1.937	1.933	1.936	1.936	1.942	1.931	1.937	1.933	1.934	1.930	1.935
Ti	0.001	0.000	0.000	0.000	0.000	0.000	0.000	0.000	0.000	0.000	0.000	0.000	0.000	0.001	0.001	0.001	0.000	0.000	0.000	0.000
Al	0.433	0.446	0.425	0.411	0.389	0.375	0.367	0.357	0.358	0.348	0.342	0.343	0.330	0.324	0.335	0.335	0.337	0.331	0.337	0.337
Cr	0.001	0.000	0.000	0.000	0.001	0.000	0.000	0.001	0.001	0.000	0.001	0.000	0.000	0.001	0.001	0.000	0.000	0.002	0.000	0.001
Fe2+	0.086	0.086	0.088	0.087	0.093	0.100	0.095	0.102	0.100	0.106	0.105	0.104	0.114	0.106	0.106	0.098	0.101	0.108	0.108	0.104
Mn	0.000	0.001	0.001	0.001	0.001	0.001	0.001	0.000	0.002	0.001	0.001	0.000	0.003	0.002	0.000	0.000	0.001	0.000	0.000	0.001
Ni	0.003	0.005	0.003	0.004	0.005	0.004	0.002	0.004	0.003	0.003	0.004	0.005	0.003	0.004	0.003	0.005	0.004	0.004	0.004	0.004
Mg	0.602	0.575	0.588	0.606	0.606	0.623	0.616	0.622	0.633	0.634	0.643	0.637	0.643	0.643	0.649	0.649	0.649	0.658	0.656	0.650
Ca	0.743	0.739	0.745	0.736	0.737	0.745	0.745	0.747	0.754	0.746	0.753	0.759	0.756	0.764	0.762	0.760	0.766	0.752	0.760	0.756
Na	0.235	0.245	0.241	0.242	0.242	0.230	0.229	0.228	0.230	0.224	0.226	0.218	0.223	0.221	0.222	0.221	0.209	0.218	0.213	0.213
K	0.001	0.000	0.000	0.000	0.000	0.000	0.000	0.000	0.000	0.000	0.000	0.000	0.000	0.000	0.000	0.000	0.000	0.001	0.001	0.000
Sum	4.003	3.998	3.999	4.002	4.000	4.002	3.992	3.998	4.008	4.000	4.008	4.002	4.010	4.006	4.011	4.005	4.002	4.008	4.009	4.002
Mg#	87.50	86.99	86.98	87.45	86.70	86.17	86.64	85.91	86.36	85.68	85.96	85.96	84.94	85.85	85.96	86.88	86.53	85.90	85.86	86.21
Al IV	0.100	0.101	0.092	0.085	0.074	0.073	0.069	0.065	0.065	0.062	0.059	0.063	0.054	0.053	0.058	0.058	0.064	0.057	0.062	0.063
Al VI	0.333	0.346	0.333	0.327	0.315	0.303	0.298	0.292	0.294	0.286	0.284	0.281	0.277	0.271	0.277	0.277	0.273	0.274	0.276	0.275

1904-9 Cpx II, profile 515

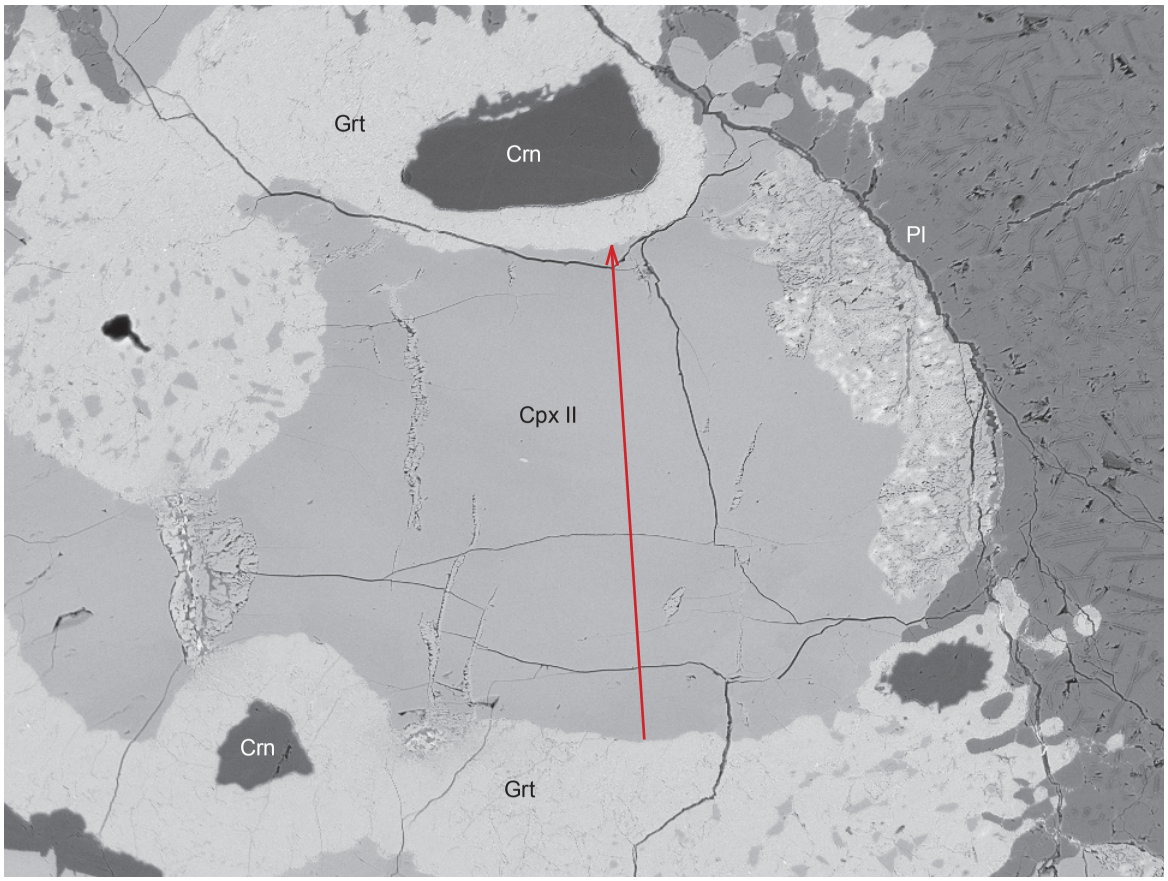
	210	220	230	240	250	260	270	280	290	300	310	320	330	340	350	360	370	380	390	400
SiO2	53.23	53.28	53.34	53.21	53.40	53.43	53.15	52.94	53.01	53.45	53.27	53.14	53.44	53.80	53.47	53.50	53.28	53.56	53.69	53.39
TiO2	0.02	0.02	0.02	0.01	0.02	0.01	0.04	0.02	0.03	0.04	0.00	0.00	0.03	0.03	0.02	0.01	0.01	0.03	0.03	0.05
Al2O3	7.76	7.75	7.69	7.79	7.85	7.86	7.87	7.78	7.74	7.88	7.83	7.84	7.87	7.91	7.74	7.81	7.73	7.87	7.82	7.89
Cr2O3	0.03	0.01	0.03	0.00	0.05	0.00	0.00	0.03	0.05	0.00	0.00	0.02	0.00	0.00	0.01	0.02	0.00	0.00	0.00	0.00
FeO	3.40	3.59	3.56	3.57	3.68	3.60	3.63	3.65	3.46	3.54	3.30	3.58	3.56	3.49	3.67	3.80	3.52	3.50	3.52	3.50
MnO	0.03	0.11	0.00	0.00	0.00	0.04	0.02	0.05	0.00	0.00	0.01	0.00	0.04	0.00	0.00	0.01	0.04	0.03	0.00	0.00
NiO	0.13	0.13	0.11	0.16	0.14	0.16	0.12	0.12	0.16	0.12	0.13	0.15	0.15	0.11	0.11	0.16	0.15	0.11	0.17	0.17
MgO	11.89	12.04	11.92	12.13	12.04	11.97	12.05	11.94	11.89	11.95	12.03	11.93	11.95	12.05	12.08	12.02	12.03	11.92	11.88	12.00
CaO	19.49	19.56	19.49	19.66	19.65	19.59	19.67	19.69	19.59	19.48	19.60	19.54	19.59	19.65	19.74	19.80	19.59	19.71	19.65	19.70
Na2O	3.10	3.03	3.00	2.97	3.06	2.94	3.06	2.99	2.91	3.07	2.98	3.01	3.05	3.08	2.95	3.06	3.01	2.98	3.00	2.95
K2O	0.00	0.00	0.02	0.00	0.02	0.02	0.00	0.00	0.02	0.00	0.00	0.00	0.00	0.02	0.00	0.00	0.00	0.01	0.01	0.01
Total	99.08	99.51	99.17	99.52	99.92	99.63	99.61	99.21	98.85	99.51	99.14	99.19	99.67	100.14	99.78	100.19	99.36	99.72	99.76	99.66
Si	1.938	1.933	1.940	1.931	1.931	1.935	1.928	1.929	1.935	1.937	1.936	1.933	1.935	1.937	1.935	1.931	1.935	1.937	1.940	1.933
Ti	0.001	0.000	0.000	0.000	0.000	0.000	0.001	0.001	0.001	0.001	0.000	0.000	0.001	0.001	0.000	0.000	0.000	0.001	0.001	0.001
Al	0.333	0.332	0.330	0.333	0.335	0.336	0.336	0.334	0.333	0.336	0.335	0.336	0.336	0.336	0.330	0.332	0.331	0.335	0.333	0.337
Cr	0.001	0.000	0.001	0.000	0.002	0.000	0.000	0.001	0.001	0.000	0.000	0.000	0.000	0.000	0.000	0.000	0.000	0.000	0.000	0.000
Fe2	0.104	0.109	0.108	0.108	0.111	0.109	0.110	0.111	0.106	0.107	0.100	0.109	0.108	0.105	0.111	0.115	0.107	0.106	0.106	0.106
Mn	0.001	0.003	0.000	0.000	0.000	0.001	0.001	0.002	0.000	0.000	0.000	0.000	0.001	0.000	0.000	0.000	0.001	0.001	0.000	0.000
Ni	0.004	0.004	0.003	0.005	0.004	0.005	0.003	0.003	0.005	0.003	0.004	0.004	0.004	0.003	0.003	0.005	0.004	0.003	0.005	0.005
Mg	0.645	0.651	0.646	0.656	0.649	0.646	0.652	0.648	0.647	0.645	0.652	0.647	0.645	0.647	0.651	0.647	0.651	0.643	0.640	0.648
Ca	0.760	0.761	0.760	0.764	0.761	0.760	0.764	0.768	0.766	0.756	0.763	0.762	0.760	0.758	0.765	0.766	0.763	0.764	0.761	0.764
Na	0.218	0.213	0.212	0.209	0.215	0.206	0.215	0.211	0.206	0.216	0.210	0.212	0.214	0.215	0.207	0.214	0.212	0.209	0.210	0.207
K	0.000	0.000	0.001	0.000	0.001	0.001	0.000	0.000	0.001	0.000	0.000	0.000	0.000	0.001	0.000	0.000	0.000	0.001	0.000	0.000
Sum	4.004	4.007	4.001	4.007	4.009	4.000	4.011	4.009	4.000	4.002	4.001	4.004	4.004	4.002	4.003	4.010	4.005	3.999	3.997	4.001
Mg#	86.11	85.66	85.68	85.86	85.39	85.56	85.56	85.38	85.92	85.77	86.70	85.58	85.66	86.04	85.43	84.91	85.88	85.85	85.79	85.94
Al IV	0.059	0.060	0.059	0.062	0.061	0.065	0.062	0.063	0.065	0.061	0.063	0.062	0.062	0.061	0.062	0.059	0.060	0.064	0.063	0.066
Al VI	0.274	0.273	0.271	0.271	0.275	0.272	0.275	0.271	0.269	0.275	0.273	0.274	0.274	0.275	0.269	0.273	0.272	0.272	0.271	0.271

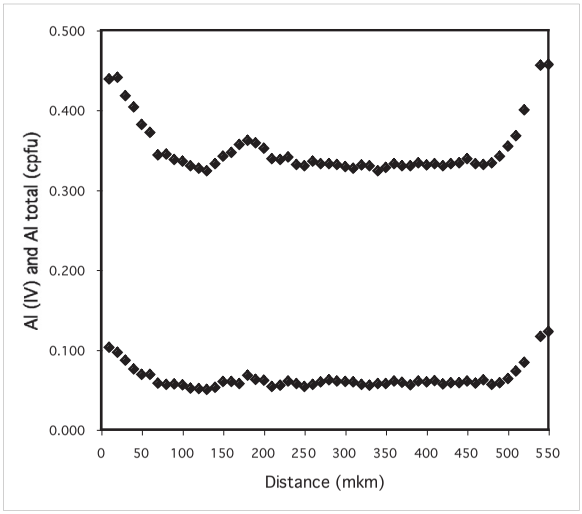
1904-9 Cpx II, profile 515

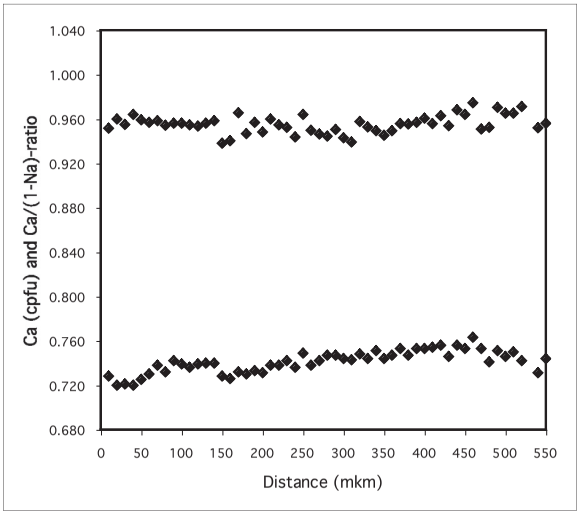
	410	420	430	440	450	460	470	480	490	500	510	520	530
SiO2	53.31	53.59	53.28	53.41	53.47	53.29	53.67	53.35	53.19	52.73	52.40	52.22	52.26
TiO2	0.01	0.02	0.00	0.01	0.02	0.00	0.03	0.00	0.03	0.00	0.01	0.00	0.03
Al2O3	7.81	7.84	7.98	7.95	7.89	8.00	8.30	8.66	9.22	9.50	10.53	10.85	10.64
Cr2O3	0.02	0.03	0.03	0.02	0.04	0.04	0.02	0.00	0.01	0.00	0.00	0.02	0.03
FeO	3.35	3.34	3.18	3.41	3.32	3.18	3.28	3.20	2.99	2.80	2.93	2.83	2.71
MnO	0.01	0.05	0.01	0.02	0.05	0.00	0.03	0.00	0.04	0.00	0.07	0.00	0.05
NiO	0.18	0.13	0.15	0.12	0.15	0.16	0.12	0.14	0.16	0.16	0.16	0.17	0.14
MgO	11.91	11.95	11.81	12.02	12.19	12.06	11.94	11.61	11.48	11.32	10.96	10.96	11.26
CaO	19.83	19.66	19.53	19.68	19.72	19.71	19.61	19.53	19.30	19.41	19.27	19.48	19.61
Na2O	3.09	2.97	3.11	3.10	3.07	2.96	3.01	3.13	3.22	3.30	3.39	3.25	3.08
K2O	0.00	0.00	0.01	0.01	0.00	0.00	0.00	0.01	0.00	0.00	0.03	0.00	0.04
Total	99.50	99.55	99.09	99.75	99.92	99.41	100.01	99.63	99.62	99.21	99.74	99.76	99.84
Si	1.934	1.940	1.937	1.932	1.931	1.931	1.932	1.928	1.919	1.911	1.890	1.882	1.882
Ti	0.000	0.000	0.000	0.000	0.001	0.000	0.001	0.000	0.001	0.000	0.000	0.000	0.001
Al	0.334	0.334	0.342	0.339	0.336	0.342	0.352	0.369	0.392	0.406	0.447	0.461	0.451
Cr	0.001	0.001	0.001	0.001	0.001	0.001	0.001	0.000	0.000	0.000	0.000	0.000	0.001
Fe2+	0.102	0.101	0.097	0.103	0.100	0.096	0.099	0.097	0.090	0.085	0.088	0.085	0.082
Mn	0.000	0.001	0.000	0.001	0.001	0.000	0.001	0.000	0.001	0.000	0.002	0.000	0.001
Ni	0.005	0.004	0.004	0.003	0.004	0.005	0.003	0.004	0.005	0.005	0.005	0.005	0.004
Mg	0.644	0.645	0.640	0.648	0.656	0.652	0.641	0.625	0.617	0.611	0.590	0.589	0.604
Ca	0.771	0.763	0.761	0.763	0.763	0.766	0.757	0.756	0.746	0.753	0.745	0.752	0.756
Na	0.217	0.208	0.219	0.218	0.215	0.208	0.210	0.219	0.225	0.232	0.237	0.227	0.215
K	0.000	0.000	0.000	0.001	0.000	0.000	0.000	0.000	0.000	0.000	0.001	0.000	0.002
Sum	4.007	3.997	4.001	4.007	4.008	4.001	3.996	3.998	3.997	4.002	4.005	4.001	4.000
Mg#	86.33	86.46	86.84	86.28	86.77	87.17	86.62	86.57	87.27	87.79	87.02	87.39	88.05
Al IV	0.059	0.064	0.062	0.061	0.062	0.068	0.073	0.075	0.085	0.087	0.105	0.117	0.119
Al VI	0.275	0.271	0.280	0.279	0.274	0.275	0.280	0.294	0.308	0.319	0.343	0.344	0.333

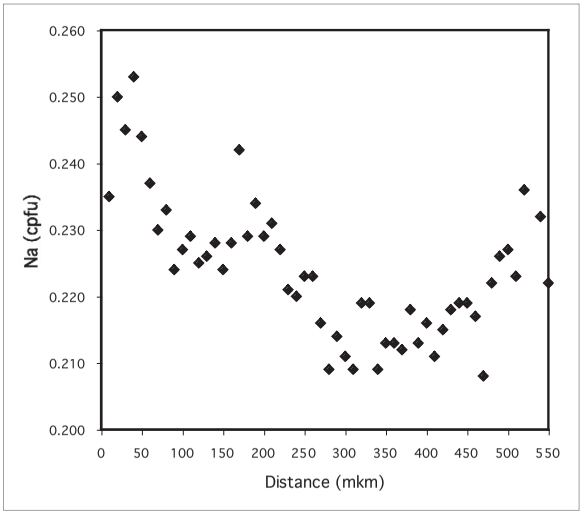
1904-9 Cpx II, profile 515

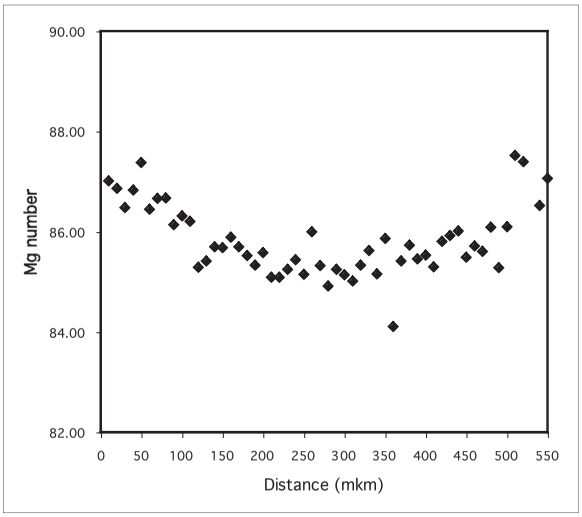
1904-9 Cpx II, profile 540











	10	20	30	40	50	60	70	80	90	100	110	120	130	140	150	160	170	180	190	200
SiO2	53.08	53.00	53.44	53.45	53.99	53.93	53.73	54.15	53.77	53.96	54.01	54.02	54.04	54.02	54.03	53.74	53.82	53.68	53.85	53.69
TiO2	0.05	0.03	0.02	0.01	0.01	0.02	0.04	0.02	0.01	0.03	0.03	0.00	0.03	0.00	0.02	0.00	0.02	0.03	0.00	0.01
Al2O3	10.39	10.43	9.90	9.56	9.05	8.81	8.08	8.13	7.94	7.92	7.77	7.72	7.63	7.86	8.05	8.15	8.41	8.51	8.49	8.28
Cr2O3	0.01	0.00	0.00	0.00	0.02	0.05	0.01	0.04	0.00	0.03	0.03	0.01	0.00	0.03	0.00	0.03	0.01	0.03	0.04	0.02
FeO	2.97	3.00	3.11	3.11	2.96	3.26	3.26	3.26	3.43	3.38	3.48	3.76	3.68	3.59	3.57	3.50	3.50	3.53	3.60	3.57
MnO	0.04	0.01	0.08	0.03	0.01	0.03	0.02	0.00	0.00	0.00	0.02	0.04	0.00	0.02	0.00	0.03	0.00	0.01	0.05	0.05
NiO	0.15	0.12	0.18	0.16	0.12	0.12	0.12	0.17	0.13	0.13	0.16	0.16	0.14	0.11	0.18	0.14	0.09	0.10	0.18	0.17
MgO	11.15	11.13	11.13	11.47	11.53	11.70	11.94	11.88	12.00	11.96	12.24	12.22	12.09	12.06	11.92	11.98	11.71	11.64	11.74	11.92
CaO	18.96	18.73	18.76	18.73	18.88	19.03	19.07	19.00	19.18	19.13	19.08	19.20	19.17	19.20	18.86	18.76	18.97	18.87	19.05	18.94
Na2O	3.39	3.59	3.52	3.64	3.51	3.41	3.28	3.35	3.20	3.24	3.28	3.23	3.23	3.27	3.21	3.25	3.46	3.28	3.37	3.28
K2O	0.01	0.01	0.01	0.00	0.00	0.00	0.01	0.01	0.00	0.01	0.02	0.01	0.00	0.00	0.01	0.00	0.00	0.00	0.01	0.01
Total	100.19	100.03	100.14	100.16	100.07	100.37	99.54	100.00	99.67	99.79	100.11	100.38	100.02	100.15	99.85	99.57	100.00	99.66	100.38	99.92
Si	1.902	1.902	1.916	1.917	1.935	1.932	1.941	1.946	1.942	1.946	1.943	1.942	1.947	1.943	1.947	1.941	1.937	1.937	1.933	1.935
Ti	0.001	0.001	0.000	0.000	0.000	0.001	0.001	0.000	0.000	0.001	0.001	0.000	0.001	0.000	0.001	0.000	0.000	0.001	0.000	0.000
Al	0.439	0.441	0.418	0.404	0.382	0.372	0.344	0.345	0.338	0.336	0.330	0.327	0.324	0.333	0.342	0.347	0.357	0.362	0.359	0.352
Cr	0.000	0.000	0.000	0.000	0.000	0.001	0.000	0.001	0.000	0.001	0.001	0.000	0.000	0.001	0.000	0.001	0.000	0.001	0.001	0.000
Fe2+	0.089	0.090	0.093	0.093	0.089	0.098	0.099	0.098	0.104	0.102	0.105	0.113	0.111	0.108	0.107	0.106	0.105	0.106	0.108	0.108
Mn	0.001	0.000	0.002	0.001	0.000	0.001	0.000	0.000	0.000	0.000	0.000	0.001	0.000	0.000	0.000	0.001	0.000	0.000	0.002	0.002
Ni	0.004	0.003	0.005	0.005	0.003	0.003	0.003	0.005	0.004	0.004	0.005	0.005	0.004	0.003	0.005	0.004	0.003	0.003	0.005	0.005
Mg	0.596	0.595	0.595	0.613	0.616	0.625	0.643	0.637	0.646	0.643	0.656	0.655	0.650	0.647	0.640	0.645	0.629	0.626	0.628	0.641
Ca	0.728	0.720	0.721	0.720	0.725	0.730	0.738	0.732	0.742	0.739	0.736	0.739	0.740	0.740	0.728	0.726	0.732	0.730	0.733	0.731
Na	0.235	0.250	0.245	0.253	0.244	0.237	0.230	0.233	0.224	0.227	0.229	0.225	0.226	0.228	0.224	0.228	0.242	0.229	0.234	0.229
K	0.000	0.000	0.000	0.000	0.000	0.000	0.000	0.000	0.000	0.000	0.001	0.000	0.000	0.000	0.000	0.000	0.000	0.000	0.001	0.000
Sum	3.995	4.002	3.996	4.007	3.995	3.999	4.001	3.997	4.001	3.998	4.006	4.007	4.003	4.004	3.994	3.999	4.005	3.995	4.004	4.003
Mg#	87.01	86.86	86.48	86.83	87.38	86.45	86.66	86.67	86.13	86.31	86.20	85.29	85.41	85.70	85.68	85.89	85.69	85.52	85.33	85.58
Al IV	0.103	0.097	0.087	0.076	0.069	0.069	0.058	0.057	0.057	0.056	0.052	0.051	0.050	0.053	0.060	0.060	0.058	0.068	0.063	0.062
Al VI	0.336	0.345	0.332	0.329	0.313	0.303	0.286	0.289	0.281	0.280	0.279	0.276	0.274	0.280	0.282	0.287	0.300	0.294	0.297	0.291

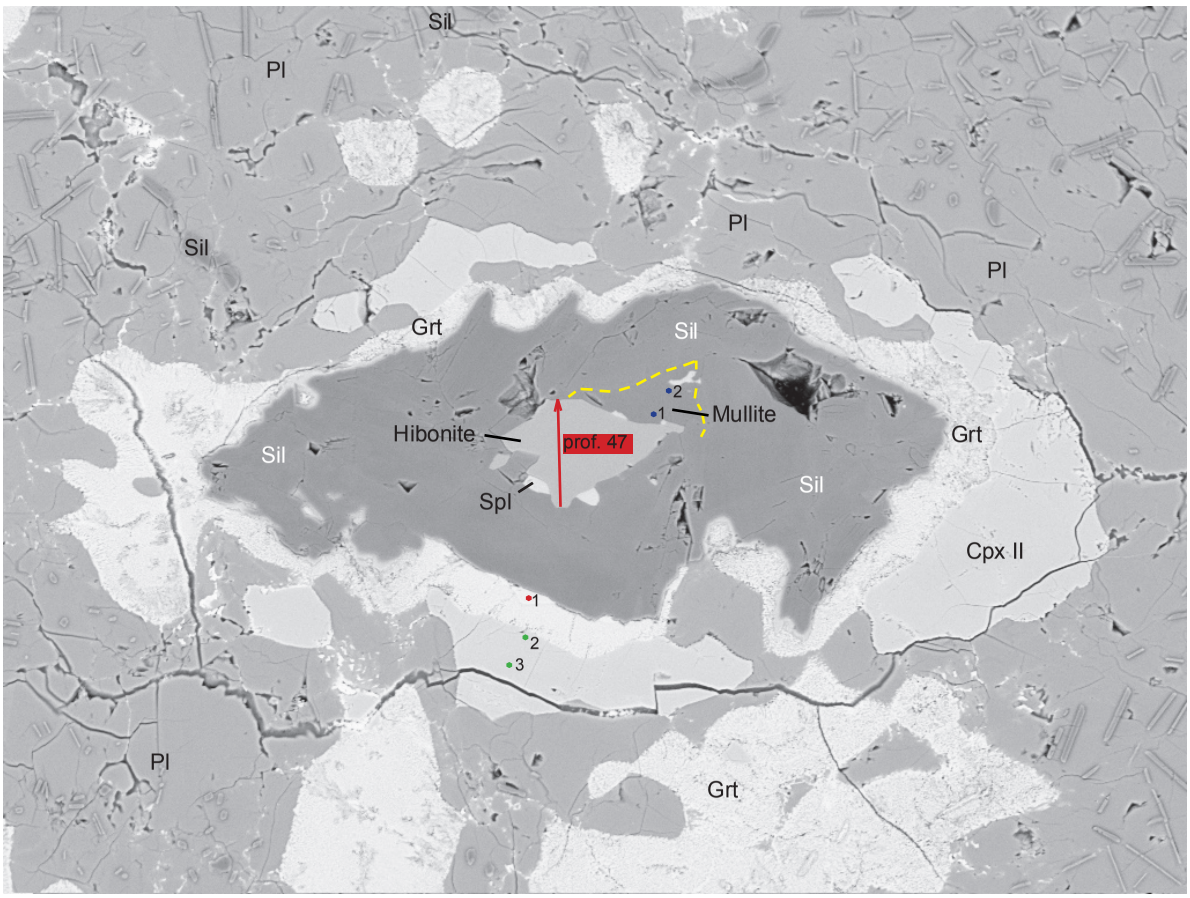
1904-9 Cpx II, profile 540

	210	220	230	240	250	260	270	280	290	300	310	320	330	340	350	360	370	380	390	400
SiO2	53.92	53.76	53.61	53.66	53.62	53.79	53.78	53.73	53.41	53.70	53.44	53.55	53.81	53.36	53.67	53.25	53.62	53.43	53.26	53.49
TiO2	0.00	0.00	0.02	0.02	0.01	0.02	0.05	0.01	0.03	0.02	0.01	0.00	0.02	0.01	0.00	0.00	0.00	0.00	0.00	0.02
Al2O3	8.00	7.95	8.02	7.78	7.74	7.89	7.83	7.85	7.76	7.74	7.64	7.78	7.77	7.56	7.69	7.79	7.76	7.72	7.81	7.76
Cr2O3	0.00	0.02	0.03	0.02	0.03	0.01	0.00	0.01	0.04	0.01	0.03	0.02	0.01	0.04	0.00	0.02	0.00	0.01	0.00	0.05
FeO	3.73	3.69	3.72	3.70	3.68	3.52	3.70	3.86	3.74	3.81	3.80	3.78	3.68	3.76	3.57	4.10	3.70	3.60	3.68	3.63
MnO	0.05	0.00	0.05	0.05	0.00	0.02	0.00	0.00	0.03	0.08	0.06	0.02	0.04	0.05	0.00	0.04	0.00	0.03	0.08	0.02
NiO	0.18	0.14	0.15	0.12	0.20	0.12	0.14	0.11	0.14	0.12	0.15	0.11	0.13	0.11	0.14	0.11	0.15	0.12	0.13	0.16
MgO	11.91	11.86	12.03	12.18	11.90	12.09	12.11	12.15	12.08	12.26	12.15	12.34	12.31	12.06	12.14	12.13	12.19	12.10	12.17	12.05
CaO	19.15	19.06	19.19	19.00	19.30	19.08	19.20	19.34	19.23	19.26	19.09	19.36	19.29	19.27	19.16	19.23	19.46	19.22	19.39	19.42
Na2O	3.31	3.24	3.16	3.14	3.17	3.18	3.09	2.98	3.04	3.02	2.97	3.14	3.13	2.96	3.03	3.04	3.02	3.10	3.03	3.07
K2O	0.00	0.02	0.00	0.01	0.00	0.00	0.01	0.00	0.01	0.00	0.00	0.00	0.00	0.01	0.00	0.01	0.00	0.00	0.01	0.00
Total	100.25	99.74	99.99	99.69	99.65	99.72	99.91	100.03	99.51	100.02	99.33	100.11	100.18	99.19	99.39	99.71	99.90	99.33	99.55	99.68
Si	1.940	1.943	1.934	1.940	1.941	1.942	1.940	1.937	1.937	1.937	1.941	1.932	1.937	1.941	1.945	1.931	1.937	1.940	1.932	1.937
Ti	0.000	0.000	0.000	0.001	0.000	0.000	0.001	0.000	0.001	0.001	0.000	0.000	0.000	0.000	0.000	0.000	0.000	0.000	0.000	0.001
Al	0.339	0.338	0.341	0.332	0.330	0.336	0.333	0.333	0.332	0.329	0.327	0.331	0.330	0.324	0.328	0.333	0.330	0.330	0.334	0.331
Cr	0.000	0.001	0.001	0.001	0.001	0.000	0.000	0.000	0.001	0.000	0.001	0.001	0.000	0.001	0.000	0.001	0.000	0.000	0.000	0.002
Fe2+	0.112	0.112	0.112	0.112	0.112	0.106	0.112	0.116	0.113	0.115	0.116	0.114	0.111	0.114	0.108	0.124	0.112	0.109	0.112	0.110
Mn	0.002	0.000	0.002	0.001	0.000	0.001	0.000	0.000	0.001	0.002	0.002	0.000	0.001	0.001	0.000	0.001	0.000	0.001	0.002	0.001
Ni	0.005	0.004	0.004	0.003	0.006	0.003	0.004	0.003	0.004	0.004	0.004	0.003	0.004	0.003	0.004	0.003	0.004	0.003	0.004	0.005
Mg	0.639	0.639	0.647	0.657	0.642	0.651	0.651	0.653	0.653	0.659	0.658	0.663	0.661	0.654	0.656	0.656	0.656	0.655	0.658	0.650
Ca	0.738	0.738	0.742	0.736	0.749	0.738	0.742	0.747	0.747	0.744	0.743	0.748	0.744	0.751	0.744	0.747	0.753	0.747	0.753	0.753
Na	0.231	0.227	0.221	0.220	0.223	0.223	0.216	0.209	0.214	0.211	0.209	0.219	0.219	0.209	0.213	0.213	0.212	0.218	0.213	0.216
K	0.000	0.001	0.000	0.000	0.000	0.000	0.000	0.000	0.000	0.000	0.000	0.000	0.000	0.001	0.000	0.000	0.000	0.000	0.000	0.000
Sum	4.006	4.002	4.005	4.004	4.004	4.001	4.000	4.000	4.003	4.003	4.000	4.012	4.007	4.001	3.997	4.009	4.004	4.004	4.008	4.004
Mg#	85.09	85.09	85.24	85.44	85.15	86.00	85.32	84.92	85.25	85.14	85.01	85.33	85.62	85.16	85.86	84.10	85.42	85.73	85.45	85.53
Al IV	0.054	0.056	0.061	0.058	0.054	0.057	0.060	0.062	0.061	0.060	0.060	0.057	0.056	0.058	0.058	0.061	0.059	0.056	0.061	0.060
Al VI	0.285	0.283	0.281	0.275	0.276	0.280	0.274	0.271	0.272	0.269	0.268	0.275	0.275	0.267	0.271	0.273	0.271	0.274	0.274	0.272

1904-9 Cpx II, profile 540

	410	420	430	440	450	460	470	480	490	500	510	520	530	540	550
SiO2	53.59	53.78	53.74	53.48	53.53	53.46	53.79	53.98	53.62	53.78	53.45	53.35	41.91	52.79	52.24
TiO2	0.02	0.00	0.04	0.03	0.01	0.02	0.01	0.01	0.01	0.00	0.01	0.00	0.02	0.02	0.00
Al2O3	7.79	7.78	7.84	7.85	7.96	7.81	7.82	7.89	8.06	8.41	8.67	9.48	13.00	10.83	10.77
Cr2O3	0.01	0.00	0.00	0.00	0.02	0.00	0.00	0.05	0.04	0.05	0.02	0.13	0.06	0.30	0.39
FeO	3.68	3.58	3.54	3.53	3.64	3.56	3.64	3.52	3.69	3.44	3.03	2.97	1.06	3.04	2.92
MnO	0.00	0.00	0.02	0.00	0.00	0.09	0.01	0.00	0.04	0.08	0.05	0.00	0.05	0.00	0.03
NiO	0.12	0.15	0.15	0.11	0.16	0.15	0.15	0.22	0.17	0.11	0.12	0.12		0.16	0.13
MgO	11.93	12.17	12.14	12.22	12.03	12.02	12.17	12.25	11.97	11.94	11.88	11.56	3.30	10.95	11.03
CaO	19.43	19.60	19.30	19.53	19.45	19.71	19.49	19.26	19.46	19.40	19.42	19.31	11.01	19.08	19.29
Na2O	3.01	3.08	3.11	3.13	3.13	3.10	2.97	3.20	3.24	3.26	3.19	3.40	0.98	3.34	3.18
K2O	0.00	0.03	0.00	0.00	0.00	0.00	0.00	0.00	0.00	0.01	0.01	0.00	0.19	0.00	0.01
Total	99.56	100.17	99.86	99.89	99.92	99.93	100.06	100.36	100.29	100.47	99.85	100.33	71.64	100.50	100.00
Si	1.941	1.937	1.939	1.932	1.933	1.933	1.938	1.938	1.931	1.929	1.926	1.912		1.888	1.879
Ti	0.000	0.000	0.001	0.001	0.000	0.000	0.000	0.000	0.000	0.000	0.000	0.000		0.000	0.000
Al	0.333	0.330	0.333	0.334	0.339	0.333	0.332	0.334	0.342	0.355	0.368	0.400		0.456	0.457
Cr	0.000	0.000	0.000	0.000	0.001	0.000	0.000	0.001	0.001	0.001	0.001	0.004		0.009	0.011
Fe2+	0.111	0.108	0.107	0.107	0.110	0.108	0.110	0.106	0.111	0.103	0.091	0.089		0.091	0.088
Mn	0.000	0.000	0.000	0.000	0.000	0.003	0.000	0.000	0.001	0.003	0.002	0.000		0.000	0.001
Ni	0.003	0.004	0.004	0.003	0.005	0.004	0.004	0.006	0.005	0.003	0.004	0.003		0.005	0.004
Mg	0.644	0.653	0.653	0.658	0.648	0.648	0.654	0.656	0.643	0.638	0.638	0.617		0.584	0.592
Ca	0.754	0.756	0.746	0.756	0.753	0.763	0.753	0.741	0.751	0.746	0.750	0.742		0.731	0.744
Na	0.211	0.215	0.218	0.219	0.219	0.217	0.208	0.222	0.226	0.227	0.223	0.236		0.232	0.222
K	0.000	0.001	0.000	0.000	0.000	0.000	0.000	0.000	0.000	0.001	0.000	0.000		0.000	0.000
Sum	3.998	4.006	4.002	4.010	4.007	4.009	3.999	4.005	4.011	4.006	4.001	4.004		3.995	3.998
Mg#	85.30	85.81	85.92	86.01	85.49	85.71	85.60	86.09	85.28	86.10	87.52	87.39		86.52	87.06
Al IV	0.061	0.057	0.059	0.059	0.061	0.058	0.062	0.057	0.059	0.064	0.073	0.084		0.117	0.123
Al VI	0.272	0.273	0.275	0.276	0.279	0.275	0.270	0.278	0.284	0.291	0.295	0.316		0.340	0.334

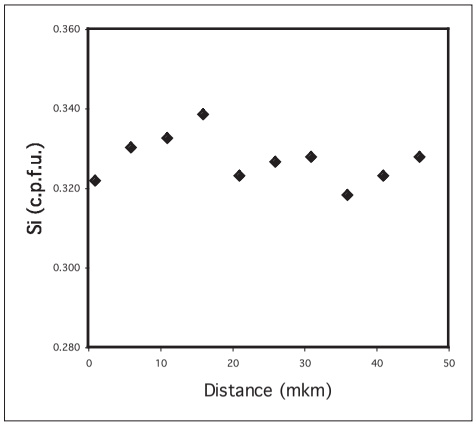
1904-9 Cpx II, profile 540

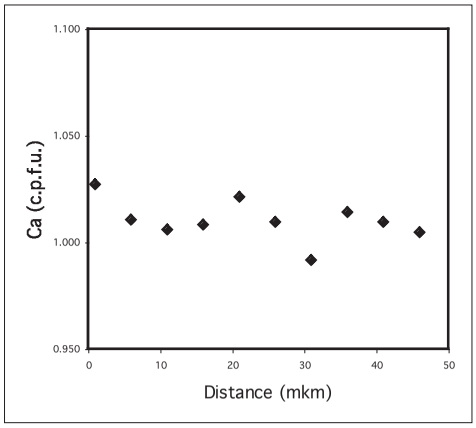


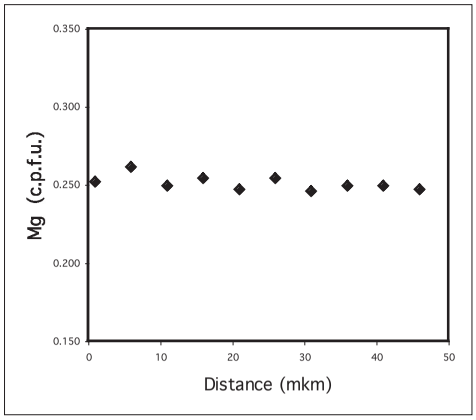
1904-9 Hibonite, profile 47

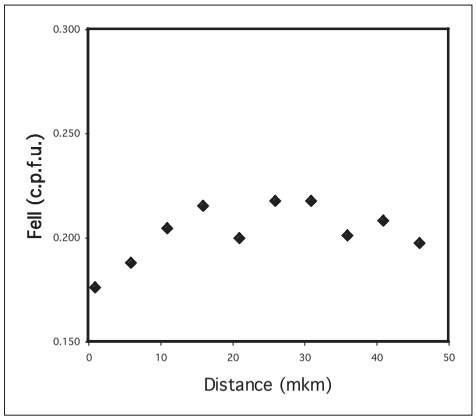
	1	6	11	16	21	26	31	36	41	46
SiO2	2.85	2.94	2.96	3.02	2.88	2.91	2.93	2.85	2.89	2.93
TiO2	0.24	0.25	0.22	0.26	0.16	0.19	0.20	0.20	0.24	0.25
Al2O3	84.59	84.93	84.76	84.81	84.84	84.82	85.24	85.23	84.94	84.95
Cr2O3	0.06	0.03	0.09	0.10	0.10	0.12	0.11	0.06	0.05	0.06
FeO	1.87	2.00	2.18	2.30	2.12	2.32	2.33	2.15	2.22	2.10
MnO	0.02	0.00	0.02	0.03	0.00	0.03	0.00	0.00	0.00	0.02
ZnO	0.15	0.26	0.12	0.18	0.18	0.22	0.27	0.26	0.26	0.19
MgO	1.50	1.57	1.49	1.52	1.48	1.53	1.48	1.50	1.49	1.48
CaO	8.52	8.42	8.37	8.42	8.50	8.41	8.29	8.48	8.42	8.37
Na2O	0.02	0.00	0.01	0.03	0.02	0.02	0.04	0.00	0.03	0.01
K2O	0.00	0.01	0.00	0.00	0.01	0.00	0.00	0.01	0.00	0.01
Total	99.82	100.41	100.20	100.67	100.28	100.56	100.89	100.73	100.53	100.37
Si	0.322	0.330	0.333	0.338	0.323	0.327	0.328	0.318	0.323	0.328
Ti	0.020	0.021	0.018	0.021	0.014	0.015	0.017	0.017	0.020	0.021
Al	11.224	11.209	11.210	11.179	11.220	11.197	11.211	11.223	11.210	11.217
Cr	0.005	0.002	0.008	0.008	0.008	0.011	0.010	0.005	0.005	0.005
Fe2	0.176	0.188	0.204	0.215	0.200	0.217	0.217	0.201	0.208	0.197
Mn	0.002	0.000	0.002	0.002	0.000	0.002	0.000	0.000	0.000	0.002
Zn	0.012	0.021	0.010	0.015	0.014	0.018	0.023	0.021	0.021	0.015
Mg	0.252	0.261	0.249	0.254	0.247	0.254	0.246	0.249	0.249	0.247
Ca	1.027	1.011	1.006	1.008	1.021	1.009	0.992	1.014	1.009	1.005
Na	0.005	0.001	0.001	0.007	0.005	0.005	0.008	0.001	0.006	0.001
K	0.000	0.001	0.000	0.000	0.001	0.000	0.000	0.001	0.000	0.002
Sum	13.046	13.045	13.041	13.049	13.053	13.057	13.049	13.052	13.052	13.041
O	19	19	19	19	19	19	19	19	19	19

1904-9 Hibonite, profile 47







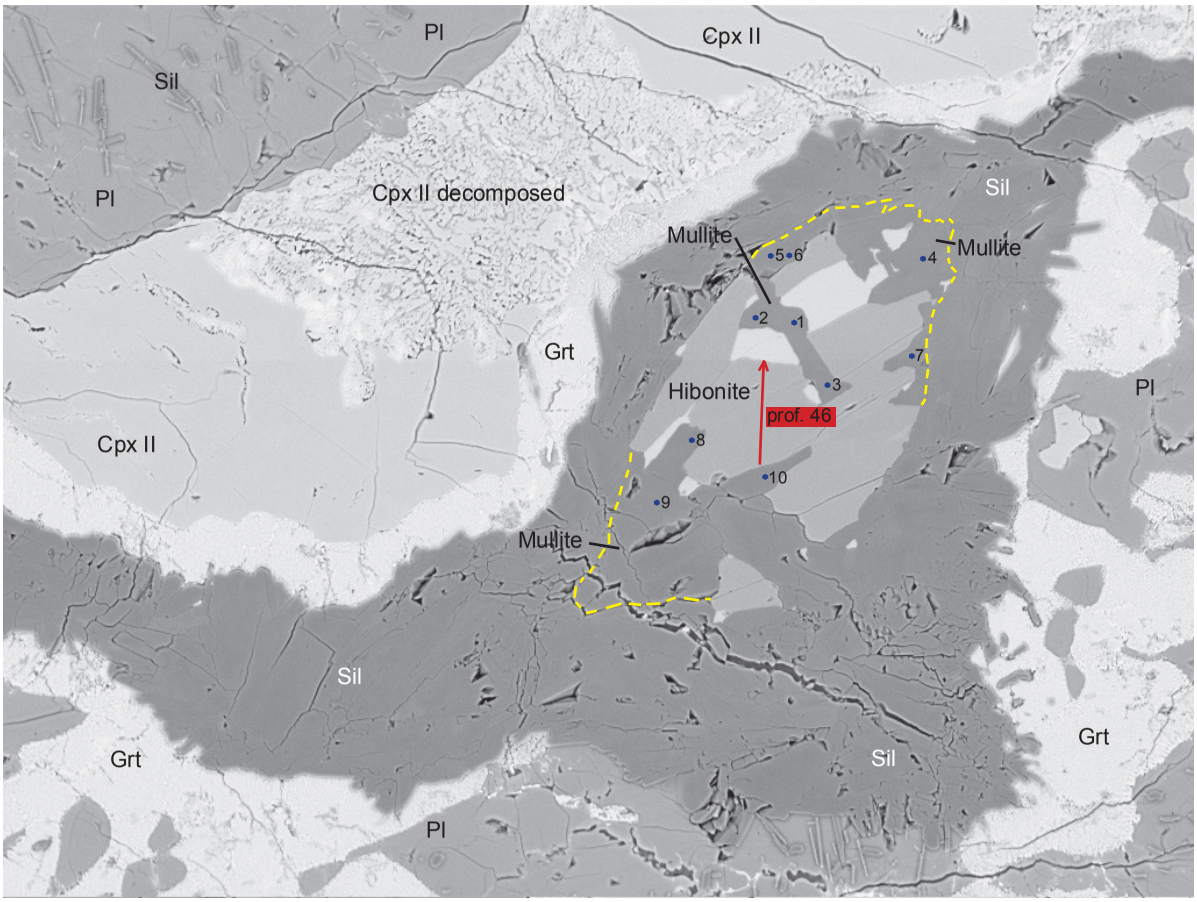


1904-9 Mullite Al2SiO5*Al2O3, an. 1 & 2

	1	2
SiO2	22.50	22.28
TiO2	0.04	0.00
Al2O3	77.16	77.02
Cr2O3	0.10	0.12
FeO	0.36	0.31
MnO	0.00	0.00
ZnO	0.00	0.05
MgO	0.02	0.02
CaO	0.03	0.00
Na2O	0.00	0.00
K2O	0.01	0.01
Total	100.21	99.82
Si	0.988	0.983
Ti	0.001	0.000
Al	3.995	4.005
Cr	0.003	0.004
Fe3+	0.013	0.011
Mn	0.000	0.000
Zn	0.000	0.001
Mg	0.002	0.001
Ca	0.002	0.000
Na	0.000	0.000
K	0.000	0.001
Sum	5.005	5.007
O	8.000	8.000

1904-9 Grt (1) and Cpx (2 & 3)

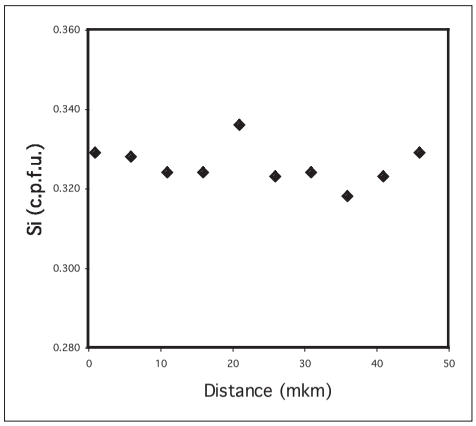
	1 Grt	2 Cpx	3 Cpx
SiO2	40.08	51.74	51.33
TiO2	0.03	0.01	0.01
Al2O3	22.81	10.73	11.75
Cr2O3	0.03	0.04	0.00
FeO	14.41	2.93	2.84
MnO	0.20	0.03	0.01
NiO	0.07	0.20	0.10
MgO	11.45	11.51	11.01
CaO	11.45	19.89	19.73
Na2O	0.01	2.88	3.04
K2O	0.01	0.00	0.00
Total	100.52	99.97	99.82
Si	2.965	1.865	1.851
Ti	0.002	0.000	0.000
Al	1.989	0.456	0.499
Cr	0.002	0.001	0.000
Fe2	0.891	0.088	0.086
Mn	0.012	0.001	0.000
Ni	0.004	0.006	0.003
Mg	1.263	0.619	0.592
Ca	0.908	0.768	0.762
Na	0.001	0.202	0.212
K	0.000	0.000	0.000
Sum	8.038	4.007	4.005

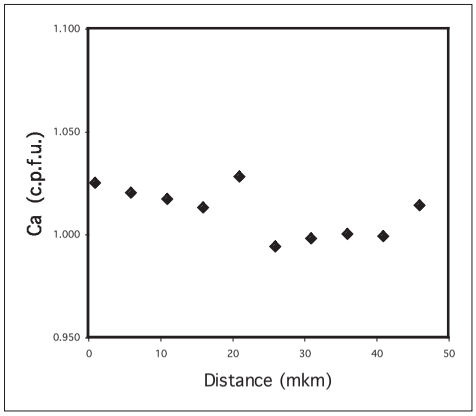


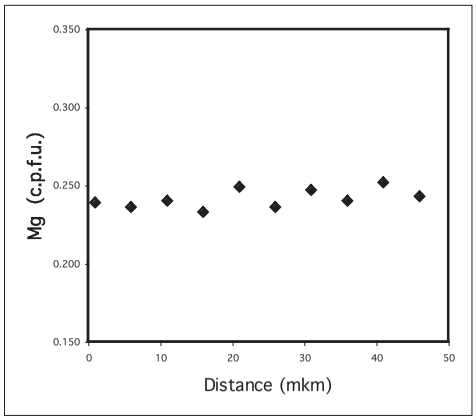
1904-9 Hibonite, profile 46

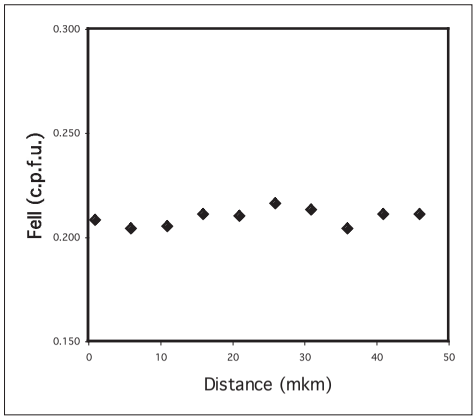
	1	6	11	16	21	26	31	36	41	46
SiO2	2.91	2.91	2.87	2.86	2.98	2.88	2.87	2.83	2.87	2.92
TiO2	0.02	0.07	0.12	0.09	0.02	0.06	0.06	0.09	0.10	0.10
Al2O3	84.42	84.62	84.15	84.09	84.15	84.78	84.33	84.79	84.45	84.39
Cr2O3	0.09	0.22	0.28	0.19	0.23	0.25	0.15	0.25	0.29	0.18
FeO	2.20	2.17	2.17	2.23	2.23	2.30	2.25	2.17	2.24	2.24
MnO	0.01	0.06	0.02	0.00	0.00	0.01	0.00	0.00	0.00	0.00
ZnO	0.13	0.18	0.21	0.16	0.19	0.10	0.21	0.17	0.29	0.22
MgO	1.42	1.41	1.43	1.38	1.49	1.41	1.47	1.43	1.50	1.45
CaO	8.48	8.47	8.39	8.35	8.50	8.25	8.24	8.30	8.28	8.40
Na2O	0.03	0.00	0.02	0.03	0.04	0.00	0.02	0.01	0.02	0.02
K2O	0.02	0.00	0.01	0.02	0.00	0.01	0.00	0.00	0.00	0.00
Total	99.74	100.11	99.65	99.40	99.83	100.04	99.59	100.03	100.03	99.92
Si	0.329	0.328	0.324	0.324	0.336	0.323	0.324	0.318	0.323	0.329
Ti	0.002	0.006	0.010	0.007	0.002	0.005	0.006	0.007	0.008	0.008
Al	11.225	11.215	11.208	11.224	11.190	11.235	11.230	11.237	11.208	11.209
Cr	0.008	0.019	0.025	0.017	0.020	0.023	0.013	0.021	0.026	0.017
Fe2+	0.208	0.204	0.205	0.211	0.210	0.216	0.213	0.204	0.211	0.211
Mn	0.001	0.006	0.001	0.000	0.000	0.000	0.000	0.000	0.000	0.000
Zn	0.011	0.014	0.018	0.014	0.015	0.008	0.018	0.014	0.024	0.019
Mg	0.239	0.236	0.240	0.233	0.249	0.236	0.247	0.240	0.252	0.243
Ca	1.025	1.020	1.017	1.013	1.028	0.994	0.998	1.000	0.999	1.014
Na	0.007	0.000	0.005	0.007	0.008	0.001	0.004	0.002	0.005	0.005
K	0.002	0.000	0.001	0.002	0.000	0.002	0.000	0.000	0.000	0.000
Sum	13.057	13.049	13.053	13.053	13.061	13.045	13.052	13.046	13.055	13.053
O	19	19	19	19	19	19	19	19	19	19

1904-9 Hibonite, profile 46









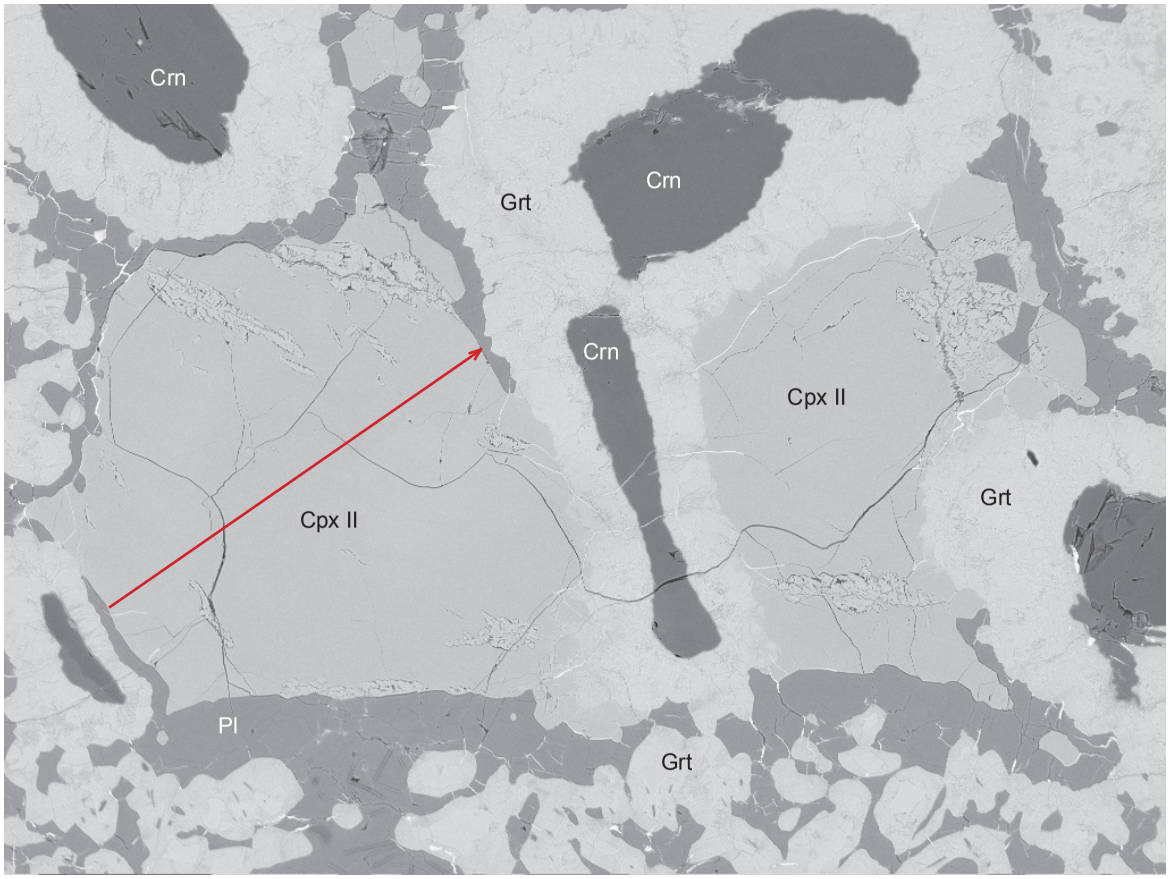
1904-9 Mullite
Al2SiO5*Al2O3, an. 1-10

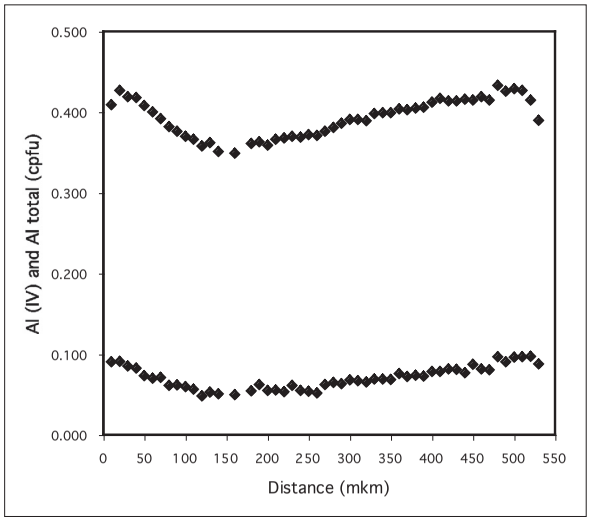
	1	2	3	4	5
SiO2	22.83	22.41	22.83	22.54	22.57
TiO2	0.00	0.03	0.00	0.00	0.00
Al2O3	76.54	77.28	76.94	76.88	76.61
Cr2O3	0.39	0.29	0.37	0.26	0.27
FeO	0.36	0.44	0.42	0.38	0.39
MnO	0.01	0.00	0.02	0.02	0.02
NiO	0.00	0.03	0.05	0.00	0.02
MgO	0.04	0.05	0.01	0.05	0.03
CaO	0.00	0.01	0.05	0.01	0.01
Na2O	0.00	0.01	0.00	0.00	0.00
K2O	0.01	0.00	0.01	0.02	0.00
Total	100.17	100.55	100.70	100.16	99.90
Si	1.004	0.982	0.999	0.991	0.995
Ti	0.000	0.001	0.000	0.000	0.000
Al	3.966	3.993	3.969	3.985	3.981
Cr	0.014	0.010	0.013	0.009	0.009
Fe3+	0.013	0.016	0.015	0.014	0.014
Fe2+	0.000	0.000	0.000	0.000	0.000
Mn	0.000	0.000	0.001	0.001	0.001
Ni	0.000	0.001	0.002	0.000	0.001
Mg	0.003	0.003	0.001	0.003	0.002
Ca	0.000	0.000	0.002	0.000	0.000
Na	0.000	0.001	0.000	0.000	0.000
K	0.000	0.000	0.001	0.001	0.000
Sum	5.000	5.008	5.002	5.005	5.003

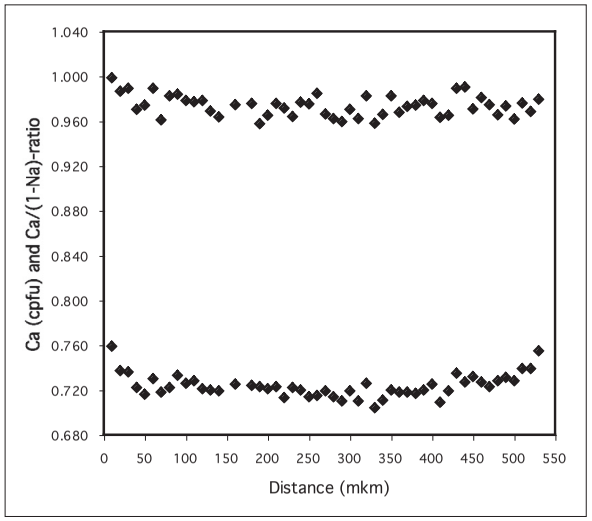
	6	7	8	9	10
SiO2	22.47	22.31	22.46	22.25	22.64
TiO2	0.00	0.00	0.00	0.02	0.01
Al2O3	76.79	76.57	76.84	76.76	76.63
Cr2O3	0.40	0.35	0.18	0.35	0.29
FeO	0.44	0.40	0.37	0.31	0.35
MnO	0.00	0.00	0.00	0.00	0.02
NiO	0.01	0.00	0.01	0.01	0.01
MgO	0.03	0.02	0.03	0.01	0.03
CaO	0.02	0.01	0.08	0.00	0.02
Na2O	0.00	0.02	0.00	0.00	0.01
K2O	0.00	0.00	0.00	0.00	0.00
Total	100.16	99.68	99.97	99.71	100.01
Si	0.989	0.986	0.990	0.983	0.997
Ti	0.000	0.000	0.000	0.001	0.000
Al	3.983	3.989	3.990	3.997	3.977
Cr	0.014	0.012	0.006	0.012	0.010
Fe3+	0.016	0.015	0.014	0.011	0.013
Fe2+	0.000	0.000	0.000	0.000	0.000
Mn	0.000	0.000	0.000	0.000	0.001
Ni	0.000	0.000	0.000	0.000	0.000
Mg	0.002	0.001	0.002	0.001	0.002
Ca	0.001	0.000	0.004	0.000	0.001
Na	0.000	0.002	0.000	0.000	0.001
K	0.000	0.000	0.000	0.000	0.000
Sum	5.005	5.006	5.006	5.006	5.003
O	8	8	8	8	8

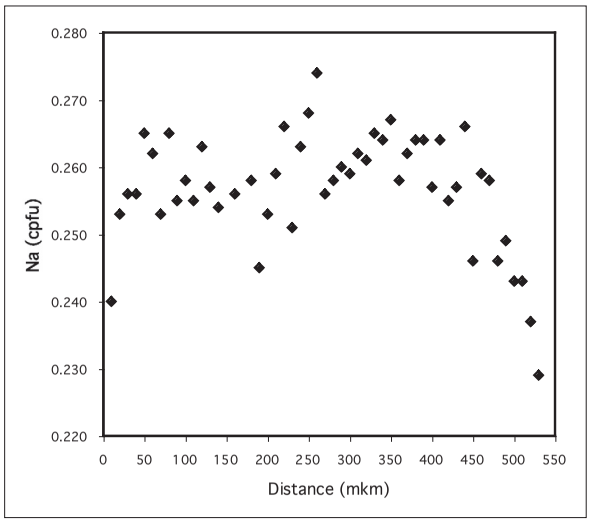
Ca-Al granulite 1906-2

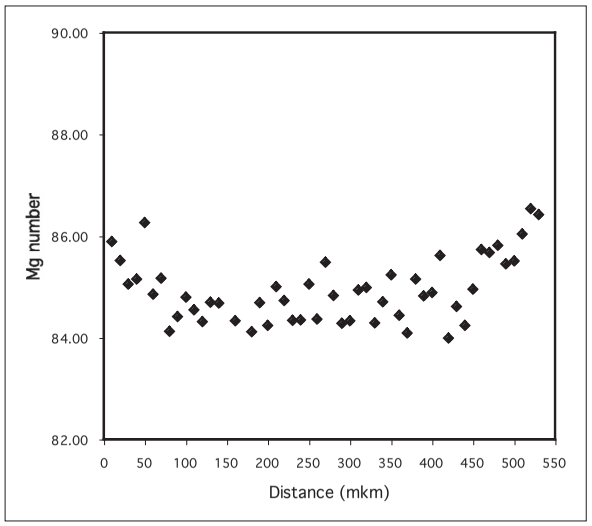
1906-2 Cpx II, profile 525











	10	20	30	40	50	60	70	80	90	100	110	120	130	140	150	160	170	180	190	200
SiO2	51.76	52.12	52.11	52.53	52.72	52.88	53.04	52.67	53.08	53.00	52.93	53.25	53.29	53.31	52.38	53.19	52.32	53.07	53.18	53.21
TiO2	0.03	0.04	0.06	0.00	0.01	0.01	0.04	0.02	0.01	0.06	0.04	0.01	0.01	0.05	0.09	0.06	0.04	0.04	0.07	0.05
Al2O3	9.56	10.03	9.79	9.80	9.55	9.44	9.20	8.93	8.86	8.67	8.57	8.40	8.49	8.24	8.63	8.17	8.54	8.51	8.53	8.43
Cr2O3	0.34	0.21	0.13	0.14	0.09	0.09	0.06	0.10	0.06	0.10	0.04	0.07	0.04	0.08	0.05	0.10	0.07	0.13	0.09	0.07
FeO	3.35	3.39	3.49	3.50	3.19	3.65	3.58	3.86	3.86	3.73	3.80	3.86	3.77	3.83	4.05	3.90	3.97	4.05	3.80	3.93
MnO	0.01	0.02	0.00	0.05	0.01	0.01	0.00	0.00	0.07	0.00	0.00	0.04	0.02	0.04	0.07	0.02	0.00	0.04	0.01	0.02
NiO	0.14	0.17	0.10	0.08	0.14	0.14	0.15	0.17	0.12	0.16	0.12	0.21	0.11	0.13	0.13	0.12	0.16	0.13	0.10	0.12
MgO	11.46	11.29	11.14	11.27	11.26	11.49	11.51	11.46	11.71	11.68	11.63	11.66	11.70	11.89	12.51	11.74	12.60	12.03	11.80	11.79
CaO	19.49	19.03	18.93	18.63	18.42	18.93	18.54	18.56	18.99	18.72	18.73	18.59	18.56	18.54	17.53	18.65	17.99	18.76	18.64	18.62
Na2O	3.40	3.62	3.64	3.65	3.77	3.75	3.62	3.76	3.65	3.68	3.63	3.75	3.66	3.62	3.54	3.64	3.34	3.69	3.50	3.61
K2O	0.01	0.01	0.01	0.02	0.00	0.00	0.03	0.01	0.00	0.00	0.01	0.02	0.00	0.00	0.06	0.01	0.07	0.00	0.00	0.01
Total	99.53	99.91	99.41	99.66	99.15	100.38	99.77	99.53	100.41	99.79	99.48	99.85	99.65	99.72	99.03	99.59	99.10	100.45	99.71	99.84
Si	1.882	1.884	1.893	1.900	1.912	1.902	1.915	1.912	1.911	1.918	1.921	1.927	1.929	1.930		1.929		1.912	1.924	1.924
Ti	0.001	0.001	0.002	0.000	0.000	0.000	0.001	0.001	0.000	0.002	0.001	0.000	0.000	0.001		0.002		0.001	0.002	0.001
Al	0.409	0.427	0.419	0.418	0.408	0.400	0.392	0.382	0.376	0.370	0.366	0.358	0.362	0.351		0.349		0.361	0.363	0.359
Cr	0.010	0.006	0.004	0.004	0.003	0.002	0.002	0.003	0.002	0.003	0.001	0.002	0.001	0.002		0.003		0.004	0.002	0.002
Fe2+	0.102	0.103	0.106	0.106	0.097	0.110	0.108	0.117	0.116	0.113	0.115	0.117	0.114	0.116		0.118		0.122	0.115	0.119
Mn	0.000	0.000	0.000	0.001	0.000	0.000	0.000	0.000	0.002	0.000	0.000	0.001	0.001	0.001		0.001		0.001	0.000	0.000
Ni	0.004	0.005	0.003	0.002	0.004	0.004	0.004	0.005	0.004	0.005	0.004	0.006	0.003	0.004		0.003		0.004	0.003	0.003
Mg	0.621	0.608	0.603	0.608	0.609	0.616	0.620	0.620	0.628	0.630	0.629	0.629	0.631	0.641		0.635		0.646	0.636	0.636
Ca	0.759	0.737	0.736	0.722	0.716	0.730	0.718	0.722	0.733	0.726	0.728	0.721	0.720	0.719		0.725		0.724	0.723	0.721
Na	0.240	0.253	0.256	0.256	0.265	0.262	0.253	0.265	0.255	0.258	0.255	0.263	0.257	0.254		0.256		0.258	0.245	0.253
K	0.000	0.000	0.001	0.001	0.000	0.000	0.001	0.000	0.000	0.000	0.001	0.001	0.000	0.000		0.001		0.000	0.000	0.000
Sum	4.028	4.025	4.023	4.018	4.015	4.027	4.014	4.027	4.027	4.024	4.022	4.025	4.018	4.019		4.021		4.033	4.014	4.020
Mg#	85.89	85.51	85.05	85.15	86.26	84.85	85.16	84.12	84.41	84.79	84.54	84.32	84.70	84.68		84.33		84.11	84.69	84.24
Al IV	0.091	0.091	0.085	0.083	0.073	0.070	0.071	0.061	0.062	0.060	0.057	0.048	0.053	0.051		0.050		0.055	0.062	0.055
Al VI	0.319	0.336	0.334	0.336	0.335	0.330	0.321	0.321	0.315	0.311	0.310	0.310	0.309	0.301		0.300		0.307	0.301	0.304

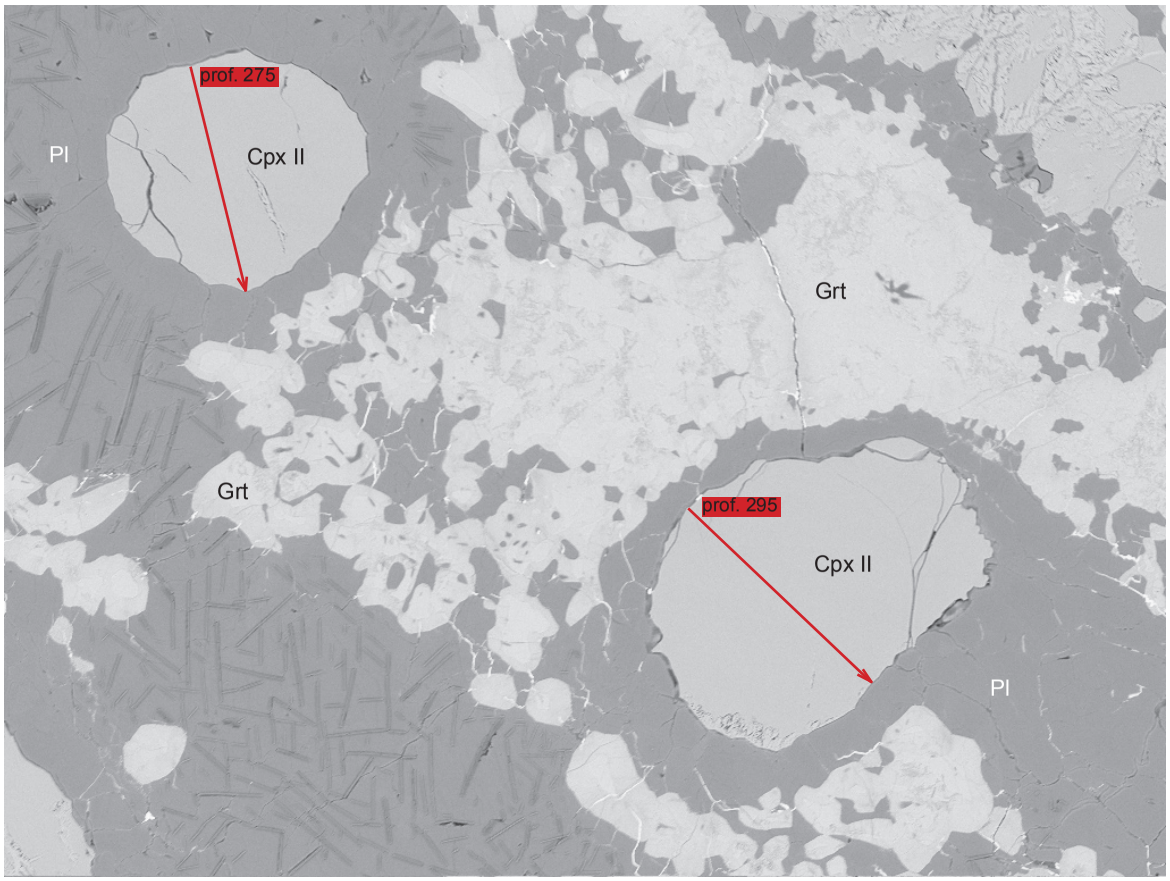
1906-2 Cpx II, profile 525

	210	220	230	240	250	260	270	280	290	300	310	320	330	340	350	360	370	380	390	400
SiO2	52.98	53.20	53.20	53.17	53.31	53.07	53.10	53.12	52.82	53.02	53.04	52.71	52.94	52.67	52.89	52.89	53.02	53.06	52.81	52.47
TiO2	0.03	0.04	0.00	0.04	0.02	0.03	0.04	0.07	0.02	0.05	0.06	0.04	0.03	0.00	0.04	0.02	0.04	0.05	0.04	0.00
Al2O3	8.56	8.66	8.68	8.67	8.74	8.70	8.81	8.97	9.02	9.18	9.19	9.09	9.35	9.34	9.37	9.52	9.51	9.53	9.56	9.65
Cr2O3	0.05	0.11	0.10	0.06	0.06	0.13	0.08	0.12	0.03	0.05	0.08	0.06	0.11	0.11	0.12	0.11	0.07	0.13	0.07	0.08
FeO	3.66	3.83	3.89	3.84	3.65	3.84	3.55	3.70	3.83	3.75	3.65	3.58	3.81	3.71	3.52	3.77	3.86	3.48	3.62	3.59
MnO	0.05	0.01	0.01	0.03	0.02	0.00	0.00	0.06	0.04	0.01	0.07	0.00	0.01	0.03	0.00	0.07	0.00	0.00	0.05	0.03
NiO	0.11	0.16	0.13	0.14	0.12	0.15	0.10	0.14	0.14	0.14	0.13	0.17	0.13	0.18	0.15	0.14	0.15	0.10	0.17	0.15
MgO	11.62	11.88	11.71	11.60	11.63	11.61	11.68	11.63	11.50	11.29	11.53	11.40	11.46	11.47	11.36	11.42	11.46	11.20	11.34	11.34
CaO	18.58	18.46	18.65	18.60	18.46	18.45	18.53	18.47	18.25	18.55	18.36	18.67	18.19	18.31	18.61	18.62	18.67	18.56	18.63	18.70
Na2O	3.68	3.81	3.59	3.76	3.83	3.90	3.64	3.69	3.69	3.69	3.75	3.72	3.78	3.75	3.81	3.70	3.77	3.77	3.78	3.66
K2O	0.01	0.00	0.01	0.00	0.00	0.01	0.00	0.00	0.03	0.00	0.02	0.01	0.00	0.01	0.00	0.00	0.01	0.00	0.02	0.00
Total	99.33	100.16	99.98	99.90	99.83	99.89	99.53	99.96	99.35	99.71	99.87	99.44	99.82	99.58	99.87	100.25	100.56	99.88	100.09	99.65
Si	1.924	1.918	1.921	1.922	1.925	1.919	1.922	1.917	1.918	1.917	1.915	1.912	1.912	1.908	1.910	1.904	1.904	1.913	1.904	1.900
Ti	0.001	0.001	0.000	0.001	0.001	0.001	0.001	0.002	0.000	0.001	0.002	0.001	0.001	0.000	0.001	0.001	0.001	0.001	0.001	0.000
Al	0.366	0.368	0.370	0.369	0.372	0.371	0.376	0.381	0.386	0.391	0.391	0.389	0.398	0.399	0.399	0.404	0.403	0.405	0.406	0.412
Cr	0.002	0.003	0.003	0.002	0.002	0.004	0.002	0.003	0.001	0.002	0.002	0.002	0.003	0.003	0.003	0.003	0.002	0.004	0.002	0.002
Fe2+	0.111	0.115	0.117	0.116	0.110	0.116	0.107	0.112	0.116	0.113	0.110	0.109	0.115	0.112	0.106	0.113	0.116	0.105	0.109	0.109
Mn	0.002	0.000	0.000	0.001	0.000	0.000	0.000	0.002	0.001	0.000	0.002	0.000	0.000	0.001	0.000	0.002	0.000	0.000	0.001	0.001
Ni	0.003	0.005	0.004	0.004	0.004	0.004	0.003	0.004	0.004	0.004	0.004	0.005	0.004	0.005	0.004	0.004	0.004	0.003	0.005	0.004
Mg	0.629	0.638	0.630	0.625	0.626	0.626	0.630	0.626	0.622	0.608	0.620	0.617	0.617	0.620	0.612	0.613	0.613	0.602	0.609	0.612
Ca	0.723	0.713	0.722	0.720	0.714	0.715	0.719	0.714	0.710	0.719	0.710	0.726	0.704	0.711	0.720	0.718	0.718	0.717	0.720	0.725
Na	0.259	0.266	0.251	0.263	0.268	0.274	0.256	0.258	0.260	0.259	0.262	0.261	0.265	0.264	0.267	0.258	0.262	0.264	0.264	0.257
K	0.000	0.000	0.000	0.000	0.000	0.000	0.000	0.000	0.001	0.000	0.001	0.001	0.000	0.000	0.000	0.000	0.001	0.000	0.001	0.000
Sum	4.021	4.028	4.019	4.023	4.022	4.030	4.016	4.018	4.019	4.014	4.019	4.022	4.019	4.023	4.022	4.021	4.024	4.013	4.023	4.022
Mg#	85.00	84.73	84.34	84.35	85.05	84.37	85.48	84.82	84.28	84.33	84.93	84.99	84.29	84.70	85.24	84.44	84.09	85.15	84.82	84.88
Al IV	0.056	0.054	0.061	0.055	0.054	0.052	0.062	0.065	0.063	0.068	0.067	0.066	0.069	0.069	0.069	0.076	0.072	0.074	0.073	0.079
Al VI	0.311	0.315	0.309	0.314	0.318	0.320	0.314	0.316	0.323	0.323	0.324	0.324	0.329	0.330	0.331	0.329	0.331	0.332	0.334	0.334

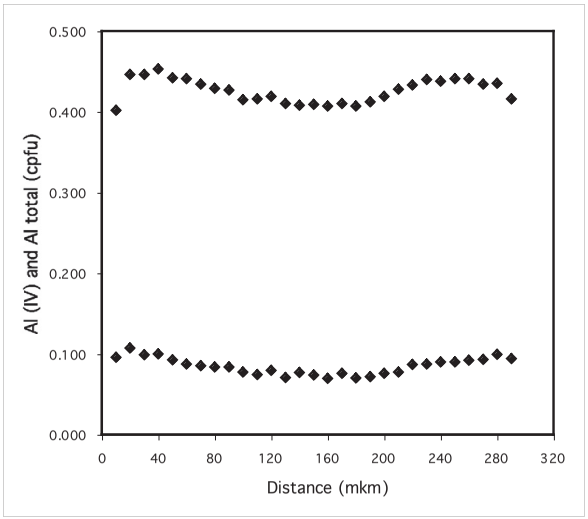
1906-2 Cpx II, profile 525

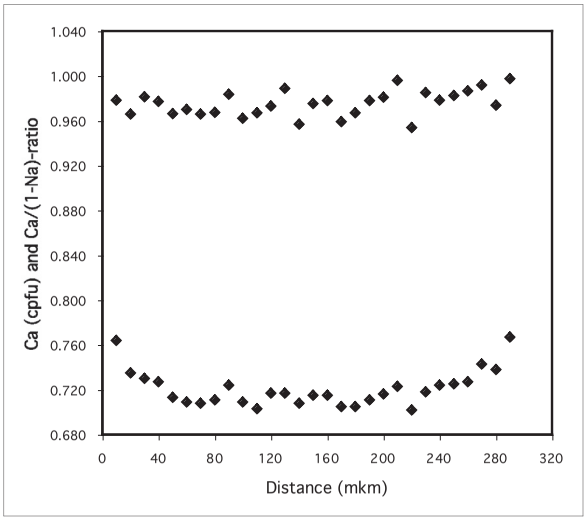
	410	420	430	440	450	460	470	480	490	500	510	520	530
SiO2	52.40	53.01	52.28	52.53	52.71	52.33	52.80	52.13	52.37	52.49	52.67	52.48	52.58
TiO2	0.03	0.02	0.04	0.05	0.02	0.01	0.02	0.04	0.01	0.03	0.04	0.07	0.03
Al2O3	9.71	9.77	9.69	9.78	9.76	9.80	9.77	10.14	10.01	10.06	10.11	9.77	9.18
Cr2O3	0.08	0.07	0.11	0.09	0.10	0.11	0.12	0.14	0.15	0.15	0.28	0.42	0.45
FeO	3.36	3.78	3.63	3.76	3.55	3.34	3.34	3.31	3.42	3.35	3.25	3.17	3.29
MnO	0.01	0.02	0.03	0.00	0.02	0.00	0.00	0.02	0.00	0.05	0.00	0.02	0.06
NiO	0.11	0.16	0.17	0.15	0.13	0.17	0.15	0.16	0.17	0.10	0.13	0.11	0.17
MgO	11.18	11.15	11.21	11.23	11.23	11.22	11.23	11.20	11.24	11.05	11.29	11.49	11.72
CaO	18.16	18.66	18.93	18.82	18.95	18.69	18.69	18.74	18.87	18.80	19.24	19.14	19.55
Na2O	3.74	3.66	3.66	3.80	3.52	3.69	3.68	3.50	3.55	3.47	3.50	3.40	3.27
K2O	0.00	0.00	0.00	0.01	0.00	0.00	0.01	0.00	0.01	0.00	0.01	0.00	0.01
Total	98.79	100.30	99.75	100.21	100.00	99.35	99.80	99.37	99.81	99.54	100.51	100.06	100.31
Si	1.908	1.906	1.894	1.894	1.901	1.898	1.905	1.890	1.892	1.899	1.890	1.891	1.895
Ti	0.001	0.001	0.001	0.001	0.001	0.000	0.000	0.001	0.000	0.001	0.001	0.002	0.001
Al	0.417	0.414	0.414	0.416	0.415	0.419	0.415	0.433	0.426	0.429	0.427	0.415	0.390
Cr	0.002	0.002	0.003	0.003	0.003	0.003	0.004	0.004	0.004	0.004	0.008	0.012	0.013
Fe2+	0.102	0.114	0.110	0.113	0.107	0.101	0.101	0.100	0.103	0.101	0.098	0.096	0.099
Mn	0.000	0.000	0.001	0.000	0.000	0.000	0.000	0.001	0.000	0.001	0.000	0.001	0.002
Ni	0.003	0.005	0.005	0.004	0.004	0.005	0.004	0.005	0.005	0.003	0.004	0.003	0.005
Mg	0.607	0.598	0.605	0.604	0.604	0.607	0.604	0.605	0.605	0.596	0.604	0.617	0.630
Ca	0.709	0.719	0.735	0.727	0.732	0.727	0.723	0.728	0.731	0.728	0.739	0.739	0.755
Na	0.264	0.255	0.257	0.266	0.246	0.259	0.258	0.246	0.249	0.243	0.243	0.237	0.229
K	0.000	0.000	0.000	0.001	0.000	0.000	0.000	0.000	0.000	0.000	0.001	0.000	0.000
Sum	4.013	4.013	4.025	4.028	4.013	4.020	4.014	4.013	4.017	4.006	4.014	4.012	4.018
Mg#	85.61	83.99	84.62	84.24	84.95	85.73	85.67	85.82	85.45	85.51	86.04	86.54	86.42
Al IV	0.079	0.082	0.081	0.077	0.087	0.082	0.081	0.097	0.091	0.096	0.097	0.097	0.088
Al VI	0.339	0.333	0.333	0.339	0.328	0.338	0.335	0.337	0.336	0.333	0.331	0.318	0.302

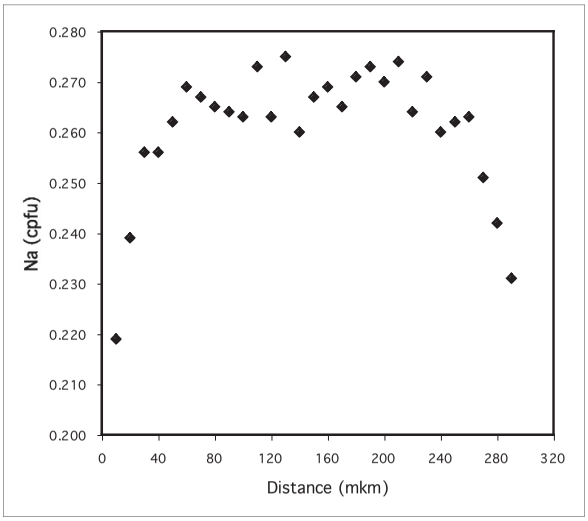
1906-2 Cpx II, profile 525

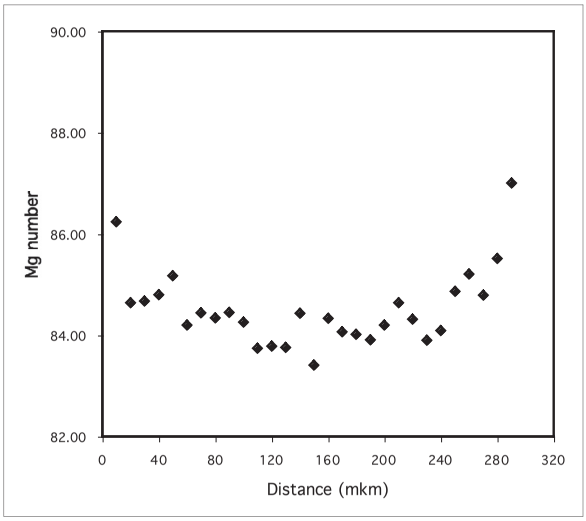


1906-2 Cpx II, profile 275









1906-2 Cpx II, profile 275

	10	20	30	40	50	60	70	80	90	100	110	120
SiO2	51.94	52.06	52.02	52.19	52.15	52.22	52.64	52.59	51.93	52.60	52.59	52.53
TiO2	0.08	0.06	0.07	0.05	0.05	0.03	0.04	0.05	0.04	0.02	0.04	0.04
Al2O3	9.38	10.43	10.43	10.65	10.31	10.32	10.18	10.05	9.91	9.70	9.71	9.81
Cr2O3	0.13	0.09	0.11	0.08	0.11	0.03	0.06	0.02	0.07	0.04	0.10	0.05
FeO	3.31	3.50	3.47	3.44	3.35	3.64	3.58	3.61	3.58	3.67	3.75	3.81
MnO	0.00	0.00	0.00	0.01	0.05	0.06	0.02	0.00	0.01	0.01	0.08	0.04
NiO	0.15	0.17	0.14	0.11	0.13	0.16	0.12	0.13	0.13	0.19	0.10	0.17
MgO	11.68	10.81	10.73	10.77	10.80	10.84	10.89	10.87	10.87	10.97	10.82	11.01
CaO	19.60	18.92	18.78	18.79	18.31	18.24	18.30	18.33	18.49	18.21	18.05	18.48
Na2O	3.11	3.41	3.63	3.65	3.71	3.82	3.81	3.78	3.73	3.73	3.88	3.75
K2O	0.00	0.00	0.00	0.02	0.01	0.00	0.01	0.00	0.00	0.00	0.00	0.01
Total	99.37	99.44	99.39	99.77	98.96	99.36	99.64	99.44	98.75	99.12	99.12	99.71
Si	1.888	1.887	1.887	1.885	1.897	1.895	1.902	1.905	1.897	1.911	1.912	1.902
Ti	0.002	0.002	0.002	0.001	0.001	0.001	0.001	0.001	0.001	0.001	0.001	0.001
Al	0.402	0.446	0.446	0.453	0.442	0.441	0.434	0.429	0.427	0.415	0.416	0.419
Cr	0.004	0.003	0.003	0.002	0.003	0.001	0.002	0.001	0.002	0.001	0.003	0.002
Fe2	0.101	0.106	0.105	0.104	0.102	0.110	0.108	0.109	0.109	0.111	0.114	0.115
Mn	0.000	0.000	0.000	0.000	0.001	0.002	0.001	0.000	0.000	0.000	0.002	0.001
Ni	0.005	0.005	0.004	0.003	0.004	0.005	0.003	0.004	0.004	0.005	0.003	0.005
Mg	0.633	0.584	0.580	0.580	0.586	0.586	0.586	0.587	0.592	0.594	0.587	0.594
Ca	0.764	0.735	0.730	0.727	0.713	0.709	0.708	0.711	0.724	0.709	0.703	0.717
Na	0.219	0.239	0.256	0.256	0.262	0.269	0.267	0.265	0.264	0.263	0.273	0.263
K	0.000	0.000	0.000	0.001	0.000	0.000	0.001	0.000	0.000	0.000	0.000	0.001
Sum	4.016	4.007	4.014	4.014	4.011	4.018	4.013	4.012	4.020	4.011	4.014	4.019
Mg#	86.24	84.64	84.67	84.80	85.17	84.20	84.44	84.34	84.45	84.26	83.74	83.78
Al IV	0.096	0.107	0.099	0.100	0.093	0.088	0.085	0.084	0.084	0.078	0.074	0.080
Al VI	0.307	0.339	0.348	0.353	0.350	0.354	0.349	0.346	0.344	0.338	0.342	0.340

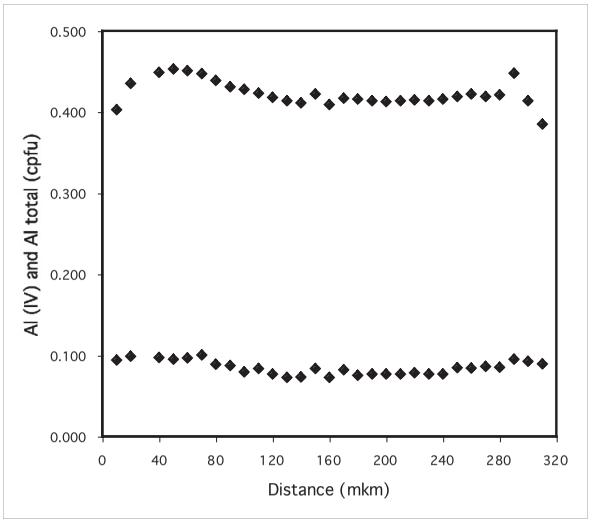
	130	140	150	160	170	180	190	200	210	220	230	240
SiO2	52.63	52.84	52.38	52.92	53.00	52.95	52.72	52.77	52.51	52.61	52.30	52.70
TiO2	0.07	0.06	0.07	0.01	0.07	0.04	0.05	0.02	0.01	0.06	0.04	0.05
Al2O3	9.62	9.55	9.54	9.56	9.61	9.56	9.65	9.83	10.04	10.15	10.30	10.34
Cr2O3	0.05	0.08	0.06	0.02	0.10	0.06	0.07	0.09	0.03	0.08	0.14	0.05
FeO	3.81	3.67	3.91	3.64	3.72	3.73	3.74	3.63	3.50	3.61	3.64	3.63
MnO	0.08	0.05	0.00	0.00	0.00	0.05	0.02	0.04	0.05	0.03	0.03	0.01
NiO	0.14	0.09	0.11	0.20	0.13	0.11	0.13	0.12	0.17	0.14	0.13	0.18
MgO	11.00	11.15	11.03	10.98	10.97	11.02	10.90	10.87	10.84	10.85	10.60	10.75
CaO	18.50	18.26	18.36	18.46	18.19	18.19	18.31	18.49	18.65	18.11	18.51	18.78
Na2O	3.91	3.70	3.79	3.84	3.78	3.86	3.88	3.85	3.91	3.76	3.86	3.73
K2O	0.01	0.01	0.01	0.00	0.00	0.00	0.01	0.02	0.00	0.01	0.01	0.02
Total	99.81	99.45	99.25	99.64	99.57	99.55	99.47	99.71	99.71	99.39	99.55	100.24
Si	1.905	1.913	1.905	1.914	1.916	1.916	1.911	1.908	1.899	1.905	1.895	1.896
Ti	0.002	0.002	0.002	0.000	0.002	0.001	0.001	0.001	0.000	0.001	0.001	0.001
Al	0.410	0.408	0.409	0.407	0.410	0.407	0.412	0.419	0.428	0.433	0.440	0.438
Cr	0.002	0.002	0.002	0.001	0.003	0.002	0.002	0.002	0.001	0.002	0.004	0.001
Fe2	0.115	0.111	0.119	0.110	0.112	0.113	0.113	0.110	0.106	0.109	0.110	0.109
Mn	0.002	0.001	0.000	0.000	0.000	0.002	0.000	0.001	0.001	0.001	0.001	0.000
Ni	0.004	0.003	0.003	0.006	0.004	0.003	0.004	0.003	0.005	0.004	0.004	0.005
Mg	0.593	0.602	0.598	0.592	0.591	0.594	0.589	0.586	0.584	0.586	0.573	0.576
Ca	0.717	0.708	0.715	0.715	0.705	0.705	0.711	0.716	0.723	0.702	0.718	0.724
Na	0.275	0.260	0.267	0.269	0.265	0.271	0.273	0.270	0.274	0.264	0.271	0.260
K	0.000	0.000	0.001	0.000	0.000	0.000	0.000	0.001	0.000	0.000	0.000	0.001
Sum	4.025	4.010	4.021	4.016	4.008	4.014	4.017	4.016	4.023	4.008	4.018	4.013
Mg#	83.76	84.43	83.40	84.33	84.07	84.02	83.90	84.20	84.64	84.32	83.89	84.09
Al IV	0.071	0.077	0.074	0.070	0.076	0.070	0.072	0.076	0.078	0.087	0.088	0.090
Al VI	0.340	0.331	0.336	0.338	0.334	0.337	0.341	0.343	0.351	0.347	0.353	0.348

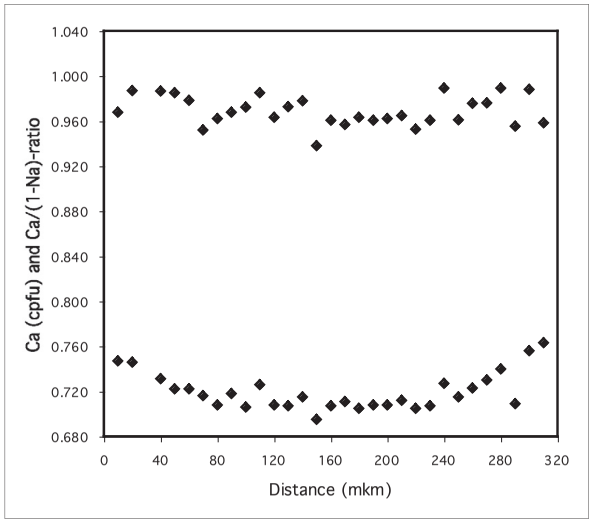
1906-2 Cpx II, profile 275

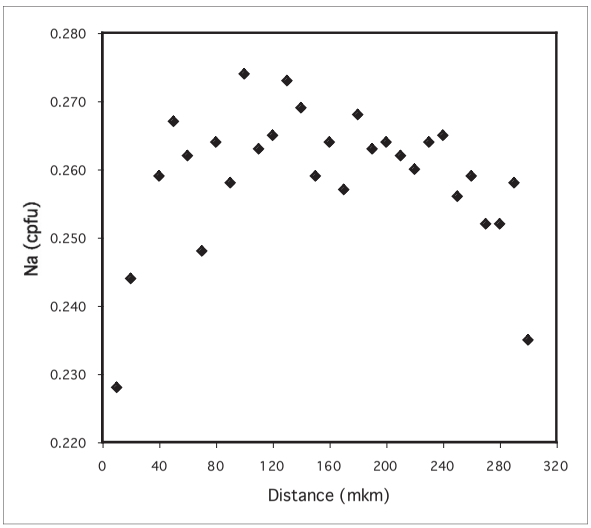
	250	260	270	280	290
SiO2	52.41	52.31	52.22	52.13	52.12
TiO2	0.02	0.07	0.04	0.07	0.04
Al2O3	10.35	10.33	10.20	10.21	9.75
Cr2O3	0.02	0.07	0.03	0.08	0.05
FeO	3.45	3.31	3.52	3.39	3.04
MnO	0.00	0.00	0.02	0.00	0.00
NiO	0.13	0.13	0.17	0.14	0.15
MgO	10.81	10.67	10.96	11.17	11.40
CaO	18.72	18.73	19.19	19.05	19.77
Na2O	3.73	3.75	3.58	3.46	3.28
K2O	0.00	0.00	0.00	0.00	0.00
Total	99.63	99.37	99.94	99.68	99.58
Si	1.895	1.896	1.887	1.886	1.888
Ti	0.000	0.002	0.001	0.002	0.001
Al	0.441	0.441	0.434	0.435	0.416
Cr	0.001	0.002	0.001	0.002	0.001
Fe2+	0.104	0.100	0.106	0.102	0.092
Mn	0.000	0.000	0.001	0.000	0.000
Ni	0.004	0.004	0.005	0.004	0.004
Mg	0.583	0.576	0.591	0.602	0.616
Ca	0.725	0.727	0.743	0.738	0.767
Na	0.262	0.263	0.251	0.242	0.231
K	0.000	0.000	0.000	0.000	0.000
Sum	4.015	4.012	4.020	4.015	4.017
Mg#	84.86	85.21	84.79	85.51	87.01
Al IV	0.090	0.092	0.093	0.100	0.094
Al VI	0.351	0.349	0.341	0.336	0.322

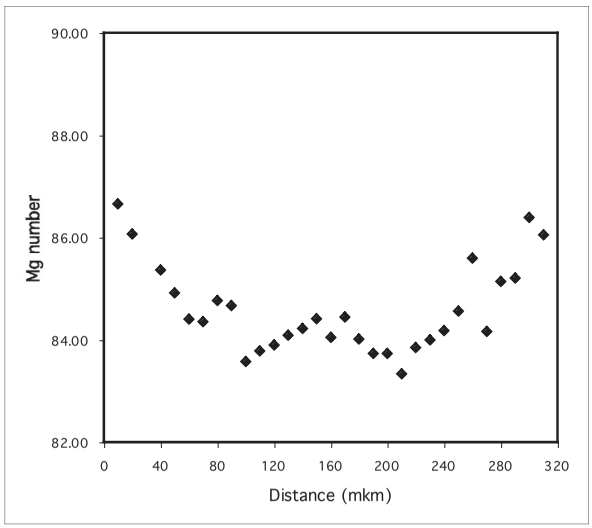
1906-2 Cpx II, profile 275

1906-2 Cpx II, profile 295









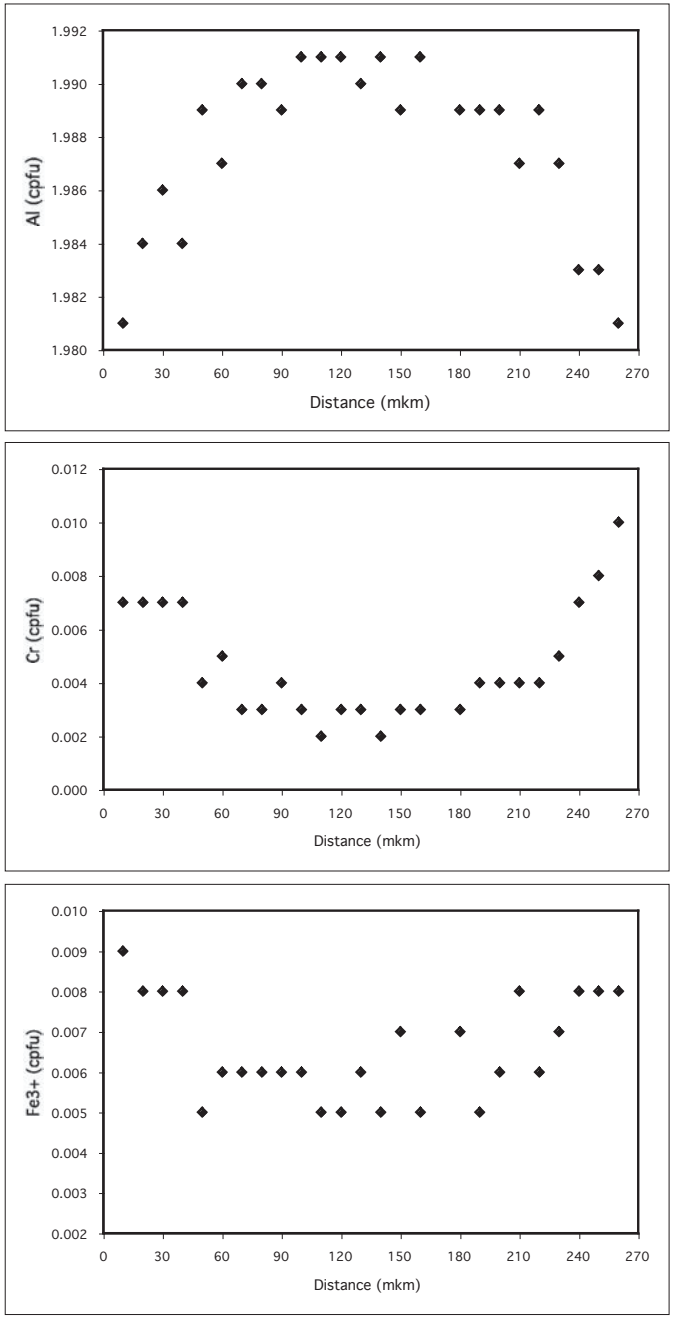
	10	20	30	40	50	60	70	80	90	100	110	120
SiO2	52.42	52.09	48.90	51.91	52.15	51.92	52.43	52.30	52.33	52.52	52.50	52.67
TiO2	0.09	0.08	0.07	0.04	0.06	0.05	0.01	0.04	0.00	0.03	0.07	0.03
Al2O3	9.42	10.16	10.57	10.49	10.61	10.53	10.53	10.27	10.07	10.04	9.93	9.78
Cr2O3	0.23	0.07	0.11	0.05	0.06	0.05	0.09	0.03	0.07	0.10	0.10	0.02
FeO	3.13	3.16	3.93	3.34	3.38	3.52	3.64	3.49	3.51	3.83	3.77	3.77
MnO	0.02	0.00	0.09	0.03	0.00	0.00	0.06	0.07	0.01	0.01	0.00	0.01
NiO	0.16	0.17	0.15	0.17	0.14	0.09	0.11	0.12	0.14	0.13	0.10	0.16
MgO	11.41	10.96	12.51	10.90	10.64	10.68	11.04	10.90	10.91	10.94	10.93	11.00
CaO	19.23	19.18	16.23	18.81	18.60	18.54	18.54	18.22	18.46	18.21	18.74	18.25
Na2O	3.25	3.46	2.61	3.68	3.79	3.71	3.55	3.75	3.67	3.91	3.76	3.77
K2O	0.00	0.00	0.04	0.00	0.01	0.01	0.01	0.00	0.00	0.00	0.00	0.02
Total	99.36	99.33	95.19	99.42	99.43	99.11	100.01	99.17	99.17	99.74	99.89	99.47
Si	1.901	1.890		1.883	1.889	1.888	1.889	1.898	1.901	1.900	1.898	1.908
Ti	0.003	0.002		0.001	0.001	0.001	0.000	0.001	0.000	0.001	0.002	0.001
Al	0.403	0.435		0.449	0.453	0.451	0.447	0.439	0.431	0.428	0.423	0.418
Cr	0.007	0.002		0.002	0.002	0.002	0.002	0.001	0.002	0.003	0.003	0.000
Fe2+	0.095	0.096		0.101	0.102	0.107	0.110	0.106	0.107	0.116	0.114	0.114
Mn	0.001	0.000		0.001	0.000	0.000	0.002	0.002	0.000	0.000	0.000	0.000
Ni	0.005	0.005		0.005	0.004	0.003	0.003	0.004	0.004	0.004	0.003	0.005
Mg	0.617	0.593		0.589	0.574	0.579	0.593	0.590	0.591	0.590	0.589	0.594
Ca	0.747	0.746		0.731	0.722	0.722	0.716	0.708	0.718	0.706	0.726	0.708
Na	0.228	0.244		0.259	0.267	0.262	0.248	0.264	0.258	0.274	0.263	0.265
K	0.000	0.000		0.000	0.000	0.000	0.000	0.000	0.000	0.000	0.000	0.001
Sum	4.006	4.011		4.020	4.015	4.015	4.010	4.012	4.012	4.021	4.019	4.015
Mg#	86.66	86.07		85.36	84.91	84.40	84.35	84.77	84.67	83.57	83.78	83.90
Al IV	0.094	0.099		0.097	0.095	0.097	0.101	0.089	0.088	0.080	0.084	0.077
Al VI	0.309	0.337		0.352	0.358	0.355	0.347	0.350	0.344	0.349	0.340	0.341

1906-2 Cpx II, profile 295

	130	140	150	160	170	180	190	200	210	220	230	240
SiO2	53.00	52.97	52.65	53.02	52.80	52.39	52.56	52.67	52.55	52.58	52.71	52.25
TiO2	0.04	0.05	0.02	0.01	0.06	0.03	0.03	0.04	0.05	0.02	0.04	0.03
Al2O3	9.74	9.65	9.87	9.59	9.78	9.68	9.68	9.68	9.68	9.70	9.68	9.70
Cr2O3	0.06	0.08	0.08	0.00	0.07	0.04	0.02	0.09	0.02	0.05	0.07	0.07
FeO	3.71	3.65	3.65	3.70	3.65	3.75	3.85	3.82	3.92	3.79	3.72	3.68
MnO	0.02	0.07	0.07	0.01	0.02	0.03	0.00	0.03	0.03	0.08	0.05	0.05
NiO	0.13	0.16	0.16	0.16	0.15	0.12	0.21	0.11	0.11	0.14	0.12	0.11
MgO	11.00	10.91	11.11	10.94	11.07	11.03	11.13	11.04	11.00	11.03	10.97	11.01
CaO	18.28	18.47	17.88	18.22	18.36	18.06	18.21	18.23	18.32	18.13	18.21	18.65
Na2O	3.90	3.84	3.68	3.76	3.67	3.79	3.75	3.75	3.72	3.70	3.76	3.77
K2O	0.00	0.00	0.01	0.00	0.00	0.03	0.00	0.00	0.00	0.00	0.01	0.02
Total	99.89	99.85	99.17	99.42	99.64	98.96	99.44	99.46	99.39	99.21	99.31	99.33
Si	1.912	1.912	1.910	1.920	1.909	1.908	1.906	1.909	1.907	1.910	1.912	1.900
Ti	0.001	0.001	0.001	0.000	0.001	0.001	0.001	0.001	0.001	0.000	0.001	0.001
Al	0.414	0.411	0.422	0.409	0.417	0.416	0.414	0.413	0.414	0.415	0.414	0.416
Cr	0.002	0.002	0.002	0.000	0.002	0.001	0.001	0.003	0.000	0.002	0.002	0.002
Fe2	0.112	0.110	0.111	0.112	0.110	0.114	0.117	0.116	0.119	0.115	0.113	0.112
Mn	0.000	0.002	0.002	0.000	0.001	0.001	0.000	0.001	0.001	0.002	0.001	0.001
Ni	0.004	0.005	0.005	0.005	0.004	0.004	0.006	0.003	0.003	0.004	0.003	0.003
Mg	0.592	0.587	0.601	0.590	0.597	0.599	0.602	0.597	0.595	0.597	0.593	0.596
Ca	0.707	0.715	0.695	0.707	0.711	0.705	0.708	0.708	0.712	0.705	0.707	0.727
Na	0.273	0.269	0.259	0.264	0.257	0.268	0.263	0.264	0.262	0.260	0.264	0.265
K	0.000	0.000	0.000	0.000	0.000	0.001	0.000	0.000	0.000	0.000	0.000	0.001
Sum	4.016	4.014	4.007	4.007	4.009	4.017	4.017	4.014	4.015	4.012	4.012	4.024
Mg#	84.09	84.22	84.41	84.05	84.44	84.01	83.73	83.73	83.33	83.85	83.99	84.18
Al IV	0.073	0.073	0.084	0.073	0.082	0.075	0.077	0.077	0.077	0.079	0.077	0.077
Al VI	0.342	0.338	0.339	0.337	0.335	0.341	0.337	0.336	0.337	0.337	0.337	0.339

	250	260	270	280	290	300	310
SiO2	52.73	52.21	52.47	52.31	52.72	52.34	52.68
TiO2	0.07	0.06	0.07	0.06	0.04	0.07	0.06
Al2O3	9.84	9.83	9.83	9.86	10.53	9.68	9.01
Cr2O3	0.06	0.03	0.07	0.01	0.03	0.07	0.00
FeO	3.59	3.31	3.65	3.43	3.31	3.14	3.32
MnO	0.00	0.05	0.08	0.02	0.04	0.04	0.02
NiO	0.10	0.12	0.12	0.08	0.13	0.19	0.18
MgO	11.07	11.05	10.94	11.03	10.72	11.16	11.53
CaO	18.44	18.52	18.83	19.05	18.34	19.46	19.63
Na2O	3.64	3.67	3.58	3.59	3.68	3.34	2.90
K2O	0.00	0.01	0.01	0.01	0.07	0.00	0.14
Total	99.55	98.85	99.64	99.45	99.62	99.49	99.47
Si	1.907	1.902	1.900	1.897	1.902	1.897	1.911
Ti	0.002	0.002	0.002	0.001	0.001	0.002	0.002
Al	0.419	0.422	0.419	0.421	0.448	0.414	0.385
Cr	0.002	0.001	0.002	0.000	0.001	0.002	0.000
Fe2+	0.109	0.101	0.111	0.104	0.100	0.095	0.101
Mn	0.000	0.001	0.002	0.001	0.001	0.001	0.000
Ni	0.003	0.004	0.003	0.002	0.004	0.006	0.005
Mg	0.597	0.600	0.590	0.596	0.576	0.603	0.623
Ca	0.715	0.723	0.730	0.740	0.709	0.756	0.763
Na	0.256	0.259	0.252	0.252	0.258	0.235	0.204
K	0.000	0.000	0.001	0.001	0.003	0.000	0.006
Sum	4.008	4.015	4.013	4.017	4.003	4.010	4.000
Mg#	84.56	85.59	84.17	85.14	85.21	86.39	86.05
Al IV	0.085	0.084	0.086	0.085	0.095	0.093	0.090
Al VI	0.335	0.338	0.333	0.336	0.353	0.322	0.296

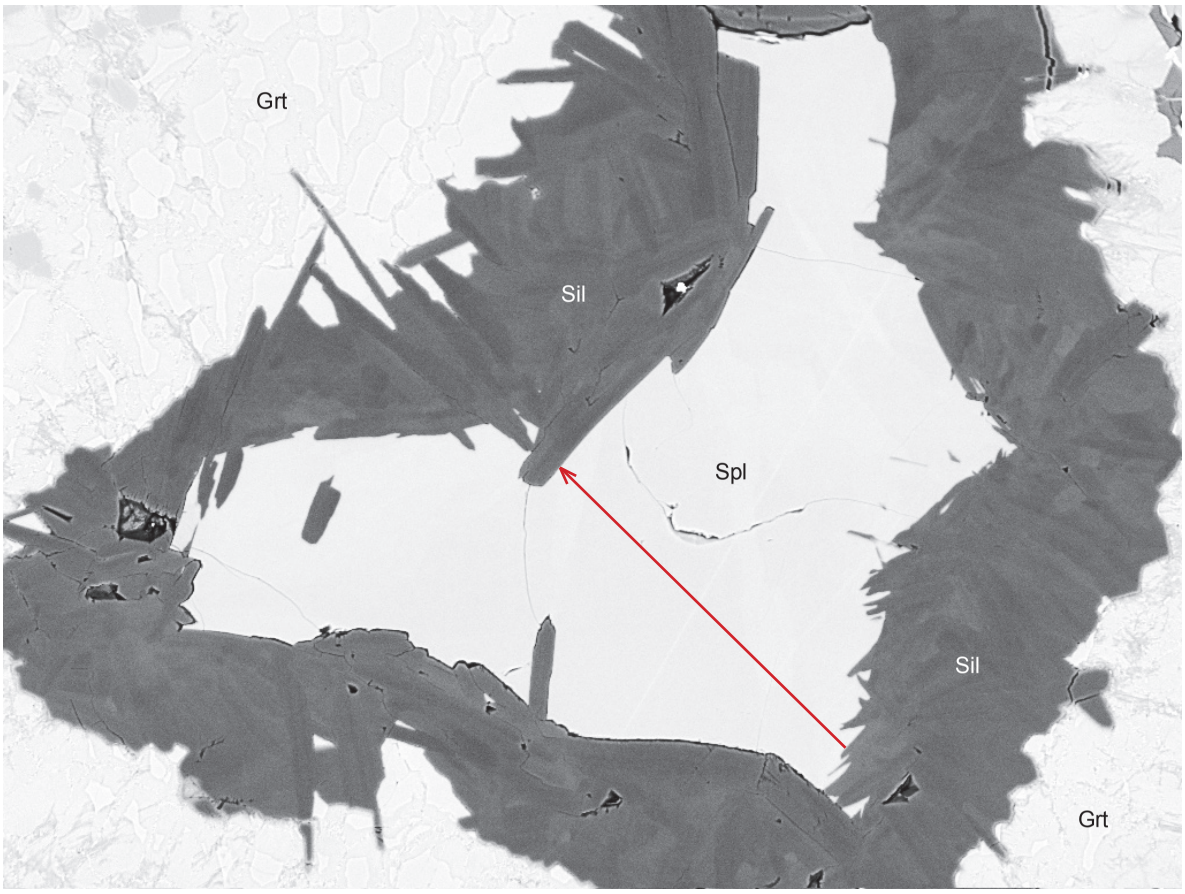
	10	20	30	40	50	60	70	80	90	100
SiO2	0.04	0.00	0.00	0.04	0.02	0.05	0.01	0.00	0.00	0.00
TiO2	0.03	0.01	0.00	0.00	0.06	0.01	0.00	0.01	0.02	0.00
Al2O3	97.66	98.11	98.68	98.70	98.71	98.78	98.81	98.70	98.86	98.74
Cr2O3	0.54	0.54	0.49	0.50	0.31	0.36	0.24	0.23	0.27	0.20
FeO	0.64	0.53	0.54	0.57	0.39	0.44	0.42	0.45	0.44	0.41
MnO	0.02	0.00	0.00	0.00	0.00	0.04	0.00	0.00	0.01	0.00
NiO	0.05	0.02	0.00	0.00	0.02	0.00	0.02	0.00	0.00	0.00
MgO	0.00	0.02	0.00	0.00	0.01	0.00	0.02	0.01	0.01	0.00
CaO	0.05	0.00	0.01	0.00	0.00	0.00	0.00	0.01	0.01	0.00
Na2O	0.00	0.01	0.00	0.01	0.00	0.00	0.02	0.00	0.01	0.01
K2O	0.00	0.01	0.00	0.00	0.00	0.01	0.00	0.00	0.00	0.00
Total	99.03	99.24	99.72	99.84	99.52	99.69	99.54	99.40	99.63	99.37
Si	0.001	0.000	0.000	0.001	0.000	0.001	0.000	0.000	0.000	0.000
Ti	0.000	0.000	0.000	0.000	0.001	0.000	0.000	0.000	0.000	0.000
Al	1.981	1.984	1.986	1.984	1.989	1.987	1.990	1.990	1.989	1.991
Cr	0.007	0.007	0.007	0.007	0.004	0.005	0.003	0.003	0.004	0.003
Fe3+	0.009	0.008	0.008	0.008	0.005	0.006	0.006	0.006	0.006	0.006
Fe2+	0.000	0.000	0.000	0.000	0.001	0.000	0.000	0.000	0.000	0.000
Mn	0.000	0.000	0.000	0.000	0.000	0.001	0.000	0.000	0.000	0.000
Ni	0.001	0.000	0.000	0.000	0.000	0.000	0.000	0.000	0.000	0.000
Mg	0.000	0.000	0.000	0.000	0.000	0.000	0.000	0.000	0.000	0.000
Ca	0.001	0.000	0.000	0.000	0.000	0.000	0.000	0.000	0.000	0.000
Na	0.000	0.000	0.000	0.000	0.000	0.000	0.001	0.000	0.000	0.000
K	0.000	0.000	0.000	0.000	0.000	0.000	0.000	0.000	0.000	0.000
Sum	2.000	2.001	2.000	2.000	2.000	2.000	2.001	2.000	2.000	2.000

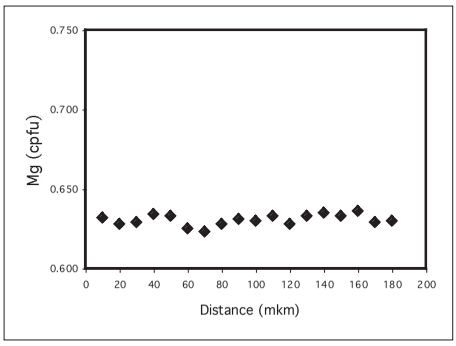


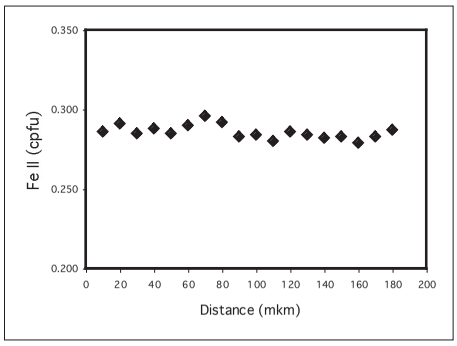
1906-2 Corundum, profile 248

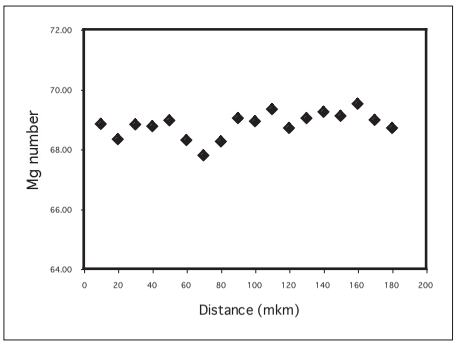
	110	120	130	140	150	160	170	180	190	200	210	220	230	240	250	260
SiO2	0.02	0.00	0.00	0.01	0.03	0.03	0.23	0.03	0.06	0.02	0.01	0.03	0.05	0.02	0.02	0.04
TiO2	0.03	0.00	0.03	0.02	0.00	0.03	0.04	0.01	0.02	0.00	0.03	0.01	0.00	0.04	0.02	0.00
Al2O3	98.73	98.91	99.05	98.95	98.93	99.06	98.42	99.07	98.88	98.76	99.08	98.71	99.02	98.98	99.15	99.36
Cr2O3	0.14	0.23	0.23	0.17	0.22	0.21	0.18	0.23	0.29	0.32	0.28	0.27	0.34	0.53	0.56	0.71
Fe2O3	0.00	0.00	0.00	0.00	0.00	0.00	0.00	0.00	0.00	0.00	0.00	0.00	0.00	0.00	0.00	
FeO	0.33	0.35	0.43	0.40	0.47	0.39	0.45	0.50	0.41	0.39	0.56	0.43	0.52	0.55	0.55	0.55
MnO	0.01	0.00	0.06	0.00	0.00	0.00	0.01	0.01	0.00	0.02	0.01	0.01	0.00	0.03	0.00	0.00
NiO	0.00	0.01	0.00	0.00	0.00	0.00	0.02	0.01	0.00	0.02	0.03	0.00	0.00	0.00	0.02	0.00
MgO	0.01	0.02	0.00	0.00	0.00	0.00	0.08	0.00	0.00	0.00	0.01	0.01	0.00	0.02	0.02	0.00
CaO	0.01	0.00	0.00	0.01	0.03	0.00	0.00	0.01	0.01	0.00	0.00	0.00	0.01	0.01	0.02	0.02
Na2O	0.03	0.00	0.01	0.00	0.01	0.00	0.00	0.01	0.01	0.00	0.00	0.00	0.01	0.00	0.00	0.00
K2O	0.00	0.02	0.01	0.00	0.03	0.01	0.00	0.00	0.00	0.00	0.00	0.00	0.01	0.01	0.00	0.01
Total	99.32	99.54	99.82	99.56	99.71	99.73	99.44	99.87	99.67	99.54	100.02	99.47	99.95	100.18	100.36	100.69
Si	0.000	0.000	0.000	0.000	0.000	0.000	0.004	0.000	0.001	0.000	0.000	0.001	0.001	0.000	0.000	0.001
Ti	0.000	0.000	0.000	0.000	0.000	0.000	0.001	0.000	0.000	0.000	0.000	0.000	0.000	0.001	0.000	0.000
Al	1.991	1.991	1.990	1.991	1.989	1.991	1.984	1.989	1.989	1.989	1.987	1.989	1.987	1.983	1.983	1.981
Cr	0.002	0.003	0.003	0.002	0.003	0.003	0.002	0.003	0.004	0.004	0.004	0.004	0.005	0.007	0.008	0.010
Fe3	0.005	0.005	0.006	0.005	0.007	0.005	0.005	0.007	0.005	0.006	0.008	0.006	0.007	0.008	0.008	0.008
Fe2	0.000	0.000	0.000	0.000	0.000	0.001	0.002	0.000	0.001	0.000	0.000	0.000	0.000	0.000	0.000	0.000
Mn	0.000	0.000	0.001	0.000	0.000	0.000	0.000	0.000	0.000	0.000	0.000	0.000	0.000	0.000	0.000	0.000
Ni	0.000	0.000	0.000	0.000	0.000	0.000	0.000	0.000	0.000	0.000	0.000	0.000	0.000	0.000	0.000	0.000
Mg	0.000	0.000	0.000	0.000	0.000	0.000	0.002	0.000	0.000	0.000	0.000	0.000	0.000	0.000	0.001	0.000
Ca	0.000	0.000	0.000	0.000	0.001	0.000	0.000	0.000	0.000	0.000	0.000	0.000	0.000	0.000	0.000	0.000
Na	0.001	0.000	0.000	0.000	0.000	0.000	0.000	0.000	0.000	0.000	0.000	0.000	0.000	0.000	0.000	0.000
K	0.000	0.000	0.000	0.000	0.001	0.000	0.000	0.000	0.000	0.000	0.000	0.000	0.000	0.000	0.000	0.000
Sum	2.001	2.000	2.001	2.000	2.001	2.000	2.000	2.000	2.000	2.000	2.000	2.000	2.000	2.000	2.000	2.000

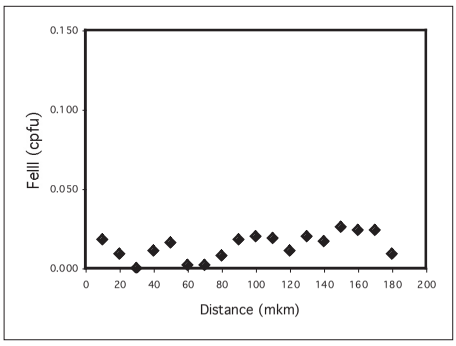
1906-2 Spinel, profile 175

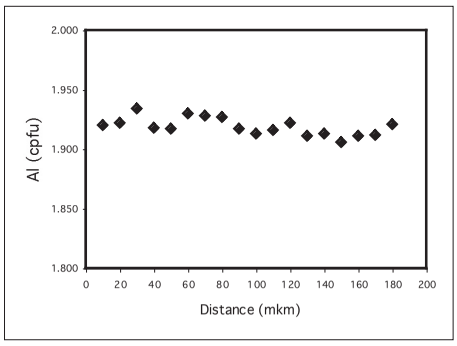


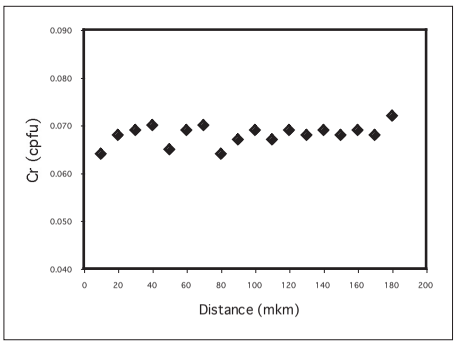


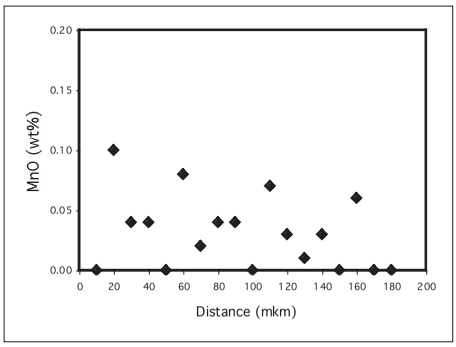


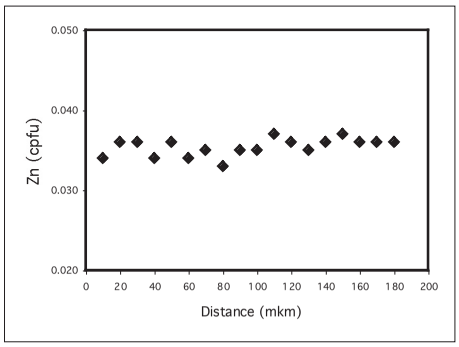


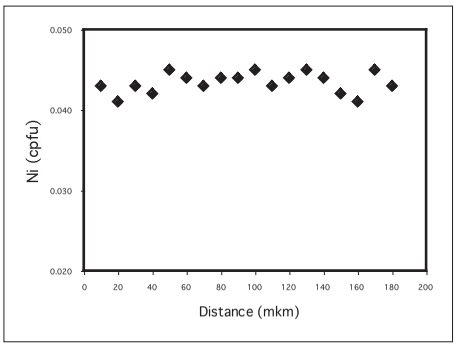








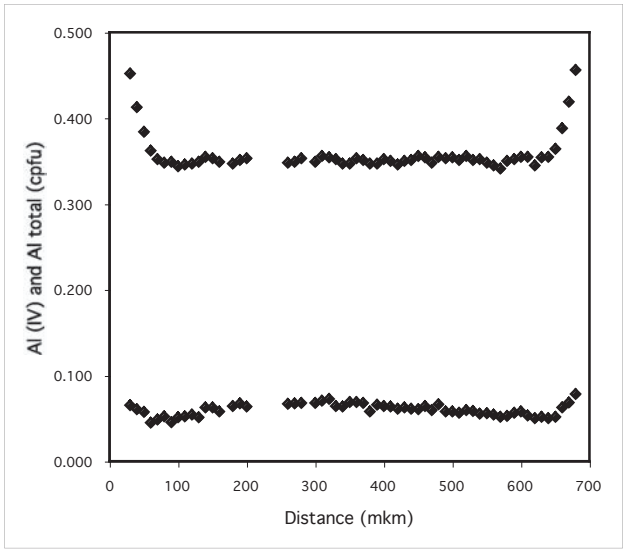


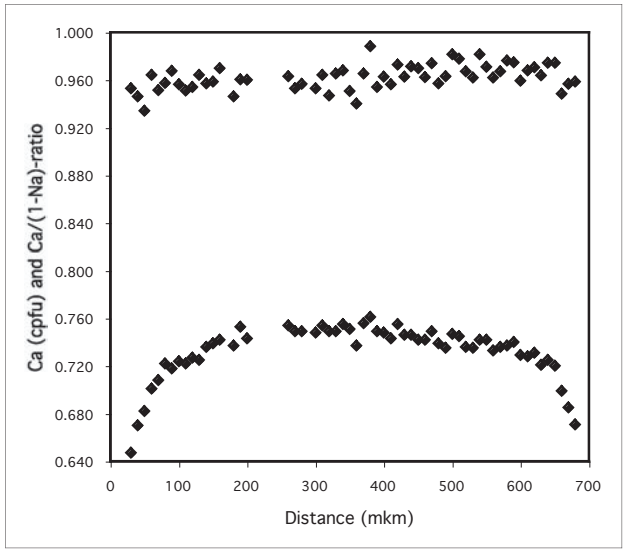


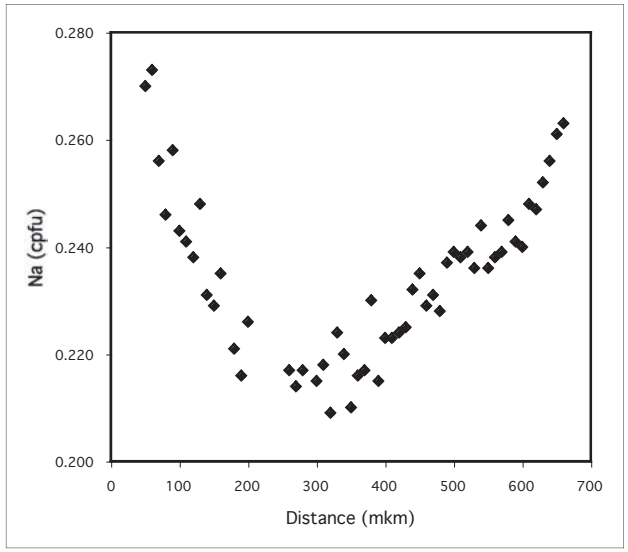
	10	20	30	40	50	60	70	80	90	100	110	120	130	140	150	160	170	180
SiO2	0.02	0.03	0.02	0.02	0.03	0.01	0.02	0.02	0.00	0.00	0.00	0.02	0.04	0.03	0.03	0.00	0.00	0.00
TiO2	0.00	0.00	0.00	0.04	0.00	0.03	0.05	0.02	0.01	0.03	0.00	0.00	0.00	0.01	0.04	0.00	0.00	0.00
V2O3	0.00	0.04	0.02	0.03	0.05	0.02	0.01	0.02	0.04	0.02	0.04	0.02	0.00	0.03	0.00	0.00	0.00	0.00
Al2O3	63.19	63.01	63.07	62.90	63.06	63.28	63.42	62.89	63.08	62.83	63.07	63.29	62.62	62.48	62.74	63.06	62.89	63.18
Cr2O3	3.13	3.35	3.36	3.40	3.21	3.38	3.43	3.11	3.27	3.38	3.28	3.40	3.33	3.35	3.34	3.40	3.31	3.54
FeO	14.10	13.86	13.12	13.82	13.95	13.49	13.80	13.83	13.94	14.03	13.87	13.76	14.06	13.78	14.35	14.10	14.22	13.72
MnO	0.00	0.10	0.04	0.04	0.00	0.08	0.02	0.04	0.04	0.00	0.07	0.03	0.01	0.03	0.00	0.06	0.00	0.00
NiO	2.08	1.96	2.06	2.01	2.15	2.11	2.05	2.10	2.13	2.19	2.09	2.12	2.15	2.10	2.03	1.99	2.18	2.07
ZnO	1.79	1.87	1.85	1.77	1.90	1.79	1.84	1.74	1.84	1.86	1.96	1.88	1.85	1.86	1.92	1.89	1.89	1.87
MgO	16.44	16.28	16.21	16.43	16.45	16.21	16.20	16.19	16.41	16.37	16.48	16.36	16.40	16.39	16.47	16.59	16.34	16.38
CaO	0.00	0.01	0.00	0.00	0.00	0.00	0.00	0.01	0.01	0.00	0.00	0.00	0.00	0.00	0.00	0.00	0.00	0.00
Na2O	0.05	0.03	0.04	0.03	0.03	0.05	0.04	0.02	0.06	0.04	0.05	0.07	0.03	0.02	0.07	0.07	0.07	0.04
K2O	0.01	0.00	0.00	0.00	0.00	0.00	0.01	0.00	0.00	0.02	0.00	0.00	0.00	0.02	0.00	0.00	0.01	0.01
Total	100.82	100.53	99.79	100.50	100.83	100.44	100.90	99.97	100.83	100.77	100.91	100.93	100.50	100.11	100.97	101.15	100.91	100.81
Si	0.001	0.001	0.000	0.000	0.001	0.000	0.001	0.000	0.000	0.000	0.000	0.001	0.001	0.001	0.001	0.000	0.000	0.000
Ti	0.000	0.000	0.000	0.001	0.000	0.001	0.001	0.000	0.000	0.001	0.000	0.000	0.000	0.000	0.001	0.000	0.000	0.000
V	0.000	0.001	0.000	0.001	0.001	0.000	0.000	0.000	0.001	0.000	0.001	0.000	0.000	0.001	0.000	0.000	0.000	0.000
Al	1.920	1.922	1.934	1.918	1.917	1.930	1.928	1.927	1.917	1.913	1.916	1.922	1.911	1.913	1.906	1.911	1.912	1.921
Cr	0.064	0.068	0.069	0.070	0.065	0.069	0.070	0.064	0.067	0.069	0.067	0.069	0.068	0.069	0.068	0.069	0.068	0.072
Fe3+	0.018	0.009	0.000	0.011	0.016	0.002	0.002	0.008	0.018	0.020	0.019	0.011	0.020	0.017	0.026	0.024	0.024	0.009
Fe2+	0.286	0.291	0.285	0.288	0.285	0.290	0.296	0.292	0.283	0.284	0.280	0.286	0.284	0.282	0.283	0.279	0.283	0.287
Mn	0.000	0.002	0.001	0.001	0.000	0.002	0.000	0.001	0.001	0.000	0.001	0.001	0.000	0.001	0.000	0.001	0.000	0.000
Ni	0.043	0.041	0.043	0.042	0.045	0.044	0.043	0.044	0.044	0.045	0.043	0.044	0.045	0.044	0.042	0.041	0.045	0.043
Zn	0.034	0.036	0.036	0.034	0.036	0.034	0.035	0.033	0.035	0.035	0.037	0.036	0.035	0.036	0.037	0.036	0.036	0.036
Mg	0.632	0.628	0.629	0.634	0.633	0.625	0.623	0.628	0.631	0.630	0.633	0.628	0.633	0.635	0.633	0.636	0.629	0.630
Ca	0.000	0.000	0.000	0.000	0.000	0.000	0.000	0.000	0.000	0.000	0.000	0.000	0.000	0.000	0.000	0.000	0.000	0.000
Na	0.002	0.001	0.002	0.002	0.001	0.002	0.002	0.001	0.003	0.002	0.002	0.003	0.002	0.001	0.004	0.003	0.003	0.002
K	0.000	0.000	0.000	0.000	0.000	0.000	0.000	0.000	0.000	0.001	0.000	0.000	0.000	0.001	0.000	0.000	0.000	0.000
Sum	3.000	3.000	2.999	3.000	3.000	3.000	3.000	3.000	3.000	3.000	3.000	3.000	3.000	3.000	3.000	3.000	3.000	3.000
100*Mg/(Mg+Fe2+)	68.85	68.34	68.82	68.76	68.95	68.31	67.79	68.26	69.04	68.93	69.33	68.71	69.03	69.25	69.10	69.51	68.97	68.70

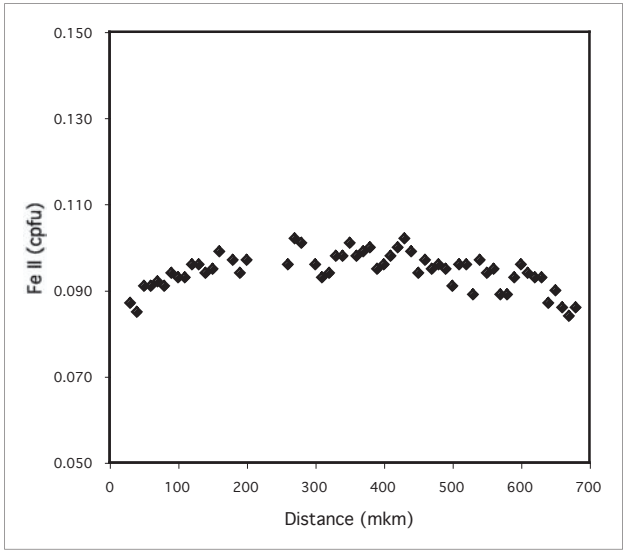
1906-2 Spinel, profile 175

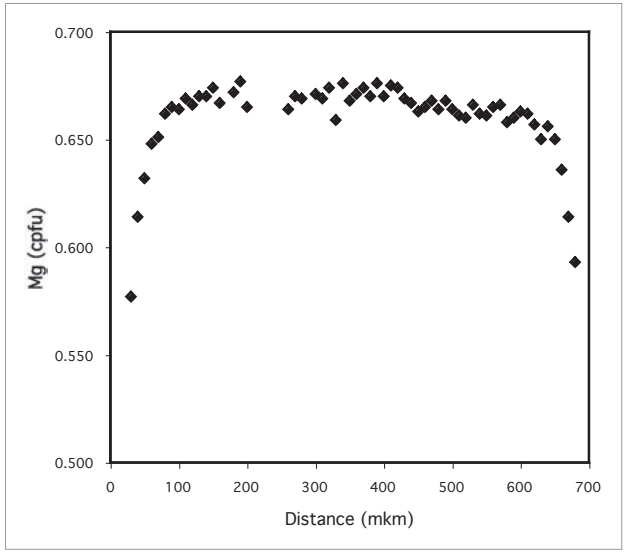
Mg-Al granulite 1904-3

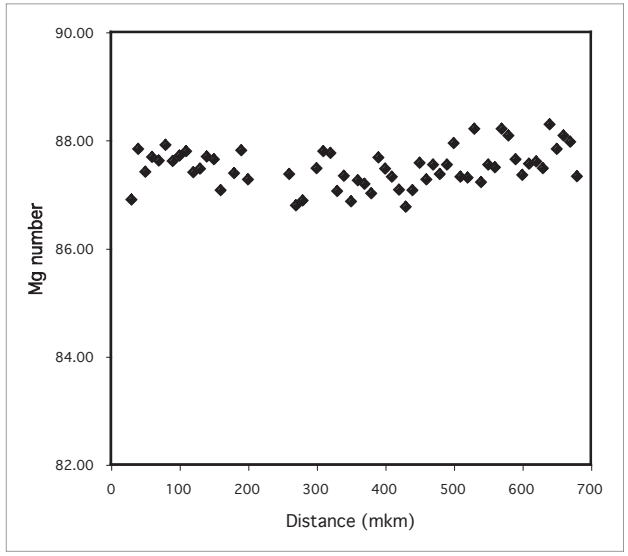






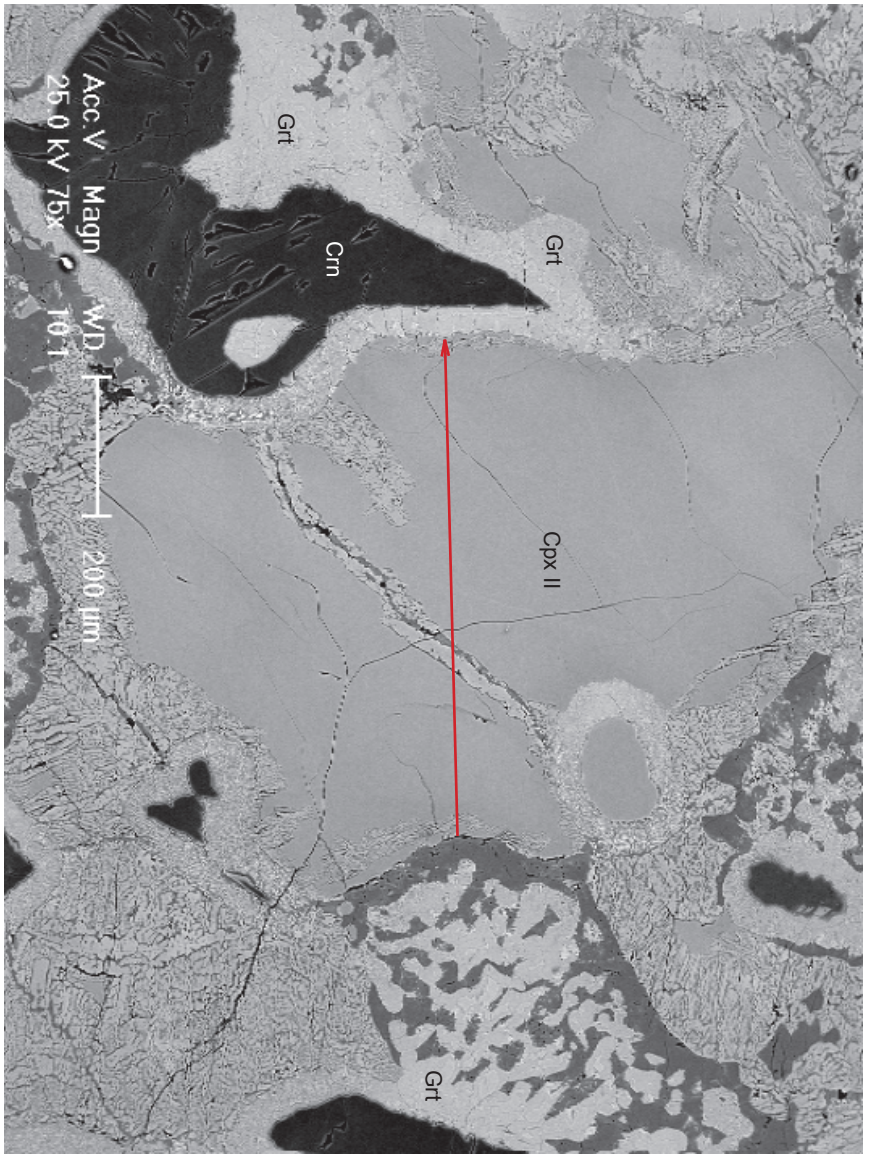






1904-3 Cpx II, profile 655

	30	40	50	60	70	80	90	100	110	120	130
SiO2	54.16	54.20	54.36	54.50	54.35	54.30	54.30	54.35	54.16	54.13	53.87
TiO2	0.00	0.01	0.01	0.01	0.00	0.03	0.01	0.02	0.00	0.01	0.00
Al2O3	10.82	9.83	9.12	8.63	8.34	8.27	8.33	8.19	8.22	8.23	8.27
Cr2O3	0.03	0.00	0.02	0.03	0.02	0.02	0.01	0.02	0.01	0.00	0.05
FeO	2.95	2.85	3.04	3.05	3.07	3.06	3.18	3.10	3.11	3.20	3.20
MnO	0.01	0.04	0.00	0.01	0.03	0.02	0.03	0.05	0.05	0.05	0.04
NiO	0.06	0.09	0.12	0.08	0.12	0.09	0.12	0.09	0.14	0.07	0.07
MgO	10.91	11.57	11.88	12.22	12.22	12.45	12.53	12.50	12.56	12.50	12.55
CaO	17.02	17.56	17.84	18.39	18.48	18.88	18.83	18.94	18.86	18.99	18.89
Na2O	4.66	4.23	3.91	3.96	3.69	3.55	3.75	3.51	3.48	3.43	3.57
K2O	0.01	0.00	0.00	0.00	0.01	0.00	0.00	0.00	0.01	0.00	0.00
Total	100.62	100.38	100.31	100.88	100.32	100.68	101.07	100.76	100.58	100.61	100.51
Si	1.923	1.931	1.940	1.939	1.944	1.937	1.932	1.938	1.935	1.934	1.929
Ti	0.000	0.000	0.000	0.000	0.000	0.001	0.000	0.000	0.000	0.000	0.000
Al	0.452	0.413	0.384	0.362	0.352	0.348	0.349	0.344	0.346	0.347	0.349
Cr	0.001	0.000	0.001	0.001	0.001	0.001	0.000	0.001	0.000	0.000	0.001
Fe2+	0.087	0.085	0.091	0.091	0.092	0.091	0.094	0.093	0.093	0.096	0.096
Mn	0.000	0.001	0.000	0.000	0.001	0.000	0.001	0.002	0.001	0.002	0.001
Ni	0.002	0.002	0.003	0.002	0.003	0.003	0.003	0.003	0.004	0.002	0.002
Mg	0.577	0.614	0.632	0.648	0.651	0.662	0.665	0.664	0.669	0.666	0.670
Ca	0.647	0.670	0.682	0.701	0.708	0.722	0.718	0.724	0.722	0.727	0.725
Na	0.321	0.292	0.270	0.273	0.256	0.246	0.258	0.243	0.241	0.238	0.248
K	0.001	0.000	0.000	0.000	0.000	0.000	0.000	0.000	0.001	0.000	0.000
Sum	4.011	4.009	4.003	4.016	4.008	4.011	4.022	4.011	4.012	4.011	4.020
Mg#	86.90	87.84	87.41	87.69	87.62	87.92	87.62	87.71	87.80	87.40	87.47
Al IV	0.066	0.061	0.058	0.045	0.049	0.053	0.046	0.051	0.052	0.055	0.051
Al VI	0.387	0.353	0.327	0.317	0.304	0.296	0.304	0.293	0.294	0.293	0.298



1904-3 Cpx II, profile 655

	140	150	160	170	180	190	200	210	220	230	240	250	260	270	280	290	300	310	320	330
SiO2	53.69	53.96	53.74	53.35	54.08	53.51	53.81	51.48	51.16	52.86	51.44	53.67	53.50	53.61	53.70	50.16	53.60	53.22	53.45	53.74
TiO2	0.00	0.00	0.03	0.04	0.03	0.00	0.01	0.00	0.05	0.03	0.02	0.02	0.00	0.01	0.00	0.04	0.05	0.04	0.01	0.01
Al2O3	8.41	8.43	8.26	10.21	8.25	8.31	8.40	5.60	6.57	5.36	20.81	21.86	8.21	8.28	8.37	8.59	8.25	8.40	8.35	8.33
Cr2O3	0.02	0.08	0.00	0.03	0.03	0.00	0.04	0.00	0.00	0.00	0.00	0.00	0.10	0.04	0.00	0.03	0.00	0.04	0.01	0.02
FeO	3.15	3.18	3.29	3.84	3.25	3.12	3.25	6.52	4.38	3.34	7.00	8.12	3.20	3.42	3.36	3.14	3.19	3.09	3.12	3.26
MnO	0.01	0.03	0.00	0.05	0.02	0.04	0.10	0.11	0.00	0.00	0.10	0.08	0.08	0.07	0.03	0.04	0.05	0.02	0.07	0.00
NiO	0.13	0.08	0.09		0.12	0.17	0.13						0.09	0.11	0.10		0.07	0.12	0.14	0.14
MgO	12.54	12.70	12.50	10.73	12.64	12.66	12.50	15.09	13.50	14.90	4.41	3.49	12.39	12.55	12.56	10.66	12.55	12.47	12.57	12.33
CaO	19.18	19.38	19.34	17.01	19.29	19.60	19.43	19.38	20.70	22.71	6.52	4.40	19.59	19.53	19.56	18.17	19.45	19.54	19.46	19.51
Na2O	3.32	3.32	3.39	2.63	3.20	3.10	3.27	0.53	0.82	1.08	0.85	1.95	3.11	3.08	3.13	2.56	3.10	3.12	2.99	3.22
K2O	0.01	0.01	0.00	0.13	0.00	0.00	0.00	0.14	0.13	0.01	0.30	0.34	0.01	0.01	0.00	0.05	0.00	0.01	0.00	0.00
Total	100.46	101.17	100.64	98.05	100.88	100.51	100.95	98.95	97.43	100.37	91.49	93.97	100.29	100.71	100.81	93.51	100.30	100.06	100.16	100.57
Si	1.923	1.921	1.924		1.929	1.918	1.921						1.923	1.920	1.920		1.924	1.916	1.921	1.925
Ti	0.000	0.000	0.001		0.001	0.000	0.000						0.000	0.000	0.000		0.001	0.001	0.000	0.000
Al	0.355	0.353	0.349		0.347	0.351	0.353						0.348	0.349	0.353		0.349	0.356	0.354	0.352
Cr	0.001	0.002	0.000		0.001	0.000	0.001						0.003	0.001	0.000		0.000	0.001	0.000	0.001
Fe2+	0.094	0.095	0.099		0.097	0.094	0.097						0.096	0.102	0.101		0.096	0.093	0.094	0.098
Mn	0.000	0.001	0.000		0.000	0.001	0.003						0.002	0.002	0.001		0.002	0.001	0.002	0.000
Ni	0.004	0.002	0.003		0.003	0.005	0.004						0.003	0.003	0.003		0.002	0.003	0.004	0.004
Mg	0.670	0.674	0.667		0.672	0.677	0.665						0.664	0.670	0.669		0.671	0.669	0.674	0.659
Ca	0.736	0.739	0.742		0.737	0.753	0.743						0.754	0.749	0.749		0.748	0.754	0.749	0.749
Na	0.231	0.229	0.235		0.221	0.216	0.226						0.217	0.214	0.217		0.215	0.218	0.209	0.224
K	0.000	0.001	0.000		0.000	0.000	0.000						0.000	0.001	0.000		0.000	0.000	0.000	0.000
Sum	4.014	4.017	4.019		4.008	4.014	4.015						4.010	4.012	4.012		4.008	4.013	4.006	4.010
Mg#	87.70	87.65	87.08		87.39	87.81	87.27						87.37	86.79	86.88		87.48	87.80	87.76	87.05
Al IV	0.063	0.063	0.058		0.065	0.068	0.064						0.067	0.068	0.068		0.068	0.071	0.073	0.065
Al VI	0.293	0.291	0.291		0.283	0.284	0.289						0.281	0.282	0.285		0.281	0.286	0.282	0.288

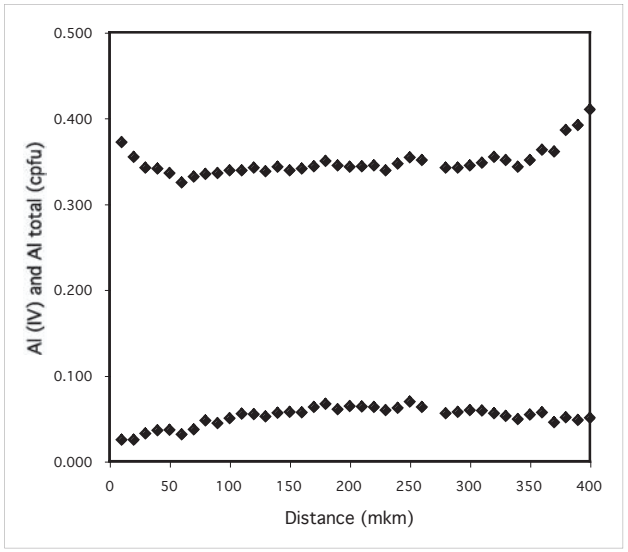
1904-3 Cpx II, profile 655

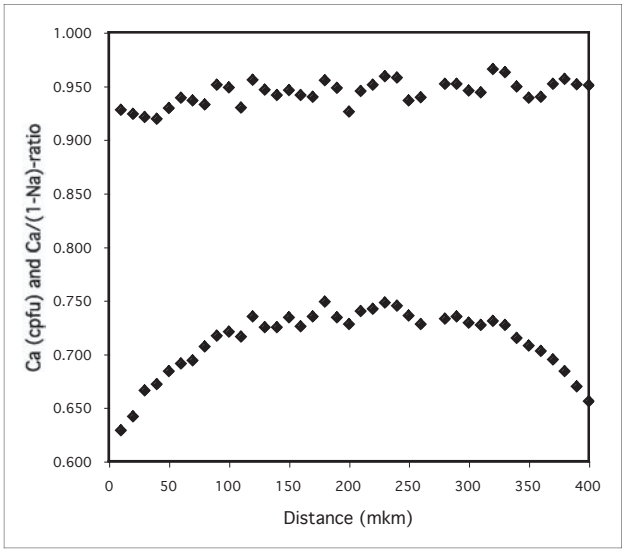
	340	350	360	370	380	390	400	410	420	430	440	450	460	470	480	490	500	510	520	530
SiO2	53.60	53.32	53.67	53.37	53.53	53.53	53.59	53.56	53.38	53.48	53.63	53.47	53.66	53.65	53.72	53.57	53.49	53.61	53.73	53.84
TiO2	0.01	0.00	0.00	0.04	0.00	0.01	0.00	0.02	0.01	0.00	0.03	0.00	0.03	0.03	0.06	0.00	0.01	0.00	0.02	0.02
Al2O3	8.23	8.16	8.36	8.31	8.23	8.19	8.33	8.28	8.17	8.26	8.33	8.41	8.39	8.25	8.41	8.34	8.36	8.30	8.44	8.30
Cr2O3	0.00	0.04	0.02	0.01	0.02	0.00	0.00	0.00	0.02	0.00	0.03	0.01	0.06	0.01	0.06	0.01	0.02	0.02	0.04	0.00
FeO	3.28	3.35	3.28	3.30	3.33	3.18	3.22	3.28	3.33	3.40	3.31	3.13	3.23	3.17	3.21	3.16	3.03	3.20	3.22	2.98
MnO	0.08	0.01	0.01	0.02	0.00	0.00	0.05	0.02	0.03	0.11	0.08	0.01	0.03	0.08	0.01	0.00	0.02	0.00	0.06	0.04
NiO	0.06	0.10	0.13	0.13	0.08	0.14	0.08	0.09	0.11	0.11	0.06	0.14	0.11	0.12	0.12	0.11	0.07	0.09	0.15	0.10
MgO	12.67	12.41	12.54	12.60	12.56	12.61	12.53	12.62	12.59	12.50	12.50	12.36	12.47	12.52	12.44	12.47	12.40	12.36	12.37	12.45
CaO	19.69	19.42	19.18	19.67	19.84	19.46	19.46	19.31	19.63	19.41	19.45	19.27	19.35	19.52	19.26	19.08	19.42	19.37	19.19	19.14
Na2O	3.17	3.00	3.10	3.12	3.32	3.09	3.20	3.20	3.21	3.23	3.34	3.37	3.30	3.33	3.29	3.40	3.44	3.42	3.44	3.39
K2O	0.01	0.00	0.01	0.00	0.01	0.01	0.00	0.00	0.01	0.00	0.00	0.01	0.00	0.01	0.00	0.00	0.01	0.01	0.02	0.00
Total	100.80	99.81	100.29	100.56	100.90	100.21	100.46	100.37	100.48	100.49	100.75	100.16	100.61	100.68	100.58	100.14	100.25	100.38	100.68	100.25
Si	1.918	1.925	1.925	1.914	1.916	1.924	1.921	1.922	1.917	1.920	1.919	1.922	1.921	1.921	1.923	1.925	1.922	1.924	1.923	1.930
Ti	0.000	0.000	0.000	0.001	0.000	0.000	0.000	0.000	0.000	0.000	0.001	0.000	0.001	0.001	0.002	0.000	0.000	0.000	0.001	0.001
Al	0.347	0.347	0.353	0.351	0.347	0.347	0.352	0.350	0.346	0.350	0.351	0.356	0.354	0.348	0.355	0.353	0.354	0.351	0.356	0.351
Cr	0.000	0.001	0.001	0.000	0.000	0.000	0.000	0.000	0.001	0.000	0.001	0.000	0.002	0.000	0.002	0.000	0.001	0.001	0.001	0.000
Fe2+	0.098	0.101	0.098	0.099	0.100	0.095	0.096	0.098	0.100	0.102	0.099	0.094	0.097	0.095	0.096	0.095	0.091	0.096	0.096	0.089
Mn	0.002	0.000	0.000	0.001	0.000	0.000	0.001	0.001	0.001	0.003	0.002	0.000	0.001	0.002	0.000	0.000	0.000	0.000	0.002	0.001
Ni	0.002	0.003	0.004	0.004	0.002	0.004	0.002	0.003	0.003	0.003	0.002	0.004	0.003	0.003	0.003	0.003	0.002	0.003	0.004	0.003
Mg	0.676	0.668	0.671	0.674	0.670	0.676	0.670	0.675	0.674	0.669	0.667	0.663	0.665	0.668	0.664	0.668	0.664	0.661	0.660	0.666
Ca	0.755	0.751	0.737	0.756	0.761	0.749	0.748	0.743	0.755	0.746	0.746	0.742	0.742	0.749	0.739	0.735	0.747	0.745	0.736	0.735
Na	0.220	0.210	0.216	0.217	0.230	0.215	0.223	0.223	0.224	0.225	0.232	0.235	0.229	0.231	0.228	0.237	0.239	0.238	0.239	0.236
K	0.000	0.000	0.000	0.000	0.001	0.000	0.000	0.000	0.001	0.000	0.000	0.000	0.000	0.000	0.000	0.000	0.000	0.001	0.001	0.000
Sum	4.019	4.006	4.006	4.017	4.026	4.010	4.014	4.014	4.022	4.018	4.020	4.017	4.015	4.020	4.011	4.016	4.021	4.019	4.018	4.012
Mg#	87.34	86.87	87.26	87.19	87.01	87.68	87.47	87.32	87.08	86.77	87.08	87.58	87.27	87.55	87.37	87.55	87.95	87.32	87.30	88.21
Al IV	0.064	0.069	0.069	0.068	0.058	0.066	0.065	0.064	0.061	0.063	0.061	0.061	0.065	0.060	0.067	0.058	0.058	0.057	0.060	0.059
Al VI	0.284	0.278	0.284	0.283	0.289	0.281	0.288	0.287	0.285	0.288	0.290	0.296	0.290	0.289	0.289	0.295	0.296	0.295	0.297	0.293

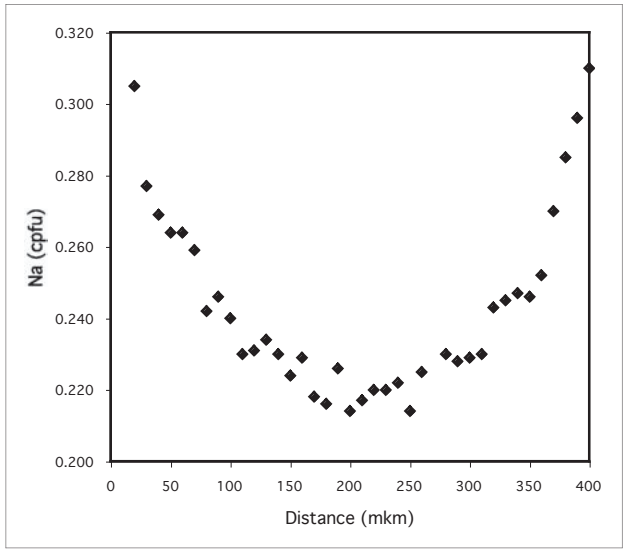
1904-3 Cpx II, profile 655

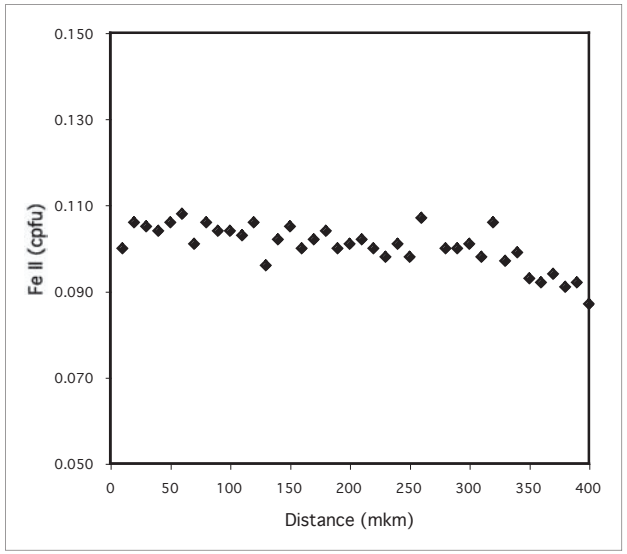
	540	550	560	570	580	590	600	610	620	630	640	650	660	670	680
SiO2	53.92	53.91	53.95	53.85	53.84	53.67	53.88	53.63	54.08	54.26	53.84	54.08	53.90	53.82	53.72
TiO2	0.03	0.00	0.03	0.02	0.03	0.03	0.00	0.00	0.02	0.02	0.00	0.00	0.01	0.02	0.00
Al2O3	8.39	8.25	8.17	8.06	8.29	8.31	8.43	8.38	8.18	8.41	8.38	8.67	9.19	9.95	10.91
Cr2O3	0.02	0.00	0.01	0.03	0.00	0.00	0.03	0.00	0.00	0.03	0.04	0.01	0.02	0.00	0.04
FeO	3.25	3.16	3.16	2.95	2.97	3.11	3.20	3.14	3.10	3.11	2.91	3.00	2.87	2.82	2.88
MnO	0.01	0.06	0.03	0.00	0.05	0.01	0.04	0.02	0.01	0.03	0.05	0.07	0.06	0.04	0.01
NiO	0.08	0.07	0.07	0.11	0.09	0.13	0.12	0.10	0.11	0.08	0.09	0.11	0.11	0.11	0.11
MgO	12.46	12.39	12.44	12.43	12.30	12.34	12.44	12.35	12.32	12.22	12.25	12.22	11.91	11.54	11.20
CaO	19.43	19.36	19.10	19.10	19.17	19.25	19.03	18.89	19.06	18.86	18.86	18.85	18.22	17.90	17.66
Na2O	3.54	3.40	3.43	3.43	3.53	3.47	3.46	3.56	3.56	3.64	3.68	3.78	3.79	4.10	4.36
K2O	0.00	0.00	0.01	0.00	0.01	0.00	0.00	0.00	0.00	0.01	0.00	0.00	0.00	0.01	0.00
Total	101.15	100.58	100.40	99.98	100.28	100.31	100.63	100.07	100.44	100.67	100.09	100.78	100.06	100.32	100.90
Si	1.921	1.929	1.933	1.936	1.931	1.926	1.927	1.928	1.936	1.937	1.933	1.929	1.930	1.921	1.906
Ti	0.001	0.000	0.001	0.000	0.001	0.001	0.000	0.000	0.001	0.000	0.000	0.000	0.000	0.001	0.000
Al	0.352	0.348	0.345	0.341	0.350	0.352	0.355	0.355	0.345	0.354	0.355	0.364	0.388	0.419	0.456
Cr	0.001	0.000	0.000	0.001	0.000	0.000	0.001	0.000	0.000	0.001	0.001	0.000	0.000	0.000	0.001
Fe2+	0.097	0.094	0.095	0.089	0.089	0.093	0.096	0.094	0.093	0.093	0.087	0.090	0.086	0.084	0.086
Mn	0.000	0.002	0.001	0.000	0.001	0.000	0.001	0.001	0.000	0.001	0.001	0.002	0.002	0.001	0.000
Ni	0.002	0.002	0.002	0.003	0.003	0.004	0.004	0.003	0.003	0.002	0.003	0.003	0.003	0.003	0.003
Mg	0.662	0.661	0.665	0.666	0.658	0.660	0.663	0.662	0.657	0.650	0.656	0.650	0.636	0.614	0.593
Ca	0.742	0.742	0.733	0.736	0.737	0.740	0.729	0.728	0.731	0.721	0.725	0.720	0.699	0.685	0.671
Na	0.244	0.236	0.238	0.239	0.245	0.241	0.240	0.248	0.247	0.252	0.256	0.261	0.263	0.284	0.300
K	0.000	0.000	0.000	0.000	0.001	0.000	0.000	0.000	0.000	0.000	0.000	0.000	0.000	0.000	0.000
Sum	4.023	4.015	4.013	4.012	4.016	4.018	4.015	4.018	4.014	4.012	4.017	4.020	4.007	4.011	4.015
Mg#	87.22	87.55	87.50	88.21	88.09	87.65	87.35	87.57	87.60	87.48	88.29	87.84	88.09	87.97	87.33
Al IV	0.056	0.056	0.055	0.052	0.053	0.057	0.058	0.054	0.050	0.052	0.050	0.052	0.063	0.069	0.079
Al VI	0.297	0.292	0.291	0.290	0.297	0.296	0.297	0.302	0.295	0.303	0.305	0.313	0.326	0.351	0.378

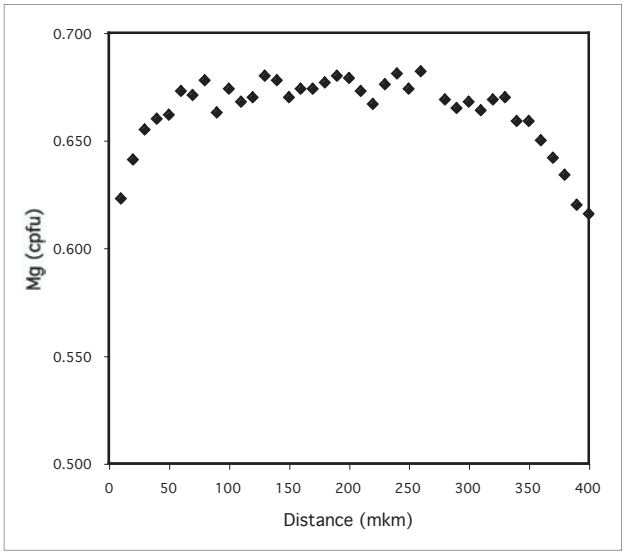
1904-3 Cpx II, profile 655

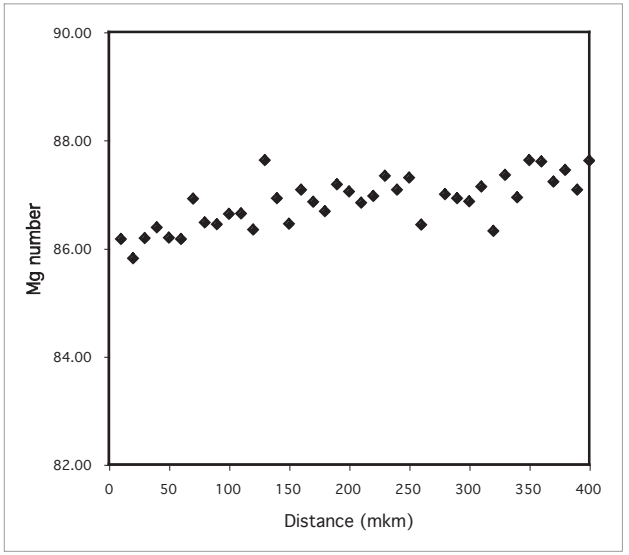












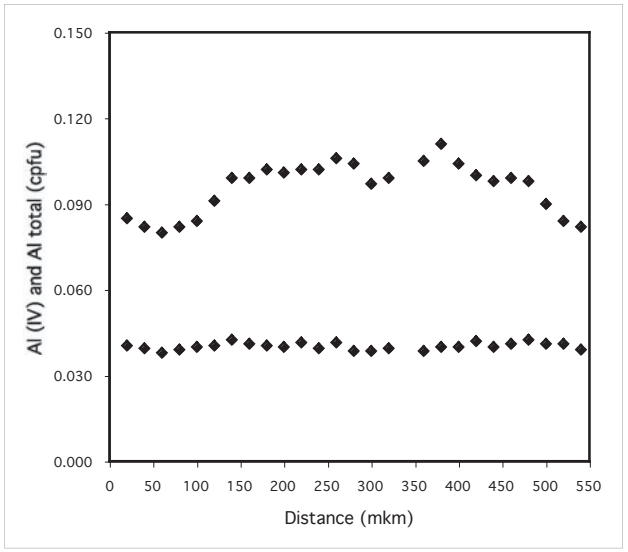
1904-3 Cpx II, profile 394

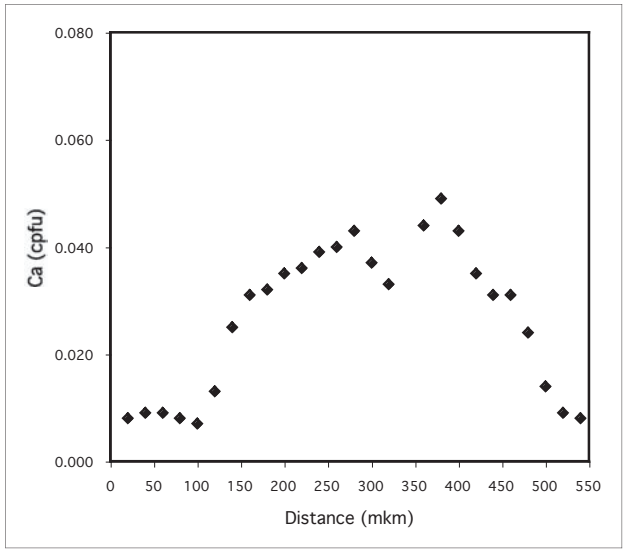
	10	20	30	40	50	60	70	80	90	100	110	120	130	140	150	160	170	180	190	200
SiO2	55.03	54.92	54.88	55.01	54.65	54.63	54.56	54.17	54.22	53.89	54.22	53.67	53.84	53.77	54.08	53.88	53.80	53.24	53.54	54.11
TiO2	0.00	0.00	0.02	0.00	0.01	0.03	0.00	0.02	0.00	0.01	0.02	0.02	0.00	0.01	0.00	0.05	0.01	0.00	0.04	0.00
Al2O3	8.86	8.44	8.13	8.13	7.98	7.73	7.87	7.93	7.95	8.01	8.02	8.09	7.97	8.12	8.05	8.07	8.13	8.26	8.14	8.14
Cr2O3	0.00	0.03	0.00	0.00	0.03	0.04	0.03	0.05	0.01	0.03	0.00	0.00	0.00	0.00	0.00	0.00	0.00	0.00	0.00	0.00
FeO	3.34	3.56	3.53	3.51	3.55	3.63	3.39	3.55	3.46	3.48	3.45	3.52	3.20	3.40	3.51	3.34	3.41	3.45	3.33	3.37
MnO	0.04	0.07	0.04	0.06	0.07	0.09	0.05	0.05	0.03	0.04	0.00	0.02	0.04	0.08	0.05	0.02	0.00	0.04	0.07	0.03
NiO	0.08	0.10	0.14	0.07	0.09	0.10	0.11	0.06	0.08	0.09	0.10	0.09	0.12	0.14	0.14	0.09	0.11	0.11	0.08	0.10
MgO	11.72	12.05	12.31	12.44	12.42	12.66	12.58	12.70	12.42	12.60	12.51	12.52	12.68	12.69	12.58	12.61	12.61	12.62	12.70	12.74
CaO	16.47	16.79	17.42	17.62	17.87	18.07	18.11	18.43	18.67	18.75	18.65	19.09	18.83	18.87	19.16	18.88	19.14	19.42	19.07	19.02
Na2O	4.65	4.41	4.01	3.89	3.81	3.82	3.74	3.48	3.54	3.45	3.32	3.32	3.36	3.31	3.23	3.30	3.14	3.09	3.24	3.08
K2O	0.00	0.01	0.00	0.00	0.01	0.01	0.00	0.01	0.01	0.01	0.00	0.02	0.00	0.00	0.01	0.00	0.00	0.00	0.00	0.00
Total	100.19	100.37	100.48	100.73	100.48	100.81	100.44	100.45	100.38	100.35	100.30	100.35	100.04	100.38	100.80	100.23	100.34	100.23	100.20	100.59
Si	1.963	1.960	1.958	1.957	1.953	1.949	1.951	1.940	1.943	1.934	1.943	1.928	1.935	1.929	1.932	1.933	1.930	1.916	1.924	1.934
Ti	0.000	0.000	0.000	0.000	0.000	0.001	0.000	0.000	0.000	0.000	0.001	0.000	0.000	0.000	0.000	0.001	0.000	0.000	0.001	0.000
Al	0.372	0.355	0.342	0.341	0.336	0.325	0.332	0.335	0.336	0.339	0.339	0.342	0.338	0.343	0.339	0.341	0.344	0.350	0.345	0.343
Cr	0.000	0.001	0.000	0.000	0.001	0.001	0.001	0.002	0.000	0.001	0.000	0.000	0.000	0.000	0.000	0.000	0.000	0.000	0.000	0.000
Fe2+	0.100	0.106	0.105	0.104	0.106	0.108	0.101	0.106	0.104	0.104	0.103	0.106	0.096	0.102	0.105	0.100	0.102	0.104	0.100	0.101
Mn	0.001	0.002	0.001	0.002	0.002	0.003	0.001	0.001	0.001	0.001	0.000	0.001	0.001	0.002	0.001	0.001	0.000	0.001	0.002	0.001
Ni	0.002	0.003	0.004	0.002	0.003	0.003	0.003	0.002	0.002	0.003	0.003	0.003	0.003	0.004	0.004	0.003	0.003	0.003	0.002	0.003
Mg	0.623	0.641	0.655	0.660	0.662	0.673	0.671	0.678	0.663	0.674	0.668	0.670	0.680	0.678	0.670	0.674	0.674	0.677	0.680	0.679
Ca	0.629	0.642	0.666	0.672	0.684	0.691	0.694	0.707	0.717	0.721	0.716	0.735	0.725	0.725	0.734	0.726	0.735	0.749	0.734	0.728
Na	0.322	0.305	0.277	0.269	0.264	0.264	0.259	0.242	0.246	0.240	0.230	0.231	0.234	0.230	0.224	0.229	0.218	0.216	0.226	0.214
K	0.000	0.001	0.000	0.000	0.000	0.001	0.000	0.000	0.001	0.000	0.000	0.001	0.000	0.000	0.000	0.000	0.000	0.000	0.000	0.000
Sum	4.012	4.015	4.009	4.007	4.011	4.019	4.013	4.013	4.012	4.017	4.003	4.017	4.013	4.014	4.010	4.009	4.007	4.016	4.015	4.002
Mg#	86.17	85.81	86.18	86.39	86.20	86.17	86.92	86.48	86.44	86.63	86.64	86.34	87.63	86.92	86.45	87.08	86.86	86.68	87.18	87.05
Al IV	0.025	0.025	0.033	0.036	0.037	0.032	0.037	0.048	0.045	0.050	0.056	0.055	0.052	0.057	0.058	0.057	0.063	0.067	0.061	0.065
Al VI	0.347	0.330	0.310	0.305	0.300	0.294	0.295	0.288	0.292	0.289	0.284	0.287	0.286	0.287	0.282	0.284	0.281	0.283	0.285	0.279

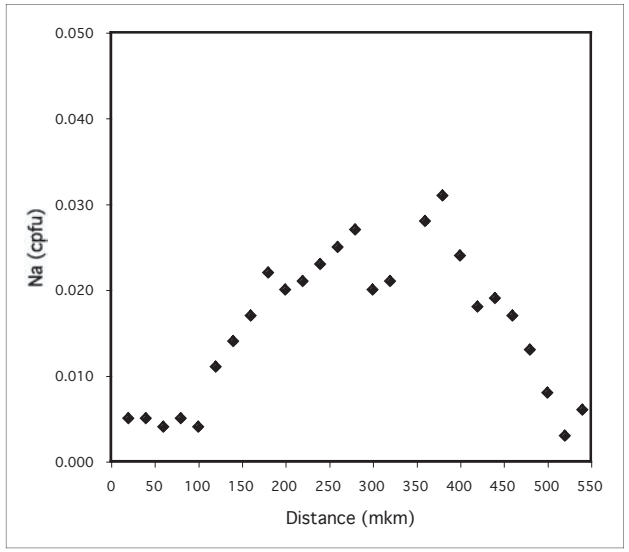
1904-3 Cpx II, profile 394

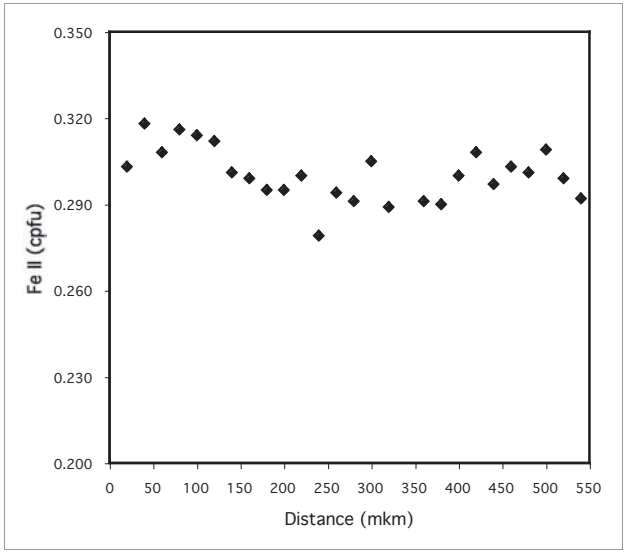
	210	220	230	240	250	260	270	280	290	300	310	320	330	340	350	360	370	380	390	400
SiO2	53.54	53.64	53.71	53.61	53.69	54.17	53.18	53.78	54.21	54.11	54.03	53.36	53.89	54.30	54.26	54.14	54.48	54.27	54.76	54.79
TiO2	0.00	0.00	0.01	0.00	0.00	0.01	0.02	0.01	0.00	0.05	0.00	0.00	0.00	0.04	0.04	0.03	0.02	0.00	0.00	0.00
Al2O3	8.09	8.15	8.03	8.22	8.37	8.41	8.83	8.07	8.14	8.19	8.24	8.38	8.33	8.15	8.32	8.59	8.58	9.20	9.39	9.87
Cr2O3	0.00	0.02	0.04	0.02	0.00	0.04	0.00	0.01	0.02	0.03	0.01	0.03	0.00	0.00	0.06	0.02	0.00	0.04	0.00	0.05
FeO	3.39	3.33	3.28	3.38	3.28	3.61	3.29	3.34	3.35	3.37	3.27	3.51	3.25	3.31	3.11	3.06	3.15	3.05	3.11	2.96
MnO	0.03	0.00	0.08	0.03	0.06	0.04	0.05	0.02	0.06	0.05	0.03	0.00	0.01	0.04	0.09	0.00	0.03	0.04	0.09	0.00
NiO	0.11	0.13	0.09	0.09	0.09	0.13	0.06	0.10	0.15	0.10	0.06	0.11	0.12	0.10	0.12	0.11	0.12	0.09	0.06	0.09
MgO	12.54	12.45	12.64	12.77	12.61	12.93	11.95	12.48	12.52	12.56	12.42	12.49	12.57	12.36	12.36	12.18	12.08	11.96	11.75	11.72
CaO	19.17	19.24	19.47	19.44	19.16	19.19	18.74	19.04	19.23	19.05	18.93	18.98	18.99	18.66	18.48	18.31	18.17	17.93	17.66	17.34
Na2O	3.10	3.15	3.16	3.20	3.07	3.28	3.08	3.30	3.30	3.31	3.31	3.49	3.53	3.56	3.55	3.63	3.90	4.14	4.32	4.53
K2O	0.00	0.01	0.01	0.01	0.01	0.02	0.06	0.00	0.01	0.00	0.00	0.01	0.00	0.00	0.00	0.00	0.00	0.00	0.00	0.01
Total	99.97	100.11	100.51	100.77	100.35	101.83	99.26	100.15	100.98	100.82	100.30	100.37	100.69	100.52	100.39	100.08	100.53	100.71	101.13	101.36
Si	1.929	1.929	1.926	1.918	1.925	1.918		1.933	1.933	1.931	1.936	1.918	1.927	1.941	1.940	1.939	1.944	1.932	1.939	1.933
Ti	0.000	0.000	0.000	0.000	0.000	0.000		0.000	0.000	0.001	0.000	0.000	0.000	0.001	0.001	0.001	0.000	0.000	0.000	0.000
Al	0.344	0.345	0.339	0.347	0.354	0.351		0.342	0.342	0.345	0.348	0.355	0.351	0.343	0.351	0.363	0.361	0.386	0.392	0.410
Cr	0.000	0.001	0.001	0.000	0.000	0.001		0.000	0.001	0.001	0.000	0.001	0.000	0.000	0.002	0.001	0.000	0.001	0.000	0.001
Fe2+	0.102	0.100	0.098	0.101	0.098	0.107		0.100	0.100	0.101	0.098	0.106	0.097	0.099	0.093	0.092	0.094	0.091	0.092	0.087
Mn	0.001	0.000	0.002	0.001	0.002	0.001		0.001	0.002	0.002	0.001	0.000	0.000	0.001	0.003	0.000	0.001	0.001	0.003	0.000
Ni	0.003	0.004	0.003	0.003	0.003	0.004		0.003	0.004	0.003	0.002	0.003	0.003	0.003	0.003	0.003	0.004	0.002	0.002	0.003
Mg	0.673	0.667	0.676	0.681	0.674	0.682		0.669	0.665	0.668	0.664	0.669	0.670	0.659	0.659	0.650	0.642	0.634	0.620	0.616
Ca	0.740	0.742	0.748	0.745	0.736	0.728		0.733	0.735	0.729	0.727	0.731	0.727	0.715	0.708	0.703	0.695	0.684	0.670	0.656
Na	0.217	0.220	0.220	0.222	0.214	0.225		0.230	0.228	0.229	0.230	0.243	0.245	0.247	0.246	0.252	0.270	0.285	0.296	0.310
K	0.000	0.000	0.001	0.001	0.001	0.001		0.000	0.000	0.000	0.000	0.001	0.000	0.000	0.000	0.000	0.000	0.000	0.000	0.000
Sum	4.008	4.008	4.014	4.019	4.005	4.019		4.011	4.010	4.009	4.005	4.026	4.021	4.009	4.006	4.004	4.010	4.017	4.013	4.016
Mg#	86.84	86.96	87.34	87.08	87.31	86.44		87.00	86.93	86.87	87.14	86.32	87.35	86.94	87.63	87.60	87.23	87.45	87.08	87.62
Al IV	0.064	0.063	0.060	0.062	0.070	0.063		0.056	0.058	0.060	0.059	0.056	0.053	0.049	0.055	0.057	0.046	0.051	0.048	0.051
Al VI	0.281	0.282	0.280	0.285	0.285	0.288		0.286	0.285	0.286	0.289	0.299	0.298	0.294	0.297	0.306	0.316	0.335	0.344	0.360

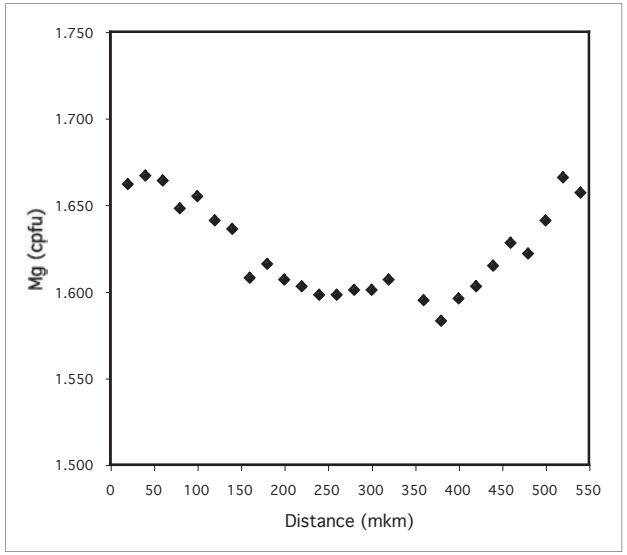
1904-3 Cpx II, profile 394

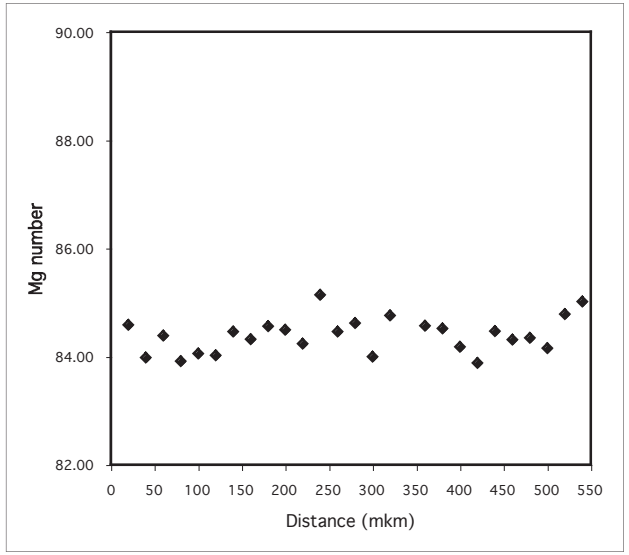






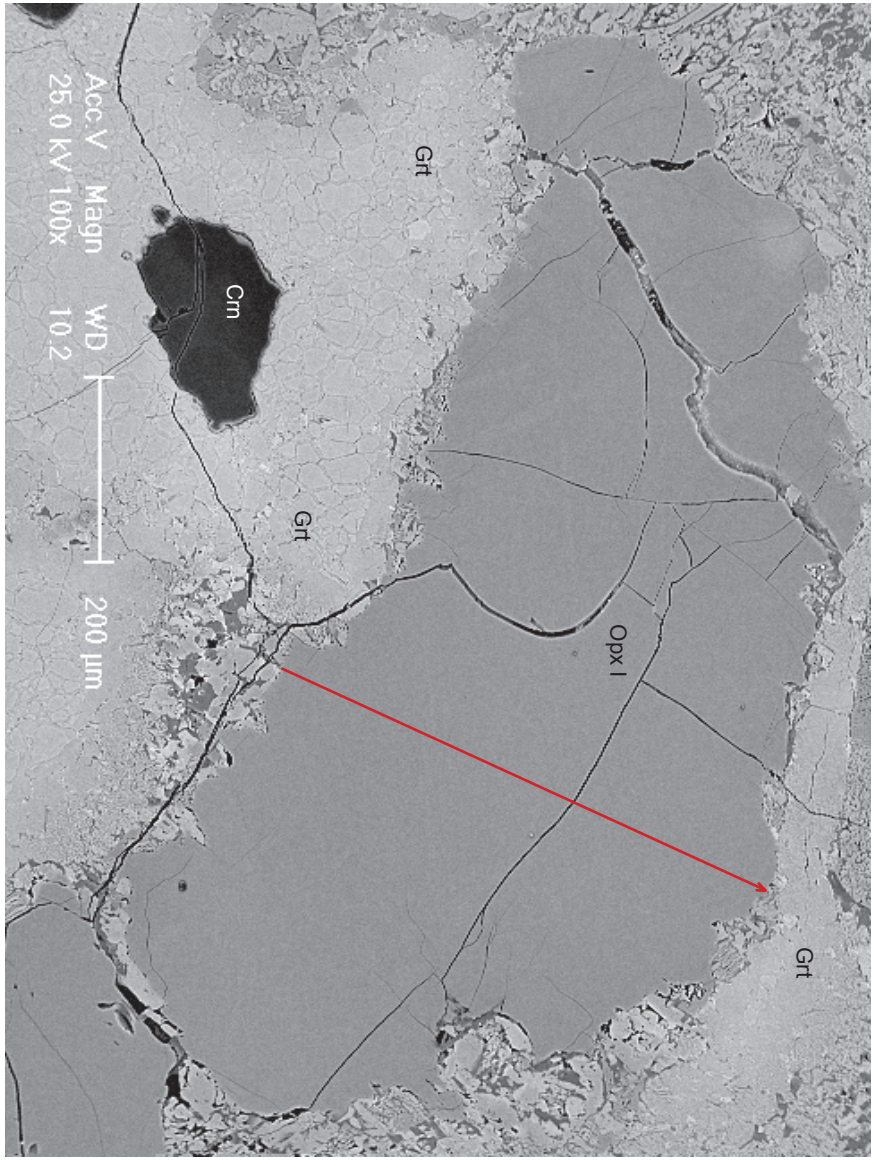






1904-3 Opx I, defocused beam, profile 523

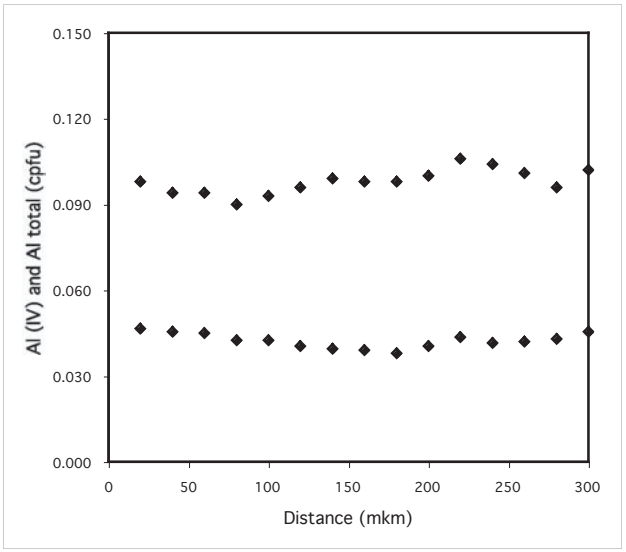
	20	40	60	80	100	120	140	160	180	200
SiO2	55.61	55.66	55.57	55.81	55.54	55.51	55.30	55.62	55.38	55.56
TiO2	0.00	0.02	0.00	0.03	0.00	0.00	0.00	0.00	0.00	0.00
Al2O3	2.07	2.01	1.94	1.99	2.05	2.20	2.39	2.40	2.46	2.44
Cr2O3	0.03	0.00	0.01	0.01	0.00	0.04	0.00	0.02	0.04	0.02
FeO	10.36	10.92	10.53	10.85	10.74	10.65	10.26	10.20	10.05	10.07
MnO	0.06	0.01	0.05	0.08	0.06	0.01	0.00	0.05	0.04	0.07
NiO	0.22	0.25	0.28	0.22	0.25	0.26	0.22	0.22	0.24	0.25
MgO	31.88	32.14	31.90	31.71	31.72	31.46	31.30	30.81	30.92	30.77
CaO	0.22	0.24	0.23	0.22	0.18	0.36	0.66	0.84	0.85	0.92
Na2O	0.07	0.07	0.05	0.07	0.05	0.16	0.20	0.25	0.32	0.30
K2O	0.01	0.00	0.00	0.03	0.00	0.00	0.01	0.00	0.00	0.01
Total	100.51	101.33	100.55	101.03	100.59	100.65	100.35	100.40	100.29	100.41
Si	1.944	1.936	1.944	1.946	1.944	1.942	1.938	1.948	1.942	1.946
Ti	0.000	0.001	0.000	0.001	0.000	0.000	0.000	0.000	0.000	0.000
Al	0.085	0.082	0.080	0.082	0.084	0.091	0.099	0.099	0.102	0.101
Cr	0.001	0.000	0.000	0.000	0.000	0.001	0.000	0.000	0.001	0.000
Fe2+	0.303	0.318	0.308	0.316	0.314	0.312	0.301	0.299	0.295	0.295
Mn	0.002	0.000	0.002	0.002	0.002	0.000	0.000	0.002	0.001	0.002
Ni	0.006	0.007	0.008	0.006	0.007	0.007	0.006	0.006	0.007	0.007
Mg	1.662	1.667	1.664	1.648	1.655	1.641	1.636	1.608	1.616	1.607
Ca	0.008	0.009	0.009	0.008	0.007	0.013	0.025	0.031	0.032	0.035
Na	0.005	0.005	0.004	0.005	0.004	0.011	0.014	0.017	0.022	0.020
K	0.000	0.000	0.000	0.001	0.000	0.000	0.000	0.000	0.000	0.001
Sum	4.015	4.025	4.018	4.016	4.016	4.018	4.019	4.011	4.017	4.013
Mg#	84.58	83.98	84.38	83.91	84.05	84.02	84.46	84.32	84.56	84.49
Al IV	0.041	0.040	0.038	0.039	0.040	0.041	0.043	0.041	0.041	0.040
Al VI	0.045	0.043	0.042	0.043	0.044	0.051	0.057	0.058	0.062	0.061

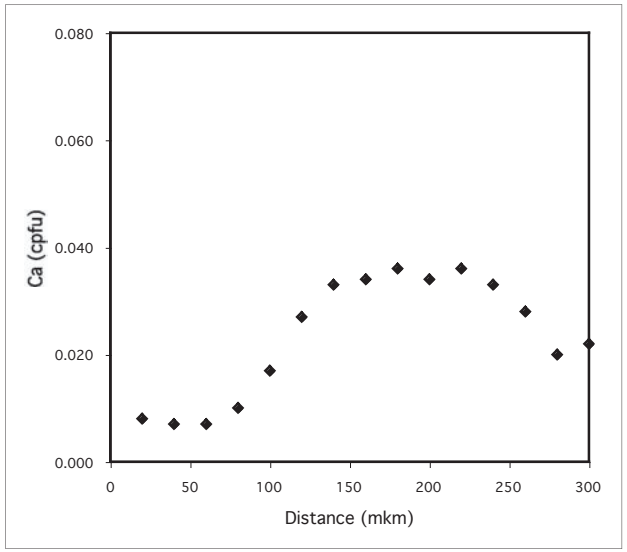


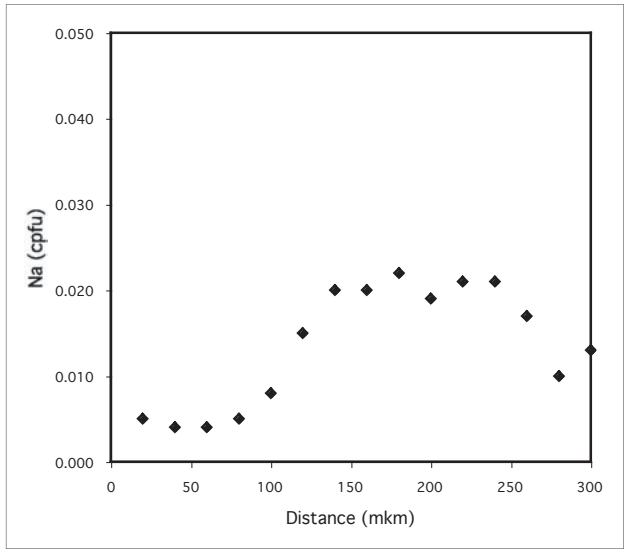
1904-3 Opx I, defocused beam, profile 523

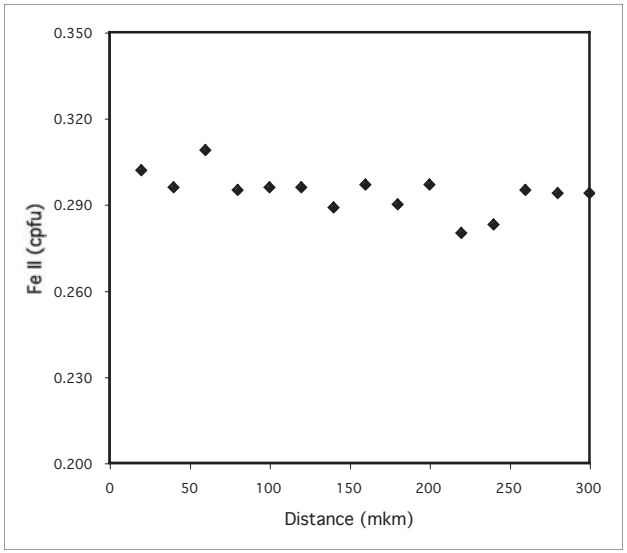
	220	240	260	280	300	320	340	360	380	400	420	440	460	480	500	520	540
SiO2	55.43	55.48	55.05	55.11	55.60	55.51	54.78	55.58	55.27	55.35	55.15	55.47	55.33	55.40	55.48	55.44	55.66
TiO2	0.02	0.01	0.00	0.01	0.00	0.01	0.00	0.00	0.00	0.00	0.03	0.02	0.00	0.00	0.00	0.00	0.02
Al2O3	2.46	2.45	2.54	2.50	2.36	2.39	4.26	2.54	2.69	2.53	2.42	2.38	2.40	2.38	2.19	2.04	1.97
Cr2O3	0.02	0.02	0.07	0.00	0.00	0.02	0.00	0.01	0.02	0.00	0.00	0.00	0.00	0.00	0.01	0.02	0.01
FeO	10.23	9.45	9.97	9.87	10.41	9.85	9.71	9.92	9.87	10.23	10.46	10.13	10.36	10.26	10.54	10.20	9.96
MnO	0.02	0.04	0.08	0.10	0.03	0.11	0.09	0.03	0.07	0.05	0.08	0.12	0.05	0.07	0.03	0.08	0.07
NiO	0.22	0.22	0.28	0.28	0.25	0.21	0.25	0.21	0.25	0.24	0.26	0.25	0.30	0.21	0.26	0.25	0.22
MgO	30.64	30.41	30.39	30.45	30.68	30.69	28.82	30.55	30.21	30.52	30.53	30.92	31.23	30.99	31.43	31.88	31.66
CaO	0.96	1.04	1.05	1.13	0.98	0.87	1.52	1.16	1.29	1.13	0.92	0.84	0.82	0.64	0.37	0.23	0.22
Na2O	0.31	0.33	0.37	0.39	0.30	0.31	0.33	0.41	0.45	0.35	0.27	0.28	0.24	0.19	0.12	0.04	0.09
K2O	0.00	0.02	0.01	0.00	0.01	0.00	0.02	0.00	0.02	0.00	0.01	0.02	0.00	0.00	0.00	0.00	0.00
Total	100.31	99.45	99.81	99.84	100.62	99.96	99.79	100.40	100.13	100.39	100.12	100.43	100.74	100.15	100.43	100.19	99.88
Si	1.945	1.956	1.942	1.943	1.946	1.950		1.946	1.943	1.942	1.942	1.944	1.935	1.945	1.944	1.944	1.954
Ti	0.001	0.000	0.000	0.000	0.000	0.000		0.000	0.000	0.000	0.001	0.001	0.000	0.000	0.000	0.000	0.001
Al	0.102	0.102	0.106	0.104	0.097	0.099		0.105	0.111	0.104	0.100	0.098	0.099	0.098	0.090	0.084	0.082
Cr	0.000	0.001	0.002	0.000	0.000	0.001		0.000	0.001	0.000	0.000	0.000	0.000	0.000	0.000	0.001	0.000
Fe2+	0.300	0.279	0.294	0.291	0.305	0.289		0.291	0.290	0.300	0.308	0.297	0.303	0.301	0.309	0.299	0.292
Mn	0.000	0.001	0.002	0.003	0.001	0.003		0.001	0.002	0.001	0.002	0.004	0.001	0.002	0.001	0.002	0.002
Ni	0.006	0.006	0.008	0.008	0.007	0.006		0.006	0.007	0.007	0.007	0.007	0.008	0.006	0.007	0.007	0.006
Mg	1.603	1.598	1.598	1.601	1.601	1.607		1.595	1.583	1.596	1.603	1.615	1.628	1.622	1.641	1.666	1.657
Ca	0.036	0.039	0.040	0.043	0.037	0.033		0.044	0.049	0.043	0.035	0.031	0.031	0.024	0.014	0.009	0.008
Na	0.021	0.023	0.025	0.027	0.020	0.021		0.028	0.031	0.024	0.018	0.019	0.017	0.013	0.008	0.003	0.006
K	0.000	0.001	0.000	0.000	0.000	0.000		0.000	0.001	0.000	0.000	0.001	0.000	0.000	0.000	0.000	0.000
Sum	4.014	4.005	4.017	4.019	4.015	4.010		4.015	4.017	4.017	4.017	4.016	4.023	4.012	4.015	4.015	4.008
Mg#	84.24	85.14	84.46	84.62	84.00	84.76		84.57	84.52	84.18	83.88	84.47	84.31	84.35	84.15	84.78	85.02
Al IV	0.042	0.040	0.042	0.039	0.039	0.040		0.039	0.040	0.040	0.042	0.040	0.041	0.043	0.041	0.041	0.039
Al VI	0.061	0.063	0.065	0.066	0.059	0.060		0.067	0.071	0.064	0.058	0.058	0.058	0.056	0.049	0.043	0.043

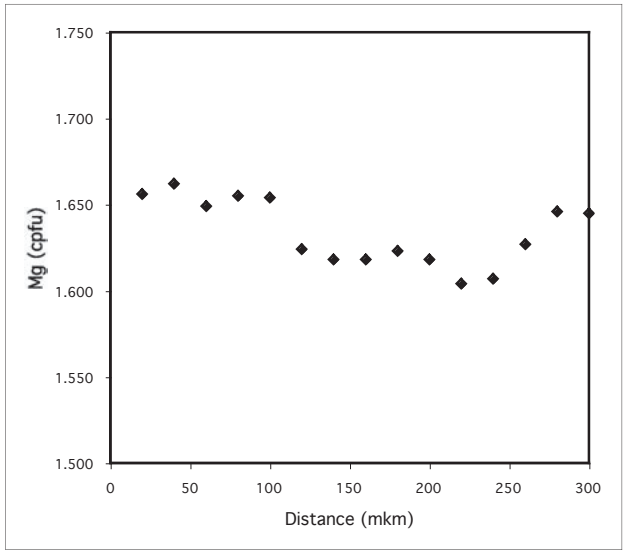
1904-3 Opx I, defocused beam, profile 523

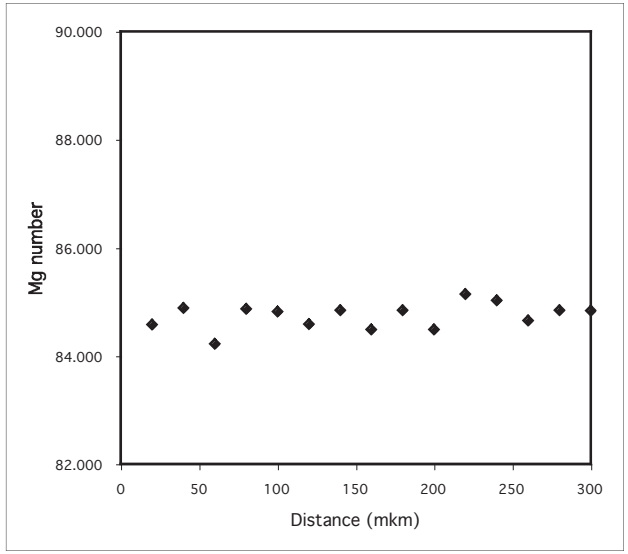






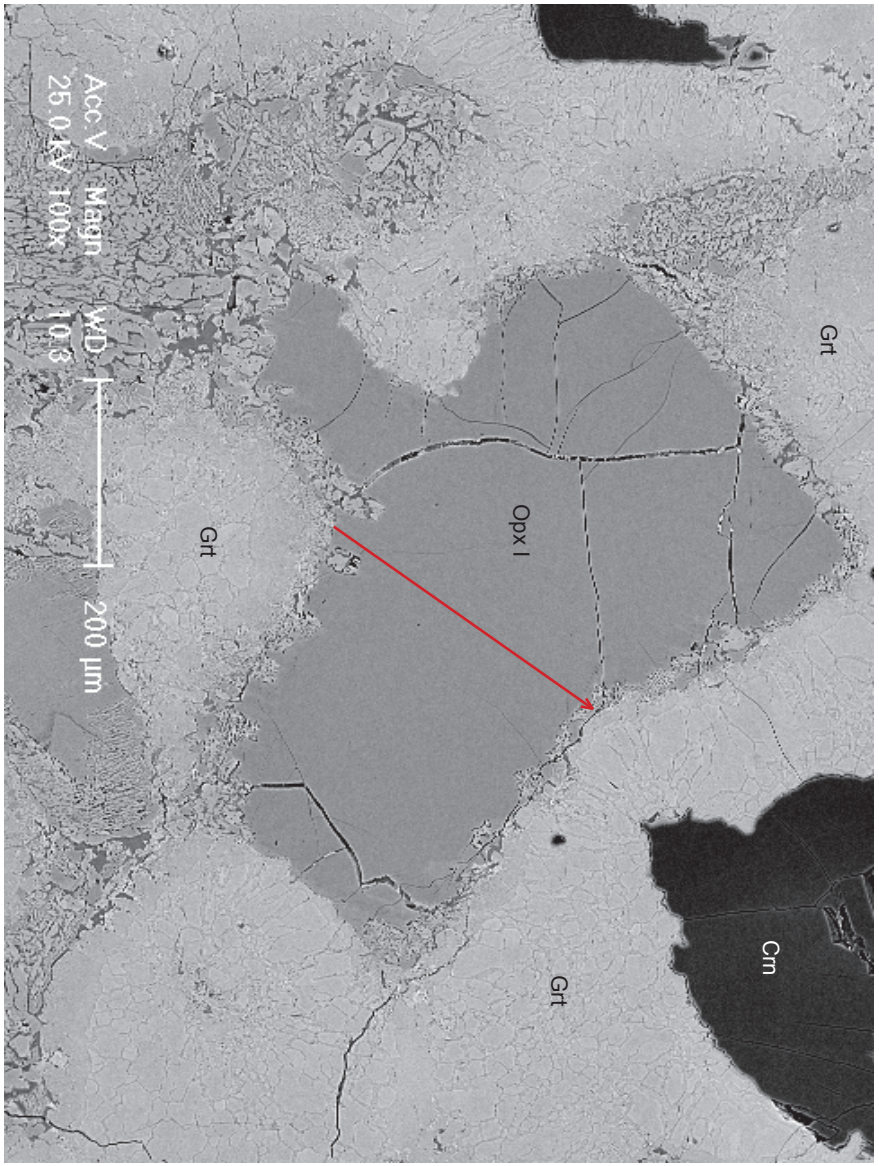






1904-3 Opx I, defocused beam, profile 311

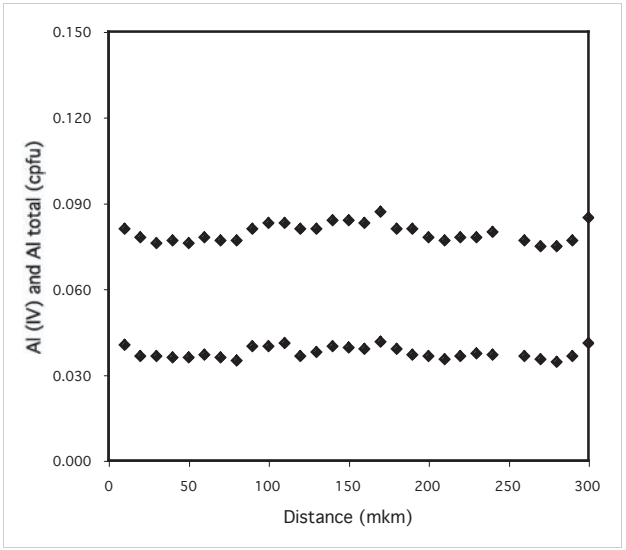
	20	40	60	80	100	120	140	160	180	200
SiO2	55.34	55.51	55.65	55.73	55.55	55.76	55.85	55.57	55.75	55.59
TiO2	0.00	0.01	0.00	0.02	0.00	0.01	0.00	0.01	0.00	0.00
Al2O3	2.36	2.27	2.30	2.19	2.27	2.35	2.40	2.39	2.38	2.43
Cr2O3	0.02	0.02	0.01	0.00	0.02	0.00	0.01	0.01	0.01	0.01
FeO	10.30	10.11	10.59	10.09	10.12	10.15	9.92	10.15	9.96	10.17
MnO	0.00	0.04	0.13	0.02	0.04	0.11	0.08	0.03	0.03	0.05
NiO	0.23	0.23	0.21	0.25	0.24	0.26	0.24	0.25	0.28	0.28
MgO	31.69	31.87	31.73	31.79	31.76	31.24	31.14	31.06	31.25	31.10
CaO	0.22	0.20	0.19	0.26	0.44	0.72	0.89	0.92	0.98	0.92
Na2O	0.08	0.07	0.06	0.07	0.11	0.23	0.30	0.29	0.33	0.28
K2O	0.01	0.00	0.00	0.01	0.00	0.00	0.00	0.00	0.00	0.00
Total	100.24	100.32	100.87	100.42	100.55	100.83	100.84	100.67	100.95	100.83
Si	1.939	1.942	1.940	1.947	1.941	1.945	1.946	1.942	1.942	1.941
Ti	0.000	0.000	0.000	0.000	0.000	0.000	0.000	0.000	0.000	0.000
Al	0.098	0.094	0.094	0.090	0.093	0.096	0.099	0.098	0.098	0.100
Cr	0.000	0.001	0.000	0.000	0.000	0.000	0.000	0.000	0.000	0.000
Fe2+	0.302	0.296	0.309	0.295	0.296	0.296	0.289	0.297	0.290	0.297
Mn	0.000	0.001	0.004	0.001	0.001	0.003	0.002	0.001	0.001	0.001
Ni	0.007	0.006	0.006	0.007	0.007	0.007	0.007	0.007	0.008	0.008
Mg	1.656	1.662	1.649	1.655	1.654	1.624	1.618	1.618	1.623	1.618
Ca	0.008	0.007	0.007	0.010	0.017	0.027	0.033	0.034	0.036	0.034
Na	0.005	0.004	0.004	0.005	0.008	0.015	0.020	0.020	0.022	0.019
K	0.000	0.000	0.000	0.000	0.000	0.000	0.000	0.000	0.000	0.000
Sum	4.015	4.013	4.014	4.010	4.016	4.015	4.015	4.018	4.020	4.019
Mg#	84.58	84.88	84.22	84.87	84.82	84.58	84.85	84.49	84.84	84.49
Al IV	0.047	0.046	0.045	0.043	0.043	0.041	0.040	0.039	0.038	0.041
Al VI	0.052	0.049	0.049	0.048	0.051	0.056	0.060	0.059	0.060	0.060

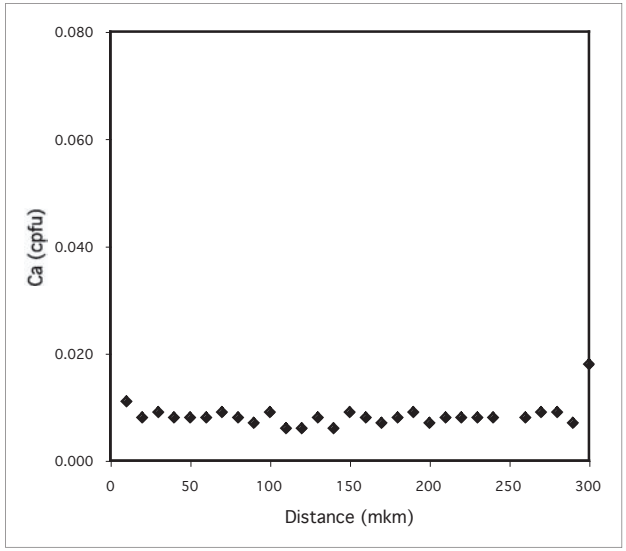


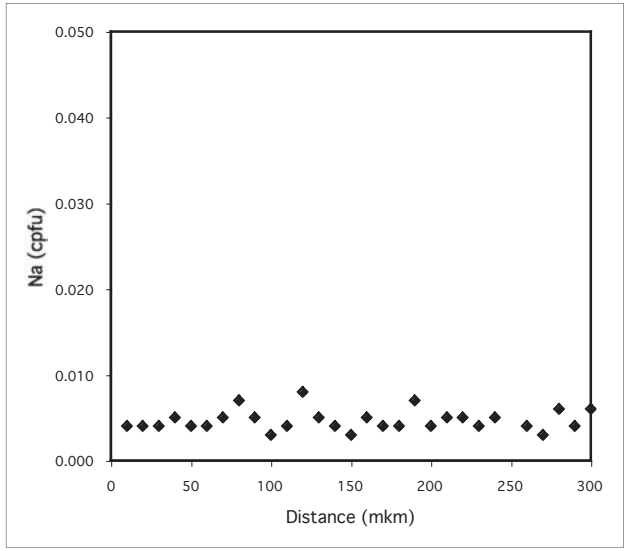
1904-3 Opx I, defocused beam, profile 311

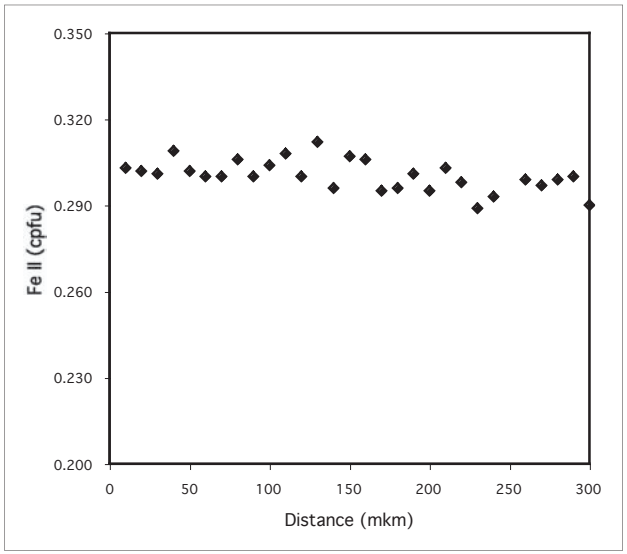
	220	240	260	280	300
SiO2	55.58	55.38	55.40	55.45	55.23
TiO2	0.01	0.00	0.01	0.01	0.03
Al2O3	2.56	2.50	2.45	2.34	2.48
Cr2O3	0.06	0.00	0.00	0.00	0.01
FeO	9.55	9.62	10.07	10.05	10.03
MnO	0.03	0.07	0.08	0.08	0.05
NiO	0.29	0.29	0.29	0.23	0.23
MgO	30.68	30.60	31.17	31.56	31.49
CaO	0.97	0.88	0.74	0.54	0.58
Na2O	0.31	0.30	0.25	0.15	0.19
K2O	0.00	0.00	0.01	0.00	0.01
Total	100.03	99.63	100.44	100.40	100.32
Si	1.949	1.950	1.940	1.940	1.935
Ti	0.000	0.000	0.000	0.000	0.001
Al	0.106	0.104	0.101	0.096	0.102
Cr	0.002	0.000	0.000	0.000	0.000
Fe2+	0.280	0.283	0.295	0.294	0.294
Mn	0.001	0.002	0.002	0.002	0.002
Ni	0.008	0.008	0.008	0.006	0.006
Mg	1.604	1.607	1.627	1.646	1.645
Ca	0.036	0.033	0.028	0.020	0.022
Na	0.021	0.021	0.017	0.010	0.013
K	0.000	0.000	0.000	0.000	0.000
Sum	4.007	4.008	4.018	4.016	4.020
Mg#	85.14	85.03	84.65	84.85	84.84
Al IV	0.044	0.042	0.042	0.043	0.046
Al VI	0.063	0.063	0.059	0.053	0.057

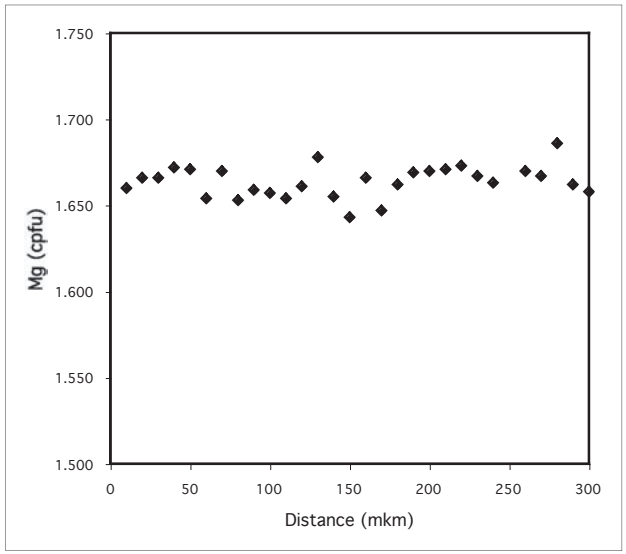
1904-3 Opx I, defocused beam, profile 311

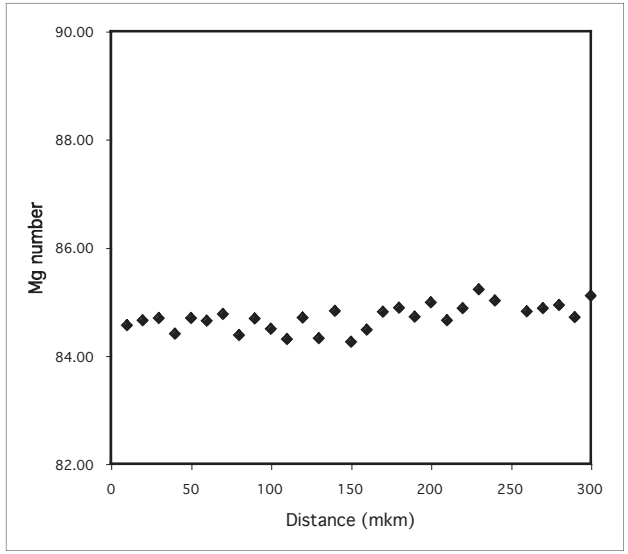






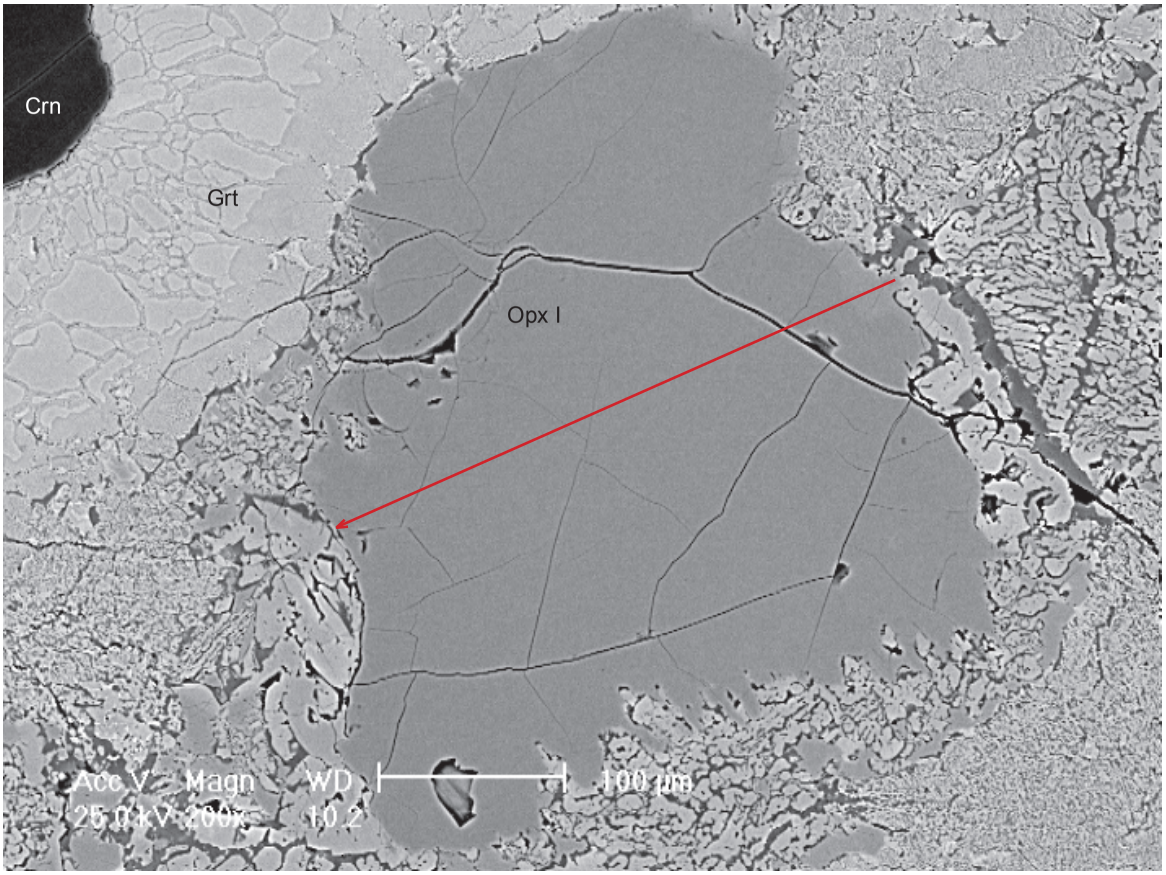






1904-3 Opx II, profile 310

1904-3 Opx II, profile 310

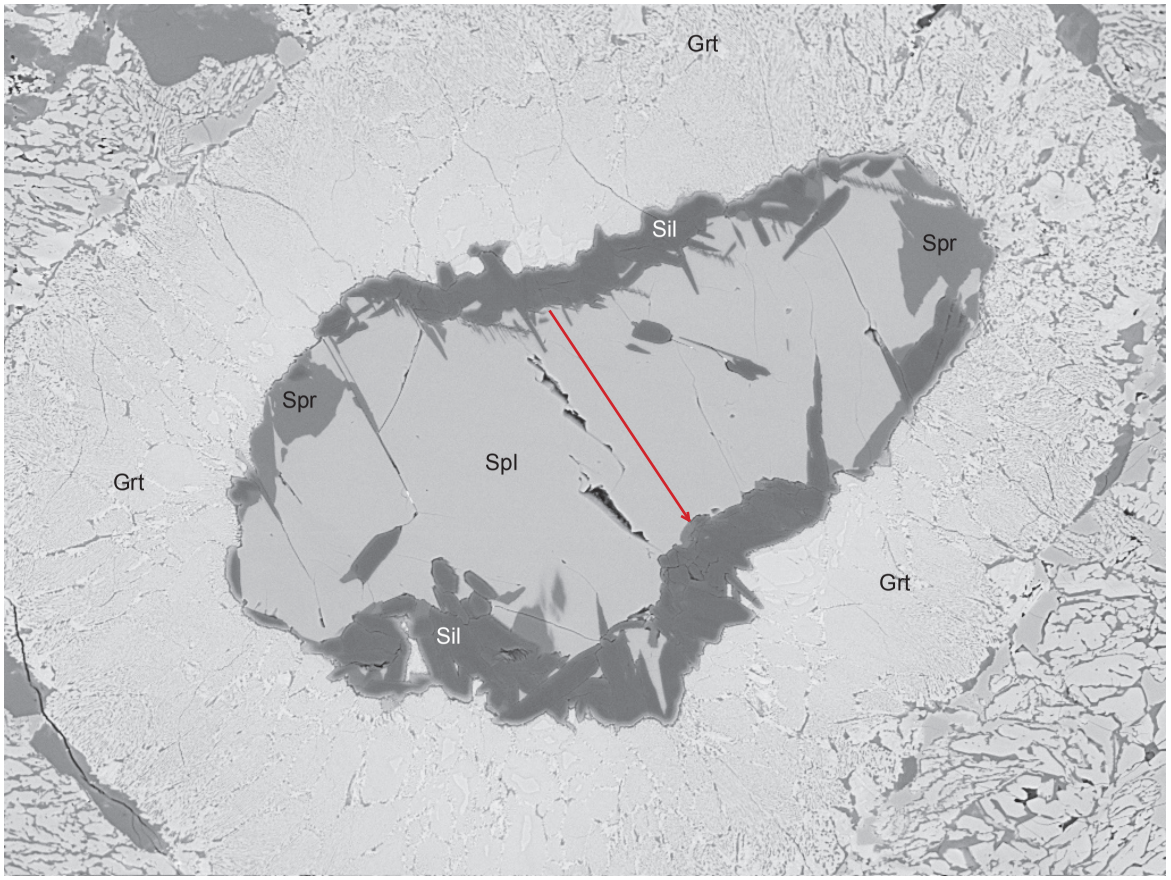


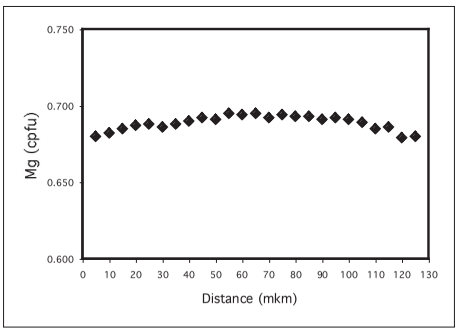
	Cpx	Cpx	10	20	30	40	50	60	70	80
SiO2	55.41	55.11	56.03	56.03	56.48	55.43	55.81	55.91	55.92	56.37
TiO2	0.01	0.00	0.04	0.01	0.00	0.00	0.00	0.00	0.00	0.01
Al2O3	9.61	9.65	1.98	1.90	1.86	1.86	1.84	1.89	1.88	1.88
Cr2O3	0.03	0.02	0.06	0.00	0.03	0.01	0.04	0.00	0.00	0.00
FeO	3.28	3.23	10.43	10.41	10.41	10.53	10.35	10.26	10.29	10.56
MnO	0.03	0.00	0.06	0.16	0.04	0.01	0.05	0.04	0.08	0.09
NiO	0.08	0.12	0.29	0.28	0.23	0.22	0.25	0.27	0.24	0.26
MgO	11.59	11.41	32.09	32.19	32.36	32.00	32.15	31.73	32.18	32.02
CaO	16.00	15.95	0.30	0.22	0.24	0.21	0.21	0.20	0.24	0.21
Na2O	5.06	5.21	0.06	0.06	0.06	0.07	0.06	0.06	0.08	0.10
K2O	0.02	0.00	0.00	0.02	0.00	0.00	0.01	0.00	0.00	0.00
Total	101.10	100.70	101.34	101.28	101.72	100.33	100.77	100.35	100.90	101.49
Si	1.956	1.954	1.944	1.946	1.950	1.943	1.946	1.955	1.947	1.952
Ti	0.000	0.000	0.001	0.000	0.000	0.000	0.000	0.000	0.000	0.000
Al	0.400	0.403	0.081	0.078	0.076	0.077	0.076	0.078	0.077	0.077
Cr	0.001	0.000	0.002	0.000	0.001	0.000	0.001	0.000	0.000	0.000
Fe2+	0.097	0.096	0.303	0.302	0.301	0.309	0.302	0.300	0.300	0.306
Mn	0.001	0.000	0.002	0.005	0.001	0.000	0.001	0.001	0.002	0.003
Ni	0.002	0.003	0.008	0.008	0.006	0.006	0.007	0.007	0.007	0.007
Mg	0.610	0.603	1.660	1.666	1.666	1.672	1.671	1.654	1.670	1.653
Ca	0.605	0.606	0.011	0.008	0.009	0.008	0.008	0.008	0.009	0.008
Na	0.346	0.358	0.004	0.004	0.004	0.005	0.004	0.004	0.005	0.007
K	0.001	0.000	0.000	0.001	0.000	0.000	0.001	0.000	0.000	0.000
Sum	4.017	4.024	4.016	4.018	4.014	4.021	4.018	4.008	4.017	4.012
Mg#	86.28	86.27	84.56	84.65	84.70	84.40	84.69	84.65	84.77	84.38
Al IV	0.027	0.023	0.041	0.037	0.037	0.036	0.036	0.037	0.036	0.035
Al VI	0.373	0.381	0.041	0.042	0.040	0.041	0.040	0.041	0.041	0.042

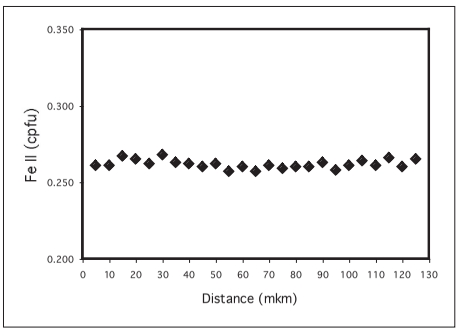
	90	100	110	120	130	140	150	160	170	180	190
SiO2	56.14	56.01	56.13	55.68	55.46	56.18	55.84	55.85	56.25	56.24	55.78
TiO2	0.02	0.01	0.03	0.01	0.01	0.00	0.00	0.00	0.00	0.00	0.01
Al2O3	1.98	2.04	2.03	1.97	1.98	2.06	2.05	2.02	2.13	1.98	1.98
Cr2O3	0.06	0.00	0.03	0.00	0.01	0.01	0.03	0.00	0.00	0.04	0.01
FeO	10.32	10.48	10.64	10.25	10.70	10.17	10.49	10.53	10.14	10.22	10.35
MnO	0.03	0.07	0.06	0.08	0.12	0.08	0.00	0.10	0.04	0.08	0.01
NiO	0.27	0.27	0.31	0.25	0.23	0.26	0.23	0.33	0.31	0.22	0.28
MgO	32.04	31.99	32.00	31.85	32.28	31.94	31.53	32.16	31.80	32.15	32.15
CaO	0.19	0.23	0.16	0.16	0.21	0.16	0.25	0.21	0.18	0.21	0.24
Na2O	0.07	0.05	0.06	0.11	0.08	0.06	0.05	0.07	0.06	0.06	0.10
K2O	0.00	0.01	0.01	0.00	0.00	0.00	0.07	0.00	0.00	0.00	0.00
Total	101.12	101.14	101.45	100.36	101.06	100.91	100.54	101.27	100.91	101.21	100.89
Si	1.949	1.946	1.946	1.949	1.934	1.953	1.952	1.941	1.955	1.950	1.943
Ti	0.001	0.000	0.001	0.000	0.000	0.000	0.000	0.000	0.000	0.000	0.000
Al	0.081	0.083	0.083	0.081	0.081	0.084	0.084	0.083	0.087	0.081	0.081
Cr	0.002	0.000	0.001	0.000	0.000	0.000	0.001	0.000	0.000	0.001	0.000
Fe2+	0.300	0.304	0.308	0.300	0.312	0.296	0.307	0.306	0.295	0.296	0.301
Mn	0.001	0.002	0.002	0.002	0.003	0.002	0.000	0.003	0.001	0.002	0.000
Ni	0.007	0.007	0.009	0.007	0.006	0.007	0.007	0.009	0.009	0.006	0.008
Mg	1.659	1.657	1.654	1.661	1.678	1.655	1.643	1.666	1.647	1.662	1.669
Ca	0.007	0.009	0.006	0.006	0.008	0.006	0.009	0.008	0.007	0.008	0.009
Na	0.005	0.003	0.004	0.008	0.005	0.004	0.003	0.005	0.004	0.004	0.007
K	0.000	0.000	0.000	0.000	0.000	0.000	0.003	0.000	0.000	0.000	0.000
Sum	4.011	4.013	4.014	4.014	4.028	4.007	4.009	4.020	4.004	4.011	4.019
Mg#	84.69	84.50	84.30	84.70	84.32	84.83	84.26	84.48	84.81	84.88	84.72
Al IV	0.040	0.040	0.041	0.037	0.038	0.040	0.040	0.039	0.042	0.039	0.037
Al VI	0.041	0.043	0.042	0.045	0.043	0.044	0.045	0.044	0.046	0.042	0.044

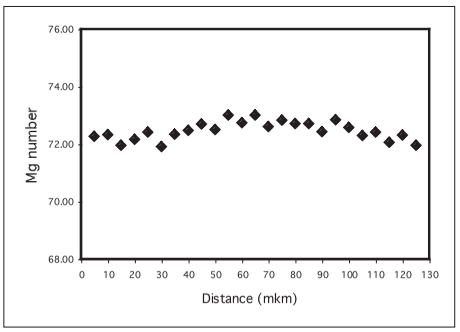
	200	210	220	230	240	250	260	270	280	290	300
SiO2	56.07	56.10	55.89	56.13	55.99	54.21	56.15	56.17	55.56	55.78	55.84
TiO2	0.01	0.02	0.00	0.02	0.00	0.01	0.00	0.01	0.01	0.01	0.04
Al2O3	1.91	1.88	1.90	1.90	1.95	2.38	1.87	1.84	1.81	1.88	2.08
Cr2O3	0.00	0.00	0.00	0.03	0.00	0.00	0.00	0.00	0.00	0.04	0.03
FeO	10.13	10.47	10.23	9.94	10.05	10.77	10.31	10.24	10.23	10.27	9.94
MnO	0.01	0.09	0.04	0.06	0.06	0.06	0.06	0.02	0.03	0.08	0.04
NiO	0.22	0.29	0.27	0.30	0.26	0.26	0.30	0.28	0.26	0.26	0.28
MgO	32.20	32.35	32.23	32.14	31.99	31.01	32.29	32.18	32.36	31.90	31.92
CaO	0.18	0.20	0.22	0.22	0.20	0.26	0.21	0.23	0.25	0.19	0.47
Na2O	0.05	0.07	0.08	0.06	0.07	0.11	0.06	0.05	0.08	0.07	0.09
K2O	0.02	0.02	0.00	0.00	0.03	0.04	0.00	0.02	0.01	0.02	0.00
Total	100.80	101.50	100.87	100.79	100.61	99.09	101.26	101.04	100.60	100.49	100.71
Si	1.951	1.944	1.946	1.953	1.952		1.948	1.951	1.941	1.950	1.946
Ti	0.000	0.000	0.000	0.000	0.000		0.000	0.000	0.000	0.000	0.001
Al	0.078	0.077	0.078	0.078	0.080		0.077	0.075	0.075	0.077	0.085
Cr	0.000	0.000	0.000	0.001	0.000		0.000	0.000	0.000	0.001	0.001
Fe2+	0.295	0.303	0.298	0.289	0.293		0.299	0.297	0.299	0.300	0.290
Mn	0.000	0.003	0.001	0.002	0.002		0.002	0.001	0.001	0.002	0.001
Ni	0.006	0.008	0.008	0.008	0.007		0.008	0.008	0.007	0.007	0.008
Mg	1.670	1.671	1.673	1.667	1.663		1.670	1.667	1.686	1.662	1.658
Ca	0.007	0.008	0.008	0.008	0.008		0.008	0.009	0.009	0.007	0.018
Na	0.004	0.005	0.005	0.004	0.005		0.004	0.003	0.006	0.004	0.006
K	0.001	0.001	0.000	0.000	0.001		0.000	0.001	0.000	0.001	0.000
Sum	4.012	4.020	4.018	4.010	4.011		4.016	4.013	4.024	4.013	4.013
Mg#	84.99	84.65	84.88	85.22	85.02		84.81	84.88	84.94	84.71	85.11
Al IV	0.037	0.036	0.037	0.038	0.037		0.037	0.036	0.035	0.037	0.041
Al VI	0.042	0.042	0.042	0.041	0.043		0.041	0.040	0.041	0.041	0.044

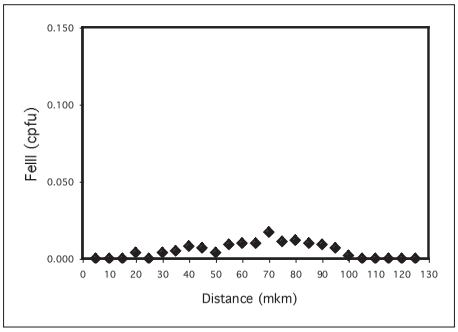
1904-3 Spinel, profile 121

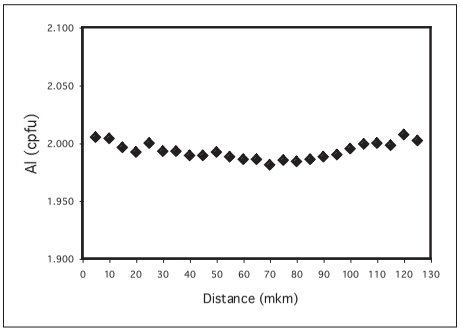


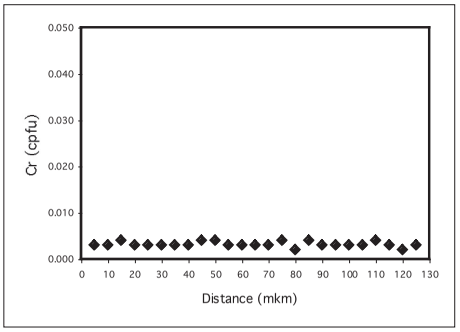


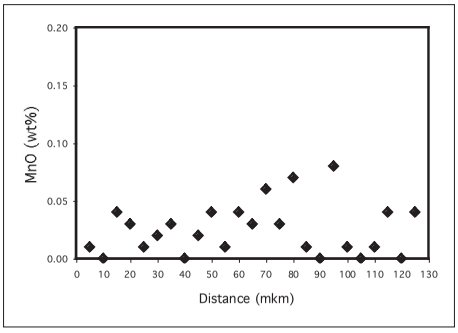


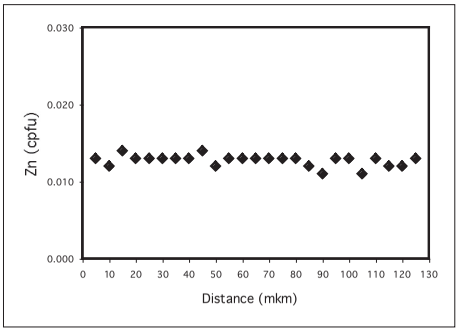


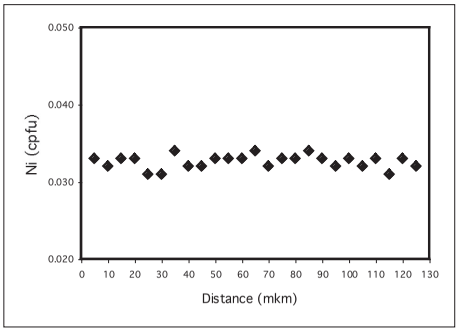












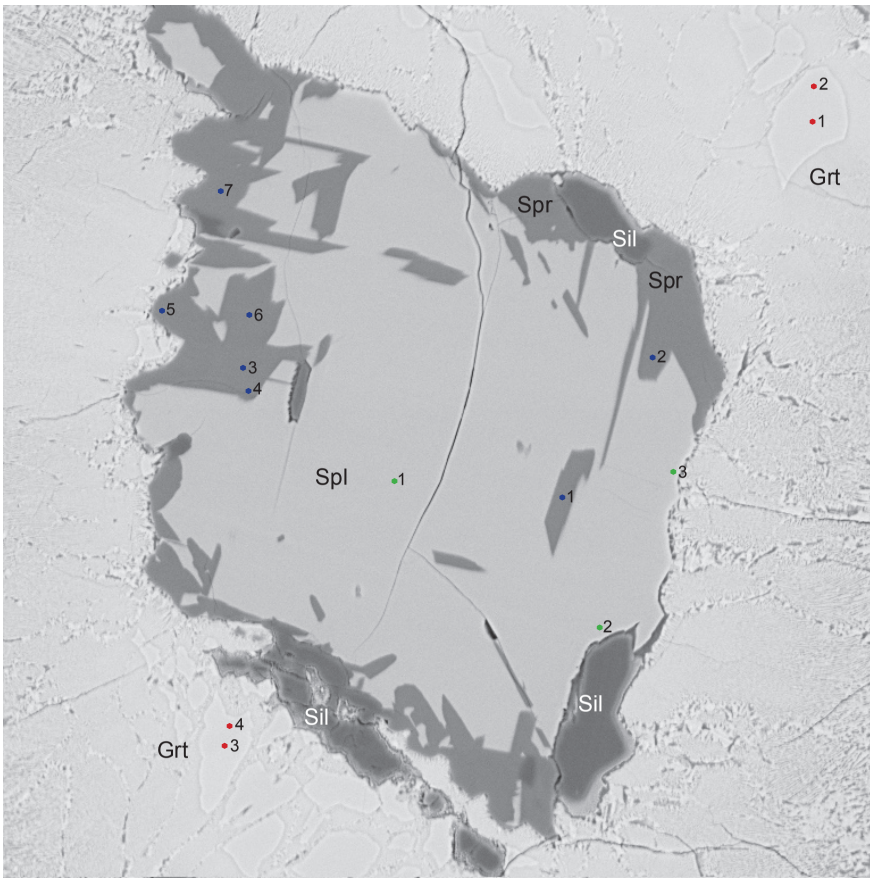
1904-3 Spinel, profile 121

	5	10	15	20	25	30	35	40	45	50	55	60
SiO2	0.02	0.01	0.01	0.03	0.02	0.01	0.00	0.01	0.01	0.02	0.01	0.01
TiO2	0.00	0.00	0.01	0.00	0.00	0.01	0.00	0.00	0.00	0.01	0.01	0.00
V2O3	0.00	0.00	0.01	0.00	0.00	0.00	0.00	0.01	0.00	0.00	0.01	0.03
Al2O3	67.42	67.37	67.24	67.18	67.11	67.16	67.10	67.14	67.04	66.91	66.96	66.92
Cr2O3	0.15	0.17	0.18	0.16	0.14	0.15	0.15	0.17	0.18	0.21	0.14	0.14
FeO	12.37	12.39	12.65	12.79	12.41	12.89	12.71	12.88	12.69	12.58	12.61	12.80
MnO	0.01	0.00	0.04	0.03	0.01	0.02	0.03	0.00	0.02	0.04	0.01	0.04
NiO	1.63	1.59	1.62	1.62	1.53	1.54	1.66	1.60	1.58	1.63	1.62	1.62
ZnO	0.68	0.63	0.74	0.70	0.67	0.72	0.70	0.71	0.74	0.66	0.70	0.67
MgO	18.08	18.12	18.24	18.31	18.24	18.27	18.32	18.43	18.45	18.35	18.50	18.49
CaO	0.00	0.00	0.00	0.00	0.00	0.00	0.00	0.00	0.00	0.00	0.00	0.00
Na2O	0.01	0.02	0.01	0.03	0.04	0.01	0.01	0.01	0.01	0.01	0.02	0.00
K2O	0.00	0.00	0.01	0.00	0.00	0.01	0.00	0.01	0.00	0.01	0.01	0.00
Total	100.36	100.32	100.76	100.85	100.18	100.80	100.69	100.98	100.73	100.44	100.61	100.74
Si	0.001	0.000	0.000	0.001	0.000	0.000	0.000	0.000	0.000	0.000	0.000	0.000
Ti	0.000	0.000	0.000	0.000	0.000	0.000	0.000	0.000	0.000	0.000	0.000	0.000
V	0.000	0.000	0.000	0.000	0.000	0.000	0.000	0.000	0.000	0.000	0.000	0.001
Al	2.005	2.004	1.996	1.992	2.000	1.993	1.993	1.989	1.989	1.992	1.988	1.986
Cr	0.003	0.003	0.004	0.003	0.003	0.003	0.003	0.003	0.004	0.004	0.003	0.003
Fe3+	0.000	0.000	0.000	0.004	0.000	0.004	0.005	0.008	0.007	0.004	0.009	0.010
Fe2+	0.261	0.261	0.267	0.265	0.262	0.268	0.263	0.262	0.260	0.262	0.257	0.260
Mn	0.000	0.000	0.001	0.001	0.000	0.000	0.001	0.000	0.000	0.001	0.000	0.001
Ni	0.033	0.032	0.033	0.033	0.031	0.031	0.034	0.032	0.032	0.033	0.033	0.033
Zn	0.013	0.012	0.014	0.013	0.013	0.013	0.013	0.013	0.014	0.012	0.013	0.013
Mg	0.680	0.682	0.685	0.687	0.688	0.686	0.688	0.690	0.692	0.691	0.695	0.694
Ca	0.000	0.000	0.000	0.000	0.000	0.000	0.000	0.000	0.000	0.000	0.000	0.000
Na	0.001	0.001	0.000	0.001	0.002	0.001	0.001	0.001	0.001	0.001	0.001	0.000
K	0.000	0.000	0.000	0.000	0.000	0.000	0.000	0.000	0.000	0.000	0.000	0.000
Sum	2.996	2.996	3.000	3.000	2.999	3.000	3.000	3.000	3.000	3.000	3.000	3.000
Mg#	72.26	72.32	71.95	72.16	72.42	71.91	72.34	72.48	72.69	72.51	73.00	72.75

	65	70	75	80	85	90	95	100	105	110	115	120	125
SiO2	0.02	0.00	0.01	0.02	0.00	0.01	0.02	0.02	0.02	0.01	0.02	0.02	0.04
TiO2	0.01	0.00	0.00	0.01	0.00	0.00	0.00	0.00	0.00	0.00	0.02	0.00	0.00
V2O3	0.00	0.00	0.00	0.00	0.01	0.01	0.02	0.00	0.00	0.01	0.00	0.02	0.00
Al2O3	66.92	66.88	66.89	66.86	66.85	67.08	66.88	66.88	67.00	67.03	67.09	67.40	67.57
Cr2O3	0.13	0.16	0.19	0.12	0.18	0.16	0.17	0.17	0.14	0.18	0.16	0.12	0.13
FeO	12.72	13.20	12.82	12.91	12.83	12.94	12.54	12.43	12.46	12.35	12.58	12.33	12.58
MnO	0.03	0.06	0.03	0.07	0.01	0.00	0.08	0.01	0.00	0.01	0.04	0.00	0.04
NiO	1.66	1.58	1.61	1.61	1.67	1.64	1.59	1.60	1.55	1.61	1.52	1.61	1.56
ZnO	0.69	0.71	0.69	0.70	0.63	0.61	0.68	0.68	0.60	0.72	0.66	0.66	0.71
MgO	18.50	18.46	18.49	18.46	18.43	18.43	18.38	18.31	18.25	18.15	18.21	18.03	18.13
CaO	0.00	0.00	0.00	0.00	0.00	0.00	0.00	0.00	0.00	0.00	0.00	0.00	0.00
Na2O	0.01	0.01	0.01	0.01	0.01	0.01	0.04	0.03	0.01	0.02	0.02	0.02	0.02
K2O	0.00	0.00	0.00	0.00	0.00	0.01	0.00	0.01	0.00	0.02	0.00	0.00	0.00
Total	100.69	101.07	100.73	100.77	100.62	100.91	100.39	100.14	100.03	100.11	100.32	100.21	100.80
Si	0.000	0.000	0.000	0.000	0.000	0.000	0.001	0.000	0.000	0.000	0.000	0.000	0.001
Ti	0.000	0.000	0.000	0.000	0.000	0.000	0.000	0.000	0.000	0.000	0.000	0.000	0.000
V	0.000	0.000	0.000	0.000	0.000	0.000	0.000	0.000	0.000	0.000	0.000	0.000	0.000
Al	1.986	1.981	1.985	1.984	1.986	1.988	1.990	1.995	1.999	2.000	1.998	2.007	2.002
Cr	0.003	0.003	0.004	0.002	0.004	0.003	0.003	0.003	0.003	0.004	0.003	0.002	0.003
Fe3	0.010	0.017	0.011	0.012	0.010	0.009	0.007	0.002	0.000	0.000	0.000	0.000	0.000
Fe2	0.257	0.261	0.259	0.260	0.260	0.263	0.258	0.261	0.264	0.261	0.266	0.260	0.265
Mn	0.001	0.001	0.001	0.001	0.000	0.000	0.002	0.000	0.000	0.000	0.001	0.000	0.001
Ni	0.034	0.032	0.033	0.033	0.034	0.033	0.032	0.033	0.032	0.033	0.031	0.033	0.032
Zn	0.013	0.013	0.013	0.013	0.012	0.011	0.013	0.013	0.011	0.013	0.012	0.012	0.013
Mg	0.695	0.692	0.694	0.693	0.693	0.691	0.692	0.691	0.689	0.685	0.686	0.679	0.680
Ca	0.000	0.000	0.000	0.000	0.000	0.000	0.000	0.000	0.000	0.000	0.000	0.000	0.000
Na	0.001	0.001	0.001	0.000	0.001	0.001	0.002	0.001	0.001	0.001	0.001	0.001	0.001
K	0.000	0.000	0.000	0.000	0.000	0.000	0.000	0.000	0.000	0.001	0.000	0.000	0.000
Sum	3.000	3.000	3.000	3.000	3.000	3.000	3.000	3.000	2.999	2.999	2.999	2.995	2.997
Mg#	73.00	72.61	72.82	72.72	72.72	72.43	72.84	72.58	72.30	72.41	72.06	72.31	71.96

1904-3 Spinel, an. 1-3

	1	2	3
SiO2	0.00	0.02	0.02
TiO2	0.01	0.01	0.00
V2O3	0.01	0.00	0.01
Al2O3	66.55	67.14	66.60
Cr2O3	0.19	0.20	0.25
FeO	13.30	13.53	13.68
MnO	0.00	0.03	0.02
NiO	1.74	1.50	1.58
ZnO	0.81	0.79	0.85
MgO	17.79	17.70	17.63
CaO	0.00	0.00	0.01
Na2O	0.02	0.05	0.01
K2O	0.03	0.00	0.00
Total	100.47	100.94	100.65
Si	0.000	0.000	0.000
Ti	0.000	0.000	0.000
V	0.000	0.000	0.000
Al	1.989	1.996	1.989
Cr	0.004	0.004	0.005
Fe3+	0.009	0.001	0.006
Fe2+	0.273	0.284	0.284
Mn	0.000	0.001	0.000
Ni	0.035	0.030	0.032
Zn	0.015	0.015	0.016
Mg	0.672	0.666	0.666
Ca	0.000	0.000	0.000
Na	0.001	0.002	0.001
K	0.001	0.000	0.000
Sum	3.000	3.000	3.000



1904-3 Sapphirine, an. 1-7

	1	2	3	4	5	6	7
SiO2	11.21	11.17	11.25	11.19	11.71	11.59	11.48
TiO2	0.01	0.02	0.04	0.05	0.00	0.00	0.04
Al2O3	66.41	66.19	66.30	66.52	66.04	66.46	66.60
Cr2O3	0.06	0.14	0.07	0.17	0.10	0.08	0.07
FeO	4.18	4.29	4.07	3.99	4.21	3.90	4.03
MnO	0.04	0.00	0.01	0.01	0.04	0.01	0.01
NiO	0.52	0.53	0.53	0.55	0.52	0.50	0.50
MgO	17.35	17.05	17.30	17.26	17.67	17.45	17.55
CaO	0.01	0.00	0.03	0.00	0.02	0.02	0.00
Na2O	0.01	0.02	0.00	0.02	0.02	0.02	0.01
K2O	0.00	0.00	0.02	0.01	0.00	0.01	0.01
Total	99.81	99.41	99.62	99.75	100.33	100.06	100.31
Si	1.321	1.322	1.327	1.318	1.372	1.360	1.344
Ti	0.001	0.002	0.003	0.004	0.000	0.000	0.003
Al	9.222	9.232	9.219	9.235	9.122	9.187	9.191
Cr	0.005	0.013	0.006	0.015	0.009	0.008	0.006
Fe2+	0.412	0.425	0.401	0.393	0.413	0.382	0.395
Mn	0.004	0.000	0.001	0.001	0.004	0.001	0.001
Ni	0.050	0.051	0.051	0.052	0.049	0.048	0.047
Mg	3.047	3.009	3.043	3.030	3.087	3.052	3.064
Ca	0.001	0.000	0.004	0.000	0.003	0.002	0.001
Na	0.002	0.004	0.000	0.004	0.004	0.005	0.003
K	0.000	0.000	0.002	0.001	0.000	0.002	0.002
Sum	14.065	14.056	14.058	14.054	14.064	14.046	14.057

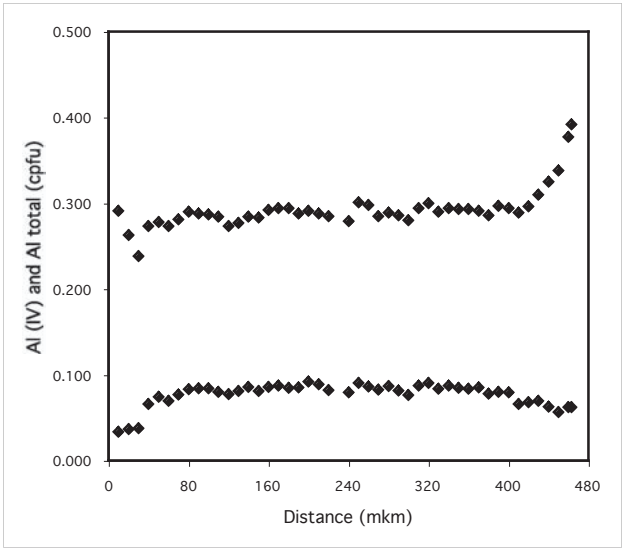
1904-3 Garnet, an. 1-4

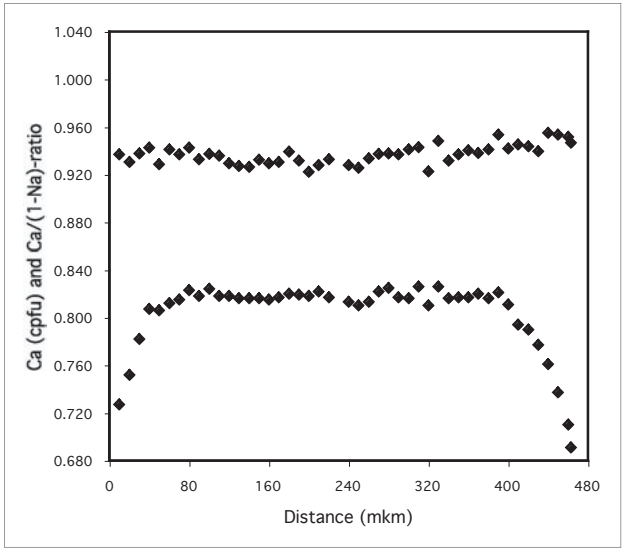
	1	2	3	4
SiO2	40.77	40.50	40.64	40.50
TiO2	0.01	0.00	0.02	0.02
Al2O3	23.38	23.45	23.34	23.46
Cr2O3	0.00	0.00	0.00	0.03
FeO	15.26	15.13	14.88	15.09
MnO	0.23	0.26	0.24	0.21
NiO	0.00	0.01	0.02	0.01
MgO	16.68	16.62	16.53	16.57
CaO	5.00	4.80	4.92	4.84
Na2O	0.00	0.02	0.00	0.00
K2O	0.00	0.00	0.01	0.02
Total	101.33	100.81	100.60	100.74
Si	2.946	2.941	2.953	2.941
Ti	0.000	0.000	0.001	0.001
Al	1.992	2.006	1.999	2.008
Cr	0.000	0.000	0.000	0.002
Fe3+	0.000	0.000	0.000	0.000
Fe2+	0.922	0.918	0.904	0.916
Mn	0.014	0.016	0.015	0.013
Ni	0.000	0.001	0.001	0.000
Mg	1.796	1.799	1.791	1.794
Ca	0.386	0.373	0.383	0.377
Na	0.000	0.003	0.000	0.000
K	0.000	0.000	0.001	0.002
Sum	8.058	8.058	8.047	8.054
Mg#	66.1	66.2	66.5	66.2

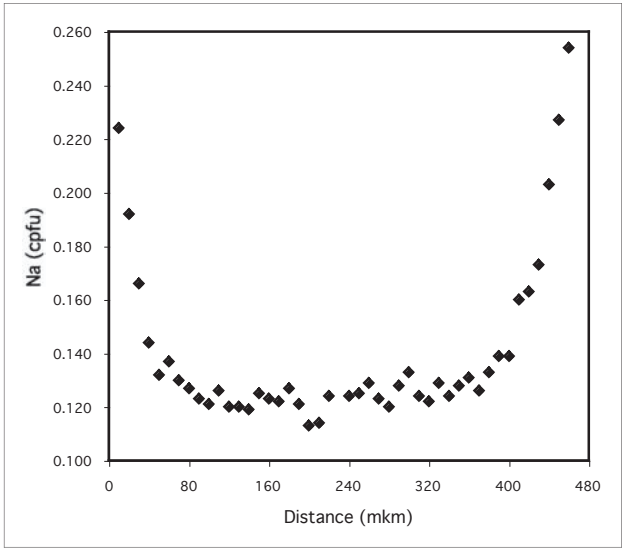
1904-3 Corundum, profile 174

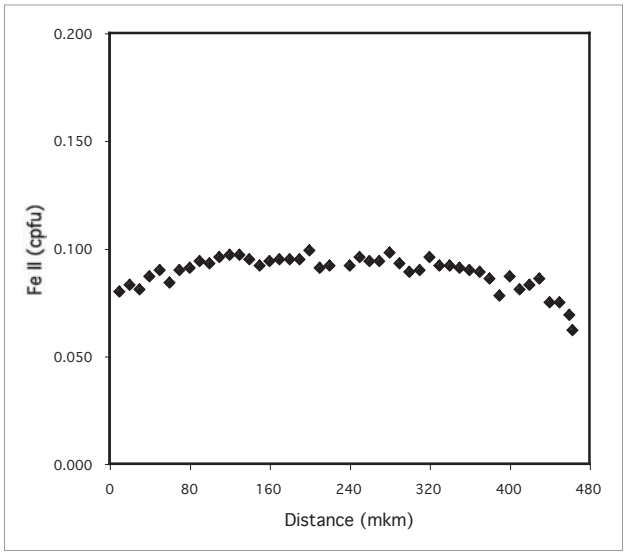
	10	20	30	40	50	60	70	80	90	100	110	120	130	140	150	160	170	180
SiO2	0.02	0.03	0.01	0.01	0.02	0.01	0.05	0.04	0.03	0.00	0.02	0.04	0.02	0.04	0.04	0.03	0.01	0.02
TiO2	0.00	0.00	0.02	0.00	0.00	0.00	0.00	0.01	0.01	0.00	0.00	0.00	0.01	0.01	0.02	0.00	0.00	0.00
Al2O3	99.19	99.25	99.34	99.26	99.02	99.35	99.45	99.17	99.32	99.08	99.31	99.38	99.44	99.08	98.93	99.05	99.30	99.16
Cr2O3	0.09	0.10	0.06	0.07	0.06	0.05	0.02	0.09	0.04	0.06	0.03	0.05	0.04	0.07	0.04	0.13	0.10	0.20
FeO	0.46	0.42	0.38	0.31	0.25	0.33	0.30	0.30	0.24	0.22	0.27	0.30	0.30	0.32	0.39	0.30	0.36	0.40
MnO	0.03	0.00	0.00	0.04	0.01	0.01	0.03	0.00	0.00	0.02	0.00	0.00	0.00	0.00	0.03	0.00	0.04	0.04
MgO	0.00	0.01	0.00	0.01	0.00	0.01	0.01	0.00	0.01	0.01	0.01	0.00	0.00	0.01	0.02	0.01	0.01	0.00
CaO	0.01	0.02	0.00	0.00	0.01	0.01	0.02	0.00	0.00	0.00	0.00	0.00	0.01	0.01	0.03	0.00	0.00	0.00
Na2O	0.00	0.00	0.00	0.01	0.00	0.01	0.00	0.01	0.00	0.00	0.00	0.01	0.00	0.02	0.00	0.00	0.00	0.00
K2O	0.00	0.01	0.01	0.01	0.01	0.00	0.00	0.02	0.01	0.00	0.00	0.01	0.01	0.00	0.02	0.00	0.00	0.00
Total	99.81	99.84	99.83	99.72	99.38	99.78	99.89	99.65	99.65	99.41	99.64	99.79	99.85	99.56	99.51	99.53	99.83	99.83
Si	0.000	0.001	0.000	0.000	0.000	0.000	0.001	0.001	0.001	0.000	0.000	0.001	0.000	0.001	0.001	0.001	0.000	0.000
Ti	0.000	0.000	0.000	0.000	0.000	0.000	0.000	0.000	0.000	0.000	0.000	0.000	0.000	0.000	0.000	0.000	0.000	0.000
Al	1.991	1.992	1.993	1.994	1.995	1.994	1.994	1.993	1.995	1.996	1.995	1.994	1.994	1.993	1.991	1.993	1.993	1.991
Cr	0.001	0.001	0.001	0.001	0.001	0.001	0.000	0.001	0.001	0.001	0.000	0.001	0.001	0.001	0.001	0.002	0.001	0.003
Fe3+	0.007	0.006	0.005	0.004	0.004	0.005	0.004	0.004	0.003	0.003	0.004	0.004	0.004	0.005	0.006	0.004	0.005	0.006
Fe2+	0.000	0.000	0.000	0.000	0.000	0.000	0.000	0.000	0.000	0.000	0.000	0.000	0.000	0.000	0.000	0.000	0.000	0.000
Mn	0.000	0.000	0.000	0.001	0.000	0.000	0.000	0.000	0.000	0.000	0.000	0.000	0.000	0.000	0.000	0.000	0.001	0.001
Mg	0.000	0.000	0.000	0.000	0.000	0.000	0.000	0.000	0.000	0.000	0.000	0.000	0.000	0.000	0.001	0.000	0.000	0.000
Ca	0.000	0.000	0.000	0.000	0.000	0.000	0.000	0.000	0.000	0.000	0.000	0.000	0.000	0.000	0.001	0.000	0.000	0.000
Na	0.000	0.000	0.000	0.000	0.000	0.000	0.000	0.000	0.000	0.000	0.000	0.000	0.000	0.001	0.000	0.000	0.000	0.000
K	0.000	0.000	0.000	0.000	0.000	0.000	0.000	0.000	0.000	0.000	0.000	0.000	0.000	0.000	0.000	0.000	0.000	0.000
Sum	2.000	2.000	2.000	2.001	2.000	2.000	2.000	2.000	2.000	2.000	2.000	2.000	2.000	2.000	2.000	2.000	2.000	2.000

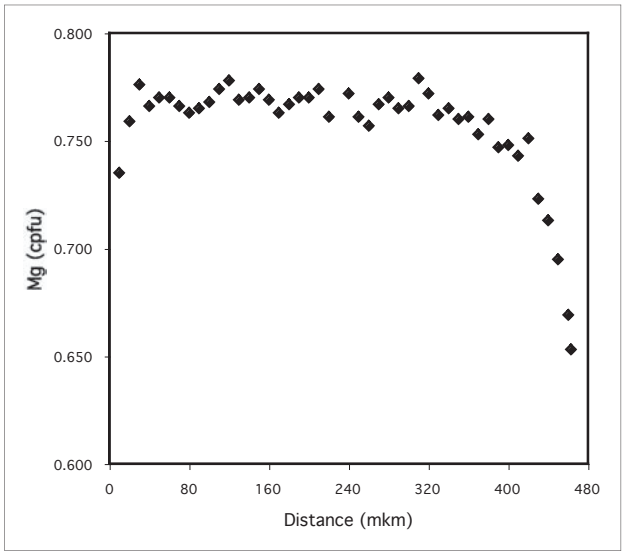
Mg-Al granulite 1904-7

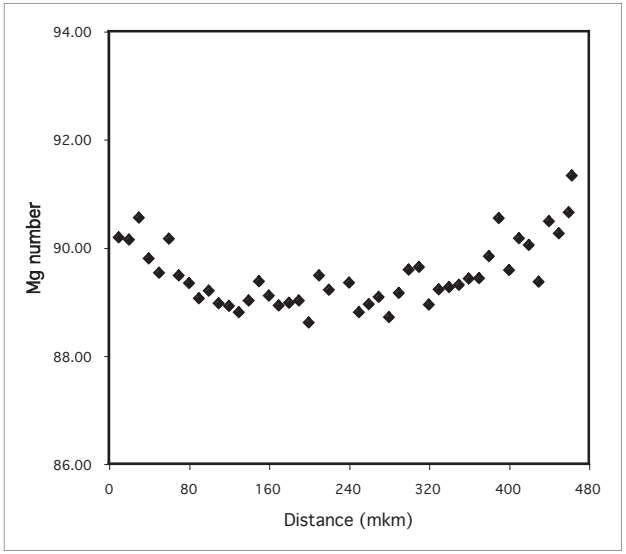












1904-7 Cpx II, profile 454

	10	20	30	40	50	60	70	80	90	100	110	120	130	140	150	160	170	180	190	200
SiO2	55.32	55.19	54.97	54.20	53.84	53.96	53.81	53.62	53.50	53.31	53.46	53.57	53.61	53.75	53.42	53.50	53.33	53.28	53.36	53.44
TiO2	0.02	0.01	0.02	0.03	0.02	0.05	0.05	0.03	0.03	0.05	0.04	0.03	0.06	0.06	0.06	0.04	0.04	0.05	0.05	0.06
Al2O3	7.01	6.29	5.67	6.52	6.60	6.49	6.69	6.90	6.84	6.80	6.74	6.47	6.56	6.77	6.72	6.94	6.98	7.00	6.84	6.94
Cr2O3	0.01	0.06	0.04	0.03	0.02	0.05	0.02	0.02	0.03	0.00	0.01	0.04	0.02	0.07	0.04	0.01	0.02	0.00	0.03	0.06
FeO	2.70	2.81	2.71	2.93	3.03	2.83	3.03	3.04	3.14	3.09	3.22	3.25	3.23	3.19	3.08	3.14	3.17	3.19	3.17	3.34
MnO	0.06	0.05	0.06	0.04	0.03	0.06	0.11	0.05	0.05	0.02	0.11	0.09	0.08	0.14	0.10	0.10	0.03	0.10	0.10	0.09
NiO	0.06	0.03	0.03	0.06	0.08	0.06	0.05	0.00	0.04	0.09	0.06	0.07	0.01	0.06	0.06	0.02	0.10	0.07	0.04	0.08
MgO	13.97	14.37	14.62	14.46	14.46	14.48	14.42	14.36	14.35	14.39	14.55	14.61	14.43	14.53	14.53	14.45	14.32	14.41	14.45	14.50
CaO	19.23	19.82	20.49	21.20	21.05	21.26	21.35	21.55	21.36	21.49	21.39	21.36	21.30	21.43	21.30	21.33	21.31	21.43	21.38	21.44
Na2O	3.28	2.80	2.40	2.09	1.90	1.98	1.88	1.84	1.78	1.74	1.81	1.73	1.73	1.73	1.80	1.77	1.76	1.84	1.74	1.63
K2O	0.00	0.00	0.00	0.00	0.02	0.00	0.00	0.00	0.00	0.00	0.00	0.02	0.00	0.00	0.01	0.00	0.02	0.01	0.01	0.00
Total	101.67	101.43	101.02	101.57	101.06	101.20	101.40	101.41	101.10	100.99	101.39	101.25	101.03	101.72	101.13	101.30	101.09	101.39	101.17	101.58
Si	1.952	1.955	1.958	1.926	1.923	1.924	1.917	1.911	1.912	1.909	1.908	1.915	1.918	1.911	1.910	1.909	1.908	1.902	1.908	1.904
Ti	0.000	0.000	0.001	0.001	0.001	0.001	0.001	0.001	0.001	0.001	0.001	0.001	0.002	0.002	0.002	0.001	0.001	0.001	0.001	0.002
Al	0.291	0.263	0.238	0.273	0.278	0.273	0.281	0.290	0.288	0.287	0.284	0.273	0.277	0.284	0.283	0.292	0.294	0.294	0.288	0.291
Cr	0.000	0.002	0.001	0.001	0.001	0.001	0.001	0.001	0.001	0.000	0.000	0.001	0.001	0.002	0.001	0.000	0.001	0.000	0.001	0.002
Fe2+	0.080	0.083	0.081	0.087	0.090	0.084	0.090	0.091	0.094	0.093	0.096	0.097	0.097	0.095	0.092	0.094	0.095	0.095	0.095	0.099
Mn	0.002	0.001	0.002	0.001	0.001	0.002	0.003	0.002	0.001	0.001	0.003	0.003	0.002	0.004	0.003	0.003	0.001	0.003	0.003	0.003
Ni	0.002	0.001	0.001	0.002	0.002	0.002	0.001	0.000	0.001	0.003	0.002	0.002	0.000	0.002	0.002	0.000	0.003	0.002	0.001	0.002
Mg	0.735	0.759	0.776	0.766	0.770	0.770	0.766	0.763	0.765	0.768	0.774	0.778	0.769	0.770	0.774	0.769	0.763	0.767	0.770	0.770
Ca	0.727	0.752	0.782	0.807	0.806	0.812	0.815	0.823	0.818	0.824	0.818	0.818	0.816	0.816	0.816	0.815	0.817	0.820	0.819	0.818
Na	0.224	0.192	0.166	0.144	0.132	0.137	0.130	0.127	0.123	0.121	0.126	0.120	0.120	0.119	0.125	0.123	0.122	0.127	0.121	0.113
K	0.000	0.000	0.000	0.000	0.001	0.000	0.000	0.000	0.000	0.000	0.000	0.001	0.000	0.000	0.001	0.000	0.001	0.000	0.000	0.000
Sum	4.014	4.008	4.005	4.008	4.004	4.006	4.006	4.007	4.004	4.007	4.012	4.008	4.002	4.004	4.009	4.006	4.005	4.013	4.007	4.004
Mg#	90.18	90.14	90.55	89.80	89.53	90.16	89.49	89.34	89.06	89.20	88.97	88.91	88.80	89.02	89.38	89.11	88.93	88.98	89.02	88.61
Al IV	0.034	0.037	0.038	0.066	0.074	0.070	0.077	0.083	0.084	0.084	0.080	0.078	0.081	0.086	0.081	0.086	0.087	0.085	0.085	0.092
Al VI	0.258	0.227	0.201	0.207	0.204	0.204	0.204	0.207	0.204	0.203	0.204	0.196	0.196	0.199	0.202	0.207	0.207	0.210	0.203	0.199

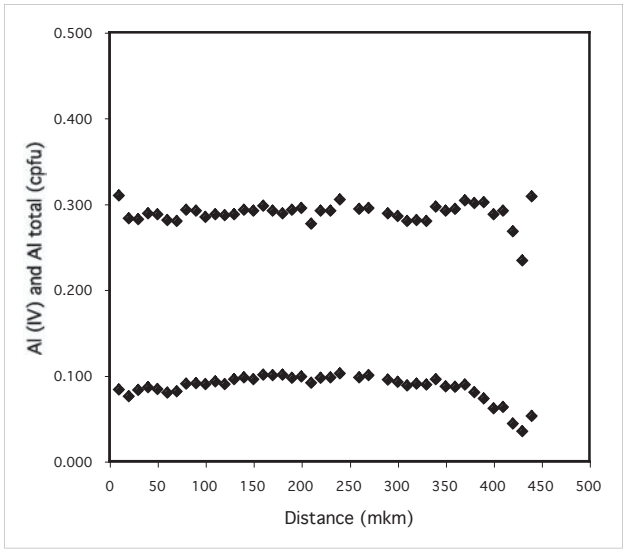
1904-7 Cpx II, profile 454

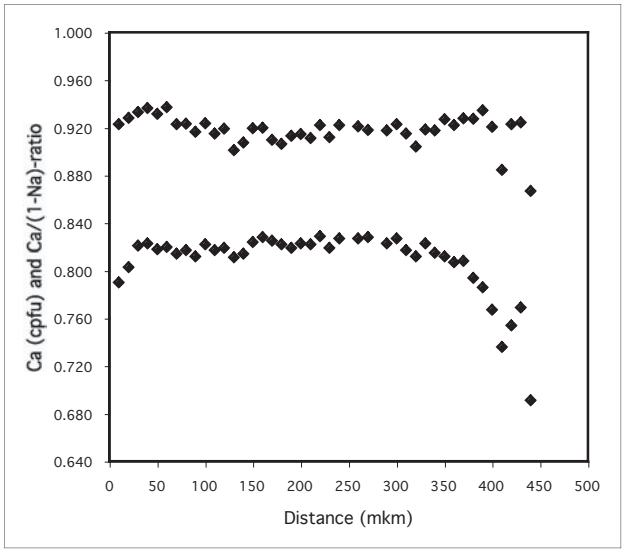
	210	220	230	240	250	260	270	280	290	300	310	320	330	340	350	360	370	380	390	400
SiO2	53.20	53.63	52.34	53.80	53.37	53.57	53.75	53.40	53.51	53.78	52.52	53.46	53.64	53.67	53.66	53.60	53.70	53.85	53.70	53.89
TiO2	0.05	0.03	0.05	0.06	0.06	0.05	0.04	0.05	0.07	0.07	0.06	0.04	0.07	0.04	0.03	0.06	0.03	0.03	0.04	0.02
Al2O3	6.80	6.76	8.46	6.65	7.16	7.10	6.81	6.89	6.79	6.66	6.92	7.16	6.93	7.01	6.98	6.97	6.94	6.80	7.05	7.02
Cr2O3	0.08	0.04	0.03	0.00	0.03	0.03	0.03	0.08	0.03	0.08	0.00	0.05	0.07	0.07	0.06	0.03	0.11	0.02	0.02	0.06
FeO	3.03	3.08	3.45	3.08	3.20	3.16	3.15	3.30	3.10	3.00	2.99	3.23	3.10	3.10	3.06	3.01	2.99	2.88	2.62	2.91
MnO	0.08	0.13	0.10	0.10	0.11	0.09	0.07	0.05	0.15	0.06	0.10	0.06	0.12	0.08	0.06	0.04	0.04	0.05	0.04	0.06
NiO	0.02	0.06	0.08	0.02	0.02	0.04	0.02	0.01	0.09	0.12	0.03	0.10	0.09	0.03	0.05	0.05	0.08	0.09	0.01	0.06
MgO	14.47	14.29	14.65	14.52	14.30	14.27	14.47	14.50	14.37	14.43	14.46	14.56	14.40	14.44	14.32	14.33	14.18	14.30	14.03	14.10
CaO	21.38	21.34	20.69	21.27	21.17	21.31	21.58	21.61	21.35	21.40	21.34	21.27	21.70	21.43	21.41	21.41	21.47	21.37	21.47	21.27
Na2O	1.65	1.79	1.77	1.79	1.80	1.87	1.79	1.73	1.84	1.93	1.77	1.77	1.87	1.80	1.86	1.90	1.83	1.92	2.01	2.02
K2O	0.00	0.00	0.00	0.00	0.00	0.00	0.01	0.00	0.01	0.00	0.00	0.00	0.00	0.01	0.00	0.00	0.01	0.01	0.00	0.00
Total	100.76	101.15	101.61	101.29	101.22	101.49	101.71	101.60	101.30	101.53	100.19	101.71	101.98	101.68	101.48	101.39	101.37	101.31	100.99	101.40
Si	1.908	1.916		1.918	1.906	1.908	1.911	1.903	1.911	1.915	1.897	1.901	1.904	1.908	1.911	1.910	1.914	1.919	1.917	1.918
Ti	0.001	0.001		0.002	0.002	0.001	0.001	0.001	0.002	0.002	0.002	0.001	0.002	0.001	0.001	0.002	0.001	0.001	0.001	0.001
Al	0.288	0.285		0.279	0.301	0.298	0.285	0.289	0.286	0.280	0.294	0.300	0.290	0.294	0.293	0.293	0.291	0.286	0.297	0.294
Cr	0.002	0.001		0.000	0.001	0.001	0.001	0.002	0.001	0.002	0.000	0.001	0.002	0.002	0.002	0.001	0.003	0.001	0.000	0.002
Fe2+	0.091	0.092		0.092	0.096	0.094	0.094	0.098	0.093	0.089	0.090	0.096	0.092	0.092	0.091	0.090	0.089	0.086	0.078	0.087
Mn	0.002	0.004		0.003	0.003	0.003	0.002	0.002	0.004	0.002	0.003	0.002	0.003	0.003	0.002	0.001	0.001	0.001	0.001	0.002
Ni	0.001	0.002		0.000	0.001	0.001	0.001	0.000	0.002	0.003	0.001	0.003	0.003	0.001	0.001	0.001	0.002	0.003	0.000	0.002
Mg	0.774	0.761		0.772	0.761	0.757	0.767	0.770	0.765	0.766	0.779	0.772	0.762	0.765	0.760	0.761	0.753	0.760	0.747	0.748
Ca	0.822	0.817		0.813	0.810	0.813	0.822	0.825	0.817	0.816	0.826	0.810	0.826	0.816	0.817	0.817	0.820	0.816	0.821	0.811
Na	0.114	0.124		0.124	0.125	0.129	0.123	0.120	0.128	0.133	0.124	0.122	0.129	0.124	0.128	0.131	0.126	0.133	0.139	0.139
K	0.000	0.000		0.000	0.000	0.000	0.000	0.000	0.000	0.000	0.000	0.000	0.000	0.000	0.000	0.000	0.000	0.000	0.000	0.000
Sum	4.003	4.002		4.002	4.004	4.006	4.007	4.010	4.008	4.009	4.016	4.008	4.012	4.006	4.006	4.007	4.001	4.004	4.003	4.003
Mg#	89.48	89.21		89.35	88.80	88.95	89.08	88.71	89.16	89.59	89.64	88.94	89.23	89.26	89.31	89.42	89.43	89.83	90.55	89.58
Al IV	0.089	0.082		0.080	0.091	0.086	0.083	0.087	0.082	0.077	0.087	0.091	0.084	0.087	0.085	0.084	0.085	0.078	0.080	0.080
Al VI	0.199	0.203		0.200	0.211	0.212	0.203	0.203	0.205	0.204	0.207	0.210	0.207	0.207	0.209	0.210	0.206	0.208	0.217	0.215

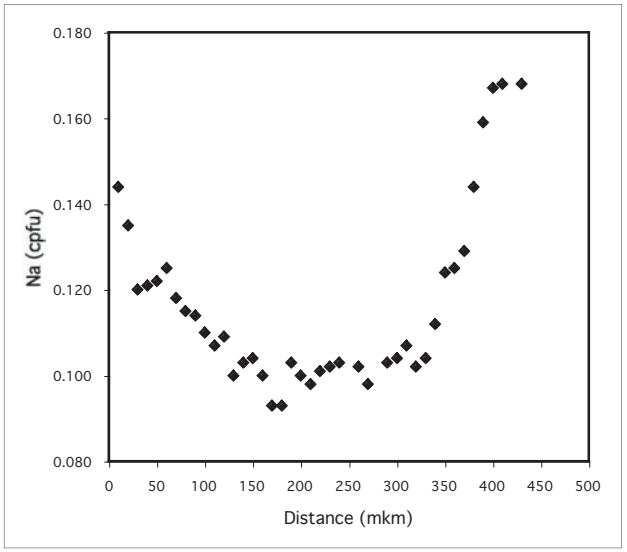
1904-7 Cpx II, profile 454

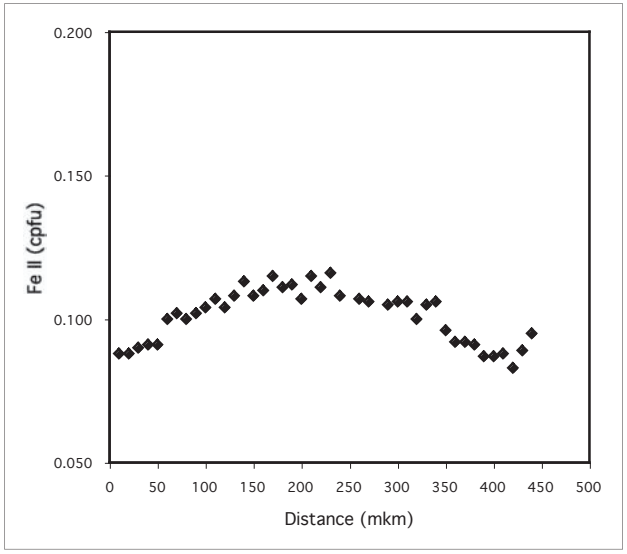
	410	420	430	440	450	460	463
SiO2	54.36	54.21	54.56	54.32	54.86	54.63	54.80
TiO2	0.05	0.04	0.06	0.02	0.03	0.03	0.04
Al2O3	6.91	7.07	7.45	7.76	8.15	9.07	9.44
Cr2O3	0.03	0.03	0.00	0.04	0.04	0.01	0.00
FeO	2.72	2.81	2.90	2.53	2.53	2.35	2.11
MnO	0.06	0.00	0.05	0.03	0.03	0.06	0.05
NiO	0.06	0.12	0.10	0.07	0.11	0.00	0.07
MgO	14.03	14.21	13.72	13.48	13.22	12.71	12.42
CaO	20.85	20.80	20.52	20.01	19.52	18.79	18.30
Na2O	2.33	2.38	2.53	2.96	3.33	3.71	3.96
K2O	0.00	0.00	0.00	0.00	0.01	0.02	0.01
Total	101.39	101.66	101.89	101.22	101.83	101.40	101.20
Si	1.931	1.922	1.928	1.928	1.933	1.927	1.932
Ti	0.001	0.001	0.001	0.001	0.001	0.001	0.001
Al	0.289	0.296	0.310	0.325	0.338	0.377	0.392
Cr	0.001	0.001	0.000	0.001	0.001	0.000	0.000
Fe2+	0.081	0.083	0.086	0.075	0.075	0.069	0.062
Mn	0.002	0.000	0.002	0.001	0.001	0.002	0.001
Ni	0.002	0.003	0.003	0.002	0.003	0.000	0.002
Mg	0.743	0.751	0.723	0.713	0.695	0.669	0.653
Ca	0.794	0.790	0.777	0.761	0.737	0.710	0.691
Na	0.160	0.163	0.173	0.203	0.227	0.254	0.270
K	0.000	0.000	0.000	0.000	0.001	0.001	0.000
Sum	4.003	4.011	4.002	4.010	4.011	4.011	4.006
Mg#	90.17	90.05	89.37	90.48	90.26	90.65	91.33
Al IV	0.066	0.068	0.070	0.063	0.057	0.062	0.062
Al VI	0.223	0.228	0.241	0.263	0.282	0.315	0.330

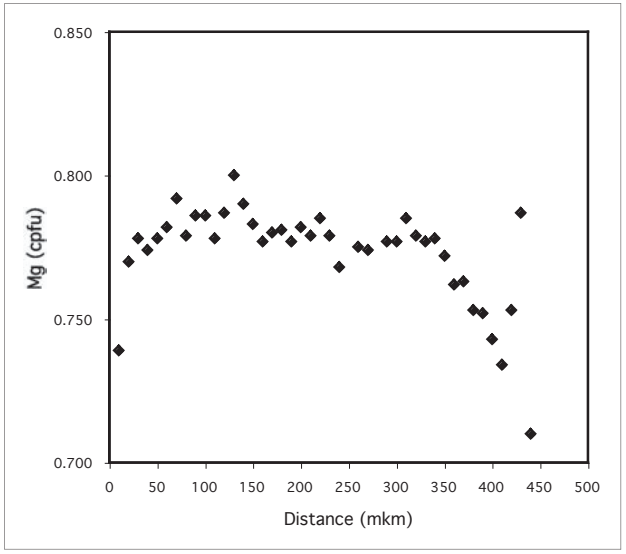
1904-7 Cpx II, profile 454

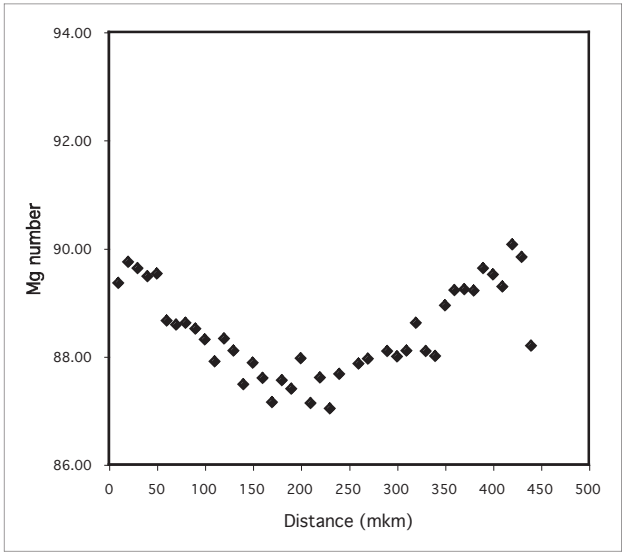












1904-7 Cpx II, profile 432

	10	20	30	40	50	60	70	80	90	100	110	120	130	140	150	160	170	180	190	200
SiO2	53.25	53.38	53.20	52.98	52.89	52.62	52.69	52.43	52.30	52.69	52.95	52.60	52.54	52.53	51.99	52.34	52.34	52.62	52.56	52.56
TiO2	0.04	0.06	0.06	0.06	0.03	0.08	0.02	0.03	0.06	0.07	0.08	0.05	0.04	0.06	0.05	0.06	0.04	0.07	0.07	0.06
Al2O3	7.31	6.68	6.67	6.81	6.78	6.59	6.58	6.85	6.82	6.72	6.81	6.74	6.76	6.91	6.82	7.00	6.84	6.81	6.89	6.95
Cr2O3	0.07	0.01	0.00	0.00	0.00	0.03	0.03	0.03	0.00	0.04	0.03	0.03	0.05	0.02	0.04	0.06	0.01	0.07	0.04	0.02
FeO	2.91	2.92	2.99	3.01	3.02	3.30	3.36	3.29	3.36	3.46	3.57	3.43	3.58	3.76	3.55	3.66	3.81	3.68	3.72	3.55
MnO	0.05	0.03	0.07	0.10	0.06	0.08	0.03	0.10	0.05	0.11	0.12	0.12	0.12	0.10	0.06	0.15	0.10	0.08	0.15	0.11
NiO	0.02	0.01	0.03	0.00	0.07	0.07	0.06	0.02	0.00	0.09	0.01	0.03	0.00	0.00	0.03	0.05	0.00	0.06	0.01	0.03
MgO	13.76	14.35	14.52	14.43	14.48	14.52	14.70	14.41	14.52	14.65	14.53	14.63	14.87	14.72	14.44	14.45	14.45	14.53	14.44	14.56
CaO	20.46	20.84	21.33	21.35	21.18	21.19	21.01	21.04	20.85	21.31	21.23	21.17	20.97	21.09	21.14	21.42	21.28	21.28	21.19	21.32
Na2O	2.06	1.93	1.72	1.73	1.74	1.79	1.69	1.64	1.61	1.58	1.54	1.56	1.43	1.48	1.48	1.43	1.33	1.33	1.47	1.43
K2O	0.07	0.02	0.00	0.01	0.00	0.01	0.01	0.00	0.00	0.01	0.01	0.02	0.00	0.01	0.01	0.00	0.01	0.01	0.03	0.00
Total	99.99	100.22	100.60	100.48	100.27	100.29	100.17	99.84	99.57	100.72	100.88	100.39	100.36	100.67	99.60	100.60	100.19	100.54	100.56	100.58
Si	1.919	1.921	1.911	1.906	1.907	1.902	1.904	1.901	1.900	1.897	1.901	1.898	1.896	1.892	1.893	1.888	1.895	1.897	1.896	1.894
Ti	0.001	0.002	0.002	0.002	0.001	0.002	0.000	0.001	0.002	0.002	0.002	0.001	0.001	0.002	0.001	0.001	0.001	0.002	0.002	0.001
Al	0.310	0.283	0.282	0.289	0.288	0.281	0.280	0.293	0.292	0.285	0.288	0.287	0.288	0.293	0.292	0.298	0.292	0.289	0.293	0.295
Cr	0.002	0.000	0.000	0.000	0.000	0.001	0.001	0.001	0.000	0.001	0.001	0.001	0.001	0.001	0.001	0.002	0.000	0.002	0.001	0.000
Fe2+	0.088	0.088	0.090	0.091	0.091	0.100	0.102	0.100	0.102	0.104	0.107	0.104	0.108	0.113	0.108	0.110	0.115	0.111	0.112	0.107
Mn	0.001	0.001	0.002	0.003	0.002	0.002	0.001	0.003	0.002	0.003	0.004	0.004	0.004	0.003	0.002	0.005	0.003	0.003	0.005	0.003
Ni	0.001	0.000	0.001	0.000	0.002	0.002	0.002	0.001	0.000	0.003	0.000	0.001	0.000	0.000	0.001	0.001	0.000	0.002	0.000	0.001
Mg	0.739	0.770	0.778	0.774	0.778	0.782	0.792	0.779	0.786	0.786	0.778	0.787	0.800	0.790	0.783	0.777	0.780	0.781	0.777	0.782
Ca	0.790	0.803	0.821	0.823	0.818	0.820	0.814	0.817	0.812	0.822	0.817	0.819	0.811	0.814	0.824	0.828	0.825	0.822	0.819	0.823
Na	0.144	0.135	0.120	0.121	0.122	0.125	0.118	0.115	0.114	0.110	0.107	0.109	0.100	0.103	0.104	0.100	0.093	0.093	0.103	0.100
K	0.003	0.001	0.000	0.000	0.000	0.001	0.000	0.000	0.000	0.000	0.000	0.001	0.000	0.000	0.000	0.000	0.000	0.000	0.001	0.000
Sum	3.998	4.003	4.006	4.008	4.009	4.018	4.014	4.009	4.009	4.013	4.006	4.011	4.008	4.011	4.011	4.011	4.005	4.002	4.007	4.007
Mg#	89.36	89.74	89.63	89.48	89.53	88.66	88.59	88.62	88.51	88.31	87.91	88.33	88.11	87.49	87.88	87.60	87.15	87.56	87.40	87.96
Al IV	0.084	0.076	0.083	0.086	0.084	0.080	0.082	0.091	0.091	0.090	0.093	0.090	0.096	0.098	0.096	0.101	0.101	0.101	0.097	0.099
Al VI	0.227	0.208	0.199	0.203	0.204	0.201	0.199	0.203	0.201	0.195	0.195	0.197	0.193	0.196	0.197	0.197	0.192	0.188	0.196	0.197

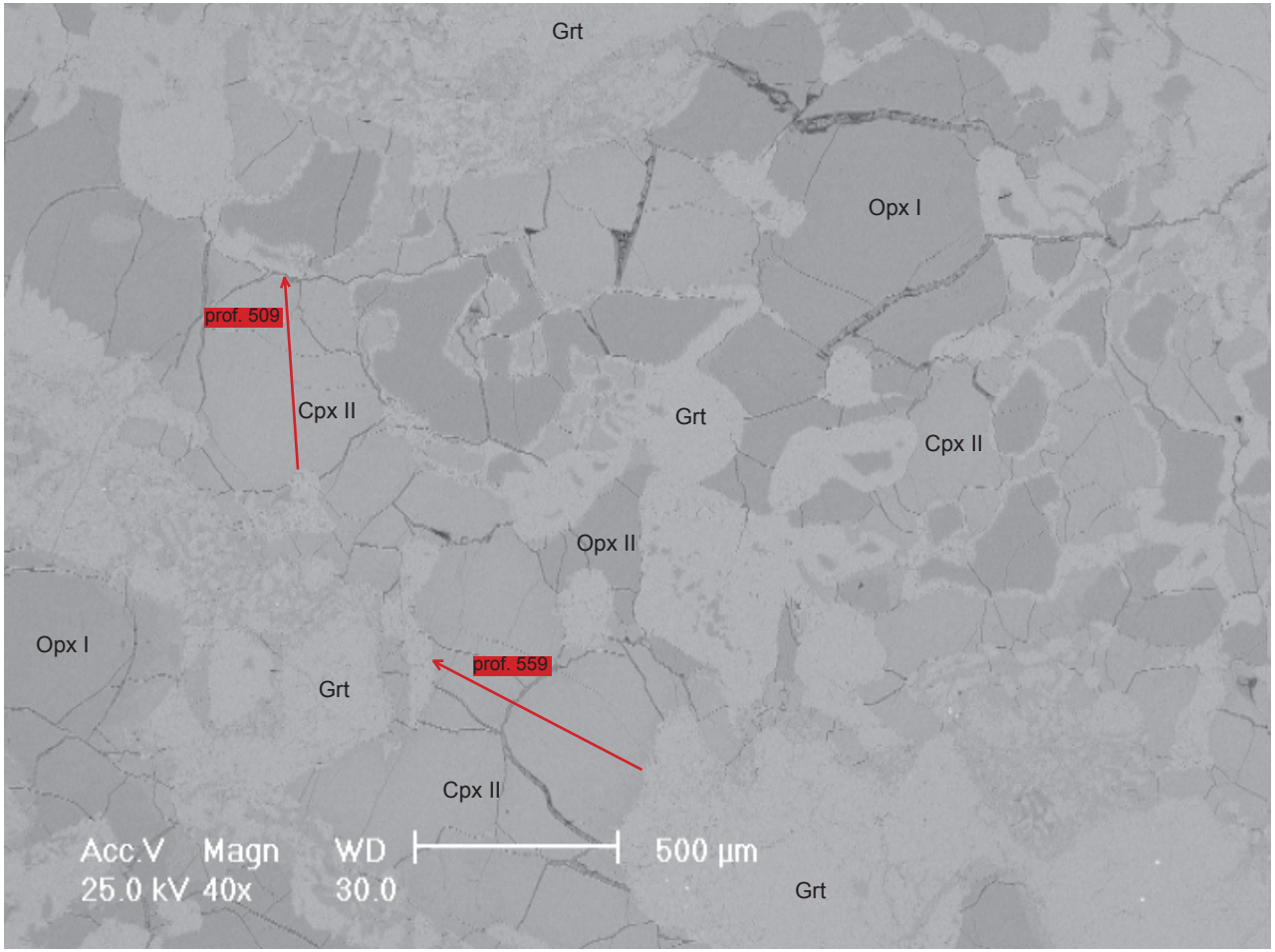
1904-7 Cpx II, profile 432

	210	220	230	240	250	260	270	280	290	300	310	320	330	340	350	360	370	380	390	400
SiO2	52.88	52.20	52.68	52.36	53.74	52.61	52.54	53.07	52.88	52.69	53.24	53.39	52.96	52.70	53.14	53.42	53.23	53.74	53.60	54.62
TiO2	0.05	0.05	0.07	0.05	0.02	0.06	0.09	0.03	0.06	0.04	0.06	0.05	0.07	0.06	0.06	0.07	0.05	0.07	0.06	0.04
Al2O3	6.53	6.85	6.91	7.16	5.75	6.94	6.94	6.53	6.83	6.74	6.65	6.65	6.59	7.02	6.93	6.96	7.20	7.16	7.17	6.88
Cr2O3	0.07	0.03	0.03	0.02	0.05	0.05	0.05	0.01	0.08	0.04	0.00	0.01	0.00	0.07	0.06	0.01	0.06	0.00	0.00	0.02
FeO	3.81	3.68	3.88	3.59	7.76	3.55	3.50	3.77	3.50	3.53	3.53	3.35	3.48	3.51	3.22	3.07	3.08	3.04	2.90	2.94
MnO	0.09	0.13	0.17	0.14	0.13	0.14	0.12	0.11	0.11	0.10	0.09	0.15	0.05	0.11	0.15	0.05	0.05	0.09	0.07	0.02
NiO	0.03	0.07	0.07	0.01	0.09	0.05	0.06	0.03	0.06	0.06	0.05	0.10	0.03	0.00	0.07	0.01	0.08	0.05	0.03	0.03
MgO	14.51	14.56	14.56	14.27	21.52	14.43	14.41	16.12	14.51	14.46	14.72	14.59	14.46	14.51	14.46	14.25	14.31	14.17	14.09	14.03
CaO	21.29	21.39	21.27	21.38	11.30	21.45	21.43	19.38	21.39	21.41	21.30	21.15	21.31	21.16	21.17	21.00	21.07	20.79	20.51	20.14
Na2O	1.40	1.44	1.46	1.47	0.80	1.47	1.40	1.38	1.48	1.49	1.54	1.47	1.50	1.60	1.79	1.80	1.87	2.08	2.29	2.42
K2O	0.00	0.00	0.00	0.00	0.01	0.00	0.01	0.00	0.01	0.00	0.00	0.00	0.01	0.00	0.01	0.00	0.00	0.00	0.01	0.01
Total	100.67	100.41	101.09	100.46	101.18	100.75	100.55	100.42	100.89	100.56	101.21	100.91	100.46	100.74	101.03	100.64	101.01	101.19	100.73	101.15
Si	1.905	1.888	1.892	1.890		1.894	1.894		1.899	1.900	1.905	1.913	1.909	1.895	1.903	1.915	1.904	1.916	1.918	1.941
Ti	0.001	0.001	0.002	0.001		0.001	0.002		0.001	0.001	0.002	0.001	0.002	0.002	0.002	0.002	0.001	0.002	0.002	0.001
Al	0.277	0.292	0.292	0.305		0.294	0.295		0.289	0.286	0.280	0.281	0.280	0.297	0.292	0.294	0.304	0.301	0.302	0.288
Cr	0.002	0.001	0.001	0.001		0.001	0.001		0.002	0.001	0.000	0.000	0.000	0.002	0.002	0.000	0.002	0.000	0.000	0.000
Fe2+	0.115	0.111	0.116	0.108		0.107	0.106		0.105	0.106	0.106	0.100	0.105	0.106	0.096	0.092	0.092	0.091	0.087	0.087
Mn	0.003	0.004	0.005	0.004		0.004	0.004		0.003	0.003	0.003	0.004	0.002	0.003	0.004	0.001	0.002	0.003	0.002	0.001
Ni	0.001	0.002	0.002	0.000		0.002	0.002		0.002	0.002	0.001	0.003	0.001	0.000	0.002	0.000	0.002	0.001	0.001	0.001
Mg	0.779	0.785	0.779	0.768		0.775	0.774		0.777	0.777	0.785	0.779	0.777	0.778	0.772	0.762	0.763	0.753	0.752	0.743
Ca	0.822	0.829	0.819	0.827		0.827	0.828		0.823	0.827	0.817	0.812	0.823	0.815	0.812	0.807	0.808	0.794	0.786	0.767
Na	0.098	0.101	0.102	0.103		0.102	0.098		0.103	0.104	0.107	0.102	0.104	0.112	0.124	0.125	0.129	0.144	0.159	0.167
K	0.000	0.000	0.000	0.000		0.000	0.001		0.000	0.000	0.000	0.000	0.001	0.000	0.000	0.000	0.000	0.000	0.001	0.000
Sum	4.003	4.015	4.010	4.007		4.008	4.004		4.005	4.008	4.006	3.996	4.002	4.009	4.010	3.998	4.007	4.004	4.009	3.997
Mg#	87.14	87.61	87.04	87.67		87.87	87.95		88.10	88.00	88.10	88.62	88.10	88.01	88.94	89.23	89.24	89.22	89.63	89.52
Al IV	0.092	0.097	0.098	0.103		0.098	0.101		0.095	0.093	0.089	0.091	0.090	0.096	0.087	0.087	0.090	0.081	0.073	0.062
Al VI	0.186	0.195	0.195	0.203		0.197	0.195		0.194	0.194	0.192	0.191	0.191	0.202	0.205	0.208	0.215	0.221	0.229	0.227

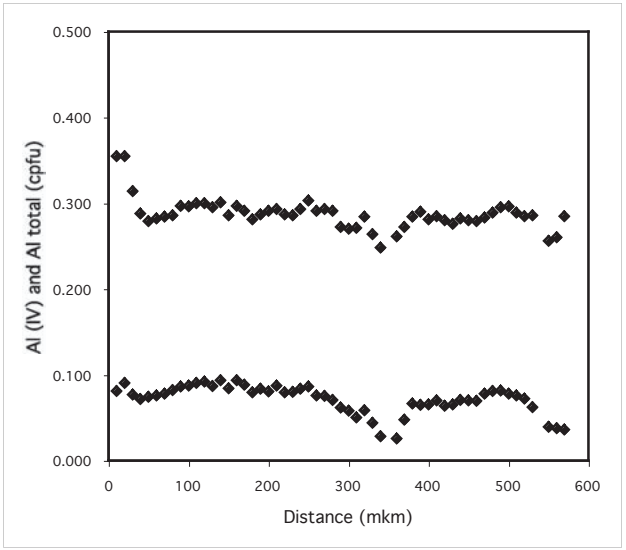
1904-7 Cpx II, profile 432

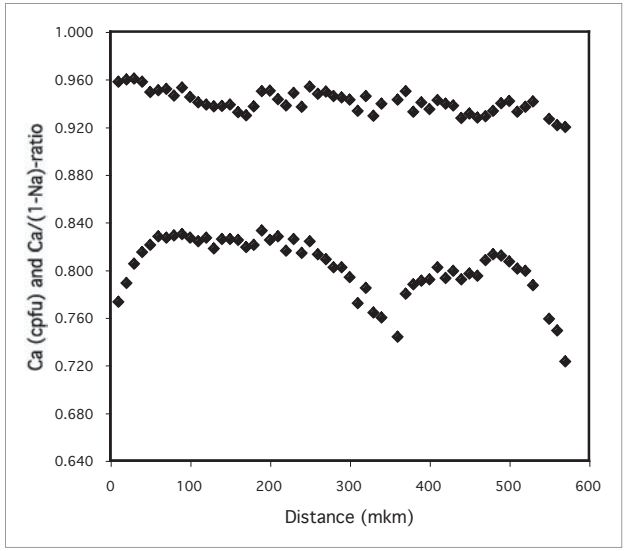
	410	420	430	440
SiO2	54.43	55.05	54.51	55.00
TiO2	0.03	0.03	0.03	0.02
Al2O3	6.88	6.39	5.53	7.32
Cr2O3	0.03	0.03	0.05	0.04
FeO	2.92	2.79	2.96	3.19
MnO	0.06	0.05	0.07	0.01
NiO	0.07	0.03	0.03	0.00
MgO	13.70	14.22	14.70	13.32
CaO	19.10	19.81	19.99	18.04
Na2O	2.41	2.66	2.41	2.93
K2O	0.02	0.00	0.00	0.06
Total	99.67	101.07	100.30	99.93
Si	1.957	1.956		1.967
Ti	0.001	0.001		0.001
Al	0.292	0.268		0.309
Cr	0.001	0.001		0.001
Fe2+	0.088	0.083		0.095
Mn	0.002	0.002		0.000
Ni	0.002	0.001		0.000
Mg	0.734	0.753		0.710
Ca	0.736	0.754		0.691
Na	0.168	0.183		0.203
K	0.001	0.000		0.003
Sum	3.981	4.001		3.980
Mg#	89.29	90.07		88.20
Al IV	0.063	0.044		0.053
Al VI	0.229	0.224		0.256

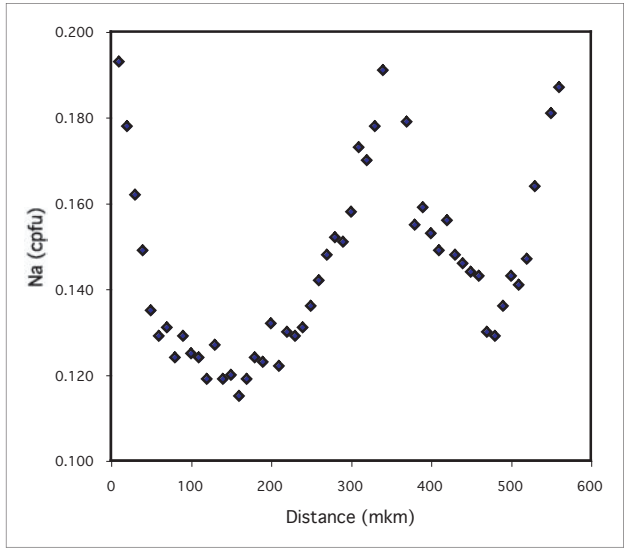
1904-7 Cpx II, profile 432

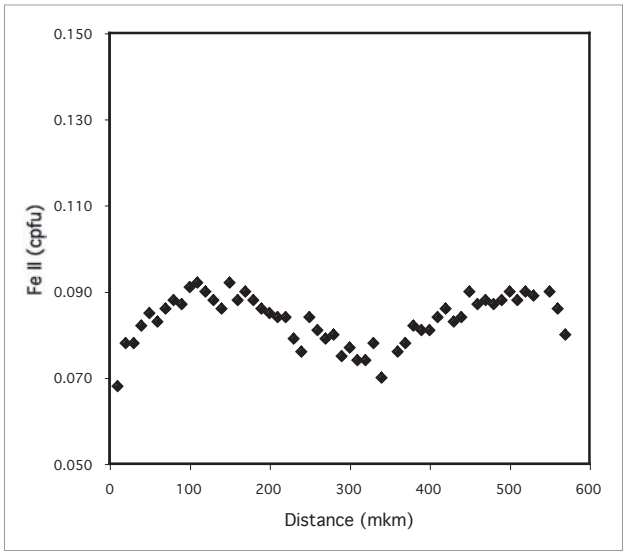


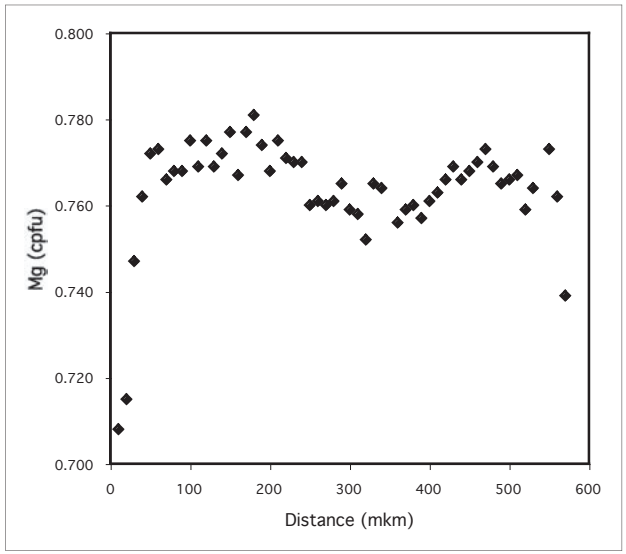
1904-7 Cpx II, profiles 559 and 509

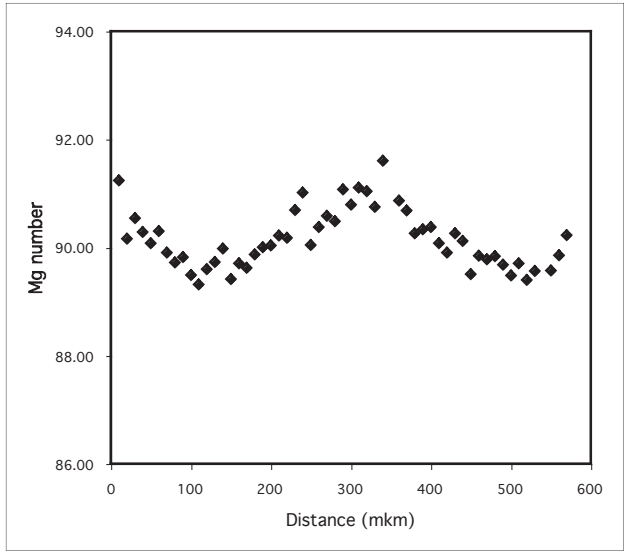












1904-7 Cpx II, profile 559

	10	20	30	40	50	60	70	80	90	100	110	120	130	140	150	160	170	180	190	200
SiO2	53.58	52.92	53.17	53.46	53.43	53.44	53.41	53.47	53.07	52.75	52.84	52.70	53.14	52.84	53.05	53.16	53.16	53.00	53.07	53.02
TiO2	0.01	0.05	0.04	0.04	0.06	0.02	0.03	0.05	0.05	0.04	0.06	0.04	0.05	0.06	0.05	0.06	0.06	0.05	0.04	0.05
Al2O3	8.45	8.42	7.42	6.82	6.61	6.70	6.75	6.81	7.03	6.97	7.10	7.08	6.99	7.11	6.76	7.02	6.89	6.61	6.78	6.88
Cr2O3	0.01	0.07	0.01	0.06	0.03	0.00	0.04	0.02	0.07	0.02	0.03	0.08	0.10	0.02	0.00	0.03	0.04	0.04	0.04	0.02
FeO	2.29	2.62	2.59	2.72	2.84	2.79	2.89	2.95	2.92	3.01	3.05	2.99	2.96	2.85	3.07	2.93	3.01	2.91	2.88	2.82
MnO	0.05	0.06	0.07	0.02	0.06	0.06	0.04	0.04	0.07	0.08	0.07	0.07	0.11	0.06	0.02	0.03	0.09	0.03	0.06	0.09
NiO	0.07	0.07	0.07	0.00	0.06	0.08	0.08	0.06	0.02	0.06	0.06	0.09	0.14	0.10	0.07	0.03	0.09	0.02	0.05	0.05
MgO	13.33	13.40	13.98	14.28	14.45	14.51	14.37	14.43	14.41	14.45	14.37	14.47	14.41	14.40	14.51	14.35	14.56	14.54	14.46	14.33
CaO	20.27	20.57	20.97	21.25	21.39	21.62	21.58	21.67	21.64	21.46	21.41	21.48	21.32	21.45	21.48	21.46	21.34	21.27	21.68	21.44
Na2O	2.80	2.57	2.33	2.14	1.95	1.86	1.89	1.79	1.86	1.79	1.78	1.70	1.83	1.71	1.72	1.65	1.72	1.77	1.76	1.90
K2O	0.01	0.00	0.01	0.00	0.02	0.02	0.00	0.00	0.00	0.00	0.00	0.03	0.00	0.00	0.01	0.00	0.00	0.01	0.00	0.01
Total	100.88	100.75	100.66	100.80	100.89	101.10	101.08	101.28	101.15	100.64	100.76	100.72	101.04	100.61	100.74	100.71	100.96	100.25	100.83	100.62
Si	1.908	1.894	1.906	1.915	1.914	1.911	1.911	1.909	1.899	1.897	1.897	1.894	1.903	1.899	1.905	1.906	1.904	1.910	1.904	1.905
Ti	0.000	0.001	0.001	0.001	0.002	0.000	0.001	0.001	0.001	0.001	0.002	0.001	0.001	0.002	0.001	0.002	0.002	0.001	0.001	0.001
Al	0.355	0.355	0.314	0.288	0.279	0.282	0.284	0.286	0.297	0.296	0.300	0.300	0.295	0.301	0.286	0.297	0.291	0.281	0.287	0.291
Cr	0.000	0.002	0.000	0.002	0.001	0.000	0.001	0.000	0.002	0.001	0.001	0.002	0.003	0.001	0.000	0.001	0.001	0.001	0.001	0.001
Fe2+	0.068	0.078	0.078	0.082	0.085	0.083	0.086	0.088	0.087	0.091	0.092	0.090	0.088	0.086	0.092	0.088	0.090	0.088	0.086	0.085
Mn	0.001	0.002	0.002	0.001	0.002	0.002	0.001	0.001	0.002	0.002	0.002	0.002	0.003	0.002	0.001	0.001	0.003	0.001	0.002	0.003
Ni	0.002	0.002	0.002	0.000	0.002	0.002	0.002	0.002	0.001	0.002	0.002	0.003	0.004	0.003	0.002	0.001	0.003	0.001	0.001	0.001
Mg	0.708	0.715	0.747	0.762	0.772	0.773	0.766	0.768	0.768	0.775	0.769	0.775	0.769	0.772	0.777	0.767	0.777	0.781	0.774	0.768
Ca	0.773	0.789	0.805	0.815	0.821	0.828	0.827	0.829	0.830	0.827	0.824	0.827	0.818	0.826	0.826	0.825	0.819	0.821	0.833	0.825
Na	0.193	0.178	0.162	0.149	0.135	0.129	0.131	0.124	0.129	0.125	0.124	0.119	0.127	0.119	0.120	0.115	0.119	0.124	0.123	0.132
K	0.000	0.000	0.000	0.000	0.001	0.001	0.000	0.000	0.000	0.000	0.000	0.001	0.000	0.000	0.000	0.000	0.000	0.001	0.000	0.001
Sum	4.011	4.016	4.017	4.014	4.013	4.012	4.012	4.008	4.015	4.016	4.012	4.014	4.011	4.009	4.010	4.001	4.008	4.010	4.012	4.014
Mg#	91.24	90.16	90.55	90.28	90.08	90.30	89.91	89.72	89.82	89.49	89.31	89.60	89.73	89.98	89.41	89.71	89.62	89.87	90.00	90.04
Al IV	0.081	0.091	0.077	0.072	0.074	0.076	0.078	0.082	0.086	0.087	0.091	0.092	0.087	0.094	0.084	0.094	0.089	0.080	0.084	0.081
Al VI	0.274	0.265	0.237	0.217	0.205	0.206	0.206	0.204	0.211	0.209	0.210	0.208	0.209	0.208	0.202	0.204	0.203	0.202	0.204	0.211

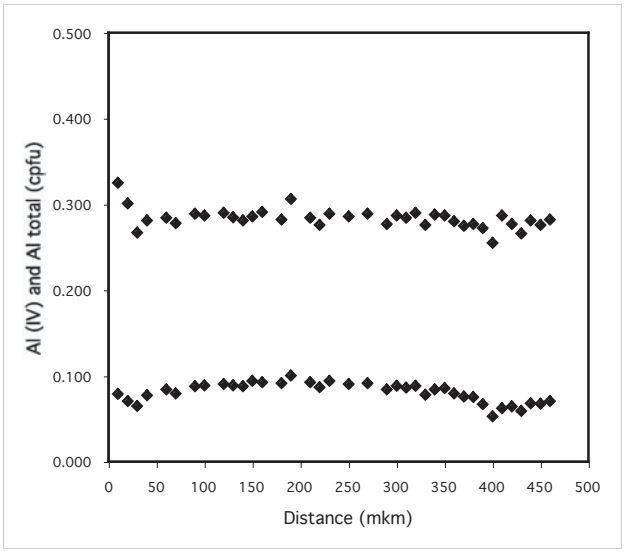
1904-7 Cpx II, profile 559

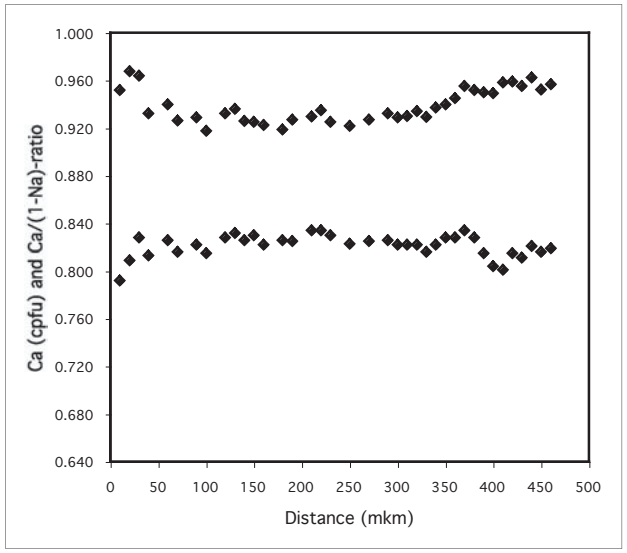
	210	220	230	240	250	260	270	280	290	300	310	320	330	340	350	360	370	380	390	400
SiO2	53.29	53.45	53.46	53.55	53.19	53.81	53.55	53.72	54.30	54.37	54.88	54.42	55.00	55.38	45.48	55.15	54.45	53.87	53.81	54.13
TiO2	0.07	0.05	0.05	0.06	0.07	0.04	0.07	0.04	0.04	0.04	0.04	0.05	0.02	0.01	0.01	0.01	0.03	0.06	0.01	0.04
Al2O3	6.97	6.81	6.78	6.96	7.19	6.94	6.96	6.92	6.48	6.43	6.47	6.76	6.32	5.92	29.34	6.22	6.49	6.73	6.88	6.69
Cr2O3	0.04	0.00	0.03	0.09	0.04	0.04	0.03	0.00	0.00	0.06	0.01	0.03	0.00	0.01	0.00	0.06	0.00	0.01	0.01	0.02
FeO	2.81	2.82	2.63	2.56	2.80	2.71	2.63	2.69	2.52	2.59	2.50	2.47	2.61	2.35	0.19	2.55	2.63	2.74	2.72	2.73
MnO	0.07	0.05	0.04	0.09	0.05	0.02	0.05	0.03	0.05	0.06	0.06	0.04	0.03	0.07	0.01	0.01	0.07	0.04	0.01	0.02
NiO	0.00	0.08	0.05	0.00	0.01	0.07	0.07	0.01	0.04	0.03	0.04	0.01	0.10	0.05	0.05	0.06	0.11	0.10	0.04	0.06
MgO	14.56	14.46	14.44	14.47	14.25	14.34	14.26	14.28	14.40	14.28	14.32	14.17	14.46	14.43	0.13	14.26	14.30	14.24	14.19	14.31
CaO	21.66	21.29	21.54	21.27	21.50	21.33	21.12	20.95	21.00	20.78	20.28	20.59	20.10	19.98	8.57	19.53	20.45	20.54	20.64	20.73
Na2O	1.76	1.87	1.86	1.90	1.96	2.06	2.13	2.20	2.18	2.29	2.51	2.46	2.59	2.78	0.23	3.05	2.60	2.24	2.29	2.21
K2O	0.01	0.01	0.00	0.02	0.00	0.00	0.00	0.01	0.00	0.00	0.00	0.00	0.00	0.01	3.94	0.03	0.00	0.01	0.01	0.01
Total	101.25	100.89	100.90	100.96	101.05	101.38	100.88	100.85	101.00	100.94	101.12	101.01	101.22	101.00	87.95	100.93	101.14	100.57	100.61	100.97
Si	1.902	1.913	1.913	1.912	1.902	1.915	1.915	1.920	1.935	1.939	1.949	1.937	1.952	1.967	1.759	1.961	1.939	1.929	1.926	1.931
Ti	0.002	0.001	0.001	0.002	0.002	0.001	0.002	0.001	0.001	0.001	0.001	0.001	0.001	0.000	0.000	0.000	0.001	0.002	0.000	0.001
Al	0.293	0.287	0.286	0.293	0.303	0.291	0.293	0.291	0.272	0.270	0.271	0.284	0.264	0.248	1.337	0.261	0.272	0.284	0.290	0.281
Cr	0.001	0.000	0.001	0.002	0.001	0.001	0.001	0.000	0.000	0.002	0.000	0.001	0.000	0.000	0.000	0.002	0.000	0.000	0.000	0.001
Fe2+	0.084	0.084	0.079	0.076	0.084	0.081	0.079	0.080	0.075	0.077	0.074	0.074	0.078	0.070	0.006	0.076	0.078	0.082	0.081	0.081
Mn	0.002	0.001	0.001	0.003	0.001	0.001	0.002	0.001	0.001	0.002	0.002	0.001	0.001	0.002	0.000	0.000	0.002	0.001	0.000	0.001
Ni	0.000	0.002	0.001	0.000	0.000	0.002	0.002	0.000	0.001	0.001	0.001	0.000	0.003	0.001	0.001	0.002	0.003	0.003	0.001	0.002
Mg	0.775	0.771	0.770	0.770	0.760	0.761	0.760	0.761	0.765	0.759	0.758	0.752	0.765	0.764	0.008	0.756	0.759	0.760	0.757	0.761
Ca	0.828	0.816	0.826	0.814	0.824	0.813	0.809	0.802	0.802	0.794	0.772	0.785	0.764	0.760	0.355	0.744	0.780	0.788	0.791	0.792
Na	0.122	0.130	0.129	0.131	0.136	0.142	0.148	0.152	0.151	0.158	0.173	0.170	0.178	0.191	0.017	0.211	0.179	0.155	0.159	0.153
K	0.001	0.000	0.000	0.001	0.000	0.000	0.000	0.000	0.000	0.000	0.000	0.000	0.000	0.001	0.194	0.001	0.000	0.000	0.001	0.000
Sum	4.010	4.007	4.007	4.005	4.012	4.009	4.010	4.010	4.003	4.003	4.001	4.005	4.005	4.005	3.678	4.013	4.014	4.005	4.008	4.004
Mg#	90.22	90.18	90.69	91.02	90.05	90.38	90.58	90.49	91.07	90.79	91.11	91.04	90.75	91.61	57.14	90.87	90.68	90.26	90.33	90.38
Al IV	0.088	0.080	0.080	0.084	0.086	0.076	0.075	0.071	0.062	0.058	0.050	0.059	0.044	0.028	0.563	0.026	0.048	0.067	0.065	0.066
Al VI	0.206	0.208	0.206	0.210	0.217	0.215	0.218	0.221	0.211	0.212	0.221	0.226	0.220	0.220	0.774	0.236	0.225	0.218	0.225	0.216

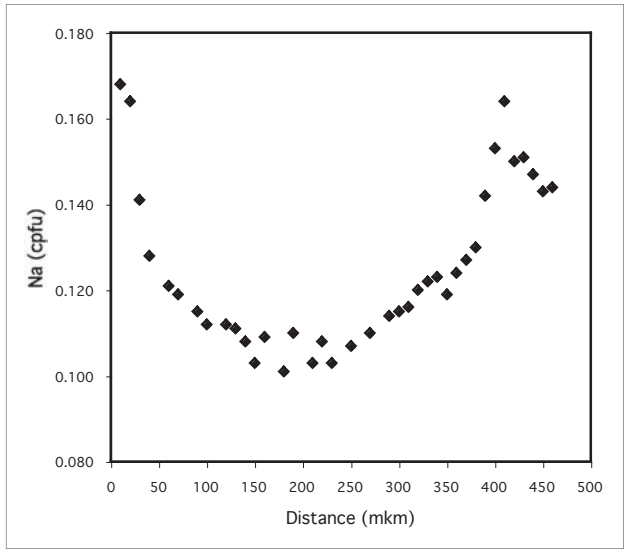
1904-7 Cpx II, profile 559

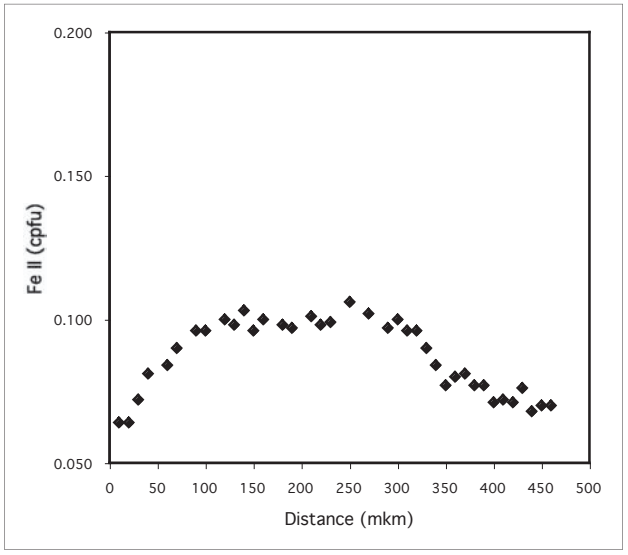
	410	420	430	440	450	460	470	480	490	500	510	520	530	540	550	560	570
SiO2	53.74	54.13	54.06	54.12	53.81	53.99	53.48	53.35	53.36	53.41	53.35	53.81	53.93	49.93	54.73	54.98	55.27
TiO2	0.07	0.04	0.05	0.06	0.06	0.03	0.05	0.05	0.04	0.04	0.07	0.09	0.05	0.02	0.04	0.02	0.01
Al2O3	6.76	6.67	6.57	6.71	6.63	6.62	6.69	6.83	6.99	7.04	6.82	6.77	6.80	18.34	6.10	6.21	6.82
Cr2O3	0.00	0.03	0.02	0.04	0.00	0.02	0.02	0.01	0.07	0.02	0.00	0.06	0.01	0.03	0.05	0.01	0.02
FeO	2.80	2.88	2.78	2.83	3.00	2.91	2.94	2.89	2.94	3.03	2.94	3.03	2.98	1.50	3.03	2.89	2.71
MnO	0.10	0.07	0.06	0.07	0.04	0.06	0.04	0.07	0.09	0.04	0.08	0.01	0.06	0.00	0.05	0.02	0.05
NiO	0.06	0.02	0.02	0.04	0.03	0.05	0.02	0.07	0.11	0.10	0.03	0.05	0.03	0.01	0.01	0.02	0.07
MgO	14.32	14.43	14.46	14.43	14.41	14.48	14.45	14.38	14.35	14.38	14.32	14.27	14.37	6.02	14.56	14.36	13.99
CaO	20.95	20.81	20.91	20.77	20.81	20.80	21.04	21.14	21.20	21.08	20.80	20.91	20.60	12.28	19.90	19.64	19.04
Na2O	2.15	2.26	2.14	2.11	2.08	2.07	1.87	1.85	1.96	2.07	2.03	2.12	2.38	1.14	2.62	2.71	3.12
K2O	0.00	0.01	0.00	0.00	0.00	0.00	0.00	0.00	0.00	0.00	0.00	0.00	0.00	1.31	0.01	0.00	0.01
Total	100.94	101.35	101.07	101.19	100.86	101.02	100.60	100.63	101.10	101.20	100.44	101.12	101.20	90.56	101.10	100.86	101.10
Si	1.921	1.926	1.928	1.927	1.924	1.927	1.918	1.914	1.908	1.907	1.917	1.921	1.922		1.949	1.958	1.959
Ti	0.002	0.001	0.001	0.002	0.002	0.001	0.001	0.001	0.001	0.001	0.002	0.002	0.001		0.001	0.001	0.000
Al	0.285	0.280	0.276	0.282	0.280	0.279	0.283	0.289	0.295	0.296	0.289	0.285	0.286		0.256	0.260	0.285
Cr	0.000	0.001	0.001	0.001	0.000	0.001	0.001	0.000	0.002	0.001	0.000	0.002	0.000		0.001	0.000	0.001
Fe2+	0.084	0.086	0.083	0.084	0.090	0.087	0.088	0.087	0.088	0.090	0.088	0.090	0.089		0.090	0.086	0.080
Mn	0.003	0.002	0.002	0.002	0.001	0.002	0.001	0.002	0.003	0.001	0.003	0.000	0.002		0.001	0.001	0.002
Ni	0.002	0.001	0.001	0.001	0.001	0.001	0.001	0.002	0.003	0.003	0.001	0.001	0.001		0.000	0.001	0.002
Mg	0.763	0.766	0.769	0.766	0.768	0.770	0.773	0.769	0.765	0.766	0.767	0.759	0.764		0.773	0.762	0.739
Ca	0.802	0.793	0.799	0.792	0.797	0.795	0.808	0.813	0.812	0.807	0.801	0.799	0.787		0.759	0.749	0.723
Na	0.149	0.156	0.148	0.146	0.144	0.143	0.130	0.129	0.136	0.143	0.141	0.147	0.164		0.181	0.187	0.214
K	0.000	0.000	0.000	0.000	0.000	0.000	0.000	0.000	0.000	0.000	0.000	0.000	0.000		0.000	0.000	0.000
Sum	4.010	4.011	4.006	4.003	4.006	4.005	4.004	4.005	4.011	4.015	4.008	4.007	4.015		4.012	4.005	4.005
Mg#	90.08	89.91	90.26	90.12	89.51	89.85	89.78	89.84	89.68	89.49	89.71	89.40	89.57		89.57	89.86	90.23
Al IV	0.070	0.064	0.066	0.071	0.070	0.070	0.078	0.081	0.082	0.078	0.076	0.072	0.062		0.039	0.038	0.036
Al VI	0.215	0.217	0.211	0.212	0.210	0.210	0.205	0.208	0.214	0.218	0.213	0.213	0.224		0.217	0.223	0.249

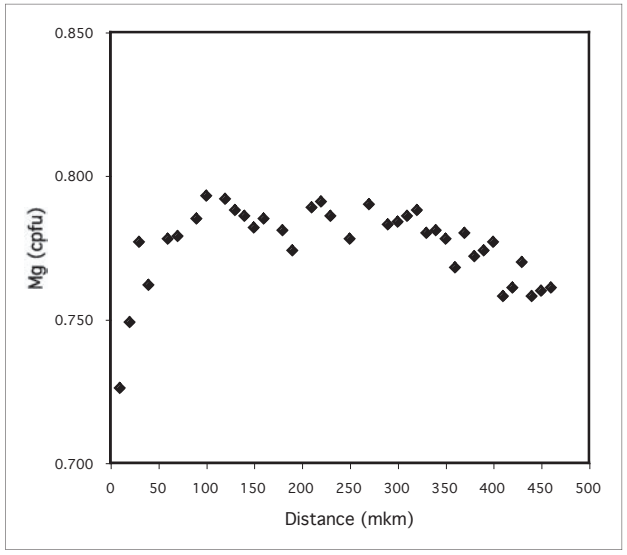
1904-7 Cpx II, profile 559

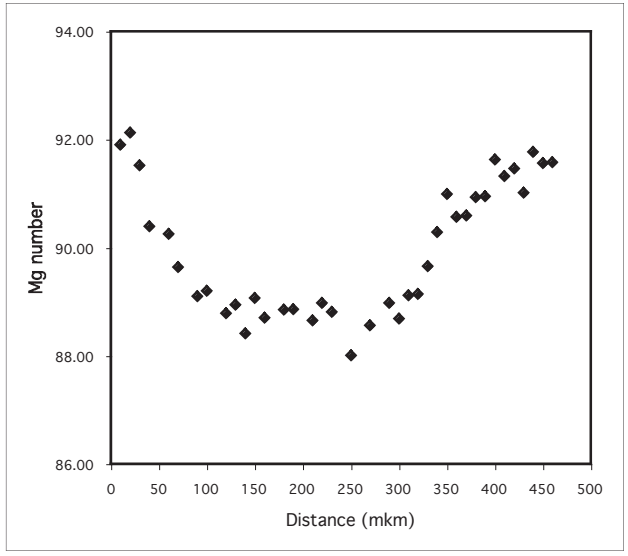












1904-7 Cpx II, profile 509

	10	20	30	40	50	60	70	80	90	100	110	120	130	140	150	160	170	180	190	200
SiO2	54.30	53.69	53.37	53.72	53.61	53.28	53.42	53.27	52.83	52.74	53.08	52.40	52.57	52.94	52.88	52.85	53.60	53.33	52.57	53.47
TiO2	0.03	0.05	0.07	0.04	0.05	0.05	0.01	0.04	0.03	0.07	0.03	0.04	0.04	0.05	0.06	0.05	0.04	0.04	0.07	0.04
Al2O3	7.79	7.16	6.29	6.66	7.15	6.74	6.59	6.58	6.83	6.76	6.31	6.82	6.70	6.64	6.76	6.89	6.16	6.70	7.22	5.83
Cr2O3	0.02	0.07	0.02	0.05	0.01	0.09	0.00	0.01	0.01	0.01	0.03	0.03	0.07	0.02	0.03	0.04	0.05	0.02	0.04	0.06
FeO	2.17	2.15	2.40	2.70	27.77	2.80	3.01	3.16	3.18	3.18	3.97	3.33	3.24	3.42	3.18	3.32	3.59	3.28	3.23	5.95
MnO	0.05	0.02	0.05	0.04	0.05	0.04	0.10	0.12	0.06	0.12	0.12	0.09	0.12	0.11	0.12	0.12	0.14	0.11	0.10	0.13
NiO	0.08	0.06	0.03	0.08	0.02	0.00	0.12	0.03	0.07	0.01	0.05	0.08	0.02	0.06	0.09	0.04	0.02	0.10	0.01	0.03
MgO	13.77	14.08	14.47	14.26	16.02	14.58	14.58	15.22	14.66	14.77	17.25	14.72	14.67	14.68	14.60	14.68	16.42	14.65	14.43	18.77
CaO	20.90	21.15	21.46	21.18	20.89	21.54	21.25	20.67	21.35	21.11	17.72	21.41	21.54	21.47	21.55	21.38	19.88	21.56	21.40	16.11
Na2O	2.45	2.37	2.02	1.85	2.07	1.74	1.71	1.59	1.66	1.60	1.45	1.61	1.58	1.55	1.49	1.56	1.31	1.46	1.58	0.98
K2O	0.03	0.00	0.02	0.03	0.00	0.00	0.00	0.00	0.00	0.01	0.01	0.00	0.01	0.00	0.01	0.00	0.00	0.01	0.00	0.00
Total	101.59	100.80	100.19	100.61	127.64	100.86	100.81	100.69	100.69	100.38	100.02	100.51	100.56	100.97	100.78	100.92	101.21	101.27	100.66	101.38
Si	1.920	1.917	1.922	1.925		1.908	1.915		1.899	1.901		1.890	1.895	1.901	1.900	1.896		1.906	1.891	
Ti	0.001	0.001	0.002	0.001		0.001	0.000		0.001	0.002		0.001	0.001	0.001	0.002	0.001		0.001	0.002	
Al	0.325	0.301	0.267	0.281		0.284	0.278		0.289	0.287		0.290	0.285	0.281	0.286	0.291		0.282	0.306	
Cr	0.000	0.002	0.001	0.001		0.003	0.000		0.000	0.000		0.001	0.002	0.001	0.001	0.001		0.001	0.001	
Fe2+	0.064	0.064	0.072	0.081		0.084	0.090		0.096	0.096		0.100	0.098	0.103	0.096	0.100		0.098	0.097	
Mn	0.002	0.001	0.001	0.001		0.001	0.003		0.002	0.004		0.003	0.004	0.003	0.004	0.004		0.003	0.003	
Ni	0.002	0.002	0.001	0.002		0.000	0.003		0.002	0.000		0.002	0.001	0.002	0.003	0.001		0.003	0.000	
Mg	0.726	0.749	0.777	0.762		0.778	0.779		0.785	0.793		0.792	0.788	0.786	0.782	0.785		0.781	0.774	
Ca	0.792	0.809	0.828	0.813		0.826	0.816		0.822	0.815		0.828	0.832	0.826	0.830	0.822		0.826	0.825	
Na	0.168	0.164	0.141	0.128		0.121	0.119		0.115	0.112		0.112	0.111	0.108	0.103	0.109		0.101	0.110	
K	0.001	0.000	0.001	0.001		0.000	0.000		0.000	0.001		0.000	0.000	0.000	0.000	0.000		0.001	0.000	
Sum	4.001	4.011	4.013	3.998		4.007	4.005		4.013	4.010		4.019	4.016	4.011	4.007	4.010		4.002	4.009	
Mg#	91.90	92.13	91.52	90.39		90.26	89.64		89.10	89.20		88.79	88.94	88.41	89.07	88.70		88.85	88.86	
Al IV	0.079	0.071	0.065	0.078		0.084	0.080		0.088	0.089		0.091	0.089	0.088	0.094	0.093		0.092	0.101	
Al VI	0.246	0.231	0.202	0.204		0.200	0.199		0.201	0.198		0.200	0.196	0.193	0.192	0.199		0.191	0.206	

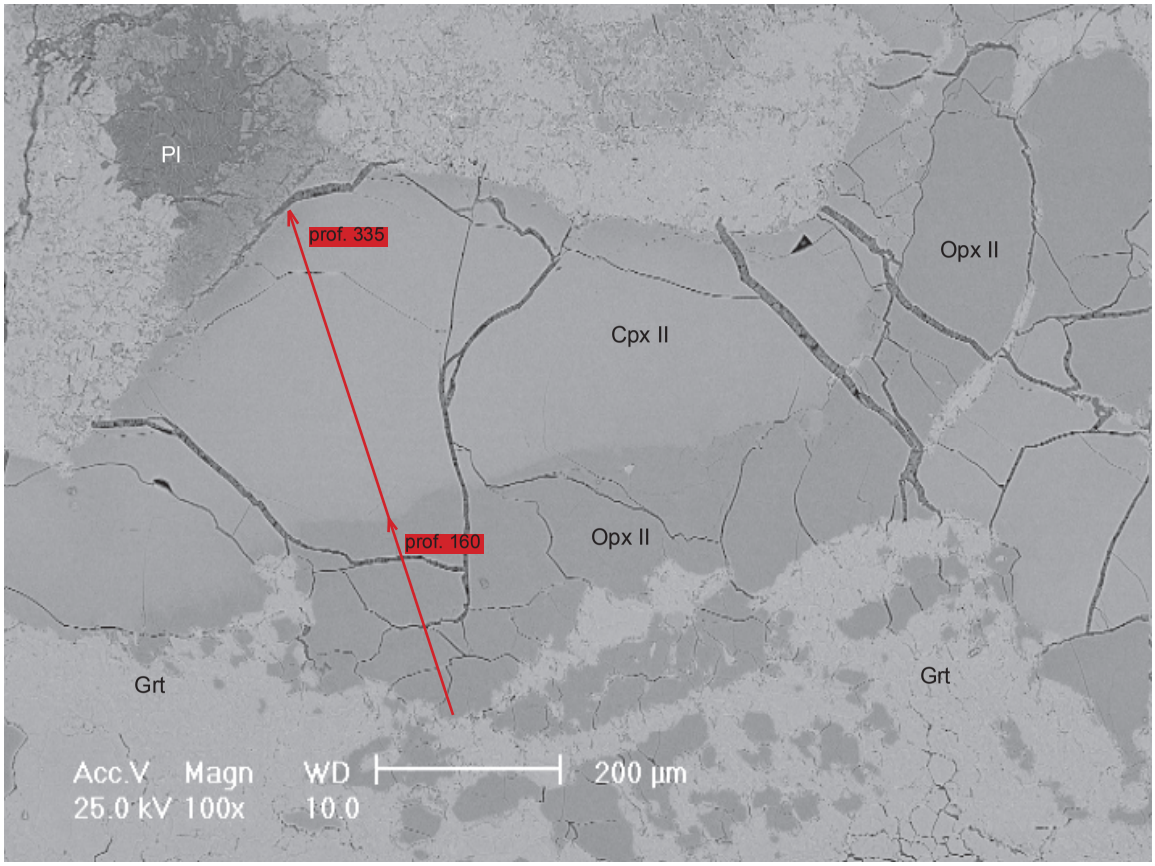
1904-7 Cpx II, profile 509

	210	220	230	240	250	260	270	280	290	300	310	320	330	340	350	360	370	380	390	400
SiO2	52.59	52.73	52.60	49.27	53.20	8.00	52.66	8.00	53.27	52.86	52.70	52.52	53.60	53.39	53.23	53.73	53.33	53.63	53.85	54.28
TiO2	0.08	0.07	0.05	0.05	0.04	0.01	0.04	0.03	0.06	0.06	0.05	0.10	0.05	0.04	0.07	0.05	0.04	0.04	0.02	0.03
Al2O3	6.69	6.51	6.80	9.42	6.78	5.93	6.82	5.41	6.57	6.79	6.69	6.83	6.55	6.83	6.79	6.65	6.51	6.58	6.46	6.04
Cr2O3	0.01	0.03	0.00	0.07	0.01	0.02	0.05	0.03	0.05	0.02	0.07	0.04	0.02	0.02	0.01	0.04	0.04	0.03	0.05	0.06
FeO	3.36	3.26	3.28	3.87	3.54	8.86	3.40	6.49	3.24	3.34	3.19	3.18	3.01	2.80	2.57	2.67	2.70	2.59	2.59	2.36
MnO	0.10	0.17	0.05	0.10	0.11	0.19	0.08	0.15	0.06	0.06	0.02	0.05	0.00	0.05	0.05	0.04	0.07	0.00	0.06	0.05
NiO	0.02	0.05	0.05	0.12	0.08	0.12	0.01	0.11	0.06	0.04	0.08	0.02	0.09	0.06	0.10	0.09	0.08	0.07	0.07	0.07
MgO	14.68	14.74	14.61	14.83	14.61	24.23	14.73	20.80	14.66	14.63	14.62	14.65	14.64	14.67	14.55	14.43	14.60	14.48	14.54	14.58
CaO	21.61	21.63	21.49	20.63	21.49	7.91	21.41	13.91	21.53	21.37	21.27	21.28	21.31	21.48	21.55	21.64	21.73	21.60	21.31	21.00
Na2O	1.48	1.55	1.48	1.56	1.55	0.68	1.58	0.92	1.64	1.65	1.66	1.72	1.76	1.77	1.72	1.79	1.83	1.88	2.06	2.21
K2O	0.00	0.00	0.00	0.03	0.01	0.02	0.00	0.01	0.00	0.00	0.00	0.00	0.00	0.01	0.01	0.01	0.00	0.01	0.00	0.00
Total	100.60	100.74	100.42	99.96	101.40	100.79	100.79	102.15	101.14	100.80	100.35	100.39	101.04	101.12	100.65	101.12	100.94	100.92	101.01	100.70
Si	1.895	1.898	1.897		1.901		1.894		1.907	1.899	1.901	1.895	1.916	1.907	1.909	1.918	1.910	1.918	1.923	1.941
Ti	0.002	0.002	0.001		0.001		0.001		0.002	0.002	0.001	0.003	0.001	0.001	0.002	0.001	0.001	0.001	0.001	0.001
Al	0.284	0.276	0.289		0.286		0.289		0.277	0.287	0.284	0.290	0.276	0.288	0.287	0.280	0.275	0.277	0.272	0.255
Cr	0.000	0.001	0.000		0.000		0.002		0.001	0.001	0.002	0.001	0.000	0.001	0.000	0.001	0.001	0.001	0.002	0.002
Fe2+	0.101	0.098	0.099		0.106		0.102		0.097	0.100	0.096	0.096	0.090	0.084	0.077	0.080	0.081	0.077	0.077	0.071
Mn	0.003	0.005	0.002		0.003		0.003		0.002	0.002	0.001	0.001	0.000	0.002	0.002	0.001	0.002	0.000	0.002	0.002
Ni	0.001	0.001	0.001		0.002		0.000		0.002	0.001	0.002	0.000	0.003	0.002	0.003	0.002	0.002	0.002	0.002	0.002
Mg	0.789	0.791	0.786		0.778		0.790		0.783	0.784	0.786	0.788	0.780	0.781	0.778	0.768	0.780	0.772	0.774	0.777
Ca	0.834	0.834	0.830		0.823		0.825		0.826	0.822	0.822	0.822	0.816	0.822	0.828	0.828	0.834	0.828	0.815	0.804
Na	0.103	0.108	0.103		0.107		0.110		0.114	0.115	0.116	0.120	0.122	0.123	0.119	0.124	0.127	0.130	0.142	0.153
K	0.000	0.000	0.000		0.000		0.000		0.000	0.000	0.000	0.000	0.000	0.000	0.001	0.000	0.000	0.000	0.000	0.000
Sum	4.012	4.016	4.009		4.008		4.015		4.009	4.012	4.012	4.017	4.005	4.009	4.005	4.002	4.014	4.007	4.011	4.007
Mg#	88.65	88.98	88.81		88.01		88.57		88.98	88.69	89.12	89.14	89.66	90.29	90.99	90.57	90.59	90.93	90.95	91.63
Al IV	0.093	0.087	0.094		0.091		0.092		0.084	0.089	0.086	0.089	0.078	0.084	0.086	0.080	0.076	0.075	0.067	0.053
Al VI	0.192	0.190	0.195		0.196		0.198		0.193	0.199	0.198	0.202	0.198	0.204	0.202	0.201	0.200	0.202	0.205	0.202

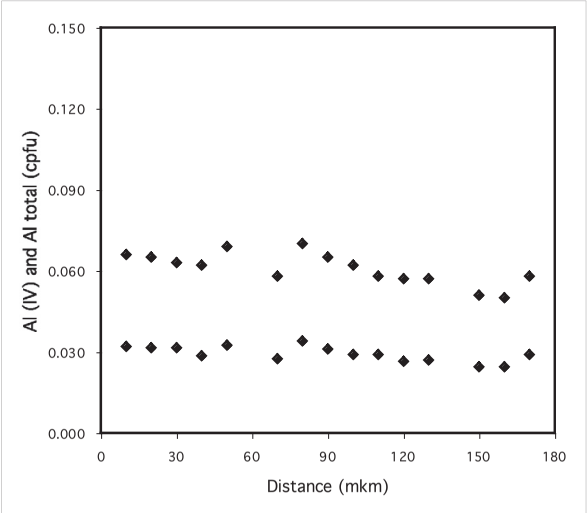
1904-7 Cpx II, profile 509

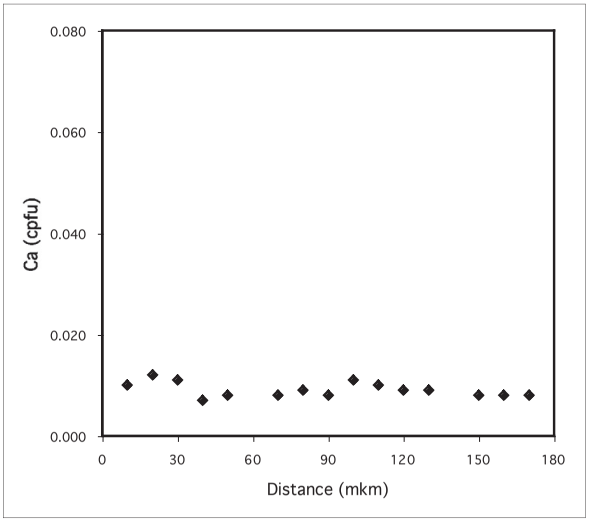
	410	420	430	440	450	460	470	480	490	500	510	520
SiO2	53.41	53.77	53.93	53.73	54.21	53.88	53.48	53.50	52.84	54.05	53.80	54.48
TiO2	0.04	0.03	0.03	0.05	0.02	0.03	0.03	0.03	0.03	0.02	0.05	0.04
Al2O3	6.75	6.56	6.29	6.64	6.57	6.70	6.80	6.55	6.50	6.66	6.51	6.81
Cr2O3	0.01	0.00	0.03	0.04	0.00	0.03	0.00	0.00	0.00	0.00	0.03	0.04
FeO	2.38	2.35	2.53	2.28	2.34	2.34	2.36	2.29	2.44	2.29	2.24	2.06
MnO	0.05	0.01	0.03	0.02	0.03	0.05	0.05	0.01	0.00	0.02	0.05	0.02
NiO	0.07	0.00	0.08	0.06	0.06	0.08	0.09	0.04	0.03	0.06	0.02	0.06
MgO	14.12	14.23	14.43	14.19	14.31	14.30	14.16	14.33	14.29	14.15	14.05	14.04
CaO	20.75	21.21	21.13	21.37	21.36	21.40	21.31	21.28	21.20	20.99	20.67	20.70
Na2O	2.35	2.16	2.17	2.11	2.07	2.08	2.14	2.15	2.12	2.31	2.47	2.66
K2O	0.02	0.00	0.00	0.01	0.01	0.01	0.00	0.00	0.00	0.01	0.00	0.00
Total	99.95	100.32	100.67	100.51	100.99	100.88	100.42	100.18	99.46	100.57	99.89	100.90
Si	1.925	1.930	1.931	1.926	1.932	1.925	1.920	1.924	1.917	1.934	1.937	1.939
Ti	0.001	0.001	0.001	0.001	0.001	0.001	0.001	0.001	0.001	0.001	0.001	0.001
Al	0.287	0.277	0.266	0.281	0.276	0.282	0.288	0.278	0.278	0.281	0.276	0.286
Cr	0.000	0.000	0.001	0.001	0.000	0.001	0.000	0.000	0.000	0.000	0.001	0.001
Fe2+	0.072	0.071	0.076	0.068	0.070	0.070	0.071	0.069	0.074	0.069	0.067	0.061
Mn	0.001	0.000	0.001	0.001	0.001	0.002	0.001	0.000	0.000	0.001	0.002	0.001
Ni	0.002	0.000	0.002	0.002	0.002	0.002	0.003	0.001	0.001	0.002	0.001	0.002
Mg	0.758	0.761	0.770	0.758	0.760	0.761	0.758	0.768	0.773	0.755	0.754	0.745
Ca	0.801	0.815	0.811	0.821	0.816	0.819	0.820	0.820	0.824	0.804	0.798	0.789
Na	0.164	0.150	0.151	0.147	0.143	0.144	0.149	0.150	0.149	0.161	0.172	0.183
K	0.001	0.000	0.000	0.001	0.000	0.000	0.000	0.000	0.000	0.000	0.000	0.000
Sum	4.013	4.006	4.010	4.006	4.001	4.006	4.010	4.011	4.017	4.006	4.009	4.008
Mg#	91.33	91.47	91.02	91.77	91.57	91.58	91.44	91.76	91.26	91.63	91.84	92.43
Al IV	0.062	0.065	0.059	0.068	0.068	0.071	0.071	0.065	0.066	0.061	0.054	0.053
Al VI	0.225	0.213	0.207	0.213	0.209	0.212	0.218	0.213	0.213	0.220	0.223	0.233

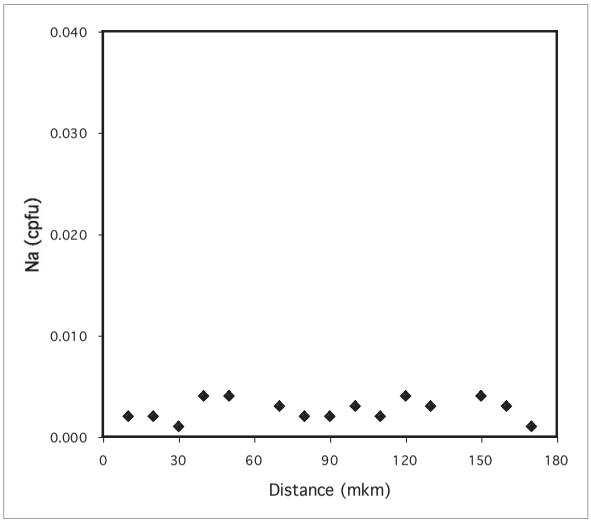
1904-7 Cpx II, profile 509

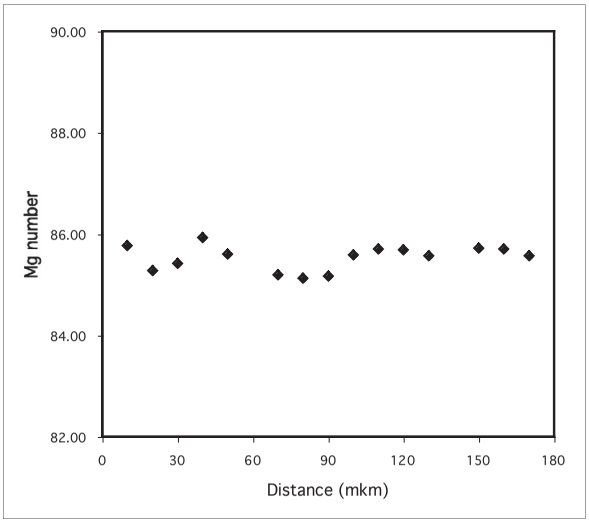


1904-7 Opx II, profile 160



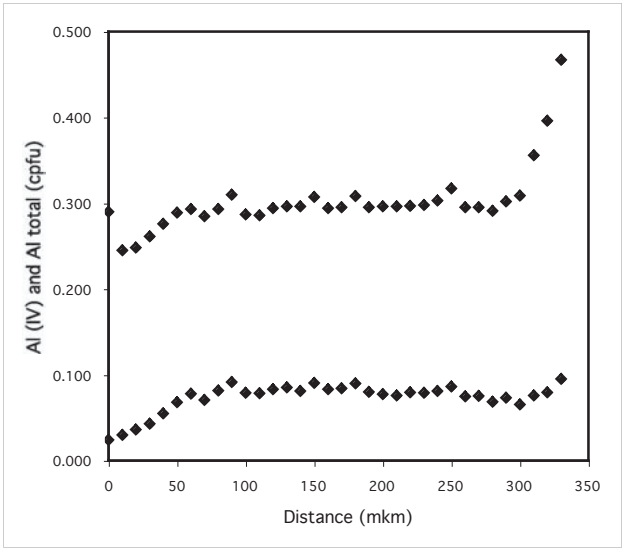


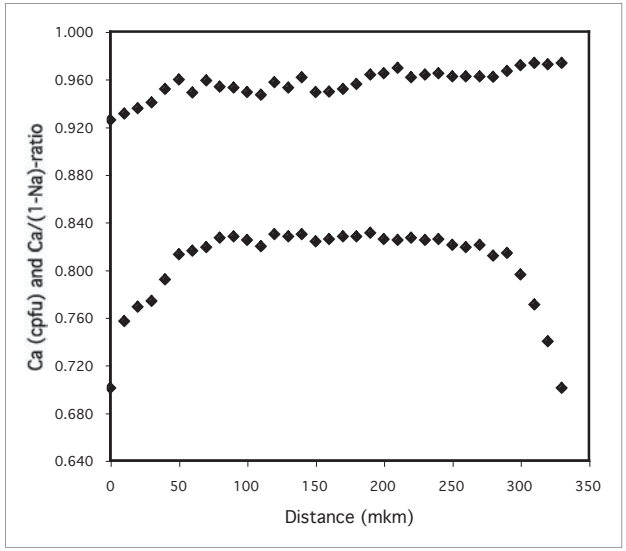


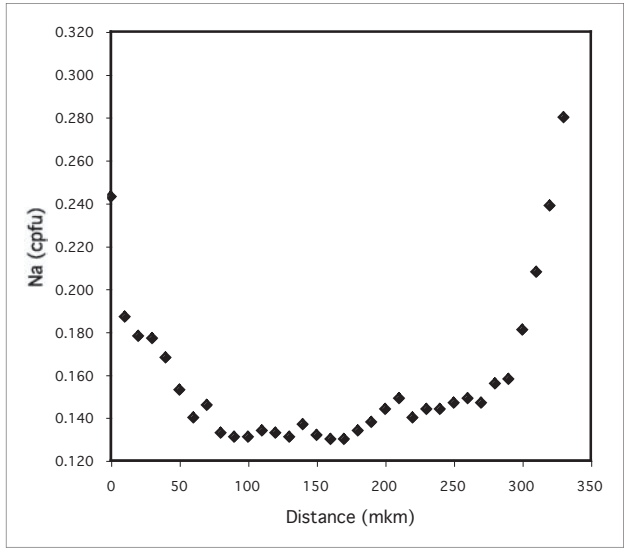


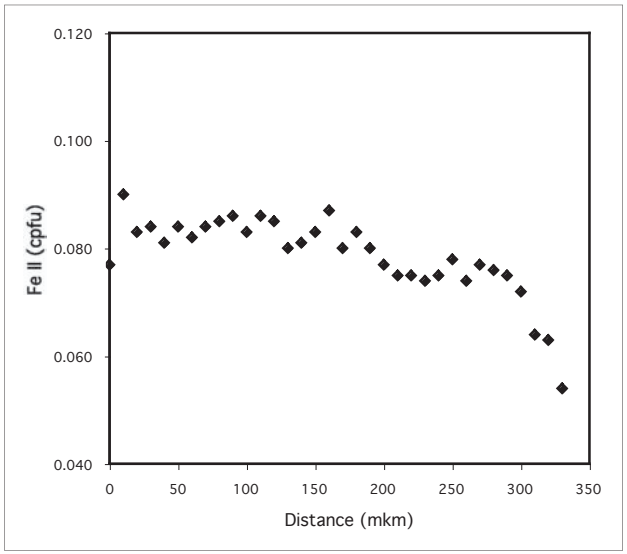
	10	20	30	40	50	60	70	80	90	100	110	120	130	140	150	160	170
SiO2	57.03	57.00	56.79	56.40	56.35	46.02	56.33	56.23	56.80	56.97	56.60	56.87	56.30	45.65	56.34	56.52	57.13
TiO2	0.00	0.01	0.00	0.00	0.02	0.00	0.00	0.00	0.01	0.00	0.04	0.02	0.01	0.00	0.02	0.03	0.01
Al2O3	1.63	1.60	1.56	1.53	1.69	15.30	1.42	1.72	1.60	1.54	1.41	1.39	1.38	25.98	1.24	1.22	1.44
Cr2O3	0.00	0.01	0.03	0.00	0.00	0.00	0.00	0.03	0.00	0.01	0.02	0.02	0.01	0.00	0.04	0.00	0.03
FeO	9.74	10.16	10.01	9.56	9.86	7.99	10.17	10.13	10.13	9.89	9.75	9.78	9.89	0.47	9.78	9.84	9.87
MnO	0.10	0.08	0.10	0.03	0.05	0.13	0.08	0.06	0.07	0.04	0.07	0.05	0.10	0.01	0.04	0.05	0.03
NiO	0.15	0.16	0.20	0.12	0.13		0.18	0.07	0.16	0.17	0.18	0.11	0.16		0.16	0.12	0.22
MgO	32.97	33.03	32.89	32.79	32.82	13.39	32.83	32.54	32.62	32.90	32.74	32.78	32.89	0.49	32.92	33.10	32.86
CaO	0.26	0.33	0.30	0.20	0.22	3.14	0.21	0.24	0.23	0.30	0.28	0.23	0.24	8.36	0.22	0.22	0.23
Na2O	0.03	0.03	0.02	0.06	0.06	0.08	0.04	0.03	0.03	0.04	0.04	0.06	0.04	0.21	0.07	0.05	0.02
K2O	0.00	0.00	0.01	0.01	0.00	0.95	0.00	0.02	0.01	0.01	0.00	0.00	0.00	3.16	0.01	0.00	0.00
Total	101.92	102.42	101.91	100.68	101.21	87.03	101.26	101.07	101.66	101.88	101.12	101.32	101.05	84.33	100.84	101.13	101.84
Si	1.958	1.952	1.954	1.959	1.951		1.953	1.951	1.959	1.958	1.960	1.964	1.954		1.958	1.958	1.964
Ti	0.000	0.000	0.000	0.000	0.000		0.000	0.000	0.000	0.000	0.001	0.000	0.000		0.001	0.001	0.000
Al	0.066	0.065	0.063	0.062	0.069		0.058	0.070	0.065	0.062	0.058	0.057	0.057		0.051	0.050	0.058
Cr	0.000	0.000	0.001	0.000	0.000		0.000	0.001	0.000	0.000	0.000	0.000	0.000		0.001	0.000	0.001
Fe2+	0.280	0.291	0.288	0.278	0.285		0.295	0.294	0.292	0.284	0.282	0.282	0.287		0.284	0.285	0.284
Mn	0.003	0.002	0.003	0.001	0.002		0.002	0.002	0.002	0.001	0.002	0.001	0.003		0.001	0.002	0.001
Ni	0.004	0.004	0.005	0.003	0.004		0.005	0.002	0.004	0.005	0.005	0.003	0.005		0.004	0.003	0.006
Mg	1.688	1.686	1.687	1.698	1.694		1.697	1.683	1.677	1.686	1.690	1.688	1.702		1.705	1.709	1.684
Ca	0.010	0.012	0.011	0.007	0.008		0.008	0.009	0.008	0.011	0.010	0.009	0.009		0.008	0.008	0.008
Na	0.002	0.002	0.001	0.004	0.004		0.003	0.002	0.002	0.003	0.002	0.004	0.003		0.004	0.003	0.001
K	0.000	0.000	0.000	0.001	0.000		0.000	0.001	0.001	0.001	0.000	0.000	0.000		0.001	0.000	0.000
Sum	4.010	4.016	4.015	4.012	4.016		4.020	4.015	4.010	4.012	4.011	4.009	4.019		4.018	4.018	4.007
Mg#	85.77	85.28	85.42	85.93	85.60		85.19	85.13	85.17	85.58	85.70	85.69	85.57		85.72	85.71	85.57
Al IV	0.032	0.032	0.032	0.029	0.033		0.028	0.034	0.031	0.029	0.029	0.027	0.027		0.025	0.025	0.029
Al VI	0.034	0.034	0.032	0.034	0.037		0.031	0.036	0.034	0.033	0.029	0.031	0.030		0.027	0.026	0.029

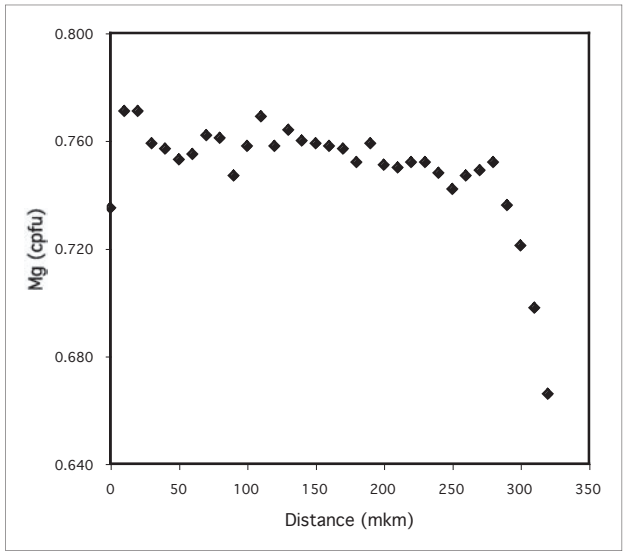
1904-7 Opx II, profile 160

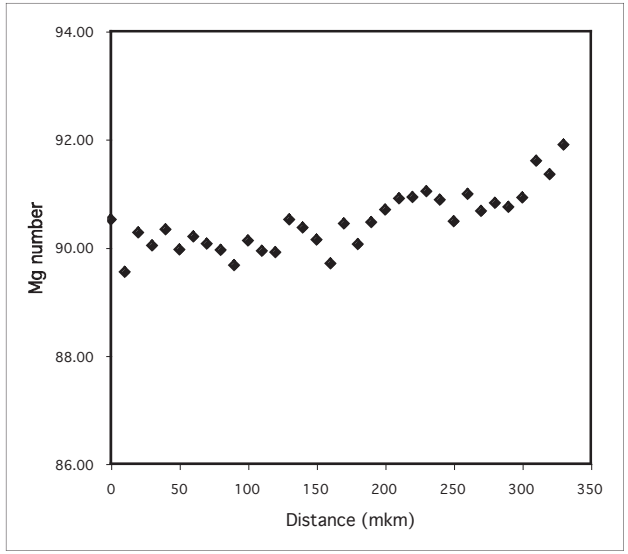












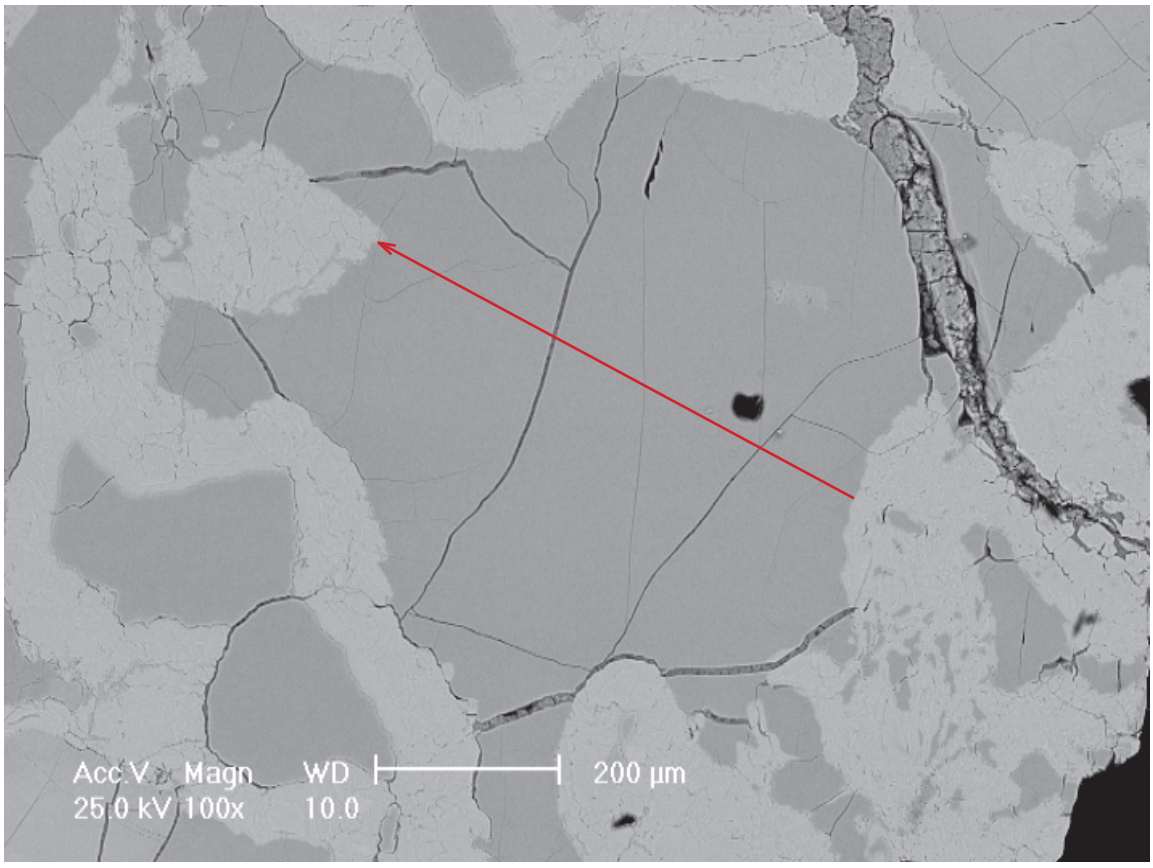
1904-7 Cpx II, profile 335

	10	20	30	40	50	60	70	80	90	100	110	120	130	140	150	160	170	180	190	200
SiO2	55.22	54.43	54.48	54.06	53.60	53.37	53.13	53.40	52.99	52.83	53.07	53.06	52.97	52.98	52.90	52.71	52.94	53.01	52.69	52.96
TiO2	0.01	0.03	0.04	0.03	0.03	0.02	0.07	0.03	0.03	0.06	0.02	0.07	0.06	0.07	0.05	0.07	0.03	0.05	0.08	0.05
Al2O3	6.93	5.79	5.85	6.15	6.49	6.83	6.89	6.75	6.92	7.31	6.75	6.73	6.93	6.98	6.97	7.24	6.93	6.94	7.26	6.95
Cr2O3	0.02	0.00	0.01	0.01	0.03	0.00	0.00	0.01	0.04	0.05	0.05	0.05	0.09	0.03	0.03	0.06	0.00	0.03	0.06	0.03
FeO	2.60	3.00	2.75	2.80	2.70	2.81	2.72	2.81	2.82	2.88	2.74	2.84	2.83	2.67	2.70	2.74	2.88	2.65	2.76	2.64
MnO	0.04	0.05	0.07	0.01	0.06	0.01	0.02	0.12	0.07	0.09	0.04	0.09	0.02	0.04	0.06	0.03	0.05	0.06	0.08	0.02
NiO	0.07	0.07	0.07	0.05	0.04	0.03	0.05	0.01	0.10	0.07	0.09	0.03	0.03	0.00	0.06	0.07	0.04	0.07	0.06	0.05
MgO	13.88	14.38	14.41	14.12	14.09	14.06	14.05	14.25	14.19	13.95	14.08	14.32	14.13	14.24	14.16	14.12	14.10	14.09	14.01	14.14
CaO	18.41	19.64	20.00	20.04	20.52	21.10	21.13	21.33	21.47	21.52	21.34	21.25	21.53	21.48	21.52	21.34	21.39	21.45	21.45	21.54
Na2O	3.52	2.69	2.56	2.53	2.41	2.20	2.00	2.10	1.90	1.88	1.87	1.92	1.91	1.88	1.96	1.89	1.86	1.86	1.93	1.98
K2O	0.00	0.01	0.00	0.00	0.01	0.00	0.01	0.00	0.00	0.00	0.00	0.00	0.02	0.00	0.00	0.00	0.00	0.00	0.00	0.00
Total	100.69	100.07	100.24	99.80	99.98	100.40	100.07	100.81	100.55	100.65	100.05	100.37	100.51	100.36	100.42	100.28	100.23	100.21	100.36	100.35
Si	1.963	1.958	1.955	1.949	1.932	1.919	1.916	1.914	1.906	1.899	1.916	1.911	1.906	1.906	1.904	1.899	1.909	1.910	1.898	1.907
Ti	0.000	0.001	0.001	0.001	0.001	0.000	0.002	0.001	0.001	0.001	0.000	0.002	0.002	0.002	0.001	0.002	0.001	0.001	0.002	0.001
Al	0.290	0.245	0.248	0.261	0.276	0.289	0.293	0.285	0.293	0.310	0.287	0.286	0.294	0.296	0.296	0.307	0.294	0.295	0.308	0.295
Cr	0.001	0.000	0.000	0.000	0.001	0.000	0.000	0.000	0.001	0.002	0.002	0.001	0.002	0.001	0.001	0.002	0.000	0.001	0.002	0.001
Fe2	0.077	0.090	0.083	0.084	0.081	0.084	0.082	0.084	0.085	0.086	0.083	0.086	0.085	0.080	0.081	0.083	0.087	0.080	0.083	0.080
Mn	0.001	0.001	0.002	0.000	0.002	0.000	0.001	0.004	0.002	0.003	0.001	0.003	0.001	0.001	0.002	0.001	0.001	0.002	0.002	0.001
Ni	0.002	0.002	0.002	0.001	0.001	0.001	0.001	0.000	0.003	0.002	0.003	0.001	0.001	0.000	0.002	0.002	0.001	0.002	0.002	0.001
Mg	0.735	0.771	0.771	0.759	0.757	0.753	0.755	0.762	0.761	0.747	0.758	0.769	0.758	0.764	0.760	0.759	0.758	0.757	0.752	0.759
Ca	0.701	0.757	0.769	0.774	0.792	0.813	0.816	0.819	0.827	0.828	0.825	0.820	0.830	0.828	0.830	0.824	0.826	0.828	0.828	0.831
Na	0.243	0.187	0.178	0.177	0.168	0.153	0.140	0.146	0.133	0.131	0.131	0.134	0.133	0.131	0.137	0.132	0.130	0.130	0.134	0.138
K	0.000	0.000	0.000	0.000	0.001	0.000	0.001	0.000	0.000	0.000	0.000	0.000	0.001	0.000	0.000	0.000	0.000	0.000	0.000	0.000
Sum	4.013	4.013	4.009	4.008	4.013	4.013	4.006	4.015	4.012	4.010	4.005	4.011	4.012	4.009	4.014	4.010	4.008	4.006	4.012	4.013
Mg#	90.52	89.55	90.28	90.04	90.33	89.96	90.20	90.07	89.95	89.68	90.13	89.94	89.92	90.52	90.37	90.14	89.70	90.44	90.06	90.46
Al IV	0.024	0.030	0.036	0.043	0.055	0.068	0.078	0.071	0.082	0.092	0.079	0.079	0.083	0.085	0.081	0.091	0.083	0.084	0.090	0.080
Al VI	0.266	0.215	0.212	0.218	0.221	0.221	0.215	0.215	0.212	0.219	0.208	0.208	0.211	0.211	0.215	0.217	0.211	0.211	0.218	0.215

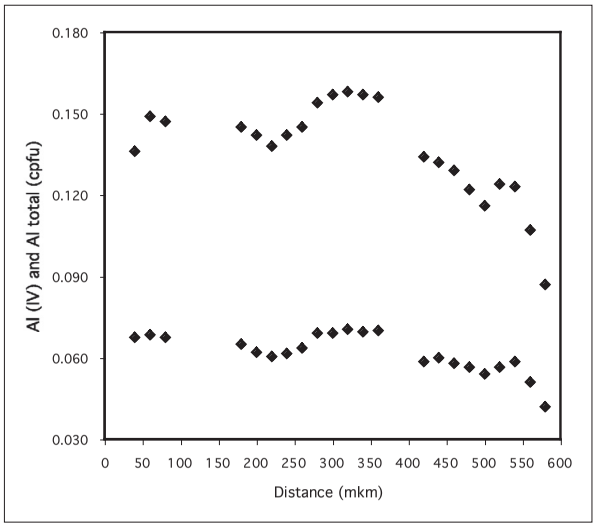
1904-7 Cpx II, profile 335

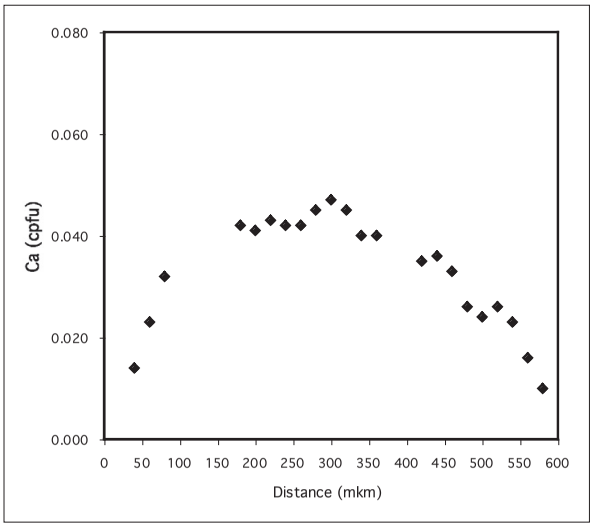
	210	220	230	240	250	260	270	280	290	300	310	320	330	340
SiO2	53.14	53.04	53.06	53.14	53.03	52.85	53.36	53.36	53.37	53.21	53.44	53.41	53.44	53.23
TiO2	0.05	0.07	0.05	0.07	0.04	0.05	0.04	0.04	0.04	0.03	0.03	0.05	0.03	0.05
Al2O3	6.99	6.97	7.00	7.03	7.15	7.48	6.97	6.98	6.85	7.11	7.28	8.43	9.44	11.15
Cr2O3	0.03	0.00	0.03	0.05	0.03	0.01	0.04	0.00	0.01	0.01	0.05	0.04	0.00	0.03
FeO	2.56	2.48	2.47	2.45	2.49	2.60	2.45	2.56	2.53	2.49	2.39	2.13	2.13	1.82
MnO	0.03	0.01	0.00	0.05	0.04	0.06	0.06	0.06	0.01	0.07	0.01	0.01	0.07	0.04
NiO	0.06	0.05	0.06	0.00	0.00	0.04	0.00	0.05	0.03	0.04	0.02	0.04	0.08	0.08
MgO	14.01	13.96	13.99	14.03	13.93	13.83	13.94	13.99	14.02	13.69	13.43	13.07	12.54	11.56
CaO	21.43	21.35	21.43	21.40	21.41	21.28	21.27	21.33	21.07	21.06	20.60	20.09	19.38	18.40
Na2O	2.07	2.13	2.00	2.07	2.07	2.11	2.14	2.11	2.24	2.26	2.59	3.00	3.46	4.07
K2O	0.01	0.00	0.02	0.01	0.00	0.00	0.00	0.00	0.01	0.00	0.00	0.00	0.00	0.00
Total	100.38	100.07	100.12	100.30	100.20	100.31	100.28	100.49	100.20	99.98	99.82	100.27	100.57	100.43
Si	1.911	1.913	1.912	1.911	1.910	1.902	1.918	1.916	1.920	1.919	1.926	1.912	1.905	1.892
Ti	0.001	0.002	0.001	0.002	0.001	0.001	0.001	0.001	0.001	0.001	0.001	0.001	0.001	0.001
Al	0.296	0.296	0.297	0.298	0.303	0.317	0.295	0.295	0.291	0.302	0.309	0.356	0.396	0.467
Cr	0.001	0.000	0.001	0.001	0.001	0.000	0.001	0.000	0.000	0.000	0.001	0.001	0.000	0.001
Fe2	0.077	0.075	0.075	0.074	0.075	0.078	0.074	0.077	0.076	0.075	0.072	0.064	0.063	0.054
Mn	0.001	0.000	0.000	0.001	0.001	0.002	0.002	0.002	0.000	0.002	0.000	0.000	0.002	0.001
Ni	0.002	0.001	0.002	0.000	0.000	0.001	0.000	0.002	0.001	0.001	0.000	0.001	0.002	0.002
Mg	0.751	0.750	0.752	0.752	0.748	0.742	0.747	0.749	0.752	0.736	0.721	0.698	0.666	0.613
Ca	0.826	0.825	0.827	0.825	0.826	0.821	0.819	0.821	0.812	0.814	0.796	0.771	0.740	0.701
Na	0.144	0.149	0.140	0.144	0.144	0.147	0.149	0.147	0.156	0.158	0.181	0.208	0.239	0.280
K	0.000	0.000	0.001	0.001	0.000	0.000	0.000	0.000	0.000	0.000	0.000	0.000	0.000	0.000
Sum	4.011	4.012	4.008	4.010	4.009	4.012	4.007	4.009	4.011	4.008	4.008	4.012	4.016	4.013
Mg#	90.70	90.91	90.93	91.04	90.89	90.49	90.99	90.68	90.82	90.75	90.92	91.60	91.36	91.90
Al IV	0.078	0.076	0.080	0.079	0.081	0.086	0.075	0.075	0.069	0.073	0.066	0.076	0.080	0.095
Al VI	0.219	0.221	0.218	0.219	0.222	0.231	0.221	0.220	0.223	0.229	0.244	0.281	0.317	0.372

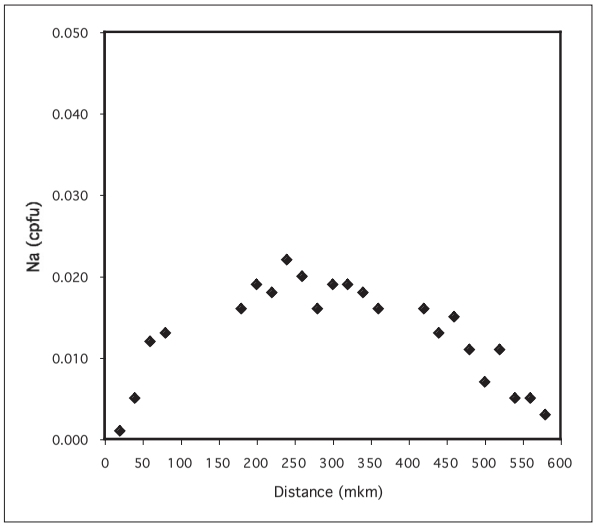
1904-7 Cpx II, profile 335

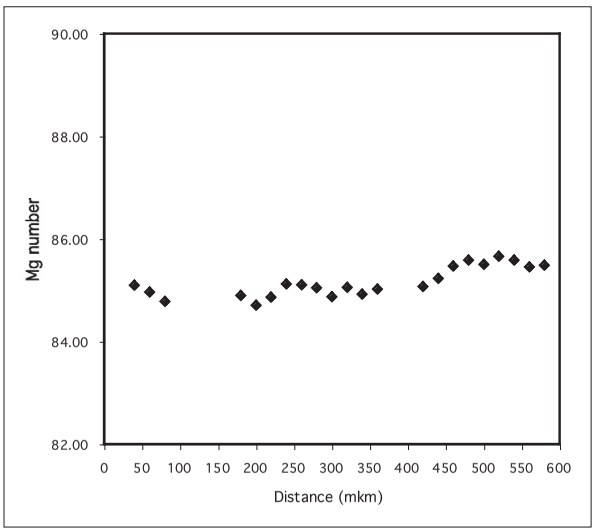


1904-7 Opx I, defocused beam, profile 558







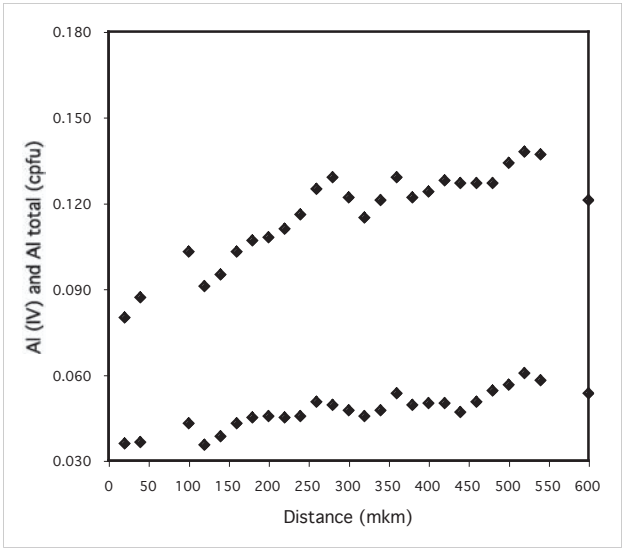


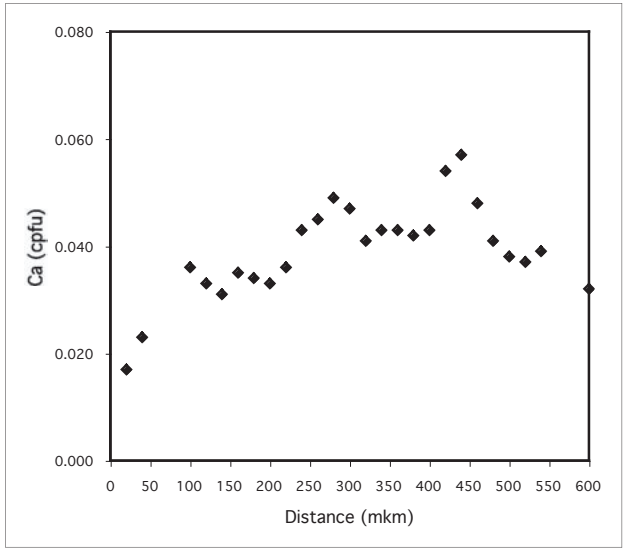
	20	40	60	80	100	120	140	160	180	200	220	240	260	280	300	320	340	360	380	400
SiO2	46.14	52.99	52.61	52.70	52.83	52.82	52.46	53.20	53.01	53.22	53.04	53.42	53.49	53.11	53.17	53.45	53.24	52.82	52.46	52.46
TiO2	0.01	0.02	0.01	0.00	0.03	0.00	0.00	0.01	0.01	0.01	0.00	0.03	0.02	0.00	0.00	0.02	0.00	0.01	0.00	0.00
Al2O3	14.11	3.24	3.51	3.49	3.39	3.80	4.37	3.51	3.44	3.38	3.27	3.38	3.45	3.67	3.74	3.78	3.74	3.71	5.98	6.14
Cr2O3	0.01	0.06	0.00	0.03	0.02	0.00	0.02	0.00	0.05	0.03	0.03	0.02	0.00	0.00	0.01	0.01	0.01	0.00	0.02	0.00
FeO	2.31	9.92	9.81	9.95	0.20	0.05	9.33	9.38	9.82	10.00	9.80	9.62	9.58	9.63	9.73	9.61	9.70	9.70	8.77	8.77
MnO	0.17	0.10	0.10	0.12	0.11	0.06	0.08	0.11	0.06	0.07	0.08	0.11	0.05	0.06	0.13	0.08	0.10	0.06	0.10	0.07
NiO	0.00	0.11	0.17	0.08	0.14	0.16	0.16	3.47	0.15	0.17	0.13	0.12	0.12	0.13	0.11	0.19	0.12	0.08	0.16	0.16
MgO	24.15	31.74	31.14	31.10	31.19	30.49	29.56	31.53	30.94	31.04	30.80	30.84	30.67	30.68	30.67	30.67	30.67	30.89	27.75	27.37
CaO	2.20	0.37	0.61	0.82	0.90	1.12	1.28	1.05	1.09	1.09	1.13	1.10	1.11	1.17	1.23	1.18	1.06	1.05	1.66	1.68
Na2O	0.02	0.07	0.17	0.19	0.21	0.27	0.22	0.25	0.23	0.27	0.26	0.32	0.30	0.24	0.28	0.27	0.26	0.23	0.29	0.26
K2O	0.01	0.00	0.01	0.00	0.00	0.05	0.11	0.00	0.00	0.00	0.00	0.01	0.01	0.00	0.00	0.00	0.00	0.00	0.45	0.45
Total	99.12	98.62	98.13	98.49	99.02	98.83	97.60	102.52	98.80	99.28	98.54	98.98	98.81	98.68	99.08	99.26	98.89	98.57	97.64	97.37
Si	1.755	1.892	1.889	1.888					1.892	1.892	1.898	1.901	1.905	1.895	1.892	1.896	1.896	1.888		
Ti	0.000	0.001	0.000	0.000					0.000	0.000	0.000	0.001	0.001	0.000	0.000	0.001	0.000	0.000		
Al	0.633	0.136	0.149	0.147					0.145	0.142	0.138	0.142	0.145	0.154	0.157	0.158	0.157	0.156		
Cr	0.000	0.002	0.000	0.001					0.001	0.001	0.001	0.001	0.000	0.000	0.000	0.000	0.000	0.000		
Fe2+	0.074	0.296	0.295	0.298					0.293	0.297	0.293	0.286	0.285	0.287	0.290	0.285	0.289	0.290		
Mn	0.005	0.003	0.003	0.003					0.002	0.002	0.002	0.003	0.002	0.002	0.004	0.002	0.003	0.002		
Ni	0.000	0.003	0.005	0.002					0.004	0.005	0.004	0.004	0.003	0.004	0.003	0.005	0.003	0.002		
Mg	1.370	1.690	1.667	1.660					1.647	1.645	1.643	1.636	1.628	1.632	1.627	1.622	1.628	1.646		
Ca	0.090	0.014	0.023	0.032					0.042	0.041	0.043	0.042	0.042	0.045	0.047	0.045	0.040	0.040		
Na	0.001	0.005	0.012	0.013					0.016	0.019	0.018	0.022	0.020	0.016	0.019	0.019	0.018	0.016		
K	0.000	0.000	0.000	0.000					0.000	0.000	0.000	0.000	0.000	0.000	0.000	0.000	0.000	0.000		
Sum	3.929	4.041	4.042	4.045					4.042	4.045	4.041	4.038	4.032	4.036	4.039	4.033	4.034	4.041		
Mg#	94.88	85.10	84.96	84.78					84.90	84.71	84.87	85.12	85.10	85.04	84.87	85.06	84.92	85.02		
Al IV	0.316	0.068	0.069	0.068					0.065	0.062	0.061	0.062	0.064	0.069	0.069	0.071	0.070	0.070		
Al VI	0.317	0.069	0.081	0.080					0.080	0.080	0.078	0.081	0.082	0.085	0.088	0.088	0.088	0.086		

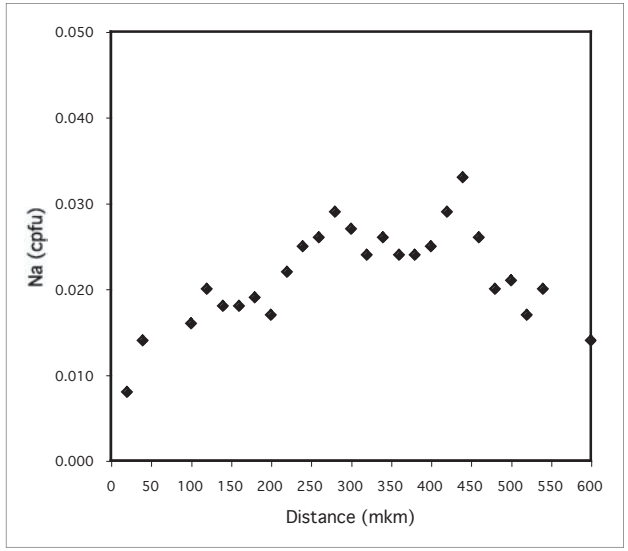
1904-7 Opx I, defocused beam, profile 558

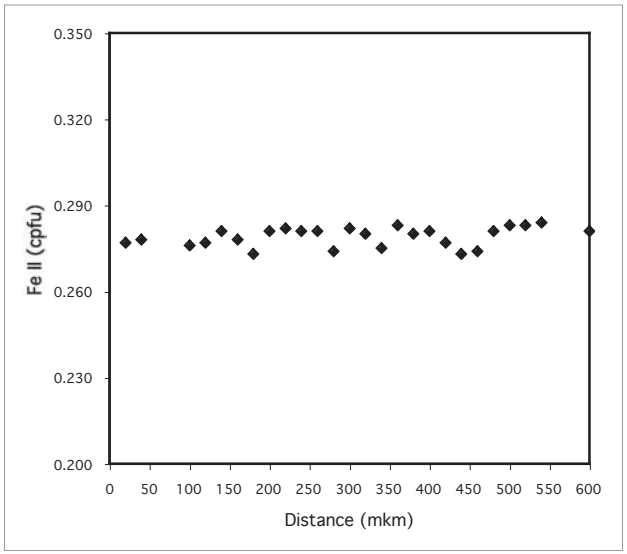
	420	440	460	480	500	520	540	560	580
SiO2	53.83	53.63	53.90	54.30	54.66	54.11	53.95	54.58	54.98
TiO2	0.01	0.00	0.03	0.02	0.01	0.02	0.01	0.00	0.00
Al2O3	3.21	3.14	3.10	2.95	2.81	2.98	2.95	2.57	2.10
Cr2O3	0.01	0.04	0.02	0.06	0.00	0.00	0.03	0.00	0.00
FeO	9.82	9.67	9.58	9.55	9.62	9.43	9.52	9.75	9.83
MnO	0.03	0.08	0.05	0.09	0.07	0.04	0.07	0.08	0.08
NiO	0.18	0.14	0.09	0.21	0.13	0.11	0.16	0.13	0.13
MgO	31.35	31.28	31.57	31.77	31.87	31.60	31.69	32.12	32.51
CaO	0.94	0.95	0.87	0.70	0.63	0.70	0.61	0.41	0.27
Na2O	0.23	0.18	0.22	0.16	0.10	0.16	0.07	0.07	0.04
K2O	0.02	0.01	0.00	0.00	0.01	0.04	0.04	0.00	0.00
Total	99.62	99.12	99.43	99.79	99.90	99.19	99.10	99.72	99.94
Si	1.903	1.904	1.906	1.912	1.920	1.915	1.912	1.922	1.931
Ti	0.000	0.000	0.001	0.000	0.000	0.001	0.000	0.000	0.000
Al	0.134	0.132	0.129	0.122	0.116	0.124	0.123	0.107	0.087
Cr	0.000	0.001	0.000	0.002	0.000	0.000	0.001	0.000	0.000
Fe2+	0.290	0.287	0.283	0.281	0.283	0.279	0.282	0.287	0.289
Mn	0.001	0.002	0.002	0.003	0.002	0.001	0.002	0.002	0.002
Ni	0.005	0.004	0.003	0.006	0.004	0.003	0.005	0.004	0.004
Mg	1.652	1.656	1.664	1.668	1.669	1.667	1.674	1.686	1.702
Ca	0.035	0.036	0.033	0.026	0.024	0.026	0.023	0.016	0.010
Na	0.016	0.013	0.015	0.011	0.007	0.011	0.005	0.005	0.003
K	0.001	0.000	0.000	0.000	0.001	0.002	0.002	0.000	0.000
Sum	4.038	4.036	4.036	4.031	4.025	4.029	4.029	4.027	4.027
Mg#	85.07	85.23	85.46	85.58	85.50	85.66	85.58	85.45	85.48
Al IV	0.059	0.060	0.058	0.057	0.054	0.057	0.059	0.051	0.042
Al VI	0.076	0.072	0.071	0.066	0.062	0.068	0.065	0.056	0.045

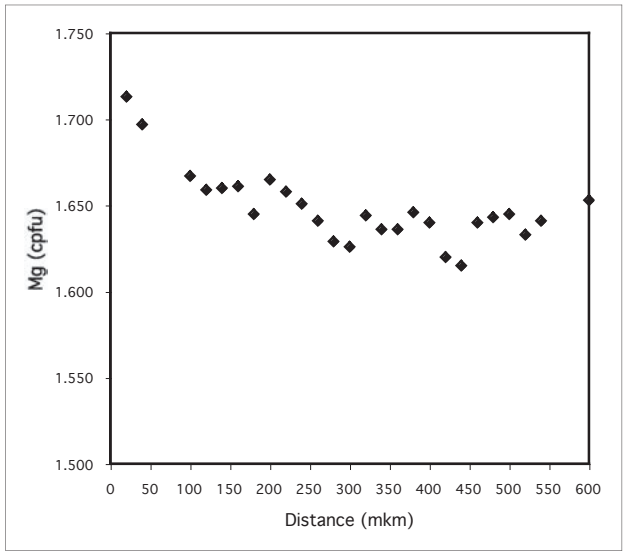
1904-7 Opx I, defocused beam, profile 558

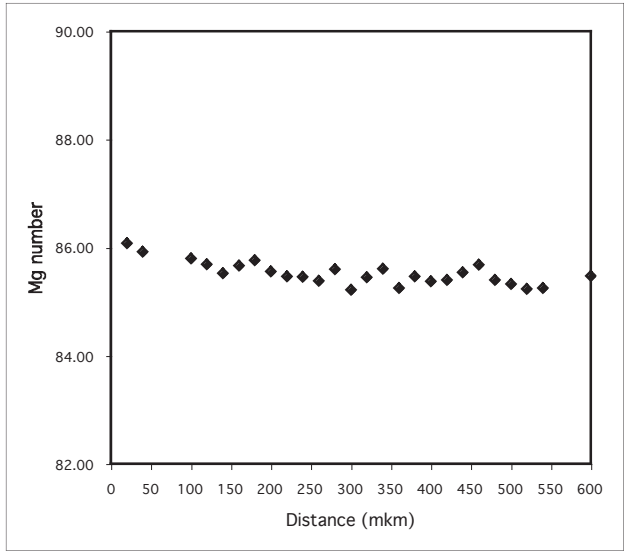












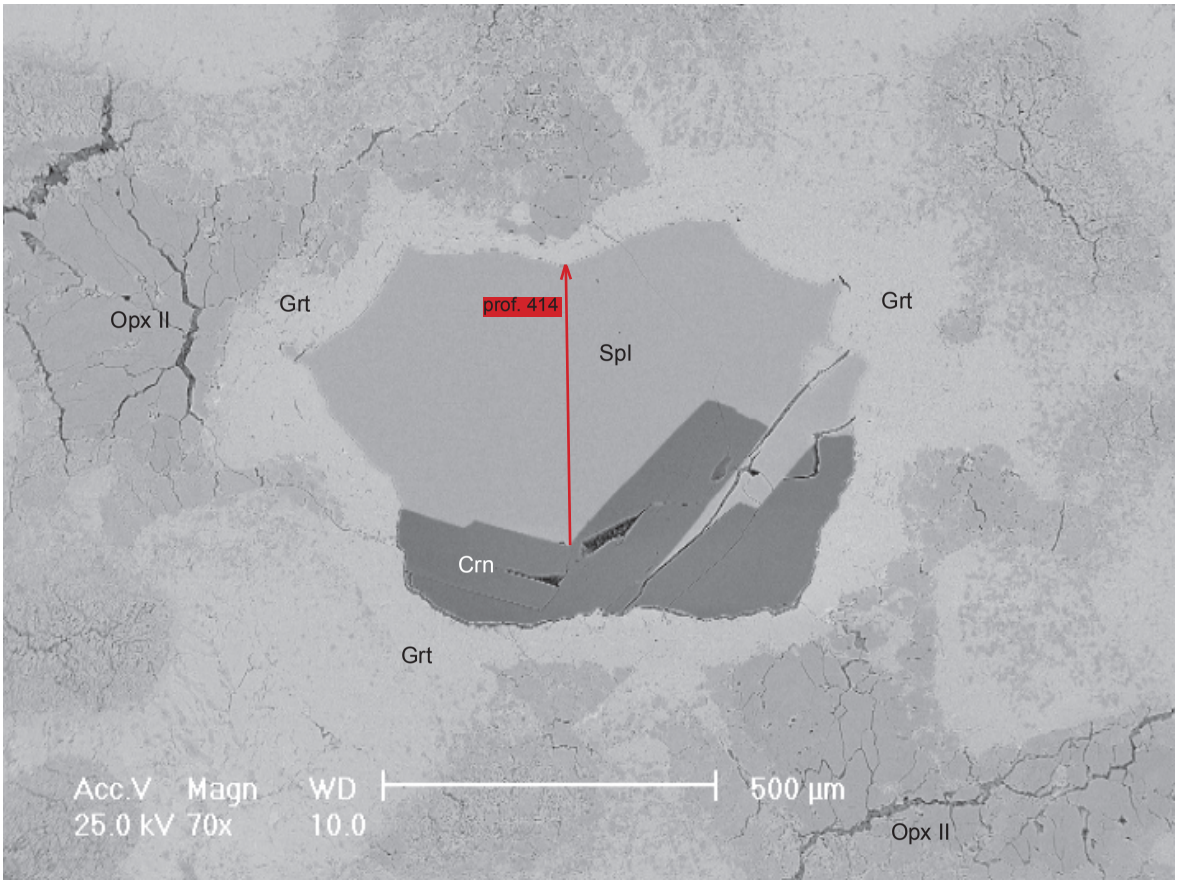
1904-7 Opx I, defocused beam, profile 584

	20	40	60	80	100	120	140	160	180	200	220	240	260	280	300	320	340	360	380	400
SiO2	54.71	54.53	54.97	54.26	54.16	55.29	55.27	54.42	54.84	54.33	54.05	54.18	54.01	53.95	54.10	54.22	54.01	53.85	53.89	54.00
TiO2	0.00	0.01	0.01	0.00	0.00	0.00	0.01	0.01	0.02	0.00	0.02	0.01	0.02	0.01	0.00	0.00	0.00	0.03	0.00	0.03
Al2O3	1.93	2.09	2.78	3.87	2.45	2.21	2.32	2.47	2.57	2.60	2.66	2.78	3.00	3.09	2.92	2.76	2.90	3.08	2.92	2.97
Cr2O3	0.00	0.01	0.00	0.02	0.00	0.00	0.01	0.04	0.00	0.02	0.03	0.00	0.00	0.00	0.02	0.00	0.00	0.00	0.02	0.00
FeO	9.39	9.41	8.99	8.70	9.29	9.46	9.62	9.41	9.26	9.49	9.49	9.52	9.48	9.22	9.52	9.44	9.26	9.54	9.43	9.48
MnO	0.09	0.09	0.07	0.07	0.03	0.06	0.08	0.10	0.05	0.07	0.05	0.07	0.08	0.07	0.07	0.08	0.07	0.07	0.07	0.12
NiO	0.23	0.22	0.19	0.20	0.26	0.15	0.18	0.21	0.22	0.24	0.20	0.20	0.16	0.11	0.18	0.23	0.29	0.22	0.21	0.17
MgO	32.57	32.21	31.12	29.58	31.47	31.73	31.84	31.49	31.29	31.59	31.32	31.34	31.08	30.77	30.75	31.12	30.88	30.91	31.08	31.06
CaO	0.44	0.60	1.03	1.36	0.94	0.88	0.84	0.92	0.91	0.87	0.96	1.13	1.19	1.29	1.24	1.08	1.12	1.12	1.10	1.13
Na2O	0.11	0.21	0.24	0.29	0.24	0.29	0.26	0.26	0.28	0.25	0.32	0.37	0.37	0.43	0.40	0.35	0.37	0.35	0.35	0.37
K2O	0.00	0.00	0.03	0.05	0.02	0.00	0.00	0.00	0.00	0.02	0.00	0.00	0.00	0.01	0.00	0.00	0.00	0.01	0.01	0.01
Total	99.48	99.39	99.42	98.40	98.85	100.08	100.43	99.33	99.43	99.49	99.09	99.60	99.40	98.96	99.20	99.29	98.90	99.18	99.08	99.34
Si	1.930	1.927			1.925	1.939	1.933	1.926	1.934	1.920	1.919	1.915	1.912	1.916	1.920	1.921	1.920	1.912	1.914	1.913
Ti	0.000	0.000			0.000	0.000	0.000	0.000	0.001	0.000	0.000	0.000	0.001	0.000	0.000	0.000	0.000	0.001	0.000	0.001
Al	0.080	0.087			0.103	0.091	0.095	0.103	0.107	0.108	0.111	0.116	0.125	0.129	0.122	0.115	0.121	0.129	0.122	0.124
Cr	0.000	0.000			0.000	0.000	0.000	0.001	0.000	0.001	0.001	0.000	0.000	0.000	0.000	0.000	0.000	0.000	0.001	0.000
Fe2+	0.277	0.278			0.276	0.277	0.281	0.278	0.273	0.281	0.282	0.281	0.281	0.274	0.282	0.280	0.275	0.283	0.280	0.281
Mn	0.003	0.003			0.001	0.002	0.002	0.003	0.001	0.002	0.002	0.002	0.003	0.002	0.002	0.002	0.002	0.002	0.002	0.004
Ni	0.006	0.006			0.007	0.004	0.005	0.006	0.006	0.007	0.006	0.006	0.004	0.003	0.005	0.007	0.008	0.006	0.006	0.005
Mg	1.713	1.697			1.667	1.659	1.660	1.661	1.645	1.665	1.658	1.651	1.641	1.629	1.626	1.644	1.636	1.636	1.646	1.640
Ca	0.017	0.023			0.036	0.033	0.031	0.035	0.034	0.033	0.036	0.043	0.045	0.049	0.047	0.041	0.043	0.043	0.042	0.043
Na	0.008	0.014			0.016	0.020	0.018	0.018	0.019	0.017	0.022	0.025	0.026	0.029	0.027	0.024	0.026	0.024	0.024	0.025
K	0.000	0.000			0.001	0.000	0.000	0.000	0.000	0.001	0.000	0.000	0.000	0.001	0.000	0.000	0.000	0.000	0.000	0.001
Sum	4.034	4.036			4.032	4.026	4.028	4.031	4.021	4.034	4.036	4.039	4.037	4.034	4.033	4.034	4.032	4.035	4.037	4.037
Mg#	86.08	85.92			85.80	85.69	85.52	85.66	85.77	85.56	85.46	85.46	85.38	85.60	85.22	85.45	85.61	85.25	85.46	85.37
Al IV	0.036	0.037			0.043	0.036	0.039	0.043	0.045	0.046	0.045	0.046	0.051	0.050	0.048	0.046	0.048	0.054	0.050	0.050
Al VI	0.044	0.051			0.060	0.056	0.057	0.060	0.062	0.063	0.066	0.071	0.075	0.080	0.075	0.070	0.074	0.076	0.073	0.074

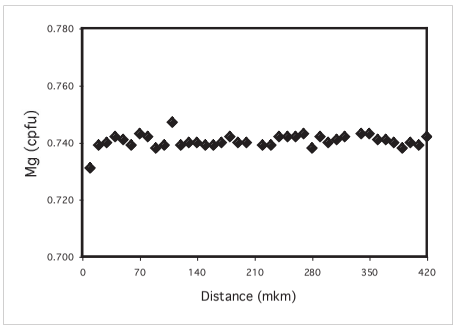
1904-7 Opx I, defocused beam, profile 584

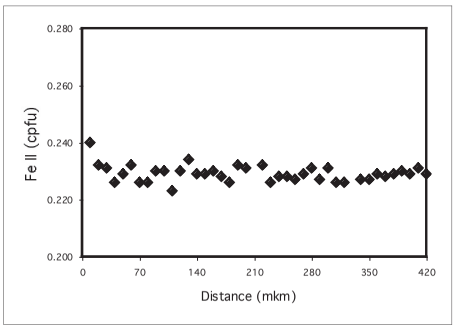
	420	440	460	480	500	520	540	560	580	600
SiO2	54.15	54.12	53.76	53.82	53.71	53.69	53.77	52.24	52.70	54.10
TiO2	0.01	0.00	0.02	0.03	0.01	0.01	0.01	0.02	0.01	0.01
Al2O3	3.08	3.04	3.03	3.04	3.20	3.29	3.28	6.54	5.98	2.89
Cr2O3	0.03	0.00	0.00	0.00	0.01	0.01	0.00	0.02	0.00	0.00
FeO	9.37	9.19	9.21	9.48	9.54	9.52	9.59	8.22	8.70	9.46
MnO	0.06	0.10	0.05	0.11	0.10	0.07	0.05	0.01	0.11	0.08
NiO	0.16	0.21	0.21	0.28	0.17	0.13	0.24	0.14	0.18	0.18
MgO	30.70	30.53	30.92	31.05	31.08	30.76	31.05	26.29	27.21	31.27
CaO	1.43	1.49	1.26	1.09	1.00	0.97	1.04	1.80	1.62	0.84
Na2O	0.43	0.48	0.38	0.29	0.30	0.25	0.29	0.26	0.28	0.20
K2O	0.00	0.00	0.00	0.00	0.00	0.01	0.03	0.34	0.24	0.00
Total	99.42	99.17	98.81	99.18	99.14	98.70	99.34	95.87	97.05	99.03
Si	1.917	1.920	1.913	1.910	1.907	1.912	1.906			1.919
Ti	0.000	0.000	0.000	0.001	0.000	0.000	0.000			0.000
Al	0.128	0.127	0.127	0.127	0.134	0.138	0.137			0.121
Cr	0.001	0.000	0.000	0.000	0.000	0.000	0.000			0.000
Fe2+	0.277	0.273	0.274	0.281	0.283	0.283	0.284			0.281
Mn	0.002	0.003	0.001	0.003	0.003	0.002	0.001			0.002
Ni	0.005	0.006	0.006	0.008	0.005	0.004	0.007			0.005
Mg	1.620	1.615	1.640	1.643	1.645	1.633	1.641			1.653
Ca	0.054	0.057	0.048	0.041	0.038	0.037	0.039			0.032
Na	0.029	0.033	0.026	0.020	0.021	0.017	0.020			0.014
K	0.000	0.000	0.000	0.000	0.000	0.000	0.001			0.000
Sum	4.033	4.033	4.036	4.035	4.036	4.027	4.036			4.027
Mg#	85.40	85.54	85.68	85.40	85.32	85.23	85.25			85.47
Al IV	0.050	0.047	0.051	0.055	0.057	0.061	0.058			0.054
Al VI	0.078	0.080	0.077	0.073	0.078	0.078	0.079			0.068

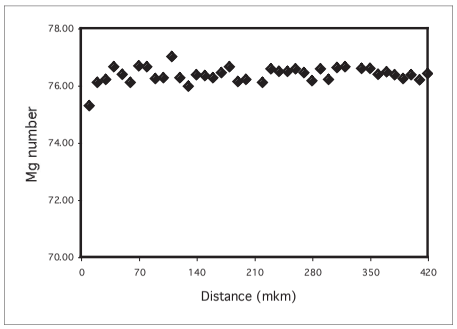
1904-7 Opx I, defocused beam, profile 584

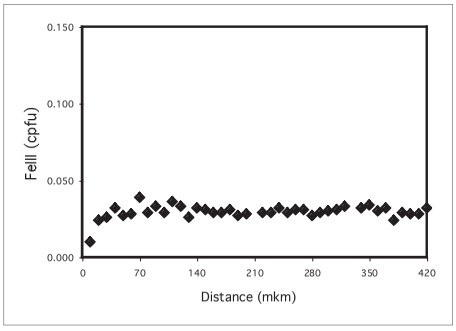


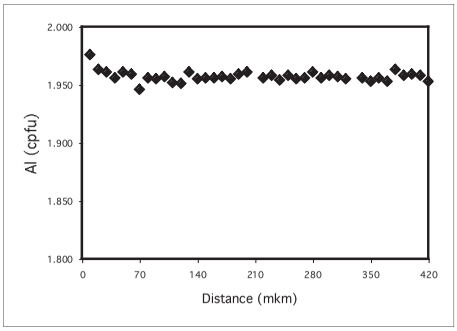
1904-7 Spinel, profile 414

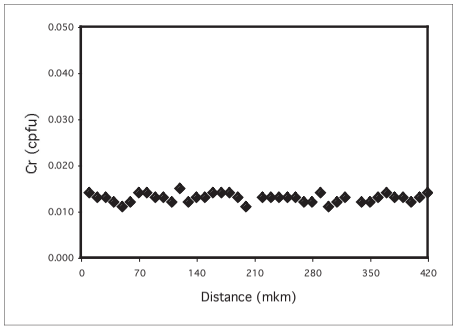


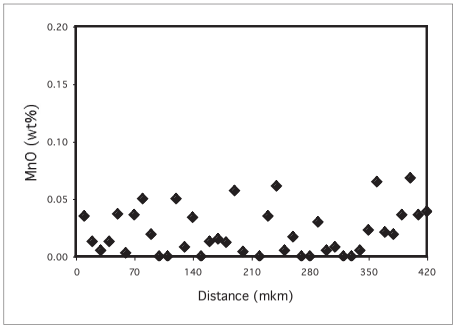


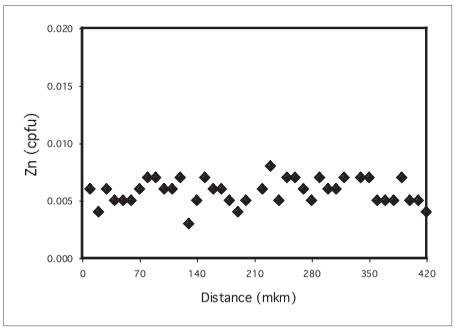


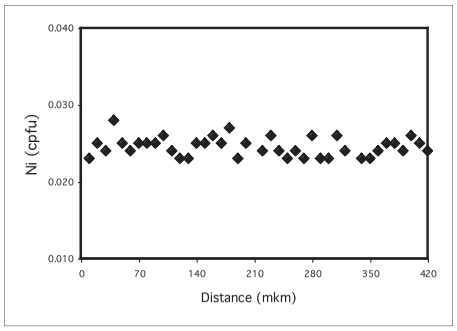












1904-7 Spinel, profile 414

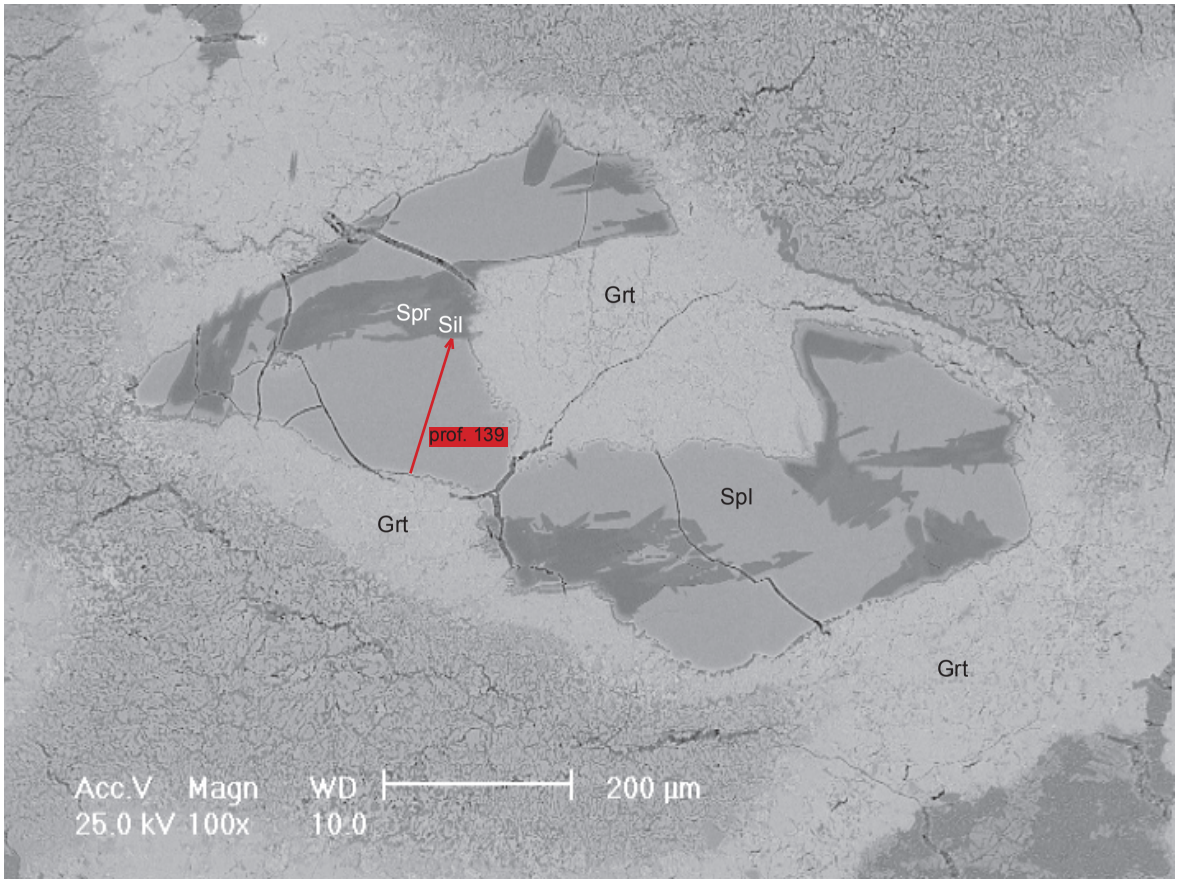
	10	20	30	40	50	60	70	80	90	100	110
SiO2	0.01	0.00	0.00	0.00	0.00	0.00	0.01	0.00	0.00	0.03	0.00
TiO2	0.01	0.00	0.01	0.00	0.01	0.00	0.01	0.00	0.00	0.00	0.00
Al2O3	66.14	66.14	65.79	65.62	65.66	65.61	65.76	66.12	66.21	66.05	65.95
Cr2O3	0.68	0.66	0.66	0.61	0.56	0.61	0.71	0.73	0.64	0.64	0.61
FeO	11.77	12.15	12.14	12.20	12.07	12.29	12.61	12.16	12.52	12.32	12.31
MnO	0.04	0.01	0.01	0.01	0.04	0.00	0.04	0.05	0.02	0.00	0.00
NiO	1.13	1.22	1.16	1.35	1.23	1.19	1.23	1.21	1.23	1.27	1.19
ZnO	0.31	0.20	0.32	0.24	0.27	0.25	0.30	0.36	0.40	0.34	0.33
MgO	19.35	19.70	19.62	19.69	19.61	19.56	19.85	19.81	19.76	19.72	19.96
CaO	0.00	0.00	0.00	0.00	0.00	0.00	0.00	0.00	0.00	0.00	0.00
Total	99.44	100.08	99.72	99.73	99.44	99.52	100.53	100.45	100.79	100.38	100.34
Si	0.000	0.000	0.000	0.000	0.000	0.000	0.000	0.000	0.000	0.001	0.000
Ti	0.000	0.000	0.000	0.000	0.000	0.000	0.000	0.000	0.000	0.000	0.000
Al	1.976	1.963	1.961	1.956	1.961	1.959	1.946	1.956	1.955	1.957	1.952
Cr	0.014	0.013	0.013	0.012	0.011	0.012	0.014	0.014	0.013	0.013	0.012
Fe3+	0.010	0.024	0.026	0.032	0.027	0.028	0.039	0.029	0.033	0.029	0.036
Fe2+	0.240	0.232	0.231	0.226	0.229	0.232	0.226	0.226	0.230	0.230	0.223
Mn	0.001	0.000	0.000	0.000	0.001	0.000	0.001	0.001	0.000	0.000	0.000
Ni	0.023	0.025	0.024	0.028	0.025	0.024	0.025	0.025	0.025	0.026	0.024
Zn	0.006	0.004	0.006	0.005	0.005	0.005	0.006	0.007	0.007	0.006	0.006
Mg	0.731	0.739	0.740	0.742	0.741	0.739	0.743	0.742	0.738	0.739	0.747
Ca	0.000	0.000	0.000	0.000	0.000	0.000	0.000	0.000	0.000	0.000	0.000
Sum	3.000	3.000	3.000	3.000	3.000	3.000	3.000	3.000	3.000	3.000	3.000
Mg#	75.3	76.1	76.2	76.7	76.4	76.1	76.7	76.7	76.2	76.3	77.0

	120	130	140	150	160	170	180	190	200	210	220
SiO2	0.00	0.01	0.00	0.01	0.01	0.01	0.00	0.02	0.00	0.02	0.03
TiO2	0.01	0.01	0.00	0.00	0.00	0.00	0.00	0.01	0.01	0.00	0.02
Al2O3	65.87	65.94	65.91	66.17	66.01	65.94	66.07	66.12	66.04	65.86	66.05
Cr2O3	0.77	0.62	0.63	0.64	0.72	0.68	0.69	0.64	0.57	0.63	0.64
FeO	12.49	12.36	12.44	12.43	12.28	12.22	12.25	12.29	12.28	12.22	12.45
MnO	0.05	0.01	0.03	0.00	0.01	0.02	0.01	0.06	0.00	0.52	0.00
NiO	1.15	1.12	1.23	1.22	1.27	1.26	1.32	1.16	1.22	1.24	1.19
ZnO	0.39	0.18	0.27	0.37	0.32	0.35	0.28	0.22	0.26	0.35	0.34
MgO	19.72	19.67	19.72	19.78	19.70	19.71	19.81	19.74	19.70	19.90	19.72
CaO	0.00	0.00	0.00	0.00	0.00	0.00	0.00	0.01	0.00	0.01	0.00
Total	100.44	99.92	100.24	100.61	100.33	100.18	100.45	100.28	100.08	100.75	100.43
Si	0.000	0.000	0.000	0.000	0.000	0.000	0.000	0.000	0.000		0.001
Ti	0.000	0.000	0.000	0.000	0.000	0.000	0.000	0.000	0.000		0.000
Al	1.951	1.961	1.955	1.956	1.956	1.957	1.955	1.959	1.961		1.956
Cr	0.015	0.012	0.013	0.013	0.014	0.014	0.014	0.013	0.011		0.013
Fe3	0.033	0.026	0.032	0.031	0.029	0.029	0.031	0.027	0.028		0.029
Fe2	0.230	0.234	0.229	0.229	0.230	0.228	0.226	0.232	0.231		0.232
Mn	0.001	0.000	0.001	0.000	0.000	0.000	0.000	0.001	0.000		0.000
Ni	0.023	0.023	0.025	0.025	0.026	0.025	0.027	0.023	0.025		0.024
Zn	0.007	0.003	0.005	0.007	0.006	0.006	0.005	0.004	0.005		0.006
Mg	0.739	0.740	0.740	0.739	0.739	0.740	0.742	0.740	0.740		0.739
Ca	0.000	0.000	0.000	0.000	0.000	0.000	0.000	0.000	0.000		0.000
Sum	3.000	3.000	3.000	3.000	3.000	3.000	3.000	3.000	3.000		3.000
Mg#	76.3	76.0	76.4	76.3	76.3	76.4	76.7	76.13	76.21		76.11

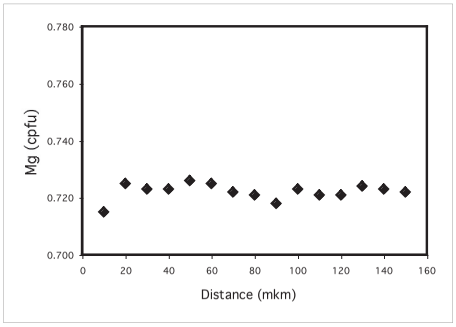
1904-7 Spinel, profile 414

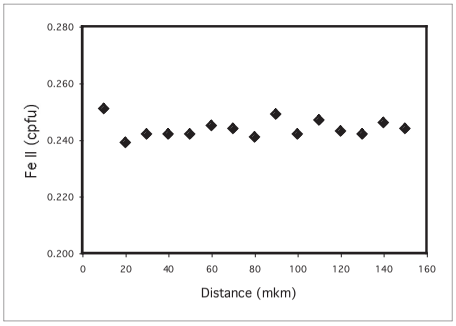
	230	240	250	260	270	280	290	300	310	320	330
SiO2	0.01	0.01	0.00	0.01	0.02	0.01	0.02	0.01	0.00	0.00	0.01
TiO2	0.00	0.00	0.01	0.00	0.01	0.00	0.00	0.00	0.00	0.00	0.00
Al2O3	65.95	65.94	66.12	65.86	66.08	66.17	66.01	66.19	66.19	66.23	65.78
Cr2O3	0.63	0.66	0.64	0.67	0.59	0.60	0.69	0.57	0.60	0.65	7.34
FeO	12.12	12.35	12.24	12.25	12.37	12.24	12.18	12.43	12.28	12.37	12.28
MnO	0.04	0.06	0.01	0.02	0.00	0.00	0.03	0.01	0.01	0.00	0.00
NiO	1.29	1.20	1.12	1.20	1.16	1.28	1.15	1.15	1.30	1.21	1.19
ZnO	0.41	0.28	0.40	0.37	0.30	0.28	0.40	0.34	0.33	0.40	0.32
MgO	19.69	19.79	19.82	19.76	19.84	19.69	19.80	19.76	19.82	19.87	20.15
CaO	0.00	0.00	0.00	0.00	0.00	0.01	0.00	0.00	0.00	0.00	0.00
Total	100.15	100.29	100.36	100.14	100.37	100.28	100.28	100.46	100.53	100.72	107.06
Si	0.000	0.000	0.000	0.000	0.000	0.000	0.000	0.000	0.000	0.000	
Ti	0.000	0.000	0.000	0.000	0.000	0.000	0.000	0.000	0.000	0.000	
Al	1.958	1.954	1.958	1.955	1.956	1.961	1.956	1.958	1.957	1.955	
Cr	0.013	0.013	0.013	0.013	0.012	0.012	0.014	0.011	0.012	0.013	
Fe3	0.029	0.032	0.029	0.031	0.031	0.027	0.029	0.030	0.031	0.033	
Fe2	0.226	0.228	0.228	0.227	0.229	0.231	0.227	0.231	0.226	0.226	
Mn	0.001	0.001	0.000	0.000	0.000	0.000	0.001	0.000	0.000	0.000	
Ni	0.026	0.024	0.023	0.024	0.023	0.026	0.023	0.023	0.026	0.024	
Zn	0.008	0.005	0.007	0.007	0.006	0.005	0.007	0.006	0.006	0.007	
Mg	0.739	0.742	0.742	0.742	0.743	0.738	0.742	0.740	0.741	0.742	
Ca	0.000	0.000	0.000	0.000	0.000	0.000	0.000	0.000	0.000	0.000	
Sum	3.000	3.000	3.000	3.000	3.000	3.000	3.000	3.000	3.000	3.000	
Mg#	76.58	76.49	76.49	76.57	76.44	76.16	76.57	76.21	76.63	76.65	

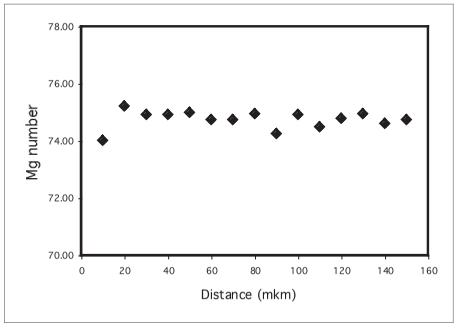
	340	350	360	370	380	390	400	410	420
SiO2	0.00	0.00	0.02	0.01	0.01	0.00	0.00	0.02	0.00
TiO2	0.00	0.01	0.01	0.00	0.00	0.00	0.02	0.00	0.01
Al2O3	66.10	65.96	66.03	65.98	66.24	66.21	66.28	66.38	65.92
Cr2O3	0.63	0.59	0.64	0.73	0.65	0.66	0.61	0.66	0.72
FeO	12.33	12.45	12.34	12.40	12.05	12.32	12.25	12.39	12.39
MnO	0.01	0.02	0.07	0.02	0.02	0.04	0.07	0.04	0.04
NiO	1.14	1.15	1.19	1.26	1.23	1.19	1.27	1.22	1.20
ZnO	0.36	0.36	0.28	0.27	0.29	0.38	0.24	0.26	0.21
MgO	19.86	19.82	19.76	19.79	19.75	19.74	19.78	19.80	19.81
CaO	0.00	0.00	0.00	0.00	0.00	0.00	0.00	0.00	0.00
Total	100.43	100.38	100.34	100.47	100.25	100.54	100.52	100.77	100.32
Si	0.000	0.000	0.000	0.000	0.000	0.000	0.000	0.000	0.000
Ti	0.000	0.000	0.000	0.000	0.000	0.000	0.000	0.000	0.000
Al	1.956	1.953	1.956	1.953	1.963	1.958	1.959	1.958	1.953
Cr	0.012	0.012	0.013	0.014	0.013	0.013	0.012	0.013	0.014
Fe3	0.032	0.034	0.030	0.032	0.024	0.029	0.028	0.028	0.032
Fe2	0.227	0.227	0.229	0.228	0.229	0.230	0.229	0.231	0.229
Mn	0.000	0.000	0.001	0.000	0.000	0.001	0.001	0.001	0.001
Ni	0.023	0.023	0.024	0.025	0.025	0.024	0.026	0.025	0.024
Zn	0.007	0.007	0.005	0.005	0.005	0.007	0.005	0.005	0.004
Mg	0.743	0.743	0.741	0.741	0.740	0.738	0.740	0.739	0.742
Ca	0.000	0.000	0.000	0.000	0.000	0.000	0.000	0.000	0.000
Sum	3.000	3.000	3.000	3.000	3.000	3.000	3.000	3.000	3.000
Mg#	76.60	76.60	76.39	76.47	76.37	76.24	76.37	76.19	76.42

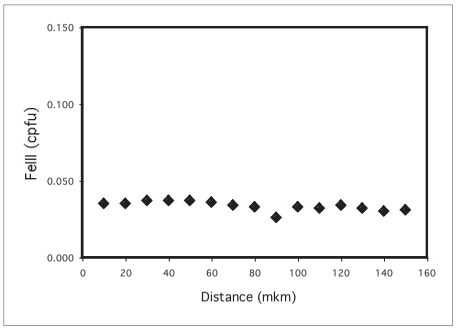


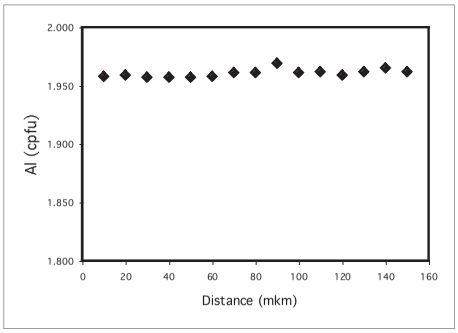
1904-7 Spinel, profile 139

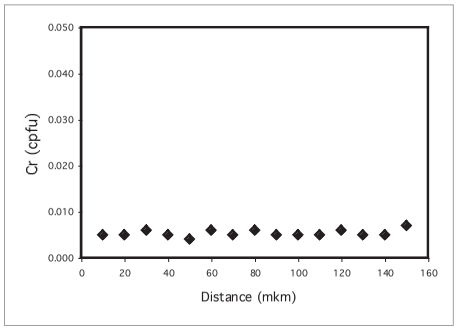


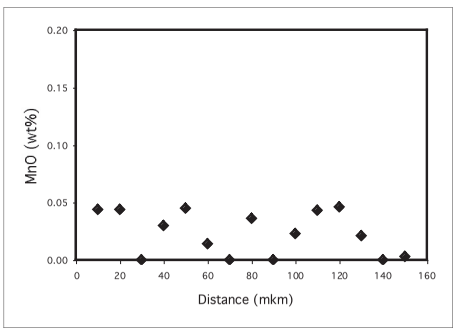


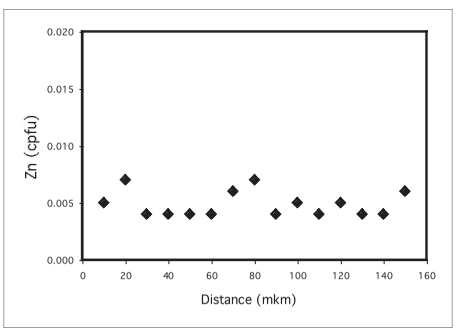


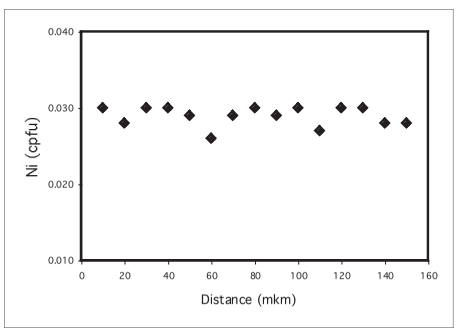








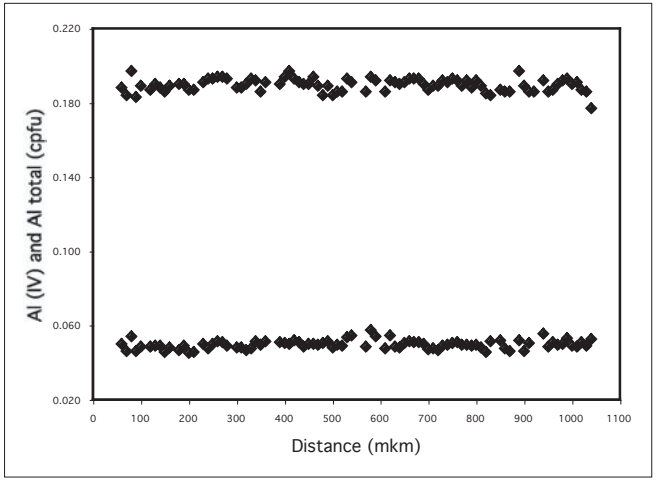


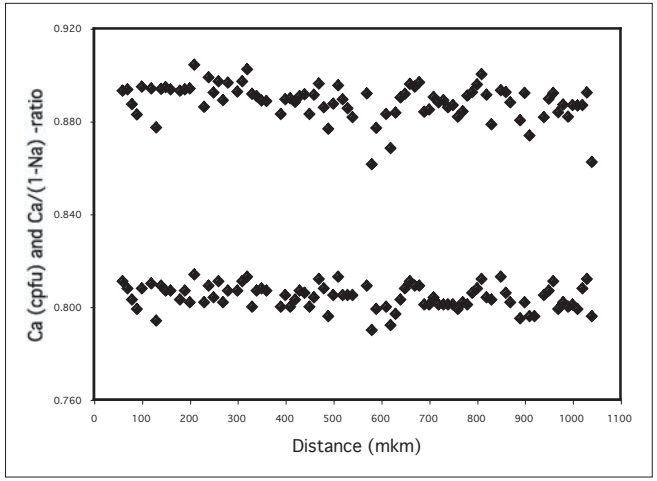


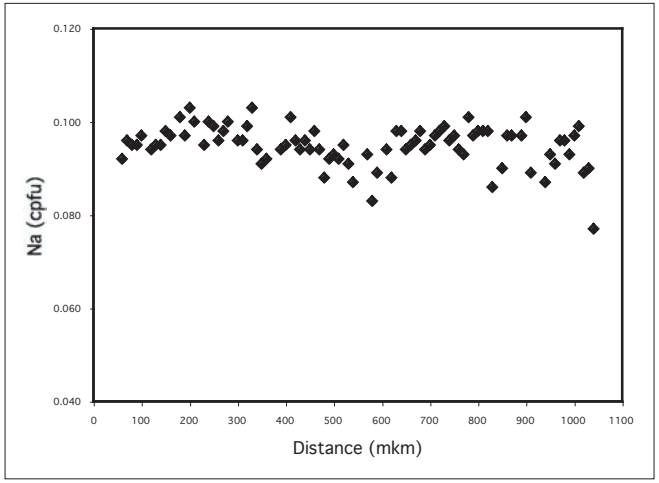
	10	20	30	40	50	60	70	80	90	100	110	120	130	140	150
SiO2	0.05	0.00	0.00	0.01	0.02	0.01	0.00	0.00	0.00	0.01	0.01	0.01	0.01	0.01	0.00
TiO2	0.00	0.01	0.01	0.00	0.00	0.00	0.01	0.01	0.00	0.00	0.01	0.00	0.02	0.00	0.00
Al2O3	65.56	65.78	65.88	65.86	65.68	65.92	65.95	66.25	66.53	66.20	65.90	65.92	65.94	66.07	66.15
Cr2O3	0.24	0.26	0.28	0.25	0.22	0.29	0.23	0.30	0.27	0.27	0.26	0.30	0.26	0.24	0.33
FeO	13.45	12.98	13.24	13.24	13.19	13.30	13.17	13.06	13.10	13.10	13.18	13.14	12.96	13.05	13.09
MnO	0.04	0.04	0.00	0.03	0.05	0.01	0.00	0.04	0.00	0.02	0.04	0.05	0.02	0.00	0.00
NiO	1.46	1.38	1.50	1.47	1.41	1.29	1.41	1.50	1.43	1.48	1.35	1.50	1.47	1.36	1.36
ZnO	0.27	0.39	0.23	0.24	0.19	0.24	0.31	0.37	0.20	0.29	0.23	0.29	0.22	0.22	0.34
MgO	18.92	19.23	19.25	19.24	19.25	19.29	19.19	19.25	19.18	19.29	19.14	19.17	19.25	19.22	19.24
CaO	0.01	0.00	0.01	0.00	0.00	0.00	0.00	0.00	0.01	0.00	0.00	0.00	0.00	0.00	0.00
Total	100.00	100.07	100.40	100.34	100.01	100.34	100.28	100.79	100.72	100.67	100.12	100.38	100.14	100.16	100.53
Si	0.001	0.000	0.000	0.000	0.001	0.000	0.000	0.000	0.000	0.000	0.000	0.000	0.000	0.000	0.000
Ti	0.000	0.000	0.000	0.000	0.000	0.000	0.000	0.000	0.000	0.000	0.000	0.000	0.000	0.000	0.000
Al	1.958	1.959	1.957	1.957	1.957	1.958	1.961	1.961	1.969	1.961	1.962	1.959	1.962	1.965	1.962
Cr	0.005	0.005	0.006	0.005	0.004	0.006	0.005	0.006	0.005	0.005	0.005	0.006	0.005	0.005	0.007
Fe3+	0.035	0.035	0.037	0.037	0.037	0.036	0.034	0.033	0.026	0.033	0.032	0.034	0.032	0.030	0.031
Fe2+	0.251	0.239	0.242	0.242	0.242	0.245	0.244	0.241	0.249	0.242	0.247	0.243	0.242	0.246	0.244
Mn	0.001	0.001	0.000	0.001	0.001	0.000	0.000	0.001	0.000	0.000	0.001	0.001	0.000	0.000	0.000
Ni	0.030	0.028	0.030	0.030	0.029	0.026	0.029	0.030	0.029	0.030	0.027	0.030	0.030	0.028	0.028
Zn	0.005	0.007	0.004	0.004	0.004	0.004	0.006	0.007	0.004	0.005	0.004	0.005	0.004	0.004	0.006
Mg	0.715	0.725	0.723	0.723	0.726	0.725	0.722	0.721	0.718	0.723	0.721	0.721	0.724	0.723	0.722
Ca	0.000	0.000	0.000	0.000	0.000	0.000	0.000	0.000	0.000	0.000	0.000	0.000	0.000	0.000	0.000
Sum	3.000	3.000	3.000	3.000	3.000	3.000	3.000	3.000	3.000	3.000	3.000	3.000	3.000	3.000	3.000
Mg#	74.0	75.2	74.9	74.9	75.0	74.7	74.7	74.9	74.3	74.9	74.5	74.8	74.9	74.6	74.7

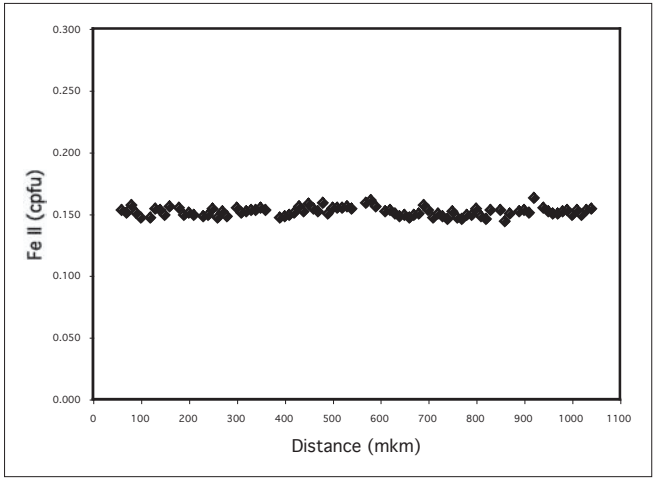
1904-7 Spinel, profile 139

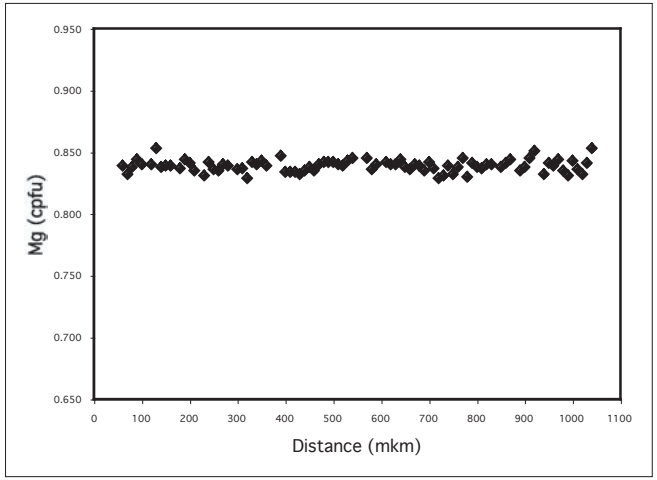
Websterite 1910-11

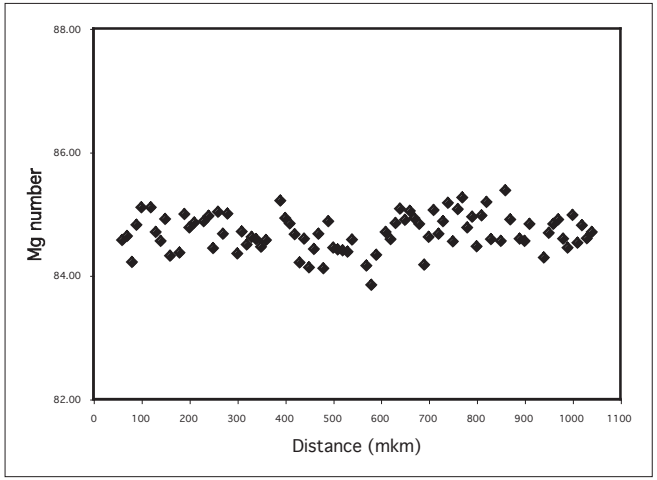












1910-11 Cpx I, profile 1070

	50	60	70	80	90	100	110	120	130	140	150	160	170	180	190	200	210	220	230	240
SiO2	51.58	52.69	53.02	52.48	52.79	52.77	52.63	52.80	53.34	52.90	52.94	52.75	52.34	52.87	52.90	52.82	52.60	51.44	52.81	52.73
TiO2	0.62	0.09	0.08	0.10	0.05	0.09	0.06	0.07	0.08	0.10	0.05	0.08	0.10	0.09	0.08	0.08	0.07	0.08	0.08	0.05
Al2O3	2.99	4.36	4.27	4.56	4.23	4.38	4.52	4.32	4.45	4.36	4.32	4.38	4.76	4.42	4.41	4.35	4.33	4.95	4.42	4.47
Cr2O3	0.12	0.02	0.00	0.01	0.00	0.04	0.02	0.01	0.00	0.00	0.06	0.01	0.01	0.03	0.03	0.06	0.00	0.00	0.01	0.00
FeO	10.22	5.00	4.95	5.12	4.89	4.79	4.77	4.79	5.11	5.02	4.89	5.09	5.01	5.07	4.87	4.94	4.85	4.86	4.83	4.87
MnO	0.24	0.05	0.09	0.05	0.06	0.06	0.04	0.01	0.06	0.08	0.05	0.11	0.02	0.04	0.04	0.05	0.03	0.05	0.01	0.01
MgO	17.81	15.37	15.26	15.32	15.40	15.39	15.06	15.36	15.81	15.40	15.40	15.39	14.77	15.37	15.51	15.41	15.24	14.49	15.18	15.45
CaO	15.60	20.66	20.62	20.42	20.29	20.60	20.39	20.62	20.50	20.69	20.61	20.59	19.99	20.51	20.64	20.45	20.69	19.20	20.39	20.65
Na2O	0.10	1.30	1.36	1.34	1.33	1.37	1.37	1.32	1.36	1.35	1.38	1.37	1.38	1.42	1.37	1.45	1.41	1.28	1.33	1.41
K2O	0.01	0.02	0.01	0.01	0.00	0.00	0.00	0.00	0.01	0.02	0.01	0.01	0.03	0.01	0.00	0.00	0.00	0.04	0.00	0.00
Total	99.30	99.56	99.66	99.41	99.03	99.48	98.85	99.30	100.71	99.93	99.71	99.78	98.40	99.82	99.85	99.60	99.21	96.39	99.06	99.63
Si		1.930	1.939	1.926	1.941	1.932		1.936	1.930	1.931	1.935	1.929		1.931	1.930	1.933	1.933		1.939	1.929
Ti		0.002	0.002	0.003	0.002	0.002		0.002	0.002	0.003	0.001	0.002		0.002	0.002	0.002	0.002		0.002	0.001
Al		0.188	0.184	0.197	0.183	0.189		0.187	0.190	0.188	0.186	0.189		0.190	0.190	0.187	0.187		0.191	0.193
Cr		0.001	0.000	0.000	0.000	0.001		0.000	0.000	0.000	0.002	0.000		0.001	0.001	0.002	0.000		0.000	0.000
Fe2+		0.153	0.151	0.157	0.151	0.147		0.147	0.154	0.153	0.149	0.156		0.155	0.149	0.151	0.149		0.148	0.149
Mn		0.002	0.003	0.001	0.002	0.002		0.000	0.002	0.003	0.002	0.003		0.001	0.001	0.002	0.001		0.000	0.000
Mg		0.839	0.832	0.838	0.844	0.840		0.840	0.853	0.838	0.839	0.839		0.837	0.844	0.841	0.835		0.831	0.842
Ca		0.811	0.808	0.803	0.799	0.808		0.810	0.794	0.809	0.807	0.807		0.803	0.807	0.802	0.814		0.802	0.809
Na		0.092	0.096	0.095	0.095	0.097		0.094	0.095	0.095	0.098	0.097		0.101	0.097	0.103	0.100		0.095	0.100
K		0.001	0.000	0.000	0.000	0.000		0.000	0.001	0.001	0.001	0.000		0.001	0.000	0.000	0.000		0.000	0.000
Sum		4.020	4.015	4.021	4.017	4.019		4.016	4.021	4.021	4.019	4.023		4.022	4.021	4.022	4.022		4.010	4.023
Mg#		84.58	84.64	84.22	84.82	85.11		85.11	84.71	84.56	84.92	84.32		84.38	84.99	84.78	84.86		84.88	84.96
Al IV		0.050	0.046	0.054	0.046	0.049		0.049	0.049	0.049	0.046	0.048		0.047	0.049	0.045	0.046		0.050	0.048
Al VI		0.138	0.138	0.143	0.137	0.141		0.139	0.141	0.139	0.141	0.141		0.144	0.141	0.142	0.142		0.141	0.146

1910-11 Cpx I, profile 1070

	250	260	270	280	290	300	310	320	330	340	350	360	370	380	390	400	410	420	430	440
SiO2	52.67	52.55	52.49	52.71	50.15	52.69	52.78	52.84	52.92	52.73	52.80	52.77	52.65	52.93	52.91	52.84	52.74	52.73	52.80	52.94
TiO2	0.06	0.07	0.11	0.07	0.11	0.08	0.09	0.05	0.06	0.08	0.08	0.07	0.08	0.08	0.10	0.05	0.08	0.09	0.09	0.05
Al2O3	4.47	4.49	4.48	4.47	5.23	4.36	4.37	4.42	4.49	4.47	4.32	4.43	5.00	4.56	4.43	4.49	4.56	4.47	4.43	4.41
Cr2O3	0.07	0.03	0.03	0.02	0.00	0.00	0.00	0.01	0.03	0.05	0.00	0.03	0.03	0.02	0.03	0.03	0.03	0.04	0.00	0.02
FeO	5.03	4.79	4.94	4.84	4.56	5.06	4.94	4.96	5.02	5.02	5.08	5.00	4.98	5.18	4.81	4.85	4.86	4.94	5.09	4.97
MnO	0.03	0.06	0.04	0.03	0.02	0.07	0.04	0.08	0.04	0.07	0.05	0.01	0.09	0.11	0.05	0.03	0.04	0.05	0.07	0.08
MgO	15.30	15.24	15.34	15.36	13.44	15.29	15.34	15.21	15.49	15.41	15.46	15.38	14.83	15.35	15.55	15.29	15.27	15.26	15.26	15.33
CaO	20.48	20.59	20.39	20.57	17.47	20.55	20.67	20.75	20.47	20.61	20.63	20.58	19.48	19.99	20.44	20.51	20.39	20.43	20.60	20.59
Na2O	1.39	1.35	1.38	1.41	1.09	1.35	1.35	1.40	1.46	1.32	1.29	1.30	1.24	1.17	1.32	1.34	1.42	1.36	1.33	1.36
K2O	0.00	0.00	0.02	0.00	0.05	0.00	0.00	0.01	0.01	0.00	0.00	0.02	0.08	0.02	0.01	0.01	0.02	0.00	0.02	0.01
Total	99.49	99.16	99.23	99.46	92.12	99.44	99.58	99.72	99.99	99.74	99.71	99.59	98.46	99.40	99.65	99.43	99.40	99.35	99.69	99.76
Si	1.930	1.931	1.928	1.931		1.932	1.932	1.933	1.929	1.928	1.931	1.931			1.933	1.935	1.932	1.933	1.931	1.934
Ti	0.002	0.002	0.003	0.002		0.002	0.002	0.001	0.002	0.002	0.002	0.002			0.003	0.001	0.002	0.003	0.003	0.001
Al	0.193	0.194	0.194	0.193		0.188	0.188	0.190	0.193	0.192	0.186	0.191			0.190	0.194	0.197	0.193	0.191	0.190
Cr	0.002	0.001	0.001	0.001		0.000	0.000	0.000	0.001	0.001	0.000	0.001			0.001	0.001	0.001	0.001	0.000	0.001
Fe2+	0.154	0.147	0.152	0.148		0.155	0.151	0.152	0.153	0.153	0.155	0.153			0.147	0.148	0.149	0.151	0.156	0.152
Mn	0.001	0.002	0.001	0.001		0.002	0.001	0.003	0.001	0.002	0.002	0.000			0.001	0.001	0.001	0.001	0.002	0.002
Mg	0.836	0.835	0.840	0.839		0.836	0.837	0.829	0.842	0.840	0.843	0.839			0.847	0.834	0.834	0.834	0.832	0.835
Ca	0.804	0.811	0.802	0.807		0.807	0.811	0.813	0.800	0.807	0.808	0.807			0.800	0.805	0.800	0.803	0.807	0.806
Na	0.099	0.096	0.098	0.100		0.096	0.096	0.099	0.103	0.094	0.091	0.092			0.094	0.095	0.101	0.096	0.094	0.096
K	0.000	0.000	0.001	0.000		0.000	0.000	0.000	0.000	0.000	0.000	0.001			0.001	0.001	0.001	0.000	0.001	0.000
Sum	4.020	4.018	4.021	4.021		4.019	4.019	4.020	4.024	4.020	4.019	4.017			4.016	4.014	4.018	4.015	4.018	4.018
Mg#	84.44	85.03	84.68	85.01		84.36	84.72	84.51	84.62	84.59	84.47	84.58			85.21	84.93	84.84	84.67	84.21	84.60
Al IV	0.050	0.052	0.051	0.049		0.048	0.048	0.047	0.048	0.052	0.050	0.052			0.051	0.051	0.050	0.052	0.051	0.049
Al VI	0.143	0.143	0.143	0.144		0.140	0.140	0.144	0.146	0.141	0.137	0.140			0.139	0.144	0.147	0.141	0.140	0.142

1910-11 Cpx I, profile 1070

	450	460	470	480	490	500	510	520	530	540	550	560	570	580	590	600	610	620	630	640
SiO2	52.97	52.63	52.77	52.65	53.17	52.96	52.78	52.81	52.54	52.77	52.20	52.57	52.68	53.05	52.73	52.57	52.89	52.85	52.71	52.77
TiO2	0.09	0.08	0.07	0.08	0.10	0.07	0.09	0.10	0.07	0.06	0.05	0.08	0.08	0.09	0.10	0.08	0.09	0.09	0.06	0.06
Al2O3	4.42	4.48	4.38	4.25	4.40	4.27	4.32	4.30	4.45	4.43	4.34	4.54	4.31	4.52	4.45	4.61	4.32	4.44	4.41	4.40
Cr2O3	0.00	0.00	0.03	0.04	0.01	0.03	0.04	0.02	0.03	0.04	0.02	0.04	0.00	0.01	0.01	0.00	0.02	0.04	0.02	0.01
FeO	5.17	5.01	4.99	5.20	4.91	5.08	5.06	5.08	5.10	5.02	5.31	5.52	5.19	5.29	5.11	4.86	4.96	4.99	4.87	4.83
MnO	0.05	0.02	0.06	0.04	0.06	0.03	0.08	0.11	0.08	0.01	0.06	0.05	0.04	0.05	0.05	0.07	0.03	0.04	0.07	0.07
MgO	15.40	15.26	15.42	15.40	15.51	15.46	15.41	15.37	15.42	15.49	15.24	15.57	15.49	15.36	15.37	15.01	15.43	15.36	15.35	15.47
CaO	20.47	20.47	20.74	20.56	20.39	20.58	20.74	20.53	20.50	20.55	20.23	20.26	20.62	20.20	20.34	19.39	20.40	20.16	20.26	20.46
Na2O	1.32	1.38	1.33	1.23	1.30	1.31	1.30	1.34	1.28	1.23	1.18	1.02	1.31	1.18	1.26	1.14	1.33	1.24	1.38	1.38
K2O	0.00	0.00	0.02	0.01	0.00	0.00	0.00	0.00	0.00	0.00	0.00	0.01	0.00	0.00	0.01	0.01	0.01	0.00	0.00	0.01
Total	99.89	99.34	99.80	99.45	99.85	99.78	99.81	99.65	99.47	99.59	98.63	99.67	99.72	99.74	99.43	97.74	99.47	99.19	99.13	99.45
Si	1.933	1.931	1.929	1.931	1.937	1.935	1.930	1.933	1.927	1.930			1.928	1.936	1.932		1.936	1.938	1.936	1.932
Ti	0.002	0.002	0.002	0.002	0.003	0.002	0.002	0.003	0.002	0.002			0.002	0.002	0.003		0.002	0.002	0.002	0.002
Al	0.190	0.194	0.189	0.184	0.189	0.184	0.186	0.186	0.193	0.191			0.186	0.194	0.192		0.186	0.192	0.191	0.190
Cr	0.000	0.000	0.001	0.001	0.000	0.001	0.001	0.001	0.001	0.001			0.000	0.000	0.000		0.000	0.001	0.000	0.000
Fe2+	0.158	0.154	0.152	0.159	0.150	0.155	0.155	0.155	0.156	0.154			0.159	0.161	0.156		0.152	0.153	0.150	0.148
Mn	0.001	0.001	0.002	0.001	0.002	0.001	0.002	0.003	0.003	0.000			0.001	0.001	0.002		0.001	0.001	0.002	0.002
Mg	0.838	0.835	0.840	0.842	0.842	0.842	0.840	0.839	0.843	0.845			0.845	0.836	0.840		0.842	0.840	0.840	0.844
Ca	0.800	0.804	0.812	0.808	0.796	0.805	0.813	0.805	0.805	0.805			0.809	0.790	0.799		0.800	0.792	0.797	0.803
Na	0.094	0.098	0.094	0.088	0.092	0.093	0.092	0.095	0.091	0.087			0.093	0.083	0.089		0.094	0.088	0.098	0.098
K	0.000	0.000	0.001	0.000	0.000	0.000	0.000	0.000	0.000	0.000			0.000	0.000	0.001		0.001	0.000	0.000	0.000
Sum	4.016	4.019	4.022	4.018	4.011	4.018	4.020	4.019	4.020	4.015			4.023	4.006	4.014		4.015	4.007	4.016	4.020
Mg#	84.14	84.43	84.68	84.12	84.88	84.45	84.42	84.41	84.38	84.58			84.16	83.85	84.34		84.71	84.59	84.85	85.08
Al IV	0.050	0.050	0.050	0.051	0.052	0.048	0.050	0.049	0.054	0.055			0.049	0.058	0.054		0.048	0.055	0.049	0.048
Al VI	0.140	0.144	0.140	0.134	0.138	0.136	0.137	0.137	0.140	0.137			0.138	0.137	0.138		0.139	0.138	0.143	0.142

III

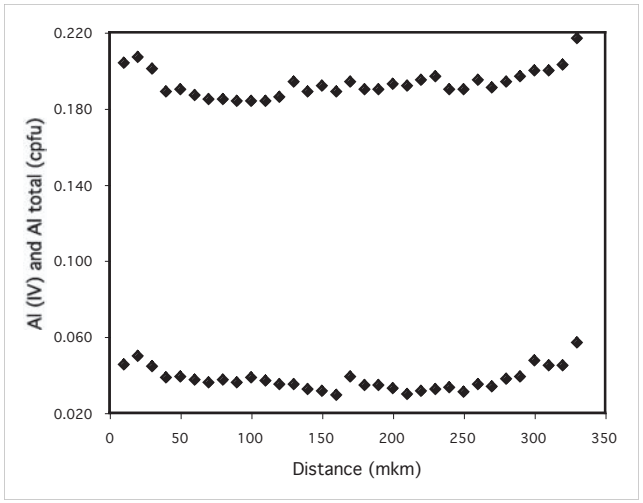
1910-11 Cpx I, profile 1070

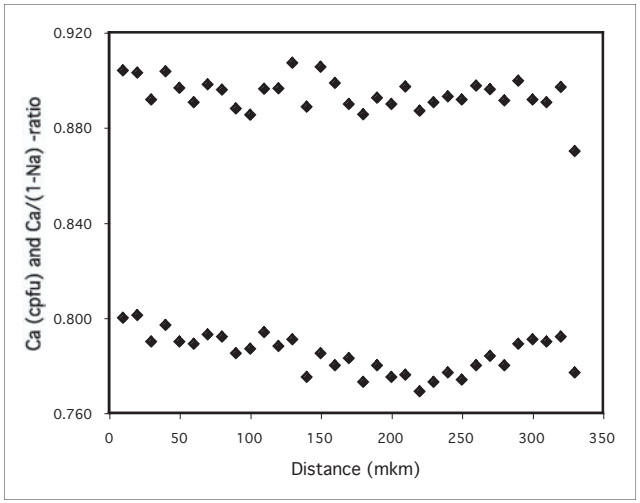
	650	660	670	680	690	700	710	720	730	740	750	760	770	780	790	800	810	820	830	840
SiO2	52.93	52.80	52.82	52.55	52.80	52.94	52.88	52.89	52.94	52.80	53.03	52.84	52.91	52.84	52.82	52.61	52.83	52.83	53.08	52.57
TiO2	0.07	0.08	0.08	0.11	0.07	0.04	0.07	0.04	0.09	0.08	0.07	0.07	0.07	0.10	0.11	0.06	0.07	0.09	0.06	0.08
Al2O3	4.43	4.48	4.47	4.46	4.39	4.34	4.39	4.38	4.46	4.41	4.49	4.44	4.39	4.44	4.36	4.43	4.39	4.27	4.27	4.54
Cr2O3	0.01	0.04	0.02	0.02	0.02	0.02	0.02	0.01	0.02	0.00	0.03	0.00	0.01	0.06	0.03	0.03	0.03	0.00	0.03	0.03
FeO	4.87	4.82	4.89	4.87	5.12	5.02	4.81	4.90	4.85	4.76	5.00	4.80	4.77	4.87	4.86	5.03	4.85	4.75	5.01	5.12
MnO	0.03	0.05	0.03	0.05	0.08	0.03	0.05	0.03	0.03	0.06	0.01	0.07	0.04	0.07	0.04	0.04	0.06	0.00	0.05	0.01
MgO	15.38	15.35	15.42	15.34	15.29	15.45	15.33	15.16	15.24	15.35	15.30	15.34	15.50	15.20	15.42	15.34	15.36	15.34	15.41	15.21
CaO	20.63	20.71	20.68	20.58	20.42	20.45	20.50	20.37	20.43	20.40	20.49	20.34	20.46	20.40	20.57	20.58	20.74	20.43	20.50	20.19
Na2O	1.33	1.33	1.35	1.38	1.33	1.35	1.36	1.37	1.40	1.35	1.37	1.33	1.31	1.43	1.37	1.37	1.38	1.37	1.22	1.12
K2O	0.01	0.01	0.00	0.00	0.01	0.01	0.02	0.00	0.00	0.00	0.00	0.01	0.02	0.00	0.00	0.00	0.00	0.00	0.00	0.00
Total	99.69	99.66	99.76	99.36	99.52	99.62	99.42	99.15	99.43	99.21	99.78	99.23	99.47	99.41	99.58	99.48	99.70	99.08	99.61	98.86
Si	1.934	1.930	1.930	1.928	1.934	1.936	1.936	1.941	1.938	1.936	1.935	1.937	1.935	1.936	1.932	1.929	1.932	1.940	1.940	
Ti	0.002	0.002	0.002	0.003	0.002	0.001	0.002	0.001	0.002	0.002	0.002	0.002	0.002	0.003	0.003	0.002	0.002	0.002	0.002	
Al	0.191	0.193	0.193	0.193	0.190	0.187	0.189	0.189	0.192	0.191	0.193	0.192	0.189	0.192	0.188	0.192	0.189	0.185	0.184	
Cr	0.000	0.001	0.001	0.001	0.000	0.000	0.000	0.000	0.001	0.000	0.001	0.000	0.000	0.002	0.001	0.001	0.001	0.000	0.001	
Fe2+	0.149	0.147	0.149	0.150	0.157	0.153	0.147	0.150	0.148	0.146	0.152	0.147	0.146	0.149	0.149	0.154	0.148	0.146	0.153	
Mn	0.001	0.001	0.001	0.002	0.002	0.001	0.001	0.001	0.001	0.002	0.000	0.002	0.001	0.002	0.001	0.001	0.002	0.000	0.001	
Mg	0.838	0.836	0.840	0.839	0.835	0.842	0.837	0.829	0.831	0.839	0.832	0.838	0.845	0.830	0.841	0.838	0.837	0.840	0.840	
Ca	0.808	0.811	0.809	0.809	0.801	0.801	0.804	0.801	0.801	0.801	0.801	0.799	0.802	0.801	0.806	0.808	0.812	0.804	0.803	
Na	0.094	0.095	0.096	0.098	0.094	0.095	0.097	0.098	0.099	0.096	0.097	0.094	0.093	0.101	0.097	0.098	0.098	0.098	0.086	
K	0.000	0.000	0.000	0.000	0.000	0.000	0.001	0.000	0.000	0.000	0.000	0.000	0.001	0.000	0.000	0.000	0.000	0.000	0.000	
Sum	4.016	4.018	4.020	4.021	4.016	4.017	4.016	4.011	4.013	4.014	4.014	4.012	4.015	4.015	4.019	4.022	4.021	4.014	4.009	
Mg#	84.90	85.05	84.93	84.83	84.17	84.62	85.06	84.68	84.88	85.18	84.55	85.08	85.27	84.78	84.95	84.48	84.97	85.19	84.59	
Al IV	0.051	0.052	0.051	0.051	0.050	0.047	0.048	0.047	0.049	0.050	0.051	0.051	0.050	0.050	0.049	0.050	0.048	0.046	0.052	
Al VI	0.141	0.142	0.142	0.142	0.140	0.140	0.142	0.143	0.143	0.142	0.143	0.141	0.140	0.143	0.139	0.143	0.141	0.140	0.133	

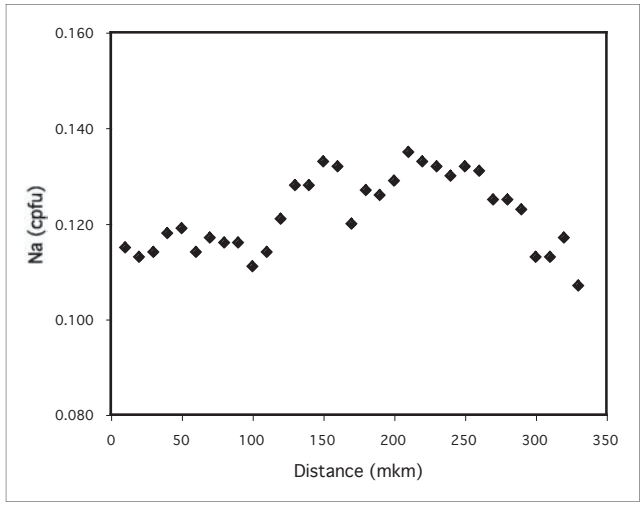
1910-11 Cpx I, profile 1070

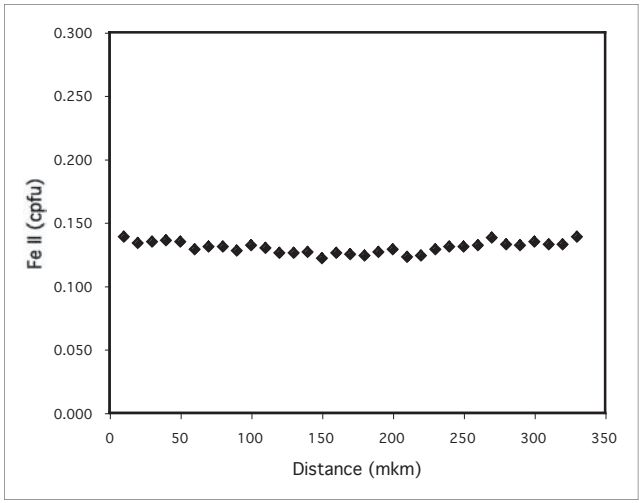
	850	860	870	880	890	900	910	920	930	940	950	960	970	980	990	1000	1010	1020	1030	1040
SiO2	52.80	52.87	52.91	53.83	52.67	52.70	52.88	52.82	51.86	52.88	52.72	52.92	53.09	52.85	52.97	52.76	52.84	53.10	52.69	53.13
TiO2	0.10	0.10	0.04	0.07	0.07	0.06	0.07	0.10	0.12	0.09	0.08	0.09	0.08	0.07	0.09	0.06	0.11	0.08	0.05	0.08
Al2O3	4.33	4.30	4.32	4.40	4.54	4.36	4.32	4.30	4.84	4.46	4.31	4.34	4.43	4.45	4.48	4.40	4.44	4.35	4.29	4.11
Cr2O3	0.02	0.03	0.04	0.03	0.01	0.01	0.03	0.00	0.03	0.02	0.00	0.00	0.03	0.00	0.00	0.03	0.00	0.00	0.01	0.04
FeO	5.00	4.72	4.89	4.92	4.95	5.00	4.94	5.31	5.69	5.08	4.96	4.92	4.91	4.96	5.00	4.86	5.01	4.86	4.97	5.05
MnO	0.05	0.06	0.02	0.07	0.00	0.05	0.10	0.08	0.07	0.10	0.07	0.03	0.09	0.05	0.07	0.11	0.03	0.05	0.03	0.09
MgO	15.36	15.41	15.47	15.80	15.26	15.32	15.48	15.58	15.18	15.27	15.39	15.41	15.55	15.31	15.24	15.44	15.31	15.27	15.38	15.65
CaO	20.74	20.53	20.45	20.33	20.22	20.39	20.27	20.27	19.16	20.54	20.54	20.73	20.50	20.46	20.44	20.41	20.38	20.63	20.66	20.32
Na2O	1.27	1.36	1.36	1.30	1.37	1.43	1.25	0.98	0.81	1.23	1.31	1.28	1.37	1.35	1.32	1.36	1.39	1.26	1.27	1.09
K2O	0.00	0.03	0.00	0.02	0.00	0.00	0.01	0.00	0.00	0.00	0.00	0.00	0.00	0.00	0.00	0.00	0.01	0.00	0.00	0.00
Total	99.65	99.40	99.50	100.77	99.10	99.31	99.36	99.44	97.75	99.67	99.38	99.71	100.04	99.51	99.60	99.42	99.53	99.60	99.35	99.56
Si	1.932	1.936	1.936		1.934	1.934	1.937			1.933	1.933	1.934	1.933	1.934	1.936	1.933	1.934	1.940	1.933	1.942
Ti	0.003	0.003	0.001		0.002	0.002	0.002			0.003	0.002	0.003	0.002	0.002	0.003	0.002	0.003	0.002	0.001	0.002
Al	0.187	0.186	0.186		0.197	0.189	0.186			0.192	0.186	0.187	0.190	0.192	0.193	0.190	0.191	0.187	0.186	0.177
Cr	0.001	0.001	0.001		0.000	0.000	0.001			0.000	0.000	0.000	0.001	0.000	0.000	0.001	0.000	0.000	0.000	0.001
Fe2+	0.153	0.144	0.150		0.152	0.153	0.151			0.155	0.152	0.150	0.150	0.152	0.153	0.149	0.153	0.149	0.153	0.154
Mn	0.001	0.002	0.001		0.000	0.001	0.003			0.003	0.002	0.001	0.003	0.002	0.002	0.003	0.001	0.002	0.001	0.003
Mg	0.838	0.841	0.844		0.835	0.838	0.845			0.832	0.841	0.839	0.844	0.835	0.831	0.843	0.836	0.832	0.841	0.853
Ca	0.813	0.806	0.802		0.795	0.802	0.796			0.805	0.807	0.811	0.799	0.802	0.800	0.801	0.799	0.808	0.812	0.796
Na	0.090	0.097	0.097		0.097	0.101	0.089			0.087	0.093	0.091	0.096	0.096	0.093	0.097	0.099	0.089	0.090	0.077
K	0.000	0.001	0.000		0.000	0.000	0.001			0.000	0.000	0.000	0.000	0.000	0.000	0.000	0.001	0.000	0.000	0.000
Sum	4.017	4.017	4.017		4.014	4.021	4.012			4.011	4.018	4.016	4.018	4.015	4.011	4.019	4.017	4.009	4.018	4.005
Mg#	84.56	85.38	84.91		84.60	84.56	84.84			84.30	84.69	84.83	84.91	84.60	84.45	84.98	84.53	84.81	84.61	84.71
Al IV	0.052	0.048	0.046		0.052	0.046	0.051			0.056	0.049	0.051	0.050	0.050	0.053	0.049	0.049	0.051	0.049	0.053
Al VI	0.135	0.139	0.140		0.145	0.143	0.136			0.137	0.138	0.136	0.141	0.142	0.140	0.141	0.143	0.136	0.137	0.125

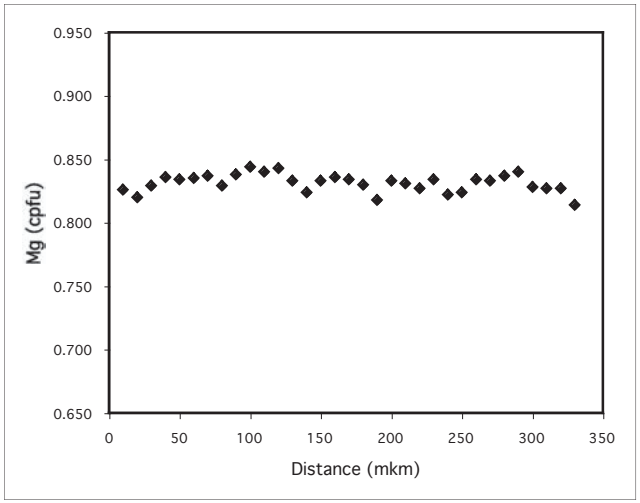
1910-11 Cpx I, profile 1070

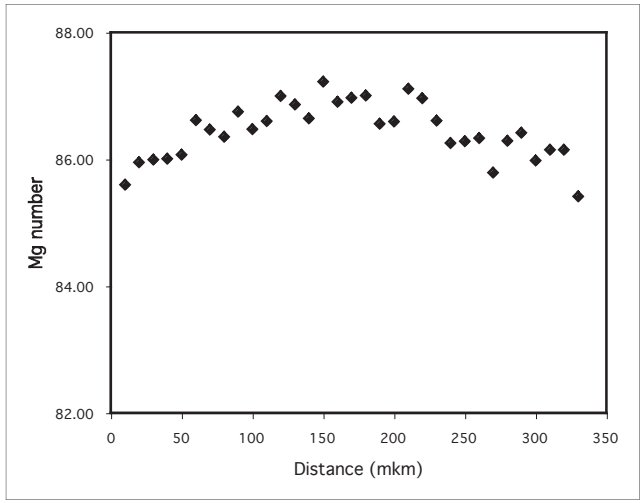












1910-11 Cpx II, profile 330

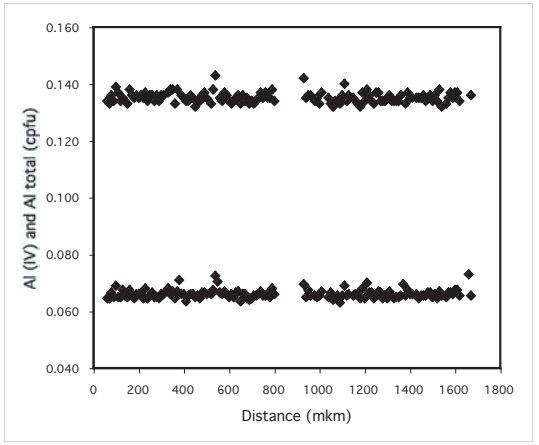
	10	20	30	40	50	60	70	80	90	100	110	120	130	140	150	160	170	180	190	200
SiO2	53.08	53.15	53.77	53.39	53.67	53.49	53.78	53.66	53.69	53.99	53.68	53.77	53.49	54.17	53.57	53.84	53.79	54.28	54.02	53.89
TiO2	0.04	0.10	0.03	0.10	0.10	0.05	0.06	0.09	0.07	0.06	0.06	0.08	0.08	0.05	0.07	0.04	0.06	0.08	0.08	0.06
Al2O3	4.76	4.84	4.73	4.42	4.45	4.37	4.34	4.32	4.29	4.34	4.30	4.36	4.54	4.44	4.49	4.42	4.55	4.47	4.45	4.52
Cr2O3	0.01	0.00	0.01	0.00	0.04	0.01	0.00	0.08	0.01	0.00	0.01	0.03	0.02	0.06	0.00	0.04	0.00	0.05	0.08	0.03
FeO	4.56	4.41	4.47	4.46	4.48	4.23	4.33	4.33	4.21	4.36	4.27	4.17	4.15	4.20	4.00	4.17	4.12	4.10	4.20	4.27
MnO	0.09	0.06	0.05	0.00	0.07	0.14	0.00	0.01	0.10	0.03	0.02	0.03	0.03	0.06	0.08	0.06	0.04	0.05	0.03	0.01
NiO	0.12	0.12	0.12	0.10	0.12	0.17	0.10	0.11	0.09	0.12	0.11	0.15	0.09	0.14	0.11	0.12	0.12	0.09	0.08	0.13
MgO	15.22	15.13	15.42	15.43	15.47	15.39	15.49	15.31	15.44	15.69	15.53	15.63	15.38	15.29	15.37	15.49	15.45	15.44	15.14	15.45
CaO	20.53	20.55	20.44	20.48	20.37	20.22	20.43	20.36	20.14	20.36	20.43	20.31	20.31	20.01	20.16	20.10	20.17	20.00	20.08	19.98
Na2O	1.62	1.61	1.62	1.68	1.70	1.61	1.67	1.65	1.64	1.59	1.62	1.72	1.82	1.82	1.88	1.88	1.71	1.81	1.80	1.84
K2O	0.00	0.00	0.00	0.00	0.00	0.00	0.00	0.00	0.00	0.00	0.01	0.00	0.02	0.00	0.01	0.02	0.00	0.00	0.02	0.02
Total	100.02	99.96	100.66	100.05	100.46	99.68	100.19	99.91	99.67	100.53	100.04	100.24	99.92	100.22	99.72	100.16	100.00	100.38	99.96	100.19
Si	1.932	1.933	1.940	1.940	1.942	1.948	1.948	1.950	1.953	1.949	1.948	1.946	1.943	1.958	1.948	1.950	1.949	1.957	1.958	1.950
Ti	0.001	0.003	0.001	0.003	0.003	0.001	0.002	0.002	0.002	0.002	0.002	0.002	0.002	0.001	0.002	0.001	0.002	0.002	0.002	0.001
Al	0.204	0.207	0.201	0.189	0.190	0.187	0.185	0.185	0.184	0.184	0.184	0.186	0.194	0.189	0.192	0.189	0.194	0.190	0.190	0.193
Cr	0.000	0.000	0.000	0.000	0.001	0.000	0.000	0.002	0.000	0.000	0.000	0.001	0.001	0.002	0.000	0.001	0.000	0.002	0.002	0.001
Fe2+	0.139	0.134	0.135	0.136	0.135	0.129	0.131	0.131	0.128	0.132	0.130	0.126	0.126	0.127	0.122	0.126	0.125	0.124	0.127	0.129
Mn	0.003	0.002	0.002	0.000	0.002	0.004	0.000	0.000	0.003	0.001	0.001	0.001	0.001	0.002	0.002	0.002	0.001	0.002	0.001	0.000
Ni	0.004	0.003	0.003	0.003	0.003	0.005	0.003	0.003	0.003	0.003	0.003	0.004	0.003	0.004	0.003	0.003	0.004	0.002	0.002	0.004
Mg	0.826	0.820	0.829	0.836	0.834	0.835	0.837	0.829	0.838	0.844	0.840	0.843	0.833	0.824	0.833	0.836	0.834	0.830	0.818	0.833
Ca	0.800	0.801	0.790	0.797	0.790	0.789	0.793	0.792	0.785	0.787	0.794	0.788	0.791	0.775	0.785	0.780	0.783	0.773	0.780	0.775
Na	0.115	0.113	0.114	0.118	0.119	0.114	0.117	0.116	0.116	0.111	0.114	0.121	0.128	0.128	0.133	0.132	0.120	0.127	0.126	0.129
K	0.000	0.000	0.000	0.000	0.000	0.000	0.000	0.000	0.000	0.000	0.000	0.000	0.001	0.000	0.000	0.001	0.000	0.000	0.001	0.001
Sum	4.022	4.017	4.015	4.022	4.019	4.014	4.016	4.012	4.011	4.013	4.016	4.018	4.022	4.009	4.021	4.021	4.012	4.008	4.007	4.017
Mg#	85.60	85.95	86.00	86.01	86.07	86.62	86.47	86.35	86.75	86.48	86.60	87.00	86.86	86.65	87.23	86.90	86.97	87.00	86.56	86.59
Al IV	0.046	0.050	0.045	0.039	0.039	0.038	0.036	0.038	0.036	0.039	0.037	0.035	0.035	0.033	0.032	0.030	0.039	0.035	0.035	0.033
Al VI	0.159	0.157	0.157	0.151	0.151	0.150	0.149	0.148	0.148	0.146	0.147	0.151	0.159	0.157	0.161	0.160	0.155	0.156	0.156	0.160

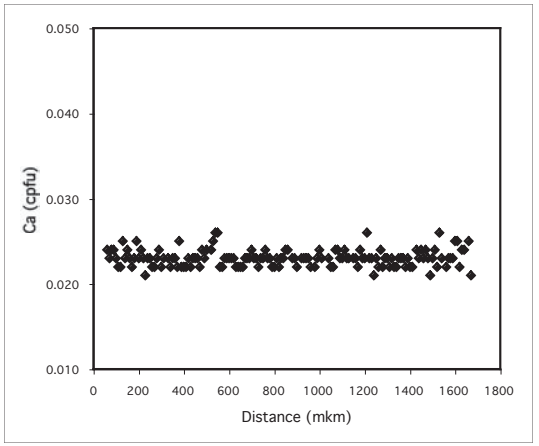
1910-11 Cpx II, profile 330

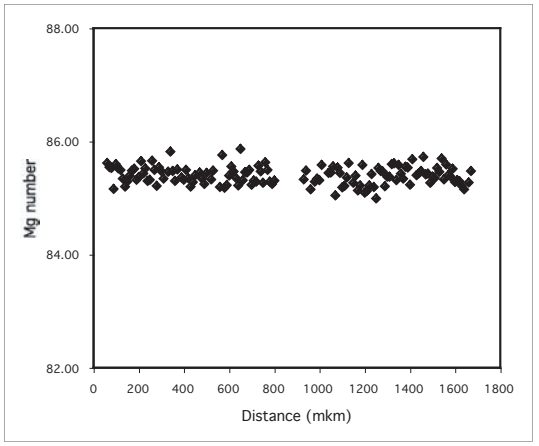
	210	220	230	240	250	260	270	280	290	300	310	320	330
SiO2	53.83	53.98	53.95	53.70	53.87	53.72	53.38	53.44	53.41	53.43	53.73	53.14	53.43
TiO2	0.03	0.03	0.02	0.09	0.08	0.10	0.02	0.10	0.09	0.13	0.07	0.06	0.07
Al2O3	4.49	4.56	4.62	4.43	4.43	4.57	4.46	4.53	4.61	4.67	4.69	4.72	5.07
Cr2O3	0.02	0.00	0.00	0.04	0.00	0.01	0.01	0.03	0.01	0.00	0.01	0.00	0.00
FeO	4.06	4.07	4.26	4.29	4.31	4.36	4.53	4.37	4.37	4.45	4.39	4.36	4.57
MnO	0.00	0.00	0.04	0.03	0.03	0.01	0.06	0.02	0.04	0.09	0.01	0.06	0.07
NiO	0.08	0.13	0.15	0.10	0.07	0.09	0.14	0.14	0.16	0.14	0.12	0.13	0.15
MgO	15.34	15.31	15.50	15.14	15.22	15.47	15.34	15.45	15.56	15.30	15.35	15.20	15.04
CaO	19.96	19.81	19.99	19.92	19.89	20.11	20.08	20.03	20.32	20.34	20.40	20.25	19.97
Na2O	1.91	1.90	1.89	1.85	1.87	1.87	1.76	1.78	1.76	1.61	1.61	1.65	1.53
K2O	0.00	0.02	0.00	0.00	0.00	0.00	0.00	0.00	0.00	0.00	0.02	0.00	0.00
Total	99.72	99.80	100.42	99.58	99.77	100.30	99.78	99.88	100.32	100.16	100.40	99.57	99.88
Si	1.955	1.957	1.948	1.955	1.957	1.944	1.944	1.943	1.935	1.938	1.943	1.939	1.941
Ti	0.001	0.001	0.000	0.003	0.002	0.003	0.001	0.003	0.002	0.004	0.002	0.002	0.002
Al	0.192	0.195	0.197	0.190	0.190	0.195	0.191	0.194	0.197	0.200	0.200	0.203	0.217
Cr	0.001	0.000	0.000	0.001	0.000	0.000	0.000	0.001	0.000	0.000	0.000	0.000	0.000
Fe2+	0.123	0.124	0.129	0.131	0.131	0.132	0.138	0.133	0.132	0.135	0.133	0.133	0.139
Mn	0.000	0.000	0.001	0.001	0.001	0.000	0.002	0.000	0.001	0.003	0.000	0.002	0.002
Ni	0.002	0.004	0.004	0.003	0.002	0.003	0.004	0.004	0.005	0.004	0.004	0.004	0.004
Mg	0.831	0.827	0.834	0.822	0.824	0.834	0.833	0.837	0.840	0.828	0.827	0.827	0.814
Ca	0.776	0.769	0.773	0.777	0.774	0.780	0.784	0.780	0.789	0.791	0.790	0.792	0.777
Na	0.135	0.133	0.132	0.130	0.132	0.131	0.125	0.125	0.123	0.113	0.113	0.117	0.107
K	0.000	0.001	0.000	0.000	0.000	0.000	0.000	0.000	0.000	0.000	0.001	0.000	0.000
Sum	4.016	4.012	4.019	4.012	4.012	4.021	4.022	4.020	4.025	4.015	4.012	4.017	4.003
Mg#	87.11	86.96	86.60	86.25	86.28	86.34	85.79	86.29	86.42	85.98	86.15	86.15	85.41
Al IV	0.030	0.032	0.033	0.034	0.031	0.035	0.034	0.038	0.039	0.048	0.045	0.045	0.057
Al VI	0.162	0.164	0.165	0.157	0.159	0.160	0.157	0.156	0.158	0.153	0.155	0.158	0.160

1910-11 Cpx II, profile 330

	60	70	80	90	100	110	120	130	140	150
SiO2	54.71	54.35	54.29	54.76	54.43	54.77	54.52	54.51	54.63	54.38
TiO2	0.01	0.04	0.05	0.01	0.03	0.01	0.03	0.03	0.05	0.00
Al2O3	3.24	3.20	3.29	3.25	3.36	3.33	3.22	3.24	3.24	3.22
Cr2O3	0.02	0.01	0.01	0.01	0.03	0.00	0.00	0.03	0.00	0.05
FeO	9.44	9.55	9.56	9.78	9.51	9.50	9.52	9.61	9.72	9.74
MnO	0.09	0.08	0.08	0.08	0.08	0.02	0.08	0.10	0.06	0.08
MgO	31.50	31.71	31.65	31.55	31.67	31.52	31.42	31.39	31.43	31.65
CaO	0.65	0.62	0.63	0.63	0.60	0.60	0.59	0.65	0.61	0.65
Na2O	0.09	0.09	0.07	0.06	0.06	0.10	0.08	0.05	0.06	0.07
K2O	0.00	0.01	0.00	0.00	0.01	0.01	0.01	0.00	0.02	0.00
Total	99.75	99.66	99.63	100.13	99.77	99.86	99.47	99.63	99.82	99.83
Si	1.921	1.913	1.911	1.918	1.912	1.920	1.920	1.918	1.919	1.912
Ti	0.000	0.001	0.001	0.000	0.001	0.000	0.001	0.001	0.001	0.000
Al	0.134	0.133	0.136	0.134	0.139	0.137	0.134	0.135	0.134	0.133
Cr	0.001	0.000	0.000	0.000	0.001	0.000	0.000	0.001	0.000	0.001
Fe2+	0.277	0.281	0.281	0.287	0.279	0.279	0.280	0.283	0.286	0.286
Mn	0.003	0.003	0.002	0.002	0.002	0.001	0.002	0.003	0.002	0.002
Mg	1.649	1.663	1.661	1.647	1.658	1.648	1.650	1.647	1.646	1.659
Ca	0.024	0.023	0.024	0.024	0.023	0.022	0.022	0.025	0.023	0.024
Na	0.006	0.006	0.005	0.004	0.004	0.007	0.006	0.003	0.004	0.004
K	0.000	0.000	0.000	0.000	0.000	0.000	0.000	0.000	0.001	0.000
Sum	4.015	4.023	4.022	4.016	4.020	4.014	4.015	4.015	4.015	4.023
Mg#	85.62	85.55	85.53	85.16	85.60	85.52	85.49	85.34	85.20	85.30
Al IV	0.065	0.065	0.067	0.065	0.069	0.065	0.065	0.068	0.066	0.065
Al VI	0.070	0.069	0.070	0.069	0.070	0.072	0.069	0.068	0.069	0.068







1910-11 Opx I, profile 1670

	160	170	180	190	200	210	220	230	240	250	260	270	280	290	300	310	320	330	340
SiO2	54.79	54.77	54.70	54.68	54.44	54.60	54.63	54.74	54.73	54.86	54.77	54.70	54.65	54.90	54.57	54.53	54.32	54.59	54.59
TiO2	0.05	0.03	0.01	0.04	0.03	0.01	0.00	0.02	0.00	0.02	0.03	0.02	0.01	0.02	0.01	0.03	0.05	0.05	0.01
Al2O3	3.35	3.29	3.27	3.29	3.26	3.28	3.26	3.32	3.24	3.29	3.30	3.24	3.29	3.26	3.29	3.28	3.59	3.32	3.32
Cr2O3	0.04	0.00	0.00	0.00	0.00	0.03	0.01	0.00	0.05	0.05	0.05	0.03	0.01	0.00	0.03	0.00	0.00	0.05	0.03
FeO	9.66	9.56	9.55	9.66	9.67	9.43	9.56	9.55	9.73	9.69	9.41	9.58	9.81	9.54	9.57	9.68	9.46	9.57	9.30
MnO	0.08	0.10	0.06	0.08	0.07	0.08	0.09	0.06	0.11	0.07	0.06	0.04	0.09	0.08	0.05	0.12	0.09	0.07	0.09
MgO	31.66	31.58	31.63	31.48	31.63	31.57	31.47	31.68	31.71	31.56	31.52	31.68	31.70	31.67	31.58	31.59	30.38	31.59	31.52
CaO	0.60	0.59	0.61	0.68	0.62	0.65	0.62	0.57	0.61	0.60	0.59	0.60	0.62	0.65	0.59	0.60	0.66	0.62	0.57
Na2O	0.09	0.09	0.08	0.09	0.08	0.07	0.07	0.05	0.09	0.09	0.08	0.07	0.09	0.07	0.07	0.08	0.08	0.06	0.09
K2O	0.01	0.01	0.01	0.00	0.00	0.00	0.02	0.00	0.00	0.00	0.01	0.01	0.00	0.01	0.01	0.01	0.03	0.01	0.01
Total	100.32	100.02	99.92	99.99	99.80	99.72	99.72	99.99	100.26	100.21	99.81	99.94	100.27	100.19	99.76	99.93	98.65	99.93	99.53
Si	1.915	1.919	1.918	1.917	1.913	1.918	1.919	1.917	1.915	1.919	1.921	1.918	1.913	1.919	1.917	1.914		1.915	1.919
Ti	0.001	0.001	0.000	0.001	0.001	0.000	0.000	0.001	0.000	0.000	0.001	0.000	0.000	0.000	0.000	0.001		0.001	0.000
Al	0.138	0.136	0.135	0.136	0.135	0.136	0.135	0.137	0.134	0.136	0.136	0.134	0.136	0.134	0.136	0.136		0.137	0.138
Cr	0.001	0.000	0.000	0.000	0.000	0.001	0.000	0.000	0.001	0.001	0.001	0.001	0.000	0.000	0.001	0.000		0.001	0.001
Fe2+	0.282	0.280	0.280	0.283	0.284	0.277	0.281	0.280	0.285	0.283	0.276	0.281	0.287	0.279	0.281	0.284		0.281	0.273
Mn	0.002	0.003	0.002	0.002	0.002	0.002	0.003	0.002	0.003	0.002	0.002	0.001	0.003	0.002	0.002	0.004		0.002	0.003
Mg	1.649	1.649	1.653	1.645	1.657	1.653	1.648	1.654	1.654	1.645	1.648	1.656	1.654	1.651	1.654	1.653		1.652	1.652
Ca	0.023	0.022	0.023	0.025	0.023	0.024	0.023	0.021	0.023	0.023	0.022	0.022	0.023	0.024	0.022	0.023		0.023	0.022
Na	0.006	0.006	0.006	0.006	0.005	0.005	0.005	0.003	0.006	0.006	0.006	0.005	0.006	0.005	0.004	0.006		0.004	0.006
K	0.000	0.001	0.000	0.000	0.000	0.000	0.001	0.000	0.000	0.000	0.000	0.000	0.000	0.000	0.001	0.000		0.000	0.001
Sum	4.017	4.016	4.017	4.017	4.021	4.016	4.016	4.015	4.020	4.015	4.013	4.017	4.022	4.015	4.017	4.020		4.017	4.015
Mg#	85.40	85.48	85.51	85.32	85.37	85.65	85.43	85.52	85.30	85.32	85.65	85.49	85.21	85.54	85.48	85.34		85.46	85.82
Al IV	0.068	0.066	0.065	0.066	0.066	0.066	0.065	0.068	0.065	0.066	0.067	0.065	0.065	0.065	0.066	0.066		0.068	0.066
Al VI	0.071	0.071	0.071	0.070	0.069	0.070	0.071	0.069	0.070	0.071	0.070	0.069	0.071	0.070	0.070	0.070		0.069	0.072

1910-11 Opx I, profile 1670

	350	360	370	380	390	400	410	420	430	440	450	460	470	480	490	500	510	520	530
SiO2	54.76	54.46	54.74	54.47	55.06	55.11	54.85	54.63	54.72	54.79	54.81	54.76	54.94	54.79	54.66	54.94	53.97	54.80	54.77
TiO2	0.04	0.01	0.04	0.00	0.03	0.04	0.01	0.03	0.04	0.02	0.02	0.03	0.01	0.03	0.02	0.01	0.04	0.03	0.02
Al2O3	3.34	3.21	3.34	3.53	3.32	3.29	3.26	3.26	3.29	3.29	3.20	3.25	3.25	3.30	3.31	3.28	3.53	3.23	3.34
Cr2O3	0.00	0.05	0.03	0.01	0.04	0.04	0.02	0.04	0.02	0.00	0.00	0.01	0.02	0.01	0.04	0.02	0.03	0.02	0.00
FeO	9.57	9.69	9.56	10.13	9.66	9.71	9.61	9.69	9.76	9.76	9.61	10.01	9.66	9.66	9.72	9.55	9.61	9.66	9.52
MnO	0.08	0.03	0.11	0.11	0.05	0.06	0.06	0.12	0.09	0.06	0.07	0.05	0.07	0.07	0.08	0.07	0.08	0.09	0.07
MgO	31.57	31.54	31.64	30.80	31.63	31.69	31.78	31.67	31.53	31.67	31.59	31.54	31.85	31.55	31.53	31.49	30.52	31.50	31.43
CaO	0.63	0.60	0.60	0.67	0.58	0.60	0.59	0.60	0.60	0.61	0.62	0.61	0.60	0.63	0.61	0.64	0.64	0.64	0.66
Na2O	0.08	0.07	0.09	0.07	0.09	0.10	0.09	0.08	0.08	0.07	0.06	0.08	0.09	0.07	0.08	0.05	0.07	0.06	0.07
K2O	0.01	0.01	0.01	0.00	0.03	0.01	0.03	0.00	0.00	0.00	0.00	0.01	0.01	0.00	0.02	0.00	0.02	0.01	0.00
Total	100.07	99.65	100.15	99.77	100.48	100.64	100.27	100.13	100.12	100.29	99.97	100.35	100.50	100.11	100.07	100.04	98.49	100.02	99.88
Si	1.917	1.916	1.916	1.918	1.920	1.919	1.917	1.914	1.917	1.916	1.921	1.916	1.916	1.918	1.916	1.923		1.920	1.920
Ti	0.001	0.000	0.001	0.000	0.001	0.001	0.000	0.001	0.001	0.001	0.001	0.001	0.000	0.001	0.001	0.000		0.001	0.001
Al	0.138	0.133	0.138	0.146	0.136	0.135	0.134	0.134	0.136	0.135	0.132	0.134	0.134	0.136	0.137	0.135		0.133	0.138
Cr	0.000	0.001	0.001	0.000	0.001	0.001	0.000	0.001	0.000	0.000	0.000	0.000	0.001	0.000	0.001	0.000		0.001	0.000
Fe2+	0.280	0.285	0.280	0.298	0.282	0.283	0.281	0.284	0.286	0.285	0.282	0.293	0.282	0.283	0.285	0.280		0.283	0.279
Mn	0.002	0.001	0.003	0.003	0.001	0.002	0.002	0.004	0.003	0.002	0.002	0.001	0.002	0.002	0.002	0.002		0.003	0.002
Mg	1.648	1.654	1.651	1.616	1.644	1.645	1.656	1.654	1.646	1.651	1.650	1.645	1.656	1.647	1.647	1.643		1.646	1.643
Ca	0.023	0.023	0.022	0.025	0.022	0.022	0.022	0.023	0.022	0.023	0.023	0.023	0.022	0.024	0.023	0.024		0.024	0.025
Na	0.006	0.005	0.006	0.004	0.006	0.006	0.006	0.006	0.006	0.005	0.004	0.005	0.006	0.005	0.006	0.003		0.004	0.005
K	0.000	0.000	0.001	0.000	0.001	0.000	0.001	0.000	0.000	0.000	0.000	0.000	0.000	0.000	0.001	0.000		0.000	0.000
Sum	4.016	4.019	4.017	4.011	4.014	4.015	4.019	4.020	4.017	4.018	4.015	4.019	4.019	4.015	4.018	4.011		4.014	4.013
Mg#	85.48	85.30	85.50	84.43	85.36	85.32	85.49	85.35	85.20	85.28	85.40	84.88	85.45	85.34	85.25	85.44		85.33	85.48
Al IV	0.067	0.065	0.067	0.071	0.066	0.066	0.064	0.066	0.066	0.066	0.065	0.066	0.065	0.067	0.067	0.066		0.066	0.068
Al VI	0.071	0.069	0.071	0.075	0.070	0.069	0.071	0.069	0.070	0.069	0.067	0.069	0.070	0.070	0.071	0.069		0.067	0.071

1910-11 Opx I, profile 1670

	540	550	560	570	580	590	600	610	620	630	640	650	660	670	680	690	700	710	720
SiO2	54.44	54.43	54.86	54.91	54.68	54.81	54.84	54.81	54.92	54.69	54.85	54.73	54.91	54.88	54.73	54.57	54.77	54.73	54.84
TiO2	0.06	0.02	0.05	0.03	0.04	0.03	0.02	0.04	0.01	0.03	0.02	0.01	0.00	0.02	0.00	0.02	0.02	0.04	0.05
Al2O3	3.45	3.53	3.27	3.24	3.31	3.29	3.24	3.21	3.25	3.27	3.30	3.20	3.29	3.25	3.27	3.20	3.26	3.21	3.25
Cr2O3	0.01	0.01	0.00	0.03	0.00	0.00	0.01	0.00	0.04	0.04	0.04	0.00	0.01	0.03	0.00	0.00	0.02	0.03	0.00
FeO	10.18	10.04	9.79	9.35	9.82	9.75	9.59	9.47	9.61	9.64	9.84	9.26	9.66	9.57	9.58	9.50	9.72	9.64	9.71
MnO	0.12	0.06	0.09	0.07	0.09	0.09	0.09	0.07	0.04	0.02	0.07	0.07	0.09	0.04	0.05	0.07	0.07	0.05	0.07
MgO	31.06	30.97	31.56	31.61	31.59	31.51	31.43	31.48	31.75	31.53	31.83	31.50	31.50	31.49	31.56	31.45	31.48	31.39	31.56
CaO	0.69	0.69	0.59	0.60	0.60	0.61	0.60	0.62	0.63	0.59	0.58	0.58	0.59	0.62	0.61	0.62	0.64	0.60	0.63
Na2O	0.03	0.08	0.07	0.07	0.08	0.07	0.09	0.05	0.08	0.07	0.08	0.09	0.06	0.05	0.08	0.08	0.08	0.07	0.07
K2O	0.00	0.00	0.00	0.00	0.00	0.01	0.01	0.00	0.00	0.00	0.01	0.00	0.01	0.01	0.00	0.00	0.00	0.00	0.01
Total	100.04	99.82	100.29	99.90	100.20	100.18	99.91	99.74	100.33	99.88	100.61	99.44	100.11	99.94	99.88	99.50	100.05	99.76	100.18
Si	1.913	1.915	1.918	1.923	1.914	1.918	1.923	1.924	1.918	1.919	1.913	1.925	1.921	1.923	1.919	1.921	1.919	1.922	1.919
Ti	0.002	0.000	0.001	0.001	0.001	0.001	0.001	0.001	0.000	0.001	0.001	0.000	0.000	0.000	0.000	0.000	0.000	0.001	0.001
Al	0.143	0.146	0.135	0.134	0.137	0.136	0.134	0.133	0.134	0.135	0.136	0.133	0.136	0.134	0.135	0.133	0.134	0.133	0.134
Cr	0.000	0.000	0.000	0.001	0.000	0.000	0.000	0.000	0.001	0.001	0.001	0.000	0.000	0.001	0.000	0.000	0.000	0.001	0.000
Fe2+	0.299	0.295	0.286	0.274	0.287	0.285	0.281	0.278	0.281	0.283	0.287	0.272	0.283	0.280	0.281	0.280	0.285	0.283	0.284
Mn	0.004	0.002	0.003	0.002	0.003	0.003	0.003	0.002	0.001	0.001	0.002	0.002	0.003	0.001	0.001	0.002	0.002	0.001	0.002
Mg	1.627	1.624	1.645	1.650	1.649	1.644	1.643	1.647	1.653	1.649	1.655	1.652	1.644	1.645	1.650	1.650	1.645	1.643	1.646
Ca	0.026	0.026	0.022	0.022	0.023	0.023	0.023	0.023	0.023	0.022	0.022	0.022	0.022	0.023	0.023	0.023	0.024	0.023	0.023
Na	0.002	0.005	0.004	0.005	0.005	0.005	0.006	0.003	0.005	0.005	0.005	0.006	0.004	0.003	0.006	0.005	0.005	0.005	0.005
K	0.000	0.000	0.000	0.000	0.000	0.001	0.000	0.000	0.000	0.000	0.000	0.000	0.000	0.000	0.000	0.000	0.000	0.000	0.000
Sum	4.015	4.014	4.015	4.011	4.019	4.016	4.013	4.011	4.017	4.015	4.021	4.012	4.013	4.011	4.016	4.015	4.015	4.013	4.015
Mg#	84.48	84.63	85.19	85.76	85.18	85.23	85.40	85.56	85.47	85.35	85.22	85.86	85.31	85.45	85.45	85.49	85.23	85.31	85.28
Al IV	0.073	0.071	0.067	0.066	0.067	0.066	0.065	0.066	0.065	0.067	0.067	0.064	0.066	0.066	0.065	0.064	0.065	0.066	0.066
Al VI	0.071	0.076	0.069	0.068	0.070	0.070	0.069	0.067	0.069	0.069	0.069	0.070	0.070	0.068	0.071	0.069	0.070	0.068	0.069

1910-11 Opx I, profile 1670

	730	740	750	760	770	780	790	800	810	820	830	840	850	860	870	880	890	900	910
SiO2	54.65	54.48	54.63	55.42	54.67	54.93	54.81	54.77	54.82	54.80	54.62	54.82	54.90	54.70	52.87	54.73	54.83	54.72	54.12
TiO2	0.04	0.02	0.03	0.01	0.00	0.02	0.04	0.04	0.02	0.00	0.03	0.03	0.01	0.02	0.05	0.03	0.04	0.01	0.06
Al2O3	3.27	3.31	3.27	3.35	3.25	3.28	3.33	3.25	3.18	3.30	3.32	3.28	3.30	3.26	3.41	3.27	3.28	3.27	6.15
Cr2O3	0.01	0.02	0.02	0.00	0.03	0.00	0.00	0.00	0.00	0.00	0.00	0.03	0.04	0.00	0.03	0.01	0.00	0.00	0.03
FeO	9.52	9.56	9.72	9.51	9.55	9.71	9.71	9.69	9.58	9.74	9.71	9.95	9.52	9.70	10.17	9.41	9.73	9.66	8.49
MnO	0.10	0.11	0.11	0.07	0.06	0.12	0.04	0.09	0.08	0.08	0.06	0.09	0.11	0.07	0.09	0.08	0.09	0.07	0.11
MgO	31.64	31.55	31.55	31.81	31.52	31.60	31.43	31.57	31.50	31.53	31.51	31.68	31.43	31.42	29.85	31.50	31.46	31.66	25.62
CaO	0.60	0.62	0.62	0.65	0.62	0.60	0.59	0.58	0.61	0.59	0.61	0.62	0.63	0.63	0.73	0.62	0.62	0.59	1.07
Na2O	0.07	0.09	0.09	0.07	0.07	0.07	0.06	0.06	0.08	0.06	0.07	0.06	0.07	0.08	0.06	0.07	0.07	0.09	0.07
K2O	0.01	0.01	0.01	0.01	0.00	0.00	0.00	0.00	0.00	0.01	0.00	0.00	0.03	0.00	0.00	0.02	0.00	0.00	0.13
Total	99.87	99.75	100.03	100.91	99.76	100.33	100.01	100.03	99.87	100.11	99.92	100.56	100.03	99.88	97.26	99.74	100.12	100.08	95.83
Si	1.917	1.915	1.916	1.922	1.920	1.919	1.920	1.919	1.923	1.919	1.916	1.914	1.922	1.920		1.921	1.920	1.917	
Ti	0.001	0.001	0.001	0.000	0.000	0.000	0.001	0.001	0.001	0.000	0.001	0.001	0.000	0.000		0.001	0.001	0.000	
Al	0.135	0.137	0.135	0.137	0.135	0.135	0.138	0.134	0.132	0.136	0.137	0.135	0.136	0.135		0.135	0.135	0.135	
Cr	0.000	0.001	0.000	0.000	0.001	0.000	0.000	0.000	0.000	0.000	0.000	0.001	0.001	0.000		0.000	0.000	0.000	
Fe2+	0.279	0.281	0.285	0.276	0.280	0.284	0.284	0.284	0.281	0.285	0.285	0.291	0.279	0.285		0.276	0.285	0.283	
Mn	0.003	0.003	0.003	0.002	0.002	0.003	0.001	0.003	0.002	0.002	0.002	0.003	0.003	0.002		0.002	0.003	0.002	
Mg	1.654	1.653	1.649	1.645	1.650	1.646	1.641	1.649	1.647	1.646	1.648	1.649	1.640	1.644		1.648	1.642	1.653	
Ca	0.022	0.023	0.023	0.024	0.023	0.023	0.022	0.022	0.023	0.022	0.023	0.023	0.024	0.024		0.023	0.023	0.022	
Na	0.005	0.006	0.006	0.005	0.004	0.005	0.004	0.004	0.005	0.004	0.005	0.004	0.005	0.005		0.005	0.005	0.006	
K	0.000	0.000	0.000	0.001	0.000	0.000	0.000	0.000	0.000	0.000	0.000	0.000	0.001	0.000		0.001	0.000	0.000	
Sum	4.017	4.019	4.019	4.012	4.015	4.015	4.012	4.015	4.013	4.015	4.017	4.019	4.012	4.015		4.013	4.014	4.018	
Mg#	85.57	85.47	85.26	85.63	85.49	85.28	85.25	85.31	85.43	85.24	85.26	85.00	85.46	85.23		85.65	85.21	85.38	
Al IV	0.066	0.067	0.066	0.066	0.066	0.065	0.068	0.066	0.065	0.066	0.067	0.067	0.066	0.065		0.066	0.066	0.065	
Al VI	0.069	0.070	0.070	0.072	0.069	0.070	0.070	0.068	0.068	0.070	0.070	0.068	0.071	0.070		0.070	0.069	0.071	

1910-11 Opx I, profile 1670

	920	930	940	950	960	970	980	990	1000	1010	1020	1030	1040	1050	1060	1070	1080	1090	1100
SiO2	54.76	54.83	54.89	54.75	54.89	43.15	54.62	54.77	55.13	54.67	54.61	53.96	55.08	55.11	54.89	54.75	54.76	55.07	54.54
TiO2	0.00	0.03	0.05	0.02	0.01	0.08	0.02	0.00	0.05	0.03	0.04	0.03	0.00	0.06	0.02	0.04	0.03	0.01	0.01
Al2O3	3.26	3.45	3.29	3.30	3.30	4.50	3.25	3.26	3.23	3.31	3.94	4.28	3.29	3.25	3.21	3.25	3.23	3.22	3.28
Cr2O3	0.03	0.01	0.00	0.04	0.01	0.02	0.02	0.00	0.05	0.00	0.03	0.01	0.01	0.00	0.02	0.02	0.01	0.00	0.00
FeO	9.39	9.59	9.59	10.02	9.77	9.83	9.77	9.66	9.73	9.48	9.50	9.38	9.59	9.64	9.49	9.90	9.50	9.59	9.77
MnO	0.10	0.06	0.12	0.07	0.04	0.10	0.07	0.07	0.10	0.09	0.07	0.05	0.04	0.09	0.09	0.07	0.07	0.09	0.07
MgO	31.51	31.28	31.65	31.27	31.43	19.53	31.75	31.51	31.68	31.55	30.76	29.93	31.57	31.76	31.53	31.64	31.56	31.53	31.52
CaO	0.62	0.62	0.61	0.61	0.60	0.76	0.59	0.63	0.64	0.61	1.01	0.67	0.62	0.59	0.59	0.63	0.65	0.61	0.61
Na2O	0.08	0.05	0.10	0.06	0.07	0.05	0.09	0.07	0.05	0.08	0.11	0.06	0.08	0.06	0.09	0.09	0.07	0.08	0.07
K2O	0.01	0.02	0.01	0.01	0.00	0.04	0.01	0.00	0.02	0.00	0.00	0.04	0.00	0.00	0.00	0.02	0.00	0.01	0.01
Total	99.74	99.94	100.29	100.15	100.12	78.05	100.19	99.96	100.68	99.82	100.07	98.41	100.27	100.56	99.92	100.41	99.88	100.22	99.89
Si	1.922	1.921	1.918	1.919	1.921		1.913	1.920	1.920	1.918			1.923	1.920	1.923	1.914	1.920	1.924	1.915
Ti	0.000	0.001	0.001	0.001	0.000		0.001	0.000	0.001	0.001			0.000	0.002	0.001	0.001	0.001	0.000	0.000
Al	0.135	0.142	0.135	0.136	0.136		0.134	0.135	0.133	0.137			0.135	0.133	0.132	0.134	0.134	0.133	0.136
Cr	0.001	0.000	0.000	0.001	0.000		0.001	0.000	0.001	0.000			0.000	0.000	0.000	0.001	0.000	0.000	0.000
Fe2+	0.276	0.281	0.280	0.294	0.286		0.286	0.283	0.283	0.278			0.280	0.281	0.278	0.290	0.279	0.280	0.287
Mn	0.003	0.002	0.003	0.002	0.001		0.002	0.002	0.003	0.003			0.001	0.003	0.003	0.002	0.002	0.003	0.002
Mg	1.649	1.634	1.649	1.634	1.640		1.658	1.647	1.644	1.650			1.643	1.650	1.647	1.649	1.650	1.643	1.650
Ca	0.023	0.023	0.023	0.023	0.022		0.022	0.023	0.024	0.023			0.023	0.022	0.022	0.024	0.024	0.023	0.023
Na	0.005	0.004	0.007	0.004	0.005		0.006	0.005	0.004	0.005			0.005	0.004	0.006	0.006	0.005	0.006	0.005
K	0.001	0.001	0.000	0.000	0.000		0.000	0.000	0.001	0.000			0.000	0.000	0.000	0.001	0.000	0.001	0.000
Sum	4.013	4.009	4.017	4.014	4.012		4.022	4.015	4.014	4.015			4.011	4.014	4.013	4.021	4.014	4.012	4.019
Mg#	85.66	85.33	85.48	84.75	85.15		85.29	85.34	85.31	85.58			85.44	85.45	85.56	85.04	85.54	85.44	85.18
Al IV	0.065	0.070	0.065	0.068	0.066		0.066	0.065	0.066	0.067			0.065	0.067	0.064	0.065	0.066	0.063	0.066
Al VI	0.070	0.073	0.070	0.069	0.071		0.069	0.070	0.068	0.070			0.070	0.067	0.068	0.069	0.069	0.070	0.071

1910-11 Opx I, profile 1670

	1110	1120	1130	1140	1150	1160	1170	1180	1190	1200	1210	1220	1230	1240	1250	1260	1270	1280	1290
SiO2	54.66	54.74	54.76	52.67	54.54	54.75	54.93	54.92	54.57	54.68	54.57	54.61	54.86	54.75	54.88	54.73	54.79	54.90	54.87
TiO2	0.03	0.03	0.02	0.02	0.03	0.02	0.04	0.05	0.03	0.00	0.07	0.03	0.02	0.02	0.03	0.01	0.03	0.02	0.02
Al2O3	3.38	3.24	3.29	4.55	3.26	3.24	3.23	3.22	3.30	3.24	3.35	3.29	3.24	3.23	3.32	3.30	3.25	3.27	3.25
Cr2O3	0.05	0.00	0.05	0.01	0.00	0.01	0.01	0.05	0.02	0.00	0.01	0.00	0.02	0.00	0.00	0.03	0.01	0.00	0.04
FeO	9.62	9.66	9.45	9.12	9.68	9.63	9.83	9.79	9.47	9.86	9.79	9.82	9.61	9.75	9.92	9.50	9.66	9.60	9.73
MnO	0.04	0.03	0.08	0.05	0.07	0.12	0.04	0.11	0.08	0.05	0.10	0.10	0.08	0.05	0.10	0.02	0.07	0.09	0.09
MgO	31.11	31.56	31.55	27.89	31.47	31.57	31.52	31.71	31.49	31.55	31.41	31.70	31.54	31.44	31.55	31.52	31.84	31.74	31.43
CaO	0.64	0.61	0.60	0.85	0.61	0.61	0.60	0.64	0.62	0.60	0.70	0.62	0.62	0.57	0.62	0.59	0.63	0.58	0.62
Na2O	0.07	0.08	0.07	0.10	0.07	0.07	0.05	0.09	0.06	0.07	0.03	0.08	0.07	0.06	0.10	0.06	0.05	0.06	0.09
K2O	0.01	0.00	0.00	0.07	0.01	0.00	0.01	0.00	0.00	0.00	0.00	0.01	0.00	0.00	0.00	0.00	0.00	0.02	0.00
Total	99.59	99.94	99.86	95.30	99.72	100.01	100.25	100.57	99.63	100.06	100.03	100.25	100.07	99.86	100.52	99.76	100.33	100.26	100.12
Si	1.923	1.919	1.920		1.917	1.919	1.921	1.916	1.918	1.917	1.914	1.912	1.921	1.922	1.916	1.920	1.915	1.918	1.921
Ti	0.001	0.001	0.000		0.001	0.001	0.001	0.001	0.001	0.000	0.002	0.001	0.001	0.000	0.001	0.000	0.001	0.000	0.001
Al	0.140	0.134	0.136		0.135	0.134	0.133	0.132	0.137	0.134	0.138	0.136	0.134	0.133	0.137	0.137	0.134	0.134	0.134
Cr	0.001	0.000	0.001		0.000	0.000	0.000	0.001	0.001	0.000	0.000	0.000	0.001	0.000	0.000	0.001	0.000	0.000	0.001
Fe2+	0.283	0.283	0.277		0.285	0.282	0.287	0.286	0.278	0.289	0.287	0.287	0.281	0.286	0.290	0.279	0.282	0.281	0.285
Mn	0.001	0.001	0.002		0.002	0.003	0.001	0.003	0.002	0.002	0.003	0.003	0.002	0.001	0.003	0.001	0.002	0.003	0.003
Mg	1.631	1.650	1.649		1.649	1.649	1.643	1.649	1.650	1.649	1.642	1.655	1.646	1.645	1.642	1.649	1.659	1.653	1.641
Ca	0.024	0.023	0.023		0.023	0.023	0.022	0.024	0.023	0.023	0.026	0.023	0.023	0.021	0.023	0.022	0.024	0.022	0.023
Na	0.005	0.005	0.005		0.005	0.004	0.003	0.006	0.004	0.005	0.002	0.005	0.004	0.004	0.007	0.004	0.003	0.004	0.006
K	0.000	0.000	0.000		0.001	0.000	0.000	0.000	0.000	0.000	0.000	0.000	0.000	0.000	0.000	0.000	0.000	0.001	0.000
Sum	4.009	4.016	4.013		4.017	4.016	4.013	4.019	4.014	4.018	4.016	4.022	4.014	4.013	4.018	4.013	4.019	4.016	4.014
Mg#	85.21	85.36	85.62		85.26	85.40	85.13	85.22	85.58	85.09	85.12	85.22	85.42	85.19	84.99	85.53	85.47	85.47	85.20
Al IV	0.069	0.066	0.066		0.066	0.066	0.066	0.065	0.068	0.065	0.070	0.067	0.067	0.065	0.066	0.067	0.067	0.065	0.066
Al VI	0.071	0.069	0.070		0.070	0.068	0.067	0.068	0.069	0.070	0.068	0.070	0.068	0.069	0.071	0.070	0.068	0.070	0.069

1910-11 Opx I, profile 1670

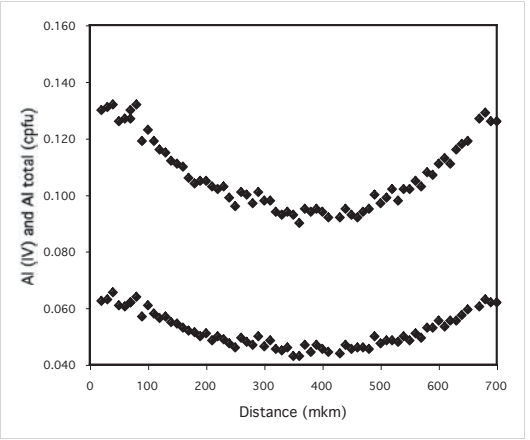
	1300	1310	1320	1330	1340	1350	1360	1370	1380	1390	1400	1410	1420	1430	1440	1450	1460	1470	1480
SiO2	54.94	54.93	54.94	54.96	55.05	55.22	54.95	54.97	54.70	54.89	55.18	55.09	53.93	55.11	54.76	54.68	55.00	55.00	54.90
TiO2	0.00	0.03	0.04	0.02	0.02	0.03	0.02	0.03	0.03	0.02	0.04	0.02	0.04	0.03	0.02	0.01	0.01	0.01	0.02
Al2O3	3.27	3.31	3.24	3.25	3.27	3.27	3.31	3.48	3.22	3.32	3.30	3.30	4.07	3.27	3.26	3.27	3.30	3.26	3.27
Cr2O3	0.00	0.02	0.00	0.00	0.03	0.03	0.00	0.00	0.00	0.03	0.00	0.00	0.02	0.00	0.02	0.02	0.03	0.02	0.01
FeO	9.60	9.66	9.47	9.42	9.73	9.47	9.52	9.48	9.49	9.50	9.81	9.46	9.19	9.58	9.58	9.58	9.40	9.66	9.50
MnO	0.03	0.10	0.08	0.10	0.05	0.10	0.09	0.07	0.08	0.06	0.09	0.10	0.09	0.12	0.09	0.09	0.10	0.05	0.09
MgO	31.39	31.60	31.55	31.45	31.75	31.51	31.34	30.94	31.57	31.51	31.74	31.80	29.43	31.47	31.54	31.66	31.70	31.73	31.27
CaO	0.60	0.58	0.62	0.60	0.58	0.61	0.63	0.62	0.59	0.61	0.59	0.60	0.70	0.63	0.61	0.64	0.60	0.64	0.61
Na2O	0.08	0.07	0.08	0.08	0.07	0.10	0.10	0.09	0.06	0.07	0.07	0.07	0.07	0.06	0.09	0.07	0.08	0.06	0.07
K2O	0.01	0.01	0.01	0.00	0.00	0.01	0.01	0.03	0.00	0.00	0.02	0.00	0.04	0.02	0.01	0.01	0.00	0.01	0.00
Total	99.92	100.31	100.02	99.87	100.54	100.36	99.96	99.70	99.74	100.01	100.81	100.43	97.57	100.30	99.98	100.02	100.22	100.42	99.73
Si	1.925	1.919	1.923	1.926	1.919	1.926	1.925	1.929	1.920	1.921	1.919	1.920		1.924	1.919	1.916	1.921	1.919	1.927
Ti	0.000	0.001	0.001	0.000	0.000	0.001	0.001	0.001	0.001	0.001	0.001	0.001		0.001	0.000	0.000	0.000	0.000	0.001
Al	0.135	0.136	0.134	0.134	0.134	0.134	0.136	0.144	0.133	0.137	0.135	0.135		0.135	0.135	0.135	0.136	0.134	0.135
Cr	0.000	0.000	0.000	0.000	0.001	0.001	0.000	0.000	0.000	0.001	0.000	0.000		0.000	0.000	0.001	0.001	0.001	0.000
Fe2+	0.281	0.282	0.277	0.276	0.284	0.276	0.279	0.278	0.279	0.278	0.285	0.276		0.280	0.281	0.281	0.275	0.282	0.279
Mn	0.001	0.003	0.002	0.003	0.001	0.003	0.003	0.002	0.002	0.002	0.003	0.003		0.003	0.003	0.003	0.003	0.001	0.003
Mg	1.640	1.646	1.646	1.642	1.650	1.638	1.636	1.618	1.652	1.644	1.645	1.652		1.638	1.648	1.654	1.651	1.651	1.636
Ca	0.023	0.022	0.023	0.022	0.022	0.023	0.023	0.023	0.022	0.023	0.022	0.022		0.024	0.023	0.024	0.023	0.024	0.023
Na	0.006	0.004	0.005	0.005	0.005	0.007	0.007	0.006	0.004	0.005	0.004	0.005		0.004	0.006	0.005	0.006	0.004	0.004
K	0.000	0.000	0.000	0.000	0.000	0.000	0.000	0.001	0.000	0.000	0.001	0.000		0.001	0.000	0.000	0.000	0.000	0.000
Sum	4.010	4.014	4.012	4.009	4.016	4.009	4.010	4.002	4.014	4.011	4.015	4.014		4.010	4.016	4.018	4.014	4.016	4.007
Mg#	85.37	85.37	85.60	85.61	85.32	85.58	85.43	85.34	85.55	85.54	85.23	85.68		85.40	85.43	85.48	85.72	85.41	85.43
Al IV	0.065	0.067	0.066	0.065	0.065	0.065	0.066	0.070	0.066	0.068	0.066	0.066		0.066	0.065	0.066	0.066	0.066	0.067
Al VI	0.071	0.069	0.069	0.070	0.069	0.069	0.071	0.075	0.068	0.070	0.069	0.069		0.069	0.071	0.070	0.071	0.069	0.069

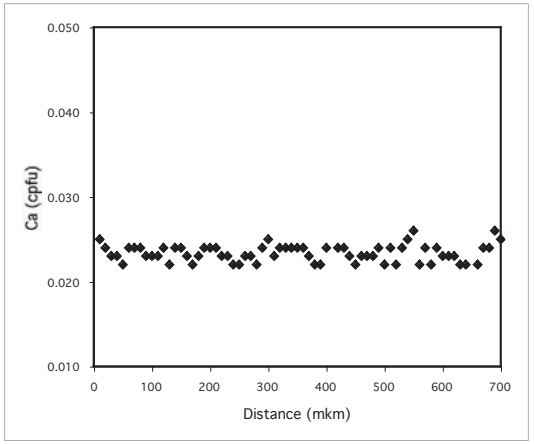
1910-11 Opx I, profile 1670

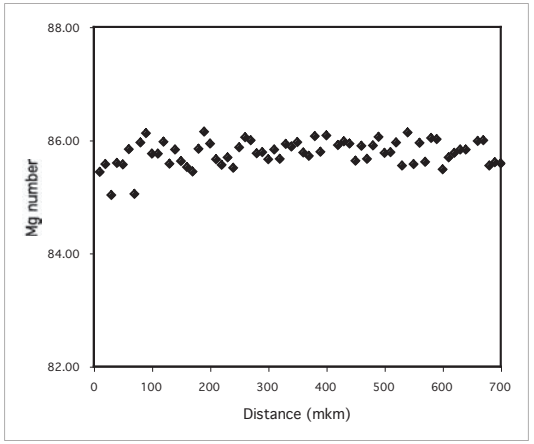
	1490	1500	1510	1520	1530	1540	1550	1560	1570	1580	1590	1600	1610	1620	1630	1640	1650	1660	1670
SiO2	54.72	54.61	55.15	54.59	54.83	54.75	54.66	54.92	54.63	54.67	54.76	54.85	54.68	54.64	54.73	54.99	55.76	54.39	54.54
TiO2	0.05	0.00	0.04	0.01	0.04	0.03	0.02	0.05	0.04	0.03	0.03	0.03	0.03	0.02	0.03	0.03	0.05	0.03	0.02
Al2O3	3.30	3.24	3.30	3.25	3.34	3.19	3.80	3.23	3.26	3.31	3.26	3.32	3.31	3.24	3.81	3.89	3.76	3.57	3.29
Cr2O3	0.00	0.03	0.03	0.00	0.01	0.04	0.00	0.00	0.02	0.02	0.00	0.00	0.03	0.00	0.01	0.00	0.01	0.07	0.01
FeO	9.72	9.64	9.59	9.63	9.53	9.39	9.52	9.52	9.64	9.67	9.51	9.70	9.66	9.77	9.60	9.48	9.23	9.53	9.61
MnO	0.05	0.06	0.06	0.07	0.07	0.05	0.08	0.10	0.05	0.05	0.06	0.08	0.10	0.09	0.07	0.07	0.09	0.05	0.08
MgO	31.58	31.56	31.33	31.93	31.41	31.60	31.09	31.68	31.69	31.66	31.49	31.56	31.45	31.79	31.00	30.50	32.13	30.95	31.71
CaO	0.56	0.61	0.63	0.60	0.68	0.60	0.85	0.59	0.62	0.61	0.61	0.66	0.66	0.59	0.63	0.65	0.61	0.65	0.57
Na2O	0.07	0.07	0.10	0.07	0.07	0.05	0.10	0.07	0.07	0.09	0.07	0.07	0.08	0.07	0.06	0.09	0.08	0.07	0.07
K2O	0.00	0.01	0.00	0.01	0.02	0.00	0.00	0.01	0.00	0.00	0.01	0.00	0.00	0.00	0.04	0.01	0.01	0.03	0.00
Total	100.05	99.82	100.23	100.16	100.01	99.68	100.10	100.16	100.02	100.11	99.80	100.25	100.00	100.22	99.97	99.72	101.72	99.34	99.90
Si	1.917	1.918	1.926	1.911	1.920	1.922		1.920	1.915	1.914	1.921	1.918	1.917	1.913	1.917	1.928		1.918	1.914
Ti	0.001	0.000	0.001	0.000	0.001	0.001		0.001	0.001	0.001	0.001	0.001	0.001	0.001	0.001	0.001		0.001	0.000
Al	0.136	0.134	0.136	0.134	0.138	0.132		0.133	0.135	0.137	0.135	0.137	0.137	0.134	0.157	0.161		0.148	0.136
Cr	0.000	0.001	0.001	0.000	0.000	0.001		0.000	0.001	0.000	0.000	0.000	0.001	0.000	0.000	0.000		0.002	0.000
Fe2+	0.285	0.283	0.280	0.282	0.279	0.276		0.278	0.283	0.283	0.279	0.284	0.283	0.286	0.281	0.278		0.281	0.282
Mn	0.002	0.002	0.002	0.002	0.002	0.001		0.003	0.002	0.002	0.002	0.002	0.003	0.003	0.002	0.002		0.001	0.002
Mg	1.649	1.652	1.632	1.667	1.640	1.654		1.651	1.656	1.653	1.647	1.645	1.644	1.659	1.619	1.594		1.627	1.659
Ca	0.021	0.023	0.024	0.022	0.026	0.023		0.022	0.023	0.023	0.023	0.025	0.025	0.022	0.024	0.024		0.025	0.021
Na	0.005	0.005	0.007	0.005	0.005	0.004		0.005	0.005	0.006	0.005	0.004	0.005	0.005	0.004	0.006		0.005	0.005
K	0.000	0.000	0.000	0.000	0.001	0.000		0.000	0.000	0.000	0.000	0.000	0.000	0.000	0.002	0.001		0.001	0.000
Sum	4.016	4.018	4.008	4.024	4.012	4.013		4.015	4.019	4.019	4.013	4.015	4.016	4.022	4.006	3.994		4.009	4.020
Mg#	85.26	85.37	85.36	85.53	85.46	85.70		85.59	85.40	85.38	85.51	85.28	85.31	85.30	85.21	85.15		85.27	85.47
Al IV	0.067	0.065	0.066	0.065	0.067	0.066		0.065	0.067	0.067	0.066	0.068	0.068	0.066	0.077	0.078		0.073	0.066
Al VI	0.070	0.069	0.070	0.070	0.071	0.067		0.068	0.069	0.071	0.069	0.070	0.070	0.069	0.081	0.083		0.075	0.071

1910-11 Opx I, profile 1670

	10	20	30	40	50	60	70	80	90	100
SiO2	55.02	55.13	55.06	55.32	55.00	55.65	54.99	55.20	55.37	55.27
TiO2	0.01	0.01	0.03	0.03	0.01	0.00	0.03	0.01	0.04	0.02
Al2O3	3.14	3.17	3.21	3.06	3.07	3.10	3.19	2.89	2.99	2.88
Cr2O3	0.03	0.03	0.08	0.02	0.00	0.02	0.02	0.01	0.02	0.00
FeO	9.49	9.41	9.82	9.37	9.41	9.29	9.76	9.18	9.06	9.27
MnO	0.10	0.01	0.08	0.07	0.13	0.05	0.06	0.10	0.09	0.01
NiO	0.27	0.26	0.25	0.21	0.29	0.18	0.25	0.21	0.28	0.21
MgO	31.23	31.28	31.31	31.20	31.31	31.59	31.15	31.52	31.60	31.31
CaO	0.67	0.63	0.62	0.61	0.59	0.65	0.65	0.63	0.62	0.60
Na2O	0.08	0.09	0.08	0.08	0.07	0.06	0.07	0.07	0.05	0.07
K2O	0.00	0.01	0.00	0.00	0.02	0.00	0.02	0.00	0.00	0.01
Total	100.03	100.02	100.53	99.96	99.90	100.58	100.19	99.80	100.12	99.65
Si	1.928	1.930	1.923	1.936	1.929	1.935	1.926	1.935	1.934	1.939
Ti	0.000	0.000	0.001	0.001	0.000	0.000	0.001	0.000	0.001	0.001
Al	0.130	0.131	0.132	0.126	0.127	0.127	0.132	0.119	0.123	0.119
Cr	0.001	0.001	0.002	0.000	0.000	0.001	0.000	0.000	0.000	0.000
Fe2+	0.278	0.275	0.287	0.274	0.276	0.270	0.286	0.269	0.265	0.272
Mn	0.003	0.000	0.002	0.002	0.004	0.001	0.002	0.003	0.003	0.000
Ni	0.007	0.007	0.007	0.006	0.008	0.005	0.007	0.006	0.008	0.006
Mg	1.631	1.632	1.630	1.628	1.637	1.637	1.627	1.647	1.645	1.638
Ca	0.025	0.024	0.023	0.023	0.022	0.024	0.024	0.024	0.023	0.023
Na	0.006	0.006	0.005	0.006	0.005	0.004	0.005	0.005	0.003	0.004
K	0.000	0.000	0.000	0.000	0.001	0.000	0.001	0.000	0.000	0.001
Sum	4.009	4.007	4.012	4.002	4.010	4.004	4.010	4.008	4.005	4.003
Mg#	85.44	85.58	85.03	85.59	85.57	85.84	85.05	85.96	86.13	85.76
Al IV	0.063	0.063	0.066	0.061	0.061	0.062	0.064	0.057	0.061	0.058
Al VI	0.068	0.068	0.067	0.065	0.067	0.065	0.068	0.062	0.062	0.061







1910-11 Opx II, profile 700

	110	120	130	140	150	160	170	180	190	200	210	220	230	240	250	260	270	280	290	300
SiO2	55.25	55.41	55.25	55.62	55.50	55.55	55.60	55.58	55.43	55.39	55.29	55.50	55.78	55.63	55.73	55.31	55.93	55.66	55.75	55.44
TiO2	0.03	0.04	0.04	0.06	0.03	0.05	0.01	0.00	0.05	0.01	0.03	0.02	0.00	0.00	0.02	0.01	0.03	0.03	0.01	0.06
Al2O3	2.79	2.78	2.71	2.69	2.66	2.59	2.54	2.53	2.53	2.49	2.48	2.50	2.41	2.32	2.44	2.42	2.37	2.45	2.39	2.37
Cr2O3	0.00	0.01	0.00	0.00	0.00	0.07	0.06	0.02	0.00	0.00	0.02	0.02	0.04	0.00	0.04	0.02	0.00	0.02	0.04	0.00
FeO	9.22	9.16	9.50	9.28	9.39	9.58	9.60	9.26	9.03	9.19	9.46	9.51	9.41	9.61	9.24	9.17	9.29	9.40	9.34	9.52
MnO	0.07	0.10	0.06	0.07	0.01	0.12	0.11	0.10	0.06	0.08	0.07	0.08	0.10	0.08	0.04	0.15	0.08	0.08	0.09	0.08
NiO	0.27	0.23	0.23	0.21	0.22	0.19	0.26	0.26	0.22	0.23	0.24	0.26	0.20	0.21	0.22	0.20	0.23	0.22	0.22	0.24
MgO	31.11	31.45	31.62	31.57	31.41	31.73	31.60	31.48	31.49	31.53	31.66	31.60	31.64	31.85	31.45	31.68	31.97	31.69	31.65	31.90
CaO	0.61	0.63	0.59	0.65	0.65	0.63	0.60	0.60	0.63	0.64	0.63	0.61	0.61	0.58	0.59	0.61	0.62	0.59	0.64	0.67
Na2O	0.07	0.04	0.06	0.07	0.08	0.09	0.04	0.07	0.06	0.09	0.06	0.09	0.07	0.06	0.07	0.07	0.07	0.05	0.09	0.07
K2O	0.01	0.00	0.00	0.02	0.01	0.01	0.00	0.01	0.02	0.00	0.02	0.00	0.00	0.00	0.00	0.01	0.00	0.01	0.01	0.00
Total	99.43	99.85	100.06	100.24	99.95	100.59	100.42	99.90	99.50	99.64	99.95	100.19	100.28	100.33	99.85	99.64	100.57	100.19	100.21	100.35
Si	1.943	1.940	1.935	1.941	1.943	1.936	1.941	1.946	1.947	1.945	1.938	1.941	1.947	1.943	1.951	1.943	1.945	1.945	1.947	1.937
Ti	0.001	0.001	0.001	0.002	0.001	0.001	0.000	0.000	0.001	0.000	0.001	0.000	0.000	0.000	0.001	0.000	0.001	0.001	0.000	0.002
Al	0.116	0.115	0.112	0.111	0.110	0.106	0.104	0.105	0.105	0.103	0.102	0.103	0.099	0.096	0.101	0.100	0.097	0.101	0.098	0.098
Cr	0.000	0.000	0.000	0.000	0.000	0.002	0.002	0.000	0.000	0.000	0.001	0.001	0.001	0.000	0.001	0.001	0.000	0.000	0.001	0.000
Fe2+	0.271	0.268	0.278	0.271	0.275	0.279	0.280	0.271	0.265	0.270	0.277	0.278	0.275	0.281	0.270	0.269	0.270	0.274	0.273	0.278
Mn	0.002	0.003	0.002	0.002	0.000	0.004	0.003	0.003	0.002	0.002	0.002	0.002	0.003	0.002	0.001	0.004	0.002	0.002	0.003	0.002
Ni	0.008	0.006	0.006	0.006	0.006	0.005	0.007	0.007	0.006	0.006	0.007	0.007	0.006	0.006	0.006	0.006	0.006	0.006	0.006	0.007
Mg	1.632	1.642	1.650	1.642	1.639	1.648	1.644	1.644	1.648	1.650	1.655	1.648	1.647	1.658	1.641	1.659	1.658	1.651	1.648	1.661
Ca	0.023	0.024	0.022	0.024	0.024	0.023	0.022	0.023	0.024	0.024	0.024	0.023	0.023	0.022	0.022	0.023	0.023	0.022	0.024	0.025
Na	0.005	0.003	0.004	0.005	0.006	0.006	0.003	0.005	0.004	0.006	0.004	0.006	0.005	0.004	0.005	0.004	0.005	0.003	0.006	0.005
K	0.000	0.000	0.000	0.001	0.000	0.000	0.000	0.000	0.001	0.000	0.001	0.000	0.000	0.000	0.000	0.001	0.000	0.000	0.000	0.000
Sum	4.001	4.003	4.011	4.005	4.004	4.012	4.007	4.004	4.002	4.007	4.012	4.010	4.005	4.011	4.000	4.009	4.008	4.006	4.006	4.015
Mg#	85.76	85.97	85.58	85.83	85.63	85.52	85.45	85.85	86.15	85.94	85.66	85.57	85.69	85.51	85.87	86.05	86.00	85.77	85.79	85.66
Al IV	0.057	0.057	0.055	0.055	0.053	0.052	0.052	0.050	0.051	0.049	0.050	0.049	0.048	0.046	0.050	0.048	0.047	0.050	0.047	0.049
Al VI	0.060	0.058	0.057	0.057	0.057	0.054	0.053	0.055	0.054	0.055	0.052	0.054	0.052	0.050	0.052	0.052	0.050	0.051	0.052	0.050

1910-11 Opx II, profile 700

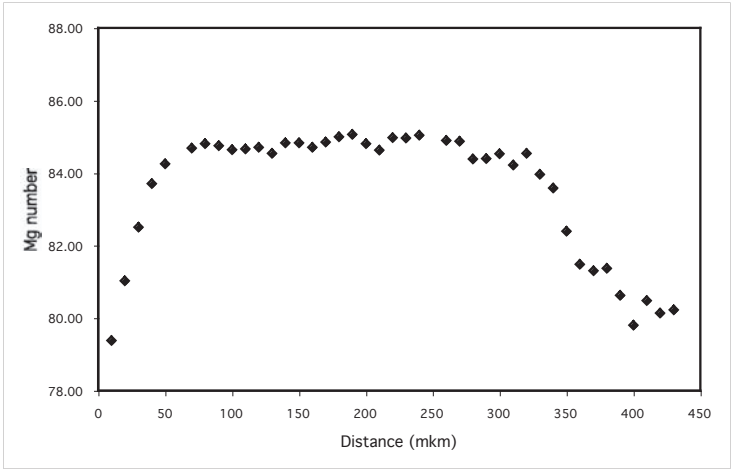
	310	320	330	340	350	360	370	380	390	400	410	420	430	440	450	460	470	480	490	500
SiO2	55.62	55.73	55.49	55.89	55.69	55.62	55.59	55.90	55.72	55.83	51.07	55.54	55.37	55.40	55.53	55.88	55.80	55.35	55.52	55.47
TiO2	0.04	0.03	0.02	0.01	0.01	0.02	0.00	0.04	0.01	0.02	0.07	0.05	0.04	0.00	0.03	0.02	0.00	0.06	0.03	0.06
Al2O3	2.27	2.27	2.28	2.27	2.19	2.30	2.27	2.32	2.29	2.24	7.78	2.24	2.29	2.24	2.24	2.28	2.31	2.42	2.34	2.41
Cr2O3	0.00	0.00	0.03	0.00	0.00	0.04	0.00	0.03	0.00	0.00	0.00	0.00	0.00	0.05	0.02	0.00	0.05	0.01	0.03	0.00
FeO	9.32	9.49	9.24	9.33	9.30	9.39	9.39	9.27	9.33	9.19	8.08	9.33	9.25	9.22	9.48	9.22	9.41	9.29	9.12	9.39
MnO	0.10	0.06	0.11	0.10	0.06	0.04	0.04	0.12	0.11	0.09	0.06	0.15	0.09	0.02	0.07	0.03	0.09	0.09	0.04	0.02
NiO	0.25	0.22	0.20	0.20	0.23	0.19	0.26	0.26	0.20	0.19	0.14	0.24	0.26	0.26	0.22	0.27	0.16	0.22	0.24	0.24
MgO	31.67	31.82	31.64	31.84	31.99	31.82	31.59	32.07	31.58	31.84	24.09	31.95	31.76	31.56	31.72	31.53	31.53	31.70	31.62	31.78
CaO	0.61	0.64	0.63	0.64	0.64	0.63	0.61	0.60	0.59	0.65	0.99	0.64	0.63	0.60	0.60	0.62	0.62	0.61	0.64	0.60
Na2O	0.07	0.08	0.05	0.10	0.06	0.06	0.07	0.05	0.05	0.05	0.08	0.09	0.04	0.04	0.04	0.06	0.07	0.05	0.07	0.05
K2O	0.01	0.00	0.00	0.00	0.00	0.01	0.01	0.01	0.00	0.02	0.12	0.00	0.02	0.01	0.00	0.00	0.00	0.01	0.01	0.03
Total	99.95	100.34	99.68	100.39	100.16	100.13	99.81	100.66	99.88	100.12	92.46	100.20	99.74	99.40	99.95	99.90	100.05	99.80	99.67	100.02
Si	1.948	1.945	1.948	1.948	1.946	1.945	1.950	1.944	1.951	1.950		1.942	1.944	1.950	1.946	1.955	1.951	1.941	1.948	1.942
Ti	0.001	0.001	0.000	0.000	0.000	0.001	0.000	0.001	0.000	0.001		0.001	0.001	0.000	0.001	0.001	0.000	0.002	0.001	0.001
Al	0.094	0.093	0.094	0.093	0.090	0.095	0.094	0.095	0.094	0.092		0.092	0.095	0.093	0.092	0.094	0.095	0.100	0.097	0.099
Cr	0.000	0.000	0.001	0.000	0.000	0.001	0.000	0.001	0.000	0.000		0.000	0.000	0.001	0.001	0.000	0.001	0.000	0.001	0.000
Fe2+	0.273	0.277	0.271	0.272	0.272	0.275	0.275	0.269	0.273	0.268		0.273	0.271	0.271	0.278	0.270	0.275	0.272	0.268	0.275
Mn	0.003	0.002	0.003	0.003	0.002	0.001	0.001	0.004	0.003	0.003		0.004	0.003	0.001	0.002	0.001	0.003	0.003	0.001	0.000
Ni	0.007	0.006	0.006	0.006	0.006	0.005	0.007	0.007	0.006	0.005		0.007	0.007	0.007	0.006	0.007	0.005	0.006	0.007	0.007
Mg	1.654	1.656	1.655	1.655	1.666	1.659	1.651	1.662	1.649	1.658		1.665	1.662	1.656	1.657	1.645	1.644	1.658	1.654	1.658
Ca	0.023	0.024	0.024	0.024	0.024	0.024	0.023	0.022	0.022	0.024		0.024	0.024	0.023	0.022	0.023	0.023	0.023	0.024	0.022
Na	0.005	0.005	0.003	0.007	0.004	0.004	0.004	0.003	0.003	0.004		0.006	0.002	0.003	0.003	0.004	0.005	0.004	0.005	0.003
K	0.000	0.000	0.000	0.000	0.000	0.000	0.001	0.001	0.000	0.001		0.000	0.001	0.000	0.000	0.000	0.000	0.000	0.000	0.001
Sum	4.007	4.010	4.006	4.008	4.011	4.009	4.006	4.009	4.003	4.006		4.014	4.010	4.005	4.008	4.000	4.002	4.009	4.005	4.010
Mg#	85.83	85.67	85.93	85.88	85.96	85.78	85.72	86.07	85.80	86.09		85.91	85.98	85.94	85.63	85.90	85.67	85.91	86.06	85.77
Al IV	0.046	0.045	0.046	0.043	0.043	0.047	0.045	0.047	0.046	0.045		0.044	0.047	0.046	0.046	0.046	0.046	0.050	0.048	0.049
Al VI	0.049	0.048	0.048	0.050	0.047	0.048	0.050	0.048	0.049	0.048		0.048	0.048	0.048	0.046	0.048	0.050	0.050	0.050	0.051

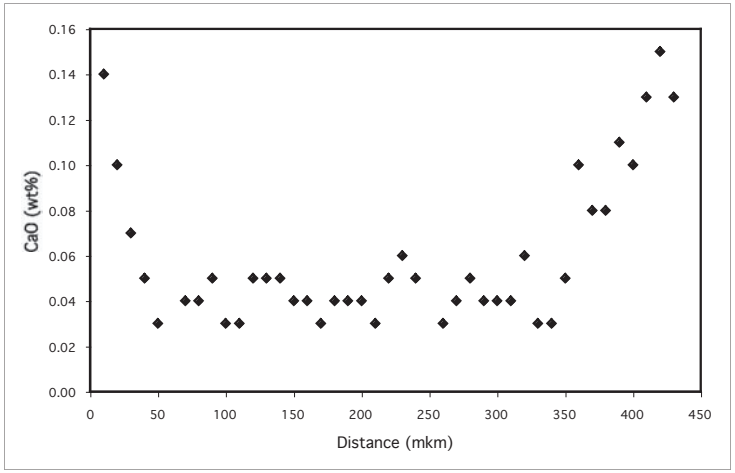
1910-11 Opx II, profile 700

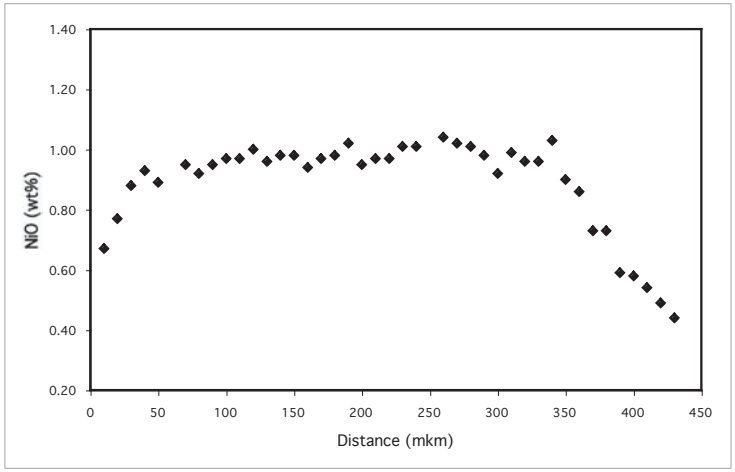
	510	520	530	540	550	560	570	580	590	600	610	620	630	640	650	660	670	680	690	700
SiO2	55.40	55.78	55.38	55.55	55.18	55.29	55.53	55.68	55.30	55.14	55.36	55.06	55.45	55.34	53.42	55.23	55.27	55.36	55.25	54.92
TiO2	0.02	0.02	0.04	0.00	0.03	0.03	0.03	0.06	0.07	0.00	0.05	0.00	0.03	0.03	0.02	0.00	0.03	0.04	0.04	0.00
Al2O3	2.46	2.39	2.48	2.47	2.54	2.49	2.63	2.61	2.68	2.73	2.69	2.80	2.87	2.89	4.71	3.09	3.13	3.07	3.05	3.14
Cr2O3	0.00	0.04	0.01	0.02	0.03	0.00	0.02	0.06	0.00	0.00	0.06	0.03	0.00	0.03	0.02	0.00	0.00	0.03	0.01	0.00
FeO	9.35	9.29	9.48	9.04	9.48	9.18	9.45	9.15	9.13	9.56	9.39	9.33	9.28	9.26	8.79	9.16	9.13	9.48	9.43	9.48
MnO	0.02	0.03	0.06	0.03	0.13	0.05	0.09	0.04	0.05	0.06	0.09	0.08	0.11	0.08	0.08	0.08	0.09	0.08	0.12	0.06
NiO	0.20	0.23	0.24	0.28	0.21	0.24	0.20	0.22	0.23	0.19	0.18	0.20	0.23	0.19	0.24	0.24	0.21	0.24	0.22	0.26
MgO	31.65	31.93	31.48	31.47	31.51	31.53	31.53	31.60	31.53	31.53	31.57	31.58	31.54	31.47	27.89	31.54	31.48	31.43	31.41	31.51
CaO	0.63	0.60	0.63	0.65	0.70	0.60	0.64	0.59	0.63	0.62	0.62	0.62	0.59	0.59	0.84	0.58	0.63	0.65	0.71	0.66
Na2O	0.08	0.07	0.06	0.08	0.09	0.08	0.06	0.10	0.07	0.08	0.06	0.09	0.07	0.05	0.05	0.08	0.08	0.06	0.05	0.07
K2O	0.00	0.00	0.00	0.02	0.00	0.00	0.00	0.00	0.00	0.00	0.00	0.00	0.01	0.01	0.06	0.02	0.00	0.02	0.01	0.01
Total	99.80	100.39	99.86	99.61	99.89	99.50	100.17	100.09	99.69	99.92	100.07	99.78	100.17	99.94	96.12	100.02	100.06	100.46	100.29	100.11
Si	1.943	1.944	1.943	1.949	1.937	1.944	1.941	1.944	1.940	1.934	1.937	1.932	1.937	1.937		1.931	1.931	1.931	1.930	1.923
Ti	0.000	0.001	0.001	0.000	0.001	0.001	0.001	0.002	0.002	0.000	0.001	0.000	0.001	0.001		0.000	0.001	0.001	0.001	0.000
Al	0.102	0.098	0.102	0.102	0.105	0.103	0.108	0.107	0.111	0.113	0.111	0.116	0.118	0.119		0.127	0.129	0.126	0.126	0.130
Cr	0.000	0.001	0.000	0.001	0.001	0.000	0.000	0.002	0.000	0.000	0.002	0.001	0.000	0.001		0.000	0.000	0.001	0.000	0.000
Fe2+	0.274	0.271	0.278	0.265	0.278	0.270	0.276	0.267	0.268	0.280	0.275	0.274	0.271	0.271		0.268	0.267	0.276	0.275	0.277
Mn	0.001	0.001	0.002	0.001	0.004	0.001	0.003	0.001	0.001	0.002	0.003	0.002	0.003	0.002		0.002	0.003	0.002	0.004	0.002
Ni	0.006	0.007	0.007	0.008	0.006	0.007	0.006	0.006	0.007	0.005	0.005	0.006	0.007	0.005		0.007	0.006	0.007	0.006	0.007
Mg	1.654	1.659	1.646	1.646	1.649	1.652	1.643	1.645	1.649	1.649	1.647	1.652	1.642	1.642		1.644	1.640	1.634	1.636	1.645
Ca	0.024	0.022	0.024	0.025	0.026	0.022	0.024	0.022	0.024	0.023	0.023	0.023	0.022	0.022		0.022	0.024	0.024	0.026	0.025
Na	0.005	0.005	0.004	0.005	0.006	0.006	0.004	0.007	0.004	0.006	0.004	0.006	0.005	0.003		0.005	0.005	0.004	0.004	0.005
K	0.000	0.000	0.000	0.001	0.000	0.000	0.000	0.000	0.000	0.000	0.000	0.000	0.000	0.000		0.001	0.000	0.001	0.000	0.001
Sum	4.009	4.008	4.007	4.003	4.013	4.007	4.006	4.003	4.005	4.012	4.007	4.012	4.006	4.004		4.008	4.006	4.007	4.008	4.015
Mg#	85.79	85.96	85.55	86.13	85.57	85.95	85.62	86.04	86.02	85.48	85.69	85.77	85.83	85.83		85.98	86.00	85.55	85.61	85.59
Al IV	0.049	0.048	0.050	0.049	0.051	0.050	0.053	0.053	0.056	0.054	0.056	0.056	0.058	0.060		0.061	0.063	0.062	0.062	0.062
Al VI	0.054	0.050	0.052	0.054	0.054	0.054	0.055	0.054	0.056	0.060	0.056	0.061	0.061	0.060		0.067	0.066	0.064	0.064	0.068

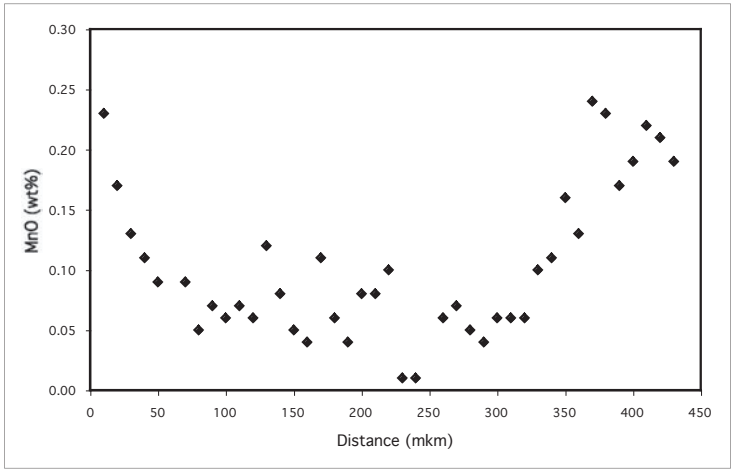
1910-11 Opx II, profile 700

	10	20	30
SiO2	39.23	39.44	39.59
TiO2	0.00	0.01	0.01
Al2O3	0.03	0.37	0.02
Cr2O3	0.02	0.02	0.00
FeO	19.18	17.54	16.51
MnO	0.23	0.17	0.13
NiO	0.67	0.77	0.88
MgO	41.44	42.07	43.60
CaO	0.14	0.10	0.07
Na2O	0.02	0.01	0.00
K2O	0.01	0.02	0.00
Total	100.96	100.51	100.80
Si	0.998	1.000	0.996
Ti	0.000	0.000	0.000
Al	0.001	0.011	0.001
Cr	0.000	0.000	0.000
Fe2+	0.408	0.372	0.347
Mn	0.005	0.004	0.003
Ni	0.014	0.016	0.018
Mg	1.571	1.589	1.636
Ca	0.004	0.003	0.002
Na	0.001	0.000	0.000
K	0.000	0.001	0.000
Sum	3.002	2.995	3.003
Mg#	79.38	81.03	82.50









1910-11 Olivine, profile 430

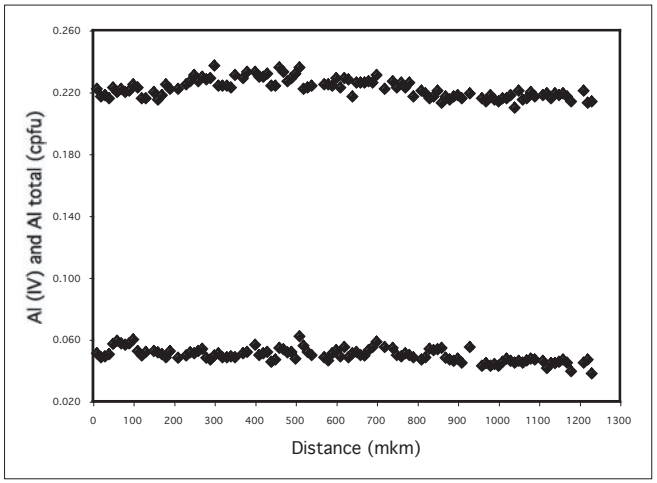
	40	50	60	70	80	90	100	110	120	130	140	150	160	170	180	190	200	210	220	230
SiO2	39.73	39.84	39.22	39.95	39.81	39.81	39.88	39.95	40.06	39.84	39.80	40.02	40.00	40.02	39.98	39.93	40.10	40.02	40.05	39.82
TiO2	0.00	0.03	0.00	0.02	0.02	0.04	0.00	0.01	0.00	0.01	0.00	0.02	0.00	0.01	0.00	0.01	0.03	0.01	0.01	0.00
Al2O3	0.04	0.03	0.13	0.06	0.06	0.08	0.07	0.05	0.03	0.03	0.03	0.03	0.02	0.02	0.03	0.03	0.02	0.03	0.02	0.04
Cr2O3	0.01	0.00	0.00	0.01	0.00	0.01	0.03	0.00	0.00	0.00	0.02	0.00	0.01	0.01	0.00	0.03	0.03	0.03	0.00	0.00
FeO	15.41	15.00	14.35	14.51	14.35	14.41	14.63	14.65	14.59	14.80	14.39	14.34	14.54	14.39	14.20	14.16	14.45	14.65	14.35	14.25
MnO	0.11	0.09	0.09	0.09	0.05	0.07	0.06	0.07	0.06	0.12	0.08	0.05	0.04	0.11	0.06	0.04	0.08	0.08	0.10	0.01
NiO	0.93	0.89	0.89	0.95	0.92	0.95	0.97	0.97	1.00	0.96	0.98	0.98	0.94	0.97	0.98	1.02	0.95	0.97	0.97	1.01
MgO	44.43	45.04	44.18	45.03	44.99	44.98	45.24	45.39	45.28	45.43	45.11	45.06	45.16	45.18	45.16	45.27	45.32	45.27	45.49	45.14
CaO	0.05	0.03	0.06	0.04	0.04	0.05	0.03	0.03	0.05	0.05	0.05	0.04	0.04	0.03	0.04	0.04	0.04	0.03	0.05	0.06
Na2O	0.01	0.03	0.01	0.01	0.01	0.00	0.00	0.04	0.00	0.01	0.00	0.00	0.00	0.00	0.01	0.00	0.02	0.01	0.02	0.00
K2O	0.00	0.02	0.02	0.02	0.00	0.00	0.03	0.00	0.00	0.00	0.01	0.00	0.02	0.00	0.00	0.01	0.00	0.00	0.00	0.00
Total	100.70	100.99	98.95	100.68	100.26	100.39	100.93	101.16	101.07	101.24	100.46	100.54	100.77	100.75	100.46	100.54	101.02	101.10	101.05	100.32
Si	0.996	0.994		0.997	0.997	0.996	0.994	0.994	0.997	0.991	0.996	1.000	0.998	0.998	0.999	0.997	0.997	0.996	0.996	0.997
Ti	0.000	0.000		0.000	0.000	0.001	0.000	0.000	0.000	0.000	0.000	0.000	0.000	0.000	0.000	0.000	0.001	0.000	0.000	0.000
Al	0.001	0.001		0.002	0.002	0.002	0.002	0.002	0.001	0.001	0.001	0.001	0.001	0.001	0.001	0.001	0.001	0.001	0.001	0.001
Cr	0.000	0.000		0.000	0.000	0.000	0.001	0.000	0.000	0.000	0.000	0.000	0.000	0.000	0.000	0.001	0.001	0.000	0.000	0.000
Fe2+	0.323	0.313		0.303	0.301	0.302	0.305	0.305	0.303	0.308	0.301	0.300	0.303	0.300	0.297	0.296	0.301	0.305	0.298	0.298
Mn	0.002	0.002		0.002	0.001	0.001	0.001	0.002	0.001	0.003	0.002	0.001	0.001	0.002	0.001	0.001	0.002	0.002	0.002	0.000
Ni	0.019	0.018		0.019	0.019	0.019	0.019	0.019	0.020	0.019	0.020	0.020	0.019	0.019	0.020	0.021	0.019	0.019	0.019	0.020
Mg	1.660	1.675		1.676	1.680	1.678	1.681	1.683	1.679	1.685	1.683	1.677	1.679	1.680	1.682	1.685	1.680	1.679	1.686	1.684
Ca	0.001	0.001		0.001	0.001	0.001	0.001	0.001	0.001	0.001	0.001	0.001	0.001	0.001	0.001	0.001	0.001	0.001	0.001	0.002
Na	0.000	0.001		0.001	0.000	0.000	0.000	0.002	0.000	0.000	0.000	0.000	0.000	0.000	0.000	0.000	0.001	0.000	0.001	0.000
K	0.000	0.001		0.001	0.000	0.000	0.001	0.000	0.000	0.000	0.000	0.000	0.001	0.000	0.000	0.000	0.000	0.000	0.000	0.000
Sum	3.003	3.006		3.002	3.001	3.002	3.005	3.006	3.003	3.008	3.004	3.000	3.002	3.001	3.001	3.002	3.002	3.004	3.004	3.003
Mg#	83.71	84.26		84.69	84.81	84.75	84.64	84.66	84.71	84.55	84.83	84.83	84.71	84.85	84.99	85.06	84.81	84.63	84.98	84.96

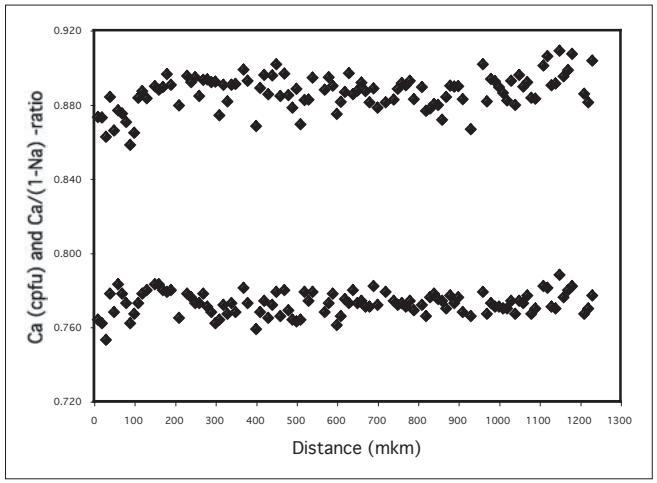
1910-11 Olivine, profile 430

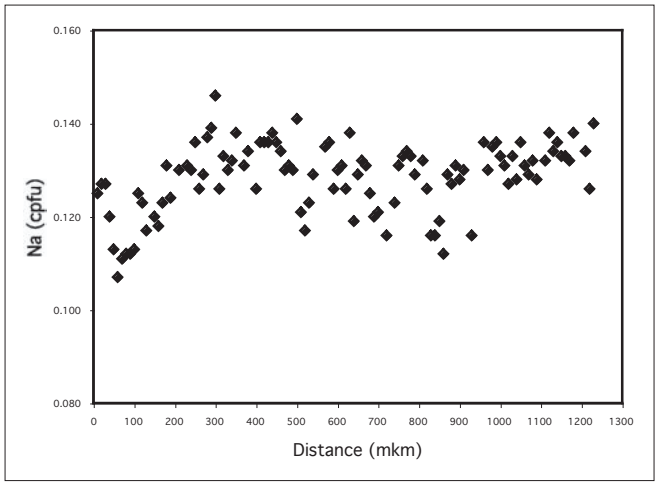
	240	250	260	270	280	290	300	310	320	330	340	350	360	370	380	390	400	410	420	430
SiO2	40.12	38.33	39.83	39.94	39.95	39.82	39.83	39.85	39.79	39.93	39.66	39.59	39.57	39.56	39.53	39.42	39.22	39.26	39.24	39.22
TiO2	0.00	0.01	0.03	0.01	0.00	0.00	0.00	0.01	0.00	0.01	0.00	0.00	0.03	0.00	0.00	0.00	0.01	0.00	0.00	0.02
Al2O3	0.03	0.07	0.03	0.03	0.02	0.04	0.03	0.03	0.03	0.03	0.03	0.03	0.37	0.02	0.03	0.03	0.03	0.03	0.03	0.05
Cr2O3	0.01	0.01	0.03	0.00	0.00	0.00	0.02	0.00	0.00	0.00	0.00	0.00	0.00	0.00	0.01	0.00	0.02	0.00	0.01	0.01
FeO	14.21	14.48	14.30	14.38	14.95	14.91	14.67	15.09	14.61	15.12	15.43	16.57	16.89	17.41	17.36	18.03	18.97	18.09	18.52	18.39
MnO	0.01	0.04	0.06	0.07	0.05	0.04	0.06	0.06	0.06	0.10	0.11	0.16	0.13	0.24	0.23	0.17	0.19	0.22	0.21	0.19
NiO	1.01	0.94	1.04	1.02	1.01	0.98	0.92	0.99	0.96	0.96	1.03	0.90	0.86	0.73	0.73	0.59	0.58	0.54	0.49	0.44
MgO	45.35	43.09	45.05	45.26	45.34	45.29	45.02	45.11	44.79	44.49	44.14	43.51	41.71	42.52	42.60	42.12	42.01	41.88	41.91	41.87
CaO	0.05	0.04	0.03	0.04	0.05	0.04	0.04	0.04	0.06	0.03	0.03	0.05	0.10	0.08	0.08	0.11	0.10	0.13	0.15	0.13
Na2O	0.01	0.00	0.03	0.01	0.01	0.00	0.01	0.01	0.00	0.00	0.02	0.01	0.00	0.00	0.00	0.03	0.00	0.02	0.00	0.02
K2O	0.00	0.00	0.01	0.00	0.01	0.00	0.00	0.00	0.00	0.00	0.01	0.00	0.02	0.00	0.00	0.00	0.00	0.00	0.02	0.01
Total	100.80	97.00	100.44	100.74	101.39	101.11	100.59	101.18	100.29	100.67	100.45	100.82	99.67	100.56	100.57	100.50	101.13	100.16	100.58	100.33
Si	0.999		0.997	0.996	0.993	0.992	0.996	0.993	0.998	1.000	0.997	0.997	1.008	1.002	1.001	1.001	0.994	1.001	0.998	0.999
Ti	0.000		0.001	0.000	0.000	0.000	0.000	0.000	0.000	0.000	0.000	0.000	0.000	0.000	0.000	0.000	0.000	0.000	0.000	0.000
Al	0.001		0.001	0.001	0.001	0.001	0.001	0.001	0.001	0.001	0.001	0.001	0.011	0.001	0.001	0.001	0.001	0.001	0.001	0.001
Cr	0.000		0.001	0.000	0.000	0.000	0.000	0.000	0.000	0.000	0.000	0.000	0.000	0.000	0.000	0.000	0.000	0.000	0.000	0.000
Fe2+	0.296		0.299	0.300	0.311	0.311	0.307	0.314	0.306	0.317	0.325	0.349	0.360	0.369	0.368	0.383	0.402	0.386	0.394	0.392
Mn	0.000		0.001	0.001	0.001	0.001	0.001	0.001	0.001	0.002	0.002	0.003	0.003	0.005	0.005	0.004	0.004	0.005	0.005	0.004
Ni	0.020		0.021	0.021	0.020	0.020	0.018	0.020	0.019	0.019	0.021	0.018	0.018	0.015	0.015	0.012	0.012	0.011	0.010	0.009
Mg	1.683		1.680	1.683	1.680	1.682	1.678	1.676	1.674	1.660	1.655	1.633	1.584	1.605	1.607	1.594	1.588	1.591	1.589	1.590
Ca	0.001		0.001	0.001	0.001	0.001	0.001	0.001	0.002	0.001	0.001	0.001	0.003	0.002	0.002	0.003	0.003	0.004	0.004	0.003
Na	0.000		0.001	0.000	0.000	0.000	0.001	0.000	0.000	0.000	0.001	0.000	0.000	0.000	0.000	0.001	0.000	0.001	0.000	0.001
K	0.000		0.000	0.000	0.000	0.000	0.000	0.000	0.000	0.000	0.000	0.000	0.001	0.000	0.000	0.000	0.000	0.000	0.001	0.000
Sum	3.001		3.003	3.003	3.007	3.007	3.004	3.007	3.002	3.000	3.003	3.003	2.987	2.998	2.999	2.999	3.005	2.999	3.002	3.000
Mg#	85.04		84.89	84.87	84.38	84.40	84.53	84.22	84.55	83.97	83.59	82.39	81.48	81.31	81.37	80.63	79.80	80.48	80.13	80.22

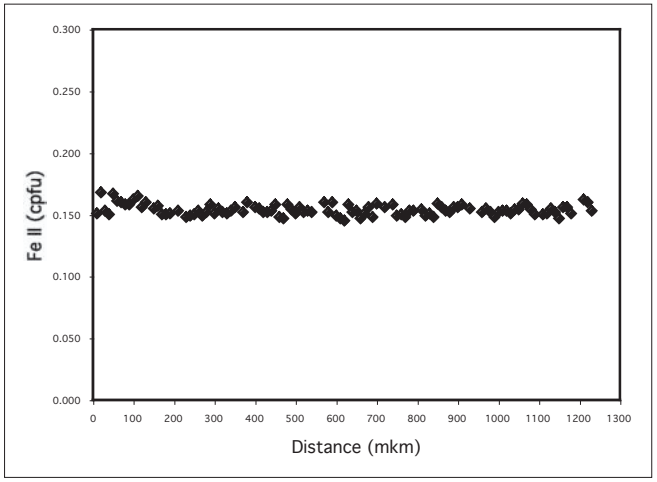
1910-11 Olivine, profile 430

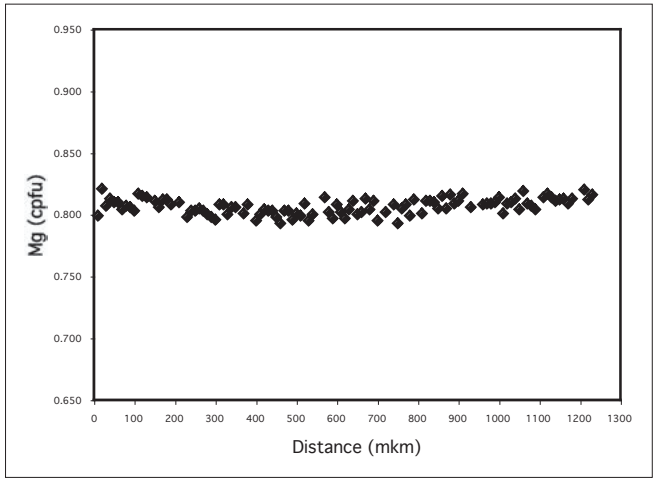
Websterite 1910-1

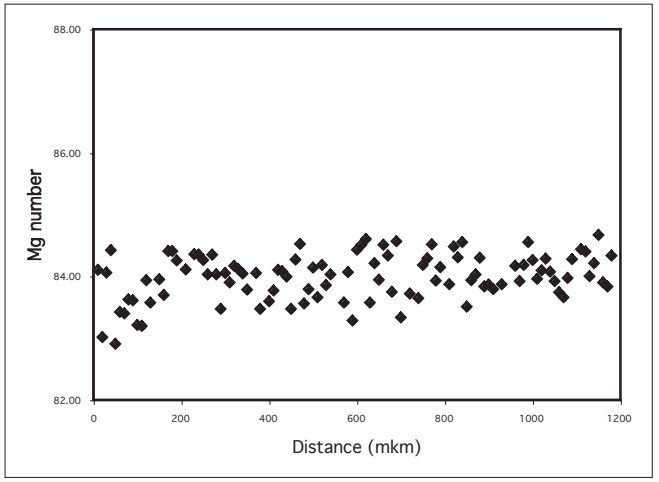












1910-1 Cpx I, profile 1230

	10	20	30	40	50	60	70	80	90	100	110	120	130	140	150	160	170	180	190	200
SiO2	53.54	52.92	53.56	52.92	53.01	52.89	52.71	52.94	53.08	52.97	52.43	52.51	52.88	52.53	52.62	52.78	52.61	52.51	52.78	52.44
TiO2	0.07	0.06	0.08	0.06	0.08	0.07	0.09	0.06	0.11	0.10	0.10	0.07	0.07	0.08	0.09	0.09	0.07	0.04	0.11	0.11
Al2O3	5.19	5.08	5.11	5.02	5.20	5.14	5.14	5.12	5.13	5.24	5.17	4.98	5.04	5.06	5.11	4.98	5.04	5.20	5.16	5.70
Cr2O3	0.02	0.10	0.10	0.04	0.05	0.05	0.01	0.04	0.03	0.07	0.07	0.05	0.03	0.09	0.07	0.07	0.07	0.03	0.04	0.02
FeO	4.98	5.51	5.04	4.89	5.49	5.29	5.21	5.17	5.17	5.33	5.40	5.08	5.27	4.96	5.07	5.15	4.90	4.90	4.94	4.91
MnO	0.04	0.08	0.05	0.09	0.11	0.09	0.04	0.08	0.03	0.11	0.00	0.04	0.06	0.04	0.03	0.08	0.06	0.07	0.08	0.03
NiO	0.10	0.06	0.09	0.04	0.07	0.04	0.08	0.10	0.09	0.07	0.12	0.04	0.07	0.10	0.04	0.07	0.06	0.02	0.07	0.06
MgO	14.79	15.14	14.93	14.92	14.96	14.92	14.72	14.83	14.80	14.78	14.98	14.88	14.98	14.71	14.87	14.78	14.86	14.86	14.86	14.35
CaO	19.68	19.55	19.39	19.87	19.72	20.06	19.84	19.76	19.49	19.64	19.72	19.78	19.98	19.67	19.97	19.98	19.84	19.83	19.95	18.06
Na2O	1.78	1.81	1.81	1.70	1.60	1.52	1.57	1.58	1.59	1.60	1.76	1.73	1.66	1.64	1.69	1.66	1.73	1.84	1.75	1.41
K2O	0.00	0.00	0.00	0.00	0.01	0.00	0.00	0.00	0.01	0.01	0.02	0.00	0.00	0.00	0.01	0.00	0.00	0.01	0.00	0.05
Total	100.16	100.31	100.16	99.55	100.28	100.06	99.40	99.68	99.52	99.92	99.77	99.17	100.05	98.89	99.58	99.62	99.23	99.31	99.74	97.13
Si	1.941	1.924	1.942	1.933	1.927	1.926	1.931	1.933	1.938	1.930	1.918	1.929	1.927		1.925	1.931	1.930	1.925	1.927	
Ti	0.002	0.002	0.002	0.002	0.002	0.002	0.002	0.002	0.003	0.003	0.003	0.002	0.002		0.002	0.002	0.002	0.001	0.003	
Al	0.222	0.217	0.218	0.216	0.223	0.220	0.222	0.220	0.221	0.225	0.223	0.216	0.216		0.220	0.215	0.218	0.225	0.222	
Cr	0.001	0.003	0.003	0.001	0.001	0.001	0.000	0.001	0.001	0.002	0.002	0.002	0.001		0.002	0.002	0.002	0.001	0.001	
Fe2+	0.151	0.168	0.153	0.150	0.167	0.161	0.160	0.158	0.158	0.162	0.165	0.156	0.160		0.155	0.157	0.150	0.150	0.151	
Mn	0.001	0.002	0.002	0.003	0.003	0.003	0.001	0.002	0.001	0.004	0.000	0.001	0.002		0.001	0.003	0.002	0.002	0.003	
Ni	0.003	0.002	0.003	0.001	0.002	0.001	0.002	0.003	0.003	0.002	0.004	0.001	0.002		0.001	0.002	0.002	0.001	0.002	
Mg	0.799	0.821	0.807	0.813	0.810	0.810	0.804	0.807	0.806	0.803	0.817	0.815	0.814		0.811	0.806	0.812	0.812	0.808	
Ca	0.764	0.762	0.753	0.778	0.768	0.783	0.778	0.773	0.762	0.767	0.773	0.778	0.780		0.783	0.783	0.780	0.779	0.780	
Na	0.125	0.127	0.127	0.120	0.113	0.107	0.111	0.112	0.112	0.113	0.125	0.123	0.117		0.120	0.118	0.123	0.131	0.124	
K	0.000	0.000	0.000	0.000	0.001	0.000	0.000	0.000	0.001	0.000	0.001	0.000	0.000		0.001	0.000	0.000	0.000	0.000	
Sum	4.009	4.028	4.010	4.017	4.017	4.014	4.011	4.011	4.006	4.011	4.031	4.023	4.021		4.021	4.019	4.021	4.027	4.021	
Mg#	84.11	83.01	84.06	84.42	82.91	83.42	83.40	83.63	83.61	83.21	83.20	83.93	83.57		83.95	83.70	84.41	84.41	84.25	
Al IV	0.051	0.049	0.049	0.051	0.057	0.059	0.058	0.057	0.058	0.060	0.053	0.050	0.052		0.053	0.052	0.051	0.049	0.053	
Al VI	0.171	0.169	0.169	0.166	0.166	0.161	0.165	0.164	0.164	0.165	0.171	0.167	0.164		0.168	0.164	0.168	0.177	0.170	

1910-1 Cpx I, profile 1230

	210	220	230	240	250	260	270	280	290	300	310	320	330	340	350	360	370	380	390	400
SiO2	53.10	52.30	52.52	52.64	52.56	52.62	52.73	52.61	52.55	52.69	52.94	52.77	53.07	52.94	52.58	49.03	52.55	52.23	52.55	52.81
TiO2	0.08	0.12	0.08	0.07	0.11	0.09	0.10	0.07	0.09	0.13	0.05	0.10	0.05	0.12	0.06	0.10	0.04	0.08	0.14	0.11
Al2O3	5.18	5.19	5.19	5.27	5.35	5.26	5.34	5.27	5.30	5.50	5.21	5.21	5.22	5.21	5.36	8.20	5.31	5.38	5.26	5.41
Cr2O3	0.01	0.02	0.05	0.08	0.03	0.00	0.03	0.04	0.01	0.00	0.06	0.00	0.07	0.04	0.01	0.01	0.08	0.03	0.05	0.04
FeO	5.04	4.88	4.81	4.87	4.90	4.99	4.87	4.97	5.15	4.95	5.08	4.97	4.95	5.03	5.09	4.86	4.96	5.23	4.79	5.09
MnO	0.04	0.07	0.04	0.00	0.00	0.01	0.03	0.01	0.05	0.02	0.02	0.02	0.07	0.00	0.12	0.03	0.08	0.06	0.08	0.07
NiO	0.08	0.09	0.05	0.05	0.09	0.05	0.10	0.08	0.02	0.12	0.05	0.07	0.05	0.09	0.09	0.05	0.08	0.06	0.06	0.08
MgO	14.93	14.73	14.56	14.71	14.72	14.72	14.76	14.64	14.59	14.62	14.83	14.83	14.72	14.84	14.78	12.61	14.69	14.76	14.38	14.56
CaO	19.61	19.68	19.74	19.77	19.71	19.68	19.87	19.63	19.55	19.47	19.53	19.72	19.62	19.82	19.59	18.19	19.92	19.66	19.73	19.35
Na2O	1.85	1.92	1.84	1.82	1.92	1.77	1.82	1.92	1.95	2.06	1.79	1.88	1.84	1.87	1.94	1.98	1.84	1.89	1.78	1.77
K2O	0.00	0.00	0.01	0.00	0.00	0.00	0.00	0.00	0.01	0.00	0.00	0.00	0.01	0.00	0.00	0.03	0.00	0.00	0.00	0.02
Total	99.91	99.00	98.86	99.28	99.38	99.19	99.65	99.24	99.26	99.57	99.55	99.58	99.68	99.97	99.64	95.07	99.54	99.37	98.81	99.32
Si	1.933		1.932	1.928	1.925	1.930	1.925	1.929	1.928	1.925	1.933	1.928	1.935	1.928	1.923		1.923	1.917		1.933
Ti	0.002		0.002	0.002	0.003	0.002	0.003	0.002	0.002	0.004	0.001	0.003	0.001	0.003	0.002		0.001	0.002		0.003
Al	0.222		0.225	0.227	0.231	0.227	0.230	0.228	0.229	0.237	0.224	0.224	0.224	0.223	0.231		0.229	0.233		0.233
Cr	0.000		0.001	0.002	0.001	0.000	0.001	0.001	0.000	0.000	0.002	0.000	0.002	0.001	0.000		0.002	0.001		0.001
Fe2+	0.153		0.148	0.149	0.150	0.153	0.149	0.152	0.158	0.151	0.155	0.152	0.151	0.153	0.156		0.152	0.160		0.156
Mn	0.001		0.001	0.000	0.000	0.000	0.001	0.000	0.001	0.001	0.001	0.000	0.002	0.000	0.004		0.003	0.002		0.002
Ni	0.002		0.001	0.001	0.003	0.001	0.003	0.002	0.000	0.004	0.001	0.002	0.001	0.003	0.003		0.002	0.002		0.002
Mg	0.810		0.798	0.803	0.803	0.805	0.803	0.800	0.798	0.796	0.808	0.808	0.800	0.806	0.806		0.801	0.808		0.795
Ca	0.765		0.778	0.776	0.773	0.773	0.778	0.771	0.768	0.762	0.764	0.772	0.767	0.773	0.768		0.781	0.773		0.759
Na	0.130		0.131	0.130	0.136	0.126	0.129	0.137	0.139	0.146	0.126	0.133	0.130	0.132	0.138		0.131	0.134		0.126
K	0.000		0.000	0.000	0.000	0.000	0.000	0.000	0.000	0.000	0.000	0.000	0.001	0.000	0.000		0.000	0.000		0.001
Sum	4.018		4.017	4.018	4.025	4.017	4.022	4.022	4.023	4.026	4.015	4.022	4.014	4.022	4.031		4.025	4.032		4.011
Mg#	84.11		84.36	84.35	84.26	84.03	84.35	84.03	83.47	84.05	83.90	84.17	84.12	84.05	83.78		84.05	83.47		83.60
Al IV	0.048		0.050	0.052	0.051	0.053	0.054	0.048	0.047	0.050	0.051	0.049	0.049	0.049	0.049		0.051	0.052		0.057
Al VI	0.174		0.176	0.176	0.180	0.175	0.176	0.180	0.182	0.188	0.173	0.176	0.176	0.174	0.183		0.178	0.181		0.177

1910-1 Cpx I, profile 1230

	410	420	430	440	450	460	470	480	490	500	510	520	530	540	550	560	570	580	590	600
SiO2	52.67	52.45	52.75	52.91	52.73	52.66	52.56	52.89	52.84	52.89	52.76	53.02	52.86	52.86	51.97	53.04	52.74	52.88	52.87	53.04
TiO2	0.09	0.10	0.11	0.09	0.11	0.11	0.06	0.11	0.09	0.06	0.15	0.12	0.09	0.08	0.09	0.13	0.12	0.06	0.09	0.10
Al2O3	5.34	5.33	5.39	5.22	5.21	5.47	5.39	5.30	5.32	5.40	5.48	5.19	5.18	5.22	6.33	4.32	5.24	5.23	5.22	5.34
Cr2O3	0.02	0.06	0.06	0.07	0.00	0.03	0.01	0.04	0.03	0.00	0.03	0.03	0.03	0.02	0.03	0.03	0.02	0.04	0.02	0.03
FeO	5.08	4.95	4.98	5.01	5.19	4.81	4.82	5.19	5.05	4.96	5.10	5.01	4.99	4.96	5.00	4.52	5.25	5.00	5.24	4.88
MnO	0.05	0.11	0.06	0.10	0.09	0.05	0.07	0.04	0.09	0.08	0.03	0.05	0.05	0.08	0.03	0.05	0.07	0.07	0.09	0.08
NiO	0.07	0.09	0.04	0.08	0.05	0.07	0.08	0.04	0.07	0.07	0.09	0.05	0.08	0.04	0.11	0.07	0.08	0.09	0.06	0.07
MgO	14.67	14.71	14.76	14.79	14.66	14.52	14.71	14.78	14.60	14.73	14.67	14.92	14.57	14.70	14.24	15.50	14.99	14.75	14.66	14.89
CaO	19.60	19.72	19.55	19.77	19.92	19.52	19.89	19.70	19.49	19.53	19.53	19.98	19.74	19.91	18.40	20.64	19.67	19.79	19.92	19.52
Na2O	1.92	1.91	1.92	1.95	1.92	1.89	1.84	1.86	1.83	1.99	1.71	1.66	1.74	1.82	1.52	1.17	1.91	1.93	1.78	1.84
K2O	0.02	0.00	0.00	0.02	0.00	0.00	0.01	0.01	0.00	0.00	0.01	0.00	0.01	0.00	0.06	0.00	0.01	0.01	0.00	0.00
Total	99.53	99.43	99.61	100.01	99.87	99.12	99.43	99.94	99.40	99.70	99.54	100.04	99.33	99.69	97.78	99.47	100.09	99.84	99.94	99.78
Si	1.927	1.922	1.926	1.927	1.925	1.930	1.924	1.927	1.933	1.929	1.927	1.928	1.935	1.930			1.921	1.929	1.928	1.931
Ti	0.003	0.003	0.003	0.002	0.003	0.003	0.002	0.003	0.002	0.002	0.004	0.003	0.002	0.002			0.003	0.002	0.002	0.003
Al	0.230	0.230	0.232	0.224	0.224	0.236	0.233	0.227	0.229	0.232	0.236	0.222	0.223	0.224			0.225	0.225	0.224	0.229
Cr	0.001	0.002	0.002	0.002	0.000	0.001	0.000	0.001	0.001	0.000	0.001	0.001	0.001	0.001			0.001	0.001	0.000	0.001
Fe2+	0.155	0.152	0.152	0.153	0.158	0.148	0.147	0.158	0.154	0.151	0.156	0.152	0.153	0.152			0.160	0.152	0.160	0.149
Mn	0.002	0.004	0.002	0.003	0.003	0.002	0.002	0.001	0.003	0.003	0.001	0.002	0.002	0.002			0.002	0.002	0.003	0.002
Ni	0.002	0.003	0.001	0.002	0.001	0.002	0.002	0.001	0.002	0.002	0.003	0.002	0.002	0.001			0.002	0.003	0.002	0.002
Mg	0.800	0.804	0.803	0.803	0.798	0.793	0.803	0.803	0.796	0.801	0.799	0.809	0.795	0.800			0.814	0.802	0.797	0.808
Ca	0.768	0.774	0.765	0.772	0.779	0.766	0.780	0.769	0.764	0.763	0.764	0.779	0.774	0.779			0.768	0.773	0.778	0.761
Na	0.136	0.136	0.136	0.138	0.136	0.134	0.130	0.131	0.130	0.141	0.121	0.117	0.123	0.129			0.135	0.136	0.126	0.130
K	0.001	0.000	0.000	0.001	0.000	0.000	0.000	0.000	0.000	0.000	0.000	0.000	0.001	0.000			0.000	0.001	0.000	0.000
Sum	4.025	4.030	4.022	4.027	4.027	4.015	4.023	4.021	4.014	4.024	4.012	4.015	4.011	4.020			4.031	4.026	4.020	4.016
Mg#	83.77	84.10	84.08	84.00	83.47	84.27	84.53	83.56	83.79	84.14	83.66	84.18	83.86	84.03			83.57	84.07	83.28	84.43
Al IV	0.050	0.051	0.052	0.046	0.047	0.055	0.054	0.052	0.052	0.048	0.062	0.056	0.052	0.050			0.049	0.047	0.051	0.053
Al VI	0.180	0.179	0.180	0.179	0.177	0.182	0.180	0.176	0.177	0.185	0.174	0.166	0.171	0.174			0.177	0.179	0.173	0.176

1910-1 Cpx I, profile 1230

	610	620	630	640	650	660	670	680	690	700	710	720	730	740	750	760	770	780	790	800
SiO2	52.90	52.84	52.66	52.94	53.18	52.73	52.79	52.79	52.66	53.15	52.22	52.88	52.51	52.65	53.17	52.86	52.76	52.92	52.99	53.25
TiO2	0.06	0.07	0.10	0.09	0.10	0.12	0.09	0.06	0.08	0.13	0.13	0.09	0.08	0.07	0.11	0.07	0.17	0.10	0.13	0.06
Al2O3	5.16	5.32	5.31	5.06	5.28	5.23	5.26	5.27	5.25	5.41	5.33	5.17	5.50	5.28	5.21	5.26	5.18	5.26	5.06	5.46
Cr2O3	0.08	0.09	0.04	0.02	0.05	0.01	0.05	0.01	0.02	0.03	0.03	0.03	0.01	0.03	0.07	0.04	0.11	0.05	0.05	0.04
FeO	4.78	4.76	5.19	4.97	5.04	4.79	4.97	5.10	4.83	5.24	5.15	5.12	5.03	5.17	4.89	4.93	4.85	5.02	5.03	5.17
MnO	0.04	0.07	0.10	0.02	0.03	0.04	0.04	0.05	0.04	0.06	0.05	0.03	0.02	0.09	0.04	0.07	0.02	0.06	0.04	0.08
NiO	0.08	0.06	0.08	0.08	0.06	0.05	0.06	0.09	0.07	0.04	0.08	0.06	0.07	0.06	0.05	0.08	0.04	0.06	0.09	0.09
MgO	14.68	14.61	14.80	14.91	14.78	14.70	14.95	14.75	14.88	14.69	14.76	14.74	14.83	14.83	14.61	14.80	14.83	14.72	14.94	14.72
CaO	19.51	19.77	19.78	19.96	19.89	19.74	19.75	19.69	19.95	19.86	19.31	19.90	19.67	19.78	19.77	19.78	19.70	19.84	19.68	18.72
Na2O	1.84	1.78	1.95	1.69	1.84	1.86	1.85	1.76	1.69	1.73	1.55	1.64	1.49	1.73	1.85	1.88	1.90	1.88	1.83	1.82
K2O	0.00	0.01	0.01	0.00	0.00	0.01	0.02	0.00	0.01	0.00	0.00	0.02	0.03	0.00	0.00	0.01	0.00	0.00	0.00	0.03
Total	99.13	99.37	100.00	99.73	100.24	99.26	99.81	99.57	99.47	100.33	98.61	99.67	99.23	99.68	99.76	99.77	99.56	99.91	99.84	99.43
Si	1.938	1.932	1.920	1.931	1.930	1.931	1.925	1.929	1.926	1.928		1.931		1.924	1.937	1.928	1.928	1.928	1.931	
Ti	0.002	0.002	0.003	0.002	0.003	0.003	0.002	0.002	0.002	0.003		0.002		0.002	0.003	0.002	0.005	0.003	0.004	
Al	0.223	0.229	0.228	0.217	0.226	0.226	0.226	0.227	0.226	0.231		0.222		0.227	0.223	0.226	0.223	0.226	0.217	
Cr	0.002	0.003	0.001	0.000	0.001	0.000	0.001	0.000	0.000	0.001		0.001		0.001	0.002	0.001	0.003	0.001	0.001	
Fe2+	0.147	0.145	0.158	0.152	0.153	0.147	0.151	0.156	0.148	0.159		0.156		0.158	0.149	0.150	0.148	0.153	0.153	
Mn	0.001	0.002	0.003	0.000	0.001	0.001	0.001	0.002	0.001	0.002		0.001		0.003	0.001	0.002	0.001	0.002	0.001	
Ni	0.002	0.002	0.002	0.002	0.002	0.001	0.002	0.003	0.002	0.001		0.002		0.002	0.001	0.002	0.001	0.002	0.003	
Mg	0.802	0.797	0.804	0.811	0.800	0.802	0.813	0.804	0.811	0.795		0.802		0.808	0.793	0.805	0.808	0.799	0.812	
Ca	0.766	0.775	0.773	0.780	0.773	0.774	0.771	0.771	0.782	0.772		0.779		0.774	0.772	0.773	0.771	0.774	0.769	
Na	0.131	0.126	0.138	0.119	0.129	0.132	0.131	0.125	0.120	0.121		0.116		0.123	0.131	0.133	0.134	0.133	0.129	
K	0.000	0.000	0.000	0.000	0.000	0.000	0.001	0.000	0.000	0.000		0.001		0.000	0.000	0.000	0.000	0.000	0.000	
Sum	4.014	4.013	4.030	4.014	4.018	4.017	4.024	4.019	4.018	4.013		4.013		4.022	4.012	4.022	4.022	4.021	4.020	
Mg#	84.51	84.61	83.58	84.22	83.95	84.51	84.34	83.75	84.57	83.33		83.72		83.64	84.18	84.29	84.52	83.93	84.15	
Al IV	0.049	0.055	0.049	0.051	0.052	0.050	0.050	0.053	0.055	0.059		0.055		0.055	0.050	0.049	0.051	0.050	0.049	
Al VI	0.174	0.174	0.180	0.166	0.174	0.176	0.177	0.174	0.171	0.173		0.167		0.173	0.173	0.177	0.172	0.176	0.169	

1910-1 Cpx I, profile 1230

	810	820	830	840	850	860	870	880	890	900	910	920	930	940	950	960	970	980	990	1000
SiO2	53.05	52.99	53.34	52.88	53.02	52.91	53.10	53.00	52.95	52.97	53.05	53.35	53.12	52.39	53.27	52.84	53.02	52.53	53.16	53.01
TiO2	0.06	0.07	0.10	0.06	0.08	0.10	0.09	0.09	0.08	0.07	0.06	0.06	0.12	0.08	0.16	0.09	0.09	0.05	0.10	0.09
Al2O3	5.14	5.08	5.06	5.02	5.14	4.95	5.06	5.01	5.05	5.08	5.05	5.21	5.10	5.08	5.25	5.01	4.96	5.02	5.01	4.99
Cr2O3	0.03	0.03	0.08	0.02	0.02	0.08	0.08	0.05	0.07	0.06	0.03	0.05	0.05	0.06	0.11	0.09	0.02	0.09	0.10	0.06
FeO	5.05	4.88	4.97	4.82	5.22	5.11	5.02	4.98	5.13	5.14	5.19	5.10	5.07	5.84	4.99	4.99	5.07	4.94	4.88	4.99
MnO	0.06	0.04	0.04	0.03	0.03	0.02	0.05	0.03	0.15	0.08	0.04	0.00	0.00	0.09	0.06	0.05	0.09	0.02	0.02	0.06
NiO	0.06	0.08	0.09	0.08	0.08	0.13	0.04	0.11	0.07	0.11	0.09	0.10	0.09	0.06	0.06	0.07	0.04	0.09	0.09	0.07
MgO	14.74	14.87	15.01	14.84	14.83	14.97	14.82	15.04	14.90	14.95	15.07	15.22	14.82	15.34	14.99	14.85	14.86	14.76	14.95	14.99
CaO	19.77	19.55	19.99	19.82	19.85	19.78	19.72	19.92	19.80	19.90	19.71	19.36	19.59	19.19	18.86	19.93	19.60	19.63	19.79	19.74
Na2O	1.86	1.77	1.65	1.64	1.69	1.59	1.82	1.80	1.85	1.81	1.84	1.70	1.64	1.53	1.75	1.92	1.83	1.89	1.93	1.88
K2O	0.00	0.02	0.00	0.00	0.00	0.01	0.00	0.00	0.00	0.03	0.01	0.03	0.01	0.00	0.03	0.01	0.00	0.02	0.01	0.01
Total	99.83	99.38	100.33	99.20	99.95	99.64	99.81	100.03	100.05	100.18	100.15	100.17	99.58	99.67	99.52	99.84	99.59	99.03	100.03	99.88
Si	1.934	1.937	1.934	1.937	1.931	1.933	1.935	1.929	1.929	1.927	1.929		1.938			1.928	1.937	1.931	1.933	1.932
Ti	0.002	0.002	0.003	0.002	0.002	0.003	0.003	0.002	0.002	0.002	0.002		0.003			0.002	0.002	0.001	0.003	0.002
Al	0.221	0.219	0.216	0.217	0.221	0.213	0.217	0.215	0.217	0.218	0.216		0.219			0.216	0.214	0.218	0.215	0.214
Cr	0.001	0.001	0.002	0.001	0.001	0.002	0.002	0.002	0.002	0.002	0.001		0.001			0.002	0.001	0.002	0.003	0.002
Fe2+	0.154	0.149	0.151	0.148	0.159	0.156	0.153	0.152	0.156	0.156	0.158		0.155			0.152	0.155	0.152	0.148	0.152
Mn	0.002	0.001	0.001	0.001	0.001	0.001	0.002	0.001	0.005	0.002	0.001		0.000			0.002	0.003	0.001	0.000	0.002
Ni	0.002	0.002	0.003	0.002	0.002	0.004	0.001	0.003	0.002	0.003	0.003		0.003			0.002	0.001	0.003	0.003	0.002
Mg	0.801	0.811	0.811	0.810	0.805	0.815	0.805	0.816	0.809	0.811	0.817		0.806			0.808	0.809	0.809	0.810	0.814
Ca	0.772	0.766	0.776	0.778	0.775	0.774	0.770	0.777	0.773	0.776	0.768		0.766			0.779	0.767	0.773	0.771	0.771
Na	0.132	0.126	0.116	0.116	0.119	0.112	0.129	0.127	0.131	0.128	0.130		0.116			0.136	0.130	0.135	0.136	0.133
K	0.000	0.001	0.000	0.000	0.000	0.000	0.000	0.000	0.000	0.001	0.001		0.000			0.000	0.000	0.001	0.000	0.001
Sum	4.021	4.015	4.013	4.012	4.016	4.013	4.017	4.024	4.026	4.026	4.026		4.007			4.027	4.019	4.026	4.022	4.025
Mg#	83.87	84.48	84.30	84.55	83.51	83.93	84.03	84.30	83.83	83.87	83.79		83.87			84.17	83.92	84.18	84.55	84.27
Al IV	0.047	0.049	0.054	0.053	0.054	0.055	0.048	0.047	0.046	0.048	0.045		0.055			0.043	0.045	0.043	0.044	0.043
Al VI	0.174	0.171	0.162	0.164	0.168	0.159	0.169	0.168	0.171	0.171	0.171		0.164			0.173	0.170	0.175	0.171	0.171

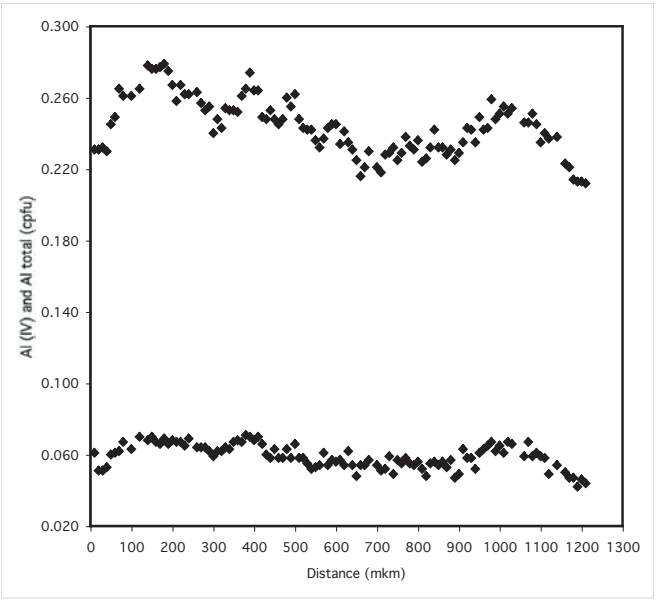
1910-1 Cpx I, profile 1230

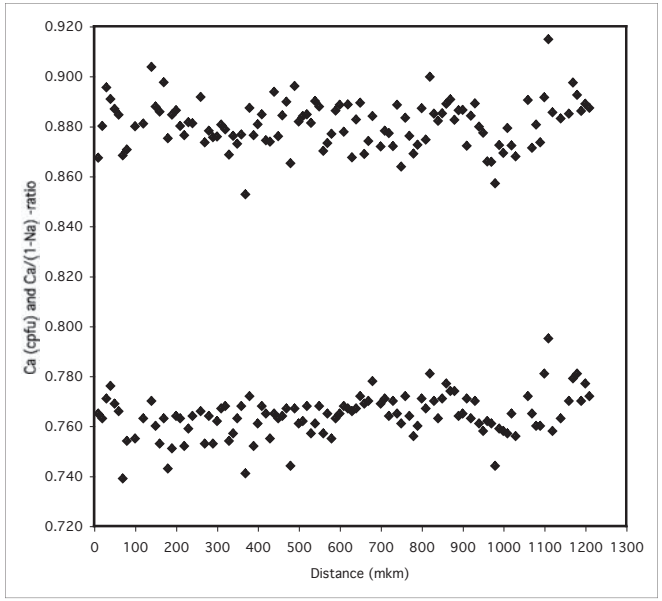
	1010	1020	1030	1040	1050	1060	1070	1080	1090	1100	1110	1120	1130	1140	1150	1160	1170	1180	1190	1200
SiO2	53.01	53.04	52.83	53.34	52.95	52.95	52.96	52.89	53.29	51.55	52.70	52.52	52.74	52.78	52.30	52.68	52.70	52.53	51.65	52.53
TiO2	0.10	0.07	0.12	0.09	0.11	0.08	0.09	0.08	0.06	0.09	0.08	0.02	0.11	0.08	0.08	0.10	0.08	0.04	0.29	0.09
Al2O3	5.00	5.01	5.06	4.90	5.15	5.03	5.03	5.12	5.07	4.85	5.07	5.08	5.02	5.09	5.03	5.08	5.04	4.94	4.36	4.99
Cr2O3	0.01	0.07	0.03	0.08	0.05	0.06	0.08	0.09	0.04	0.06	0.05	0.06	0.05	0.08	0.06	0.08	0.07	0.03	0.11	0.12
FeO	4.98	5.00	4.94	5.07	5.05	5.24	5.18	5.05	4.93	5.06	4.91	4.94	5.07	4.96	4.78	5.09	5.11	4.90	7.09	5.39
MnO	0.02	0.05	0.06	0.00	0.04	0.09	0.01	0.09	0.04	0.07	0.01	0.02	0.06	0.05	0.06	0.04	0.06	0.06	0.15	0.09
NiO	0.02	0.05	0.10	0.08	0.09	0.02	0.06	0.11	0.12	0.10	0.06	0.07	0.11	0.06	0.10	0.04	0.07	0.05	0.00	0.05
MgO	14.68	14.87	14.88	15.01	14.82	15.10	14.91	14.82	14.83	0.17	14.95	14.97	14.94	14.88	14.80	14.92	14.86	14.84	16.77	15.10
CaO	19.64	19.69	19.77	19.70	19.83	19.84	19.93	19.60	19.75	19.09	19.97	19.90	19.68	19.65	20.00	19.82	19.91	19.86	18.70	19.15
Na2O	1.84	1.79	1.88	1.82	1.92	1.86	1.83	1.86	1.82	1.92	1.86	1.95	1.90	1.92	1.86	1.88	1.86	1.93	0.45	1.20
K2O	0.01	0.00	0.00	0.00	0.00	0.00	0.01	0.00	0.00	0.01	0.01	0.01	0.01	0.00	0.00	0.01	0.02	0.00	0.01	0.03
Total	99.32	99.64	99.67	100.08	100.02	100.26	100.07	99.71	99.93	82.98	99.67	99.53	99.70	99.55	99.07	99.75	99.79	99.18	99.58	98.73
Si	1.940	1.936	1.930	1.938	1.928	1.925	1.928	1.931	1.938		1.926	1.923	1.928	1.930	1.924	1.925	1.926	1.929		
Ti	0.003	0.002	0.003	0.003	0.003	0.002	0.002	0.002	0.002		0.002	0.000	0.003	0.002	0.002	0.003	0.002	0.001		
Al	0.216	0.216	0.218	0.210	0.221	0.215	0.216	0.220	0.217		0.218	0.219	0.216	0.219	0.218	0.219	0.217	0.214		
Cr	0.000	0.002	0.001	0.002	0.001	0.002	0.002	0.003	0.001		0.002	0.002	0.002	0.002	0.002	0.002	0.002	0.001		
Fe2+	0.153	0.153	0.151	0.154	0.154	0.159	0.158	0.154	0.150		0.150	0.151	0.155	0.152	0.147	0.156	0.156	0.151		
Mn	0.001	0.002	0.002	0.000	0.001	0.003	0.000	0.003	0.001		0.000	0.001	0.002	0.002	0.002	0.001	0.002	0.002		
Ni	0.001	0.001	0.003	0.002	0.003	0.001	0.002	0.003	0.003		0.002	0.002	0.003	0.002	0.003	0.001	0.002	0.001		
Mg	0.801	0.809	0.810	0.813	0.804	0.819	0.809	0.807	0.804		0.814	0.817	0.814	0.811	0.812	0.813	0.809	0.813		
Ca	0.770	0.770	0.774	0.767	0.774	0.773	0.777	0.767	0.770		0.782	0.781	0.771	0.770	0.788	0.776	0.780	0.782		
Na	0.131	0.127	0.133	0.128	0.136	0.131	0.129	0.132	0.128		0.132	0.138	0.134	0.136	0.133	0.133	0.132	0.138		
K	0.000	0.000	0.000	0.000	0.000	0.000	0.000	0.000	0.000		0.000	0.000	0.001	0.000	0.000	0.000	0.001	0.000		
Sum	4.016	4.018	4.025	4.017	4.025	4.03	4.023	4.022	4.014		4.028	4.034	4.029	4.026	4.031	4.029	4.029	4.032		
Mg#	83.96	84.10	84.29	84.07	83.92	83.74	83.66	83.98	84.28		84.44	84.40	84.00	84.22	84.67	83.90	83.83	84.34		
Al IV	0.046	0.048	0.046	0.045	0.046	0.045	0.047	0.048	0.047		0.046	0.042	0.045	0.045	0.046	0.047	0.045	0.040		
Al VI	0.171	0.169	0.172	0.165	0.175	0.170	0.170	0.173	0.170		0.172	0.178	0.172	0.175	0.173	0.172	0.172	0.175		

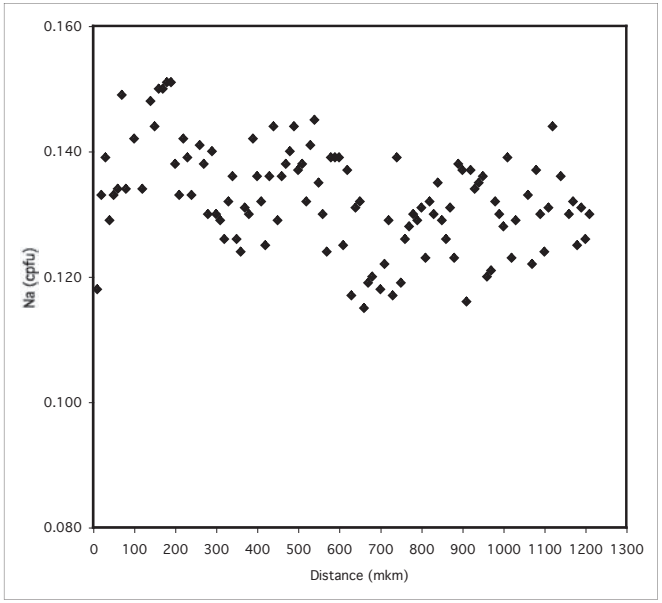
1910-1 Cpx I, profile 1230

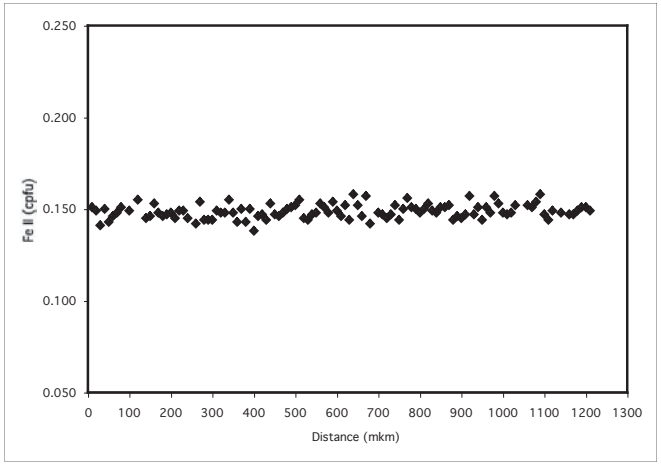
	1210	1220	1230
SiO2	52.60	52.71	52.43
TiO2	0.03	0.06	0.05
Al2O3	5.13	4.92	4.94
Cr2O3	0.03	0.09	0.01
FeO	5.31	5.22	4.98
MnO	0.07	0.03	0.01
NiO	0.05	0.03	0.04
MgO	15.06	14.86	14.87
CaO	19.60	19.59	19.71
Na2O	1.90	1.78	1.97
K2O	0.00	0.00	0.01
Total	99.78	99.29	99.02
Si	1.922	1.933	1.929
Ti	0.001	0.002	0.001
Al	0.221	0.213	0.214
Cr	0.001	0.003	0.000
Fe2+	0.162	0.160	0.153
Mn	0.002	0.001	0.000
Ni	0.001	0.001	0.001
Mg	0.820	0.812	0.816
Ca	0.767	0.770	0.777
Na	0.134	0.126	0.140
K	0.000	0.000	0.000
Sum	4.031	4.021	4.031
Mg#	83.50	83.54	84.21
Al IV	0.045	0.047	0.038
Al VI	0.176	0.166	0.176

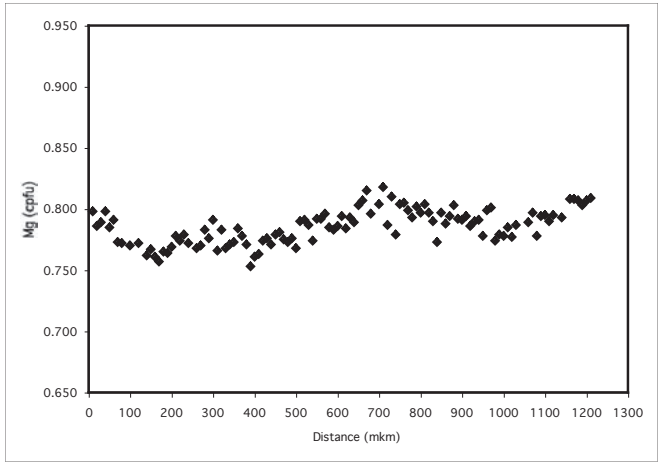
1910-1 Cpx I, profile 1230

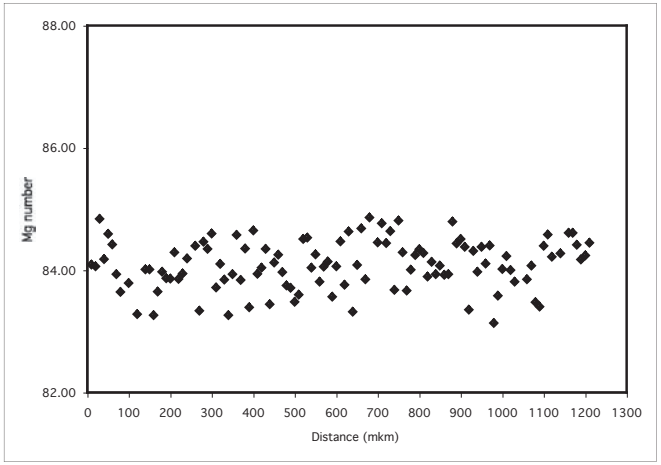












1910-1 Cpx I-II, profile 1210

	10	20	30	40	50	60	70	80	90	100	110	120	130	140	150	160	170	180	190	200
SiO2	53.62	53.57	53.22	53.26	53.19	53.25	53.19	53.02	53.14	53.03	53.40	52.78	48.33	52.35	52.96	52.84	52.71	53.00	52.95	53.10
TiO2	0.12	0.06	0.15	0.09	0.10	0.11	0.09	0.13	0.11	0.08	0.07	0.13	0.11	0.11	0.14	0.12	0.09	0.15	0.11	0.12
Al2O3	5.42	5.42	5.40	5.37	5.72	5.86	6.20	6.09	4.95	6.09	6.77	6.19	10.94	6.46	6.48	6.45	6.46	6.54	6.43	6.26
Cr2O3	0.06	0.07	0.04	0.05	0.03	0.03	0.09	0.04	0.04	0.07	0.06	0.05	0.07	0.02	0.00	0.08	0.01	0.04	0.04	0.04
FeO	5.00	4.90	4.64	4.94	4.72	4.82	4.88	4.99	4.91	4.89	4.89	5.10	5.51	4.74	4.81	5.05	4.86	4.81	4.84	4.89
MnO	0.05	0.05	0.06	0.00	0.04	0.06	0.05	0.12	0.07	0.05	0.00	0.10	0.08	0.03	0.02	0.06	0.09	0.10	0.09	0.10
MgO	14.83	14.56	14.57	14.77	14.51	14.68	14.31	14.26	15.11	14.22	14.30	14.26	10.79	14.01	14.21	14.07	13.96	14.16	14.14	14.27
CaO	19.78	19.66	19.79	19.99	19.78	19.79	19.03	19.36	20.72	19.39	18.31	19.60	14.47	19.68	19.59	19.37	19.58	19.15	19.33	19.73
Na2O	1.69	1.89	1.98	1.83	1.88	1.91	2.12	1.90	1.50	2.01	1.82	1.91	0.14	2.10	2.05	2.14	2.13	2.15	2.15	1.97
K2O	0.00	0.01	0.01	0.00	0.01	0.01	0.00	0.02	0.00	0.00	0.04	0.01	0.21	0.02	0.00	0.00	0.00	0.00	0.00	0.00
Total	100.58	100.20	99.86	100.30	99.97	100.50	99.96	99.93	100.56	99.84	99.66	100.13	90.65	99.51	100.24	100.16	99.88	100.11	100.08	100.46
Si	1.935	1.940	1.935	1.930	1.931	1.924	1.929	1.926		1.927		1.917		1.911	1.917	1.917	1.917	1.920	1.920	1.920
Ti	0.003	0.001	0.004	0.002	0.003	0.003	0.002	0.003		0.002		0.004		0.003	0.004	0.003	0.002	0.004	0.003	0.003
Al	0.231	0.231	0.232	0.230	0.245	0.249	0.265	0.261		0.261		0.265		0.278	0.276	0.276	0.277	0.279	0.275	0.267
Cr	0.002	0.002	0.001	0.001	0.001	0.001	0.003	0.001		0.002		0.001		0.000	0.000	0.002	0.000	0.001	0.001	0.001
Fe2+	0.151	0.149	0.141	0.150	0.143	0.146	0.148	0.151		0.149		0.155		0.145	0.146	0.153	0.148	0.146	0.147	0.148
Mn	0.002	0.002	0.002	0.000	0.001	0.002	0.002	0.004		0.002		0.003		0.001	0.001	0.002	0.003	0.003	0.003	0.003
Mg	0.798	0.786	0.789	0.798	0.785	0.791	0.773	0.772		0.770		0.772		0.762	0.767	0.761	0.757	0.765	0.764	0.769
Ca	0.765	0.763	0.771	0.776	0.769	0.766	0.739	0.754		0.755		0.763		0.770	0.760	0.753	0.763	0.743	0.751	0.764
Na	0.118	0.133	0.139	0.129	0.133	0.134	0.149	0.134		0.142		0.134		0.148	0.144	0.150	0.150	0.151	0.151	0.138
K	0.000	0.001	0.001	0.000	0.000	0.000	0.000	0.001		0.000		0.000		0.001	0.000	0.000	0.000	0.000	0.000	0.000
Sum	4.004	4.008	4.015	4.016	4.01	4.015	4.010	4.007		4.010		4.014		4.021	4.013	4.016	4.017	4.012	4.015	4.012
Mg#	84.09	84.06	84.84	84.18	84.59	84.42	83.93	83.64		83.79		83.28		84.01	84.01	83.26	83.65	83.97	83.86	83.86
Al IV	0.061	0.051	0.051	0.053	0.060	0.061	0.062	0.067		0.063		0.070		0.068	0.070	0.067	0.066	0.069	0.066	0.068
Al VI	0.171	0.181	0.182	0.177	0.186	0.188	0.204	0.195		0.199		0.195		0.211	0.206	0.209	0.212	0.211	0.210	0.199

1910-1 Cpx I-II, profile 1210

	210	220	230	240	250	260	270	280	290	300	310	320	330	340	350	360	370	380	390	400
SiO2	52.85	53.09	52.89	52.98	53.88	53.12	53.22	52.82	53.18	53.29	53.55	53.34	53.35	53.10	53.47	53.02	53.31	53.04	53.07	53.15
TiO2	0.13	0.10	0.13	0.12	0.10	0.08	0.15	0.08	0.14	0.11	0.09	0.10	0.12	0.15	0.10	0.09	0.08	0.10	0.14	0.10
Al2O3	6.02	6.25	6.13	6.12	7.78	6.16	6.03	5.87	5.96	5.62	5.82	5.70	5.94	5.90	5.94	5.88	6.11	6.21	6.40	6.16
Cr2O3	0.02	0.07	0.02	0.05	0.06	0.07	0.05	0.01	0.04	0.04	0.03	0.03	0.00	0.02	0.04	0.05	0.00	0.03	0.03	0.05
FeO	4.77	4.92	4.89	4.78	4.73	4.69	5.07	4.72	4.72	4.74	4.92	4.87	4.89	5.10	4.90	4.70	4.94	4.71	4.95	4.54
MnO	0.09	0.01	0.04	0.04	0.03	0.00	0.02	0.08	0.04	0.04	0.04	0.04	0.05	0.00	0.09	0.06	0.02	0.10	0.04	0.00
MgO	14.34	14.34	14.39	14.25	13.86	14.22	14.24	14.39	14.33	14.62	14.20	14.50	14.20	14.22	14.36	14.47	14.38	14.29	13.91	14.04
CaO	19.56	19.37	19.50	19.62	16.11	19.73	19.39	19.53	19.35	19.59	19.78	19.79	19.37	19.44	19.70	19.71	19.06	19.90	19.34	19.52
Na2O	1.88	2.02	1.98	1.89	1.27	2.01	1.96	1.84	1.98	1.85	1.84	1.80	1.87	1.93	1.80	1.75	1.87	1.86	2.02	1.93
K2O	0.00	0.00	0.00	0.01	0.14	0.00	0.02	0.00	0.01	0.00	0.01	0.00	0.00	0.01	0.01	0.00	0.01	0.01	0.03	0.01
Total	99.66	100.18	99.98	99.86	97.95	100.07	100.13	99.32	99.75	99.89	100.26	100.16	99.79	99.87	100.39	99.73	99.79	100.26	99.93	99.51
Si	1.924	1.923	1.921	1.925		1.925	1.929	1.929	1.932	1.934	1.937	1.933	1.937	1.930	1.932	1.928	1.934	1.921	1.926	1.934
Ti	0.004	0.003	0.003	0.003		0.002	0.004	0.002	0.004	0.003	0.002	0.003	0.003	0.004	0.003	0.003	0.002	0.003	0.004	0.003
Al	0.258	0.267	0.262	0.262		0.263	0.257	0.253	0.255	0.240	0.248	0.243	0.254	0.253	0.253	0.252	0.261	0.265	0.274	0.264
Cr	0.000	0.002	0.001	0.002		0.002	0.001	0.000	0.001	0.001	0.001	0.001	0.000	0.000	0.001	0.001	0.000	0.001	0.001	0.002
Fe2	0.145	0.149	0.149	0.145		0.142	0.154	0.144	0.144	0.144	0.149	0.148	0.148	0.155	0.148	0.143	0.150	0.143	0.150	0.138
Mn	0.003	0.000	0.001	0.001		0.000	0.000	0.002	0.001	0.001	0.001	0.001	0.002	0.000	0.003	0.002	0.001	0.003	0.001	0.000
Ni	0.000	0.000	0.000	0.000		0.000	0.000	0.000	0.000	0.000	0.000	0.000	0.000	0.000	0.000	0.000	0.000	0.000	0.000	0.000
Mg	0.778	0.774	0.779	0.772		0.768	0.770	0.783	0.776	0.791	0.766	0.783	0.768	0.771	0.773	0.784	0.778	0.771	0.753	0.761
Ca	0.763	0.752	0.759	0.764		0.766	0.753	0.764	0.753	0.762	0.767	0.768	0.754	0.757	0.763	0.768	0.741	0.772	0.752	0.761
Na	0.133	0.142	0.139	0.133		0.141	0.138	0.130	0.140	0.130	0.129	0.126	0.132	0.136	0.126	0.124	0.131	0.130	0.142	0.136
K	0.000	0.000	0.000	0.000		0.000	0.001	0.000	0.000	0.000	0.000	0.000	0.000	0.000	0.000	0.000	0.001	0.000	0.001	0.000
Sum	4.009	4.011	4.014	4.007		4.010	4.007	4.008	4.006	4.007	4.000	4.006	3.999	4.007	4.002	4.005	3.999	4.009	4.005	3.999
Mg#	84.29	83.86	83.94	84.19		84.40	83.33	84.47	84.35	84.60	83.72	84.10	83.84	83.26	83.93	84.57	83.84	84.35	83.39	84.65
Al IV	0.067	0.067	0.065	0.069		0.064	0.064	0.064	0.062	0.059	0.062	0.062	0.064	0.063	0.067	0.068	0.067	0.071	0.070	0.068
Al VI	0.192	0.201	0.197	0.194		0.199	0.194	0.190	0.193	0.182	0.186	0.181	0.190	0.191	0.186	0.185	0.195	0.194	0.204	0.196

1910-1 Cpx I-II, profile 1210

	410	420	430	440	450	460	470	480	490	500	510	520	530	540	550	560	570	580	590	600
SiO2	52.99	53.13	53.33	53.07	53.04	53.32	53.14	53.10	53.07	52.81	53.07	53.18	53.49	53.30	53.01	53.51	53.32	53.24	52.96	53.25
TiO2	0.13	0.10	0.13	0.12	0.15	0.11	0.09	0.11	0.10	0.10	0.08	0.07	0.14	0.10	0.07	0.12	0.12	0.03	0.10	0.11
Al2O3	6.16	5.82	5.80	5.91	5.77	5.75	5.79	6.05	5.98	6.10	5.82	5.68	5.68	5.66	5.50	5.44	5.56	5.67	5.72	5.74
Cr2O3	0.02	0.04	0.01	0.03	0.01	0.05	0.04	0.02	0.01	0.01	0.02	0.03	0.02	0.04	0.04	0.03	0.08	0.03	0.04	0.00
FeO	4.81	4.84	4.75	5.05	4.81	4.84	4.88	4.94	4.97	4.98	5.13	4.77	4.77	4.85	4.86	5.05	4.98	4.86	5.06	4.94
MnO	0.08	0.05	0.04	0.04	0.08	0.09	0.03	0.03	0.04	0.03	0.11	0.05	0.09	0.05	0.09	0.03	0.04	0.05	0.00	0.00
MgO	14.08	14.26	14.34	14.26	14.34	14.47	14.31	14.24	14.37	14.14	14.63	14.62	14.61	14.29	14.58	14.67	14.76	14.47	14.43	14.56
CaO	19.72	19.63	19.40	19.67	19.54	19.69	19.71	19.08	19.76	19.49	19.64	19.75	19.56	19.55	19.69	19.51	19.73	19.37	19.57	19.72
Na2O	1.87	1.77	1.93	2.05	1.83	1.93	1.96	1.98	2.05	1.93	1.96	1.87	2.02	2.06	1.91	1.85	1.76	1.98	1.97	1.98
K2O	0.00	0.01	0.00	0.01	0.03	0.00	0.01	0.01	0.02	0.00	0.00	0.00	0.02	0.00	0.00	0.01	0.00	0.00	0.00	0.02
Total	99.85	99.65	99.72	100.20	99.60	100.24	99.95	99.56	100.35	99.58	100.47	100.02	100.40	99.90	99.75	100.23	100.35	99.70	99.85	100.31
Si	1.926	1.934	1.938	1.926	1.932	1.931	1.931	1.933	1.922	1.925	1.922	1.930	1.933	1.936	1.931	1.938	1.930	1.937	1.928	1.928
Ti	0.003	0.003	0.004	0.003	0.004	0.003	0.002	0.003	0.003	0.003	0.002	0.002	0.004	0.003	0.002	0.003	0.003	0.001	0.003	0.003
Al	0.264	0.249	0.248	0.253	0.248	0.245	0.248	0.260	0.255	0.262	0.248	0.243	0.242	0.242	0.236	0.232	0.237	0.243	0.245	0.245
Cr	0.001	0.001	0.000	0.001	0.000	0.001	0.001	0.001	0.000	0.000	0.001	0.001	0.001	0.001	0.001	0.001	0.002	0.001	0.001	0.000
Fe2+	0.146	0.147	0.144	0.153	0.147	0.146	0.148	0.150	0.151	0.152	0.155	0.145	0.144	0.147	0.148	0.153	0.151	0.148	0.154	0.149
Mn	0.002	0.001	0.001	0.001	0.002	0.003	0.001	0.001	0.001	0.001	0.003	0.002	0.003	0.001	0.003	0.001	0.001	0.002	0.000	0.000
Mg	0.763	0.774	0.776	0.771	0.779	0.781	0.775	0.773	0.776	0.768	0.790	0.791	0.787	0.774	0.792	0.792	0.796	0.785	0.783	0.786
Ca	0.768	0.765	0.755	0.765	0.763	0.764	0.767	0.744	0.767	0.761	0.762	0.768	0.757	0.761	0.768	0.757	0.765	0.755	0.763	0.765
Na	0.132	0.125	0.136	0.144	0.129	0.136	0.138	0.140	0.144	0.137	0.138	0.132	0.141	0.145	0.135	0.130	0.124	0.139	0.139	0.139
K	0.00	0.000	0.000	0.000	0.001	0.000	0.000	0.001	0.001	0.000	0.000	0.000	0.001	0.000	0.000	0.001	0.000	0.000	0.000	0.001
Sum	4.005	4.001	4.002	4.017	4.005	4.011	4.012	4.004	4.019	4.009	4.021	4.012	4.013	4.012	4.016	4.008	4.009	4.010	4.016	4.016
Mg#	83.94	84.04	84.35	83.44	84.13	84.25	83.97	83.75	83.71	83.48	83.60	84.51	84.53	84.04	84.26	83.81	84.05	84.14	83.56	84.06
Al IV	0.070	0.066	0.060	0.058	0.063	0.058	0.058	0.063	0.058	0.066	0.058	0.058	0.055	0.052	0.053	0.054	0.061	0.054	0.057	0.056
Al VI	0.195	0.184	0.188	0.195	0.185	0.187	0.191	0.197	0.197	0.197	0.191	0.185	0.188	0.190	0.183	0.178	0.177	0.190	0.189	0.190

1910-1 Cpx I-II, profile 1210

	610	620	630	640	650	660	670	680	690	700	710	720	730	740	750	760	770	780	790	800
SiO2	53.39	53.14	53.18	53.22	53.31	53.68	53.47	53.10	53.32	53.64	53.21	53.26	53.53	53.70	53.70	53.13	53.22	53.62	53.27	53.27
TiO2	0.11	0.09	0.09	0.10	0.06	0.11	0.08	0.07	0.03	0.08	0.11	0.06	0.10	0.08	0.10	0.08	0.10	0.09	0.06	0.10
Al2O3	5.49	5.64	5.47	5.41	5.27	5.06	5.19	5.35	6.28	5.19	5.09	5.30	5.38	5.45	5.27	5.35	5.58	5.47	5.40	5.54
Cr2O3	0.00	0.04	0.02	0.03	0.01	0.01	0.05	0.04	0.04	0.02	0.00	0.04	0.00	0.03	0.05	0.06	0.00	0.06	0.06	0.02
FeO	4.81	5.02	4.72	5.19	5.00	4.82	5.19	4.67	4.89	4.89	4.85	4.74	4.86	5.02	4.75	4.92	5.14	5.00	4.94	4.91
MnO	0.04	0.06	0.07	0.05	0.05	0.05	0.08	0.09	0.05	0.06	0.04	0.01	0.05	0.05	0.06	0.04	0.02	0.05	0.01	0.03
MgO	14.70	14.48	14.58	14.58	14.87	14.96	15.15	14.65	15.08	14.91	15.09	14.45	15.06	14.47	14.91	14.88	14.81	14.72	14.81	14.77
CaO	19.79	19.72	19.61	19.72	19.89	19.82	19.91	19.91	19.50	19.85	19.79	19.51	19.90	19.78	19.64	19.84	19.69	19.53	19.53	19.89
Na2O	1.78	1.95	1.65	1.86	1.87	1.64	1.71	1.70	1.42	1.68	1.73	1.82	1.67	1.99	1.69	1.80	1.82	1.85	1.84	1.87
K2O	0.02	0.01	0.00	0.00	0.02	0.01	0.01	0.02	0.03	0.00	0.00	0.02	0.01	0.00	0.01	0.00	0.00	0.01	0.00	0.00
Total	100.12	100.14	99.39	100.15	100.34	100.16	100.84	99.61	100.63	100.33	99.91	99.21	100.56	100.56	100.17	100.09	100.37	100.38	99.92	100.39
Si	1.935	1.929		1.933	1.932	1.944	1.929	1.935		1.940	1.934	1.946	1.932	1.940	1.943	1.929	1.927	1.938	1.935	1.928
Ti	0.003	0.002		0.003	0.002	0.003	0.002	0.002		0.002	0.003	0.002	0.003	0.002	0.003	0.002	0.003	0.002	0.002	0.003
Al	0.234	0.241		0.231	0.225	0.216	0.221	0.230		0.221	0.218	0.228	0.229	0.232	0.225	0.229	0.238	0.233	0.231	0.236
Cr	0.000	0.001		0.001	0.000	0.000	0.002	0.001		0.001	0.000	0.001	0.000	0.001	0.001	0.002	0.000	0.002	0.002	0.001
Fe2+	0.146	0.152		0.158	0.152	0.146	0.157	0.142		0.148	0.147	0.145	0.147	0.152	0.144	0.150	0.156	0.151	0.150	0.148
Mn	0.001	0.002		0.002	0.001	0.002	0.002	0.003		0.002	0.001	0.000	0.002	0.001	0.002	0.001	0.001	0.002	0.000	0.001
Mg	0.794	0.784		0.789	0.803	0.807	0.815	0.796		0.804	0.818	0.787	0.810	0.779	0.804	0.805	0.799	0.793	0.802	0.797
Ca	0.768	0.767		0.767	0.772	0.769	0.770	0.778		0.769	0.771	0.764	0.770	0.765	0.761	0.772	0.764	0.756	0.760	0.771
Na	0.125	0.137		0.131	0.132	0.115	0.119	0.120		0.118	0.122	0.129	0.117	0.139	0.119	0.126	0.128	0.130	0.129	0.131
K	0.001	0.001		0.000	0.001	0.000	0.000	0.001		0.000	0.000	0.001	0.001	0.000	0.000	0.000	0.000	0.000	0.000	0.000
Sum	4.008	4.016		4.014	4.020	4.002	4.017	4.008		4.006	4.015	4.003	4.009	4.011	4.001	4.016	4.015	4.007	4.012	4.016
Mg#	84.47	83.76		83.32	84.08	84.68	83.85	84.86		84.45	84.77	84.44	84.64	83.67	84.81	84.29	83.66	84.00	84.24	84.34
Al IV	0.057	0.054		0.054	0.048	0.054	0.054	0.057		0.054	0.051	0.052	0.059	0.049	0.057	0.055	0.058	0.055	0.054	0.056
Al VI	0.177	0.187		0.178	0.177	0.163	0.167	0.173		0.167	0.167	0.177	0.171	0.183	0.169	0.175	0.180	0.179	0.177	0.180

1910-1 Cpx I-II, profile 1210

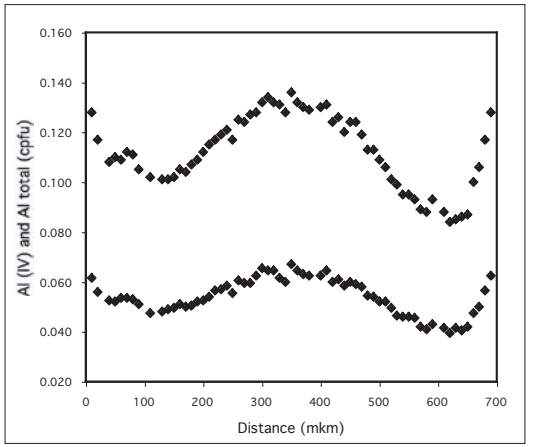
	810	820	830	840	850	860	870	880	890	900	910	920	930	940	950	960	970	980	990	1000
SiO2	53.59	53.21	53.07	53.49	53.32	53.30	53.26	53.31	53.48	53.30	53.06	53.10	52.98	53.53	53.37	53.05	53.25	52.96	53.31	53.42
TiO2	0.04	0.05	0.11	0.08	0.08	0.06	0.13	0.08	0.11	0.06	0.10	0.13	0.13	0.09	0.14	0.06	0.13	0.11	0.09	0.09
Al2O3	5.25	5.30	5.41	5.66	5.43	5.44	5.33	5.40	5.27	5.35	5.46	5.69	5.66	5.50	5.84	5.65	5.70	6.04	5.80	5.89
Cr2O3	0.01	0.01	0.06	0.04	0.04	0.07	0.04	0.04	0.04	0.07	0.02	0.02	0.04	0.02	0.02	0.00	0.00	0.05	0.08	0.06
FeO	4.97	5.04	4.90	4.87	5.00	4.99	5.02	4.75	4.81	4.77	4.83	5.17	4.85	4.99	4.76	4.96	4.88	5.15	5.07	4.88
MnO	0.06	0.09	0.03	0.00	0.06	0.09	0.11	0.01	0.05	0.13	0.04	0.09	0.10	0.00	0.04	0.04	0.06	0.04	0.00	0.00
MgO	14.91	14.75	14.54	14.30	14.77	14.58	14.70	14.85	14.63	14.60	14.61	14.54	14.58	14.67	14.40	14.74	14.85	14.24	14.43	14.42
CaO	19.78	20.10	19.72	19.63	19.86	20.00	19.94	19.93	19.65	19.63	19.73	19.66	19.76	19.64	19.53	19.55	19.62	19.04	19.56	19.55
Na2O	1.76	1.87	1.85	1.92	1.83	1.79	1.87	1.74	1.97	1.94	1.65	1.95	1.90	1.93	1.94	1.70	1.72	1.87	1.85	1.82
K2O	0.00	0.01	0.01	0.00	0.00	0.01	0.00	0.00	0.00	0.01	0.01	0.00	0.00	0.01	0.00	0.00	0.01	0.01	0.02	0.00
Total	100.36	100.42	99.71	100.00	100.38	100.32	100.40	100.11	99.99	99.85	99.49	100.36	99.98	100.38	100.05	99.75	100.22	99.48	100.20	100.14
Si	1.939	1.929	1.934	1.94	1.931	1.932	1.93	1.933	1.941	1.938	1.935	1.925	1.926	1.936	1.934	1.93	1.928	1.931	1.931	1.934
Ti	0.001	0.001	0.003	0.002	0.002	0.002	0.004	0.002	0.003	0.002	0.003	0.004	0.003	0.002	0.004	0.002	0.004	0.003	0.002	0.002
Al	0.224	0.226	0.232	0.242	0.232	0.232	0.228	0.231	0.225	0.229	0.235	0.243	0.242	0.235	0.249	0.242	0.243	0.259	0.248	0.251
Cr	0.000	0.000	0.002	0.001	0.001	0.002	0.001	0.001	0.001	0.002	0.001	0.001	0.001	0.000	0.001	0.000	0.000	0.001	0.002	0.002
Fe2+	0.150	0.153	0.149	0.148	0.151	0.151	0.152	0.144	0.146	0.145	0.147	0.157	0.147	0.151	0.144	0.151	0.148	0.157	0.153	0.148
Mn	0.002	0.003	0.001	0.000	0.002	0.003	0.003	0.000	0.001	0.004	0.001	0.003	0.003	0.000	0.001	0.001	0.002	0.001	0.000	0.000
Mg	0.804	0.797	0.790	0.773	0.797	0.788	0.794	0.803	0.792	0.791	0.794	0.786	0.790	0.791	0.778	0.799	0.801	0.774	0.779	0.778
Ca	0.767	0.781	0.770	0.763	0.771	0.777	0.774	0.774	0.764	0.765	0.771	0.763	0.770	0.761	0.758	0.762	0.761	0.744	0.759	0.758
Na	0.123	0.132	0.130	0.135	0.129	0.126	0.131	0.123	0.138	0.137	0.116	0.137	0.134	0.135	0.136	0.120	0.121	0.132	0.13	0.128
K	0.000	0.001	0.001	0.000	0.000	0.000	0.000	0.000	0.000	0.000	0.001	0.000	0.000	0.000	0.000	0.000	0.000	0.000	0.001	0.000
Sum	4.010	4.022	4.012	4.004	4.015	4.013	4.017	4.010	4.012	4.013	4.003	4.018	4.016	4.012	4.006	4.007	4.008	4.002	4.007	4.001
Mg#	84.28	83.89	84.13	83.93	84.07	83.92	83.93	84.79	84.43	84.51	84.38	83.35	84.31	83.97	84.38	84.11	84.40	83.14	83.58	84.02
Al IV	0.052	0.048	0.055	0.056	0.054	0.056	0.053	0.057	0.047	0.049	0.063	0.058	0.058	0.052	0.061	0.063	0.065	0.067	0.062	0.065
Al VI	0.173	0.179	0.178	0.186	0.178	0.176	0.175	0.175	0.178	0.180	0.173	0.186	0.185	0.183	0.188	0.179	0.178	0.192	0.187	0.187

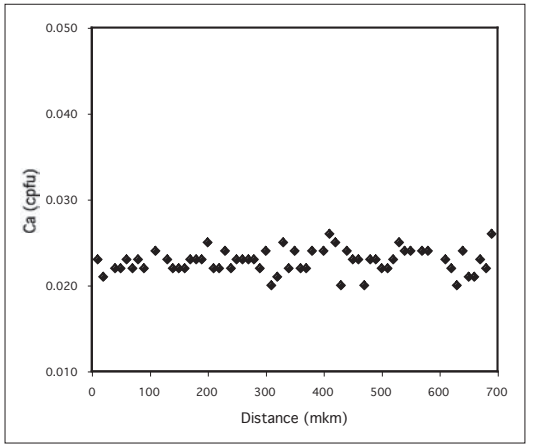
1910-1 Cpx I-II, profile 1210

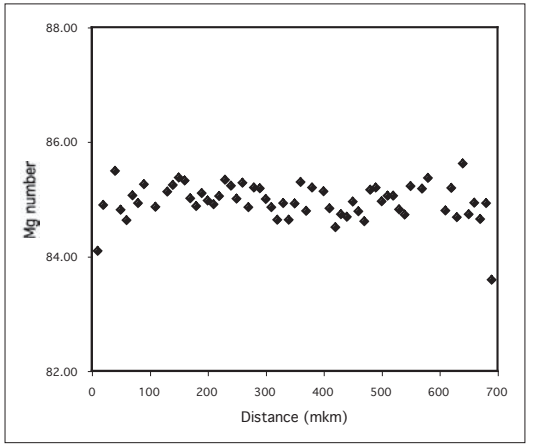
	1010	1020	1030	1040	1050	1060	1070	1080	1090	1100	1110	1120	1130	1140	1150	1160	1170	1180	1190	1200
SiO2	53.01	53.18	53.17	53.56	53.54	52.84	52.81	53.05	52.94	53.16	52.65	53.20	53.05	53.32	42.47	53.38	53.15	53.33	53.54	53.36
TiO2	0.12	0.09	0.10	0.12	0.11	0.11	0.13	0.08	0.11	0.10	0.11	0.10	0.08	0.10	0.11	0.07	0.03	0.07	0.05	0.06
Al2O3	5.97	5.86	5.95	4.50	3.26	5.73	5.72	5.86	5.72	5.50	5.60	5.53	5.11	5.58	27.82	5.24	5.15	4.99	4.98	4.97
Cr2O3	0.02	0.06	0.04	0.07	0.04	0.00	0.03	0.00	0.00	0.06	0.03	0.00	0.06	0.02	0.00	0.09	0.06	0.02	0.03	0.09
FeO	4.85	4.88	5.02	4.54	4.38	5.00	4.96	5.07	5.20	4.86	4.74	4.91	4.88	4.90	3.45	4.86	4.84	4.89	4.97	4.96
MnO	0.09	0.08	0.03	0.03	0.06	0.06	0.00	0.03	0.02	0.05	0.06	0.07	0.05	0.09	0.02	0.04	0.07	0.02	0.11	0.00
MgO	14.50	14.36	14.57	15.68	16.36	14.55	14.68	14.36	14.64	14.71	14.54	14.68	14.12	14.69	9.53	14.97	14.92	14.89	14.86	14.90
CaO	19.47	19.66	19.47	20.58	21.83	19.80	19.60	19.52	19.52	20.12	20.37	19.48	19.67	19.68	10.96	19.86	20.01	20.05	19.83	19.95
Na2O	1.98	1.75	1.83	0.99	0.79	1.88	1.73	1.94	1.84	1.76	1.85	2.04	1.70	1.94	0.85	1.86	1.88	1.77	1.86	1.79
K2O	0.02	0.00	0.00	0.05	0.01	0.05	0.00	0.02	0.00	0.01	0.02	0.03	0.02	0.03	0.20	0.00	0.00	0.00	0.02	0.02
Total	100.01	99.91	100.18	100.10	100.39	100.01	99.66	99.94	100.01	100.33	99.96	100.04	98.73	100.35	95.41	100.37	100.11	100.03	100.25	100.08
Si	1.924	1.931	1.926			1.922	1.924	1.928	1.924	1.926	1.918	1.932		1.93		1.932	1.931	1.938	1.942	1.938
Ti	0.003	0.002	0.003			0.003	0.004	0.002	0.003	0.003	0.003	0.003		0.003		0.002	0.001	0.002	0.001	0.002
Al	0.255	0.251	0.254			0.246	0.246	0.251	0.245	0.235	0.240	0.237		0.238		0.223	0.221	0.214	0.213	0.213
Cr	0.000	0.002	0.001			0.000	0.001	0.000	0.000	0.002	0.001	0.000		0.000		0.003	0.002	0.001	0.001	0.002
Fe2+	0.147	0.148	0.152			0.152	0.151	0.154	0.158	0.147	0.144	0.149		0.148		0.147	0.147	0.149	0.151	0.151
Mn	0.003	0.002	0.001			0.002	0.000	0.001	0.001	0.002	0.002	0.002		0.003		0.001	0.002	0.001	0.004	0.000
Mg	0.785	0.777	0.787			0.789	0.797	0.778	0.794	0.795	0.79	0.795		0.793		0.808	0.808	0.807	0.803	0.807
Ca	0.757	0.765	0.756			0.772	0.765	0.760	0.760	0.781	0.795	0.758		0.763		0.770	0.779	0.781	0.770	0.777
Na	0.139	0.123	0.129			0.133	0.122	0.137	0.130	0.124	0.131	0.144		0.136		0.130	0.132	0.125	0.131	0.126
K	0.001	0.000	0.000			0.002	0.000	0.001	0.000	0.001	0.001	0.001		0.001		0.000	0.000	0.000	0.001	0.001
Sum	4.015	4.002	4.008			4.020	4.010	4.013	4.015	4.015	4.024	4.02		4.017		4.018	4.023	4.015	4.016	4.016
Mg#	84.23	84.00	83.81			83.85	84.07	83.48	83.40	84.39	84.58	84.22		84.27		84.61	84.61	84.41	84.17	84.24
Al IV	0.061	0.067	0.066			0.059	0.067	0.059	0.061	0.059	0.058	0.049		0.054		0.050	0.047	0.047	0.042	0.046
Al VI	0.195	0.184	0.188			0.188	0.180	0.193	0.185	0.176	0.183	0.188		0.185		0.173	0.175	0.167	0.171	0.167

1910-1 Cpx I-II, profile 1210

	10	20	30	40	50	60	70	80	90
SiO2	55.23	55.24	49.49	55.53	55.23	55.29	55.37	55.32	55.47
TiO2	0.01	0.01	0.03	0.03	0.02	0.04	0.02	0.02	0.03
Al2O3	3.11	2.84	9.90	2.63	2.66	2.66	2.72	2.69	2.56
Cr2O3	0.02	0.03	0.03	0.03	0.04	0.03	0.02	0.04	0.03
FeO	10.51	9.96	9.21	9.56	10.06	10.19	9.85	9.95	9.76
MnO	0.15	0.03	0.07	0.06	0.07	0.08	0.02	0.07	0.10
NiO	0.18	0.20	0.12	0.16	0.18	0.21	0.18	0.15	0.12
MgO	31.17	31.37	25.19	31.57	31.50	31.53	31.48	31.47	31.65
CaO	0.62	0.56	0.60	0.60	0.60	0.61	0.60	0.60	0.58
Na2O	0.07	0.08	0.10	0.08	0.11	0.08	0.10	0.09	0.09
K2O	0.01	0.00	0.02	0.00	0.00	0.00	0.01	0.00	0.00
Total	101.07	100.32	94.76	100.24	100.46	100.71	100.36	100.40	100.39
Si	1.924	1.932		1.940	1.932	1.930	1.935	1.934	1.938
Ti	0.000	0.000		0.001	0.000	0.001	0.001	0.000	0.001
Al	0.128	0.117		0.108	0.110	0.109	0.112	0.111	0.105
Cr	0.001	0.001		0.001	0.001	0.001	0.000	0.001	0.001
Fe2+	0.306	0.291		0.279	0.294	0.298	0.288	0.291	0.285
Mn	0.004	0.001		0.002	0.002	0.002	0.000	0.002	0.003
Ni	0.005	0.006		0.004	0.005	0.006	0.005	0.004	0.003
Mg	1.618	1.636		1.644	1.642	1.641	1.640	1.640	1.648
Ca	0.023	0.021		0.022	0.022	0.023	0.022	0.023	0.022
Na	0.005	0.006		0.006	0.007	0.005	0.007	0.006	0.006
K	0.001	0.000		0.000	0.000	0.000	0.000	0.000	0.000
Sum	4.014	4.011		4.008	4.016	4.016	4.012	4.013	4.012
Mg#	84.10	84.90		85.49	84.81	84.63	85.06	84.93	85.26
Al IV	0.062	0.056		0.053	0.052	0.054	0.054	0.053	0.051
Al VI	0.067	0.061		0.056	0.058	0.056	0.059	0.058	0.054







1910-1 Opx I, profile 690

	100	110	120	130	140	150	160	170	180	190	200	210	220	230	240	250	260	270	280	290
SiO2	55.62	55.85	56.03	55.86	55.86	55.55	55.72	55.51	55.87	55.64	55.69	55.73	55.59	55.76	55.25	55.75	55.16	54.98	55.20	55.06
TiO2	0.01	0.01	0.02	0.03	0.03	0.04	0.03	0.02	0.04	0.03	0.02	0.04	0.03	0.03	0.02	0.05	0.00	0.02	0.01	0.05
Al2O3	2.62	2.49	2.47	2.45	2.45	2.48	2.55	2.53	2.63	2.66	2.73	2.81	2.85	2.89	2.94	2.87	3.04	2.99	3.09	3.12
Cr2O3	0.00	0.01	0.04	0.01	0.01	0.02	0.02	0.00	0.01	0.02	0.02	0.04	0.00	0.01	0.00	0.02	0.02	0.00	0.00	0.02
FeO	9.79	10.07	9.63	9.83	9.74	9.63	9.71	9.95	10.03	9.87	9.88	10.00	9.86	9.59	9.72	9.94	9.70	9.86	9.66	9.76
MnO	0.07	0.09	0.11	0.10	0.10	0.08	0.13	0.03	0.07	0.09	0.03	0.05	0.03	0.08	0.03	0.06	0.11	0.09	0.04	0.06
NiO	0.18	0.15	0.22	0.17	0.16	0.13	0.12	0.15	0.13	0.16	0.15	0.13	0.18	0.16	0.07	0.14	0.16	0.16	0.17	0.13
MgO	31.38	31.60	30.93	31.53	31.60	31.59	31.69	31.61	31.55	31.60	31.39	31.54	31.45	31.29	31.41	31.59	31.47	31.02	31.22	31.46
CaO	0.77	0.66	1.46	0.62	0.60	0.60	0.59	0.62	0.63	0.61	0.68	0.60	0.60	0.65	0.59	0.61	0.60	0.61	0.61	0.58
Na2O	0.16	0.11	0.16	0.09	0.08	0.08	0.08	0.09	0.11	0.11	0.14	0.14	0.09	0.09	0.09	0.11	0.08	0.10	0.10	0.09
K2O	0.00	0.00	0.00	0.02	0.01	0.00	0.00	0.00	0.03	0.00	0.00	0.02	0.01	0.01	0.00	0.00	0.00	0.00	0.01	0.01
Total	100.59	101.04	101.07	100.71	100.63	100.21	100.64	100.52	101.08	100.79	100.73	101.09	100.68	100.57	100.11	101.14	100.35	99.82	100.10	100.32
Si		1.941		1.945	1.945	1.942	1.941	1.938	1.940	1.937	1.939	1.935	1.936	1.941	1.933	1.933	1.928	1.932	1.932	1.925
Ti		0.000		0.001	0.001	0.001	0.001	0.001	0.001	0.001	0.001	0.001	0.001	0.001	0.001	0.001	0.000	0.001	0.000	0.001
Al		0.102		0.101	0.101	0.102	0.105	0.104	0.107	0.109	0.112	0.115	0.117	0.119	0.121	0.117	0.125	0.124	0.127	0.128
Cr		0.000		0.000	0.000	0.000	0.000	0.000	0.000	0.000	0.000	0.001	0.000	0.000	0.000	0.000	0.001	0.000	0.000	0.001
Fe2+		0.292		0.286	0.284	0.282	0.283	0.290	0.291	0.287	0.288	0.290	0.287	0.279	0.284	0.288	0.283	0.290	0.283	0.285
Mn		0.003		0.003	0.003	0.002	0.004	0.001	0.002	0.003	0.001	0.001	0.001	0.002	0.001	0.002	0.003	0.003	0.001	0.002
Ni		0.004		0.005	0.004	0.004	0.003	0.004	0.004	0.005	0.004	0.004	0.005	0.004	0.002	0.004	0.005	0.004	0.005	0.004
Mg		1.637		1.637	1.641	1.646	1.645	1.645	1.633	1.640	1.629	1.632	1.633	1.624	1.639	1.633	1.640	1.625	1.629	1.639
Ca		0.024		0.023	0.022	0.022	0.022	0.023	0.023	0.023	0.025	0.022	0.022	0.024	0.022	0.023	0.023	0.023	0.023	0.022
Na		0.007		0.006	0.005	0.005	0.005	0.006	0.007	0.007	0.009	0.009	0.006	0.006	0.006	0.008	0.005	0.007	0.007	0.006
K		0.000		0.001	0.000	0.000	0.000	0.000	0.001	0.000	0.000	0.001	0.000	0.001	0.000	0.000	0.000	0.000	0.001	0.000
Sum		4.012		4.007	4.007	4.008	4.009	4.013	4.010	4.011	4.009	4.011	4.008	4.002	4.009	4.010	4.012	4.009	4.008	4.013
Mg#		84.86		85.13	85.25	85.37	85.32	85.01	84.88	85.11	84.98	84.91	85.05	85.34	85.23	85.01	85.28	84.86	85.20	85.19
Al IV		0.048		0.048	0.049	0.050	0.051	0.050	0.051	0.052	0.053	0.054	0.057	0.057	0.059	0.056	0.061	0.060	0.060	0.063
Al VI		0.055		0.053	0.052	0.053	0.054	0.054	0.057	0.057	0.060	0.061	0.061	0.062	0.063	0.062	0.065	0.065	0.068	0.066

1910-1 Opx I, profile 690

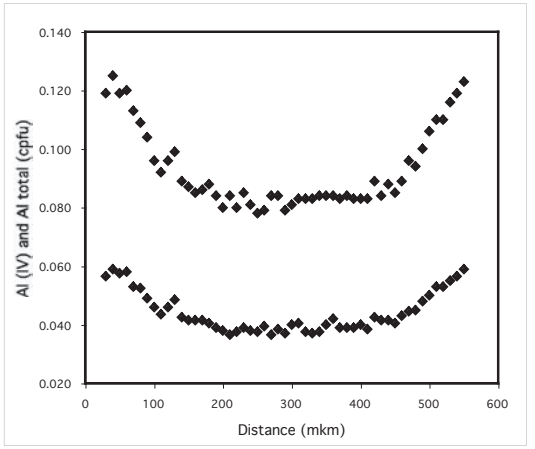
	300	310	320	330	340	350	360	370	380	390	400	410	420	430	440	450	460	470	480	490
SiO2	55.07	55.24	55.14	55.20	55.21	55.02	55.06	54.94	55.10	55.23	55.30	55.02	55.33	55.44	55.28	55.45	55.24	55.35	55.39	55.33
TiO2	0.08	0.06	0.04	0.01	0.01	0.08	0.07	0.02	0.03	0.02	0.01	0.04	0.03	0.00	0.03	0.05	0.00	0.06	0.00	0.04
Al2O3	3.20	3.28	3.22	3.19	3.11	3.32	3.20	3.17	3.14	3.13	3.16	3.18	3.02	3.06	2.92	3.02	3.00	2.90	2.74	2.73
Cr2O3	0.03	0.00	0.04	0.02	0.03	0.00	0.00	0.04	0.04	0.01	0.01	0.02	0.01	0.03	0.02	0.00	0.06	0.04	0.04	0.02
FeO	9.81	9.99	10.10	9.86	10.04	9.95	9.65	10.08	9.71	9.43	9.75	9.94	10.28	10.03	10.18	9.92	9.99	10.29	9.69	9.69
MnO	0.08	0.15	0.05	0.12	0.08	0.03	0.14	0.00	0.05	0.11	0.09	0.05	0.05	0.11	0.10	0.08	0.03	0.12	0.16	0.06
NiO	0.14	0.15	0.16	0.12	0.16	0.12	0.11	0.18	0.17	0.13	0.15	0.13	0.12	0.16	0.16	0.12	0.16	0.16	0.18	0.13
MgO	31.21	31.46	31.23	31.18	31.08	31.42	31.40	31.48	31.39	30.46	31.27	31.24	31.45	31.20	31.52	31.47	31.22	31.77	31.22	31.29
CaO	0.63	0.54	0.56	0.66	0.58	0.65	0.58	0.58	0.63	1.89	0.64	0.69	0.67	0.55	0.64	0.61	0.60	0.54	0.61	0.60
Na2O	0.09	0.11	0.08	0.12	0.13	0.10	0.09	0.10	0.10	0.22	0.07	0.08	0.09	0.08	0.09	0.09	0.12	0.11	0.08	0.12
K2O	0.00	0.00	0.01	0.00	0.00	0.00	0.03	0.01	0.00	0.00	0.01	0.00	0.01	0.00	0.00	0.00	0.01	0.00	0.00	0.00
Total	100.34	100.98	100.65	100.47	100.42	100.69	100.30	100.60	100.36	100.63	100.45	100.38	101.05	100.65	100.95	100.82	100.42	101.34	100.11	100.03
Si	1.925	1.921	1.924	1.928	1.930	1.918	1.924	1.919	1.925		1.930	1.924	1.925	1.933	1.925	1.929	1.931	1.921	1.940	1.939
Ti	0.002	0.001	0.001	0.000	0.000	0.002	0.002	0.001	0.001		0.000	0.001	0.001	0.000	0.001	0.001	0.000	0.002	0.000	0.001
Al	0.132	0.134	0.132	0.131	0.128	0.136	0.132	0.130	0.129		0.130	0.131	0.124	0.126	0.120	0.124	0.124	0.119	0.113	0.113
Cr	0.001	0.000	0.001	0.000	0.001	0.000	0.000	0.001	0.001		0.000	0.001	0.000	0.001	0.001	0.000	0.002	0.001	0.001	0.001
Fe2+	0.287	0.291	0.295	0.288	0.294	0.290	0.282	0.294	0.284		0.284	0.291	0.299	0.292	0.296	0.289	0.292	0.299	0.284	0.284
Mn	0.002	0.004	0.001	0.004	0.002	0.001	0.004	0.000	0.002		0.003	0.001	0.002	0.003	0.003	0.002	0.001	0.004	0.005	0.002
Ni	0.004	0.004	0.005	0.003	0.004	0.003	0.003	0.005	0.005		0.004	0.004	0.003	0.005	0.005	0.003	0.004	0.005	0.005	0.004
Mg	1.626	1.631	1.625	1.623	1.620	1.633	1.636	1.639	1.635		1.627	1.628	1.631	1.621	1.637	1.632	1.627	1.644	1.630	1.635
Ca	0.024	0.020	0.021	0.025	0.022	0.024	0.022	0.022	0.024		0.024	0.026	0.025	0.020	0.024	0.023	0.023	0.020	0.023	0.023
Na	0.006	0.007	0.005	0.008	0.009	0.006	0.006	0.007	0.007		0.005	0.005	0.006	0.005	0.006	0.006	0.008	0.008	0.005	0.008
K	0.000	0.000	0.001	0.000	0.000	0.000	0.001	0.000	0.000		0.000	0.000	0.000	0.000	0.000	0.000	0.000	0.000	0.000	0.000
Sum	4.009	4.014	4.011	4.010	4.010	4.015	4.011	4.018	4.012		4.007	4.012	4.016	4.007	4.017	4.010	4.011	4.021	4.006	4.008
Mg#	85.00	84.86	84.64	84.93	84.64	84.92	85.30	84.79	85.20		85.14	84.84	84.51	84.74	84.69	84.96	84.78	84.61	85.16	85.20
Al IV	0.066	0.065	0.065	0.062	0.060	0.067	0.065	0.063	0.063		0.063	0.065	0.060	0.061	0.059	0.060	0.059	0.058	0.055	0.054
Al VI	0.067	0.070	0.068	0.070	0.068	0.069	0.068	0.067	0.067		0.068	0.067	0.064	0.065	0.062	0.064	0.065	0.061	0.059	0.059

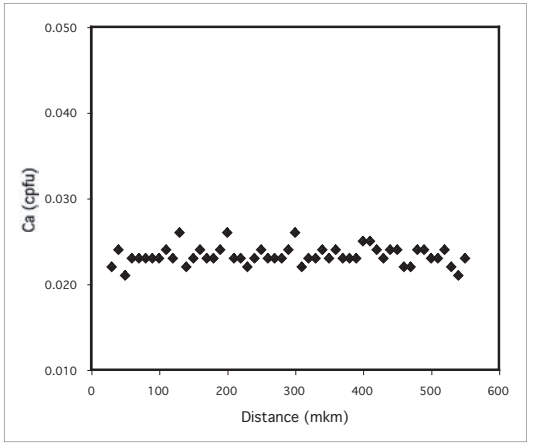
1910-1 Opx I, profile 690

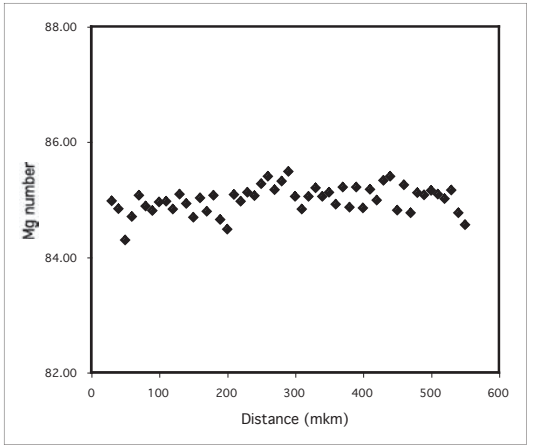
	500	510	520	530	540	550	560	570	580	590	600	610	620	630	640	650	660	670	680	690
SiO2	55.64	55.51	55.41	55.51	55.54	55.51	56.08	56.03	55.19	55.34	55.90	55.84	55.14	55.89	55.72	55.35	55.40	55.19	55.29	54.86
TiO2	0.01	0.03	0.04	0.01	0.04	0.06	0.09	0.03	0.02	0.05	0.07	0.03	0.03	0.04	0.06	0.04	0.02	0.03	0.03	0.04
Al2O3	2.66	2.59	2.46	2.41	2.32	2.30	2.27	2.18	2.12	2.25	2.17	2.15	2.03	2.07	2.08	2.11	2.42	2.57	2.85	3.09
Cr2O3	0.05	0.05	0.03	0.00	0.02	0.03	0.01	0.02	0.02	0.00	0.00	0.00	0.00	0.04	0.00	0.02	0.00	0.01	0.00	0.00
FeO	10.01	9.91	9.85	10.12	10.19	9.76	9.88	9.83	9.72	9.75	9.98	10.17	9.84	10.28	9.48	10.21	9.91	10.25	9.92	10.76
MnO	0.11	0.11	0.04	0.06	0.05	0.11	0.02	0.11	0.08	0.07	0.08	0.10	0.04	0.09	0.10	0.09	0.05	0.09	0.14	0.05
NiO	0.18	0.16	0.13	0.16	0.13	0.14	0.18	0.20	0.15	0.10	0.19	0.17	0.18	0.14	0.15	0.15	0.13	0.18	0.14	0.15
MgO	31.75	31.66	31.51	31.68	31.68	31.63	31.30	31.70	31.86	30.97	31.67	31.83	31.80	31.87	31.70	31.79	31.37	31.65	31.35	30.80
CaO	0.58	0.58	0.62	0.66	0.64	0.65	1.06	0.64	0.63	1.64	0.97	0.62	0.59	0.53	0.63	0.57	0.56	0.62	0.59	0.68
Na2O	0.09	0.08	0.08	0.09	0.08	0.09	0.09	0.10	0.10	0.14	0.03	0.10	0.11	0.07	0.09	0.09	0.08	0.11	0.09	0.08
K2O	0.00	0.00	0.00	0.00	0.00	0.00	0.00	0.01	0.00	0.01	0.00	0.01	0.00	0.00	0.02	0.01	0.00	0.00	0.01	0.00
Total	101.07	100.67	100.18	100.70	100.68	100.27	100.95	100.83	99.88	100.32	101.05	101.01	99.74	101.01	100.04	100.42	99.94	100.70	100.40	100.50
Si	1.933	1.935	1.940	1.937	1.938	1.942		1.949	1.939			1.943	1.941	1.944	1.951	1.938	1.944	1.928	1.933	1.923
Ti	0.000	0.001	0.001	0.000	0.001	0.001		0.001	0.000			0.001	0.001	0.001	0.001	0.001	0.000	0.001	0.001	0.001
Al	0.109	0.106	0.101	0.099	0.095	0.095		0.089	0.088			0.088	0.084	0.085	0.086	0.087	0.100	0.106	0.117	0.128
Cr	0.001	0.001	0.001	0.000	0.000	0.001		0.000	0.001			0.000	0.000	0.001	0.000	0.001	0.000	0.000	0.000	0.000
Fe2+	0.291	0.289	0.289	0.295	0.297	0.286		0.286	0.286			0.296	0.290	0.299	0.278	0.299	0.291	0.299	0.290	0.316
Mn	0.003	0.003	0.001	0.002	0.002	0.003		0.003	0.002			0.003	0.001	0.003	0.003	0.003	0.001	0.003	0.004	0.001
Ni	0.005	0.005	0.004	0.004	0.004	0.004		0.006	0.004			0.005	0.005	0.004	0.004	0.004	0.004	0.005	0.004	0.004
Mg	1.644	1.645	1.645	1.648	1.648	1.650		1.644	1.669			1.651	1.669	1.653	1.655	1.660	1.641	1.649	1.634	1.610
Ca	0.022	0.022	0.023	0.025	0.024	0.024		0.024	0.024			0.023	0.022	0.020	0.024	0.021	0.021	0.023	0.022	0.026
Na	0.006	0.005	0.005	0.006	0.005	0.006		0.007	0.007			0.007	0.007	0.005	0.006	0.006	0.005	0.008	0.006	0.005
K	0.000	0.000	0.000	0.000	0.000	0.000		0.000	0.000			0.000	0.000	0.000	0.001	0.000	0.000	0.000	0.000	0.000
Sum	4.015	4.013	4.010	4.016	4.015	4.012		4.009	4.020			4.016	4.020	4.014	4.008	4.020	4.008	4.022	4.011	4.014
Mg#	84.96	85.06	85.06	84.82	84.73	85.23		85.18	85.37			84.80	85.20	84.68	85.62	84.74	84.94	84.65	84.93	83.59
Al IV	0.052	0.052	0.050	0.047	0.046	0.046		0.042	0.041			0.042	0.040	0.042	0.041	0.042	0.048	0.050	0.057	0.063
Al VI	0.057	0.054	0.052	0.053	0.049	0.049		0.047	0.047			0.047	0.045	0.044	0.046	0.045	0.053	0.056	0.061	0.066

1910-1 Opx I, profile 690

	30	40	50	60	70	80	90	100	110	120	130	140	150
SiO2	55.47	55.43	55.44	55.26	55.81	55.58	55.89	55.87	55.88	56.00	55.24	56.21	55.54
TiO2	0.00	0.01	0.00	0.02	0.00	0.05	0.00	0.01	0.02	0.01	0.02	0.03	0.03
Al2O3	2.90	3.03	2.89	2.90	2.74	2.66	2.53	2.34	2.24	2.34	2.38	2.16	2.12
Cr2O3	0.04	0.00	0.05	0.00	0.00	0.03	0.05	0.03	0.00	0.06	0.06	0.01	0.00
FeO	9.83	9.91	10.40	10.05	9.79	9.98	10.05	9.91	9.96	10.02	9.76	9.96	10.20
MnO	0.09	0.15	0.09	0.08	0.12	0.11	0.04	0.12	0.13	0.06	0.08	0.10	0.13
NiO	0.20	0.10	0.12	0.16	0.10	0.17	0.18	0.21	0.14	0.12	0.17	0.18	0.15
MgO	31.16	31.07	31.32	31.24	31.26	31.45	31.44	31.39	31.54	31.49	31.22	31.52	31.60
CaO	0.59	0.64	0.56	0.62	0.62	0.61	0.61	0.62	0.65	0.62	0.61	0.58	0.61
Na2O	0.10	0.10	0.08	0.09	0.10	0.10	0.10	0.08	0.11	0.09	0.09	0.09	0.08
K2O	0.00	0.00	0.01	0.00	0.01	0.00	0.00	0.01	0.00	0.00	0.00	0.01	0.02
Total	100.37	100.43	100.95	100.41	100.54	100.73	100.88	100.58	100.66	100.82	99.69	100.85	100.49
Si	1.938	1.936	1.931	1.932	1.945	1.937	1.944	1.949	1.948	1.948	1.944	1.954	1.943
Ti	0.000	0.000	0.000	0.001	0.000	0.001	0.000	0.000	0.001	0.000	0.001	0.001	0.001
Al	0.119	0.125	0.119	0.120	0.113	0.109	0.104	0.096	0.092	0.096	0.099	0.089	0.087
Cr	0.001	0.000	0.001	0.000	0.000	0.001	0.001	0.001	0.000	0.002	0.002	0.000	0.000
Fe2+	0.287	0.289	0.303	0.294	0.285	0.291	0.292	0.289	0.290	0.292	0.287	0.290	0.298
Mn	0.003	0.004	0.003	0.002	0.004	0.003	0.001	0.004	0.004	0.002	0.002	0.003	0.004
Ni	0.006	0.003	0.003	0.004	0.003	0.005	0.005	0.006	0.004	0.003	0.005	0.005	0.004
Mg	1.623	1.617	1.626	1.628	1.624	1.634	1.630	1.632	1.639	1.633	1.638	1.634	1.648
Ca	0.022	0.024	0.021	0.023	0.023	0.023	0.023	0.023	0.024	0.023	0.026	0.022	0.023
Na	0.007	0.007	0.005	0.006	0.007	0.007	0.007	0.005	0.007	0.006	0.006	0.006	0.005
K	0.000	0.000	0.000	0.000	0.000	0.000	0.000	0.000	0.000	0.000	0.000	0.000	0.001
Sum	4.006	4.005	4.012	4.01	4.004	4.011	4.007	4.005	4.009	4.005	4.01	4.004	4.014
Mg#	84.97	84.84	84.29	84.70	85.07	84.88	84.81	84.96	84.97	84.83	85.09	84.93	84.69
Al IV	0.057	0.059	0.058	0.058	0.053	0.053	0.049	0.046	0.044	0.046	0.049	0.043	0.042
Al VI	0.063	0.066	0.062	0.062	0.060	0.057	0.055	0.050	0.049	0.050	0.051	0.047	0.046







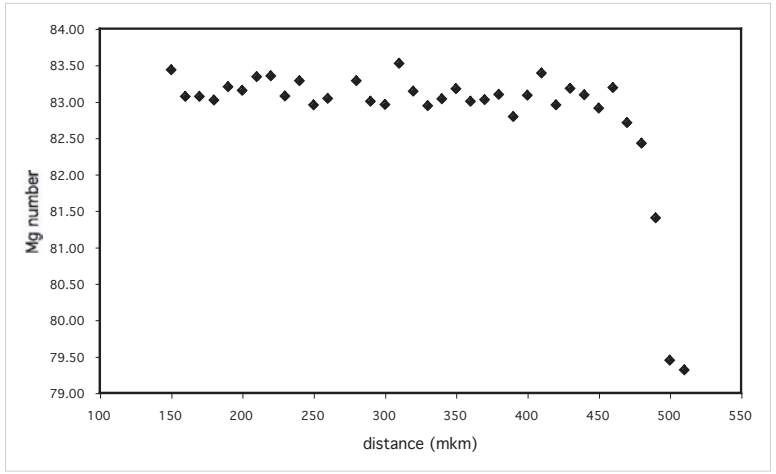
1910-1 Opx II, profile 550

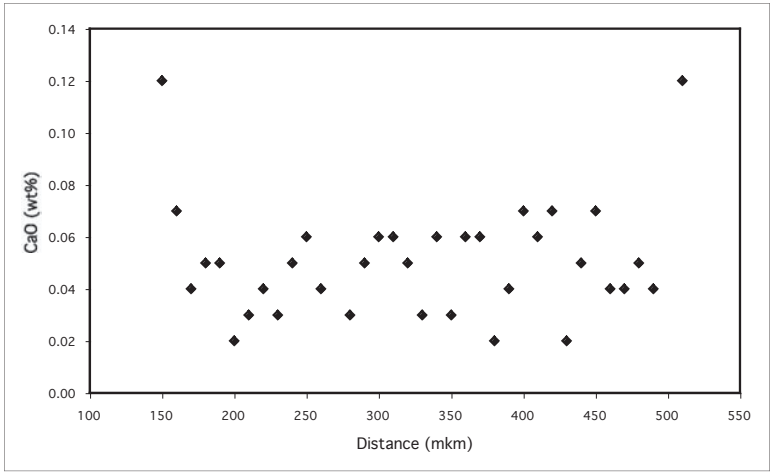
	160	170	180	190	200	210	220	230	240	250	260	270	280	290	300	310	320	330	340	350
SiO2	55.89	55.89	56.19	55.99	55.88	55.90	56.17	55.78	55.98	55.93	56.10	56.17	55.89	56.15	56.24	55.94	55.92	56.24	56.12	55.94
TiO2	0.03	0.00	0.06	0.04	0.05	0.00	0.04	0.05	0.04	0.05	0.06	0.01	0.03	0.00	0.03	0.04	0.00	0.01	0.01	0.04
Al2O3	2.07	2.09	2.14	2.04	1.94	2.03	1.94	2.05	1.97	1.90	1.92	2.02	2.02	1.92	1.97	2.01	2.00	2.01	2.05	2.02
Cr2O3	0.00	0.01	0.01	0.04	0.00	0.02	0.00	0.00	0.02	0.04	0.02	0.00	0.05	0.00	0.00	0.03	0.00	0.00	0.01	0.03
FeO	9.92	10.23	9.78	10.10	10.40	9.70	9.96	9.66	9.75	9.78	9.66	9.52	9.59	9.58	9.92	10.07	9.85	9.68	9.78	9.69
MnO	0.09	0.11	0.10	0.13	0.11	0.11	0.15	0.05	0.15	0.11	0.12	0.04	0.15	0.05	0.04	0.08	0.11	0.09	0.05	0.11
NiO	0.17	0.17	0.21	0.19	0.18	0.14	0.20	0.17	0.21	0.19	0.16	0.12	0.12	0.15	0.08	0.13	0.11	0.17	0.20	0.16
MgO	31.65	31.96	31.24	31.24	31.81	31.05	31.58	30.96	31.18	31.72	31.74	30.66	31.22	31.69	31.69	31.60	31.39	31.29	31.21	31.05
CaO	0.63	0.62	0.61	0.63	0.70	0.60	0.61	0.58	0.62	0.63	0.62	0.61	0.62	0.64	0.69	0.59	0.60	0.61	0.64	0.60
Na2O	0.06	0.05	0.16	0.13	0.09	0.17	0.11	0.13	0.12	0.09	0.07	0.16	0.14	0.07	0.05	0.07	0.12	0.13	0.14	0.11
K2O	0.00	0.00	0.00	0.00	0.00	0.00	0.01	0.00	0.00	0.01	0.00	0.01	0.00	0.00	0.00	0.01	0.00	0.00	0.00	0.00
Total	100.50	101.13	101.11	101.25	101.16	100.63	101.02	100.41	100.74	100.56	100.48	100.26	100.41	100.23	100.71	100.57	100.49	100.75	100.75	100.41
Si	1.951	1.943	1.959	1.956	1.944	1.963	1.956	1.964	1.961	1.952	1.956	1.976	1.961	1.960	1.957	1.952	1.958	1.964	1.962	1.964
Ti	0.001	0.000	0.002	0.001	0.001	0.000	0.001	0.001	0.001	0.001	0.002	0.000	0.001	0.000	0.001	0.001	0.000	0.000	0.000	0.001
Al	0.085	0.086	0.088	0.084	0.080	0.084	0.080	0.085	0.081	0.078	0.079	0.084	0.084	0.079	0.081	0.083	0.083	0.083	0.084	0.084
Cr	0.000	0.000	0.000	0.001	0.000	0.001	0.000	0.000	0.001	0.001	0.001	0.000	0.001	0.000	0.000	0.001	0.000	0.000	0.000	0.001
Fe2+	0.290	0.297	0.285	0.295	0.303	0.285	0.290	0.284	0.286	0.285	0.282	0.280	0.281	0.280	0.289	0.294	0.288	0.283	0.286	0.284
Mn	0.003	0.003	0.003	0.004	0.003	0.003	0.004	0.001	0.004	0.003	0.004	0.001	0.004	0.001	0.001	0.002	0.003	0.003	0.001	0.003
Ni	0.005	0.005	0.006	0.005	0.005	0.004	0.006	0.005	0.006	0.005	0.004	0.003	0.003	0.004	0.002	0.004	0.003	0.005	0.006	0.005
Mg	1.647	1.656	1.624	1.627	1.650	1.626	1.639	1.625	1.629	1.650	1.650	1.608	1.633	1.649	1.644	1.644	1.639	1.629	1.627	1.625
Ca	0.024	0.023	0.023	0.024	0.026	0.023	0.023	0.022	0.023	0.024	0.023	0.023	0.023	0.024	0.026	0.022	0.023	0.023	0.024	0.023
Na	0.004	0.003	0.011	0.009	0.006	0.012	0.007	0.009	0.008	0.006	0.005	0.011	0.010	0.005	0.003	0.005	0.008	0.009	0.009	0.007
K	0.000	0.000	0.000	0.000	0.000	0.000	0.000	0.000	0.000	0.000	0.000	0.000	0.000	0.000	0.000	0.000	0.000	0.000	0.000	0.000
Sum	4.010	4.016	4.001	4.006	4.018	4.001	4.006	3.996	4.000	4.005	4.006	3.986	4.001	4.002	4.004	4.008	4.005	3.999	3.999	3.997
Mg#	85.03	84.79	85.07	84.65	84.49	85.09	84.97	85.12	85.07	85.27	85.40	85.17	85.32	85.48	85.05	84.83	85.05	85.20	85.05	85.12
Al IV	0.042	0.042	0.041	0.039	0.038	0.037	0.038	0.039	0.038	0.038	0.040	0.037	0.039	0.037	0.040	0.041	0.038	0.037	0.038	0.040
Al VI	0.044	0.045	0.048	0.045	0.042	0.048	0.043	0.046	0.043	0.041	0.040	0.048	0.046	0.042	0.041	0.043	0.046	0.046	0.047	0.044

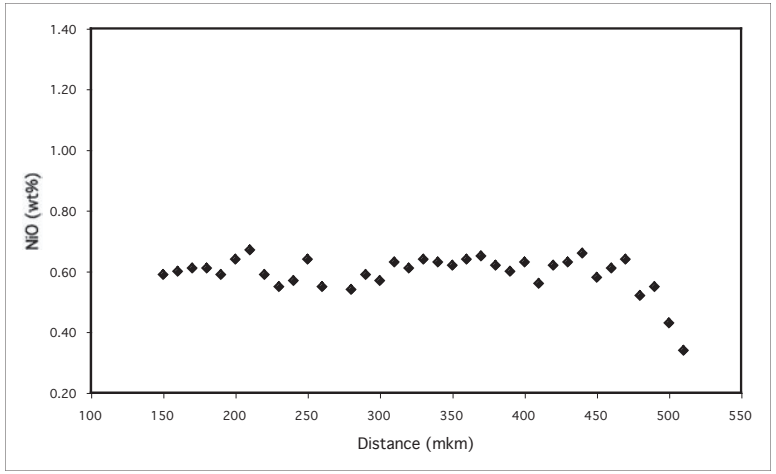
1910-1 Opx II, profile 550

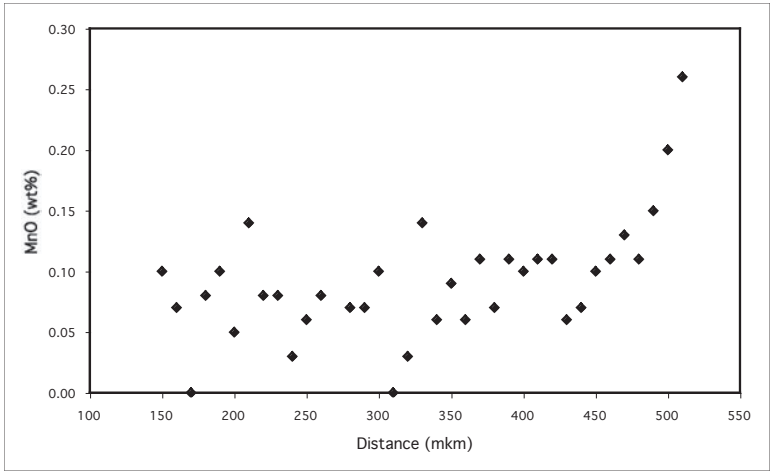
	360	370	380	390	400	410	420	430	440	450	460	470	480	490	500	510	520	530	540	550
SiO2	56.27	56.18	55.85	56.10	56.11	56.28	56.03	55.92	56.01	56.06	56.12	55.97	55.91	56.02	55.49	55.45	55.43	55.49	54.87	55.27
TiO2	0.07	0.05	0.02	0.02	0.03	0.02	0.06	0.02	0.00	0.00	0.02	0.01	0.02	0.05	0.04	0.03	0.03	0.00	0.00	0.04
Al2O3	2.05	2.02	2.03	2.03	2.03	2.03	2.16	2.04	2.15	2.08	2.16	2.34	2.29	2.43	2.56	2.66	2.66	2.82	2.87	2.99
Cr2O3	0.02	0.02	0.03	0.01	0.07	0.00	0.05	0.00	0.00	0.00	0.01	0.01	0.06	0.00	0.02	0.02	0.00	0.04	0.03	0.00
FeO	10.02	9.58	9.84	9.82	10.07	9.78	9.78	9.72	9.62	10.08	9.69	10.00	9.85	9.79	9.72	9.83	9.89	9.73	10.00	10.19
MnO	0.09	0.07	0.12	0.13	0.11	0.09	0.06	0.09	0.10	0.04	0.07	0.09	0.04	0.06	0.10	0.03	0.08	0.11	0.10	0.06
NiO	0.13	0.17	0.15	0.15	0.17	0.12	0.21	0.11	0.17	0.19	0.20	0.15	0.17	0.16	0.16	0.16	0.14	0.14	0.18	0.13
MgO	31.65	30.99	30.92	31.76	31.67	31.56	31.04	31.72	31.61	31.62	31.47	31.25	31.61	31.29	31.33	31.43	31.48	31.29	31.23	31.27
CaO	0.63	0.60	0.62	0.63	0.67	0.66	0.63	0.62	0.63	0.63	0.58	0.59	0.64	0.63	0.60	0.62	0.63	0.59	0.57	0.62
Na2O	0.08	0.12	0.13	0.10	0.10	0.12	0.13	0.05	0.08	0.06	0.08	0.10	0.12	0.09	0.13	0.11	0.09	0.09	0.11	0.10
K2O	0.01	0.00	0.01	0.00	0.00	0.00	0.00	0.00	0.01	0.00	0.01	0.00	0.01	0.01	0.00	0.01	0.01	0.02	0.00	0.00
Total	101.01	100.35	100.40	100.75	101.05	100.65	101.05	100.29	100.38	100.75	100.39	100.50	100.71	100.52	100.15	100.36	100.42	100.31	99.97	100.68
Si	1.954	1.969	1.963	1.953	1.950	1.959	1.960	1.953	1.954	1.952	1.957	1.953	1.947	1.952	1.942	1.938	1.936	1.939	1.928	1.929
Ti	0.002	0.001	0.001	0.001	0.001	0.001	0.002	0.001	0.000	0.000	0.001	0.000	0.001	0.001	0.001	0.001	0.001	0.000	0.000	0.001
Al	0.084	0.083	0.084	0.083	0.083	0.083	0.089	0.084	0.088	0.085	0.089	0.096	0.094	0.100	0.106	0.110	0.110	0.116	0.119	0.123
Cr	0.001	0.001	0.001	0.000	0.002	0.000	0.001	0.000	0.000	0.000	0.000	0.000	0.002	0.000	0.001	0.001	0.000	0.001	0.001	0.000
Fe2+	0.291	0.281	0.289	0.286	0.293	0.285	0.286	0.284	0.281	0.294	0.283	0.292	0.287	0.285	0.285	0.287	0.289	0.284	0.294	0.297
Mn	0.003	0.002	0.004	0.004	0.003	0.003	0.002	0.003	0.003	0.001	0.002	0.003	0.001	0.002	0.003	0.001	0.002	0.003	0.003	0.002
Ni	0.004	0.005	0.004	0.004	0.005	0.003	0.006	0.003	0.005	0.005	0.006	0.004	0.005	0.004	0.005	0.004	0.004	0.004	0.005	0.004
Mg	1.638	1.619	1.620	1.648	1.641	1.637	1.619	1.652	1.644	1.642	1.636	1.625	1.641	1.625	1.635	1.638	1.639	1.630	1.636	1.627
Ca	0.024	0.023	0.023	0.023	0.025	0.025	0.024	0.023	0.024	0.024	0.022	0.022	0.024	0.024	0.023	0.023	0.024	0.022	0.021	0.023
Na	0.005	0.008	0.009	0.007	0.007	0.008	0.009	0.003	0.005	0.004	0.005	0.007	0.008	0.006	0.009	0.007	0.006	0.006	0.007	0.007
K	0.000	0.000	0.000	0.000	0.000	0.000	0.000	0.000	0.000	0.000	0.000	0.000	0.000	0.000	0.000	0.000	0.000	0.001	0.000	0.000
Sum	4.006	3.992	3.998	4.009	4.01	4.004	3.998	4.006	4.004	4.007	4.001	4.002	4.01	3.999	4.01	4.01	4.011	4.006	4.014	4.013
Mg#	84.91	85.21	84.86	85.21	84.85	85.17	84.99	85.33	85.40	84.81	85.25	84.77	85.11	85.08	85.16	85.09	85.01	85.16	84.77	84.56
Al IV	0.042	0.039	0.039	0.039	0.040	0.039	0.043	0.042	0.042	0.041	0.043	0.045	0.045	0.048	0.050	0.053	0.053	0.055	0.057	0.059
Al VI	0.042	0.044	0.045	0.044	0.043	0.045	0.047	0.043	0.047	0.045	0.046	0.052	0.049	0.052	0.056	0.057	0.057	0.061	0.063	0.064

1910-1 Opx II, profile 550









1910-1 Olivine, profile 360

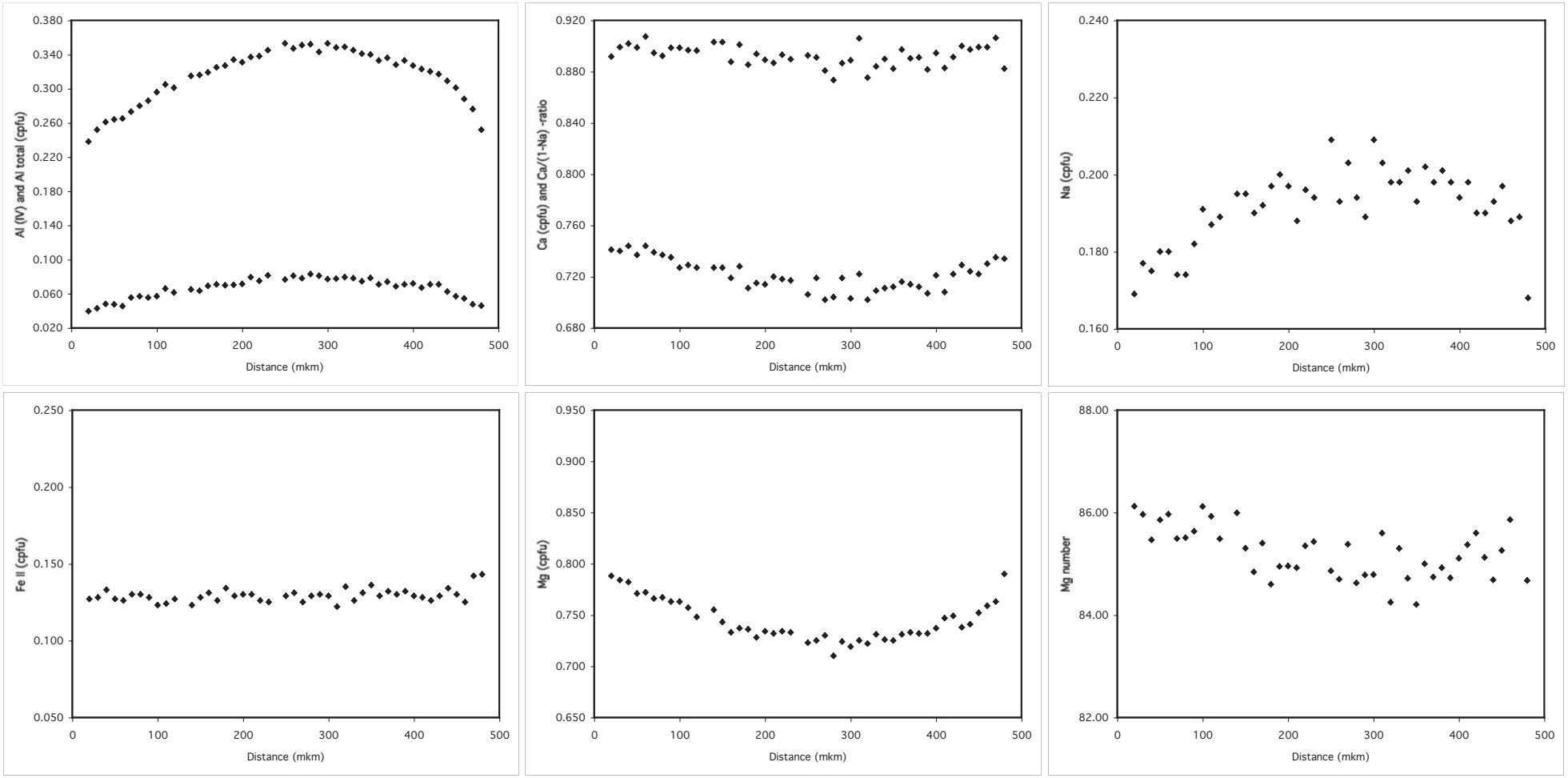
	150	160	170	180	190	200	210	220	230	240	250	260	270	280	290	300	310	320
SiO2	39.25	39.13	39.14	38.84	39.03	38.89	39.30	39.37	39.37	39.08	39.30	39.37	39.49	39.55	38.67	39.21	39.29	39.20
TiO2	0.00	0.05	0.02	0.00	0.00	0.00	0.00	0.00	0.04	0.00	0.00	0.00	0.03	0.01	0.00	0.02	0.00	0.01
Al2O3	0.02	0.03	0.03	0.01	0.02	0.01	0.02	0.01	0.01	0.00	0.02	0.03	3.61	0.02	0.02	0.01	0.02	0.01
Cr2O3	0.02	0.00	0.01	0.00	0.00	0.02	0.03	0.02	0.00	0.03	0.01	0.01	0.00	0.00	0.07	0.00	0.02	0.00
FeO	15.78	16.11	16.10	16.23	16.01	16.00	15.90	15.80	16.21	16.01	16.24	16.07	14.60	15.98	16.26	16.32	15.75	16.13
MnO	0.10	0.07	0.00	0.08	0.10	0.05	0.14	0.08	0.08	0.03	0.06	0.08	0.03	0.07	0.07	0.10	0.00	0.03
NiO	0.59	0.60	0.61	0.61	0.59	0.64	0.67	0.59	0.55	0.57	0.64	0.55	0.50	0.54	0.59	0.57	0.63	0.61
MgO	44.52	44.36	44.32	44.50	44.49	44.26	44.58	44.37	44.64	44.73	44.35	44.18	39.36	44.69	44.55	44.58	44.79	44.57
CaO	0.12	0.07	0.04	0.05	0.05	0.02	0.03	0.04	0.03	0.05	0.06	0.04	0.40	0.03	0.05	0.06	0.06	0.05
Na2O	0.00	0.03	0.00	0.00	0.01	0.00	0.00	0.01	0.01	0.03	0.00	0.00	0.04	0.00	0.00	0.01	0.00	0.00
K2O	0.00	0.01	0.00	0.00	0.01	0.00	0.00	0.00	0.00	0.01	0.00	0.02	0.05	0.00	0.01	0.00	0.00	0.02
Total	100.40	100.45	100.26	100.30	100.29	99.87	100.65	100.27	100.95	100.54	100.68	100.36	98.11	100.89	100.30	100.87	100.56	100.63
Si	0.989	0.987	0.988	0.982	0.985	0.986	0.988	0.992	0.987	0.984	0.989	0.992		0.991	0.979	0.985	0.987	0.987
Ti	0.000	0.001	0.000	0.000	0.000	0.000	0.000	0.000	0.001	0.000	0.000	0.000		0.000	0.000	0.000	0.000	0.000
Al	0.001	0.001	0.001	0.000	0.001	0.000	0.001	0.000	0.000	0.000	0.001	0.001		0.000	0.001	0.000	0.001	0.000
Cr	0.000	0.000	0.000	0.000	0.000	0.000	0.000	0.000	0.000	0.001	0.000	0.000		0.000	0.001	0.000	0.000	0.000
Fe2+	0.332	0.340	0.340	0.343	0.338	0.339	0.334	0.333	0.340	0.337	0.342	0.339		0.335	0.344	0.343	0.331	0.339
Mn	0.002	0.001	0.000	0.002	0.002	0.001	0.003	0.002	0.002	0.001	0.001	0.002		0.002	0.002	0.002	0.000	0.001
Ni	0.012	0.012	0.012	0.012	0.012	0.013	0.013	0.012	0.011	0.012	0.013	0.011		0.011	0.012	0.012	0.013	0.012
Mg	1.672	1.668	1.668	1.677	1.674	1.673	1.671	1.667	1.669	1.679	1.664	1.660		1.669	1.680	1.670	1.678	1.672
Ca	0.003	0.002	0.001	0.001	0.001	0.001	0.001	0.001	0.001	0.001	0.002	0.001		0.001	0.001	0.002	0.002	0.001
Na	0.000	0.002	0.000	0.000	0.001	0.000	0.000	0.000	0.001	0.001	0.000	0.000		0.000	0.000	0.001	0.000	0.000
K	0.000	0.000	0.000	0.000	0.000	0.000	0.000	0.000	0.000	0.000	0.000	0.001		0.000	0.000	0.000	0.000	0.001
Sum	3.011	3.013	3.011	3.018	3.015	3.014	3.011	3.008	3.012	3.016	3.011	3.007		3.009	3.021	3.015	3.012	3.013
Mg#	83.43	83.07	83.07	83.02	83.20	83.15	83.34	83.35	83.08	83.28	82.95	83.04		83.28	83.00	82.96	83.52	83.14

1910-1 Olivine, profile 360

	330	340	350	360	370	380	390	400	410	420	430	440	450	460	470	480	490	500	510
SiO2	39.37	39.45	39.19	39.22	39.10	39.53	39.32	39.35	39.35	39.28	39.30	39.21	38.21	39.31	39.09	38.90	39.05	39.67	38.35
TiO2	0.00	0.02	0.00	0.00	0.01	0.01	0.01	0.01	0.01	0.00	0.01	0.00	0.01	0.01	0.00	0.00	0.03	0.04	0.00
Al2O3	0.03	0.01	0.00	0.03	0.00	0.02	0.03	0.01	0.18	0.04	0.03	0.01	1.79	0.04	0.05	0.03	0.02	1.21	1.23
Cr2O3	0.00	0.00	0.00	0.00	0.00	0.02	0.00	0.02	0.01	0.01	0.01	0.02	0.04	0.00	0.02	0.00	0.00	0.01	0.02
FeO	16.39	16.22	16.04	16.27	16.23	16.10	16.43	16.22	15.83	16.36	15.93	16.08	15.87	16.00	16.45	16.63	17.61	18.02	18.85
MnO	0.14	0.06	0.09	0.06	0.11	0.07	0.11	0.10	0.11	0.11	0.06	0.07	0.10	0.11	0.13	0.11	0.15	0.20	0.26
NiO	0.64	0.63	0.62	0.64	0.65	0.62	0.60	0.63	0.56	0.62	0.63	0.66	0.58	0.61	0.64	0.52	0.55	0.43	0.34
MgO	44.68	44.49	44.46	44.58	44.61	44.44	44.30	44.71	44.54	44.69	44.14	44.31	43.17	44.46	44.14	43.74	43.29	39.06	40.58
CaO	0.03	0.06	0.03	0.06	0.06	0.02	0.04	0.07	0.06	0.07	0.02	0.05	0.07	0.04	0.04	0.05	0.04	0.26	0.12
Na2O	0.00	0.00	0.00	0.00	0.00	0.00	0.01	0.01	0.00	0.01	0.02	0.02	0.00	0.00	0.00	0.01	0.00	0.00	0.01
K2O	0.00	0.00	0.00	0.00	0.01	0.02	0.01	0.00	0.00	0.00	0.00	0.00	0.00	0.00	0.00	0.00	0.02	0.03	0.00
Total	101.27	100.93	100.45	100.86	100.78	100.85	100.85	101.12	100.65	101.19	100.15	100.42	99.83	100.56	100.55	99.97	100.75	98.91	99.75
Si	0.986	0.990	0.988	0.986	0.984	0.992	0.989	0.986	0.988	0.984	0.992	0.989	0.968	0.989	0.986	0.988	0.988	1.019	0.985
Ti	0.000	0.000	0.000	0.000	0.000	0.000	0.000	0.000	0.000	0.000	0.000	0.000	0.000	0.000	0.000	0.000	0.001	0.001	0.000
Al	0.001	0.000	0.000	0.001	0.000	0.001	0.001	0.000	0.005	0.001	0.001	0.000	0.053	0.001	0.001	0.001	0.001	0.036	0.037
Cr	0.000	0.000	0.000	0.000	0.000	0.000	0.000	0.000	0.000	0.000	0.000	0.000	0.001	0.000	0.000	0.000	0.000	0.000	0.000
Fe2+	0.343	0.340	0.338	0.342	0.342	0.338	0.345	0.340	0.332	0.343	0.336	0.339	0.336	0.337	0.347	0.353	0.373	0.387	0.405
Mn	0.003	0.001	0.002	0.001	0.002	0.002	0.002	0.002	0.002	0.002	0.001	0.001	0.002	0.002	0.003	0.002	0.003	0.004	0.006
Ni	0.013	0.013	0.013	0.013	0.013	0.013	0.012	0.013	0.011	0.012	0.013	0.013	0.012	0.012	0.013	0.011	0.011	0.009	0.007
Mg	1.668	1.664	1.671	1.670	1.673	1.662	1.660	1.670	1.667	1.669	1.662	1.666	1.630	1.668	1.660	1.656	1.633	1.496	1.553
Ca	0.001	0.001	0.001	0.001	0.001	0.001	0.001	0.002	0.001	0.002	0.000	0.001	0.002	0.001	0.001	0.001	0.001	0.007	0.003
Na	0.000	0.000	0.000	0.000	0.000	0.000	0.000	0.000	0.000	0.000	0.001	0.001	0.000	0.000	0.000	0.001	0.000	0.000	0.000
K	0.000	0.000	0.000	0.000	0.000	0.001	0.000	0.000	0.000	0.000	0.000	0.000	0.000	0.000	0.000	0.000	0.001	0.001	0.000
Sum	3.014	3.010	3.012	3.014	3.016	3.008	3.011	3.014	3.009	3.015	3.007	3.011	3.005	3.010	3.013	3.012	3.011	2.962	2.997
Mg#	82.94	83.03	83.18	83.00	83.03	83.10	82.79	83.08	83.39	82.95	83.18	83.09	82.91	83.19	82.71	82.43	81.41	79.45	79.32

1910-1 Olivine, profile 360

Websterite 1535-3



1535-3 Cpx II, profile 480

	20	30	40	50	60	70	80	90	100	110	120	130	140	150	160	170	180	190	200	210
SiO2	53.95	53.69	53.10	53.49	53.41	53.49	53.48	52.98	52.89	52.69	53.04	51.17	52.39	52.78	52.86	52.59	52.45	52.76	52.52	52.86
TiO2	0.19	0.20	0.16	0.20	0.13	0.22	0.13	0.12	0.14	0.21	0.18	0.12	0.15	0.11	0.16	0.15	0.16	0.12	0.12	0.19
Al2O3	5.61	5.94	6.11	6.19	6.23	6.45	6.61	6.69	6.92	7.14	7.06	8.88	7.36	7.41	7.48	7.60	7.63	7.83	7.74	7.95
Cr2O3	0.01	0.02	0.08	0.03	0.00	0.04	0.09	0.03	0.04	0.06	0.03	0.02	0.06	0.00	0.04	0.04	0.07	0.03	0.10	0.03
FeO	4.22	4.26	4.38	4.19	4.18	4.31	4.31	4.24	4.07	4.10	4.19	4.51	4.04	4.23	4.32	4.17	4.40	4.26	4.27	4.32
MnO	0.04	0.03	0.09	0.00	0.08	0.10	0.00	0.04	0.05	0.05	0.05	0.08	0.06	0.09	0.07	0.01	0.02	0.00	0.05	0.03
NiO	0.17	0.11	0.07	0.14	0.14	0.12	0.05	0.17	0.09	0.10	0.10	0.11	0.12	0.06	0.12	0.10	0.09	0.12	0.06	0.11
MgO	14.68	14.61	14.49	14.31	14.33	14.28	14.30	14.12	14.13	14.01	13.88	12.59	13.93	13.77	13.57	13.63	13.57	13.51	13.58	13.65
CaO	19.19	19.19	19.19	19.05	19.22	19.16	19.12	18.91	18.71	18.78	18.76	16.48	18.68	18.76	18.52	18.76	18.24	18.45	18.37	18.68
Na2O	2.42	2.54	2.49	2.57	2.57	2.50	2.49	2.60	2.71	2.66	2.70	2.21	2.77	2.78	2.70	2.73	2.80	2.85	2.80	2.70
K2O	0.00	0.00	0.00	0.01	0.00	0.02	0.00	0.00	0.01	0.00	0.00	0.12	0.00	0.00	0.01	0.00	0.01	0.00	0.00	0.02
Total	100.47	100.59	100.17	100.19	100.27	100.69	100.56	99.88	99.77	99.80	99.97	96.28	99.53	100.00	99.85	99.78	99.45	99.93	99.61	100.53
Si	1.943	1.933	1.923	1.932	1.929	1.924	1.924	1.920	1.917	1.910	1.919		1.904	1.910	1.914	1.906	1.908	1.908	1.906	1.901
Ti	0.005	0.005	0.004	0.005	0.003	0.006	0.003	0.003	0.004	0.006	0.005		0.004	0.003	0.004	0.004	0.004	0.003	0.003	0.005
Al	0.238	0.252	0.261	0.264	0.265	0.273	0.280	0.286	0.296	0.305	0.301		0.315	0.316	0.319	0.325	0.327	0.334	0.331	0.337
Cr	0.000	0.001	0.002	0.001	0.000	0.001	0.002	0.001	0.001	0.002	0.001		0.002	0.000	0.001	0.001	0.002	0.001	0.003	0.001
Fe2+	0.127	0.128	0.133	0.127	0.126	0.130	0.130	0.128	0.123	0.124	0.127		0.123	0.128	0.131	0.126	0.134	0.129	0.130	0.130
Mn	0.001	0.001	0.003	0.000	0.002	0.003	0.000	0.001	0.002	0.002	0.001		0.002	0.003	0.002	0.000	0.001	0.000	0.001	0.001
Ni	0.005	0.003	0.002	0.004	0.004	0.004	0.001	0.005	0.003	0.003	0.003		0.003	0.002	0.003	0.003	0.003	0.003	0.002	0.003
Mg	0.788	0.784	0.782	0.771	0.772	0.766	0.767	0.763	0.763	0.757	0.748		0.755	0.743	0.733	0.737	0.736	0.728	0.734	0.732
Ca	0.741	0.740	0.744	0.737	0.744	0.739	0.737	0.735	0.727	0.729	0.727		0.727	0.727	0.719	0.728	0.711	0.715	0.714	0.720
Na	0.169	0.177	0.175	0.180	0.180	0.174	0.174	0.182	0.191	0.187	0.189		0.195	0.195	0.190	0.192	0.197	0.200	0.197	0.188
K	0.000	0.000	0.000	0.000	0.000	0.001	0.000	0.000	0.000	0.000	0.000		0.000	0.000	0.000	0.000	0.000	0.000	0.000	0.001
Sum	4.017	4.024	4.029	4.020	4.025	4.020	4.018	4.024	4.026	4.025	4.021		4.031	4.027	4.016	4.022	4.022	4.021	4.022	4.019
Al IV	0.040	0.043	0.048	0.048	0.046	0.056	0.057	0.056	0.057	0.066	0.062		0.065	0.064	0.069	0.071	0.070	0.071	0.072	0.080
Al VI	0.199	0.209	0.213	0.217	0.220	0.218	0.223	0.231	0.239	0.239	0.240		0.250	0.253	0.250	0.254	0.257	0.264	0.260	0.258
Mg#	86.12	85.96	85.46	85.86	85.97	85.49	85.51	85.63	86.12	85.93	85.49		85.99	85.30	84.84	85.40	84.60	84.95	84.95	84.92

1535-3 Cpx II, profile 480

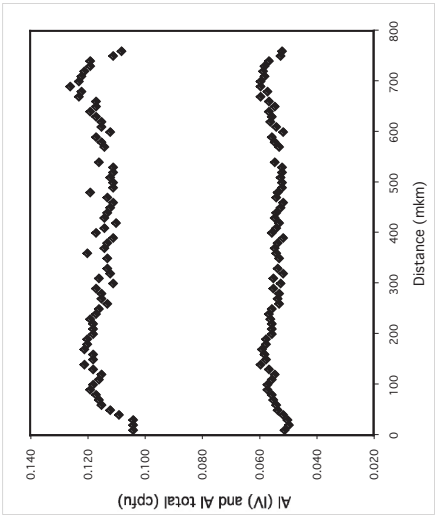
	220	230	240	250	260	270	280	290	300	310	320	330	340	350	360	370	380	390	400	410
SiO2	52.39	52.64	52.33	52.51	52.44	52.77	52.73	52.69	52.37	52.48	52.79	52.61	52.82	52.62	52.65	52.73	53.03	52.98	52.98	52.65
TiO2	0.13	0.21	0.14	0.15	0.13	0.14	0.15	0.13	0.17	0.17	0.16	0.16	0.13	0.15	0.18	0.14	0.13	0.13	0.17	0.15
Al2O3	7.90	8.12	8.37	8.30	8.15	8.26	8.24	8.05	8.27	8.17	8.22	8.11	8.02	7.97	7.83	7.90	7.74	7.83	7.71	7.54
Cr2O3	0.08	0.00	0.08	0.05	0.09	0.02	0.04	0.01	0.03	0.06	0.02	0.04	0.05	0.07	0.05	0.05	0.06	0.02	0.04	0.02
FeO	4.15	4.16	4.14	4.28	4.34	4.14	4.27	4.29	4.26	4.05	4.48	4.18	4.36	4.49	4.27	4.37	4.33	4.39	4.28	4.21
MnO	0.02	0.10	0.05	0.06	0.00	0.03	0.05	0.11	0.05	0.00	0.06	0.09	0.03	0.04	0.09	0.07	0.03	0.00	0.02	0.00
NiO	0.06	0.11	0.12	0.12	0.11	0.09	0.10	0.05	0.13	0.10	0.13	0.11	0.08	0.11	0.13	0.12	0.09	0.08	0.09	0.13
MgO	13.57	13.64	13.30	13.43	13.44	13.58	13.16	13.45	13.31	13.46	13.44	13.56	13.52	13.44	13.58	13.63	13.64	13.63	13.74	13.80
CaO	18.46	18.56	18.34	18.26	18.54	18.19	18.17	18.57	18.10	18.65	18.17	18.31	18.41	18.37	18.49	18.49	18.45	18.30	18.69	18.21
Na2O	2.79	2.77	2.64	2.99	2.75	2.90	2.77	2.70	2.97	2.90	2.83	2.82	2.87	2.76	2.89	2.83	2.89	2.83	2.78	2.81
K2O	0.01	0.00	0.02	0.00	0.00	0.00	0.02	0.00	0.02	0.01	0.00	0.00	0.00	0.00	0.00	0.01	0.00	0.02	0.00	0.00
Total	99.54	100.30	99.51	100.15	99.98	100.13	99.69	100.05	99.65	100.05	100.31	99.96	100.29	100.00	100.16	100.34	100.39	100.20	100.50	99.52
Si	1.902	1.897		1.896	1.897	1.902	1.909	1.903	1.899	1.896	1.902	1.901	1.904	1.903	1.902	1.901	1.909	1.910	1.906	1.911
Ti	0.003	0.006		0.004	0.003	0.004	0.004	0.004	0.005	0.004	0.004	0.004	0.004	0.004	0.005	0.004	0.004	0.004	0.005	0.004
Al	0.338	0.345		0.353	0.347	0.351	0.352	0.343	0.353	0.348	0.349	0.345	0.341	0.340	0.333	0.336	0.328	0.333	0.327	0.323
Cr	0.002	0.000		0.001	0.002	0.000	0.001	0.000	0.001	0.002	0.000	0.001	0.001	0.002	0.001	0.002	0.002	0.000	0.001	0.001
Fe2+	0.126	0.125		0.129	0.131	0.125	0.129	0.130	0.129	0.122	0.135	0.126	0.131	0.136	0.129	0.132	0.130	0.132	0.129	0.128
Mn	0.001	0.003		0.002	0.000	0.001	0.002	0.003	0.002	0.000	0.002	0.003	0.001	0.001	0.003	0.002	0.001	0.000	0.000	0.000
Ni	0.002	0.003		0.003	0.003	0.003	0.003	0.002	0.004	0.003	0.004	0.003	0.002	0.003	0.004	0.003	0.003	0.002	0.003	0.004
Mg	0.734	0.733		0.723	0.725	0.730	0.710	0.724	0.719	0.725	0.722	0.731	0.726	0.725	0.731	0.733	0.732	0.732	0.737	0.747
Ca	0.718	0.717		0.706	0.719	0.702	0.704	0.719	0.703	0.722	0.702	0.709	0.711	0.712	0.716	0.714	0.712	0.707	0.721	0.708
Na	0.196	0.194		0.209	0.193	0.203	0.194	0.189	0.209	0.203	0.198	0.198	0.201	0.193	0.202	0.198	0.201	0.198	0.194	0.198
K	0.000	0.000		0.000	0.000	0.000	0.001	0.000	0.001	0.000	0.000	0.000	0.000	0.000	0.000	0.000	0.000	0.001	0.000	0.000
Sum	4.023	4.022		4.028	4.021	4.020	4.008	4.016	4.024	4.026	4.018	4.020	4.022	4.019	4.027	4.025	4.023	4.019	4.022	4.022
Al IV	0.075	0.082		0.077	0.081	0.078	0.083	0.081	0.077	0.078	0.080	0.078	0.075	0.079	0.071	0.074	0.069	0.071	0.072	0.067
Al VI	0.263	0.264		0.277	0.266	0.273	0.269	0.262	0.276	0.271	0.270	0.267	0.267	0.262	0.262	0.262	0.260	0.262	0.255	0.256
Mg#	85.35	85.43		84.86	84.70	85.38	84.62	84.78	84.79	85.60	84.25	85.30	84.71	84.20	85.00	84.74	84.92	84.72	85.10	85.37

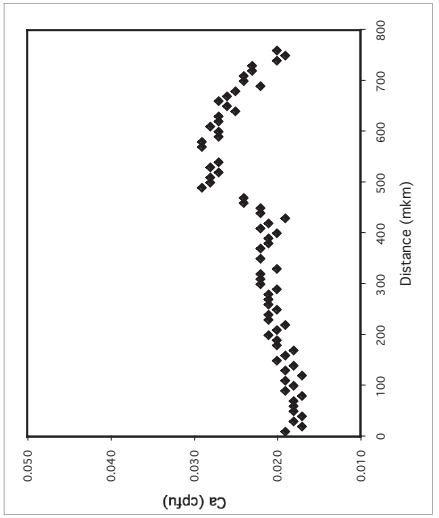
1535-3 Cpx II, profile 480

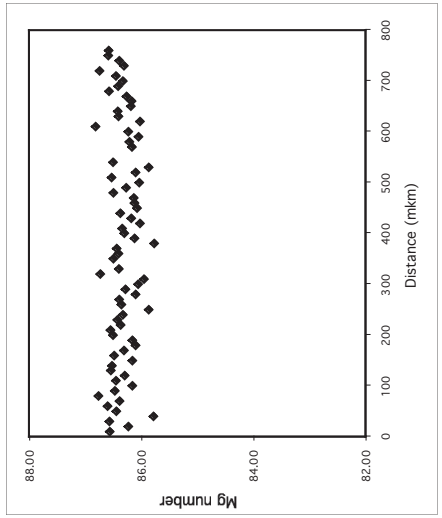
	420	430	440	450	460	470	480
SiO2	52.60	53.10	52.95	53.26	53.05	53.22	53.30
TiO2	0.20	0.21	0.15	0.15	0.17	0.12	0.14
Al2O3	7.51	7.48	7.27	7.11	6.74	6.50	5.92
Cr2O3	0.07	0.11	0.03	0.05	0.04	0.06	0.04
FeO	4.17	4.29	4.43	4.32	4.14	4.70	4.72
MnO	0.02	0.06	0.06	0.03	0.08	0.07	0.02
NiO	0.18	0.16	0.13	0.09	0.11	0.10	0.13
MgO	13.88	13.78	13.77	14.02	14.06	14.20	14.64
CaO	18.63	18.95	18.72	18.72	18.80	19.03	18.94
Na2O	2.71	2.73	2.76	2.83	2.68	2.71	2.39
K2O	0.00	0.00	0.00	0.01	0.00	0.00	0.01
Total	99.97	100.86	100.27	100.59	99.87	100.70	100.25
Si	1.904	1.906	1.912	1.916	1.922		1.928
Ti	0.005	0.006	0.004	0.004	0.004		0.004
Al	0.320	0.317	0.309	0.301	0.288		0.252
Cr	0.002	0.003	0.001	0.002	0.001		0.001
Fe2+	0.126	0.129	0.134	0.130	0.125		0.143
Mn	0.001	0.002	0.002	0.001	0.002		0.000
Ni	0.005	0.005	0.004	0.003	0.003		0.004
Mg	0.749	0.738	0.741	0.752	0.759		0.790
Ca	0.722	0.729	0.724	0.722	0.730		0.734
Na	0.190	0.190	0.193	0.197	0.188		0.168
K	0.000	0.000	0.000	0.000	0.000		0.001
Sum	4.025	4.023	4.025	4.027	4.023		4.025
Al IV	0.071	0.071	0.063	0.057	0.055		0.046
Al VI	0.249	0.246	0.247	0.244	0.234		0.206
Mg#	85.60	85.12	84.69	85.26	85.86		84.67

1535-3 Cpx II, profile 480

1535-3 Opx II, profile 760







	10	20	30	40	50	60	70	80	90	100	110	120	130	140	150	160	170	180	190	200
SiO2	56.04	56.01	55.83	55.60	55.85	55.66	55.83	55.80	55.52	55.44	55.66	55.75	55.54	55.49	55.64	55.57	55.75	55.52	55.59	55.73
TiO2	0.06	0.00	0.02	0.03	0.03	0.03	0.01	0.00	0.04	0.02	0.04	0.04	0.04	0.04	0.02	0.06	0.08	0.03	0.03	0.01
Al2O3	2.54	2.54	2.55	2.65	2.74	2.80	2.84	2.85	2.88	2.86	2.83	2.81	2.86	2.94	2.88	2.87	2.94	2.91	2.93	2.87
Cr2O3	0.03	0.05	0.04	0.02	0.00	0.00	0.02	0.00	0.00	0.08	0.00	0.04	0.06	0.00	0.03	0.00	0.04	0.00	0.02	0.01
FeO	8.88	9.12	8.95	9.38	8.94	8.88	9.03	8.69	8.91	9.10	8.92	9.02	8.85	8.86	9.07	8.85	8.96	9.10	9.12	8.81
MnO	0.05	0.08	0.14	0.08	0.10	0.11	0.08	0.06	0.10	0.07	0.10	0.05	0.07	0.05	0.04	0.06	0.03	0.04	0.01	0.06
MgO	32.02	32.01	32.33	31.75	31.95	32.13	32.11	31.89	31.95	31.78	31.93	31.90	31.90	31.93	31.71	31.82	31.68	31.61	31.89	31.64
CaO	0.51	0.46	0.48	0.46	0.47	0.47	0.48	0.45	0.51	0.48	0.51	0.47	0.51	0.47	0.54	0.50	0.49	0.52	0.54	0.55
Na2O	0.07	0.08	0.10	0.12	0.11	0.13	0.11	0.09	0.11	0.09	0.10	0.13	0.13	0.07	0.09	0.09	0.12	0.10	0.10	0.10
K2O	0.01	0.00	0.01	0.01	0.01	0.01	0.01	0.00	0.00	0.00	0.01	0.00	0.00	0.00	0.00	0.01	0.00	0.00	0.01	0.00
Total	100.19	100.36	100.45	100.09	100.20	100.21	100.50	99.82	100.02	99.92	100.08	100.19	99.96	99.84	100.03	99.83	100.08	99.83	100.24	99.79
Si	1.949	1.947	1.940	1.942	1.944	1.938	1.938	1.946	1.937	1.937	1.940	1.941	1.938	1.937	1.941	1.941	1.942	1.941	1.936	1.946
Ti	0.001	0.000	0.001	0.001	0.001	0.001	0.000	0.000	0.001	0.000	0.001	0.001	0.001	0.001	0.001	0.002	0.002	0.001	0.001	0.000
Al	0.104	0.104	0.104	0.109	0.112	0.115	0.116	0.117	0.119	0.118	0.116	0.115	0.118	0.121	0.118	0.118	0.121	0.120	0.120	0.118
Cr	0.001	0.001	0.001	0.001	0.000	0.000	0.001	0.000	0.000	0.002	0.000	0.001	0.002	0.000	0.001	0.000	0.001	0.000	0.001	0.000
Fe2+	0.258	0.265	0.260	0.274	0.260	0.258	0.262	0.253	0.260	0.266	0.260	0.263	0.258	0.259	0.265	0.259	0.261	0.266	0.266	0.257
Mn	0.001	0.002	0.004	0.002	0.003	0.003	0.002	0.002	0.003	0.002	0.003	0.001	0.002	0.001	0.001	0.002	0.001	0.001	0.000	0.002
Mg	1.661	1.659	1.675	1.653	1.658	1.667	1.662	1.658	1.661	1.655	1.659	1.656	1.659	1.662	1.649	1.657	1.645	1.647	1.655	1.647
Ca	0.019	0.017	0.018	0.017	0.018	0.018	0.018	0.017	0.019	0.018	0.019	0.017	0.019	0.018	0.020	0.019	0.018	0.020	0.020	0.021
Na	0.005	0.006	0.007	0.008	0.007	0.009	0.007	0.006	0.007	0.006	0.007	0.009	0.009	0.004	0.006	0.006	0.008	0.007	0.007	0.007
K	0.000	0.000	0.000	0.001	0.000	0.000	0.000	0.000	0.000	0.000	0.000	0.000	0.000	0.000	0.000	0.000	0.000	0.000	0.001	0.000
Sum	4.000	4.003	4.010	4.007	4.003	4.009	4.007	3.999	4.007	4.005	4.004	4.004	4.006	4.003	4.002	4.002	3.999	4.002	4.006	3.998
Al IV	0.051	0.050	0.050	0.052	0.054	0.054	0.055	0.056	0.057	0.057	0.056	0.055	0.057	0.060	0.058	0.058	0.059	0.058	0.058	0.056
Al VI	0.053	0.055	0.054	0.058	0.059	0.061	0.061	0.062	0.062	0.061	0.061	0.061	0.062	0.062	0.061	0.060	0.062	0.063	0.063	0.063
Mg#	86.56	86.23	86.56	85.78	86.44	86.60	86.38	86.76	86.47	86.15	86.45	86.29	86.54	86.52	86.15	86.48	86.31	86.10	86.15	86.50

	210	220	230	240	250	260	270	280	290	300	310	320	330	340	350	360	370	380	390	400
SiO2	55.94	55.45	55.39	55.75	55.59	55.85	55.65	55.73	55.71	55.76	55.28	55.84	55.79	55.76	55.61	55.63	55.71	55.29	55.87	55.65
TiO2	0.01	0.04	0.02	0.03	0.02	0.00	0.00	0.00	0.01	0.04	0.00	0.01	0.02	0.03	0.01	0.00	0.00	0.05	0.02	0.05
Al2O3	2.89	2.88	2.88	2.86	2.84	2.75	2.80	2.80	2.84	2.72	2.81	2.74	2.75	2.84	2.75	2.93	2.76	2.73	2.71	2.85
Cr2O3	0.00	0.00	0.02	0.03	0.01	0.01	0.01	0.02	0.03	0.04	0.04	0.00	0.06	0.00	0.00	0.04	0.03	0.04	0.01	0.02
FeO	8.82	8.97	8.93	8.94	9.43	8.91	8.94	9.23	9.04	9.26	9.22	8.72	8.92	8.85	8.87	8.77	8.87	9.35	9.17	8.97
MnO	0.14	0.14	0.02	0.04	0.05	0.08	0.05	0.06	0.11	0.06	0.08	0.07	0.08	0.09	0.11	0.06	0.02	0.04	0.11	0.09
MgO	31.78	31.87	31.88	31.73	32.13	31.63	31.87	32.04	31.86	32.07	31.60	31.99	31.78	31.29	31.87	31.18	31.67	31.62	31.98	31.74
CaO	0.55	0.52	0.56	0.57	0.55	0.57	0.57	0.57	0.52	0.58	0.60	0.59	0.55	1.14	0.59	1.54	0.58	0.56	0.56	0.54
Na2O	0.11	0.13	0.12	0.09	0.10	0.11	0.12	0.14	0.10	0.13	0.11	0.13	0.11	0.16	0.10	0.19	0.08	0.14	0.12	0.11
K2O	0.01	0.01	0.00	0.02	0.00	0.00	0.00	0.01	0.01	0.00	0.01	0.00	0.00	0.00	0.00	0.00	0.01	0.00	0.00	0.02
Total	100.24	100.00	99.82	100.05	100.72	99.91	100.01	100.59	100.24	100.65	99.75	100.09	100.05	100.16	99.90	100.33	99.74	99.83	100.54	100.03
Si	1.945	1.936	1.936	1.943	1.931	1.949	1.941	1.936	1.940	1.936	1.937	1.944	1.945		1.942		1.947	1.937	1.941	1.941
Ti	0.000	0.001	0.000	0.001	0.001	0.000	0.000	0.000	0.000	0.001	0.000	0.000	0.000		0.000		0.000	0.001	0.000	0.001
Al	0.118	0.118	0.119	0.117	0.116	0.113	0.115	0.115	0.117	0.111	0.116	0.112	0.113		0.113		0.114	0.113	0.111	0.117
Cr	0.000	0.000	0.001	0.001	0.000	0.000	0.000	0.000	0.001	0.001	0.001	0.000	0.002		0.000		0.001	0.001	0.000	0.000
Fe2+	0.256	0.262	0.261	0.261	0.274	0.260	0.261	0.268	0.263	0.269	0.270	0.254	0.260		0.259		0.259	0.274	0.267	0.262
Mn	0.004	0.004	0.001	0.001	0.002	0.002	0.002	0.002	0.003	0.002	0.002	0.002	0.002		0.003		0.001	0.001	0.003	0.003
Mg	1.647	1.659	1.661	1.648	1.664	1.645	1.657	1.660	1.654	1.660	1.651	1.660	1.651		1.659		1.650	1.651	1.656	1.650
Ca	0.020	0.019	0.021	0.021	0.020	0.021	0.021	0.021	0.020	0.022	0.022	0.022	0.020		0.022		0.022	0.021	0.021	0.020
Na	0.007	0.009	0.008	0.006	0.007	0.007	0.008	0.009	0.007	0.009	0.007	0.009	0.008		0.007		0.006	0.009	0.008	0.007
K	0.000	0.000	0.000	0.001	0.000	0.000	0.000	0.000	0.001	0.000	0.000	0.000	0.000		0.000		0.000	0.000	0.000	0.001
Sum	3.999	4.008	4.008	4.000	4.014	3.998	4.005	4.011	4.005	4.011	4.008	4.004	4.001		4.005		3.999	4.009	4.007	4.003
Al IV	0.056	0.056	0.056	0.057	0.056	0.053	0.054	0.053	0.055	0.053	0.055	0.052	0.054		0.053		0.055	0.054	0.052	0.056
Al VI	0.063	0.063	0.063	0.061	0.061	0.060	0.062	0.062	0.062	0.059	0.061	0.061	0.060		0.060		0.060	0.060	0.060	0.062
Mg#	86.55	86.36	86.42	86.33	85.86	86.35	86.39	86.10	86.28	86.05	85.94	86.73	86.39		86.50		86.43	85.77	86.12	86.30

1535-3 Opx II, profile 760

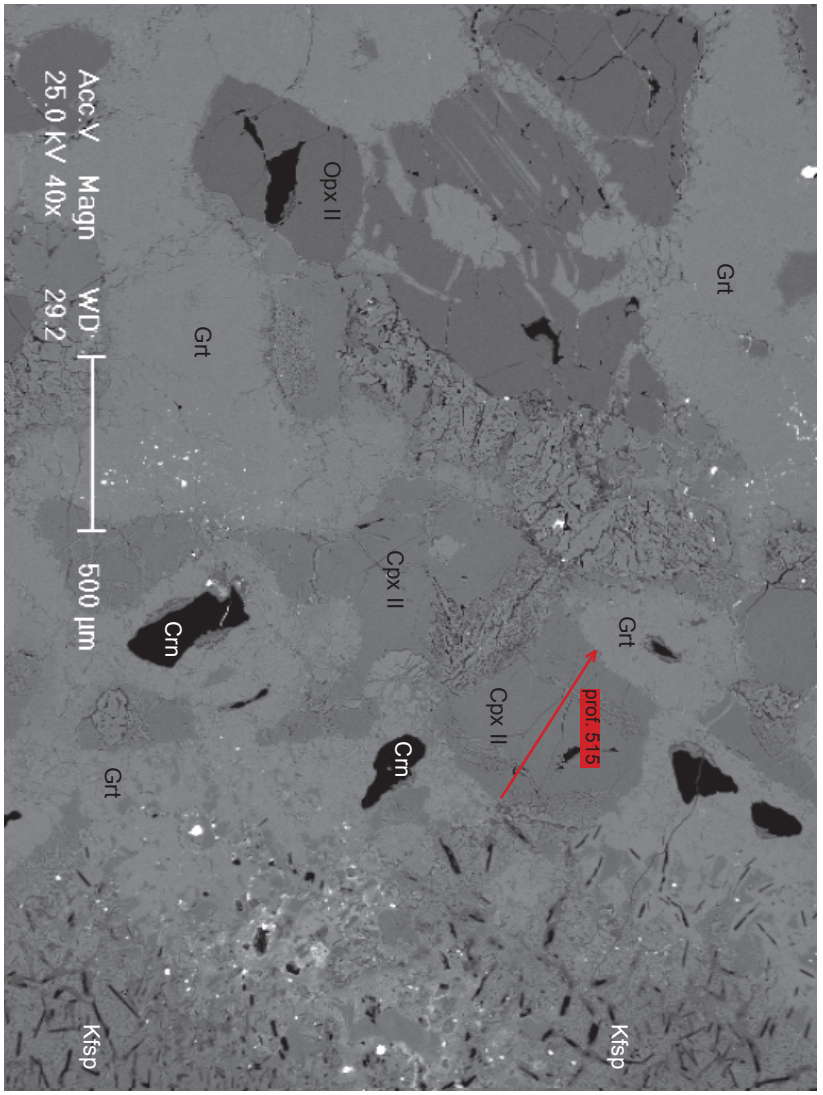
	410	420	430	440	450	460	470	480	490	500	510	520	530	540	550	560	570	580	590	600
SiO2	55.87	55.94	55.96	55.36	55.53	55.65	55.63	55.25	55.65	55.66	55.46	55.86	55.70	55.74	55.67	53.87	55.60	55.53	55.54	55.66
TiO2	0.01	0.03	0.02	0.04	0.03	0.02	0.02	0.06	0.02	0.00	0.01	0.01	0.02	0.02	0.01	0.03	0.02	0.04	0.04	0.01
Al2O3	2.77	2.69	2.79	2.75	2.72	2.69	2.74	2.88	2.70	2.70	2.71	2.70	2.71	2.81	2.79	3.12	2.77	2.78	2.84	2.74
Cr2O3	0.03	0.03	0.02	0.02	0.01	0.01	0.00	0.00	0.00	0.02	0.04	0.02	0.02	0.01	0.04	0.03	0.01	0.00	0.01	0.03
FeO	8.96	9.26	9.13	8.94	9.12	9.10	9.07	8.59	8.96	9.15	8.80	9.09	9.31	8.81	8.75	9.04	9.04	9.00	9.11	9.11
MnO	0.03	0.09	0.08	0.11	0.10	0.08	0.08	0.08	0.00	0.08	0.07	0.09	0.06	0.05	0.08	0.02	0.04	0.01	0.08	0.10
MgO	31.76	32.01	31.92	31.81	31.65	31.69	31.60	30.81	31.56	31.61	31.76	31.58	31.70	31.67	31.28	30.35	31.58	31.51	31.48	32.00
CaO	0.59	0.57	0.51	0.60	0.60	0.65	0.64	1.59	0.76	0.76	0.74	0.73	0.75	0.72	1.11	0.78	0.78	0.77	0.73	0.73
Na2O	0.11	0.11	0.10	0.12	0.13	0.12	0.11	0.23	0.10	0.12	0.12	0.10	0.14	0.12	0.15	0.13	0.15	0.12	0.12	0.14
K2O	0.00	0.01	0.01	0.00	0.00	0.01	0.00	0.01	0.01	0.00	0.00	0.02	0.00	0.02	0.02	0.01	0.01	0.01	0.00	0.02
Total	100.13	100.72	100.52	99.74	99.88	100.00	99.88	99.50	99.76	100.09	99.69	100.20	100.40	99.98	99.89	97.37	100.00	99.78	99.93	100.53
Si	1.946	1.941	1.943	1.938	1.942	1.943	1.944	1.941	1.946	1.943	1.941	1.947	1.940	1.944			1.942	1.943	1.941	1.935
Ti	0.000	0.001	0.001	0.001	0.001	0.000	0.001	0.002	0.000	0.000	0.000	0.000	0.001	0.001			0.001	0.001	0.001	0.000
Al	0.114	0.110	0.114	0.113	0.112	0.111	0.113	0.119	0.111	0.111	0.112	0.111	0.111	0.116			0.114	0.115	0.117	0.112
Cr	0.001	0.001	0.000	0.001	0.000	0.000	0.000	0.000	0.000	0.001	0.001	0.001	0.000	0.000			0.000	0.000	0.000	0.001
Fe2+	0.261	0.269	0.265	0.262	0.267	0.266	0.265	0.252	0.262	0.267	0.258	0.265	0.271	0.257			0.264	0.263	0.266	0.265
Mn	0.001	0.003	0.002	0.003	0.003	0.002	0.002	0.002	0.000	0.002	0.002	0.003	0.002	0.002			0.001	0.000	0.002	0.003
Mg	1.649	1.655	1.652	1.660	1.650	1.650	1.646	1.614	1.646	1.645	1.657	1.641	1.646	1.647			1.644	1.644	1.640	1.659
Ca	0.022	0.021	0.019	0.022	0.022	0.024	0.024	0.060	0.029	0.028	0.028	0.027	0.028	0.027			0.029	0.029	0.027	0.027
Na	0.007	0.007	0.007	0.008	0.009	0.008	0.007	0.016	0.007	0.008	0.008	0.007	0.009	0.008			0.010	0.008	0.008	0.009
K	0.000	0.000	0.000	0.000	0.000	0.000	0.000	0.000	0.000	0.000	0.000	0.001	0.000	0.001			0.000	0.000	0.000	0.001
Sum	4.000	4.007	4.003	4.008	4.006	4.005	4.003	4.006	4.001	4.005	4.006	4.002	4.008	4.002			4.006	4.003	4.003	4.013
Al IV	0.054	0.053	0.055	0.054	0.053	0.052	0.054	0.054	0.052	0.052	0.053	0.052	0.052	0.055			0.053	0.055	0.056	0.052
Al VI	0.060	0.057	0.060	0.059	0.060	0.060	0.059	0.066	0.059	0.059	0.060	0.059	0.059	0.062			0.061	0.061	0.062	0.061
Mg#	86.34	86.02	86.18	86.37	86.07	86.12	86.13	86.50	86.27	86.04	86.53	86.10	85.86	86.50			86.16	86.21	86.04	86.23

1535-3 Opx II, profile 760

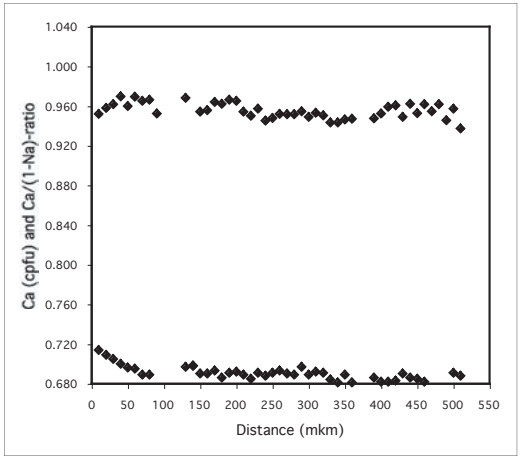
	610	620	630	640	650	660	670	680	690	700	710	720	730	740	750	760
SiO2	55.74	55.44	55.78	55.30	55.53	55.70	55.28	55.41	55.29	55.40	55.41	55.35	56.01	55.50	55.58	55.60
TiO2	0.05	0.05	0.06	0.04	0.00	0.02	0.05	0.06	0.01	0.04	0.02	0.02	0.04	0.04	0.02	0.04
Al2O3	2.79	2.79	2.86	2.88	2.84	2.84	2.98	2.97	3.05	2.99	2.96	2.91	2.92	2.89	2.70	2.61
Cr2O3	0.02	0.01	0.01	0.00	0.00	0.03	0.04	0.00	0.00	0.02	0.02	0.04	0.03	0.00	0.05	0.02
FeO	8.62	9.12	8.93	8.83	9.10	9.05	9.05	8.75	8.87	8.97	8.87	8.53	9.05	8.97	8.78	8.83
MnO	0.00	0.09	0.09	0.03	0.10	0.05	0.06	0.09	0.04	0.08	0.05	0.11	0.10	0.04	0.08	0.06
MgO	31.77	31.48	31.89	31.49	31.78	31.67	31.85	31.66	31.66	31.78	31.70	31.31	32.00	32.01	31.80	31.93
CaO	0.74	0.71	0.73	0.66	0.68	0.74	0.69	0.66	0.59	0.63	0.65	0.60	0.62	0.54	0.51	0.54
Na2O	0.12	0.08	0.12	0.12	0.12	0.10	0.11	0.15	0.11	0.09	0.09	0.11	0.09	0.11	0.13	0.09
K2O	0.02	0.00	0.00	0.00	0.01	0.01	0.01	0.01	0.01	0.00	0.00	0.01	0.00	0.00	0.00	0.02
Total	99.86	99.77	100.46	99.34	100.15	100.21	100.12	99.75	99.62	99.99	99.76	98.99	100.86	100.12	99.64	99.74
Si	1.945	1.941	1.938	1.941	1.937	1.941	1.930	1.937	1.936	1.934	1.938	1.947	1.938	1.935	1.944	1.944
Ti	0.001	0.001	0.001	0.001	0.000	0.001	0.001	0.001	0.000	0.001	0.000	0.001	0.001	0.001	0.001	0.001
Al	0.115	0.115	0.117	0.119	0.117	0.117	0.123	0.122	0.126	0.123	0.122	0.121	0.119	0.119	0.111	0.108
Cr	0.000	0.000	0.000	0.000	0.000	0.001	0.001	0.000	0.000	0.000	0.000	0.001	0.001	0.000	0.001	0.001
Fe2+	0.251	0.267	0.260	0.259	0.265	0.264	0.264	0.256	0.260	0.262	0.259	0.251	0.262	0.262	0.257	0.258
Mn	0.000	0.003	0.003	0.001	0.003	0.001	0.002	0.003	0.001	0.002	0.001	0.003	0.003	0.001	0.002	0.002
Mg	1.652	1.643	1.652	1.648	1.653	1.645	1.657	1.650	1.653	1.654	1.652	1.642	1.651	1.663	1.659	1.664
Ca	0.028	0.027	0.027	0.025	0.026	0.027	0.026	0.025	0.022	0.024	0.024	0.023	0.023	0.020	0.019	0.020
Na	0.008	0.005	0.008	0.008	0.008	0.007	0.007	0.010	0.007	0.006	0.006	0.007	0.006	0.008	0.009	0.006
K	0.001	0.000	0.000	0.000	0.000	0.000	0.000	0.000	0.000	0.000	0.000	0.000	0.000	0.000	0.000	0.001
Sum	4.001	4.003	4.006	4.002	4.009	4.003	4.011	4.005	4.005	4.007	4.004	3.996	4.004	4.009	4.003	4.004
Al IV	0.054	0.056	0.056	0.057	0.055	0.057	0.060	0.057	0.060	0.060	0.058	0.059	0.058	0.057	0.053	0.052
Al VI	0.061	0.059	0.062	0.063	0.063	0.061	0.064	0.065	0.067	0.064	0.064	0.063	0.061	0.063	0.059	0.056
Mg#	86.81	86.02	86.40	86.42	86.18	86.17	86.26	86.57	86.41	86.33	86.45	86.74	86.30	86.39	86.59	86.58

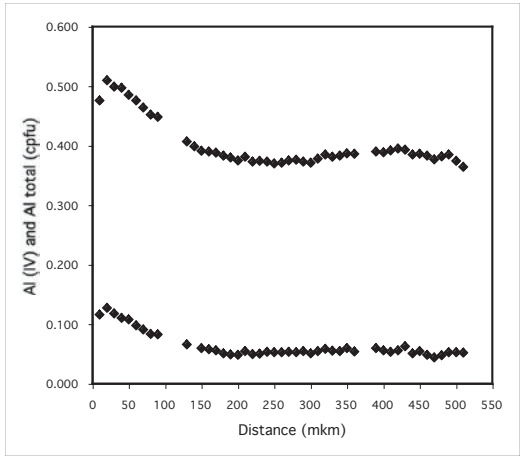
1535-3 Opx II, profile 760

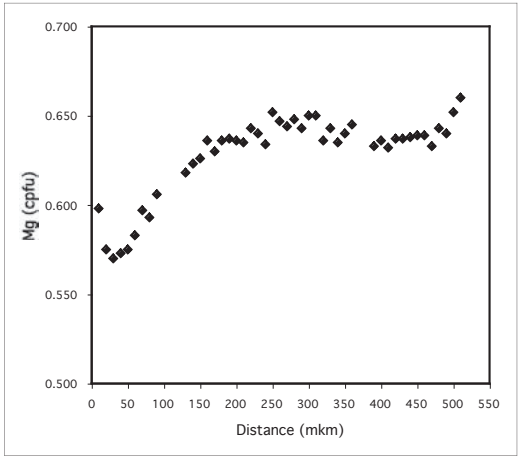
Websterite 1906-4

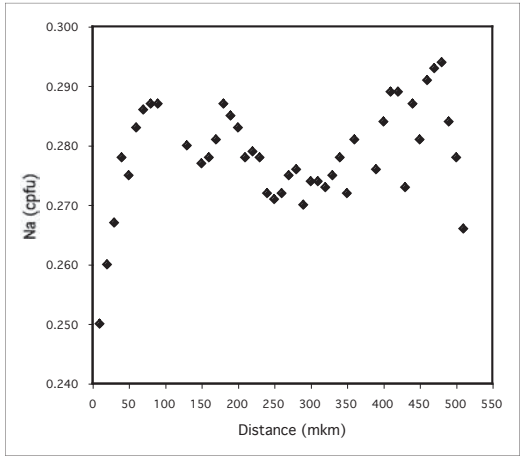


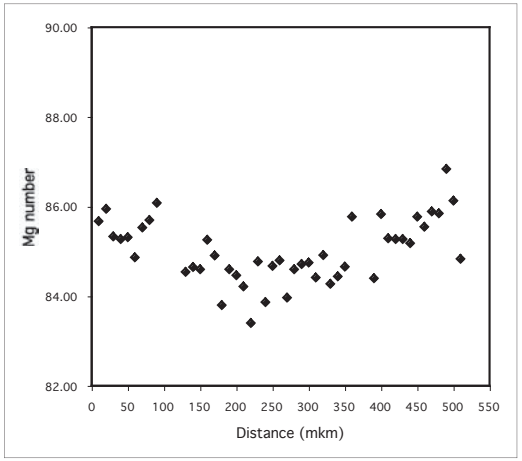
1906-4 Cpx II, profile 515

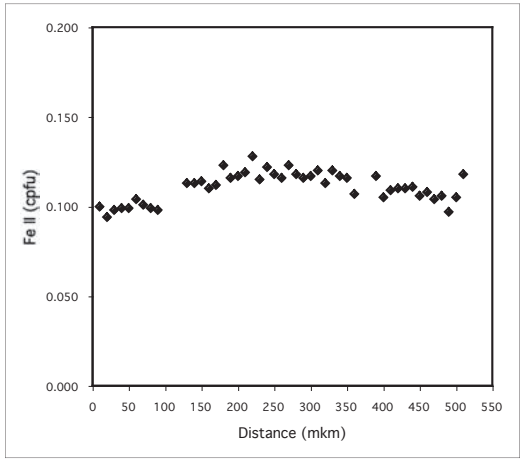












	10	20	30	40	50	60	70	80	90	100	110	120	130	140	150	160	170	180	190	200
SiO2	52.26	51.38	51.86	51.97	52.17	52.14	52.50	52.92	52.98	43.99	51.51	50.67	52.77	52.86	53.32	53.07	53.14	53.19	53.18	53.30
TiO2	0.10	0.08	0.09	0.06	0.06	0.05	0.09	0.04	0.06	0.06	0.06	0.05	0.07	0.06	0.06	0.07	0.07	0.11	0.09	0.08
Al2O3	11.27	11.97	11.74	11.74	11.45	11.21	10.97	10.71	10.61	18.66	6.02	11.31	9.56	9.36	9.21	9.16	9.13	9.02	8.93	8.83
Cr2O3	0.00	0.05	0.04	0.02	0.06	0.03	0.00	0.02	0.00	0.04	0.00	0.00	0.05	0.01	0.03	0.00	0.02	0.00	0.02	0.05
FeO	3.33	3.12	3.24	3.29	3.31	3.44	3.36	3.31	3.28	4.38	4.41	2.82	3.73	3.74	3.78	3.64	3.71	4.08	3.86	3.88
MnO	0.00	0.00	0.01	0.04	0.03	0.00	0.03	0.00	0.05	0.02	0.07	0.04	0.00	0.05	0.00	0.00	0.02	0.01	0.02	0.01
NiO	0.01	0.08	0.00	0.09	0.10	0.05	0.03	0.11	0.15		0.06		0.09	0.04	0.04	0.07	0.04	0.07	0.10	0.00
MgO	11.20	10.66	10.61	10.70	10.73	10.86	11.16	11.10	11.36	11.42	14.46	9.42	11.48	11.54	11.67	11.80	11.72	11.85	11.86	11.83
CaO	18.61	18.29	18.25	18.18	18.05	18.00	17.92	17.95	17.71	17.38	21.96	17.14	18.02	18.00	17.88	17.83	17.91	17.77	17.88	17.91
Na2O	3.60	3.71	3.82	3.99	3.94	4.05	4.11	4.14	4.14	0.91	1.10	3.17	4.00	3.83	3.97	3.96	4.01	4.12	4.08	4.04
K2O	0.01	0.00	0.01	0.00	0.00	0.00	0.01	0.00	0.01	0.26	0.03	0.07	0.01	0.00	0.01	0.02	0.00	0.01	0.01	0.01
Total	100.37	99.34	99.68	100.07	99.89	99.82	100.17	100.30	100.34	97.34	99.68	94.73	99.79	99.48	99.95	99.62	99.77	100.22	100.04	99.93
Si	1.872	1.859	1.869	1.868	1.877	1.879	1.884	1.896	1.896				1.906		1.920	1.917	1.918	1.915	1.917	1.922
Ti	0.003	0.002	0.002	0.001	0.002	0.001	0.002	0.001	0.002				0.002		0.002	0.002	0.002	0.003	0.002	0.002
Al	0.476	0.510	0.499	0.497	0.485	0.476	0.464	0.452	0.448				0.407		0.391	0.390	0.388	0.383	0.380	0.375
Cr	0.000	0.001	0.001	0.000	0.002	0.001	0.000	0.000	0.000				0.001		0.001	0.000	0.000	0.000	0.000	0.001
Fe2+	0.100	0.094	0.098	0.099	0.099	0.104	0.101	0.099	0.098				0.113		0.114	0.110	0.112	0.123	0.116	0.117
Mn	0.000	0.000	0.000	0.001	0.001	0.000	0.001	0.000	0.001				0.000		0.000	0.000	0.000	0.000	0.001	0.000
Ni	0.000	0.002	0.000	0.002	0.003	0.001	0.001	0.003	0.004				0.003		0.001	0.002	0.001	0.002	0.003	0.000
Mg	0.598	0.575	0.570	0.573	0.575	0.583	0.597	0.593	0.606				0.618		0.626	0.636	0.630	0.636	0.637	0.636
Ca	0.714	0.709	0.705	0.700	0.696	0.695	0.689	0.689	0.679				0.697		0.690	0.690	0.693	0.686	0.691	0.692
Na	0.250	0.260	0.267	0.278	0.275	0.283	0.286	0.287	0.287				0.280		0.277	0.278	0.281	0.287	0.285	0.283
K	0.000	0.000	0.001	0.000	0.000	0.000	0.000	0.000	0.000				0.000		0.000	0.001	0.000	0.000	0.001	0.001
Sum	4.012	4.013	4.012	4.021	4.015	4.023	4.025	4.021	4.022				4.028		4.021	4.025	4.026	4.035	4.033	4.029
Mg#	85.67	85.95	85.33	85.27	85.31	84.86	85.53	85.69	86.08				84.54		84.59	85.25	84.91	83.79	84.59	84.46
Al IV	0.116	0.128	0.118	0.111	0.108	0.098	0.091	0.084	0.083				0.066		0.060	0.058	0.056	0.051	0.049	0.048
Al VI	0.360	0.383	0.381	0.387	0.377	0.378	0.373	0.369	0.366				0.341		0.332	0.333	0.333	0.332	0.331	0.327

1906-4 Cpx II, profile 515

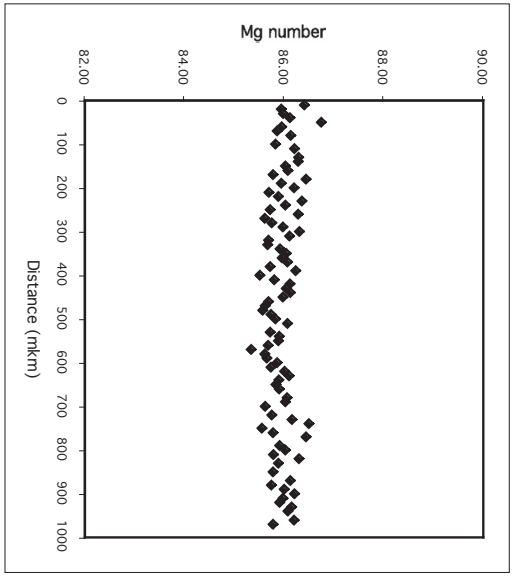
	210	220	230	240	250	260	270	280	290	300	310	320	330	340	350	360	370	380	390	400
SiO2	52.96	53.28	53.24	53.41	53.06	53.31	53.03	53.04	53.09	53.08	52.95	52.92	53.24	53.21	53.34	54.03	50.69	51.86	53.11	53.30
TiO2	0.09	0.07	0.08	0.07	0.07	0.10	0.09	0.08	0.10	0.07	0.08	0.10	0.06	0.09	0.08	0.08	0.03	0.10	0.08	0.10
Al2O3	8.91	8.78	8.79	8.76	8.67	8.72	8.80	8.84	8.76	8.69	8.89	9.02	8.96	9.01	9.14	9.22	16.60	5.07	9.17	9.15
Cr2O3	0.00	0.03	0.00	0.08	0.06	0.03	0.00	0.03	0.01	0.00	0.03	0.00	0.00	0.05	0.00	0.00	0.00	0.00	0.03	0.02
FeO	3.94	4.24	3.79	4.05	3.89	3.85	4.07	3.92	3.85	3.88	3.98	3.74	3.97	3.86	3.85	3.61	1.87	3.95	3.88	3.49
MnO	0.00	0.00	0.05	0.00	0.04	0.00	0.13	0.06	0.04	0.00	0.02	0.00	0.07	0.00	0.00	0.05	0.05	0.04	0.00	0.04
NiO	0.03	0.08	0.04	0.00	0.04	0.03	0.03	0.04	0.02	0.08	0.01	0.00	0.01	0.11	0.12	0.10	0.00	0.03	0.10	0.04
MgO	11.75	11.98	11.89	11.79	12.08	12.04	11.96	12.03	11.91	12.05	12.07	11.76	11.96	11.78	11.96	12.19	5.53	15.21	11.76	11.84
CaO	17.73	17.76	17.86	17.81	17.83	17.93	17.82	17.80	17.97	17.77	17.88	17.78	17.71	17.59	17.91	17.91	11.44	22.31	17.75	17.65
Na2O	3.96	4.00	3.96	3.89	3.86	3.89	3.92	3.94	3.86	3.91	3.91	3.89	3.94	3.97	3.91	4.07	1.82	0.73	3.94	4.07
K2O	0.00	0.00	0.00	0.01	0.00	0.01	0.00	0.00	0.00	0.00	0.00	0.01	0.00	0.01	0.01	0.02	0.11	0.05	0.00	0.00
Total	99.37	100.21	99.71	99.86	99.60	99.91	99.85	99.77	99.60	99.52	99.83	99.21	99.93	99.68	100.30	101.29	88.15	99.35	99.83	99.70
Si	1.920	1.919	1.923	1.927	1.920	1.922	1.917	1.917	1.921	1.922	1.913	1.920	1.919	1.922	1.916	1.919			1.916	1.921
Ti	0.003	0.002	0.002	0.002	0.002	0.003	0.003	0.002	0.003	0.002	0.002	0.003	0.002	0.002	0.002	0.002			0.002	0.003
Al	0.381	0.373	0.374	0.373	0.370	0.371	0.375	0.376	0.373	0.371	0.378	0.385	0.381	0.383	0.387	0.386			0.390	0.389
Cr	0.000	0.001	0.000	0.002	0.002	0.001	0.000	0.001	0.000	0.000	0.001	0.000	0.000	0.001	0.000	0.000			0.001	0.001
Fe2+	0.119	0.128	0.115	0.122	0.118	0.116	0.123	0.118	0.116	0.117	0.120	0.113	0.120	0.117	0.116	0.107			0.117	0.105
Mn	0.000	0.000	0.002	0.000	0.001	0.000	0.004	0.002	0.001	0.000	0.001	0.000	0.002	0.000	0.000	0.002			0.000	0.001
Ni	0.001	0.002	0.001	0.000	0.001	0.001	0.001	0.001	0.000	0.002	0.000	0.000	0.000	0.003	0.003	0.003			0.003	0.001
Mg	0.635	0.643	0.640	0.634	0.652	0.647	0.644	0.648	0.643	0.650	0.650	0.636	0.643	0.635	0.640	0.645			0.633	0.636
Ca	0.689	0.685	0.691	0.688	0.691	0.693	0.690	0.689	0.697	0.689	0.692	0.691	0.684	0.681	0.689	0.681			0.686	0.682
Na	0.278	0.279	0.278	0.272	0.271	0.272	0.275	0.276	0.270	0.274	0.274	0.273	0.275	0.278	0.272	0.281			0.276	0.284
K	0.000	0.000	0.000	0.000	0.000	0.001	0.000	0.000	0.000	0.000	0.000	0.001	0.000	0.001	0.000	0.001			0.000	0.000
Sum	4.026	4.032	4.026	4.020	4.028	4.026	4.031	4.030	4.025	4.028	4.032	4.022	4.026	4.023	4.025	4.027			4.024	4.023
Mg#	84.22	83.40	84.77	83.86	84.68	84.80	83.96	84.60	84.72	84.75	84.42	84.91	84.27	84.44	84.66	85.77			84.40	85.83
Al IV	0.055	0.050	0.050	0.054	0.053	0.053	0.053	0.053	0.055	0.051	0.055	0.059	0.055	0.055	0.060	0.054			0.060	0.056
Al VI	0.327	0.324	0.324	0.320	0.318	0.319	0.322	0.324	0.319	0.321	0.324	0.327	0.326	0.329	0.328	0.332			0.331	0.333

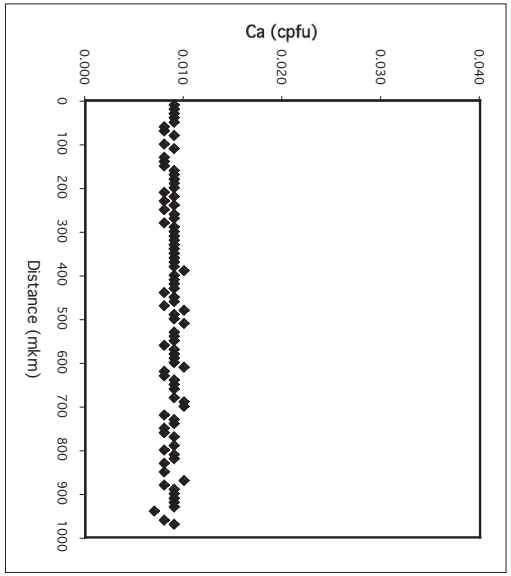
1906-4 Cpx II, profile 515

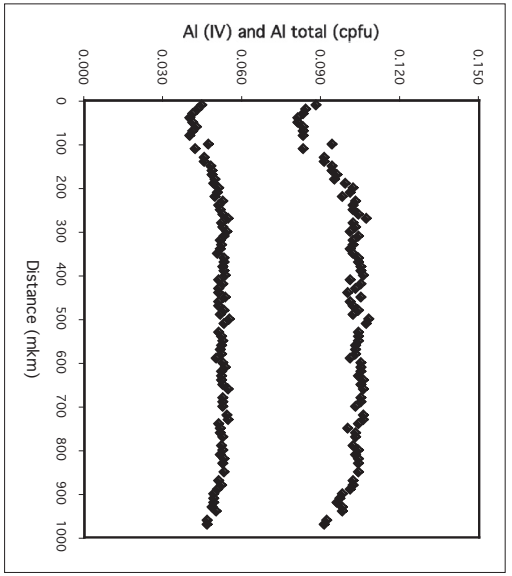
	410	420	430	440	450	460	470	480	490	500	510
SiO2	53.22	53.05	52.98	53.22	53.09	53.08	53.68	53.30	53.31	53.17	52.96
TiO2	0.09	0.10	0.10	0.09	0.07	0.08	0.09	0.11	0.09	0.14	0.14
Al2O3	9.24	9.31	9.21	9.07	9.06	8.98	8.87	8.99	9.01	8.79	8.53
Cr2O3	0.00	0.00	0.00	0.00	0.00	0.03	0.00	0.02	0.00	0.05	0.05
FeO	3.61	3.64	3.63	3.68	3.50	3.56	3.44	3.50	3.21	3.46	3.89
MnO	0.06	0.07	0.03	0.03	0.07	0.03	0.07	0.01	0.00	0.05	0.05
NiO	0.07	0.15	0.00	0.00	0.11	0.00	0.14	0.12	0.00	0.05	0.06
MgO	11.77	11.87	11.83	11.86	11.85	11.83	11.79	11.97	11.85	12.11	12.21
CaO	17.66	17.71	17.81	17.77	17.68	17.59	17.49	17.58	17.45	17.85	17.70
Na2O	4.14	4.15	3.90	4.11	4.01	4.15	4.20	4.21	4.04	3.97	3.78
K2O	0.01	0.00	0.00	0.00	0.01	0.00	0.00	0.01	0.00	0.00	0.07
Total	99.86	100.05	99.48	99.83	99.46	99.34	99.77	99.81	98.96	99.64	99.43
Si	1.918	1.910	1.916	1.919	1.920	1.922	1.933	1.921	1.931	1.920	1.920
Ti	0.002	0.003	0.003	0.002	0.002	0.002	0.002	0.003	0.002	0.004	0.004
Al	0.392	0.395	0.393	0.385	0.386	0.383	0.377	0.382	0.385	0.374	0.364
Cr	0.000	0.000	0.000	0.000	0.000	0.001	0.000	0.001	0.000	0.001	0.001
Fe2+	0.109	0.110	0.110	0.111	0.106	0.108	0.104	0.106	0.097	0.105	0.118
Mn	0.002	0.002	0.001	0.001	0.002	0.001	0.002	0.000	0.000	0.002	0.002
Ni	0.002	0.004	0.000	0.000	0.003	0.000	0.004	0.004	0.000	0.001	0.002
Mg	0.632	0.637	0.637	0.638	0.639	0.639	0.633	0.643	0.640	0.652	0.660
Ca	0.682	0.683	0.690	0.686	0.685	0.682	0.675	0.679	0.677	0.691	0.688
Na	0.289	0.289	0.273	0.287	0.281	0.291	0.293	0.294	0.284	0.278	0.266
K	0.000	0.000	0.000	0.000	0.000	0.000	0.000	0.000	0.000	0.000	0.003
Sum	4.028	4.034	4.022	4.030	4.026	4.029	4.023	4.032	4.016	4.027	4.027
Mg#	85.29	85.27	85.27	85.18	85.77	85.54	85.89	85.85	86.84	86.13	84.83
Al IV	0.054	0.056	0.063	0.051	0.055	0.049	0.044	0.048	0.053	0.053	0.052
Al VI	0.339	0.339	0.330	0.334	0.332	0.335	0.333	0.335	0.333	0.322	0.312

1906-4 Cpx II, profile 515

1906-4 Opx II, profile 957







	10	20	30	40	50	60	70	80	90	100	110	120	130	140	150	160	170	180	190	200
SiO2	55.80	55.74	55.62	55.53	55.43	55.74	55.69	55.48	50.32	55.62	55.83	55.73	55.56	55.83	55.63	55.64	55.52	55.44	55.66	55.46
TiO2	0.04	0.04	0.05	0.03	0.03	0.03	0.01	0.02	0.02	0.02	0.00	0.03	0.03	0.02	0.03	0.05	0.05	0.06	0.04	0.05
Al2O3	2.15	2.05	2.01	1.97	1.96	2.01	2.02	2.01	1.99	2.29	2.02	2.09	2.21	2.21	2.29	2.30	2.34	2.30	2.41	2.48
Cr2O3	0.00	0.01	0.01	0.00	0.05	0.00	0.01	0.00	0.00	0.05	0.06	0.00	0.01	0.03	0.00	0.07	0.03	0.01	0.00	0.00
FeO	9.17	9.56	9.50	9.36	8.91	9.51	9.55	9.36	7.70	9.57	9.31	8.65	9.26	9.18	9.44	9.36	9.58	9.06	9.44	9.23
MnO	0.04	0.13	0.06	0.06	0.07	0.03	0.05	0.00	0.10	0.03	0.09	0.08	0.03	0.07	0.09	0.11	0.11	0.01	0.09	0.00
NiO	0.03	0.07	0.10	0.20	0.14	0.19	0.08	0.11	0.09	0.15	0.14	0.08	0.20	0.12	0.13		0.12		0.20	0.14
MgO	32.67	32.75	32.66	32.61	32.66	32.56	32.56	32.60	28.15	32.53	32.59	32.50	32.67	32.42	32.60	32.51	32.33	32.37	32.40	32.38
CaO	0.25	0.24	0.23	0.25	0.24	0.21	0.23	0.24	0.26	0.22	0.23	0.23	0.22	0.21	0.23	0.24	0.23	0.25	0.24	0.23
Na2O	0.01	0.00	0.04	0.03	0.03	0.00	0.01	0.04	0.04	0.01	0.01	0.01	0.03	0.02	0.00	0.02	0.03	0.01	0.04	0.03
K2O	0.01	0.00	0.00	0.01	0.00	0.00	0.01	0.01	0.02	0.00	0.00	0.00	0.01	0.01	0.00	0.00	0.01	0.01	0.00	0.01
Total	100.17	100.60	100.29	100.06	99.51	100.30	100.21	99.87	88.69	100.50	100.30	99.39	100.23	100.10	100.44	100.55	100.33	99.79	100.52	100.01
Si	1.945	1.940	1.941	1.942	1.945	1.945	1.944	1.943		1.937	1.946		1.938	1.947	1.938	1.937	1.937	1.941	1.938	1.937
Ti	0.001	0.001	0.001	0.001	0.001	0.001	0.000	0.000		0.000	0.000		0.001	0.000	0.001	0.001	0.001	0.002	0.001	0.001
Al	0.088	0.084	0.083	0.081	0.081	0.083	0.083	0.083		0.094	0.083		0.091	0.091	0.094	0.094	0.096	0.095	0.099	0.102
Cr	0.000	0.000	0.000	0.000	0.001	0.000	0.000	0.000		0.001	0.002		0.000	0.001	0.000	0.002	0.001	0.000	0.000	0.000
Fe2+	0.267	0.278	0.277	0.274	0.261	0.277	0.279	0.274		0.279	0.271		0.270	0.268	0.275	0.273	0.279	0.265	0.275	0.270
Mn	0.001	0.004	0.002	0.002	0.002	0.001	0.001	0.000		0.001	0.003		0.001	0.002	0.003	0.003	0.003	0.000	0.003	0.000
Ni	0.001	0.002	0.003	0.006	0.004	0.005	0.002	0.003		0.004	0.004		0.006	0.003	0.004	0.007	0.003	0.007	0.006	0.004
Mg	1.697	1.699	1.699	1.700	1.708	1.694	1.694	1.702		1.689	1.694		1.699	1.686	1.693	1.687	1.682	1.689	1.681	1.686
Ca	0.009	0.009	0.009	0.009	0.009	0.008	0.008	0.009		0.008	0.009		0.008	0.008	0.008	0.009	0.009	0.009	0.009	0.009
Na	0.000	0.000	0.003	0.002	0.002	0.000	0.001	0.003		0.001	0.001		0.002	0.001	0.000	0.001	0.002	0.000	0.003	0.002
K	0.001	0.000	0.000	0.001	0.000	0.000	0.000	0.000		0.000	0.000		0.000	0.000	0.000	0.000	0.000	0.000	0.000	0.000
Sum	4.011	4.017	4.018	4.018	4.015	4.013	4.014	4.017		4.015	4.012		4.016	4.007	4.015	4.014	4.014	4.010	4.013	4.012
Mg#	86.41	85.94	85.98	86.12	86.74	85.95	85.86	86.13		85.82	86.21		86.29	86.28	86.03	86.07	85.77	86.44	85.94	86.20
Al IV	0.045	0.043	0.041	0.040	0.041	0.043	0.041	0.040		0.047	0.042		0.046	0.046	0.048	0.049	0.049	0.050	0.049	0.051
Al VI	0.044	0.041	0.042	0.041	0.040	0.041	0.042	0.043		0.047	0.041		0.046	0.046	0.046	0.046	0.048	0.046	0.050	0.051

1906-4 Opx II, profile 957

	210	220	230	240	250	260	270	280	290	300	310	320	330	340	350	360	370	380	390	400
SiO2	55.41	55.24	55.34	55.46	55.22	55.24	55.15	55.21	55.28	55.56	55.35	55.29	55.43	53.85	55.12	55.37	55.19	55.20	55.21	55.08
TiO2	0.04	0.02	0.02	0.04	0.04	0.01	0.03	0.06	0.03	0.06	0.04	0.02	0.02	0.04	0.00	0.04	0.04	0.03	0.06	0.04
Al2O3	2.45	2.37	2.49	2.48	2.48	2.51	2.59	2.48	2.50	2.45	2.52	2.49	2.48	2.38	2.46	2.52	2.51	2.54	2.54	2.57
Cr2O3	0.02	0.01	0.00	0.00	0.05	0.07	0.02	0.00	0.00	0.10	0.02	0.07	0.02	0.05	0.00	0.02	0.02	0.00	0.00	0.01
FeO	9.57	9.40	9.08	9.41	9.61	9.14	9.66	9.57	9.44	9.08	9.31	9.65	9.65	9.09	9.34	9.43	9.26	9.62	9.19	9.79
MnO	0.10	0.08	0.06	0.07	0.02	0.12	0.11	0.07	0.06	0.06	0.10	0.08	0.08	0.04	0.16	0.07	0.11	0.10	0.09	0.02
NiO	0.10	0.09	0.02	0.19	0.21	0.16	0.09	0.13	0.20	0.15	0.14	0.15	0.10	0.16	0.09	0.13	0.10	0.12	0.08	0.13
MgO	32.19	32.04	32.19	32.46	32.39	32.28	32.31	32.29	32.53	32.16	32.38	32.46	32.30	31.12	32.29	32.36	32.12	32.38	32.25	32.40
CaO	0.21	0.24	0.22	0.24	0.23	0.25	0.23	0.21	0.25	0.24	0.24	0.23	0.23	0.23	0.24	0.24	0.25	0.24	0.25	0.25
Na2O	0.02	0.01	0.00	0.02	0.03	0.01	0.02	0.03	0.00	0.00	0.02	0.02	0.07	0.01	0.01	0.02	0.01	0.01	0.02	0.01
K2O	0.00	0.00	0.00	0.02	0.00	0.00	0.00	0.01	0.00	0.01	0.01	0.00	0.00	0.00	0.00	0.01	0.00	0.02	0.00	0.00
Total	100.11	99.50	99.43	100.38	100.28	99.79	100.22	100.06	100.30	99.88	100.14	100.46	100.37	96.98	99.72	100.22	99.61	100.26	99.68	100.31
Si	1.937	1.941	1.942	1.933	1.929	1.935	1.928	1.932	1.930	1.942	1.933		1.934	1.941	1.934	1.933	1.937	1.929	1.935	1.925
Ti	0.001	0.001	0.001	0.001	0.001	0.000	0.001	0.002	0.001	0.002	0.001		0.001	0.001	0.000	0.001	0.001	0.001	0.001	0.001
Al	0.101	0.098	0.103	0.102	0.102	0.104	0.107	0.102	0.103	0.101	0.104		0.102	0.101	0.102	0.104	0.104	0.105	0.105	0.106
Cr	0.000	0.000	0.000	0.000	0.001	0.002	0.001	0.000	0.000	0.003	0.001		0.000	0.001	0.000	0.001	0.001	0.000	0.000	0.000
Fe2+	0.280	0.276	0.266	0.274	0.281	0.268	0.283	0.280	0.276	0.266	0.272		0.281	0.274	0.274	0.275	0.272	0.281	0.269	0.286
Mn	0.003	0.002	0.002	0.002	0.001	0.003	0.003	0.002	0.002	0.002	0.003		0.002	0.001	0.005	0.002	0.003	0.003	0.003	0.001
Ni	0.003	0.003	0.001	0.005	0.006	0.004	0.003	0.004	0.006	0.004	0.004		0.003	0.005	0.003	0.004	0.003	0.003	0.002	0.004
Mg	1.677	1.679	1.684	1.687	1.687	1.686	1.684	1.685	1.692	1.676	1.686		1.680	1.672	1.689	1.684	1.680	1.687	1.685	1.688
Ca	0.008	0.009	0.008	0.009	0.008	0.009	0.009	0.008	0.009	0.009	0.009		0.009	0.009	0.009	0.009	0.009	0.009	0.010	0.009
Na	0.002	0.001	0.000	0.001	0.002	0.001	0.001	0.002	0.000	0.000	0.001			0.001	0.001	0.001	0.001	0.001	0.001	0.001
K	0.000	0.000	0.000	0.001	0.000	0.000	0.000	0.000	0.000	0.000	0.000		0.000	0.000	0.000	0.000	0.000	0.001	0.000	0.000
Sum	4.012	4.009	4.006	4.016	4.019	4.012	4.018	4.017	4.018	4.005	4.014		4.017	4.007	4.016	4.014	4.010	4.019	4.012	4.021
Mg#	85.69	85.88	86.36	86.03	85.72	86.28	85.61	85.75	85.98	86.30	86.11		85.67	85.92	86.04	85.96	86.07	85.72	86.23	85.51
Al IV	0.051	0.050	0.053	0.051	0.052	0.053	0.055	0.052	0.053	0.054	0.053		0.052	0.052	0.051	0.053	0.053	0.053	0.053	0.054
Al VI	0.051	0.049	0.051	0.051	0.051	0.052	0.053	0.050	0.051	0.047	0.051		0.050	0.050	0.052	0.051	0.051	0.053	0.052	0.053

1906-4 Opx II, profile 957

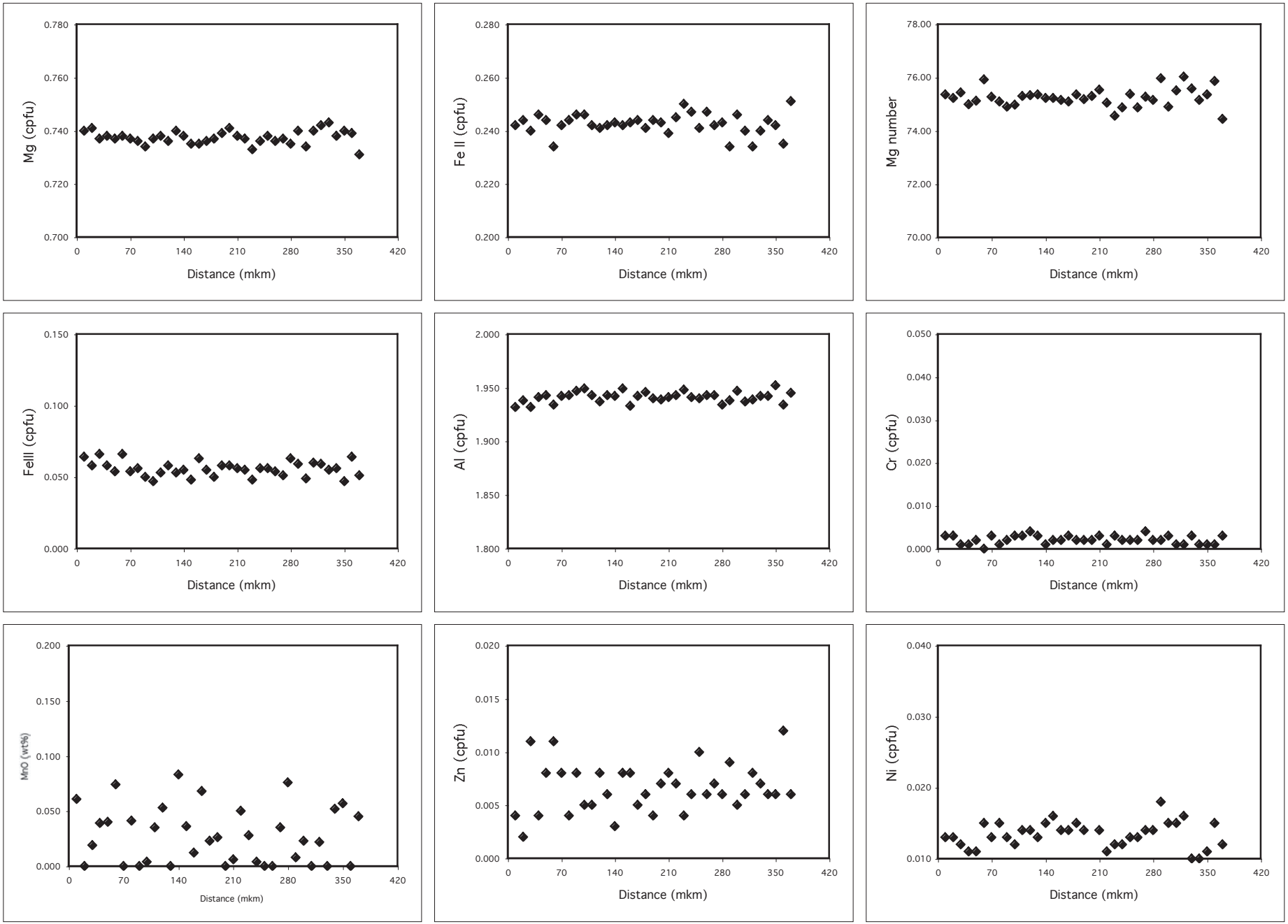
	410	420	430	440	450	460	470	480	490	500	510	520	530	540	550	560	570	580	590	600
SiO2	55.20	55.28	55.14	55.62	55.11	55.28	55.35	55.40	55.07	55.24	54.88	52.76	55.09	54.76	55.06	55.05	55.08	55.23	55.18	54.97
TiO2	0.04	0.04	0.02	0.03	0.02	0.04	0.01	0.04	0.02	0.05	0.05	0.02	0.02	0.02	0.04	0.04	0.02	0.04	0.02	0.05
Al2O3	2.45	2.54	2.50	2.42	2.54	2.45	2.49	2.54	2.46	2.61	2.58	8.28	2.50	2.50	2.50	2.49	2.49	2.50	2.45	2.54
Cr2O3	0.04	0.00	0.01	0.01	0.04	0.00	0.00	0.05	0.02	0.00	0.00	0.00	0.01	0.00	0.00	0.00	0.00	0.00	0.00	0.00
FeO	9.53	9.23	9.36	9.27	9.42	9.64	9.70	9.72	9.52	9.46	9.29	7.81	9.48	9.40	9.37	9.63	9.86	9.67	9.62	9.49
MnO	0.06	0.02	0.13	0.03	0.06	0.12	0.08	0.00	0.06	0.08	0.03	0.00	0.00	0.11	0.07	0.06	0.03	0.06	0.08	0.07
NiO	0.04	0.08	0.07	0.10	0.09	0.05	0.13		0.10	0.01	0.21	0.09	0.17	0.20	0.04	0.07	0.20	0.18	0.17	0.17
MgO	32.30	32.17	32.34	32.32	32.42	32.40	32.38	32.30	32.15	32.10	32.16	24.61	31.94	32.12	31.99	32.28	32.23	32.32	32.26	32.27
CaO	0.25	0.25	0.25	0.23	0.25	0.23	0.21	0.26	0.25	0.24	0.26	1.36	0.23	0.24	0.25	0.21	0.23	0.25	0.23	0.24
Na2O	0.03	0.01	0.05	0.01	0.01	0.01	0.01	0.02	0.03	0.00	0.05	0.04	0.02	0.01	0.01	0.02	0.04	0.02	0.02	0.02
K2O	0.01	0.01	0.00	0.00	0.00	0.01	0.00	0.00	0.01	0.01	0.00	0.66	0.01	0.00	0.00	0.00	0.00	0.00	0.00	0.00
Total	99.95	99.64	99.88	100.04	99.96	100.24	100.37	100.60	99.69	99.81	99.51	95.63	99.48	99.34	99.32	99.86	100.18	100.28	100.03	99.83
Si	1.933	1.938	1.932	1.942	1.929	1.931	1.932	1.930	1.934	1.935	1.930		1.938	1.930	1.938	1.931	1.929	1.930	1.933	1.928
Ti	0.001	0.001	0.001	0.001	0.001	0.001	0.000	0.001	0.001	0.001	0.001		0.000	0.000	0.001	0.001	0.001	0.001	0.000	0.001
Al	0.101	0.105	0.103	0.100	0.105	0.101	0.102	0.104	0.102	0.108	0.107		0.104	0.104	0.104	0.103	0.103	0.103	0.101	0.105
Cr	0.001	0.000	0.000	0.000	0.001	0.000	0.000	0.001	0.001	0.000	0.000		0.000	0.000	0.000	0.000	0.000	0.000	0.000	0.000
Fe2+	0.279	0.271	0.274	0.271	0.276	0.282	0.283	0.283	0.280	0.277	0.273		0.279	0.277	0.276	0.282	0.289	0.283	0.282	0.278
Mn	0.002	0.001	0.004	0.001	0.002	0.004	0.002	0.000	0.002	0.002	0.001		0.000	0.003	0.002	0.002	0.001	0.002	0.002	0.002
Ni	0.001	0.002	0.002	0.003	0.003	0.001	0.004	0.007	0.003	0.000	0.006		0.005	0.006	0.001	0.002	0.006	0.005	0.005	0.005
Mg	1.686	1.681	1.689	1.682	1.692	1.688	1.685	1.678	1.683	1.677	1.686		1.675	1.688	1.679	1.687	1.682	1.684	1.684	1.688
Ca	0.009	0.009	0.009	0.008	0.009	0.009	0.008	0.010	0.009	0.009	0.010		0.009	0.009	0.009	0.008	0.009	0.009	0.009	0.009
Na	0.002	0.001	0.003	0.000	0.001	0.001	0.000	0.001	0.002	0.000	0.003		0.002	0.000	0.001	0.001	0.002	0.001	0.001	0.002
K	0.000	0.001	0.000	0.000	0.000	0.000	0.000	0.000	0.000	0.000	0.000		0.000	0.000	0.000	0.000	0.000	0.000	0.000	0.000
Sum	4.016	4.009	4.017	4.008	4.018	4.018	4.017	4.017	4.015	4.010	4.017		4.011	4.018	4.010	4.017	4.020	4.018	4.017	4.019
Mg#	85.80	86.12	86.04	86.12	85.98	85.69	85.62	85.57	85.74	85.82	86.06		85.72	85.90	85.88	85.68	85.34	85.61	85.66	85.86
Al IV	0.051	0.053	0.051	0.051	0.054	0.051	0.051	0.053	0.052	0.055	0.053		0.051	0.052	0.053	0.052	0.052	0.052	0.050	0.053
Al VI	0.050	0.053	0.052	0.049	0.052	0.050	0.051	0.051	0.051	0.053	0.054		0.053	0.052	0.052	0.051	0.052	0.051	0.051	0.053

1906-4 Opx II, profile 957

	610	620	630	640	650	660	670	680	690	700	710	720	730	740	750	760	770	780	790	800
SiO2	55.16	55.16	55.15	55.30	55.07	55.02	54.78	55.17	55.12	55.22	54.17	55.17	55.14	55.40	55.38	55.17	55.03	44.58	55.29	55.06
TiO2	0.05	0.05	0.03	0.00	0.03	0.03	0.03	0.04	0.02	0.03	0.06	0.04	0.06	0.02	0.03	0.01	0.05	0.00	0.03	0.04
Al2O3	2.54	2.54	2.52	2.58	2.55	2.56	2.49	2.54	2.55	2.51	3.35	2.58	2.57	2.52	2.42	2.50	2.49	9.05	2.48	2.51
Cr2O3	0.02	0.02	0.00	0.02	0.00	0.09	0.00	0.00	0.00	0.00	0.00	0.00	0.00	0.00	0.03	0.02	0.05	0.00	0.00	0.01
FeO	9.51	9.41	9.21	9.54	9.52	9.41	9.25	9.28	9.36	9.62	9.82	9.61	9.25	8.99	9.73	9.54	9.01	5.42	9.46	9.33
MnO	0.08	0.06	0.10	0.03	0.02	0.08	0.07	0.05	0.06	0.05	0.07	0.11	0.07	0.17	0.03	0.11	0.04	0.12	0.00	0.10
NiO	0.11	0.15	0.03	0.03	0.17	0.18	0.13	0.14	0.12	0.16	0.10	0.07	0.14	0.13	0.15	0.21	0.14	0.09	0.15	0.18
MgO	32.08	32.41	32.03	32.53	32.39	32.17	32.44	32.09	32.30	32.18	30.77	32.48	32.30	32.29	32.32	32.25	32.21	20.61	32.42	32.25
CaO	0.26	0.22	0.22	0.23	0.23	0.24	0.22	0.24	0.26	0.26	0.68	0.23	0.23	0.23	0.22	0.22	0.24	7.73	0.24	0.21
Na2O	0.00	0.06	0.03	0.04	0.03	0.04	0.01	0.02	0.04	0.00	0.02	0.00	0.02	0.02	0.00	0.02	0.02	0.01	0.00	0.02
K2O	0.02	0.00	0.00	0.01	0.00	0.00	0.01	0.02	0.00	0.00	0.02	0.01	0.00	0.01	0.01	0.00	0.00	0.58	0.00	0.00
Total	99.83	100.10	99.33	100.31	100.01	99.82	99.43	99.60	99.84	100.04	99.06	100.29	99.79	99.79	100.33	100.07	99.29	88.20	100.09	99.71
Si	1.934	1.929	1.939	1.929	1.928	1.930		1.937	1.932	1.933		1.927	1.932	1.939	1.934	1.932	1.936		1.933	1.932
Ti	0.001	0.001	0.001	0.000	0.001	0.001		0.001	0.001	0.001		0.001	0.002	0.000	0.001	0.000	0.001		0.001	0.001
Al	0.105	0.105	0.104	0.106	0.105	0.106		0.105	0.105	0.103		0.106	0.106	0.104	0.100	0.103	0.103		0.102	0.104
Cr	0.001	0.001	0.000	0.001	0.000	0.003		0.000	0.000	0.000		0.000	0.000	0.000	0.001	0.001	0.001		0.000	0.000
Fe2+	0.279	0.275	0.271	0.278	0.279	0.276		0.272	0.274	0.282		0.281	0.271	0.263	0.284	0.279	0.265		0.277	0.274
Mn	0.002	0.002	0.003	0.001	0.000	0.002		0.002	0.002	0.001		0.003	0.002	0.005	0.001	0.003	0.001		0.000	0.003
Ni	0.003	0.004	0.001	0.001	0.005	0.005		0.004	0.003	0.004		0.002	0.004	0.004	0.004	0.006	0.004		0.004	0.005
Mg	1.677	1.690	1.679	1.692	1.690	1.682		1.679	1.687	1.679		1.691	1.687	1.685	1.682	1.683	1.689		1.689	1.687
Ca	0.010	0.008	0.008	0.009	0.009	0.009		0.009	0.010	0.010		0.008	0.009	0.009	0.008	0.008	0.009		0.009	0.008
Na	0.000	0.004	0.002	0.003	0.002	0.002		0.001	0.002	0.000		0.000	0.001	0.001	0.000	0.001	0.001		0.000	0.001
K	0.001	0.000	0.000	0.000	0.000	0.000		0.001	0.000	0.000		0.000	0.000	0.001	0.000	0.000	0.000		0.000	0.000
Sum	4.012	4.019	4.009	4.019	4.019	4.016		4.011	4.016	4.014		4.019	4.014	4.010	4.016	4.017	4.011		4.015	4.015
Mg#	85.74	86.01	86.10	85.89	85.83	85.90		86.06	86.03	85.62		85.75	86.16	86.50	85.55	85.78	86.44		85.91	86.03
Al IV	0.054	0.052	0.052	0.052	0.053	0.055		0.053	0.053	0.053		0.054	0.055	0.051	0.052	0.052	0.053		0.052	0.053
Al VI	0.052	0.053	0.052	0.054	0.053	0.052		0.053	0.053	0.051		0.052	0.052	0.053	0.049	0.052	0.051		0.050	0.052

1906-4 Opx II, profile 957

	810	820	830	840	850	860	870	880	890	900	910	920	930	940	950	960	970
SiO2	54.97	55.12	55.14	54.37	55.27	55.00	55.10	55.19	55.13	55.47	55.44	55.30	55.50	55.49	54.92	55.27	55.30
TiO2	0.05	0.04	0.04	0.06	0.04	0.02	0.03	0.05	0.05	0.04	0.04	0.04	0.02	0.04	0.05	0.04	0.02
Al2O3	2.48	2.50	2.51	2.77	2.51	2.64	2.48	2.48	2.45	2.38	2.34	2.34	2.39	2.37	2.46	2.21	2.21
Cr2O3	0.00	0.02	0.02	0.00	0.02	0.02	0.00	0.00	0.01	0.00	0.00	0.02	0.00	0.00	0.00	0.02	0.05
FeO	9.55	9.15	9.40	9.58	9.48	9.51	9.32	9.54	9.44	9.24	9.42	9.50	9.28	9.40	9.47	9.22	9.55
MnO	0.07	0.03	0.07	0.07	0.08	0.04	0.03	0.05	0.03	0.04	0.10	0.02	0.14	0.04	0.10	0.04	0.06
NiO	0.13	0.19	0.09	0.12	0.16	0.17	0.17	0.09	0.15	0.09	0.15	0.16		0.08	0.14	0.13	0.08
MgO	32.29	32.27	32.06	31.76	32.13	31.90	32.43	32.24	32.47	32.35	32.35	32.51	32.37	32.57	31.97	32.32	32.30
CaO	0.23	0.23	0.21	0.23	0.21	0.24	0.26	0.22	0.23	0.24	0.23	0.23	0.23	0.20	0.27	0.21	0.25
Na2O	0.02	0.02	0.01	0.02	0.02	0.02	0.03	0.00	0.01	0.02	0.02	0.00	0.02	0.00	0.04	0.01	0.02
K2O	0.00	0.00	0.02	0.02	0.01	0.01	0.00	0.00	0.01	0.00	0.01	0.00	0.00	0.01	0.01	0.00	0.01
Total	99.81	99.58	99.58	99.00	99.93	99.57	99.84	99.87	100.01	99.86	100.11	100.11	100.18	100.21	99.43	99.50	99.85
Si	1.929	1.935	1.937		1.936		1.931	1.934	1.930	1.940	1.938	1.933	1.938	1.936		1.941	1.939
Ti	0.001	0.001	0.001		0.001		0.001	0.001	0.001	0.001	0.001	0.001	0.000	0.001		0.001	0.001
Al	0.103	0.104	0.104		0.104		0.102	0.102	0.101	0.098	0.097	0.096	0.098	0.098		0.092	0.091
Cr	0.000	0.001	0.001		0.001		0.000	0.000	0.000	0.000	0.000	0.000	0.000	0.000		0.000	0.001
Fe2+	0.280	0.268	0.276		0.278		0.273	0.280	0.276	0.270	0.275	0.278	0.271	0.274		0.271	0.280
Mn	0.002	0.001	0.002		0.002		0.001	0.002	0.001	0.001	0.003	0.001	0.004	0.001		0.001	0.002
Ni	0.004	0.005	0.003		0.005		0.005	0.003	0.004	0.003	0.004	0.005	0.006	0.002		0.004	0.002
Mg	1.690	1.688	1.679		1.677		1.694	1.684	1.695	1.687	1.686	1.695	1.685	1.694		1.693	1.688
Ca	0.009	0.009	0.008		0.008		0.010	0.008	0.009	0.009	0.009	0.009	0.009	0.007		0.008	0.009
Na	0.002	0.001	0.001		0.001		0.002	0.000	0.001	0.002	0.001	0.000	0.001	0.000		0.001	0.001
K	0.000	0.000	0.001		0.000		0.000	0.000	0.001	0.000	0.000	0.000	0.000	0.000		0.000	0.000
Sum	4.019	4.013	4.011		4.012		4.018	4.014	4.019	4.010	4.014	4.017	4.013	4.014		4.012	4.015
Mg#	85.79	86.30	85.88		85.78		86.12	85.74	86.00	86.20	85.98	85.91	86.15	86.08		86.20	85.77
Al IV	0.052	0.053	0.053		0.053		0.051	0.052	0.051	0.049	0.049	0.049	0.049	0.050		0.047	0.047
Al VI	0.052	0.051	0.052		0.051		0.051	0.050	0.051	0.049	0.048	0.047	0.050	0.048		0.046	0.045



1906-4 Spinel, profile 362

	10	20	30	40	50	60	70	80	90	100	110	120	130	140	150	160	170	180	190
SiO2	0.02	0.01	0.01	0.00	0.00	0.00	0.01	0.00	0.01	0.00	0.01	0.01	0.00	0.01	0.00	0.01	0.01	0.00	0.00
TiO2	0.02	0.03	0.00	0.00	0.01	0.00	0.00	0.01	0.01	0.02	0.02	0.02	0.02	0.02	0.02	0.02	0.02	0.03	0.02
Al2O3	64.65	64.87	64.87	64.95	65.06	65.11	65.14	64.98	65.03	64.59	65.00	65.29	65.37	65.10	65.06	65.23	64.98	65.43	65.08
Cr2O3	0.13	0.13	0.06	0.06	0.12	0.02	0.14	0.06	0.10	0.14	0.14	0.19	0.15	0.07	0.11	0.12	0.13	0.11	0.09
FeO	14.43	14.23	14.47	14.32	14.03	14.24	14.01	14.14	13.90	13.70	13.88	14.19	14.01	14.08	13.63	14.54	14.06	13.82	14.25
MnO	0.06	0.00	0.02	0.04	0.04	0.07	0.00	0.04	0.00	0.00	0.04	0.05	0.00	0.08	0.04	0.01	0.07	0.02	0.03
NiO	0.63	0.64	0.59	0.53	0.53	0.74	0.66	0.75	0.63	0.57	0.70	0.70	0.62	0.72	0.77	0.72	0.69	0.75	0.68
ZnO	0.24	0.12	0.60	0.22	0.42	0.57	0.43	0.23	0.42	0.29	0.29	0.45	0.33	0.18	0.41	0.45	0.29	0.34	0.20
MgO	19.57	19.61	19.56	19.52	19.51	19.65	19.53	19.45	19.38	19.30	19.53	19.62	19.67	19.55	19.39	19.60	19.47	19.59	19.60
CaO	0.00	0.00	0.00	0.00	0.00	0.00	0.00	0.00	0.00	0.00	0.00	0.01	0.00	0.00	0.00	0.00	0.00	0.00	0.00
Total	99.76	99.63	100.19	99.64	99.73	100.41	99.92	99.67	99.49	98.61	99.61	100.53	100.18	99.81	99.43	100.69	99.70	100.09	99.95
Si	0.001	0.000	0.000	0.000	0.000	0.000	0.000	0.000	0.000	0.000	0.000	0.000	0.000	0.000	0.000	0.000	0.000	0.000	0.000
Ti	0.000	0.000	0.000	0.000	0.000	0.000	0.000	0.000	0.000	0.000	0.000	0.000	0.000	0.000	0.000	0.000	0.000	0.001	0.000
Al	1.932	1.938	1.932	1.941	1.943	1.934	1.942	1.943	1.947	1.949	1.943	1.937	1.943	1.942	1.949	1.933	1.942	1.946	1.940
Cr	0.003	0.003	0.001	0.001	0.002	0.000	0.003	0.001	0.002	0.003	0.003	0.004	0.003	0.001	0.002	0.002	0.003	0.002	0.002
Fe3+	0.064	0.058	0.066	0.058	0.054	0.066	0.054	0.056	0.050	0.047	0.053	0.058	0.053	0.055	0.048	0.063	0.055	0.050	0.058
Fe2+	0.242	0.244	0.240	0.246	0.244	0.234	0.242	0.244	0.246	0.246	0.242	0.241	0.242	0.243	0.242	0.243	0.244	0.241	0.244
Mn	0.001	0.000	0.000	0.001	0.001	0.002	0.000	0.001	0.000	0.000	0.001	0.001	0.000	0.002	0.001	0.000	0.001	0.000	0.001
Ni	0.013	0.013	0.012	0.011	0.011	0.015	0.013	0.015	0.013	0.012	0.014	0.014	0.013	0.015	0.016	0.014	0.014	0.015	0.014
Zn	0.004	0.002	0.011	0.004	0.008	0.011	0.008	0.004	0.008	0.005	0.005	0.008	0.006	0.003	0.008	0.008	0.005	0.006	0.004
Mg	0.740	0.741	0.737	0.738	0.737	0.738	0.737	0.736	0.734	0.737	0.738	0.736	0.740	0.738	0.735	0.735	0.736	0.737	0.739
Ca	0.000	0.000	0.000	0.000	0.000	0.000	0.000	0.000	0.000	0.000	0.000	0.000	0.000	0.000	0.000	0.000	0.000	0.000	0.000
Sum	3.000	3.000	3.000	3.000	3.000	3.000	3.000	3.000	3.000	3.000	3.000	3.000	3.000	3.000	3.000	3.000	3.000	3.000	3.000
Mg#	75.36	75.23	75.44	75.00	75.13	75.93	75.28	75.10	74.90	74.97	75.31	75.33	75.36	75.23	75.23	75.15	75.10	75.36	75.18

1906-4 Spinel, profile 362

	200	210	220	230	240	250	260	270	280	290	300	310	320	330	340	350	360	370
SiO2	0.00	0.00	0.01	0.00	0.03	0.02	0.01	0.02	0.00	0.02	0.02	0.02	0.02	0.02	0.00	0.00	0.01	0.03
TiO2	0.03	0.00	0.01	0.02	0.00	0.04	0.02	0.02	0.01	0.01	0.00	0.01	0.00	0.01	0.01	0.00	0.01	0.00
Al2O3	65.00	65.10	65.23	65.28	65.19	65.34	65.27	65.18	65.21	65.50	65.33	65.01	65.15	65.00	65.16	65.14	65.16	65.35
Cr2O3	0.09	0.17	0.08	0.16	0.09	0.10	0.12	0.20	0.11	0.11	0.14	0.07	0.06	0.13	0.06	0.03	0.07	0.13
FeO	14.26	13.95	14.19	14.10	14.35	14.08	14.23	13.87	14.57	13.93	13.93	14.19	13.86	13.91	14.22	13.61	14.17	14.28
MnO	0.00	0.01	0.05	0.03	0.00	0.00	0.00	0.04	0.08	0.01	0.02	0.00	0.02	0.00	0.05	0.06	0.00	0.05
NiO	0.46	0.70	0.52	0.61	0.59	0.64	0.62	0.67	0.67	0.89	0.76	0.72	0.80	0.51	0.49	0.52	0.72	0.60
ZnO	0.37	0.42	0.37	0.23	0.30	0.54	0.30	0.39	0.35	0.49	0.25	0.31	0.45	0.39	0.34	0.30	0.65	0.32
MgO	19.63	19.58	19.55	19.42	19.55	19.64	19.54	19.54	19.60	19.76	19.47	19.63	19.71	19.66	19.58	19.52	19.68	19.41
CaO	0.00	0.00	0.01	0.00	0.00	0.00	0.00	0.01	0.00	0.00	0.00	0.01	0.00	0.00	0.00	0.01	0.01	0.00
Total	99.85	99.93	100.02	99.86	100.11	100.39	100.12	99.93	100.59	100.70	99.93	99.97	100.09	99.63	99.92	99.19	100.48	100.18
Si	0.000	0.000	0.000	0.000	0.001	0.000	0.000	0.000	0.000	0.000	0.001	0.001	0.001	0.000	0.000	0.000	0.000	0.001
Ti	0.000	0.000	0.000	0.000	0.000	0.001	0.000	0.000	0.000	0.000	0.000	0.000	0.000	0.000	0.000	0.000	0.000	0.000
Al	1.939	1.941	1.943	1.948	1.941	1.940	1.943	1.943	1.934	1.938	1.947	1.937	1.939	1.942	1.942	1.952	1.934	1.945
Cr	0.002	0.003	0.001	0.003	0.002	0.002	0.002	0.004	0.002	0.002	0.003	0.001	0.001	0.003	0.001	0.001	0.001	0.003
Fe3+	0.058	0.056	0.055	0.048	0.056	0.056	0.054	0.051	0.063	0.059	0.049	0.060	0.059	0.055	0.056	0.047	0.064	0.051
Fe2+	0.243	0.239	0.245	0.250	0.247	0.241	0.247	0.242	0.243	0.234	0.246	0.240	0.234	0.240	0.244	0.242	0.235	0.251
Mn	0.000	0.000	0.001	0.001	0.000	0.000	0.000	0.001	0.002	0.000	0.000	0.000	0.000	0.000	0.001	0.001	0.000	0.001
Ni	0.009	0.014	0.011	0.012	0.012	0.013	0.013	0.014	0.014	0.018	0.015	0.015	0.016	0.010	0.010	0.011	0.015	0.012
Zn	0.007	0.008	0.007	0.004	0.006	0.010	0.006	0.007	0.006	0.009	0.005	0.006	0.008	0.007	0.006	0.006	0.012	0.006
Mg	0.741	0.738	0.737	0.733	0.736	0.738	0.736	0.737	0.735	0.740	0.734	0.740	0.742	0.743	0.738	0.740	0.739	0.731
Ca	0.000	0.000	0.000	0.000	0.000	0.000	0.000	0.000	0.000	0.000	0.000	0.000	0.000	0.000	0.000	0.000	0.000	0.000
Sum	3.000	3.000	3.000	3.000	3.000	3.000	3.000	3.000	3.000	3.000	3.000	3.000	3.000	3.000	3.000	3.000	3.000	3.000
Mg#	75.30	75.54	75.05	74.57	74.87	75.38	74.87	75.28	75.15	75.98	74.90	75.51	76.02	75.58	75.15	75.36	75.87	74.44

1906-4 Spinel, profile 362